Wayne State University Dissertations

1-1-2010

Synthesis Of Functionalized Gpi Anchors And Related Glycoconjugates

Benjamin M. Swarts
Wayne State University

Follow this and additional works at: http://digitalcommons.wayne.edu/oa_dissertations

Part of the Organic Chemistry Commons

Recommended Citation

SYNTHESIS OF FUNCTIONALIZED GPI ANCHORS
AND RELATED GLYCOCONJUGATES

by

BENJAMIN M. SWARTS

DISSERTATION

Submitted to the Graduate School

of Wayne State University,

Detroit, Michigan

in partial fulfillment of the requirements

for the degree of

DOCTOR OF PHILOSOPHY

2010

MAJOR: CHEMISTRY (Organic)

Approved by:

_____
Advisor   Date

_____

_____

_____

DEDICATION

To my parents and grandparents

for their love, support, and commitment to education

TABLE OF CONTENTS

LIST OF FIGURES

LIST OF SCHEMES

x

LIST OF TABLES

LIST OF ABBREVIATIONS

2ClTrt	2-Chlorotrityl
Ac	Acetyl
Acyl CoA	Acyl Coenzyme A
All	Allyl
AChE	Acetylcholinesterase
APase	Alkaline phosphatase
Asn	Asparagine
Asp	Aspartic acid
Boc	*tert*-butyl carbonyl
Bn	Benzyl
BSA	Bovine serum albumin
Bt	Benzotriazole
Bz	Benzoyl
CAN	Ceric ammonium nitrate
CD	Circular dichroism
ClAc	Chloroacetyl
COD	1,5-Cyclooctadiene
CSA	Camphor sulfonic acid
DAST	Diethylaminosulfur trifluoride
DBU	1,8-Diazobicycloundec-7-ene
DCC	*N,N'*-dicyclohexylcarbodiimide
DDQ	2,3-Dichloro-4,5-dicyano-1,4-benzoquinone

DMAP	4-Dimethylaminopyridine
DMF	*N,N*-Dimethylformamide
DMSO	Dimethylsulfoxide
Dol-P-Man	Dolicholphsophomannose
EDCI	*N*-(3-dimethylaminopropyl)-*N'*-ethylcarbodiimide hydrochloride
ER	Endoplasmic reticulum
ESI	Electrospray ionization
Fmoc	9-Fluorenylmethoxycarbonyl
FRET	Fluorescence resonance energy transfer
Gal	Galactose
GalNAc	*N*-Acetylgalactosamine
GDP	Guanosine diphosphate
Glc	Glucose
GlcN/GlcNH$_2$	Glucosamine
GlcNAc	*N*-Acetyl glucosamine
Gln	Glutamine
Gly	Glycine
GPI	Glycosylphosphatidylinositol
HA	Hemagglutinin
HexNAc	*N*-Acetylhexosamine
HIV	Human immunodeficiency virus
HPLC	High performance liquid chromatography
HOBt	1-Hydroxybenzotriazole

IPG	Inositol phosphoglycan
KLH	Keyhole limpet hemocyanin
Lev	Levulinoyl
MALDI	Matrix-assisted laser desportion ionization
Man	Mannose
mCPBA	*meta*-chloroperbenzoic acid
Mnt	Menthyl
MS	Mass spectrometry
NANA	Sialic acid
NIS	*N*-iodosuccinimide
NMR	Nuclear magnetic resonance
OTf	Trifluoromethanesulfonate
p-TolSCl	*para*-Toluenesulfenyl chloride
PARP	Procyclic acidic repetitive protein
Phth	Phthalimido
PIG-B	GPI mannosyltransferase III
PIG-M	GPI mannosyltransferase I
PIG-V	GPI mannosyltransferase II
Piv	Pivaloyl
PMB	*para*-Methoxybenzyl
PMTrt	*para*-Methoxytrityl
PI	Phosphatidylinositol
PI PLC	Phosphatidylinositol-specific phospholipases C

PPL	Porcine pancreas lipase
Pro	Proline
Pyr	Pyridine
RP	Reverse phase
SAR	Structure-activity relationship
SEM	2-Trimethylsilylethoxy methyl
SIV	Simian immunodeficiency virus
Ser	Serine
SPPS	Solid phase peptide synthesis
t-BuOOH	*tert*-Butyl hydroperoxide
TBAF	tetrabutylammonium fluoride
TBDPS	*tert*-Butyldiphenylsilyl
TBS	*tert*-Butyldimethylsilyl
TCP	Tetrachlorophthalimido
TES	Triethylsilyl
Tf	Trifluoromethanesulfonyl
TFE	2,2,2-Trifluoroethanol
Thr	Threonine
TMS	Trimethylsilyl
TIPS	Triisopropyl
TOF	Time of flight
Troc	2,2,2-Trichloroethoxycarbonyl
Ts	*para*-Toluenesulfonyl

TTBP	2,4,6-tri-*tert*-butylpyrimidine
UDP	Uridine diphosphate
VSG	Variant surface glycoprotein

CHAPTER 1

SYNTHESIS OF FUNCTIONALIZED GPI ANCHORS

1.1 Introduction

The anchoring of membrane proteins and glycoproteins to the cell surface by glycosylphosphatidylinositol (GPI) anchors, a structurally diverse class of complex glycolipids, is ubiquitous among eukaryotic species.[1] The discovery of this membrane-protein binding mechanism – a surprising alternative to the classic Singer-Nicolson model[2] – spanned the 1970s and 1980s, and culminated in the full characterization of the *Trypanosoma brucei* variant surface glycoprotein (VSG) GPI anchor in 1988 by Ferguson and co-workers.[3] Over the ensuing two decades, more than 30 unique GPIs were identified, which can be categorized into two classes. One class consists of non-protein-anchoring GPIs that are often found in protozoan parasites and contain the core structure **1.1** (Figure 1.1): Manα1→4GlcNH$_2$α1→6-*myo*-inositol-1-OPO$_3$-lipid.[4-5] The other class, which this dissertation will focus on, is comprised of protein-anchoring GPIs in mammals and other lower eukaryotes, which exhibit the core structure **1.2**: NH$_2$Et-OPO$_3$-6Manα1→2Manα1→6Manα1→4GlcNH$_2$α1→6-*myo*-inositol-1-OPO$_3$-lipid.[1,6-7]
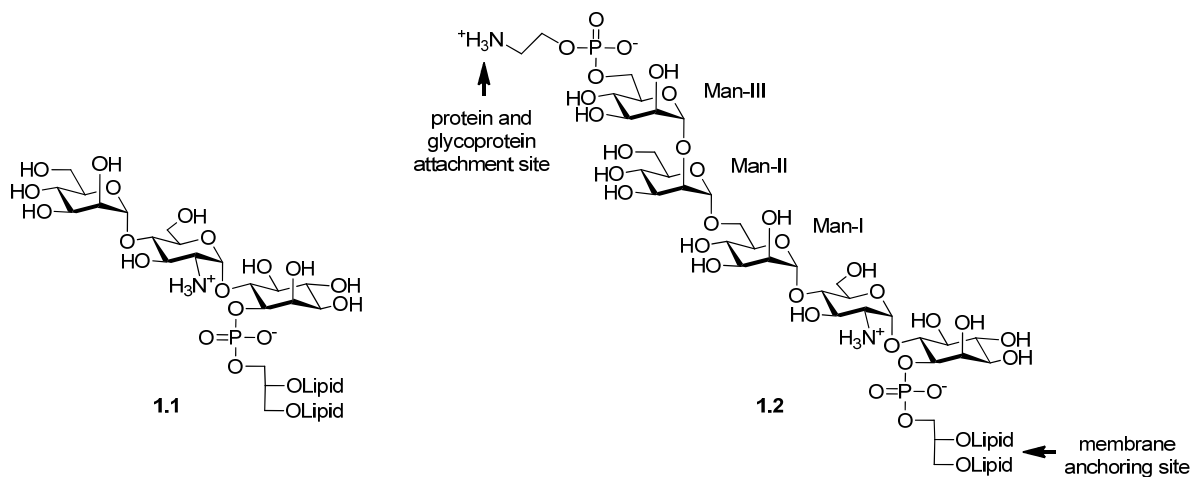
Figure 1.1. Core structures of GPIs

The primary function of GPI anchors of type **1.2** is to localize extracellular molecules, namely membrane proteins/glycoproteins, to the cell surface. This process involves covalent attachment of the protein C-terminus to the phosphoethanolamine unit at the non-reducing end of the GPI and insertion of the phosphatidylinositol lipid chains into cell membrane, thereby creating a "molecular bridge" between the protein and membrane.[3] Other biological processes that GPIs have been implicated in include cell recognition and adhesion,[8] signal transduction,[9-10] pathogenic infections,[11] and involvement in enzymatic reactions on the cell surface.[12] GPI-anchored proteins and glycoproteins are also functionally diverse, ranging from enzymes such as alkaline phosphatase (APase) and acetylcholinesterase (AChE) to cellular markers such as the human CD14 and CD52 antigens.[13] To date, more than 250 eukaryotic membrane proteins have been established as GPI-anchored,[13-14] a number that will certainly continue to grow considering that a recent study estimated that 0.5–1% of proteins encoded in the eukaryotic genome are anchored to the cell surface by GPIs.[15]

Despite significant advances in understanding the biosynthesis, structure, and function of GPI anchors, many aspects of these molecules remain a mystery. For example, the anchoring of membrane proteins could seemingly be accomplished by simpler covalent lipid modifications; the considerable structural complexity of GPIs is suggestive of additional biological responsibilities beyond providing a stable anchoring system for proteins. While evidence for some ancillary GPI functions exists, additional biological studies are required to better understand the various roles of GPIs on the cell surface. In addition, the correlations between specific structural features/diversity of GPIs and function are essentially unknown. Answering these questions necessitates

structure-activity relationship (SAR) studies aimed at probing the significance of GPI structural features, such as type of sugar unit, stereo- and regiochemistry of glycosidic bonds, lipid modifications, and additional sugar branching or phosphoethanolamine units. Furthermore, the scope of GPI anchoring has not been rigorously studied. To investigate all of these issues, it is necessary to have access to homogeneous and structurally well-defined GPIs, GPI analogs, and functionalized GPIs. However, due to the issues of structural microheterogeneity and the natural scarcity of these molecules, it is nearly impossible to obtain sufficient quantities of GPIs from natural sources, making the study of GPI anchorage quite difficult. To address this problem, chemical synthesis, although challenging and time-consuming, has become the primary means for obtaining pure samples of GPIs. While several complex GPI structures have been synthesized, the development of new synthetic methodologies is necessary for the preparation of uniquely functionalized GPIs aimed at studying various aspects of the GPI anchoring process.

The remainder of the introduction will serve as a review of various aspects of GPI anchors. The first section will provide a historical perspective on GPI anchors, including the key studies that led to their discovery. The structural properties of GPIs will then be discussed, including the first characterization of a GPI by Ferguson and subsequent identification of various structurally diverse GPIs. Next, GPI anchors will be evaluated in a purely biological context. These sections will survey GPI biosynthesis and function. Finally, the state-of-the-art in GPI chemical synthesis will be reviewed prior to a full report of the synthetic studies conducted for this dissertation.

1.1.1 Discovery of GPI Anchors

The lipid bilayer of the cell membrane functions as a permeability barrier that prevents the free extracellular/cytoplasmic exchange of water-soluble molecules, such as ions and proteins. Nearly all biological processes that occur on the cell surface involve membrane proteins, which function by associating with the lipid bilayer and facilitating signal transmission, metabolite transportation, and other vital cellular activities. Early on, protein–membrane binding was primarily attributed to the insertion of hydrophobic protein domains into the lipid bilayer,[2] and little credence was afforded to the notion that a covalently linked lipid moiety could be solely responsible for the anchoring of proteins to the membrane. However, evidence for the latter anchoring mechanism accumulated rapidly in the 1970s and 1980s, when various lipid-modified prokaryotic and eukaryotic proteins were characterized.[16] For example, protein *S*-palmitoylation[17] (addition of a C16 fatty acid) and *N*-myristoylation[18] (addition of a C14 fatty acid) are modifications of cysteine and N-terminal glycine residues, respectively, that can contribute to protein-membrane binding. Another type of membrane-anchoring protein lipidation that was identified during this time was the covalent attachment of complex glycosylated phospholipids, later designated GPI anchors, to the C-terminus carboxyl group of various membrane proteins, a discovery that was "most unusual and unexpected."[16]

The concept of membrane protein anchoring by phosphatidylinositol (PI) was independently cultivated by Low[19-21] and Ikezawa[22-23] in the late 1970s. Their work centered on the ability of a class of PI-cleaving bacterial phospholipases, termed phosphatidylinositol-specific phospholipases C (PI PLC), to release the membrane-

bound enzyme APase from various tissues. Actually, PI PLC were first shown to release APase from *Bacillus anthracis* toxins in the early 1960s,[24-27] but the significance of these results was overlooked until Low, Ikezawa, and others extensively studied purified PI PLC and found that they released a variety of membrane proteins, also including 5'-nucleotidase and AChE.[28] These observations led to the conclusion that certain proteins were covalently linked to PI, a property that enabled membrane binding by insertion of the PI lipid chains. Furthermore, the release of a protein by PI PLC could be used as a convincing marker that PI was involved in membrane anchoring, although the converse was not necessarily true, as some PI-anchored proteins were later shown to be resistant to PI PLC cleavage.[28]

The nature of the protein-PI linkage remained unclear for several years, but was unraveled from 1980-1985 as a result of characterization data accumulated for a number of PI-anchored proteins. Studies on *Torpedo* electric organ AChE,[29] human erythrocyte AChE,[30] rat brain and thymocyte Thy-1,[31-32] and *T. brucei* VSG[33-36] demonstrated that for all of these PI-PLC-positive membrane proteins, a glycosylated phosphatidylinositol structure was attached to the C-terminus amino acid via a phosphoethanolamine unit. Structural data obtained from these experiments confirmed the presence of various fragments of the GPI structure, including *myo*-inositol, phosphate, ethanolamine, and an oligosaccharide composed of glucosamine and mannose. Although the precise structure of a GPI anchor had not yet been determined, a consensus for the general structure and distribution of GPI anchors materialized in 1985.[14]

1.1.2 Structure of GPI Anchors

The first fully characterized GPI anchor was that of the *T. brucei* VSG, achieved in 1988 by Ferguson and co-workers using a combination of NMR spectroscopy, MS, chemical modification, and exoglycosidase digestion.[3] Since then, more than 30 different GPI anchors derived from various eukaryotic cells and species have been identified.[1,6] To date, all GPI anchors contain the conserved core described by structure **1.2** (Figure 1.1): $NH_2EtO-PO_3-6Man\alpha1\rightarrow2Man\alpha1\rightarrow6Man\alpha1\rightarrow4GlcNH_2\alpha1\rightarrow6$-*myo*-inositol-1-$OPO_3$-lipid.

The phosphoethanolamine-protein bridge exists in the form of an amide bond that links the GPI anchor to the C-terminal amino acid carboxyl group. This connection was confirmed by testing for dansylation of the ethanolamine NH_2-group during Edman degradation, which only occurred after removal of the protein's C-terminal amino acid.[33] The presence of non-acetylated glucosamine, which is present in all GPIs but rarely in other eukaryotic glycoconjugates, was identified by its unique propensity to undergo deamination by nitrous acid.[36] This reaction also released PI and inositol phosphate, which was evidence for the glucosamine-inositol linkage.[3] Moreover, ^{1}H NMR studies showed that the glucosamine-inositol glycosidic bond was located at the inositol 6-*O*-position and exhibited α stereochemistry. The remainder of the conserved glycan portion was determined to be a linear trimannose, also bearing α-configured anomeric centers. The phosphatidylinositol group is composed of D-*myo*-inositol derivatized at the 1-*O*-position with a phosphoglycerolipid backbone containing an sn-1,2-dilipid-3-phosphate stereochemical configuration. These assignments were aided by the action of enzymes that hydrolyze these specific moieties.[35,37]

GPI anchors exhibit a high degree of structural diversity, as summarized for various GPIs in Table 1.1 (adapted from Bertozzi[13] and Ikezawa[38]). The tetrasaccharide core can contain additional carbohydrate chains and phosphoethanolamine groups. The trimannose segment commonly exhibits additional carbohydrate branching at the Man-III 2-*O*-position and Man-I 3- and 4-*O*-positions. The former location typically is decorated with additional mannose residues in the form of a Manα1→2 linkage, while the latter two locations may contain a variety of sugars, including galactose, galactosamine, and sialic acid in the form of monosaccharides or oligosaccharides. The core glucosamine residue is rarely modified, but has been observed to carry a unique 2-aminoethylphosphonate group (similar to a phosphoethanolamine group but bearing a P-C bond) at the 6-*O*-position in the *Trypanosoma cruzi* NETNES GPI anchor. Additional phosphoethanolamine side chains are also found frequently at the Man-I 2-*O*-position and Man-II 6-*O*-position in higher eukaryotes. There is also wide variation in the composition of the lipid chains, which may be linked to the glycerol moiety via an ether or ester bond or contain unsaturation. The presence of unsaturation in the lipid chains of GPIs may have a pronounced impact on biological function. A recent study by Ferguson on highly purified *T. cruzi* GPI anchors indicated that their potent proinflammatory activity is dependent on unsaturated fatty acids, rather than saturated fatty acids, at the sn-2 position of the glycerolipid.[39] This finding demonstrates the importance of synthesis and SAR studies aimed at evaluating the importance of structural diversity among GPI anchors.

Table 1.1. Structural diversity in various GPI anchors (adapted from Bertozzi[13] and Ikezawa[38])[a]
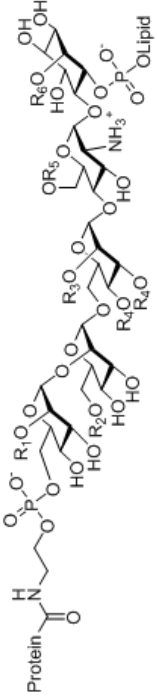
Protein[ref]	R1	R2	R3	R4	R5	R6	Lipid
Rat brain THY-1[40]	±Manα1→2	OH	PEtN	±GalNAcβ1→4	OH	OH	alkylacyl-glycerol
Human erythrocyte AChE[41-42]	OH	±PEtN	PEtN	OH	OH	palmitate	alkylacyl-glycerol
Hamster brain scrapie prion protein[43]	±Manα1→2	OH	PEtN	(±NANA)-(±Gal)-GalNAcβ1→4	OH	OH	nd
Human urine CD59[44]	±Manα1→2	OH	PEtN	±GalNAcβ1→4	OH	palmitate	nd
Mouse skel. muscle NCAM[45]	±Manα1→2	nd	PEtN	±GalNAcβ1→4	OH	OH	nd
Bovine liver 5'-nucleotidase[46]	±Manα1→2	±PEtN	PEtN	±HexNAc	OH	OH	nd
Human placental Apase[47]	OH	±PEtN	PEtN	OH	OH	OH	alkylacyl-glycerol
Human CD52[48]	±Manα1→2	±PEtN	PEtN	OH	OH	palmitate	diacyl-glycerol
Pig kidney membrane dipeptidase[49]	OH	±PEtN	PEtN	(±Galβ1→3)-±GalNAcβ1→4 or (±NANA)-GalNAcβ1→4	OH	OH	diacyl-glycerol
Human kidney membrane dipeptidase[49]	±Manα1→2	nd	PEtN	(±Galβ1→3)-±GalNAcβ1→4	OH	OH	nd
T. brucei VSG[3]	OH	OH	OH	±Galα1→2(Galα1→2Gal α1→6)Galα1→3	OH	OH	dimyristyl-glycerol
T. Cruzi 1G7[50]	±Manα1→2	OH	OH	OH	OH	OH	alkylacyl-glycerol
T. Cruzi NETNES[51]	±Manα1→2	OH	OH	OH	AEP	OH	alkylacyl-glycerol
L. major gp63[13]	OH	OH	OH	OH	OH	OH	alkylacyl-glycerol
S. cerevisiae gp125[13]	±Manα1→2Manα1→2 or ±Manα1→3Manα1→2	OH	OH	OH	OH	OH	alkylacyl-glycerol
A. fumigatis PhoAp[52]	±Manα1→3Manα1→2	OH	OH	OH	OH	OH	ceramide
P. communis arabinogalactan proteins[53]	OH	OH	OH	±GalNAcβ1→4	OH	OH	ceramide
D. discoideum PsA[13]	±Manα1→2	nd	nd	OH	OH	OH	ceramide

[a] Various side chain modifications of GPI anchors at R1–R6 and lipid linkage variations are shown. OH = no side chain known, nd = not determined, Man = mannose, Gal = galactose, GalNAc = N-acetylgalactosamine, NANA = sialic acid, HexNAc = N-acetylhexosamine, PEtN = phosphoethanolamine, AEP = 2-aminoethylphosphonate.

1.1.3 Biosynthesis of GPIs and Their Attachment to Proteins

The highly conserved core structure of GPI anchors (**1.2**) described in section 1.1.2 is shared among a wide range of species. This fact suggests that a generally conserved GPI biosynthetic pathway exists in nature.[6,40] Studies on the parasitic trypanosomes, which express large amounts of isolable GPIs, provided the first information regarding GPI biosynthesis. Trypanosome membranes were incubated with radiolabeled uridine diphosphate-*N*-acetylglucosamine (UDP-GlcNAc) and guanosine diphosphate-mannose (GDP-Man), which allowed GPI biosynthetic intermediates to be observed, thus elucidating the biosynthetic pathway.[41-42] Subsequent studies on mammal and yeast GPIs confirmed the features of this process that were conserved or species-specific.

As outlined in Figure 1.2, GPI biosynthesis starts with the transfer of a GlcNAc residue from UDP-GlcNAc to PI to form GlcNAc-PI on the cytoplasmic surface of the endoplasmic reticulum (ER), which is followed by de-*N*-acetylation of GlcNAc and then addition of a palmitoyl group to the inositol 2-*O*-position.[6] Inositol 2-*O*-palmitoylation depends on and is stimulated by the presence of acyl coenzyme A (acyl-CoA).[43] However, the attachment of a palmitoyl group is not necessary for subsequent biosynthetic steps. For example, GPI biosynthesis in the bloodstream form of *T. brucei* does not require inositol acylation.[44] Thereafter, the biosynthetic intermediate is translocated to the lumen side of the ER, where the first mannose (Man-I) is added to glucosamine by GPI mannosyltransferase I (PIG-M), with dolicholphosphomannose (Dol-P-Man) as the mannosyl donor. Subsequently, the second and third mannoses (Man-II and Man-III) are sequentially added by GPI mannosyltransferases II (PIG-V)

and III (PIG-B), respectively. In some cases, after Man-II is attached, a phosphoethanolamine moiety is added to the 2-*O*-position of Man-I.[7] It was also observed in *T. brucei* that the inositol residue can be deacylated and re-acylated once the first mannose is added,[44-45] suggesting that inositol palmitoylation is reversible.[46] For most GPIs, the last biosynthetic step is the addition of a phosphoethanolamine unit to the Man-III 6-*O*-position with phosphatidylethanolamine as the donor, though sometimes additional carbohydrate chains and/or phosphoethanolamine moieties may be added to the core glycan at this stage as well.[7] Once a phosphoethanolamine unit is added to the 6-*O*-position of Man-III, the GPI anchor may undergo attachment to target proteins.
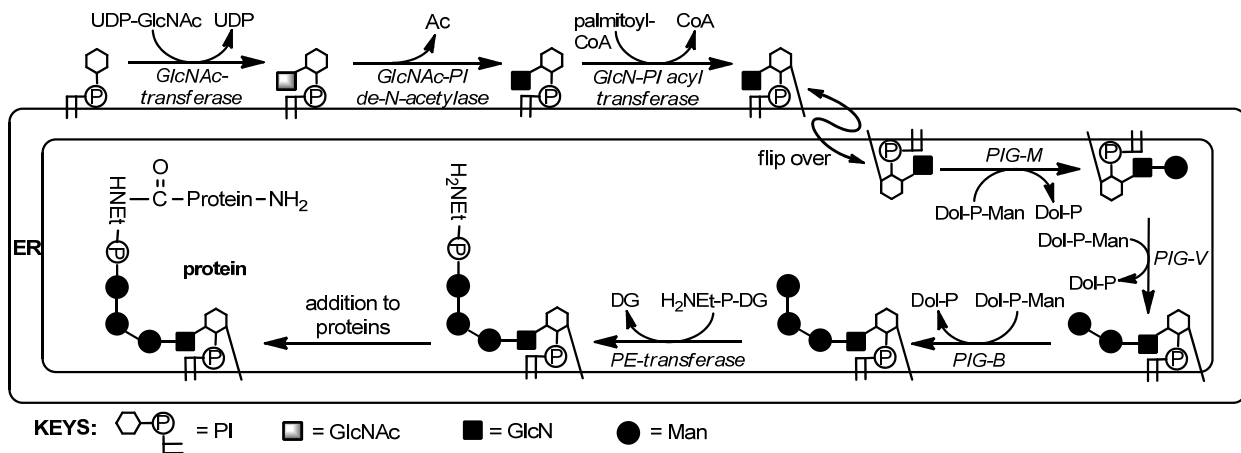
Figure 1.2. An outline of GPI biosynthesis

The attachment of GPIs to proteins also takes place in the ER lumen through a process known as GPI transamidation (Figure 1.3),[47-49] which is catalyzed by a multi-subunit transmembrane enzyme called GPI transamidase. Both the GPIs and the proteins destined for GPI attachment are anchored to the ER membrane, with the latter

being anchored via a hydrophobic peptide sequence at the C-terminus. This sequence is also the GPI attachment signal that is responsible for regulating GPI transamidation[50] and is essential for the target proteins to be recognized and coupled to GPIs by GPI transamidase. Though the GPI attachment signal is required for nascent proteins destined for GPI addition, its exact sequence can vary in different proteins.[51-54] During GPI transamidation, the C-terminal signal peptide is deleted and substituted by a GPI, thus GPIs are always linked to the polypeptide C-terminus.[50] The proteins to be GPI-linked contain another signal peptide located at the N-terminus, which directs nascent proteins to the ER but is not deleted during the transamidation process.[50] After GPIs are attached to proteins, the palmitoyl group at the inositol 2-O-position is usually removed[55] for the purpose of quality control of GPI-linked proteins. This process may also facilitate the transportation of GPI-linked proteins from the ER to the Golgi apparatus.[56] However, it is observed that some GPI-anchored proteins may retain the palmitoyl group on the inositol residue, as observed with the GPI anchors of procyclic acidic repetitive protein (PARP) of *T. brucei*, the human CD52 antigen, and human AChE.[57-66] After the GPI-linked proteins are transported to the Golgi, GPIs may be further modified through a so-called "fatty acid remodeling" process,[67-69] the details of which are not well established. Finally, the GPI-anchored proteins are delivered onto the cell surface via the trans-Golgi network.
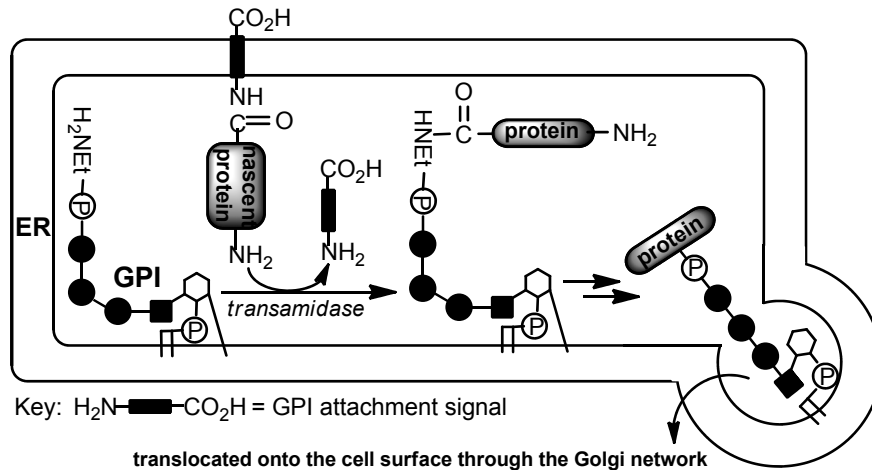
Figure 1.3. Attachment of proteins to mature GPIs to form GPI-anchored proteins

1.1.4 Biological Functions of GPI Anchors

As discussed, the primary role of GPIs is to provide a stable membrane anchoring device for cell surface proteins and glycoproteins.[1] Despite this apparent function, the questions of why certain proteins are GPI-anchored and why GPIs exhibit such a complex structure remain largely unanswered. Investigation of the various biological roles of GPIs on the cell surface has led to a better – although still murky – understanding of the significance of GPI anchoring and GPI structure.

Some unique properties of GPIs can be particularly useful for the functioning of GPI-anchored proteins and glycoproteins. For example, GPIs are thought to associate with lipid rafts, which are membrane microdomains that contain high concentrations of glycosphingolipids, cholesterol, and other lipidated biomolecules. Lipid rafts are relatively small and discrete domains where various processes such as vesicle transportation and signal transduction may occur.[13] It is hypothesized that the presence of GPIs in lipid rafts may help the sorting and localization of some GPI-anchored proteins.[70-71] For instance, GPI-linked proteins are selectively delivered onto the apical

surface in polarized mammalian cells.[72] In addition, the lateral mobility of GPIs in cell membranes and the clustered existence of GPI-linked proteins in lipid rafts can facilitate reactions on the cell surface. For example, many bacterial toxins use GPIs or GPI-anchored proteins/glycoproteins on the host cell surface to assist their aggregation and subsequent formation of porous oligomers that automatically insert into the cell membrane to kill the host cell.[73-74] Furthermore, GPIs and GPI-anchored molecules can be released relatively easily from the cell membrane, which can facilitate their shedding, shuffling, and turnover processes. This release process, mediated by endogenous PI PLC that cleave the lipid moiety of the GPI, has been suggested as a mechanism for the selective regulation of GPI-anchored proteins.[75-76] Finally, GPI anchors may have an impact on the structure of the proteins to which they are attached. A variety of studies, including circular dichroism (CD), 2D NMR spectroscopy, molecular modeling, and Förster resonance energy transfer (FRET), have confirmed this hypothesis, although the effects of GPI-induced structural/conformational changes are unclear.[77-80]

GPIs have been implicated in a number of other biological processes as well. The involvement of GPI anchors in signal transduction between the cell exterior and internal signaling molecules has been observed in some systems.[13] Notably, the enzyme-mediated release of water soluble inositol phosphoglycans (IPGs) from GPI-anchored molecules can have inhibitory or stimulatory effects on various cellular activities.[81] In addition, GPI metabolites can serve as secondary messengers involved in certain hormonal pathways,[82] possibly including insulin mediation.[83] Other processes that GPI anchors may be involved in include cellular adhesion/recognition, bacterial toxin binding, and prion disease pathogenesis.[13] The involvement of GPI anchors in

these proposed functions is controversial and requires additional studies, which would benefit greatly from access to pure and structurally defined synthetic GPI derivatives.

1.1.5 Chemical Synthesis of GPI Anchors

Obtaining homogeneous GPI anchors for biological studies is a challenging task. Like other natural glycoconjugates, each GPI anchor may be comprised of heterogeneous glycoforms,[84] a phenomenon known as microheterogeneity. This heterogeneity can be further compounded by variations in the lipid chains, such as differences in chain length and the presence of unsaturated bonds.[1] The separation of such naturally occurring complex GPI mixtures is practically impossible. Furthermore, the low abundance of these molecules in most species prevents their isolation in sufficient amounts. Thus, it is extremely difficult to obtain homogeneous GPIs and GPI-anchored proteins or glycoproteins from living cells. Consequently, the chemical synthesis of GPIs has drawn much attention from the synthetic community.

The first total synthesis of a GPI anchor, specifically a diastereomer of the natural membrane GPI anchor of *T. brucei*, was completed by Murakata and Ogawa in 1991.[85-86] Since then, numerous GPIs have been synthesized, including the GPIs of *T. brucei* by Ley,[87-88] rat brain Thy-1 by Fraser-Reid[89-90] and Schmidt,[91] *S. cerevisiae* and *T. gondii* by Schmidt,[92-94] *P. falciparum* by Fraser-Reid[95] and Seeberger,[96-97] human sperm CD52 by Guo,[98-100] and *T. cruzi* by Nikolaev.[101] These syntheses and other reports on the synthesis of partial/core structures of GPIs were covered in extensive reviews by Gigg[102] and Guo.[103] In this section, general strategies for the synthesis of GPI anchors and their components will be discussed.

1.1.5.1 Retrosynthetic Analysis of GPIs

GPI synthesis involves several different areas of chemistry, including lipid, phosphate, inositol, and carbohydrate chemistry. While this combination of chemistries poses a considerable synthetic challenge, other issues complicate GPI synthesis as well. For example, the preparation of suitably differentiated and enantiomerically pure or enriched *myo*-inositol derivatives is difficult due to the presence of six secondary hydroxyl groups and the *meso*-symmetric nature of the compound, respectively. In addition, stereoselective assembly of the glycans and regioselective introduction of the desired side chains requires careful planning. Furthermore, characterization of GPI intermediates by NMR spectroscopy, particularly if they exist as isomeric mixtures, can be difficult as well. These combined challenges render GPI synthesis a demanding task.

As described in section 1.1.3, nature uses an iterative biosynthetic process to construct GPI anchors.[7] Living systems use a series of glycosyltransferases to elongate the PI-linked glycan in a linear fashion. In the context of chemical synthesis, a convergent strategy offers a much more efficient and versatile approach. In terms of efficiency, a linear strategy involves a large number of chemical manipulation steps on valuable complex intermediates, whereas a convergent synthesis allows for a key coupling of two fragments to produce a highly elaborated GPI intermediate. A convergent approach also offers more flexibility in what types of fragments are used for the key coupling reactions, which provides an opportunity for the preparation of small libraries of related GPI derivatives for bioactivity studies. These advantages clearly support the use of a convergent strategy, which has been used in preference to a biomimetic approach in nearly all reported GPI syntheses.

A typical GPI retrosynthetic analysis used by our group is shown in Scheme 1.1. The first disconnection is often a phosphorylation reaction between fully protected GPIs of type **A** and a phosphate precursor **B** that is used to install one or more phosphoethanolamine units, including at the conserved Man-III 6-*O*-position and sometimes at other positions. This is often chosen as the final functionalization step because the stability of phosphate esters and their protecting groups (e.g., cyanoethoxy) to a wide range of glycosylation and functional group manipulation conditions is not guaranteed. Thus, the reaction conditions available for use with phosphates present can be quite limited. In addition, the presence of phosphates can significantly alter physical properties relating to solubility and separation. For instance, in the simplest case, monophosphorylation of a GPI generates a 1:1 mixture of diastereomers originating at the stereogenic phosphorus atom. These mixtures, which are often inseparable, complicate the characterization of intermediates by NMR spectroscopy, so phosphorylation reactions are usually left until the final stages of the synthesis.
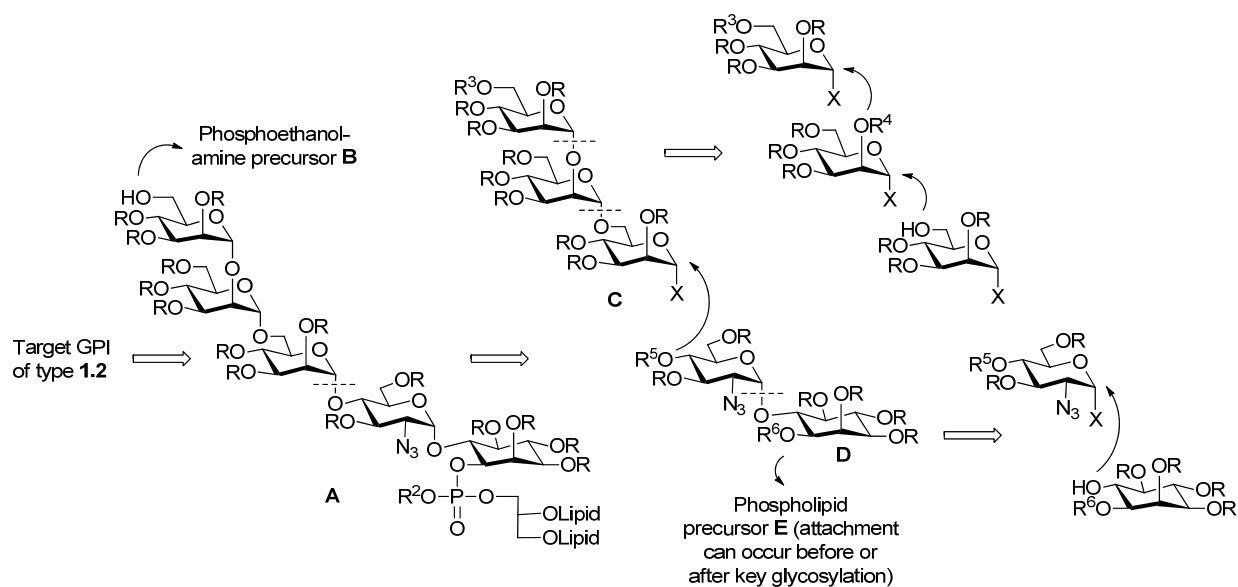
Scheme 1.1. Typical retrosynthesis of GPI anchors

In many GPI syntheses, structure **A** is prepared by a key glycosylation reaction between trimannoside glycosyl donor **C** and pseudodisaccharide glycosyl acceptor **D** (or derivatives thereof). This allows for a highly convergent synthesis that hinges on the formation of an α-mannosidic bond, which is a favorable process. Trimannoside fragment **C**, which is usually built using three suitably protected monomers, contains an orthogonal protecting group at the Man-III 6-*O*-position for later phosphorylation. In addition, any side chains present in the target GPI can be incorporated into the structure of **C**. In our lab, pseudodisaccharide **D** is formed via sequential glucosaminylation and phospholipidation of a differentially protected inositol derivative. Guo found that installation of phospholipid **E** to inositol was best performed at this point in the synthesis – rather than at a later stage – to enhance convergency and prevent an interesting but debilitating cyclization reaction between the GPI azido group and the nascent phosphite.[99] However, most GPI syntheses reported to date have successfully used late-stage phospholipidation of inositol on an advanced intermediate, so this is not always a problem. Specific approaches to each of the building blocks in Scheme 1.1, as well as strategies for their assembly, will be discussed in the following sections.

1.1.5.2 Synthesis of Differentially Protected and Optically Pure Inositols

myo-Inositol, commonly referred to as inositol in this text, is a *meso*-symmetric cyclohexanehexol compound that widely occurs in nature in both free and derivatized form. The incorporation of inositol building blocks in natural product synthesis is a demanding prospect for two reasons. First, the selective functionalization of inositol requires the differentiation of six secondary alcohols. Therefore, the regioselective

protection and deprotection of inositol derivatives is a broadly studied area in bioorganic chemistry. This topic was recently reviewed by Sureshan and Shashidhar.[104] The second challenging aspect of inositol synthesis lies in the symmetrical nature of the molecule. Derivatization of any symmetrical position of inositol will produce chirality and result in the formation of a racemic mixture (Figure 1.4). Given the ubiquity of inositol derivatives in nature, many methods have been developed for the preparation of optically pure or enriched inositols. These methods fall into three categories: (1) conversion of naturally occurring inositol derivatives into the desired structures; (2) chemical or enzymatic resolution of synthetic inositol racemates; (3) de novo synthesis of inositol derivatives from chiral pool starting materials. This section will focus on selected methods that address the preparation of building blocks commonly used in GPI synthesis, namely 1,2-*O*- and 1,2,6-*O*-differentiated inositols.
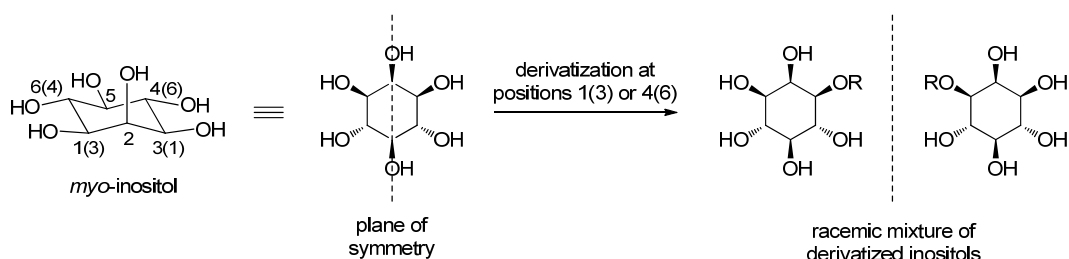
Figure 1.4. Desymmetrization of *myo*-inositol by derivatization

A useful and common starting point for many reported GPI syntheses involves the cyclohexylidenation of commercially available and inexpensive *myo*-inositol (Scheme 1.2).[105] This reaction produces an approximate 1:1:1 mixture of regioisomeric diols **1.3**, **1.4**, and **1.5**. The most GPI-relevant 1,6-*O*-differentiated product **1.5** can be

isolated using sequential recrystallization and column chromatography. The eventual resolution of racemate **1.5** has been achieved both chemically and enzymatically. The former method involves derivatization with a temporary chiral resolving reagent, such as (1*S*)-(-)-camphanic chloride, which produces a separable diastereomeric mixture. After purification of the desired diastereomer, the chiral auxiliary is cleaved to afford an enantiomerically pure inositol derivative. This method has been commonly used in the synthesis of GPI anchors by several groups, including those of Fraser-Reid,[90] Ley,[88] Martin-Lomas,[106] Ogawa,[107] Schmidt,[93] and others. The other strategy, developed by Gou et al.,[108] employed an enzymatic enantioselective resolution of (±)-**1.5** (Scheme 1.2). After stannylene acetal-directed regioselective addition of a butanoyl group to the inositol 6-*O*-position, the racemic product (±)-**1.6** was subjected to porcine pancreas lipase (PPL) digestion, which enantioselectively cleaved the ester bond. After separation of enantiomerically enriched products (-)-**1.7** and (-)-**1.8** by column chromatography, the latter was deacylated using NaOMe to give the desired enantiomer (+)-**1.7**. We have employed both chemical and enzymatic resolution in this research (see section 1.2.3). Because the 1-*O*- and 6-*O*-positions are already differentiated from the remaining hydroxyl groups in (+)-**1.7**, it is an ideal substrate for the preparation of 1,6-*O*-differentiated inositols for GPI synthesis, particularly due to the ability of its 6-*O*-position to undergo a highly regioselective stannylene acetal-directed allylation reaction, which is shown in Scheme 1.3.
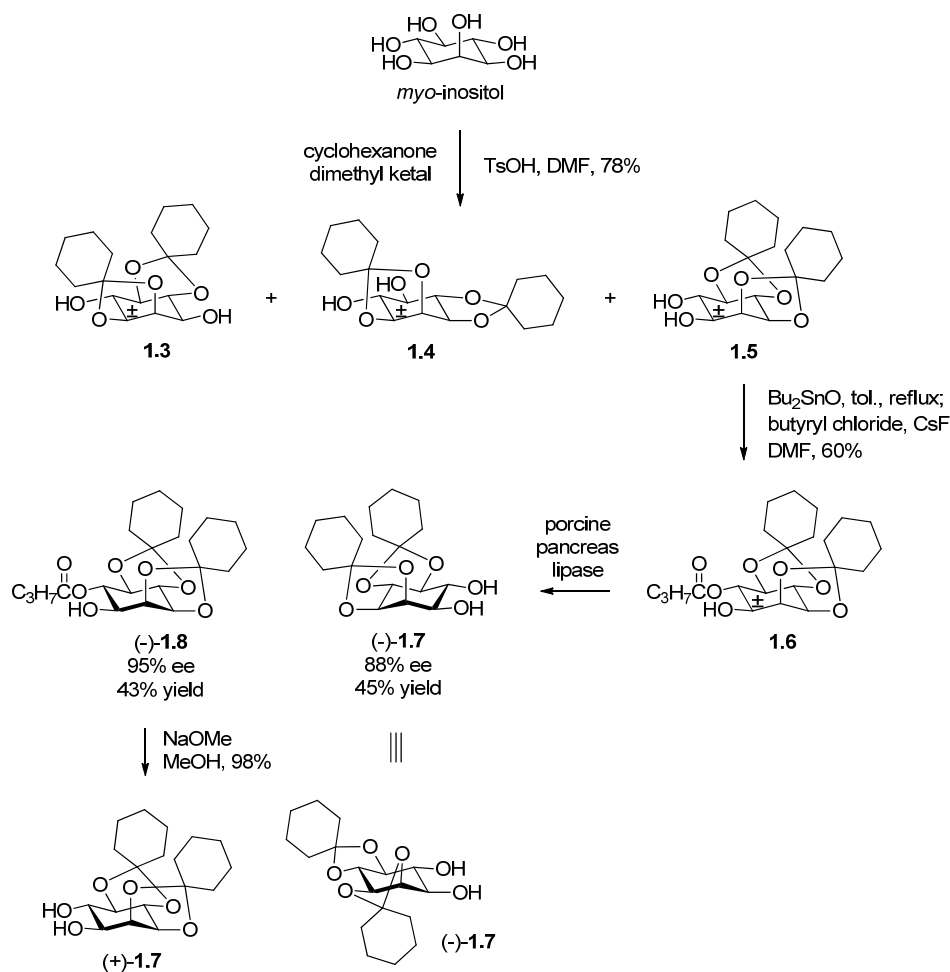
Scheme 1.2. Enzymatic resolution of a 1,6-*O*-differentiated inositol racemate

The preparation of 1,2,6-*O*-differentiated inositols, which are required for the synthesis of GPIs containing a palmitoyl group at the inositol 2-*O*-position, are more difficult to prepare. Guo developed a strategy for the conversion of both enantiomers of **1.7** to the same 1,2,6-*O*-differentiated inositol **1.12**,[109] thus eliminating the major disadvantage of enantiomeric resolutions by increasing the maximum theoretical yield from 50% to 100% (Scheme 1.3). Route A commenced with a regioselective allylation of (+)-**1.7** to provide 6-*O*-allyl inositol **1.9**, which then underwent *para*-methoxybenzylation and acid catalyzed selective removal of the *trans*-cyclohexylidene ring. The resulting diol **1.10** was then benzylated and treated with acid for a prolonged period to remove the more stable *cis*-cyclohexylidene ring, resulting in diol **1.11**. Finally, regioselective

benzylation of the 3-*O*-position provided **1.12**. Route B describes a similar pathway to **1.12** from the other enantiomer (-)-**1.7**, with analogous reactions in a different order.
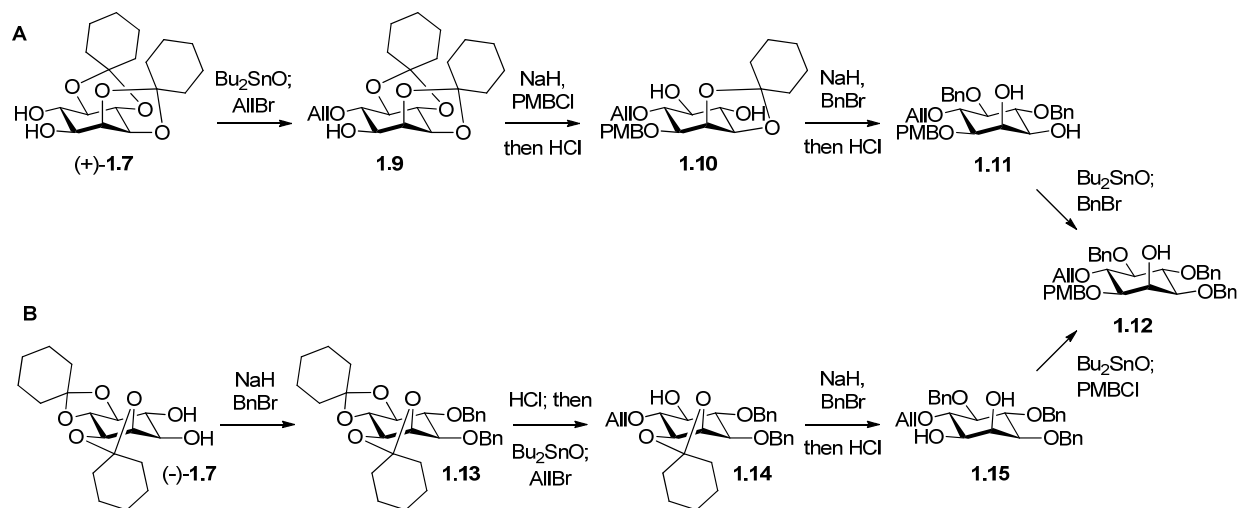
Scheme 1.3. Synthesis of a 1,2,6-*O*-differentiated inositol derivative

De novo synthesis of inositol derivatives from chiral pool starting materials offers an efficient alternative to chemical/enzymatic resolution, in which half of the material is typically lost. Our lab has made extensive use of Fraser-Reid's method for the preparation of gram-scale amounts of benzyl-protected inositol derivatives from commercially available methyl α-D-glucopyranoside (Scheme 1.4).[110] This strategy centers on an application of the Ferrier rearrangement, which was used to transform enol acetate **1.17** to polyhydroxylated cyclohexanone **1.18**. After a stereoselective reduction of the ketone and deacetylation, product **1.20** can be converted into a number of 1,2-*O*- or 1,2,6-*O*-differentiated inositol building blocks.
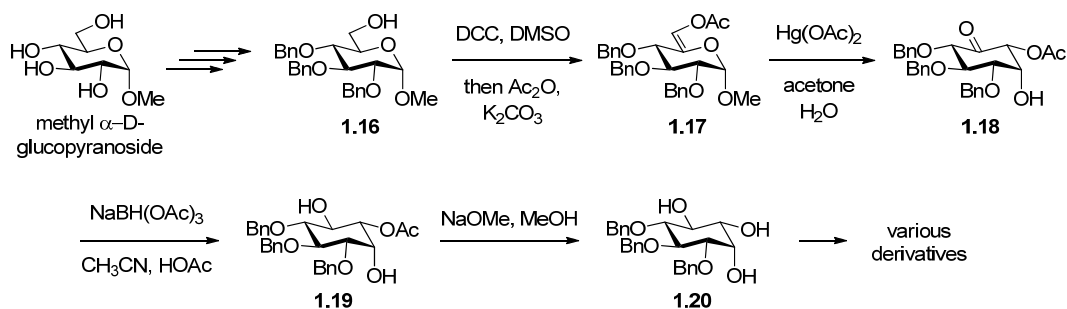
Scheme 1.4. De novo synthesis of inositol derivatives from methyl glucopyranoside

The Bertozzi lab developed a de novo synthesis of highly discriminated inositols starting from commercially available and optically pure tartrate derivative **1.21** (Scheme 1.5).[111] Key steps for this strategy included various substrate-controlled diastereoselective reactions and a ring-closing metathesis step catalyzed by Grubbs' catalyst. A final selective *para*-methoxybenzyl (PMB) ether cleavage provided 1,2,3,6-*O*-differentiated inositol **1.27**. This de novo method required only 8 steps and proceeded in an impressive 25% overall yield.
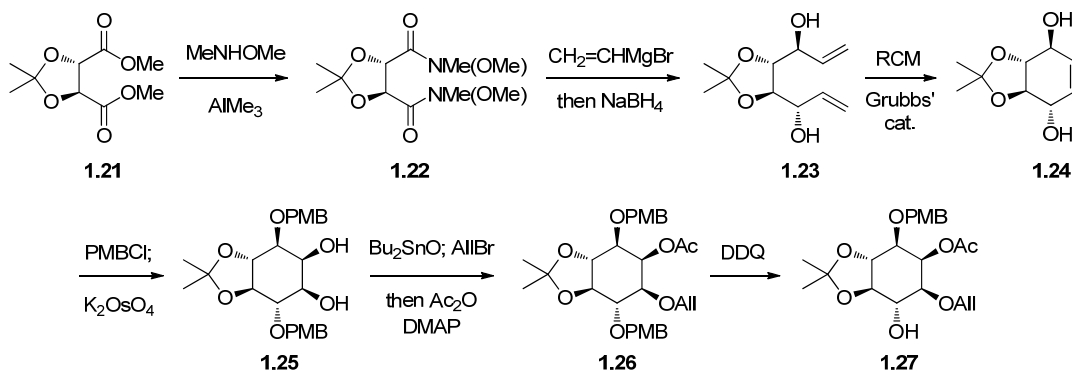
Scheme 1.5. De novo synthesis of inositol derivatives from a tartrate derivative

The procedures described above constitute a small sample of the available methods[104] for preparing discriminated inositol derivatives. However, these strategies meet the demands of most GPI syntheses, which require 1,6-*O*- and 1,2,6-*O*-differentiated inositol building blocks in optically pure form.

1.1.5.3 Synthesis of the Pseudodisaccharide Fragment

As outlined in the GPI retrosynthesis (Scheme 1.1), one of the key glycosylation components used in our GPI syntheses is pseudodisaccharide **D**. Construction of this intermediate (Scheme 1.6) requires the stepwise functionalization of a 1,6-*O*-differentiated inositol building block. In our lab, α-glycosylation of the 6-*O*-position with a glucosaminyl donor is followed by selective deprotection of the 1-*O*-position. Next, the desired phospholipid is installed at this site, and then the glucosamine 4-*O*-position is exposed to set up for the key glycosylation reaction. Alternatively, phospholipidation can be performed after the key glycosylation, as in most reported GPI syntheses.
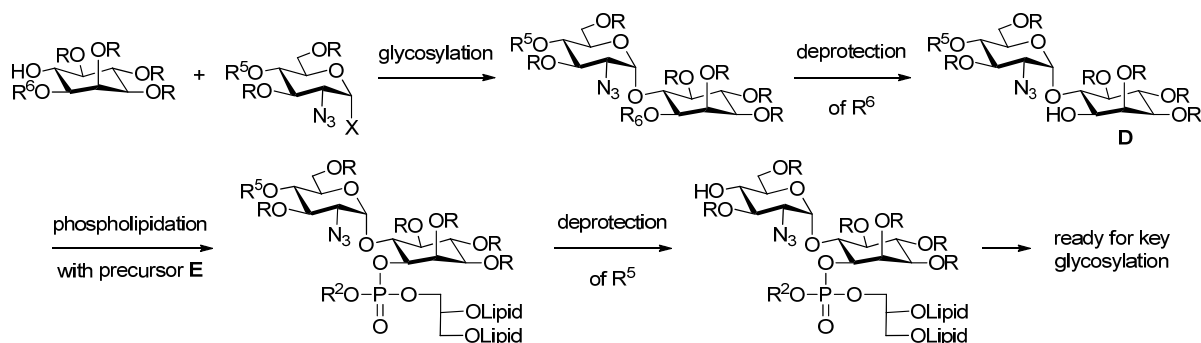
Scheme 1.6. General outline for the synthesis of pseudodisaccharide **D**

To generate the required α-glycosidic bond between a glucosaminyl donor and an inositol acceptor, several factors, such as substrate structure, protecting group

effects, and reaction conditions, must be considered. Of utmost importance for allowing, and ideally magnifying, formation of the 1,2-*cis* configured α-product is the presence of a non-participating *N*-protecting group at the glucosamine 2-position. Therefore, commonly employed amine protecting groups such as phthalimido (Phth), tetrachlorophthalimido (TCP), and various carbamates (i.e., Fmoc and Troc) cannot be used. While non-participating *N*-protecting groups are limited, the azido group has become the standard choice for GPI synthesis, as it satisfies the non-participating requirement, is stable to a range of reaction conditions, is not sterically bulky, and can be selectively removed under a variety of mild conditions. The preparations of different 1,4-*O*-differentiated glucosaminyl donors from a variety of starting materials, including anhydromannose,[112-113] D-glucal,[109,114] glucosamine hydrochloride,[115] and others[116] have been achieved using a number of methods. Our lab typically relies on elaboration of glucosamine hydrochloride to the desired building block, and we make use of Wong's copper-catalyzed diazo transfer reaction[117] to install an azido group at the 2-position.

The glycosyl donor leaving group, activation conditions, solvent, and temperature can also affect the stereochemical outcome of the reaction. Among the various glucosaminyl donors employed in this reaction have included glycosyl fluorides, bromides, and trichloroacetimidates. Several glucosamine-inositol glycosylation reaction examples are summarized in Table 1.2. In most cases, α-stereoselectivity is moderate, and the factors leading to an increase of the α-anomer are not entirely clear. However, some modifications, such as using Et_2O as the solvent or using Lemieux conditions[118] for glycosyl bromide activation, can improve stereoselectivity.

Table 1.2. Stereochemical outcomes for several glucosamine-inositol glycosylations

Donor	Acceptor	Promoter	Solvent	Yield	Ref
1.28	**1.29**	$AgClO_4$	Et_2O	α: 63% β: 22%	119
1.30	**1.31**	Bu_4NBr	CH_2Cl_2	α: 63%	98
1.32	**1.33** (-)Mnt	TMSOTf	Et_2O	α: 85% β: 0%	92
1.34	**1.35**	TMSOTf	$Et_2O/$ CH_2Cl_2	α: 46% β: 25%	120
1.36	**1.35**	TMSOTf	CH_2Cl_2	α: 65% β: 19%	121
1.37	**1.35**	TMSOTf	$CH_2Cl_2/$ n- heptane	α: 0% β: 97%	122
1.38	**1.39**	Cp_2ZrCl_2 $AgClO_4$	Et_2O	α: 48% β: trace	116
1.40	**1.31**	Cp_2ZrCl_2 $AgClO_4$	Et_2O	α: 73% β: 20%	107
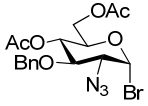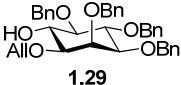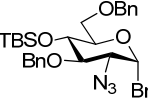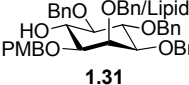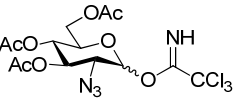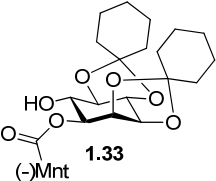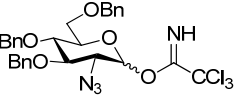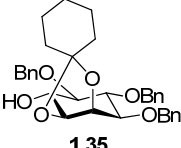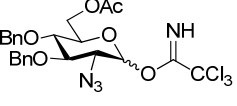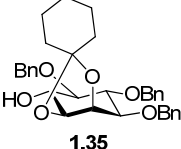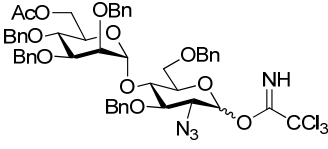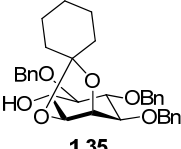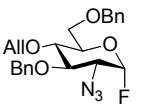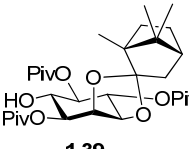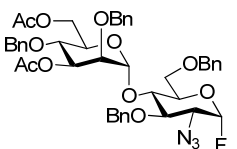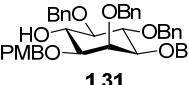
With the fully protected psuedodisaccharide **D** completed, options include elongation of the glycan chain from the glucosamine 4-*O*-position or installation of the

phospholipid moiety at the inositol 1-*O*-position. Most research groups have utilized the former method, opting to install the phospholipid at a late stage. However, as pointed out above, late stage phospholipidation performed on a fully elaborated GPI intermediate can result in an unwanted cyclization reaction.[99] Therefore, we typically proceed with selective deprotection/phosphorylation of the inositol 1-*O*-position prior to glycan advancement as the preferred assembly sequence for GPI synthesis. Phospholipidation of inositol, as well as later attachment of the phosphoethanolamine group(s), can be achieved using one of several available phosphorylation methods.

1.1.5.4 Phosphorylation Methods in GPI Synthesis

Many phosphorylation methods have been developed for the introduction of phosphates into synthetic nucleotides, GPI anchors, inositols, and other types of natural products. These methods can be classified by the oxidation state of the phosphorus atom in the reagent used. One category of reagents makes use of pentavalent phosphorus derivatives, such as $POCl_3$ and tetrabenzyl pyrophosphate, which have been used extensively in nucleotide synthesis. The other category is composed of trivalent phosphorus reagents, which can be activated under mild conditions to undergo substitution reactions, the products of which can be easily oxidized to phosphates. Two reagents in the latter category, phosphoramidites and H-phosphonates, have found widespread use in GPI synthesis (Scheme 1.7).[123-125]

A

phosphoramidite
1.41

R"OH, CH$_2$Cl$_2$, MeCN

H$^+$ (e.g. 1H-tetrazole)

phosphite
1.42

oxidation

t-BuOOH or
mCPBA

phosphate
1.43

B

1.44

H-phosphonate
1.45

pivaloyl
chloride

pyridine

mixed anhydride
1.46

R'OH

1.47

I$_2$

[O]

1.48
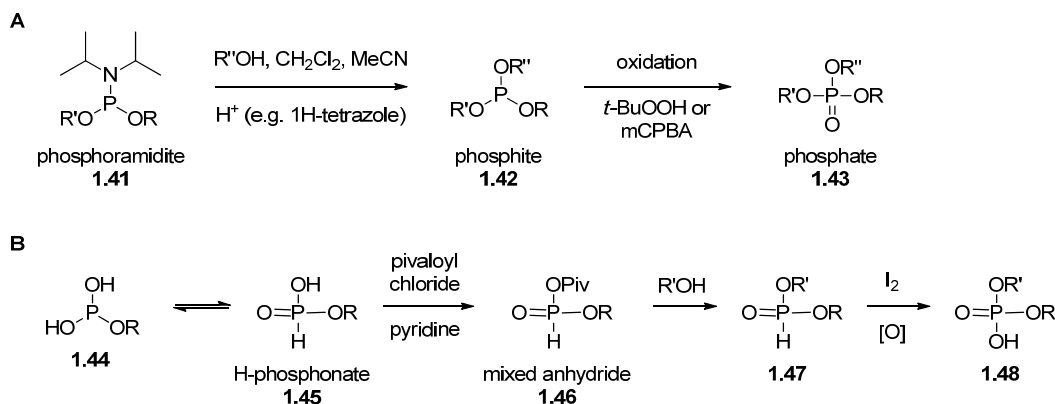
Scheme 1.7. Commonly used methods for GPI phosphorylation

Phosphoramidites of type **1.41** are activated by mild acids such as 1H-tetrazole, which protonates the diisopropylamino group. Then, displacement of diisopropylamine by an alcohol to form an intermediate phosphite **1.42** occurs. This usually fast reaction is followed by addition of an oxidant such as *tert*-butyl hydroperoxide (*t*-BuOOH) or *meta*-chloroperbenzoic acid (mCPBA), which converts the trivalent phosphite to a pentavalent phosphate **1.43**. If the three substituents around phosphorus are different, then the phosphorus atom will be chiral, and the reaction will result in the formation of an enantiomeric or diastereomeric mixture (depending on whether chirality exists in the substituents). If one of the substituents is a protecting group that is later removed to form a phosphate mono- or diester, the phosphorus atom will lose its stereogenic property. In the context of GPI synthesis, the formation of diastereomeric mixtures is a disadvantage because it complicates characterization and purification. In addition to this setback, purification of these phosphorylations can be cumbersome due to the large excess (usually 5–10 equiv) of phosphorylating reagent required. However, the speed and efficiency of the phosphoramidite method, coupled with the ability to prepare fully protected phosphates, have made it applicable to GPI synthesis.

H-Phosphonates of type **1.44** are trivalent phosphorus species that when in solution are in equilibrium with their tautomeric pentavalent form **1.45**. The latter is reactive and may be activated toward nucleophilic attack by treatment with pivaloyl chloride in dry pyridine, which results in the formation of a highly reactive mixed anhydride **1.46**. In the presence of a nucleophilic alcohol, the anhydride undergoes attack, forming H-phosphonate intermediate **1.47** along with loss of pivalic acid. Oxidation of the intermediate with water and iodine gives the desired phosphate diester **1.48**. Unlike the phosphoramidite method, usage of H-phosphonates does not generate a chiral phosphorus atom, and therefore problematic diastereomeric mixtures do not arise in GPI synthesis. However, this method produces unprotected phosphate diesters, which can complicate purification and prevent the use of various chemistries at later stages. Both phosphorylation strategies have been successfully used for attaching phospholipids and phosphoethanolamine groups to synthetic GPI intermediates.

1.1.5.5 Synthesis of the Trimannose Fragment

The conserved core of GPI anchors contains a trimannose fragment, identified as structure **C** in the retrosynthesis (Scheme 1.1). If not modified beyond the conserved core, the trimannose fragment is fairly straightforward to construct from suitably protected monomers, particularly due to the relative ease of forming α-mannosidic bonds. Scheme 1.8 depicts Guo's preparations of each mannose monomer and their assembly to form a typical non-modified trimannose fragment of type **C**.[100] The central mannose building block, Man-I, must be 1,6-*O*-differentiated for the purposes of accepting the Man-II anomeric center at the 6-*O*-position and acting as a latent glycosyl donor for the

later key glycosylation reaction. Starting from methyl α-D-mannopyranoside, four steps, including a selective hydrolysis–acetylation of the 1-*O*- and 6-*O*-positions of **1.49** to provide **1.50**, were required to obtain Man-I glycosyl acceptor **1.52**. Man-II must be 1,2-*O*-differentiated, preferably with an orthogonal acyl protecting group at the 2-*O*-position to enable neighboring group participation and thus α-stereoselectivity in glycosylation reactions. This was accomplished using intermediate 1,2-orthoester **1.55**, which can be selectively opened with trimethylsilyl chloride (TMSCl) to form 2-*O*-acetyl protected glycosyl chloride **1.56**. The Man-III building block, like Man-I, requires 1,6-*O*-differentiation, so intermediate **1.50** was useful in both preparations. Thus, **1.50** was converted to the desired Man-III glycosyl bromide **1.57** in a single step by usage of HBr/HOAc. Assembly of the trisaccharide started with a silver triflate (AgOTf)-promoted glycosylation of Man-I acceptor **1.52** with Man-II donor **1.56**. This provided α-dimannoside **1.58**, which was subjected to deacetylation with NaOMe to provide alcohol **1.59**. The final glycosylation also made use of AgOTf to activate Man-III glycosyl bromide **1.57**, resulting in α-anomer **1.60**. The Man-III 6-*O*-position protecting group was then swapped for a *tert*-butyldimethylsilyl (TBS) ether to ensure later compatibility with the inositol 2-*O*-palmitoyl acyl group.
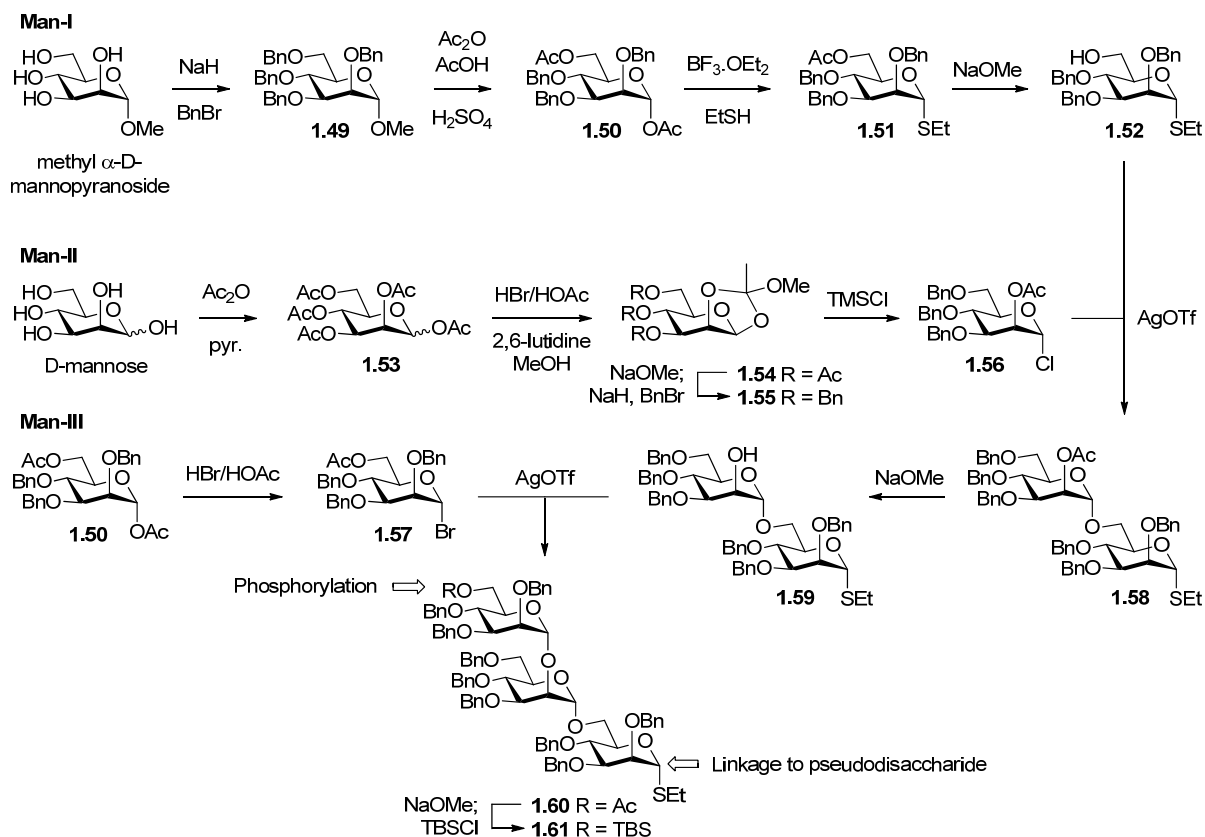
Scheme 1.8. Typical synthesis of a trimannose fragment of structure **C**

As described in Table 1.1, the trimannose core of different GPIs is structurally diverse and often contains additional sugar chains or phosphoethanolamine units or both located at various points along the glycan. Obviously, the synthesis of a modified trimannose fragment in this case would require additional positions carrying mono/oligosaccharides or orthogonal protecting groups for latent functionalization. For example, the VSG GPI anchor of *T. brucei* contains an oligogalactose moiety at the Man-I 3-*O*-position; the rat brain Thy-1 GPI anchor has GlcNAc and phosphoethanolamine units at the Man-I 4-*O*- and 2-*O*-positions, respectively; both the Thy-1 GPI anchor and the human lymphocyte CD52 GPI anchor contain additional mannose residues at the Man-III 2-*O*-position. Therefore, appropriate protecting group

tactics must be employed in the synthesis and assembly of the mannose monomers, as summarized in Scheme 1.9. In the synthesis of the *T. brucei* VSG GPI anchor, Ley and co-workers synthesized 1,3,6-*O*-differentiated Man-I building block **1.67** so that an oligogalactosyl group could be installed at the 3-*O*-position prior to mannosylation at the 6-*O*-position. Fraser-Reid employed 1,2,4,6-*O*-differentiated Man-I building block **1.71** in the synthesis of the rat brain Thy-1 GPI anchor, which allowed for the incorporation of GlcNAc and phosphoethanolamine groups. Preparation of such highly discriminated building blocks is laborious but essential for the synthesis of GPI anchors containing modified trimannose cores.

Ley's Synthesis of the *T. brucei* VSG GPI anchor Man-I monomer
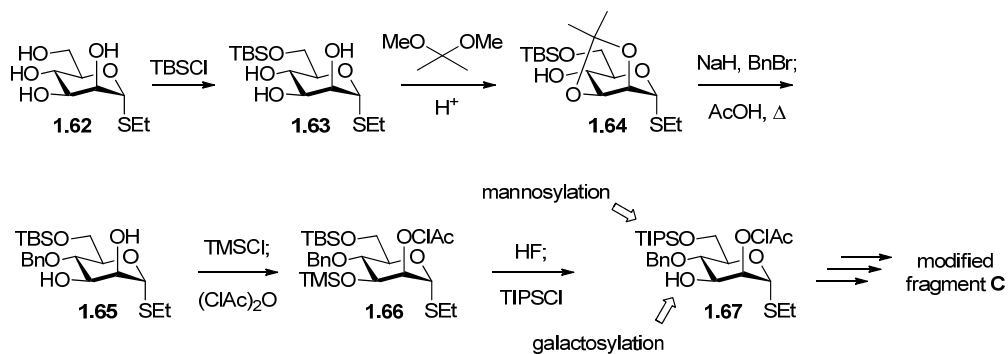
Fraser-Reid's Synthesis of the rat brain Thy-1 GPI anchor Man-I monomer
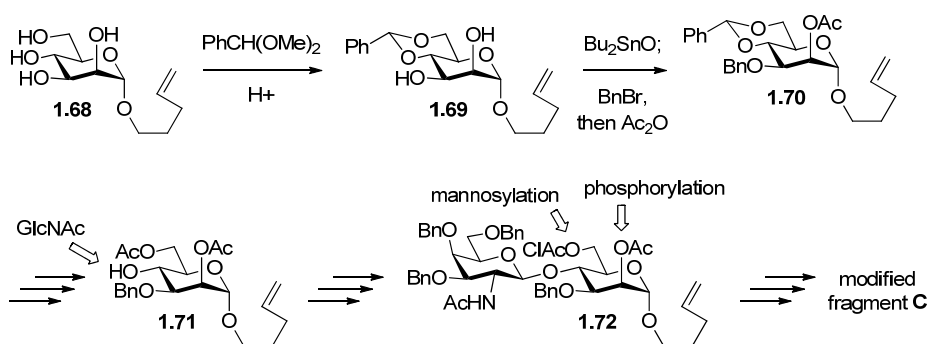
Scheme 1.9. Syntheses of modified trimannose building blocks

1.1.5.6 Assembly of GPI Anchors

There are multiple possible sequences for the assembly of GPIs from their corresponding subunits, and several factors must be taken into account when planning the synthesis. First, late-stage manipulations of valuable and complex intermediates should be minimized. When handling samples of high molecular weight on a small scale, isolated yields are generally lower, even for robust and straightforward protecting group manipulations. In addition, if a reaction fails on a complex substrate, it is difficult to amend the overall strategy and restart the synthesis. Second, time-consuming, inefficient, or difficult fragment preparations or bond formations should be accomplished at an early stage. For example, preparation of the glucosamine-inositol fragment is an arduous task and should be completed early on to streamline synthetic efficiency. Third, appropriate protecting group usage must be carefully planned. Sites on the GPI core structure that require functionalization should contain protecting groups that have well-documented orthogonality to all other protecting groups in the intermediate. Chemistries used to install or remove orthogonal protecting groups must be compatible with permanent functionalities in GPI intermediates.

Given the considerations laid out above, it is not surprising that most GPI syntheses reported to date have employed convergent strategies, such as the assembly shown in Scheme 1.1, that minimize late-stage reactions and protecting group manipulations. The first total synthesis of a GPI anchor, completed by Ogawa,[85-86] made use of a moderately convergent plan, although several glycan elongation steps were performed in a linear fashion on complex intermediates (Scheme 1.10). Ogawa's GPI assembly commenced with the convergent coupling of psuedotrisaccharide acceptor

1.73 and digalactosyl fluoride donor **1.74**. This step served to install a digalactose moiety that is observed at the Man-I 3-*O*-position in the *T. brucei* GPI anchor. NaOMe was then used to remove the Man-I 6-*O*-acetyl group, resulting in pseudopentasaccharide **1.75**. To elongate the GPI core glycan at this site, sequential mannosylation reactions were performed using monosaccharide building blocks **1.56** and **1.76**, which formed the advanced GPI intermediate **1.77**. This compound then underwent a series of manipulations to install the remaining functionalities and remove all of the protecting groups, affording the target GPI anchor. The use of linear assembly necessitated a multitude of late-stage transformations, which decreased the overall efficiency of this otherwise incredible first total synthesis of a GPI anchor. Also of note is the successful installation of the phospholipid on a fully elaborated GPI.
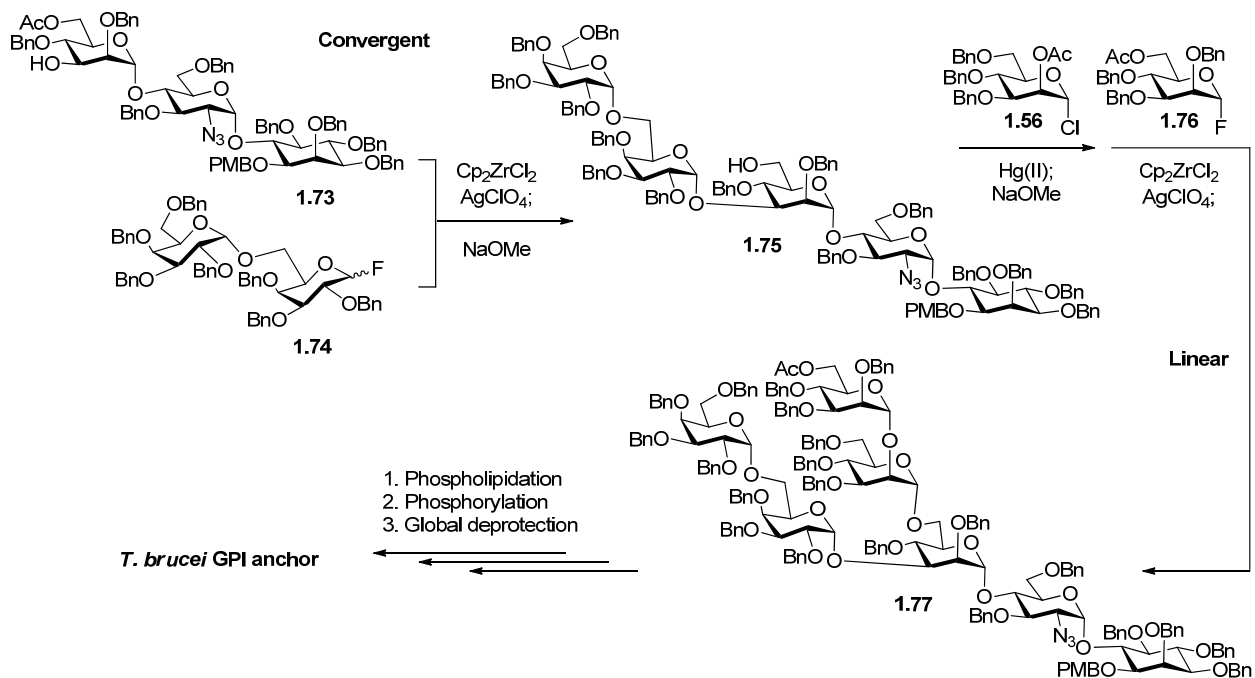
Scheme 1.10. Ogawa's synthesis of the *T. brucei* GPI anchor

In 1994, Schmidt reported a highly convergent synthesis of a *S. cerevisiae* GPI anchor, which contains a unique ceramide phospholipid and an additional mannose residue at the Man-III 2-*O*-position (Scheme 1.11).[92] The key reaction in this synthesis was a glycosylation between tetramannosyl trichloroacetimidate **1.78** and pseudodisaccharide **1.79**. These components reacted in the presence of trimethylsilyl trifluoromethansulfonate (TMSOTf) to form α-pseudohexasaccharide **1.80**, which was designed as a versatile intermediate, bearing two sites for installation of phosphoethanolamine groups and orthogonal protection at the inositol 1-*O*-position for attaching the ceramide phospholipid. Like Ogawa, Schmidt successfully performed the phospholipidation reaction at a later stage. This synthesis was highlighted by efficiency due to a convergent strategy, highly stereoselective Schmidt glycosylation reactions, and a versatile design for accessing variously modified *S. cerevisiae* GPI derivatives.
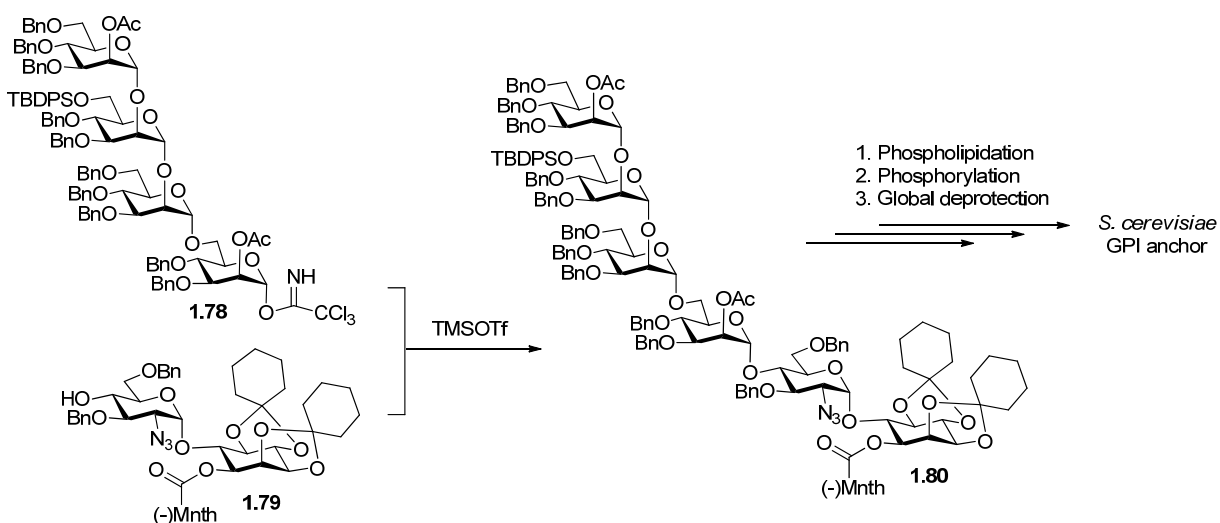
Scheme 1.11. Schmidt's synthesis of the *S. cerevisiae* GPI anchor

Fraser-Reid published the synthesis of a fully phosphorylated GPI anchor of the rat brain Thy-1 antigen in 1995,[89,119] which carried additional mannose and galactosamine residues attached to the GPI core structure (Scheme 1.12). The construction of GPI precursor **1.85** hinged on the application of their *n*-pentenyl glycoside methodology to the convergent assembly of several advanced building blocks. Thus, pseudodisaccharide **1.82** coupled with n-pentenyl disaccharide **1.81**, furnishing α-pseudotetrasaccharide **1.83** after treatment with thiourea to remove the Man-I 6-*O*-chloroacetyl (ClAc) group. This positioned the authors to attach *n*-pentenyl trimannoside **1.84** to the GPI core **1.83**, which produced the fully protected GPI intermediate **1.85**. At this point, several steps were used to sequentially introduce phosphoethanolamine groups to the Man-III 6-*O*- and Man-I 2-*O*-positions. Fraser-Reid capped this highly convergent synthesis with a late-stage phospholipidation of the inositol residue.
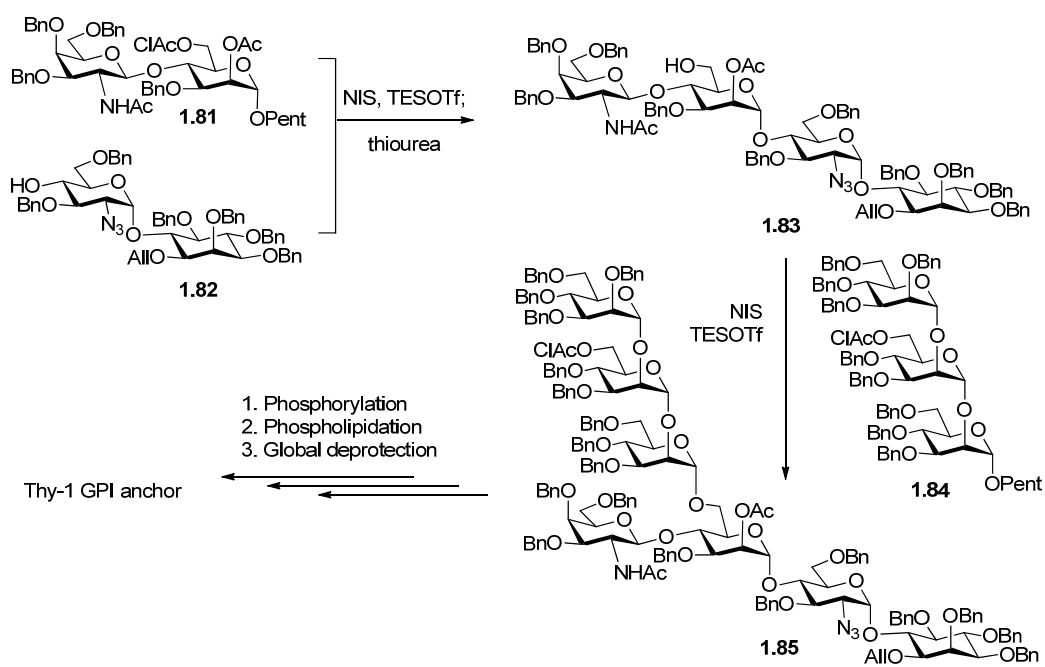
Scheme 1.12. Fraser-Reid's synthesis of the rat brain Thy-1 GPI anchor

Ley and co-workers designed a strategy for the synthesis of the *T. brucei* GPI anchor similar to those described above (Scheme 1.13).[88] While Ogawa had previously synthesized a version of this molecule, Ley enhanced its preparation by improving convergence and making use of several methodologies developed in their lab. For example, a racemic inositol intermediate was desymmetrized using a chiral bis(dihydropyran) derivative, and butanediacetals were used extensively as protecting groups in the synthesis. In terms of assembly, a key glycosylation took place between pseudodisaccharide **1.82** and pentasaccharide thioglycoside **1.86**, which made use of Ley's butanediacetal protecting groups and was activated by *N*-iodosuccinimide (NIS)/trifluoromethanesulfonic acid (TfOH). The resulting fully protected GPI intermediate **1.87** was poised for the remaining phosphorylation and global deprotection reactions.
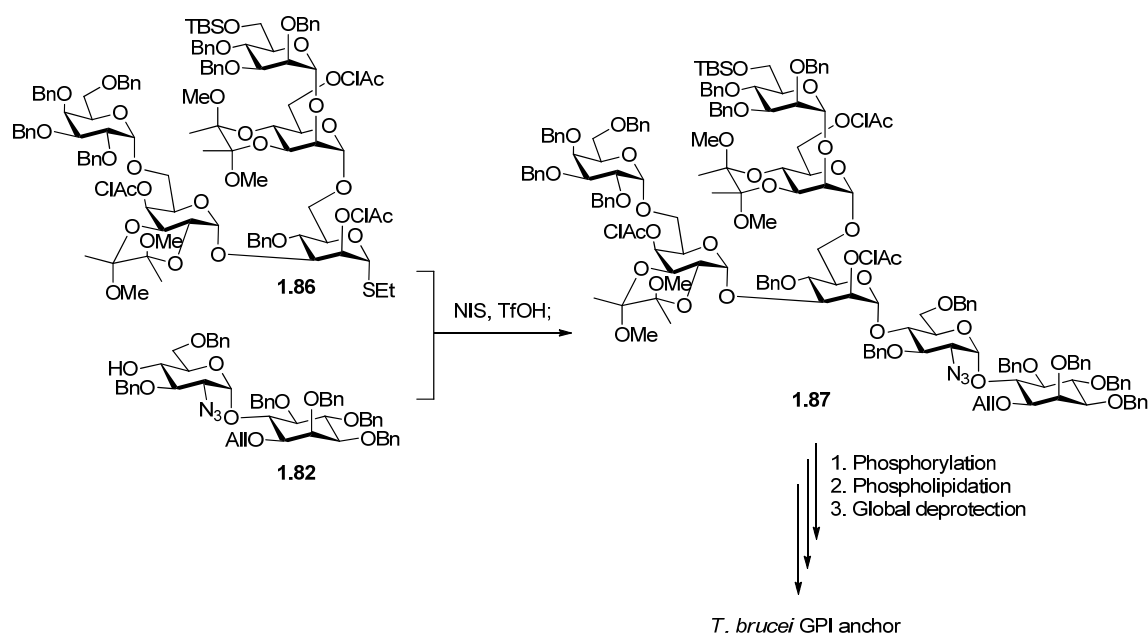
Scheme 1.13. Ley's synthesis of the *T. brucei* GPI anchor

The GPI syntheses described above all relied on late-stage installation of a phosphoglycerolipid to the inositol 1-*O*-position. While apparently this route was successfully applied in these cases, Guo uncovered an interesting problem with this strategy in the synthesis of the human sperm CD52 GPI anchor.[99] The sperm CD52 GPI anchor contains an additional palmitoyl group at the inositol 2-*O*-position, and Guo's initial plan involved early palmitoylation and late-stage installation of the phospholipid. However, upon attempting the latter reaction on fully elaborated GPI **1.88**, a novel cyclophosphoramidation reaction occurred between the glucosamine 2-azido group and the nascent inositol 1-*O*-phosphite, forming **1.89** (Scheme 1.14).
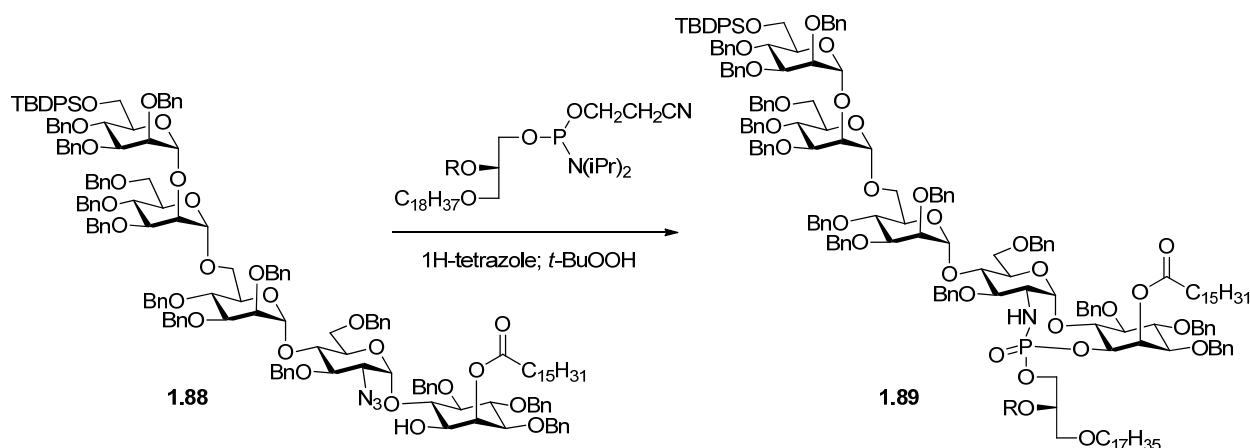
Scheme 1.14. Cyclic phosphoramidate formation observed by Guo

Because this unexpected reaction did not occur in previous GPI syntheses, it was concluded that the coexistence of the palmitoyl and trimannose groups forced the intermediate into a conformation such that this intramolecular reaction was favored. To circumvent this problem, Guo performed the phospholipidation at an earlier stage (Scheme 1.15). Therefore, pseudodisaccharide **1.90**, containing a palmitoyl group at the

inositol 2-*O*-position, underwent a smooth phospholipidation at the 1-*O*-position followed by Pd-catalyzed deallylation to give **1.91**. This product reacted with trimannose thioglycoside **1.92** in the presence of NIS/TfOH to form the desired α-pseudopentasaccharide **1.93**, which could be transformed into the target molecule in only a few more steps. Guo's modified sequence for GPI assembly prevented a dead-end cyclization reaction while also improving convergency.
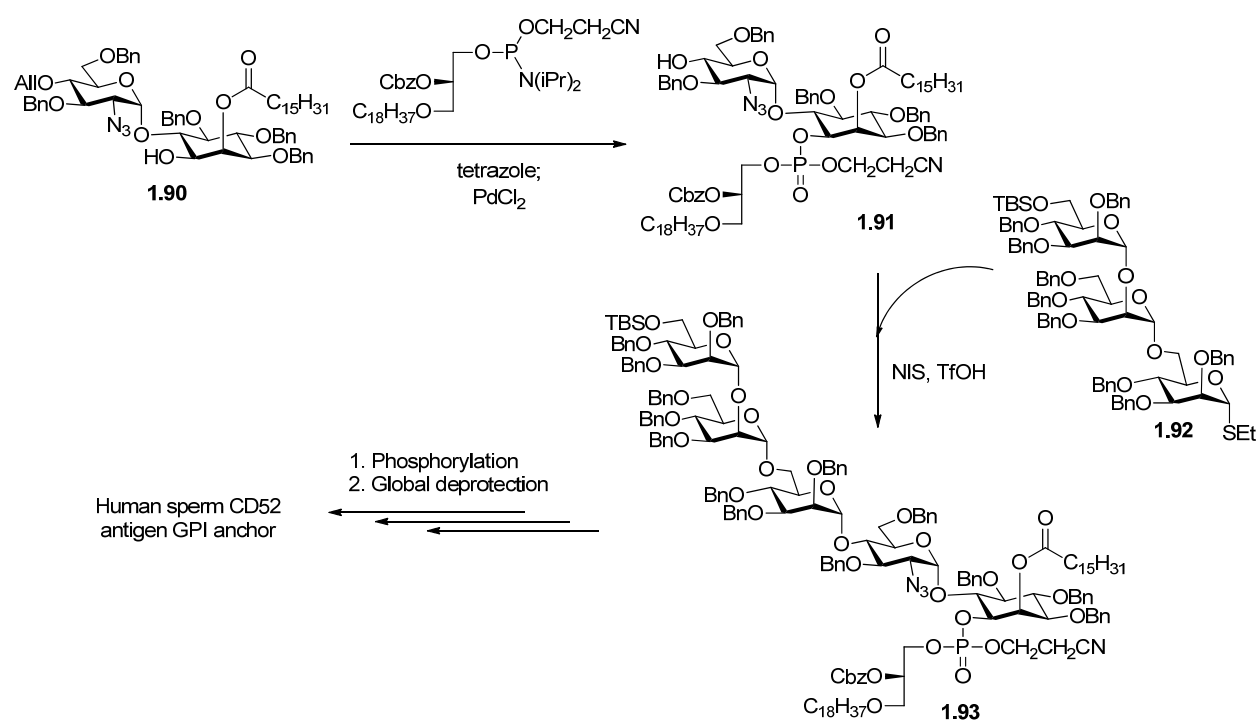
Scheme 1.15. Guo's synthesis of the human sperm CD52 antigen GPI anchor

Although convergent synthesis is the most efficient and practical way to construct GPI anchors, linear assembly is suitable for solid phase synthesis. Seeberger and co-workers synthesized an analog of the *P. falciparum* GPI anchor for testing as an anti-malarial candidate. After completing a solution phase preparation of the target

molecule,[97] their linear strategy was translated to use in an automated synthesizer (Scheme 1.16A).[126] First, a tetramannose was constructed on the surface of an octenediol-functionalized Merrifield resin **1.94** in an iterative fashion using mannosyl donors **1.95**-**1.98**. The tetramannose *n*-pentenyl glycoside **1.99** was then released from the resin using Grubbs' catalyst, and solution phase elaboration of this molecule led to a partial GPI structure lacking a phosphoglycerolipid. Martín-Lomas also employed solid phase synthesis to construct a GPI analog (Scheme 1.16B).[127] Starting from solid supported pseudodisaccharide **1.100**, the entire glycan was built up in a stepwise fashion on the solid phase. After release from the acid sensitive resin with trifluoroacetic acid (TFA), pseudopentasaccharide **1.104** was transformed into a GPI partial structure.
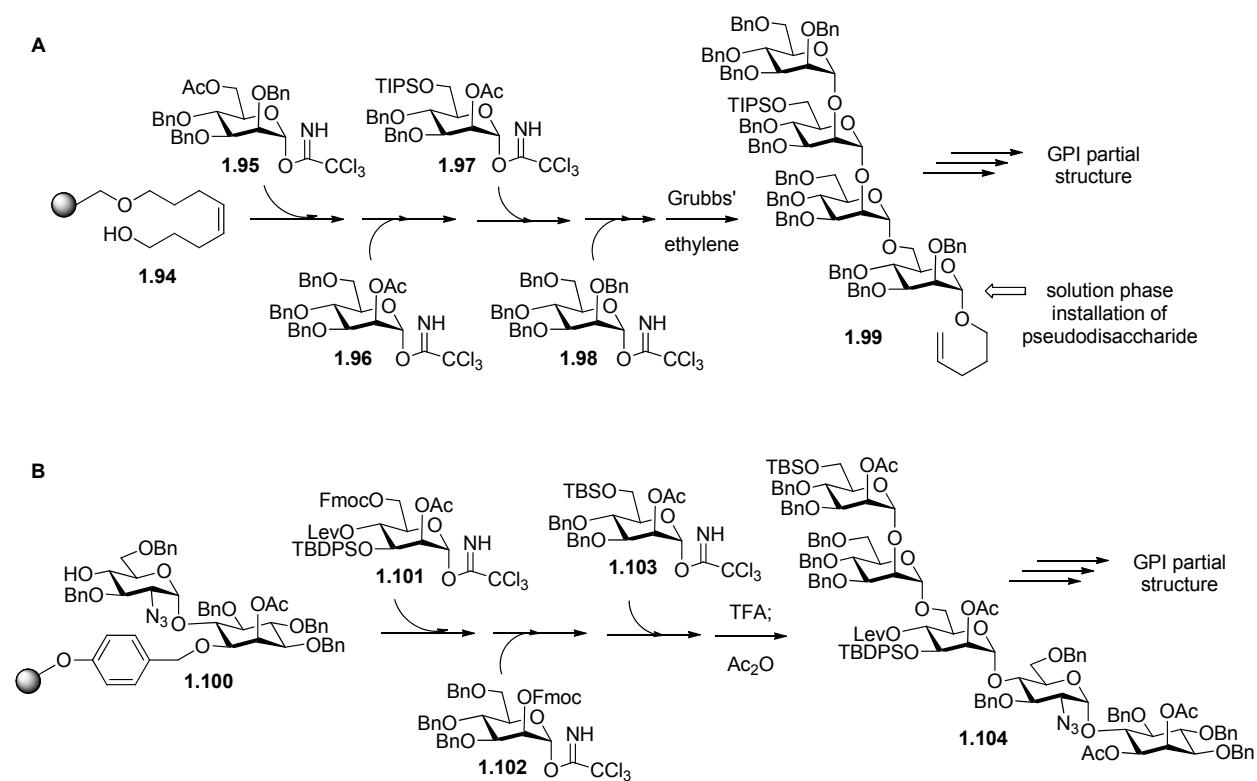
Scheme 1.16. Linear assembly of GPIs using solid phase synthesis

As demonstrated by the groups of Seeberger and Martín-Lomas, solid phase synthesis was effective for synthesizing GPI partial structures. However, solution phase preparation of the challenging glucosamine-inositol pseudodisaccharide was still required in both cases. Furthermore, the phosphoglycerolipid was omitted from the target structure in each synthesis, which points to a limitation of this method. Therefore, traditional solution phase synthesis combined with a highly convergent strategy currently represents the strongest route to synthetic GPI anchors.

In 2006, Nikolaev and co-workers published the first synthesis of a GPI anchor containing unsaturated lipid chains (Scheme 1.17),[128] which bears direct relevance to the research presented in this chapter. Up to the point of Nikolaev's publication, all GPI syntheses applied the benzyl group for global hydroxyl protection; however, this strategy is clearly incompatible with unsaturated lipids, because Pd-catalyzed hydrogenation is required to remove the benzyl groups as a final step. To address this issue, Nikolaev employed benzoyl esters for permanent protection despite the presence of an acylglycerolipid in the PI moiety, which appears to be incompatible with the conditions required for deacylation. The authors noted their hypothesis that upon global deprotection with NaOMe in MeOH, benzoyl-protected intermediates **1.105** and **1.106** could form micelles, thus mostly preventing methanolysis of the ester-linked lipid chains. However, their reported deacylation steps gave ≤ 40% yield of products **1.107** and **1.108**, thus this effect was quite limited, if operative at all. At best, the hypothesis of micellar protection of the fatty acid linkages could not take place unless the intermediate was at least partially deprotected (therefore containing a polar region), and as a result lipid cleavage would occur indiscriminately at the start of the reaction.
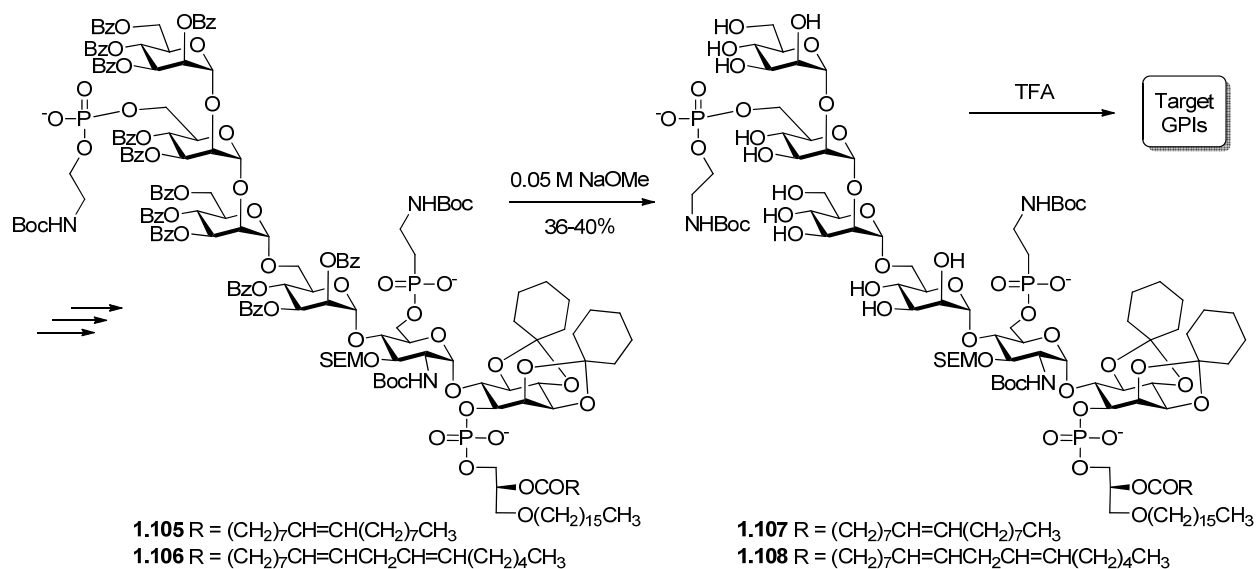
Scheme 1.17. Nikolaev's synthesis of GPI anchors bearing unsaturated lipids

Although Nikolaev's work does represent the first successful synthesis of a GPI anchor using esters for permanent hydroxyl protection, this strategy should not be relied on for future work. Ideally, such a risky and low-yielding deprotection step on a valuable and complex substrate should be avoided. The research presented in section 1.2 takes aim at the essentially unsolved issue of synthesizing functionalized GPI anchors.

1.2 Results and Discussion

1.2.1 Background and Project Design

To probe the significance of GPI structure and diversity, and to better understand the scope and mechanism of GPI anchoring, it is necessary to have access to pure and structurally defined samples of GPIs, GPI analogues, and functionalized GPIs. Advances in chemical synthesis have enabled the preparation of GPI anchors by several research groups, including ours, but limitations associated with current hydroxyl

group protection strategies in carbohydrate/GPI synthesis prevent the inclusion of certain combinations of important functional groups in the target molecule.

As described in section 1.1.5, GPI synthesis involves the elaboration of suitably protected building blocks, including monosaccharide, inositol, lipid, and phosphate precursors, into a fully protected GPI intermediate (Figure 1.5). Such an intermediate contains several types of protecting groups: an azido group is always used to mask the glucosamine 2-position; a 9-fluorenylmethoxycarbonyl (Fmoc) or *tert*-butylcarbonyl (Boc) group is commonly used to protect the primary amine of the phosphoethanolamine group; the phosphates at either end of the GPI are protected usually with a benzyl or cyanoethoxy group. Finally, the global/permanent protecting group, abbreviated as 'PG' in Figure 1.5, is employed to mask all of the nonfunctionalized hydroxyl groups in the intermediate. The choice of global protecting group at the outset of a synthesis is an important decision for several reasons. First, it will affect what other types of protection and deprotection reactions may be used throughout the synthesis. Second, protecting groups can dramatically impact reactivity and stereoselectivity in glycosylation reactions. Finally, the identity of the global protecting group will determine what conditions are required to effect a global deprotection reaction, which is the final synthetic step needed to afford the target GPI. Ideally, the global deprotection reaction will be high yielding and specific for only the protecting groups, leaving the entire desired structure intact.
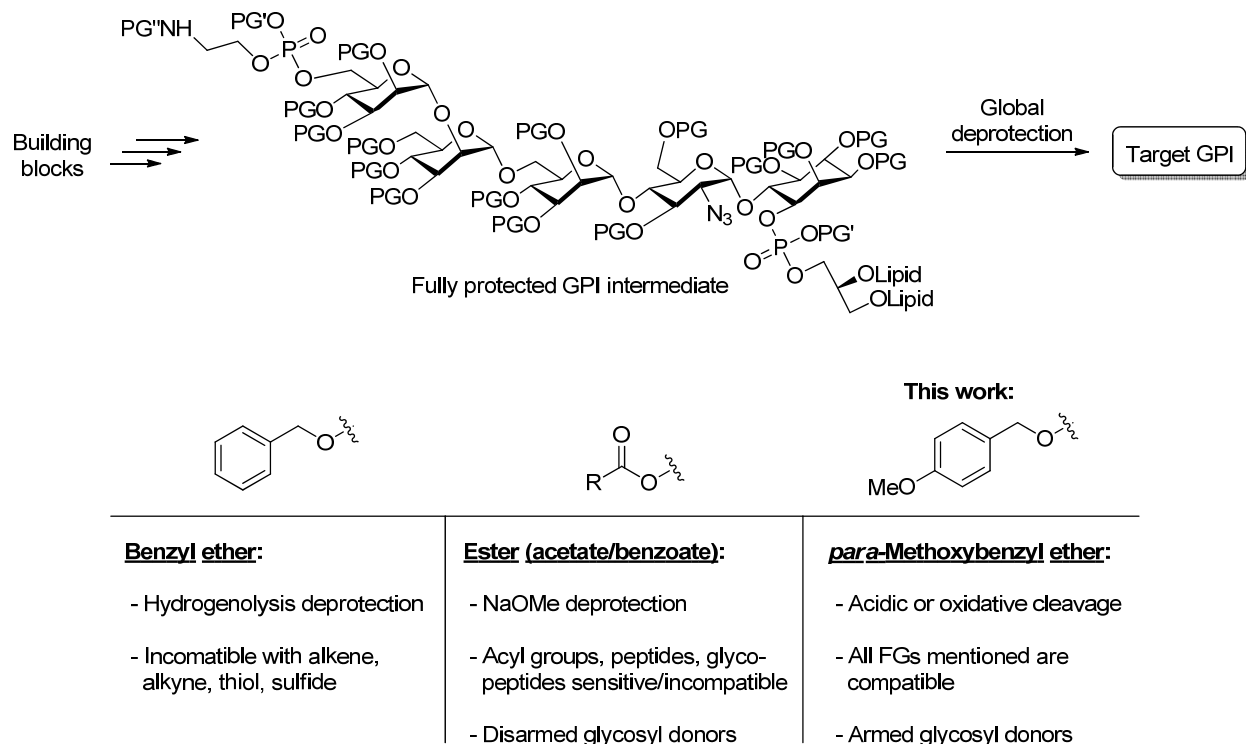
Figure 1.5. Global protecting group considerations in GPI synthesis

Two primary strategies exist for permanent hydroxyl protection in carbohydrate synthesis. Most commonly used is the benzyl ether, which is simple to install and is stable to a wide range of reaction conditions used in carbohydrate/GPI synthesis. In addition, usage of the benzyl ether has the advantage of a very mild global deprotection, which is accomplished using palladium-catalyzed hydrogenolysis. To date, all but one reported GPI synthesis have made use of the benzyl group for permanent hydroxyl protection. The primary setback to this strategy is that potentially reducible or catalyst-poisoning functional groups, such as alkenes, alkynes, thiols, and sulfides, are incompatible with hydrogenolysis global deprotection, thus preventing their incorporation into the target molecule. In the context of synthesizing naturally occurring GPI anchors, this is problematic because many GPIs contain unsaturated fatty acid

lipids, a property that is biologically important[39] yet disallows the usage of benzyl ethers for protection. Furthermore, alkenes, alkynes, thiols, and sulfides are broadly useful functional groups. Alkenes are one of the most versatile functional groups in organic chemistry and can be converted to numerous other structures. Alkynes are similarly versatile, and also have the ability to participate in the copper-catalyzed [3+2] cycloaddition "click" reaction, which is a high yielding and very chemoselective reaction that has found extensive use in all areas of chemistry and chemical biology.[129] Thiols can also participate in useful chemoselective reactions such as native chemical ligation[130] (NCL) and thiol-ene chemistry. A thioether bond is present in biotin, which is an exceptionally useful molecule due to its high binding affinity for the protein avidin, a property that allows biotinylated molecules to be separated with high efficiency from very complex mixtures. These examples illustrate the limitations of using the benzyl group for permanent protection.

An alternative to the standard benzyl ether protection strategy is usage of ester protection such as acetyl and benzoyl groups, which would be compatible with the aforementioned functional groups. However, ester global deprotection is typically carried out using NaOMe, which would clearly be problematic for other acyl groups present in the target molecule. As summarized in Table 1.1, all known GPI anchors contain at least one acyl-linked lipid. In addition, peptides and glycopeptides, which are conjugated to GPI anchors and other carbohydrates in nature, may be sensitive to treatment with NaOMe. Another potential disadvantage to this strategy is that glycosyl donors bearing multiple electron-withdrawing ester groups are termed "disarmed," and can be less reactive in glycosylation reactions.[131] Despite these apparent limitations,

Nikolaev and co-workers employed the benzoyl group for permanent protection to achieve the first synthesis of GPI anchors containing unsaturated lipid chains, as described above (Scheme 1.17).[101] Although the target molecules were obtained, the global deacylation reactions proceeded in unacceptable yields, likely due cleavage of the ester-linked lipid chains. Therefore, usage of acyl-based permanent hydroxyl protection is not particularly amenable to GPI synthesis.

Given the clear limitations of benzyl ether and ester global protection strategies in the synthesis of functionalized GPI anchors and other carbohydrates, I sought to develop a complementary strategy using the PMB group for permanent hydroxyl protection. Certainly, PMB ethers have found extensive use as orthogonal protecting groups in carbohydrate synthesis, and, to a lesser extent, as global protecting groups in simple systems such as glycosylation with monosaccharides.[132] However, one of my goals for this project was to legitimize PMB groups as candidates for permanent hydroxyl protection in complex and challenging syntheses. More importantly, I wished to access biologically relevant functionalized GPI anchors that simply could not be synthesized using current protecting group strategies. It was anticipated that PMB ethers, which can be cleaved under either acidic (e.g. 5-10% TFA) or oxidative conditions [e.g. ceric ammonium nitrate (CAN) or 2,3-dichloro-5,6-dicyano-1,4-benzoquinone (DDQ)], would provide the flexibility necessary for the incorporation of a wide range of functional groups in the target GPIs.

The target molecules for this project are depicted in Figure 1.6. Initially, I set out to prepare GPI anchors bearing unsaturated lipid chains as a proof-of-concept for the PMB protection strategy. Thus, GPI anchors **1.109** and **1.110**, each containing the core

GPI structure and a diacyloleoyl phospholipid, were designed as natural product targets. A variable phosphorylation site at the Man-I 2-*O*-position was included because the presence of an additional phosphoethanolamine unit at this site is the most commonly observed GPI structural modification in higher eukaryotes.
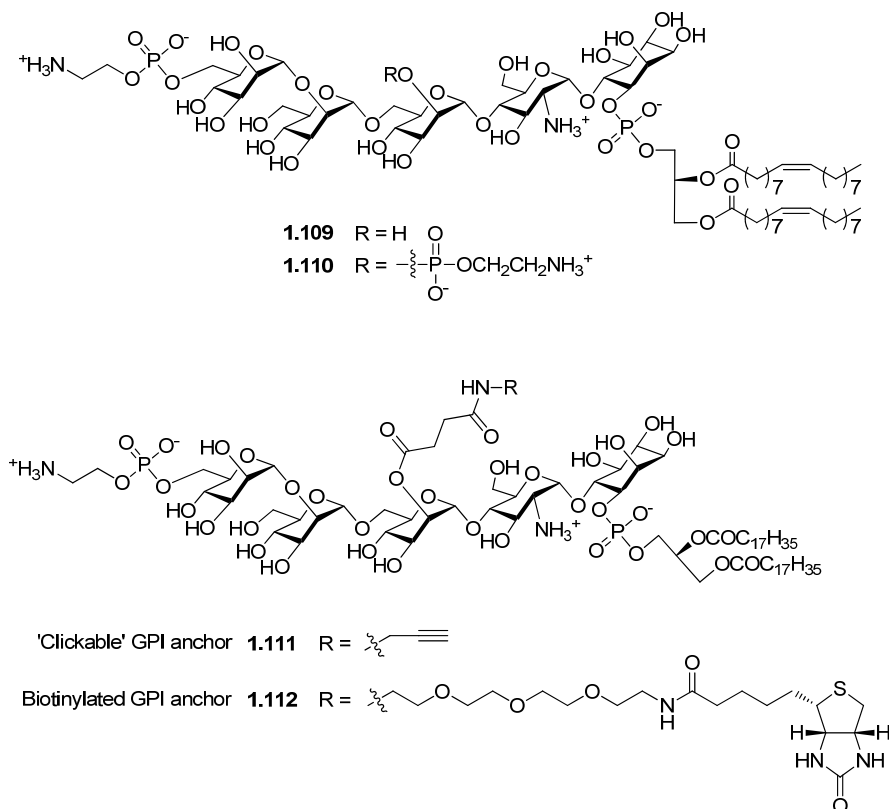
Figure 1.6. Target molecules accessible using the PMB protection strategy

Compounds **1.111** and **1.112** in Figure 1.6 represent biofunctionalized GPI anchors that will be incorporated into biological studies aimed at probing the scope and mechanism of the anchoring process, as well as at evaluating GPIs for potential therapeutic development. 'Clickable' GPI anchor **1.111** contains a short linker and alkyne functionality at the Man-I 2-*O*-position. Click tags are useful for appending

virtually any type of molecule to a substrate. For example, alkynyl GPIs, like other alkynyl sugars,[133] could be useful in a range of biological studies, from fluorescent tag labeling and cell surface visualization experiments to carrier protein conjugation for vaccine development. This utility centers on the versatility of the alkyne functional group, which is small, biologically inert, and able to undergo click reactions as described above. The fourth target GPI anchor **1.112** is quite similar in structure to **1.111**, but instead carries a biotin moiety at the 2-*O*-position. As mentioned above, biotinylated molecules can be isolated from extremely complex mixtures by using commercially available streptavidin products, which make use of the incredibly strong binding between the tetrameric protein avidin and biotin ($K_D = \sim10^{-15}$ mol/L).[134] Biotinylated GPI anchors may prove to be extremely useful for the study of GPIomics, which is the large-scale profiling of GPIs and GPI-anchored molecules in cells.

The common thread that ties target molecules **1.109**-**1.112** together is their inaccessibility by traditional synthetic strategies. The unique – but exceptionally useful – functional group combinations present in the target GPIs necessitated the development of a new global protecting group strategy, for which the PMB group was chosen.

1.2.2 Retrosynthesis

The retrosynthetic analysis for target GPI anchors **1.109**-**1.112** is outlined in Scheme 1.18. To assemble these targets, I elected to use a convergent approach, the benefits of which were described in section 1.1.5. This strategy was centered on the use of two common PMB-protected intermediates, pseudodisaccharide **1.114** and trimannose thioglycoside **1.115**, which could be applied to the synthesis of all four target

GPIs as follows: pseudodisaccharide **1.114** could undergo phospholipidation at the free inositol 1-*O*-position by using any freshly prepared phosphoramidite, thus allowing flexibility in what type of phosphoglycerolipid was installed in the GPI. After removal of the glucosamine 4-*O*-TBS group, the resulting product could participate in a key glycosylation reaction with trimannoside **1.115**, or a derivative thereof, to produce fully PMB-protected GPI intermediate **1.113**. With orthogonal protecting groups at the Man-III 6-*O*-position (PG^1) and Man-I 2-*O*-position (PG^2), compound **1.113** could undergo phosphorylation and/or functionalization at either position. Finally, removal of all protecting groups would result in the formation of the target compounds. The two common intermediates, **1.114** and **1.115**, would be formed from their corresponding suitably protected monomers **1.116**-**1.120**.
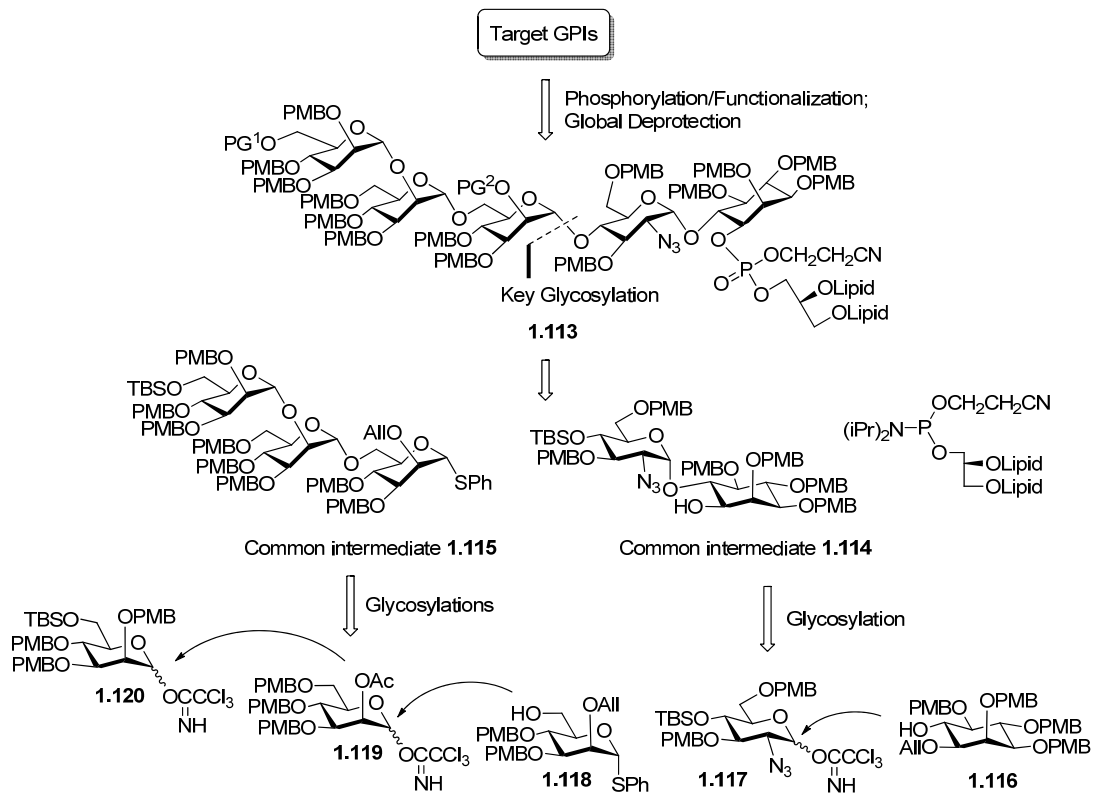
Scheme 1.18. Retrosynthesis of target GPI anchors

Several considerations were made in the planning of this synthesis. First, due to the sensitivity of PMB groups to acidic conditions, care was taken in selecting the primary glycosylation method. Various donors/activation conditions were evaluated throughout the course of this project, including glycosyl fluorides, trichloroacetimidates, and thioglycosides. The Schmidt glycosylation,[135] which makes use of trichloroacetimidate donors and catalytic TMSOTf for activation, consistently gave the best results. Second, the PMB group also required the identification and employment of protecting groups and reaction conditions with truly orthogonal properties, which turned out to be quite challenging in some cases. Finally, the functionalization site was chosen based on positions of modification in natural GPI anchors. Initially, the Man-I 3-*O*-position was used for functionalization, but eventually this was shifted to the Man-I 2-*O*-position due to a crippling side reaction (see section 1.2.6). Both of these positions are commonly modified in naturally occurring GPI anchors, and therefore no significant changes in the conformation or global structure of the GPI backbone were expected as a result of shifting the site of derivatization.

The following sections will describe the preparations – both failed and successful – of monomer building blocks **1.116**-**1.120**, including inositol, glucosamine, and mannose derivatives, and their conversion into common key intermediates pseudodisaccharide **1.114** and trimannose **1.115**. Then, separate sections will be used to detail the completion of each target molecule from the common intermediates. Finally, future directions for this research, both in terms of synthesis and biological studies, will be laid out.

1.2.3 Synthesis of Inositol Building Block 1.116

The preparation of differentially protected and optically pure inositol compounds in the context of GPI synthesis is discussed in section 1.1.5.2. For the purpose of synthesizing a suitable PMB-protected inositol derivative, I first explored the conversion of optically enriched diol (+)-**1.7** to a useful building block by using a route similar to that previously employed by Guo for the synthesis of benzyl-protected inositols.[109] Guo's strategy involved initial differentiation of the 1-*O*- and 6-*O*-positions, then installation of the permanent benzyl groups. My attempt to develop an analogous preparation is shown in scheme 1.19. First, a highly regioselective stannylene acetal-directed allylation of the 6-*O*-position provided compound **1.9** in 80% yield, thus successfully differentiating the 1-*O*- and 6-*O*-positions. Here, in the synthesis of benzyl-protected inositols (route A), an orthogonal PMB group was installed at the 1-*O*-position to provide **1.121**. This was followed by replacement of the cyclohexylidene ketals with benzyl groups by sequential treatment with AcCl/MeOH and NaH/BnBr to furnish inositol **1.122**. For such a preparation to translate successfully to the synthesis of an analogous PMB-protected inositol **1.124**, a 1-*O*-position protecting group (PG) would have to be identified that satisfied the following requirements: 1) PG must withstand treatment with strong acid (AcCl/MeOH); 2) PG must withstand treatment with strong base (NaH/PMBCl); 3) PG must be orthogonal to All, PMB, TBS, and N_3 groups; 4) PG must not be susceptible to migration from the inositol 1-*O*-position to the 2-*O*-position under acidic or basic conditions. After exploring a variety of protecting groups, it was concluded that none met these criteria, and I was forced to redesign the inositol preparation.
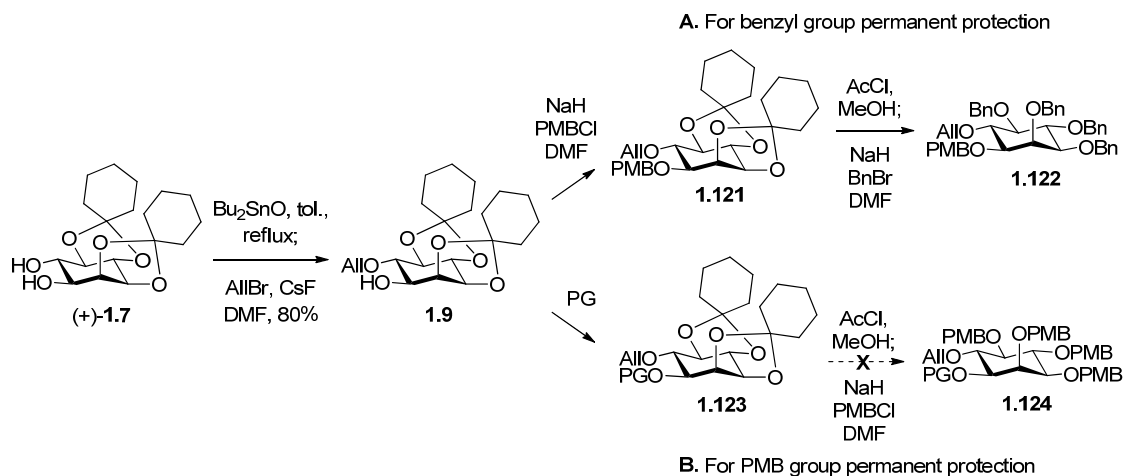
Scheme 1.19. Failed inositol preparation

Rather than immediately differentiate the 1-*O*- and 6-*O*-positions, I decided to attempt differentiation after protecting the remaining hydroxyl groups as PMB ethers (Scheme 1.20). This route also provided an opportunity to investigate a chemical resolution of the inositol racemic mixture rather than enantiomeric resolution. Thus, the racemic mixture of diol (±)-**1.5** was subjected to allylation of the 1-*O*- and 6-*O*-positions, resulting in bis(allylether) (±)-**1.125**. Then, the cyclohexylidene ketals were removed with HCl-promoted methanolysis, and the intermediate tetraol was *para*-methoxybenzylated to provide (±)-**1.126**. Deallylation of this product was quite low-yielding using standard reagents such as PdCl$_2$ (< 50%). However, the desired diol (±)-**1.127** was obtained in 85% yield when Cha's deallylation protocol[136] using cyclohexylmagnesium chloride and titanium isopropoxide was used. At this point, 1,6-*O*-differentiation was required, and I preferred to protect the 1-*O*-position regioselectively, thus leaving the 6-*O*-position free for anchoring to a chiral resolving reagent. Although the similar diol (±)-**1.7** undergoes stannylene-acetal directed allylation at the 6-*O*-position, I predicted that this regioselectivity would fortuitously swap for substrate (±)-

1.127 because of the neighboring axial substituent, which often increases nucleophilicity. On the other hand, the selectivity observed for substrate (±)-**1.7** most likely is a result of a steric effect of the molecule resulting from the rigid nature of the cyclic ketal protecting groups.[109] In the reaction, the regioselectivity fortunately did favor the desired 1-*O*-position in a 4:1 ratio (determined by HPLC), which allowed compound (±)-**1.128** to be obtained in 72% yield. This enantiomeric mixture was then reacted with the chiral resolving agent (1*S*)-(-)-camphanic chloride. The resulting mixture of diastereomers could be separated by semi-preparative HPLC, providing enantiomerically pure (-)-**1.129** in 46% yield (maximum 50%). The chiral auxiliary was then saponified in excellent yield to give the desired inositol derivative **1.116**.
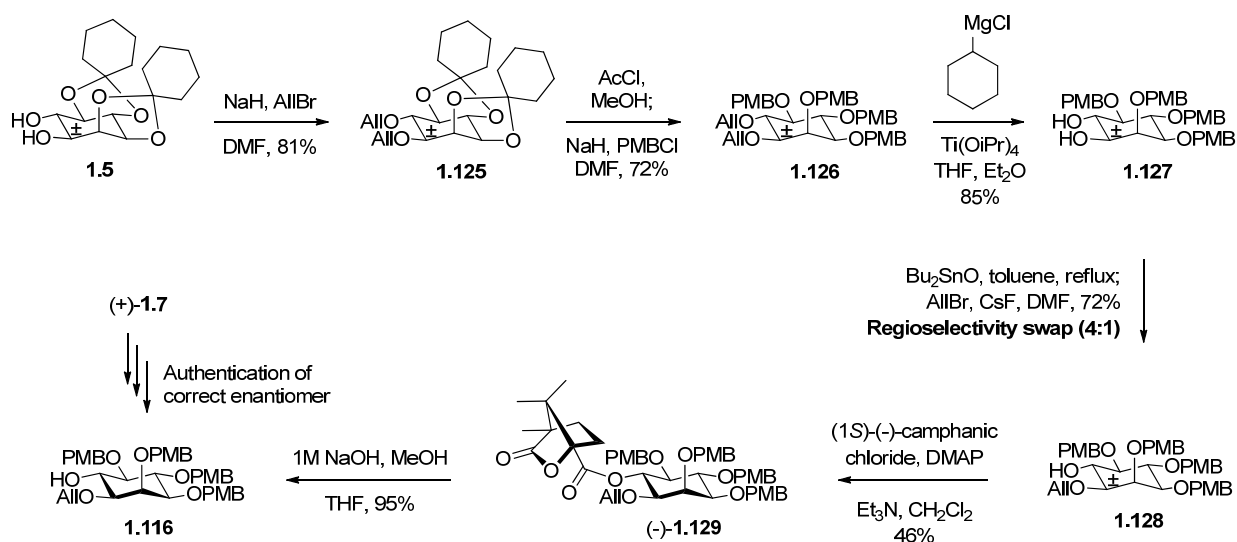
Scheme 1.20. Preparation of inositol derivative **1.116**

Because compound **1.116** and its enantiomer were generated in this procedure, the desired isomer had to be identified. To make this assignment, I performed the same procedures outlined in scheme 1.20 on enantiomerically enriched (+)-**1.7**, which allowed

access to an authentic sample of **1.116**. Comparison of optical rotation values between the authentic and unknown samples confirmed the identity of the desired enantiomer. The efficiency of the chemical resolution procedure described in scheme 1.20 compared favorably to Gou's enzymatic resolution,[108] which is commonly used in our lab to obtain enantiomerically enriched inositol derivatives. The chemical procedure required 2 steps (relating to the resolution) and gave a 44% overall yield (maximum 50%), whereas the enzymatic procedure required 3 steps and gave a 25% overall yield. However, the overall efficiency of the chemical procedure was dampened by the need for HPLC purification.

1.2.4 Synthesis of Glucosamine Building Block 1.117

The glucosamine moiety in GPI anchors contains an α-glycosidic bond to the 6-*O*-position of inositol. Achieving a highly stereoselective α-glycosylation reaction between these two subunits has been a rather difficult task in most GPI syntheses, as summarized in Table 1.2. While the presence of a non-participating protecting group at the 2-position is absolutely necessary to form a 1,2-*cis* glycosidic bond, other factors affecting stereoselectivity are not very predictable. PMB-protected glucosaminyl donor building blocks were designed to contain a non-participating azido group at the 2-position and an orthogonal TBS group masking the 4-*O*-position for later removal and glycan chain extension.

I prepared both glucosaminyl fluoride and trichloroacetimidate building blocks for the purpose of optimizing the glycosylation reaction with inositol acceptor **1.116**. Both syntheses followed nearly identical paths, beginning with commercially available

glucosamine hydrochloride. Synthesis of the trichloroacetimidate donor **1.117** is shown in Scheme 1.21. First, Wong's copper-catalyzed diazotransfer reaction[117] was used to install a non-participating azido group at the 2-position. Without purification, the intermediate was peracetylated using acetic anhydride in pyridine to provide **1.130** in 82% yield. The anomeric acetate was then replaced with an allyl ether using allyl alcohol and promoter tin(IV) chloride. After the resulting product **1.131** was deacetylated with NaOMe, the intermediate triol was reacted with *para*-anisaldehyde dimethyl acetal in the presence of catalytic camphor sulfonic acid (CSA), which resulted in the formation of 4,6-O-*para*-methoxybenzylidene-protected derivative **1.132**. PMB protection of the 3-*O*-position was followed by regioselective reductive ring opening of the *para*-methoxybenzylidene ring, providing alcohol **1.34** in 71% yield. The newly exposed 4-*O*-position hydroxyl group was then capped with TBSOTf to provide **1.135** in 85% yield. Removal of the anomeric allyl ether was inefficient using PdCl$_2$, but a two step protocol[137] involving Ir(I)-catalyzed isomerization of the allyl ether to a vinyl ether, and subsequent hydrolysis of the vinyl ether to a hydroxyl group with Hg(II) provided hemiacetal **1.136** in 85% yield. Conversion of the hemiacetal to trichloroacetimidate **1.117** took place upon treatment with trichloroacetonitrile and 1,8-diazobicycloundec-7-ene (DBU).
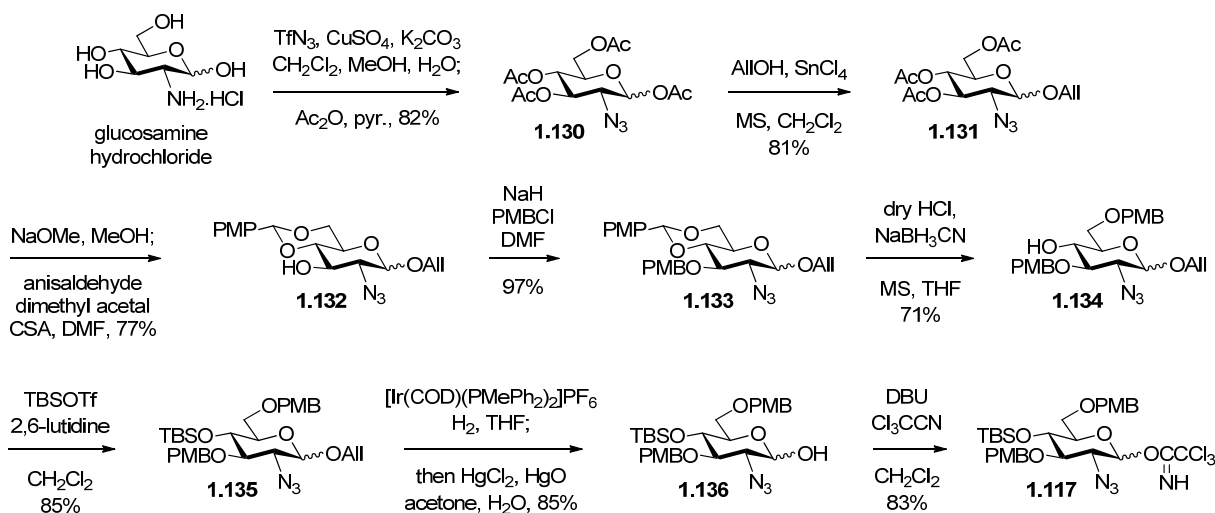
Scheme 1.21. Preparation of glucosamine derivative **1.117**

1.2.5 Synthesis of Common Pseudodisaccharide 1.114

The crucial step to forming common intermediate **1.114** was the glycosylation reaction between inositol acceptor **1.116** and a glucosaminyl donor. Various conditions using glycosyl fluorides and trichloroacetimidates were screened, and the results are shown in Table 1.3. I first evaluated glucosaminyl fluoride **1.137** (entries 1-3) because similar benzyl-protected fluoride donors required only mild activation conditions in their successful application in previous GPI syntheses. However, as reflected in entry 1, these PMB-protected glycosyl donors were quite unreactive. When performing this reaction at room temperature with any activator and stirring for days, either no reaction or only trace amounts of product **1.138** were observed. It was found, however, that upon heating the reaction to reflux in Et$_2$O, donor **1.137** reacted completely, although only moderate yields of the desired product were obtained when using Cp$_2$HfCl$_2$/AgOTf (22%) and Yb(OTf)$_3$/CaCO$_3$ (40%) as promoters (entries 2-3).

Table 1.3. Reaction conditions and results of glucosamine-inositol glycosylation
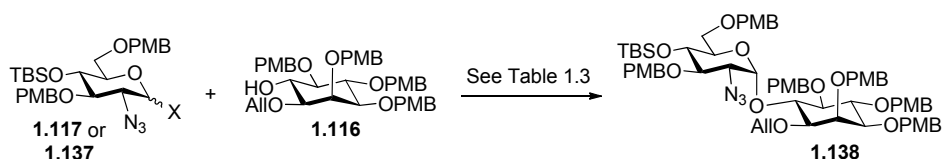
Entry	X	Conditions	Yield (α+β)	α:β ratio
1	F (**1.137**)	Any activator/solvent, ambient temp, days	NR/trace	-
2	F (**1.137**)	Cp$_2$HfCl$_2$, AgOTf, MS, Et$_2$O refluxing, overnight	22%	1:1
3	F (**1.137**)	Yb(OTf)$_3$, CaCO$_3$, MS, Et$_2$O refluxing, overnight	40%	2:1
4	OC(NH)CCl$_3$ (**1.117**)	TMSOTf (cat.), MS, CH$_2$Cl$_2$, 0 °C, 10 min	84%	1:1.6
5	OC(NH)CCl$_3$ (**1.117**)	TMSOTf (cat.), MS, Et$_2$O, 0 °C, 10 min	86%	1.2:1

The low yields of product **1.138** when using glucosaminyl fluoride donors were attributed to a side reaction that accounted for a significant portion of the mass balance (Scheme 1.22). Upon heating, donor **1.137** underwent ring flip and activation, generating oxocarbenium cation **1.139**, which possessed the proper conformation to undergo formation of 1,6-anhydro sugar **1.140**. This was a result of cleavage of the 6-*O*-PMB group and subsequent attack of the liberated primary alcohol on the electrophilic anomeric center. In the event, a significant amount of inositol acceptor **1.116** was consumed because it reacted with the newly formed PMB cation, thus resulting in the formation of fully-protected inositol derivative **1.141**.
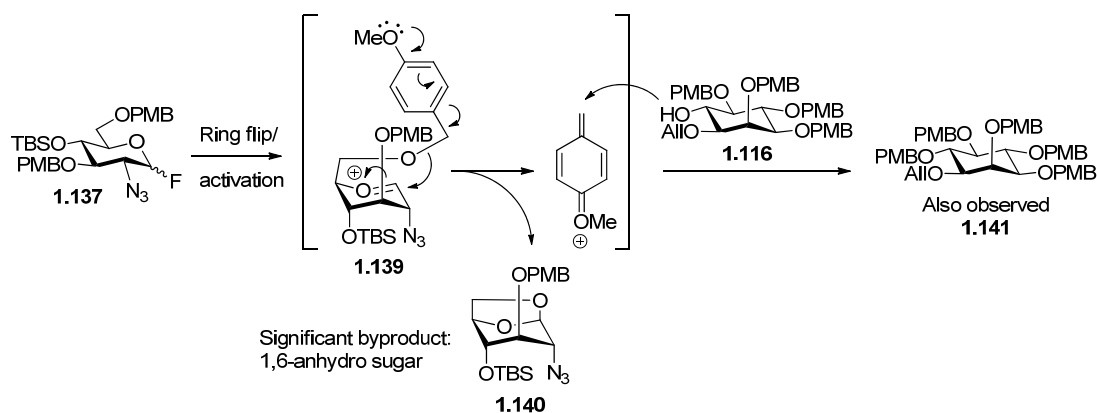
Scheme 1.22. Glucosaminyl fluoride side reaction

Given the ineffectiveness of the glycosyl fluoride donor under numerous conditions, I then turned my attention to usage of trichloroacetimidate donor **1.117** (Table 1.3, entries 4-5). I expected that the high reactivity of glycosyl trichloroacetimidates at low temperatures would suppress the side reaction discussed above. Under standard Schmidt glycosylation conditions, usage of 0.1 equiv TMSOTf at 0 °C in CH$_2$Cl$_2$, I was fortunate to observe formation of the desired pseudodisaccharide **1.138** in 84% yield. However, the α:β ratio (1:1.6) favored the undesired β-anomer. This figure was somewhat improved by changing the solvent to diethyl ether, which resulted in an 86% yield and generated the α-anomer in slight excess (α:β ratio 1.2:1). The two stereoisomers could be purified at this stage by semi-preparative HPLC, or alternatively by using silica gel column chromatography following the subsequent deallylation step. Removal of the inositol 1-*O*-allyl ether was accomplished using the one-pot Ir(I)/Hg(II) method, which provided common intermediate pseudodisaccharide **1.114** in 96% yield (Scheme 1.23). This versatile PMB protected intermediate was ready for immediate

phospholipidation at the inositol 1-*O*-position and later glycosylation at the glucosamine 4-*O*-position, thus allowing for the preparation of a diverse set of GPI anchors.
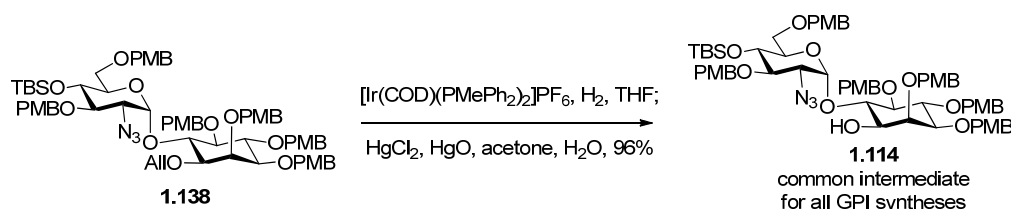
Scheme 1.23. Deallylation to form common intermediate psuedodisaccharide **1.114**

1.2.6 Synthesis of Man-I Building Block 1.118

The Man-I building block was particularly important for this synthesis because I chose this unit as the functionalization site, where alkyne- or biotin-containing groups would be attached. As discussed previously, Man-I is extensively modified in various naturally occurring GPIs. In fact, additional carbohydrate or phosphoethanolamine groups have been observed at every position of Man-I. My initial plan involved using the 3-*O*-position as the functionalization site because I predicted that the monomer preparation would be straightforward and that late-stage functionalization would be easiest due to the higher nucleophilicity of the equatorial 3-*O*-hydroxyl group. Therefore, I set out to synthesize a 1,3,6-*O*-differentiated mannoside.

In the first generation synthesis of the Man-I building block, I designed glycosyl fluoride **1.147** as the target (Scheme 1.24). I expected that diol **1.147** would undergo selective glycosylation at the primary 6-*O*-position by the Man-II glycosyl donor, leaving the 3-*O*-position discriminated for later functionalization and the anomeric fluoride ready for the later key glycosylation. Thus, mannose peracetate **1.142** was subjected to

regioselective deacetylation with benzylamine,[138] and the resulting hemiacetal **1.143** was converted in excellent yield to glycosyl fluoride **1.144** using diethylaminosulfur trifluoride (DAST). The planned pathway to **1.147** was interrupted when an unexpected reaction occurred during deacetylation. Upon treatment of fluoride **1.144** with NaOMe/MeOH, a mixture of fluoroglycoside **1.145** and methyl glycoside **1.146** were obtained from the reaction mixture (stereochemistry predicted, not determined experimentally). The undesired latter product likely resulted from displacement of the α-configured anomeric fluoride by the 2-*O*-position alkoxide, which formed an intermediate 1,2-anhydro sugar that could be opened by methoxide to give **1.146**.[139] Given this unforeseen reaction, and the low reactivity observed for other PMB-protected glycosyl fluorides, I opted to redesign the Man-I building block.
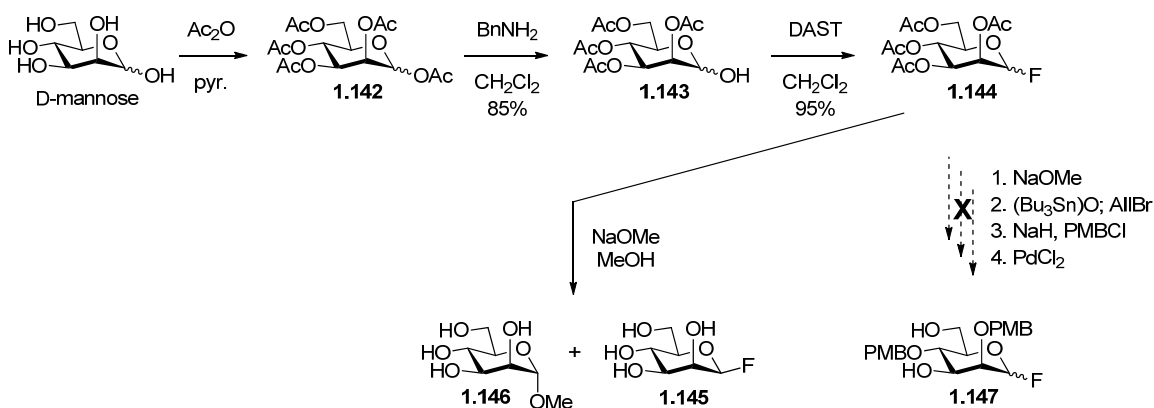
Scheme 1.24. Failed preparation of Man-I glycosyl fluoride

In the second generation Man-I synthesis, I targeted thioglycoside **1.152** (Scheme 1.25) to allow for versatility in the anomeric leaving group later on, as thioglycosides can be directly activated under numerous conditions or be converted into other glycosyl donors. Again, the preparation was started from mannose peracetate

1.142, which underwent boron trifluoride-promoted glycosylation with toluenethiol to give **1.148** in 85% yield over two steps. After deacetylation, the intermediate tetraol was selectively protected at the 6-*O*-position using the bulky reagent *para*-methoxytrityl chloride (PMTrtCl). Next, product **1.149** was regioselectively allylated at the 3-*O*-position via a stannylene acetal intermediate. The desired compound **1.150** was purified from the reaction mixture in a low but unoptimized 38% yield. The remaining hydroxyl groups at the 2-*O*- and 4-*O*-positions were protected as PMB ethers to give **1.151**, and then the very acid-labile 6-*O*-PMTrt group was selectively removed using AcOH, furnishing the desired thioglycoside **1.152** in 85% yield over two steps.
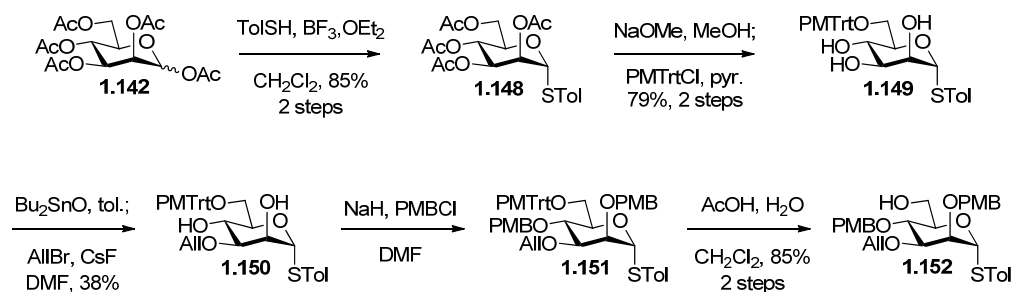
Scheme 1.25. Preparation of second generation Man-I building block

Unfortunately, the second generation Man-I building block turned out to cripple the GPI synthesis at a later stage. After elaboration of **1.152** to the desired trimannosyl trichloroacetimidate donor **1.153**, I was poised to attempt the key glycosylation reaction with phospholipidated pseudodisaccharide fragment **1.154** (Scheme 1.26). Under various reaction conditions, none of the desired pseudopentasaccharide **1.155** was formed. Instead, the entirety of the glycosyl donor was consumed by an intramolecular reaction. Upon activation with catalytic TMSOTf to form oxocarbenium cation **1.156**, the

2-*O*-PMB group was cleaved, liberating a secondary hydroxyl group that collapsed down on the neighboring electrophilic anomeric center, resulting in the formation of 1,2-anhydro sugar **1.157**.
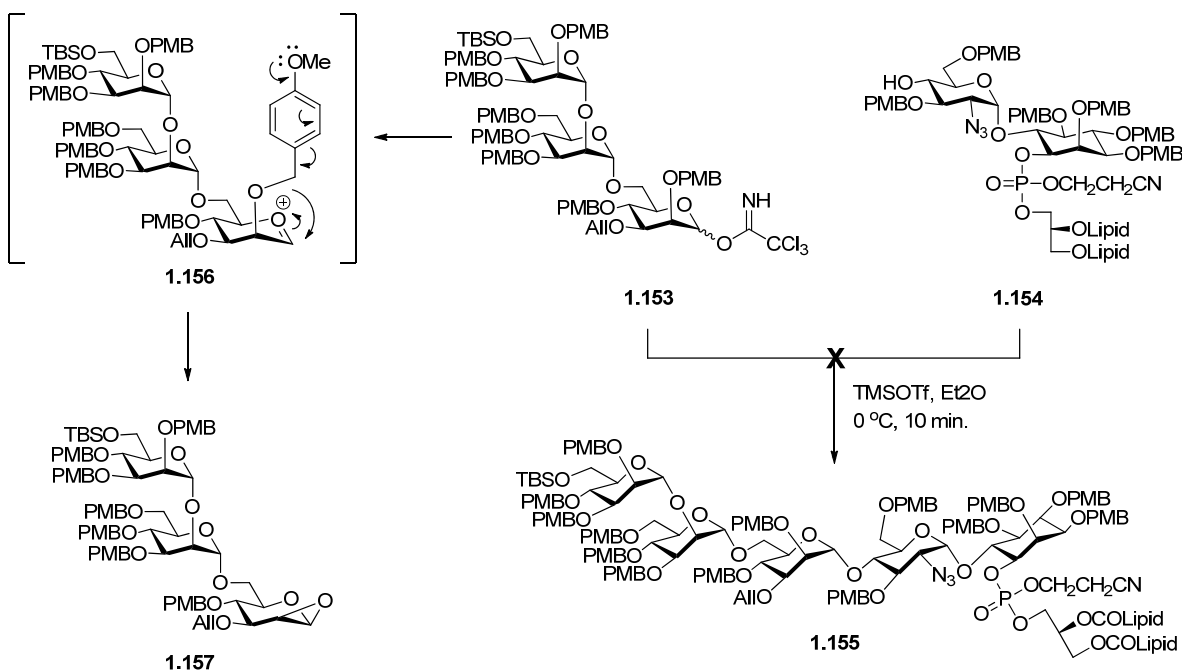
Scheme 1.26. Second generation Man-I building block disables synthesis

Because no attempted modifications of the glycosylation conditions could circumvent this side reaction when using trimannosyl donor **1.153**, I was again forced to redesign the Man-I building block. To do so, the site of functionalization was changed from the Man-I 3-*O*-position to the 2-*O*-position. In this case, the orthogonal allyl ether protecting group replaced the troublesome 2-*O*-PMB group, which should enable a successful key glycosylation. Also, because GPIs naturally contain substituents at the 2-*O*-position, no significant conformational changes were expected. Therefore, I developed a preparation of the third generation Man-I building block **1.118** (Scheme

1.27). The expedient synthesis began with a reported conversion of mannose peracetate **1.142** to 4,6-*O*-*para*-methoxybenzylidene-protected diol **1.159**.[140] Stannylene acetal-directed regioselective protection of the 3-*O*-position with a PMB group left the 2-*O*-position to be masked as an allyl ether. This two step sequence gave **1.161** in 68% yield. Finally, regioselective reductive opening of the *para*-methoxybenzylidene ring afforded the desired Man-I building block **1.118** in 82% yield.
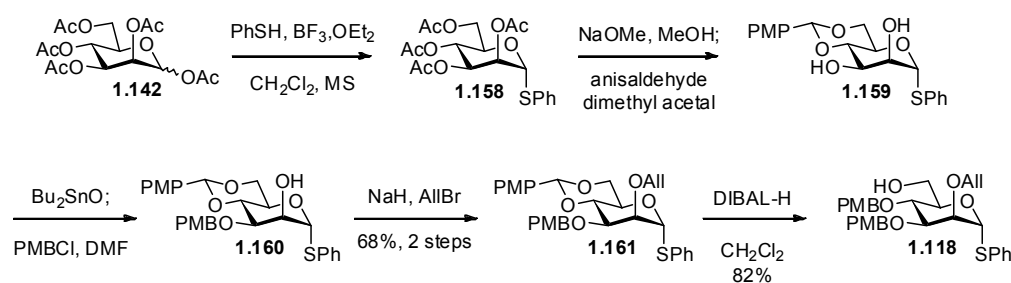
Scheme 1.27. Preparation of third generation Man-I building block **1.118**

1.2.7 Synthesis of Man-II Building Block 1.119

For the Man-II monomer, a 1,2-*O*-differentiated mannose derivative, preferably bearing a participating protecting group at the 2-*O*-position, was required. To this end, 1,2-orthoesters are very useful intermediates and were applied in the synthesis of Man-II building block **1.119** (Scheme 1.28). Thus, from mannose peracetate **1.142** a reported method[141] was used to obtain orthoester intermediate **1.163**. Deacetylation with NaOMe formed a triol intermediate that was converted to PMB-protected orthoester **1.164** in 76% yield over two steps. Next, a regioselective orthoester ring opening was carried out using acetic acid/H$_2$O. The desired hemiacetal **1.165** was generated in 70% yield, while the remainder of the mass balance was attributed to the regioisomeric anomeric acetate.

Compound **1.165** was then transformed into glycosyl trichloroacetimidate **1.119** by treatment with trichloroacetonitrile and DBU.
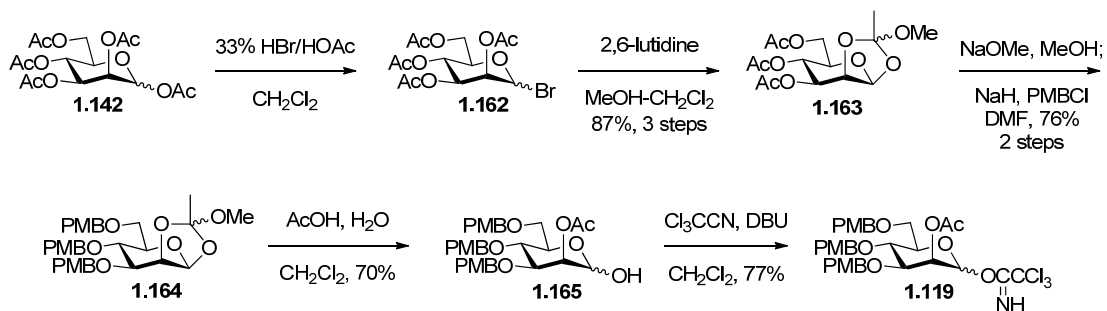
Scheme 1.28. Preparation of Man-II building block **1.119**

1.2.8 Synthesis of Man-III Building Block 1.120

The 1,6-*O*-differentiated Man-III building block **1.120** was synthesized from mannose peracetate **1.142** using the procedure shown in Scheme 1.29. First, **1.142** was converted to allyl glycoside **1.166** by BF$_3$-promoted glycosylation with allyl alcohol. Subsequent deacetylation and *para*-methoxytritylation of the primary alcohol afforded triol **1.167** in 66% yield over two steps. Next, installation of PMB groups at the 2-, 3-, and 4-*O*-positions resulted in fully protected intermediate **1.168**. The PMTrt was then replaced with a TBS group in two steps, including acidic hydrolysis of the 6-*O*-PMTrt group to give **1.169** in 94% yield, and treatment of this product with TBSCl to furnish **1.170** in 88% yield. Hydrolysis of the anomeric allyl ether with PdCl$_2$ efficiently produced hemiacetal **1.171**, which was converted to glycosyl trichloroacetimidate **1.120**, again using trichloroacetonitrile and DBU.
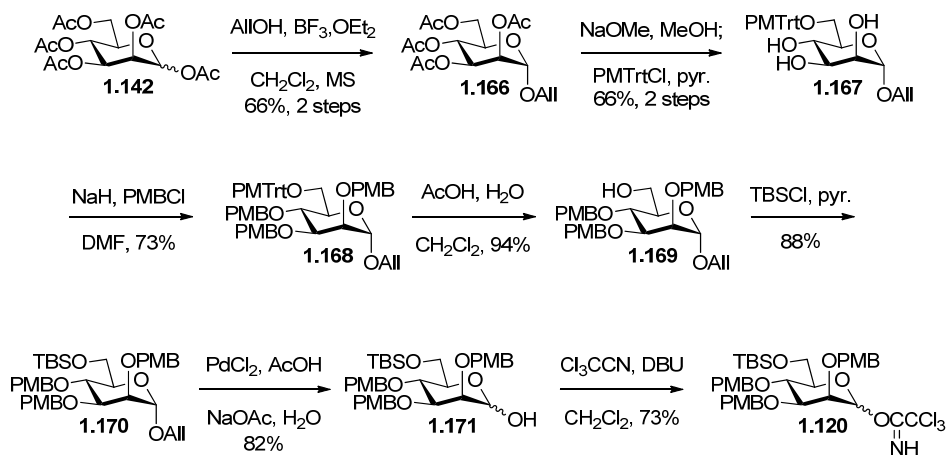
Scheme 1.29. Preparation of Man-III building block **1.120**

1.2.9 Synthesis of Common Trimannose 1.115

The synthesis of common intermediate **1.115** from mannose monomers **1.118**, **1.119**, and **1.120** was a straightforward process (Scheme 1.30), in large part due to the relative ease of forming α-mannosidic bonds. To construct each glycosidic bond, the Schmidt glycosylation was applied, which did not affect the numerous PMB groups present in the coupling partners. The first glycosylation was between Man-I acceptor **1.118** and Man-II donor **1.119**. Upon treatment of these substrates with catalytic TMSOTf, exclusively α-glycosylation took place, forming disaccharide **1.172**, which after a quick purification by column chromatography was subjected to deacetylation with K_2CO_3/MeOH. The resulting disaccharide alcohol **1.173** was formed in 66% yield over two steps and was ready for elongation at the Man-II 2-*O*-position. Thus, **1.172** was reacted with Man-III trichloroacetimidate **1.120** in the presence of TMSOTf. When CH_2Cl_2 was used as the solvent, the desired trimannose **1.115** was generated in an α:β ratio of 5:1. The stereoselectivity was improved to α-only by switching the solvent to Et_2O. Under these conditions, common intermediate **1.115** could be obtained in 76%

yield. The configurations of all three anomeric centers were established as α by the anomeric J_{CH} coupling constants (see experimental). Of note here is that no anhydro sugar derivative of **1.120** (as a result of PMB loss, e.g. Scheme 1.26) was observed.
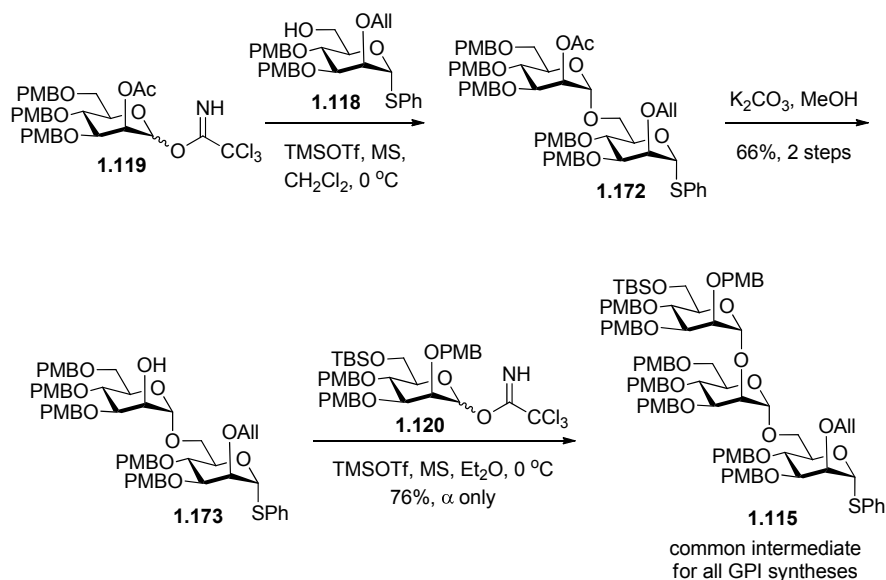
Scheme 1.30. Synthesis of common intermediate trimannose **1.115**

As outlined in the retrosynthesis (section 1.2.2), common intermediates **1.114** and **1.115** were designed to be applicable to the synthesis of all four target GPI anchors. With both PMB-protected intermediates successfully synthesized, I then turned to the assembly of the target GPIs, which will be discussed individually in the following three sections.

1.2.10 Synthesis of GPIs with Unsaturated Lipid Chains 1.109 and 1.110

Two of the synthetic targets for this project were variably phosphorylated GPI anchors bearing unsaturated lipid chains, **1.109** and **1.110**. Both targets contained

diacyloleoyl phosphoglycerolipids attached to the inositol 1-*O*-position. For the phospholipidation reaction of pseudodisaccharide **1.114**, I chose to use phosphoramidite **1.179** as the reactive phosphate precursor, and thus prepared it from optically pure glycerol derivative **1.174** (Scheme 1.31). First, the free primary alcohol was protected by a *tert*-butyldiphenylsilyl (TBDPS) group, and then the isopropylidene was removed with acetic acid, providing diol **1.176** in 66% yield over two steps. The unsaturated lipid chains were then installed in 96% yield in an acylation reaction using oleic acid, *N*-(3-dimethylaminopropyl)-*N'*-ethylcarbodiimide hydrochloride (EDCI), and catalytic 4-(dimethylamino)pyridine (DMAP). The resulting compound **1.177** was then subjected to desilylation with tetrabutylammonium fluoride (TBAF) to give alcohol **1.178** in 96% yield. This intermediate was reacted with bis(diisopropylamino)(2-cyanoethoxy)phosphine in the presence of diisopropylammonium tetrazolide to provide phosphoramidite **1.179** in 85% yield. The sensitive phosphoramidite reagent was purified quickly by a triethylamine-neutralized silica gel column and characterized by ^{1}H and ^{31}P NMR spectroscopy.
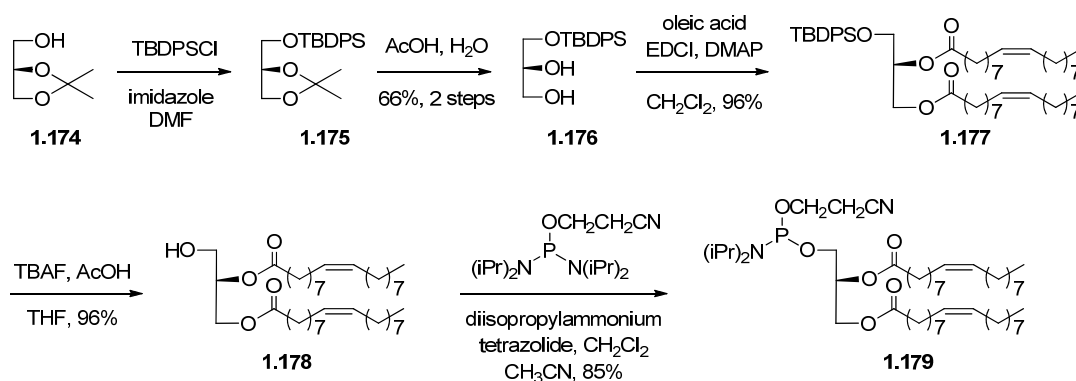
Scheme 1.31. Preparation of phospholipid precursor **1.179**

The phospholipidation of pseudodisaccharide **1.114** by phosphoramidite **1.179** was accomplished using 1H-tetrazole as a mild acidic promoter (Scheme 1.32). This resulted in the formation of trivalent phosphite intermediate **1.180**, which was chemoselectively oxidized to pentavalent phosphate **1.181** by direct addition of *t*-BuOOH to the reaction mixture at low temperature. Previous studies in our lab showed that a temperature of -40 °C was required to prevent oxidation of other alkenes present in the substrate. In this case, the double bonds in the unsaturated lipid chains were unaffected by the oxidation event. Excess *t*-BuOOH was scavenged with dimethyl sulfide prior to warming and quenching the reaction. After work-up and quick column purification, the crude product **1.181** was taken forward to the next step, removal of the glucosamine 4-*O*-TBS group. This reaction was unexpectedly difficult, as a number of commonly used desilylation reagents failed to produce the desired product **1.182**. Substrate **1.181** was unreactive toward standard conditions, TBAF buffered with acetic acid. When stronger conditions were used, the starting material decomposed unproductively. For example, unbuffered TBAF cleaved the base-labile cyanoethoxy phosphate protecting group prior to cleaving the TBS group. More acidic reagents, such as pyridine•HF, resulted in hydrolysis of multiple PMB groups prior to affecting the 4-*O*-TBS. Finally, I found that commercially available triethylamine trihydrofluoride cleanly effected the desired desilylation without compromising other protecting groups, although reaction times were unfortunately quite long (5-7 days). The resulting product **1.182** was obtained in a very acceptable 56% yield over three steps. Because this sample existed as a ~1:1 mixture of diastereomers originating from the stereogenic phosphorus atom,

semi-preparative HPLC was used to separate the two isomers. This was beneficial for the characterization of **1.182** and subsequent complex intermediates.
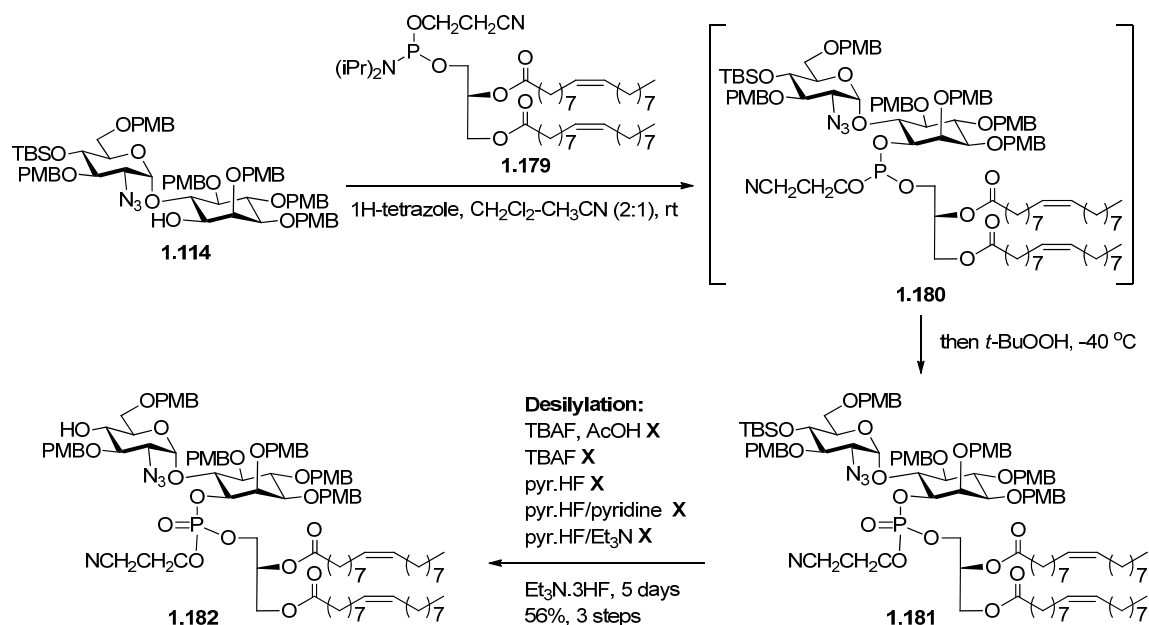
Scheme 1.32. Phospholipidation of **1.114** to install unsaturated lipid chains

At this stage, pseudodisaccharide fragment **1.182** was ready for the key glycosylation with the trimannose donor fragment. However, common trimannose intermediate **1.115** required two alterations prior to glycosylation. First, the Man-I 2-*O*-allyl group had to be swapped for a different orthogonal protecting group, because later removal of the allyl ether would likely conflict with the unsaturated lipid chains. Secondly, direct activation of the trimannose thioglycoside under various conditions was disovered to be ineffective or very low yielding. Given my success using Schmidt's trichloroacetimidate method, I decided to convert the anomeric thioether to a trichloroacetimidate.

The adjustment of trimannose intermediate **1.115**, shown in Scheme 1.33, began with selecting a suitable 2-*O*-position protecting group that would be orthogonal to the remainder of the molecule's functional groups and also provide a suitable environment for the key glycosylation reaction. I first evaluated neighboring group-participating carbonates such as 2,2,2-triclhloroethoxycarbonyl (Troc) and Fmoc, but these protecting groups were either difficult to install or were unstable to later reaction conditions. In addition, these electron-withdrawing protecting groups would disarm the trimannose donor, making for an unpredictable glycosylation reaction. I eventually chose the triethylsilyl (TES) group to protect the 2-*O*-position, expecting that the Man-III 6-*O*-TBS and Man-I 2-*O*-TES groups could be selectively removed because the former was protecting a primary alcohol, while the latter was protecting a relatively inaccessible secondary alcohol. I hoped that this potential orthogonality might provide the ability to variably phosphorylate or functionalize the GPI anchors. Thus, trimannose **1.115** underwent a 2-*O*-position protecting group swap at Man-I. Deallylation using standard protocols was ineffective, so again Cha's Ti(OiPr)$_4$–Grignard reagent method was used for the efficient removal of the Man-I 2-*O*-allyl group, which provided trimannose alcohol **1.183** in 82% yield. Installation of the TES group proceeded smoothly upon treatment with TESOTf, resulting in compound **1.184** in 90% yield. Next, the thioglycoside required converstion to a trichloroacetimidate, which was accomplished in two steps. First, hydrolysis of the anomeric thioether with NIS, AgOTf, and hindered base *tri*-tert-butylpyrimidine (TTBP) gave hemiacetal **1.185** in 74% yield. Conversion of this intermediate to the desired trimannose trichloroacetimidate **1.186** was carried out using trichloroacetonitrile and DBU.
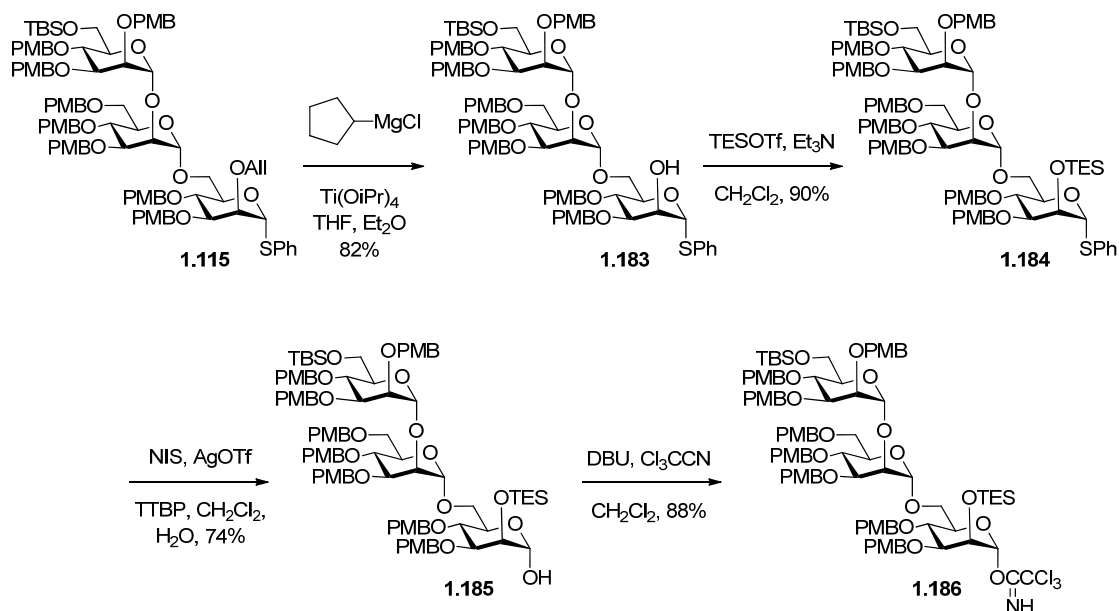
Scheme 1.33. Adjustment of trimannose **1.115** for the key glycosylation

With both key glycosylation components in hand, I carried out the pivotal reaction using standard Schmidt conditions (Scheme 1.34). Phospholipidated pseudodisaccharide acceptor **1.182** and trimannose donor **1.186** were treated with a catalytic amount of TMSOTf at 0 °C, and TLC showed nearly complete consumption of the acceptor in less than 10 minutes. After careful workup and purification, the desired α-pseudopentasaccharide **1.187** was obtained in 64% yield, while no β-isomer was detected. Configurations of anomeric positions were established as α by coupled ^{13}C NMR J_{CH} values (125 MHz): 101.80 (J_{CH} = 176 Hz, Man-1), 99.66 (J_{CH} = 175 Hz, Man-1), 99.54 (J_{CH} = 170 Hz, Man-1), 97.90 (J_{CH} = 177 Hz, GlcN$_3$-1).
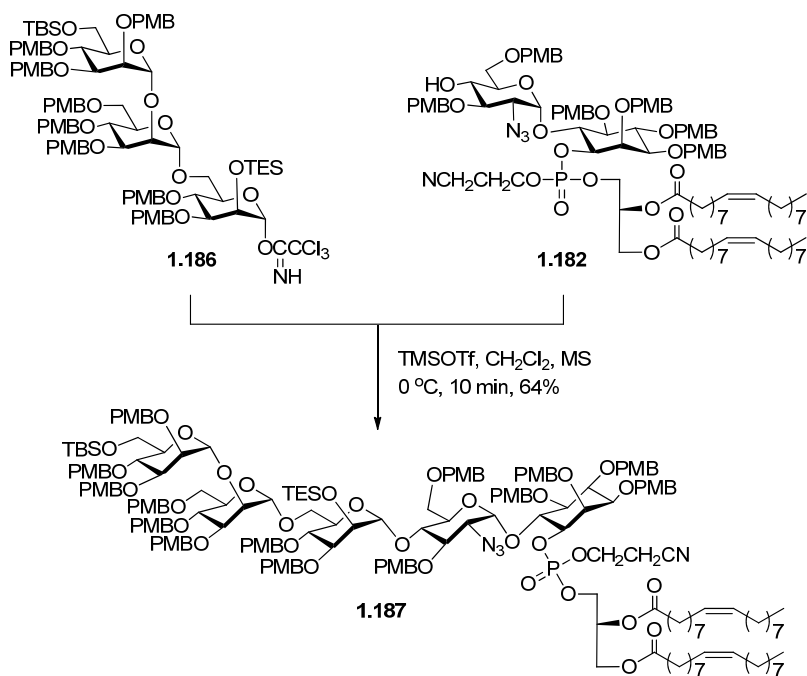
Scheme 1.34. Key glycosylation reaction

Attention was then turned to installation of phosphoethanolamine groups in the PMB-protected GPI intermediate **1.187** (Scheme 1.35). To do so with optimal flexibility, I hoped to remove the Man-III 6-*O*-TBS group selectively with triethylamine trihydrofluoride. However, this reaction proceeded without useful regioselectivity, and both silyl groups were removed after overnight treatment with Et$_3$N•3HF to provide diol **1.188** in 70% yield. Given this result, I expected to only be able to access the fully phosphorylated GPI **1.110**, an unfortunate yet acceptable occurrence. Therefore, the synthesis proceeded to the phosphorylation of **1.188** using phosphoramidite **1.189** as the phosphoethanolamine precursor. After approximately 1 hour reaction time in the presence of 1H-tetrazole, TLC showed one major product, so chemoselective oxidation with *t*-BuOOH, work-up, and sequential purifications using silica gel and size-exclusion LH-20 columns were performed. Upon analysis, the product was determined to be

singly phosphorylated GPI intermediate **1.190**, which was isolated in 50% yield (61% based on recovered starting material). Using 2D NMR spectroscopy, specifically correlation spectroscopy (COSY), I confirmed that phosphorylation occurred selectively at the primary Man-III 6-*O*-position alcohol. This fortunate result meant that I would be able to access both target GPIs **1.109** and **1.110**. Given the limited amount of material available at this stage in the synthesis, ~50-100 µg of **1.190** were taken forward to attempt the second phosphorylation reaction. Using the same conditions, but employing a larger excess of **1.189** and a longer reaction time (overnight), fully phosphorylated GPI intermediate **1.191** was formed, as detected by matrix-assisted laser desorption ionization (MALDI) MS. Given the high reactivity of phosphoramidite reagents, regioselectivity was not expected at this stage. However, the relatively low nucleophilicity of the Man-I 2-*O*-position was not surprising; this secondary hydroxyl group was also unreactive in late-stage acylation reactions (see Scheme 1.40).

The final phase of synthesizing GPIs **1.109** and **1.110** involved developing a suitable global deprotection procedure (Scheme 1.36). With fully elaborated and protected GPI intermediates **1.190** and **1.191** available, I focused on their conversion to the target molecules. Global deprotection required three sets of reaction conditions: (1) reductive, to convert the glucosamine azido group to an amine; (2) basic, to remove the Fmoc and cyanoethoxy protecting groups; (3) acidic or oxidative, to remove the global PMB protecting groups. For azide reduction, use of a heterogeneous catalyst such as Lindlar's catalyst was avoided in order to align with the overall strategy to use global deprotection conditions that would allow for the most flexibility in functional group incorporation (i.e., a thiol or sulfide could poison Lindlar's catalyst). Thus, I decided to
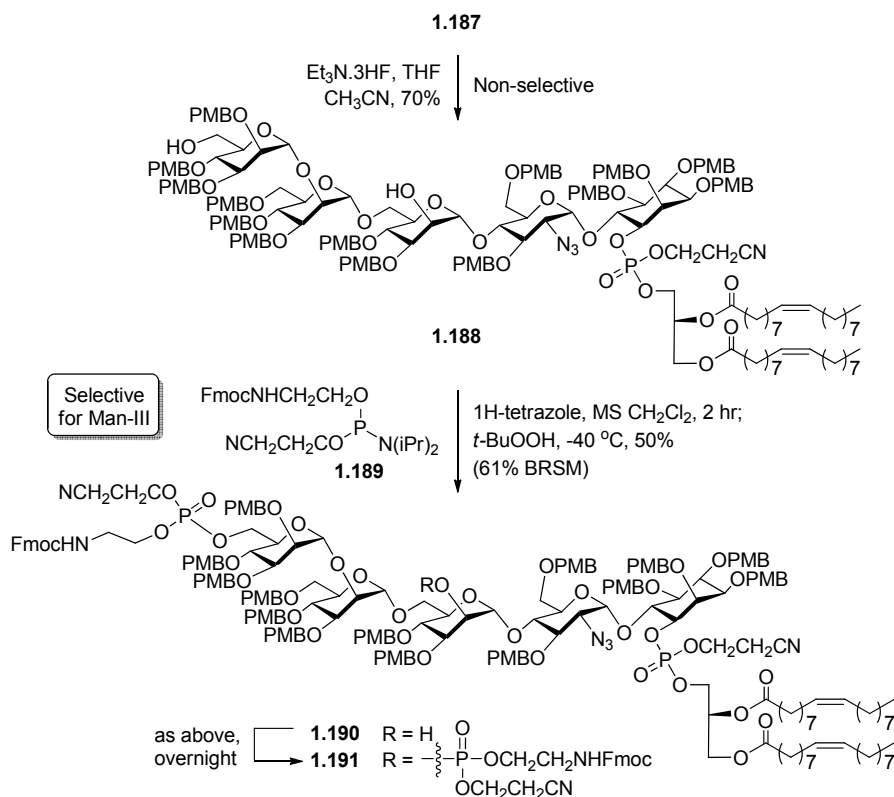
Scheme 1.35. Regioselective installation of phosphoethanolamine groups

use the combination of activated zinc and acetic acid, a very mild set of conditions for selective azide reduction. For removal of the base-labile Fmoc and cyanoethoxy groups, a low concentration of the non-nucleophilic base DBU could be used to quickly effect deprotection of the phosphates and the phosphoethanolamine primary amino groups. For PMB removal, oxidative conditions (e.g., DDQ or CAN) were ineffective, but a low concentration of TFA satisfactorily hydrolyzed all PMB groups. Thus, after extensive optimization of reaction concentrations, times, and sequence, a three-step, one-pot reaction was developed that could efficiently remove all of the protecting groups in under 4 hr: 1) zinc-mediated reduction of the azide for 2 h; 2) after filtration and evaporation, removal of the base-labile Fmoc and cyanoethoxy groups by treatment

with DBU for 1 h; 3) direct addition of 20% TFA to quench the DBU and give a final concentration of 10% TFA, which removed all PMB groups in only 30 min. The reaction mixture was then co-evaporated with toluene several times to remove volatile TFA, and purification was accomplished using a Sephadex LH-20 size exclusion column. Using this deprotection sequence, target GPI **1.109** was obtained in 81% yield after global deprotection and purification, and was subsequently characterized by NMR spectroscopy and MALDI MS. Fully phosphorylated GPI **1.110** was also successfully obtained using this global deprotection, and the microscale sample was characterized by MALDI MS.
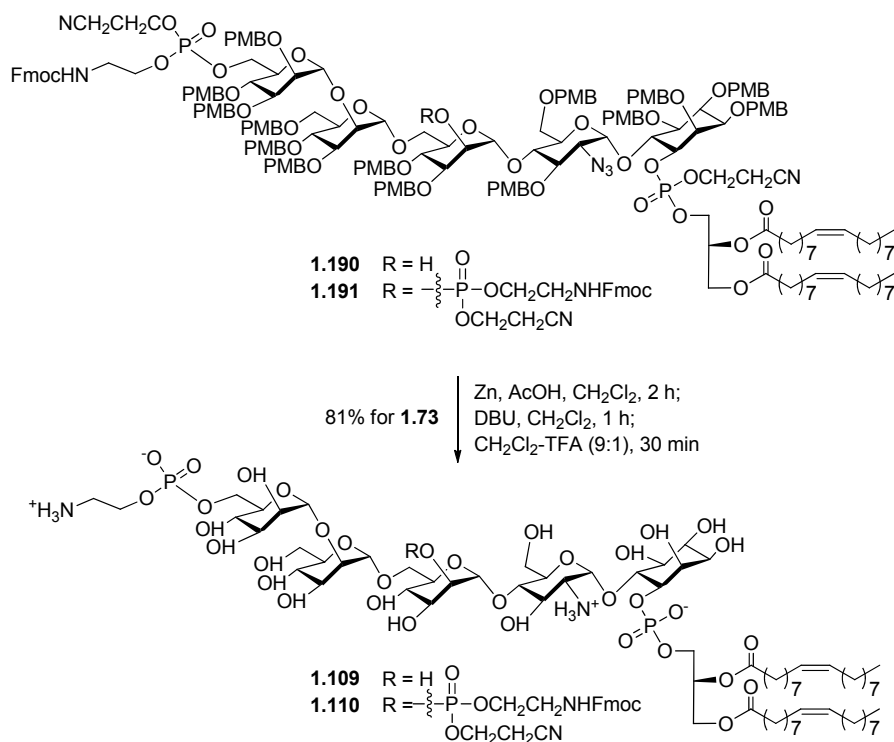
Scheme 1.36. Global deprotection to afford GPIs bearing unsaturated lipid chains

1.2.11 Synthesis of Clickable GPI 1.75

To commence the synthesis of alkyne-containing 'clickable' GPI anchor **1.111**, a diacylstearoyl glycerolipid was installed at the free inositol 1-*O*-position of common intermediate **1.114** (Scheme 1.37). The phosphorylating reagent, phosphoramidite **1.192**, was prepared in a manner identical to that shown for compound **1.179** in Scheme 1.31, and with similar yields. The phospholipidation reaction proceeded smoothly with 1H-tetrazole as the promoter and after oxidation of intermediate phosphite **1.193** to a phosphate, compound **1.194** was isolated as a ~1:1 mixture of diastereomers originating from the stereogenic phosphorus atom. I again employed triethylamine trihydrofluoride to remove the glucosamine 4-*O*-TBS group. The desilylation reaction was clean but comparably slow, requiring stirring for 7 days at room temperature. The desired phospholipidated pseudodisaccharide **1.195** was obtained in 54% yield over three steps, and separation of the two diastereomers was completed at this stage using semi-preparative HPLC.
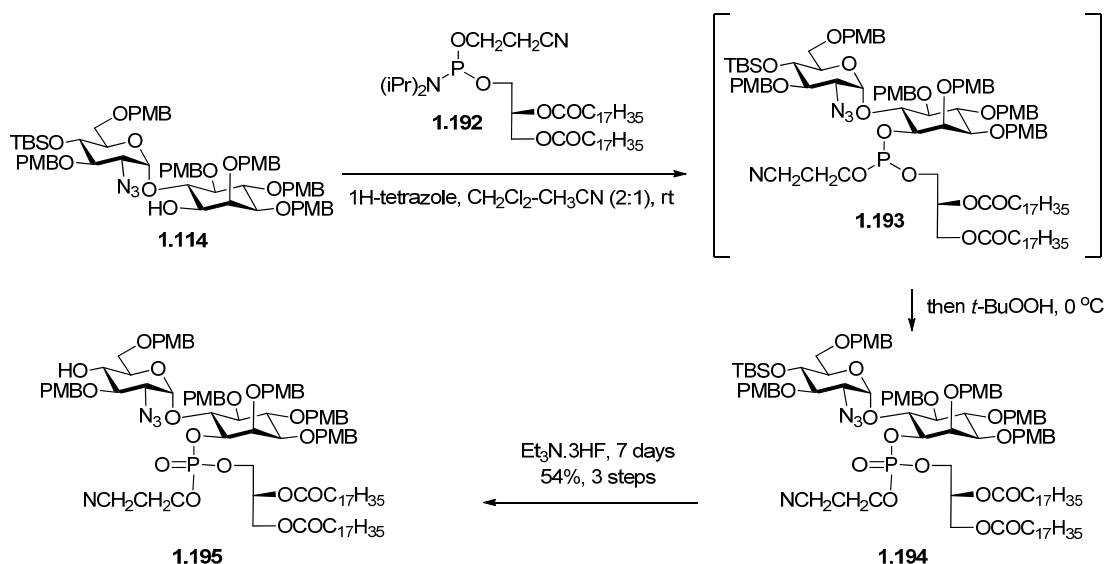
Scheme 1.37. Phospholipidation of **1.78** to install saturated lipid chains

I first attempted the key glycosylation reaction by directly activating trimannose thioglycoside **1.115** in the presence of acceptor **1.195**. Because the donor contained an allyl ether protecting group at the Man-I 2-*O*-position, an orthogonal thioether activation protocol was necessary. Thus, in lieu of the standard NIS/AgOTf combination, I made use of *para*-toluenesulfenyl chloride (*p*-TolSCl), AgOTf and TTBP, a reagent system developed by Crich.[142-143] These conditions did result in the formation of desired pseudopentasaccharide **1.197**, but in only ~20% yield, prompting me to evaluate alternative glycosylation methods. Because of prior success using the Schmidt glycosylation, trimannose thioglycoside **1.115** was converted to trichloroacetimidate **1.196** in two steps (Scheme 1.38). First, the *p*-TolSCl/AgOTf/TTBP reagent system used in combination with wet CH_2Cl_2 was applied to hydrolyze the substrate, providing the corresponding intermediate hemiacetal in 68% yield (BRSM). Treatment of this intermediate with trichloroacetonitrile and DBU gave glycosyl imidate **1.196**, which was then tested in the key glycosylation reaction. Usage of 0.1 equivalents of TMSOTf in Et_2O at 0 °C effected a successful activation of imidate **1.196**, which reacted with acceptor **1.195** efficiently to provide only the α-linked pseudopentasaccharide **1.197**. After work-up and without purification, **1.197** was treated with triethylamine trihydrofluoride in CH_3CN-THF overnight, which resulted in clean removal of the Man-III 6-*O*-TBS group. Purification at this stage gave GPI alcohol **1.198** in 81% yield over two steps, including the key glycosylation reaction. This intermediate was fully characterized using 1D/2D NMR spectroscopy and MS, and the mannosidic bonds were established as α by coupled ^{13}C NMR J_{CH} values (125 MHz): 101.09 (J_{CH} = 167 Hz, Man-1), 99.79 (J_{CH} = 174 Hz, Man-1), 99.79 (J_{CH} = 174 Hz, Man-1), 97.94 (J_{CH} = 177 Hz, $GlcN_3$-1).
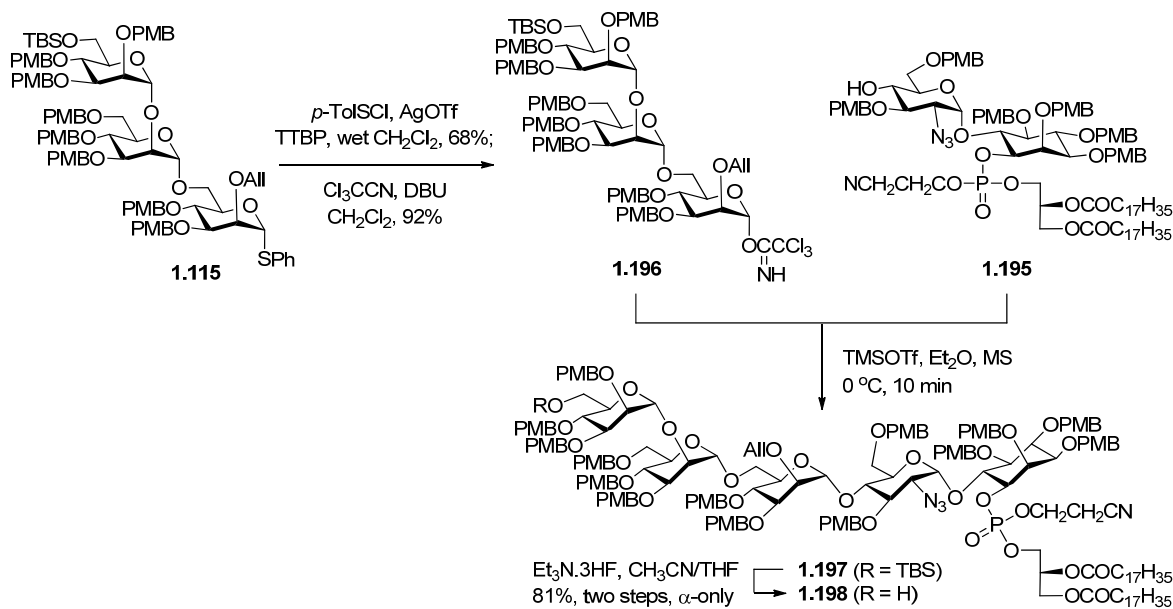
Scheme 1.38. Key glycosylation reaction

At this point, GPI intermediate **1.198** was ready for addition of a phosphoethanolamine group to the Man-III 6-*O*-position, for which phosphoramidite **1.189** was again used as the phosphorylating reagent (Scheme 1.39). The reaction was fast, quantitatively forming a phosphite intermediate in ~1 hr. After cooling the reaction mixture to -40 °C, *t*-BuOOH was used to chemoselectively oxidize the phosphite to phosphate **1.199** *in situ* without affecting the Man-I 2-*O*-allyl group. The phosphorylation process proceeded in 81% yield and, as previously, generated a ~1:1 mixture of diastereomers that were separated by semi-preparative HPLC to facilitate characterization. Next, removal of the Man-I 2-*O*-allyl group of **1.199** was realized by using the aforementioned Ir(I)/Hg(II) protocol, which afforded secondary alcohol **1.200** in 90% yield (of note: a stoichiometric amount of the iridium catalyst was required, and the isomerization reaction could not be monitored by TLC).
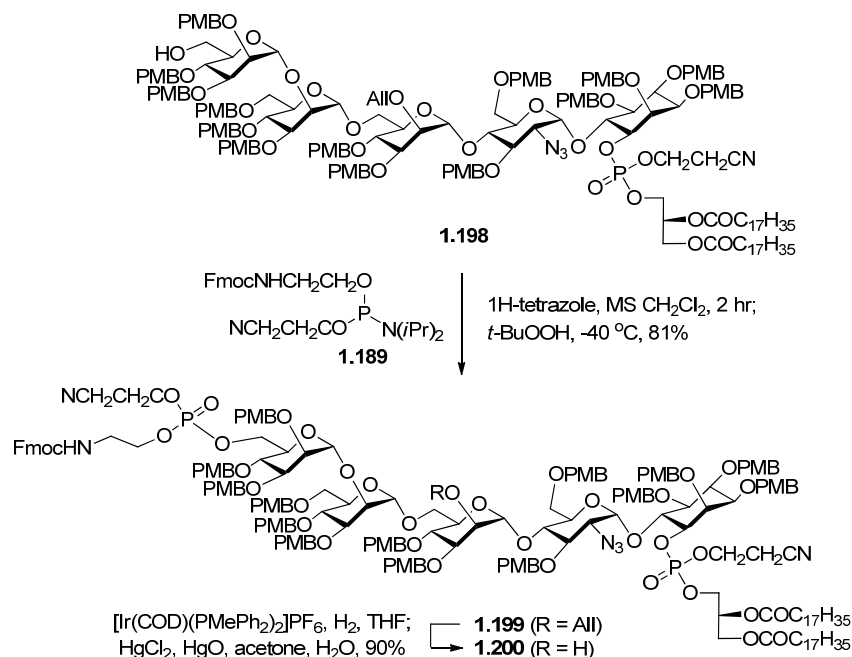
Scheme 1.39. Phosphorylation and deallylation

Installation of the alkyne 'click tag' and global deprotection to afford target GPI **1.111** are shown in Scheme 1.40. Functionalization of the Man-I 2-*O*-position proved to be a formidable task, likely a result of poor nucleophilicity, which was also encountered at this site in the synthesis of GPIs bearing unsaturated lipid chains (Scheme 1.35). Initially, direct esterification of **1.200** was attempted by using an alkyne-containing carboxylic acid (e.g., pentanoic acid) and standard coupling conditions such as EDCI and 1-hydroxybenzotriazole (HOBt) or DMAP. However, even upon heating, the desired acylation products were not observed. Difficulty was also encountered when attempting to use acid chlorides. Fortunately, I found that the substrate could undergo succinylation in 67% yield when employing a large excess of succinic anhydride, DMAP, and molecular sieves. Addition of a succinate "linker" to the GPI provided a carboxylic acid handle in intermediate **1.201**, thus allowing me to perform a much more facile
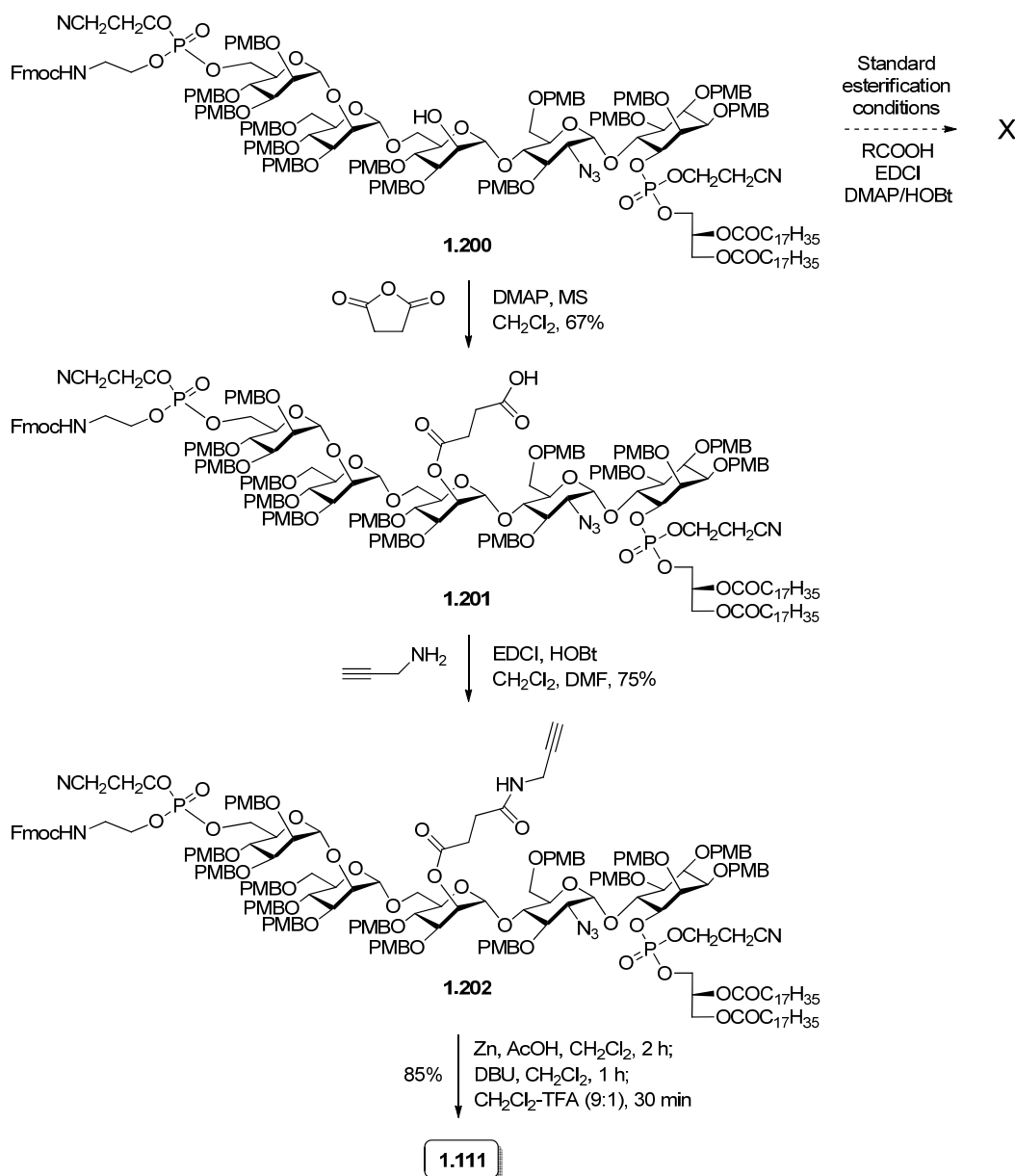
Scheme 1.40. Alkyne functionalization and deprotection to afford 'clickable' GPI

amidation reaction to install the desired alkyne functionality. Accordingly, the GPI carboxylic acid **1.201** was treated with propargyl amine under standard amide bond-forming conditions (EDCI/HOBt). This reaction successfully attached the 'clickable' alkyne functional group, furnishing fully protected GPI **1.202** in 75% yield. For the global

deprotection sequence, I employed the three-step, one-pot protocol developed previously: (1) zinc-mediated reduction of the azide for 1 h; (2) after filtration and evaporation, removal of the base-labile Fmoc and cyanoethoxy groups by treatment with DBU for 1 h; (3) direct addition of 20% TFA to quench the DBU and give a final concentration of 10% TFA, which removed all PMB groups in 30 min. After co-evaporation of the reaction mixture with toluene to remove volatile TFA, the crude material was purified using a Sephadex LH-20 size exclusion column. This protocol again proved effective, as the desired 'clickable' GPI anchor **1.111** was obtained in 85% yield over the three deprotection steps. Characterization of the target molecule was accomplished using 1D/2D NMR spectroscopy and MALDI MS.

1.2.12 Synthesis of Biotinylated GPI 1.112

After establishing a successful synthesis of clickable GPI **1.111**, the structurally analogous biotinylated GPI **1.112** could be prepared expediently from a common intermediate, GPI carboxylic acid **1.201** (Scheme 1.41). Reaction of this compound with a commercially available biotin derivative, PEG$_3$-biotin-amine **1.203**, in the presence of EDCI and HOBt provided fully protected GPI **1.204** in 70% yield. Finally, the three-step, one-pot global deprotection and subsequent purification described above were used to convert **1.204** into the target biotinylated GPI **1.112**. An isolated yield of this compound was not obtained due to a decomposition reaction that is discussed further in section 1.4. However, initial characterization of the final product using MALDI MS showed a single species corresponding to the desired compound, with no peaks relating to the starting material or intermediates.
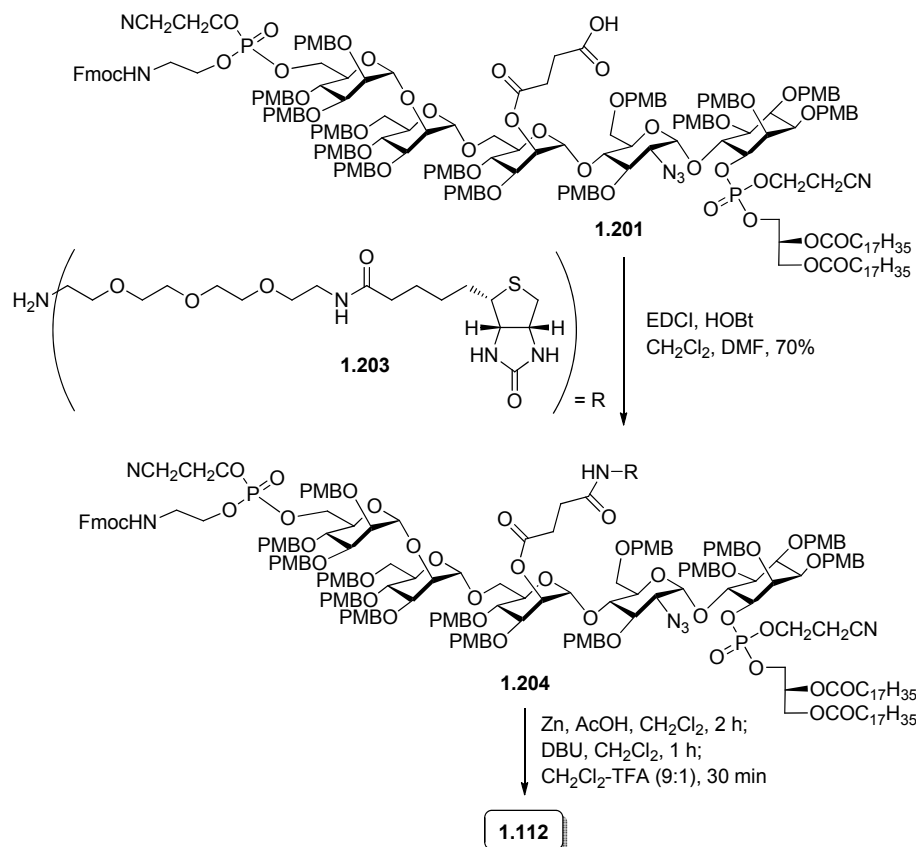
Scheme 1.41. Biotin functionalization and deprotection to afford biotinylated GPI

1.3 Conclusions

In this work, a new global protecting group strategy was developed to enable the synthesis of uniquely and usefully functionalized GPI anchors. By employing the acid-labile PMB group for permanent hydroxyl protection, a variety of functional groups that are incompatible with current protection strategies (benzyl, acetyl, benzoyl) could be incorporated into the target molecule, such as alkenes, alkynes, thiols and sulfides. To demonstrate the utility and feasibility of this methodology, four functionalized GPI anchors were synthesized, including GPIs bearing unsaturated lipid chains (**1.109** and **1.110**), an alkyne-containing 'clickable' GPI (**1.111**), and a biotinylated GPI (**1.112**).

These syntheses were highlighted by several features: (1) Employing a convergent assembly to increase efficiency and allow for easy customization of coupling partners; (2) Incorporation of several PMB-orthogonal protecting groups for late-stage selective functionalization; (3) Usage of the Schmidt glycosylation, which provided a relatively mild means for stereoselective glycosidic bond formation; (4) Development of a highly efficient three-step, one-pot global deprotection protocol that proceeded in 80-85% yield.

While the use of PMB protection greatly expands the accessibility of variously modified GPIs, the sensitivity of PMB groups to acid/oxidation complicated certain strategies and reactions. For example, I observed anydro sugar formation as a result of PMB cleavage in two key glycosylation reactions, which required redesign of the glycosyl donors. In addition, the choice of methods and reagents was limited in some cases, such as in the removal of the hindered glucosamine 4-O-TBS group, where more powerful desilylation reagents hydrolyzed PMB groups in the substrate. Furthermore, a number of strategic alterations were required to accommodate the use of PMB groups. For instance, the preparation of a suitable PMB-protected inositol derivative necessitated an overhaul of the synthetic route used in most GPI syntheses. However, despite some PMB-borne challenges and setbacks in this work, an efficient and robust strategy for the construction of functionalized GPIs was eventually developed. By demonstrating the practicality of global PMB protection in GPI synthesis, which is a difficult and complex task, this strategy should also be broadly applicable in the synthesis of other functionalized oligosaccharides.

1.4 Future Work

Future work for this project will initially involve revisiting the synthesis of the 'clickable' and biotinylated GPI anchors. I observed that upon prolonged PMB deprotection with TFA (overnight), the Man-I 2-*O*-ester bond of these molecules was slowly cleaved. Furthermore, the same decomposition reaction occurred when the GPIs were stored for extended periods (months) at -4 °C (Scheme 1.42). Because the phosphatidylinositol ester-linked lipid chains remained intact during these processes, it became clear that the Man-I 2-*O*-ester bond was particularly labile, and would clearly not be a suitable linker for GPIs to be used in biological studies.
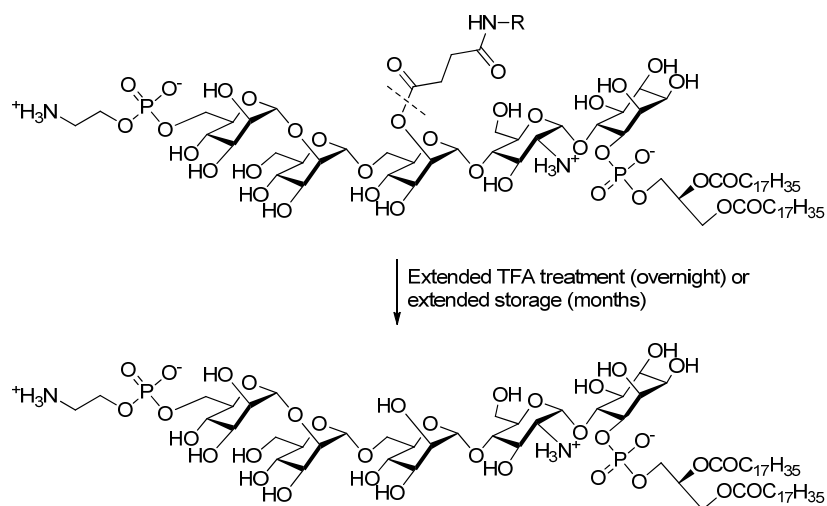
Scheme 1.42. Observed GPI decomposition

Instead, a new 'clickable' GPI anchor **1.205** containing a much more stable Man-I 2-*O*-ether linkage will be synthesized (Scheme 1.43). The pentynyl ether will be installed during monomer preparation. It will act as a protecting group for the Man-I 2-*O*-position and as a latent click functionality. In addition, this design should not only

provide a much more stable functionalized GPI but greatly improve the efficiency of the synthesis by removing three late-stage steps in the original synthesis (deallylation, succinylation, amidation). Conversion of **1.205** to biotinylated GPI anchor **1.206** using Cu-catalyzed [3+2] cycloaddition should be straightforward. This work will allow access to cell-stable functionalized GPI anchors, and I do not expect any problems to arise from this strategic modification.
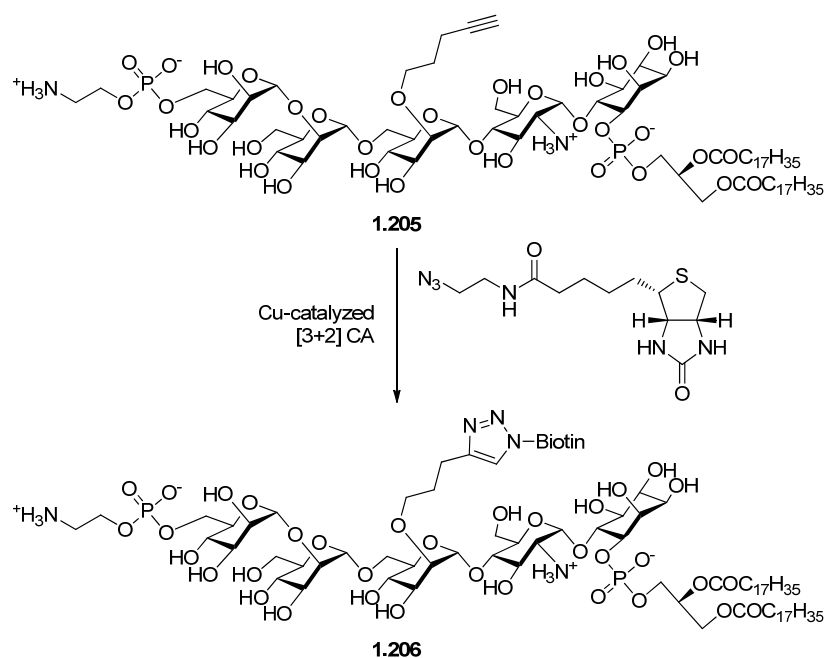
Scheme 1.43. Redesigned stable GPIs

As soon as a sufficient quantity of biofunctionalized GPIs **1.205** and **1.206** are prepared, their incorporation into various biological studies will be considered. The versatility of these two compounds, arising from the alkyne and biotin tags, should allow for their application to a broad range of studies. Although the details of such studies have not yet been established, several planned projects include:

1. Probing cell-surface GPIomics: By incubating GPI-deficient cell lines with the synthetic biotinylated GPI anchor **1.206**, the cell's intact GPI anchoring biosynthetic machinery will attach proteins/glycoproteins destined for GPI anchorage to the phosphoethanolamine unit of **1.206**. Isolation of the biotinylated GPI-anchored proteins with a streptavidin column and proteomic analysis of the resulting mixture will aid in profiling GPI-anchored molecules.

2. Visualization of GPIs on the cell surface: By 'clicking' a fluorescent label to **1.205** and other derivatives, GPI distribution on the cell surface may be determined, and structure-dependent localization of GPIs may also be studied.

3. GPI-based vaccine development: Carbohydrate-based vaccines are usually presented on carrier proteins such as BSA or KLH, a task that could be accomplished by conjugating GPI-alkynes such as **1.205** to azide-modified carrier proteins. Because GPIs are essential to various antigenic species, such as the human sperm and lymphocyte CD52 antigens, it would be interesting to identify GPI-containing epitopes for vaccine development.

These projects represent potential future applications of the biofunctionalized GPI anchors synthesized in this work, and I expect these compounds to be useful in designing other biological studies as well.

1.4 Experimental

General Methods

Materials were obtained from commercial sources without further purification unless otherwise noted. Anhydrous solvents were obtained either commercially or from an MBRAUN alumina column solvent purification system. Molecular sieves were flame-dried under hi-vacuum and used immediately after cooling. All reactions were carried out in oven-dried glassware under argon unless otherwise noted. Analytical TLC was performed on Whatman silica gel 60 Å plates (thickness 0.25 mm) and detected by UV lamp, charring with phosphomolybdic acid in EtOH, or charring with 5% H_2SO_4 in EtOH. Column chromatography was performed using Dynamic Adsorbents flash silica gel (32-63 μm). ^1H NMR spectra were recorded at 400 or 500 MHz with the chemical shifts reported in ppm (δ) relative to $CHCl_3$ (7.26 ppm), tetramethylsilane (0.00 ppm), or CH_3OH (3.30 ppm). ^{13}C NMR spectra were recorded at 100 or 125 MHz relative to the ^{13}C signal of $CDCl_3$ (77.23 ppm) or CD_3OD (49.3 ppm). ^{31}P NMR spectra were recorded at 160 MHz relative to the ^{31}P signal of phosphoric acid (0.00 ppm). Coupling constants (*J*) are reported in hertz (Hz). Mass spectrometry was performed using either a Bruker Daltonics Ultraflex MALDI TOF MS or Waters LCT Premier XE high resolution ESI MS. Optical rotation values were recorded using a Rudolph Research Analytical Autopol III automatic polarimeter. Microscale sample measurements were made using a Mettler Toledo AX205 DeltaRange balance (for max 81 g, d = 0.01 mg).

Preparation of Compounds

(±)-1,6-di-*O*-Allyl-*myo*-inositol (1.207)
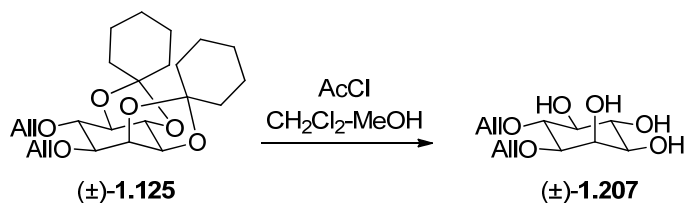
To a solution of (±)-**1.125** (9.00 g, 21.4 mmol) in anhydrous CH_2Cl_2/MeOH (2:1, 150 mL) stirring under an Ar atmosphere at rt was added acetyl chloride (1.0 mL) dropwise. After 3 h, the reaction was quenched with triethylamine and concentrated in vacuum. The crude material was purified by silica gel column chromatography to give (±)-**1.207** (5.55 g, 98%) as a white solid. NMR (500 MHz, CD_3OD): δ 5.94-5.84 (m, 2 H), 5.23 (dd, *J* = 2.0, 17.5 Hz, 1 H), 5.17 (dd, *J* = 1.5, 17 Hz, 1 H), 5.06 (dd, *J* = 1.0, 10.5 Hz, 1 H), 5.01 (dd, *J* = 1.5, 10.5 Hz, 1 H), 4.22 (ddd, *J* = 6.0, 12.5, 19.5 Hz, 2 H), 4.11 (dd, *J* = 5.5, 13 Hz, 1 H), 4.02-3.99 (m, 2 H), 3.53 (t, *J* = 9.5 Hz, 1 H), 3.47 (t, *J* = 9.5 Hz, 1 H), 3.22-3.19 (m, 1 H), 3.17 (dd, *J* = 3.0, 10 Hz, 1 H), 3.14 (t, *J* = 9.0 Hz, 1 H). ^{13}C NMR (CD_3OD, 125 MHz): δ 137.11, 136.53, 117.06, 116.54, 82.08, 81.17, 76.09, 75.27, 74.17, 73.13, 72.22, 71.11. HR ESI MS: calcd. for $C_{12}H_{20}O_6Na$ [M+Na]$^+$ *m/z*, 283.1158; found, 283.1152. To identify the desired enantiomer of compound **1.116**, an analogous route was developed starting with optically active inositol (+)-**1.7**, which was prepared using a known enzymatic resolution procedure.[108] Optical rotation for the correct enantiomer of **1.207** generated by authentication route: $[α]_D^{25}$ = -21° (*c* 1.0, CH_3OH).

(±)-1,6-di-*O*-Allyl-2,3,4,5-tetra-*O*-(*p*-methoxybenzyl)-*myo*-inositol (1.126)
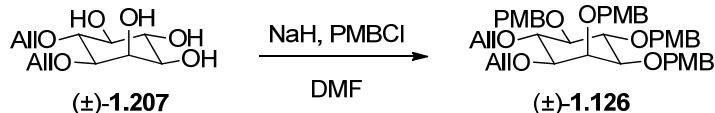
To a solution of (±)-**1.207** (5.30 g, 20.3 mmol) in anhydrous DMF (100 mL) stirring under Ar at 0 ºC was slowly added NaH (60% dispersion in mineral oil, 3.65 g, 91.4 mmol). After stirring for 30 min, *p*-methoxybenzyl chloride (10.3 mL, 98.3 mmol) was added dropwise. The reaction was stirred overnight at rt, then quenched with MeOH, diluted with EtOAc, and poured into water. The aqueous layer was extracted 3x with EtOAc, after which the combined organic layer was washed with brine, dried over Na_2SO_4, and concentrated in vacuum. The residue was purified by silica gel column chromatography to give (±)-**1.126** (11.0 g, 73%) as a syrup. ^1H NMR (500 MHz, $CDCl_3$): δ 7.35-7.25 (m, 8 H), 6.89-6.84 (m, 8 H), 6.04-5.97 (m, 1 H), 5.96-5.88 (m, 1 H), 5.31 (dd, *J* = 1.0, 17 Hz, 1 H), 5.29 (dd, *J* = 1.0, 17.5 Hz, 1 H), 5.19-5.15 (m, 2 H), 4.75-4.84 (m, 6 H), 4.60 (d, *J* = 11.5 Hz, 1 H), 4.55 (d, *J* = 11 Hz, 1 H), 4.39 (dd, *J* = 5.5, 12 Hz, 1 H), 4.31 (dd, *J* = 6.0, 12.5 Hz, 1 H), 4.13-4.05 (m, 2 H), 4.00-3.95 (m, 2 H), 3.86 (t, *J* = 9.0 Hz, 1 H), 3.83 (s, 3 H), 3.81 (s, 3 H), 3.80 (s, 6 H), 3.38 (t, *J* = 9.5 Hz, 1 H), 3.32 (dd, *J* = 2.0, 10 Hz, 1 H), 3.18 (dd, *J* = 1.5, 9.5 Hz, 1 H). ^{13}C NMR ($CDCl_3$, 125 MHz): δ 159.38, 159.34, 159.19, 135.83, 135.32, 131.50, 131.45, 131.41, 130.90, 129.91, 129.75, 129.63, 129.38, 116.72, 116.64, 113.99, 113.73, 83.71, 81.75, 81.63, 80.94, 80.89, 75.81, 75.69, 74.78, 74.19, 73.81, 72.64, 71.89, 55.51. HR ESI MS: calcd. for $C_{44}H_{52}O_{10}Na$ [M+Na]$^+$ *m/z*, 763.3458; found, 763.3448. Optical rotation for the correct enantiomer of **1.126** generated by authentication route: $[\alpha]_D^{25}$ = -9.0º (*c* 1.0, $CHCl_3$).

(±)-2,3,4,5-tetra-O-(p-Methoxybenzyl)-myo-inositol (1.127)
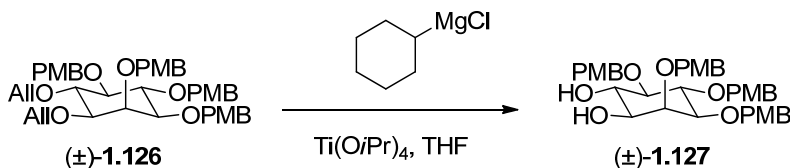
To a solution of (±)-**1.126** (10.5 g, 14.2 mmol) and titanium(IV) isopropoxide (9.20 mL, 31.2 mmol) in THF (100 mL) was slowly added cyclohexylmagnesium chloride (2.0 M solution in THF, 85 mL) via a dropping funnel under an Ar atmosphere at rt. After 2 h, the reaction was poured into 0.5 N HCl and the aqueous layer was extracted 3x with Et_2O. The combined organic layer was washed with brine, dried over Na_2SO_4, and concentrated in vacuum. The resulting residue was purified by silica gel column chromatography to obtain (±)-**1.127** (7.9 g, 85%) as a syrup. ^{1}H NMR (500 MHz, $CDCl_3$): δ 7.30-7.26 (m, 8 H), 6.89-6.85 (m, 8 H), 4.98 (d, J = 11.0 Hz, 1 H), 4.88 (d, J = 11.0 Hz, 1 H), 4.87 (d, J = 10.5 Hz, 1 H), 4.77 (d, J = 10 Hz, 1 H), 4.69 (d, J = 11 Hz, 1 H), 4.68 (d, J = 11.5 Hz, 1 H), 4.63 (d, J = 11.5 Hz, 1 H), 4.59 (d, J = 11.5 Hz, 1 H), 3.99-3.95 (m, 2 H), 3.83 (s, 3 H), 3.82 (s, 6 H), 3.81 (s, 3 H), 3.77 (t, J = 9.5 Hz, 1 H), 3.44 (dd, J = 2.0, 9.5 Hz, 1 H), 3.37-3.33 (m, 1 H), 3.28 (t, J = 9.0 Hz, 1 H). ^{13}C NMR ($CDCl_3$, 125 MHz): δ 159.48, 131.12, 129.94, 129.75, 129.67, 129.52, 114.18, 114.10, 114.05, 114.01, 82.94, 81.44, 81.37, 77.14, 75.65, 75.22, 74.71, 74.12, 73.08, 72.33, 55.52. HR ESI MS: calcd. for $C_{38}H_{44}O_{10}Na$ [M+Na]$^+$ m/z, 683.2832; found, 683.2834. Optical rotation for the correct enantiomer of **1.127** generated by authentication route: $[\alpha]_D^{25}$ = +7.0° (c 1.0, $CHCl_3$).

(±)-1-*O*-Allyl-2,3,4,5-tetra-*O*-(*p*-methoxybenzyl)-*myo*-inositol (1.128)
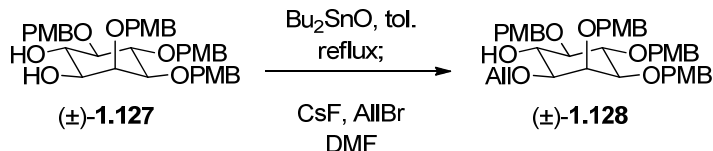
A mixture of (±)-**1.127** (7.00 g, 10.6 mmol) and dibutyltin oxide (2.90, 11.7 mmol) in anhydrous toluene (150 mL) was refluxed with azeotropic removal of water using a Dean-Stark apparatus for 2 h. After concentration in vacuum, the residue was dissolved in anhydrous DMF (100 mL) and cooled to 0 °C, after which cesium fluoride (8.2 g, 54 mmol) and allyl bromide (4.6 mL, 54 mmol) were added to the solution. After stirring overnight under an Ar atmosphere at rt, the reaction mixture was diluted with EtOAc, washed with brine, dried over Na_2SO_4, and concentrated in vacuum. After passing the crude products through a silica gel plug, the two regioisomers were separated by preparative HPLC (Waters Nova-Pak Silica 6 μm, 300 x 19 mm, eluent 33% EtOAc in hexanes, 10 mL/min, t_R = 13.4 min) to give the desired product (±)-**1.128** (5.39 g, 72%) as a white solid. ^{1}H NMR (500 MHz, CDCl$_3$): δ 7.33-7.25 (m, 8 H), 6.90-6.85 (m, 8 H), 5.94-5.86 (m, 1 H), 5.28 (dd, *J* = 1.5, 17 Hz, 1 H), 5.20 (dd, *J* = 1.0, 10 Hz, 1 H), 4.85 (d, *J* = 10.5 Hz, 1 H), 4.84 (d, *J* = 11 Hz, 1 H), 4.80-4.73 (m, 4 H), 4.63 (d, *J* = 11 Hz, 1 H), 4.57 (d, *J* = 11 Hz, 1 H), 4.10-3.97 (m, 5 H), 3.83 (s, 3 H), 3.81 (s, 6 H), 3.81 (s, 1 H), 3.35 (dd, *J* = 2.5, 9.5 Hz, 1 H), 3.34 (t, *J* = 9.0 Hz, 1 H), 3.09 (dd, *J* = 2.0, 10.0 Hz, 1 H). ^{13}C NMR (CDCl$_3$, 125 MHz): δ 159.43, 159.37, 159.26, 134.84, 131.38, 131.24, 130.81, 129.94, 129.70, 129.64, 129.41, 117.50, 114.08, 114.02, 113.98, 113.79, 83.44, 81.43, 81.19, 80.08, 75.68, 75.19, 73.82, 73.17, 72.94, 72.77, 71.32, 55.52. HR ESI MS: calcd. for $C_{41}H_{48}O_{10}Na$ [M+Na]$^+$ *m/z*, 723.3145; found, 723.3110. Optical rotation for the

correct enantiomer of **1.128** generated by authentication route: $[\alpha]_D^{25}$ = -8.5° (*c* 1.0, CHCl$_3$).

(-)-1-*O*-Allyl-6-*O*-[(1*S*)-camphanoyl]-2,3,4,5-tetra-*O*-(*p*-methoxybenzyl)-*myo*-inositol (1.129)
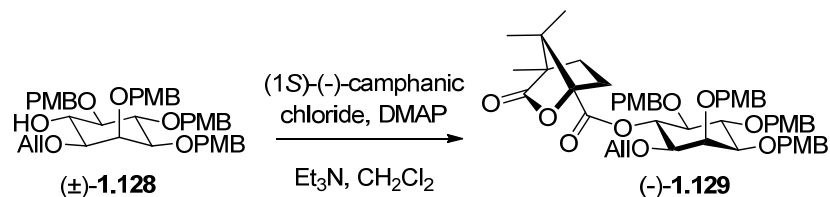
To a solution of (±)-**1.128** (5.10 g, 7.27 mmol), triethylamine (2.0 mL, 15 mmol), and 4-(dimethylamino)pyridine (300 mg) in anhydrous CH$_2$Cl$_2$ (100 mL) under an Ar atmosphere at 0 °C was added (1*S*)-(-)-camphanic chloride (freshly prepared 1.0 M solution in anhydrous CH$_2$Cl$_2$, 12.9 mL) dropwise. After stirring for 1 h, the reaction was poured into water and extracted 3x with CH$_2$Cl$_2$, after which the combined organic layer was washed with saturated aqueous NaHCO$_3$, brine, dried over Na$_2$SO$_4$, and concentrated in vacuum. The residue was then subjected to silica gel column chromatography, which gave a 1:1 mixture of diastereomers. Preparative HPLC (Waters Nova-Pak Silica 6 μm, 300 x 19 mm, eluent 25% EtOAc in hexanes, 10 mL/min, t_R = 21.4 min) was used to separate the diastereomers, affording optically pure **1.129** (2.97 g, 46%) as a white solid. ^{1}H NMR (500 MHz, CDCl$_3$): δ 7.35-7.32 (m, 2 H), 7.27-7.25 (m, 2 H), 7.21-7.18 (m, 4 H), 6.89-6.81 (m, 8 H), 5.83-5.76 (m, 1 H), 5.71 (t, *J* = 10 Hz, 1 H, 6-*O*-position shifted downfield after acylation, confirming regiochemistry of previous step), 5.24 (dd, *J* = 1.5, 17 Hz, 1 H), 5.15 (dd, *J* = 1.5, 10.5 Hz, 1 H), 4.76 (m, 4 H), 4.70 (d, *J* = 10 Hz, 1 H), 4.62 (d, *J* = 10.5 Hz, 1 H), 4.61 (d, *J* = 11 Hz, 1 H), 4.54 (d, *J* = 11.5 Hz, 1 H), 4.09 (t, *J* = 10 Hz, 1 H), 4.03 (t, *J* = 1.5 Hz, 1 H), 3.97 (dd, *J* = 5.0, 12.5 Hz, 1

H), 3.86-3.83 (m, 4 H), 3.81 (s, 3 H), 3.80 (s, 3 H), 3.79 (s, 3 H), 3.52 (t, J = 9.5 Hz, 1 H),

3.34 (dd, J = 2.5, 9.5 Hz, 1 H), 3.29 (dd, J = 2.0, 10.0 Hz, 1 H), 2.36 (ddd, J = 1.0, 4.0,

10 Hz, 1 H), 1.78-1.91 (m, 2 H), 1.59-1.64 (m, 1 H), 1.10 (s, 3 H), 1.06 (s, 3 H), 0.96 (s,

3 H). ^{13}C NMR (CDCl$_3$, 125 MHz): δ 178.94, 166.94, 159.46, 159.38, 159.29, 159.21,

134.35, 131.19, 131.01, 130.92, 130.65, 129.92, 129.75, 129.45, 129.04, 117.30,

114.02, 113.96, 113.87, 113.81, 91.53, 81.35, 81.24, 80.65, 78.01, 75.68, 75.06, 74.74,

73.74, 72.82, 72.37, 70.82, 55.54, 55.51, 55.14, 54.55, 31.12, 29.18, 16.85, 9.93. $[α]_D^{25}$

= -11° (c 1.0, CHCl$_3$). HR ESI MS: calcd. for C$_{51}$H$_{60}$O$_{13}$Na [M+Na]$^+$ m/z, 903.3932; found,

903.3889.

(-)-1-O-Allyl-2,3,4,5-tetra-O-(p-methoxybenzyl)-myo-inositol (1.116)
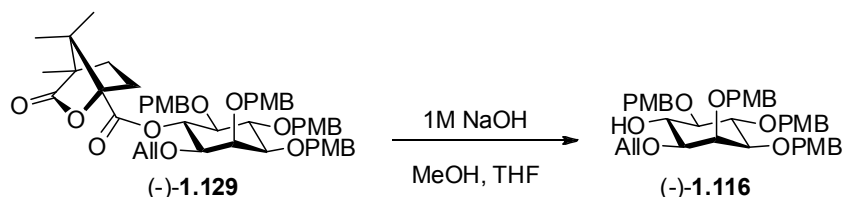
To a solution of (-)-**1.129** (400 mg, 0.45 mmol) in anhydrous THF (4 mL) was added a

2.0 M solution of NaOH in MeOH (4 mL) at rt. After stirring at rt for 3 h, the reaction was

neutralized with AcOH. After concentration, the residue was dissolved in EtOAc, and the

resulting organic layer was washed with brine 3x, dried over Na$_2$SO$_4$, and concentrated

in vacuum. The residue was purified by silica gel column chromatography to give

optically pure (-)-**9** (302 mg, 95%) as a white solid. The product was confirmed as the

correct enantiomer by comparison of optical rotation with a standard compound, which

was prepared from optically active (+)-**1.7**[108] using an identical route. (-)-**1.116**: $[α]_D^{25}$ = -

7.5º (*c* 1.0, CHCl₃), authentic standard: $[\alpha]_D^{25}$ = -8.5º (*c* 1.0, CHCl₃). All spectroscopic data for (-)-**1.116** are identical to those obtained for (±)-**1.128**.

Allyl 3,4,6-tri-*O*-acetyl-2-azido-2-deoxy-D-glucopyranoside (1.131)
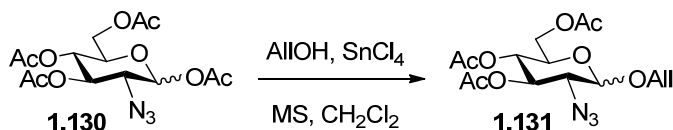
To a mixture of **1.130**[117] (3.80 g, 10.2 mmol), allyl alcohol (2.0 mL, 29 mmol), and MS 4 Å (1.0 g) in anhydrous CH_2Cl_2 stirring under Ar at 0 ºC was slowly added $SnCl_4$ (1.0 M solution in dry CH_2Cl_2, 30.0 mL). After the reaction stirred overnight at rt, additional $SnCl_4$ (1.0 M solution in dry CH_2Cl_2, 30.0 mL) was added and stirring continued for another 48 h (total ~72 h). After filtration through celite to remove MS, the reaction was quenched by pouring into cold, saturated aqueous $NaHCO_3$, which was extracted 3x with CH_2Cl_2. The combined organic layer was then washed with saturated aqueous $NaHCO_3$ and brine, dried over Na_2SO_4, and concentrated in vacuum. The residue was purified by silica gel column chromatography to give α,β-mixture **1.131** (3.0 g, 81%) as a syrup. NMR data is consistent with those reported in the literature[144] (¹H NMR and HR ESI MS spectra are included in the supplemental information). HR ESI MS: calcd. for $C_{15}H_{21}N_3O_8Na$ [M+Na]⁺ *m/z*, 394.1226; found, 394.1231.

Allyl 2-azido-2-deoxy-4,6-*O*-(*p*-methoxybenzylidene)-D-glucopyranoside (1.132)
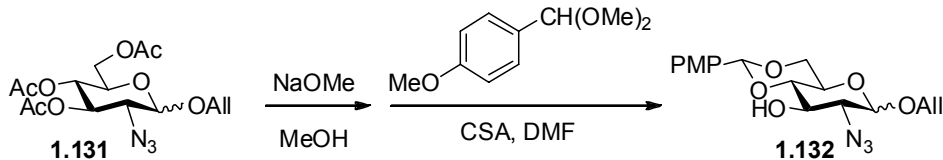
After a solution of **1.131** (2.6 g, 7.0 mmol) in 33 mL of 0.05 M NaOMe in methanol was stirred at rt for 30 min, it was neutralized to pH 6-7 using Amberlyst H$^+$ resin. The solution was filtered off and concentrated to afford a white powder (1.75 g), which was directly used for the next step. After the crude triol was dissolved in anhydrous DMF (40 mL), *p*-anisaldehyde dimethyl acetal (1.6 mL, 9.1 mmol) and camphor sulfonic acid (160 mg, 0.70 mmol) were added. The reaction was stirred for 12 h under an Ar atmosphere at rt while periodically removing MeOH under reduced pressure. After dilution with EtOAc, the organic layer was washed with saturated aqueous NaHCO$_3$ and brine, dried over Na$_2$SO$_4$, and concentrated in vacuum. The residue was purified by silica gel column chromatography to obtain α,β-mixture **1.132** (1.94 g, 77%, 2 steps) as a syrup. ^{1}H NMR (500 MHz, CDCl$_3$) of β anomer: δ 7.42-7.40 (m, 2 H), 6.92-6.89 (m, 2 H), 6.00-5.93 (m, 1 H), 5.50 (s, 1 H), 5.37 (dd, *J* = 1.5, 17 Hz, 1 H), 5.27 (dd, *J* = 1.0, 10 Hz, 1 H), 4.46 (d, *J* = 8.0 Hz, 1 H, 1-position), 4.41 (dd, *J* = 5.0, 12.5 Hz, 1 H), 4.32 (dd, *J* = 5.5, 11 Hz, 1 H), 4.18 (dd, *J* = 6.0, 12.5 Hz, 1 H), 3.81 (s, 3 H), 3.77 (t, *J* = 10 Hz, 1 H), 3.64 (dt, *J* = 2.0, 9.5 Hz, 1 H), 3.53 (t, *J* = 9.5 Hz, 1 H), 3.43 (dd, *J* = 8.0, 9.5 Hz, 1 H), 3.41-3.36 (m, 1 H), 2.82 (d, *J* = 2.0 Hz, 1 H). ^{13}C NMR (CDCl$_3$, 125 MHz) of β anomer: δ 160.56, 133.34, 129.48, 127.83, 118.49, 113.98, 102.15, 101.66, 80.80, 72.24, 70.98, 68.70, 66.62, 66.39, 55.55. [α]$_D^{25}$ of β anomer = -53° (*c* 1.0, CHCl$_3$). HR ESI MS: calcd. for C$_{17}$H$_{22}$N$_3$O$_6$ [M+H]$^+$ *m/z*, 364.1509; found, 364.1511.

Allyl 2-azido-2-deoxy-3-*O*-(*p*-methoxybenzyl)-4,6-*O*-(*p*-methoxybenzylidene)-D-glucopyranoside (1.133)

To a solution of **1.132** (1.70 g, 4.67 mmol) in anhydrous DMF (40 mL) stirring under Ar at 0 °C was slowly added NaH (60% dispersion in mineral oil, 0.92 g, 5.9 mmol). After stirring for 30 min, *p*-methoxybenzyl chloride (0.62 mL, 5.9 mmol) was added dropwise. The reaction was stirred overnight at rt, then quenched with MeOH, diluted with EtOAc, and poured into water. The aqueous layer was extracted 3x with EtOAc, after which the combined organic layer was washed with brine, dried over Na_2SO_4, and concentrated in vacuum. The residue was purified by silica gel column chromatography to give α,β-mixture **1.133** (2.20 g, 97%) as a syrup. ^{1}H NMR (500 MHz, CDCl$_3$) of β anomer: δ 7.43-7.41 (m, 2 H), 7.32-7.30 (m, 2 H), 6.94-6.87 (m, 4 H), 6.00-5.92 (m, 1 H), 5.55 (s, 1 H), 5.37 (dd, *J* = 1.5, 17.5 Hz, 1 H), 5.26 (dd, *J* = 1.5, 10.5 Hz, 1 H), 5.34 (d, *J* = 11 Hz, 1 H), 4.74 (d, *J* = 11 Hz, 1 H), 4.40 (d, *J* = 8.0 Hz, 1 H, 1-position), 4.39-4.37 (m, 1 H), 4.33 (d, *J* = 4.5, 10.5 Hz, 1 H), 4.17 (dd, *J* = 6.0, 12.5 Hz, 1 H), 3.84 (s, 3 H), 3.81 (s, 3 H), 3.79 (t, *J* = 10 Hz, 1 H), 3.69 (t, *J* = 9.5 Hz, 1 H), 3.46 (dd, *J* = 8.0, 9.5 Hz, 1 H), 3.40-3.35 (m, 1 H). ^{13}C NMR (CDCl$_3$, 125 MHz) of β anomer: δ 160.34, 159.64, 133.48, 130.18, 129.88, 127.56, 118.39, 114.03, 113.88, 101.63, 101.54, 81.77, 78.86, 74.80, 70.92, 68.77, 66.47, 66.34, 55.55, 55.51. $[\alpha]_D^{25}$ of α anomer = +12° (*c* 1.0, CHCl$_3$). HR ESI MS: calcd. for $C_{25}H_{30}N_3O_7$ [M+H]$^+$ *m/z*, 484.2084; found, 484.2097.

Allyl 2-azido-2-deoxy-3,6-di-*O*-(*p*-methoxybenzyl)-D-glucopyranoside (1.134)
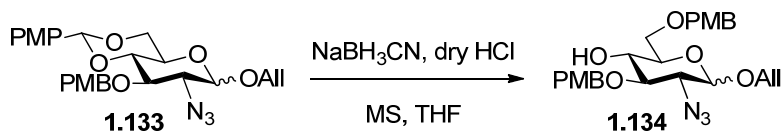
To a mixture of **1.133** (630 mg, 1.3 mmol), NaBH$_3$CN (818 mg, 13 mmol), and MS 4 Å (100 mg) in anhydrous THF (10 mL) stirring under Ar at 0 °C was added dry hydrogen chloride (1.0 M solution in Et$_2$O) dropwise until a pH of ~1 was reached. After 1 h, the reaction was filtered through celite to remove MS. The filtrate was then diluted with EtOAc and washed with saturated aqueous NaHCO$_3$ and brine, dried over Na$_2$SO$_4$, and concentrated in vacuum. The residue was purified by silica gel column chromatography to give α,β-mixture **1.134** (448 mg, 71%) as a syrup. ^{1}H NMR (500 MHz, CDCl$_3$) of β anomer: δ 7.27-7.25 (m, 2 H), 7.34-7.32 (m, 2 H), 6.92-6.88 (m, 4 H), 5.99-5.91 (m, 1 H), 5.35 (dd, *J* = 1.5, 17 Hz, 1 H), 5.23 (dd, *J* = 1.5, 10.5 Hz, 1 H), 4.85 (d, *J* = 11 Hz, 1 H), 4.72 (d, *J* = 11 Hz, 1 H), 4.54 (d, *J* = 11.5 Hz, 1 H), 4.49 (d, *J* = 11.5 Hz, 1 H), 4.39 (dd, *J* = 5.5, 13 Hz, 1 H), 4.33 (d, *J* = 8.0 Hz, 1 H, 1-position), 4.14 (dd, *J* = 6.5, 13 Hz, 1 H), 3.82 (s, 6 H), 3.70 (d, *J* = 5.0 Hz, 2 H), 3.61 (t, *J* = 9.0 Hz, 1 H), 3.42-3.37 (m, 2 H), 3.25 (t, *J* = 9.0 Hz, 1 H), 2.64 (s, broad, 1 H). ^{13}C NMR (CDCl$_3$, 125 MHz) of β anomer: δ 159.72, 159.61, 133.69, 130.44, 130.08, 129.95, 129.67, 118.03, 114.25, 114.11, 101.23, 82.39, 74.97, 74.05, 73.62, 72.47, 70.56, 70.22, 65.91, 55.52. [α]$_D^{25}$ of β anomer = -35° (*c* 1.0, CHCl$_3$). HR ESI MS: calcd. for C$_{25}$H$_{31}$N$_3$O$_7$Na [M+Na]$^+$ *m/z*, 508.2060; found, 508.2065.

Allyl 2-azido-4-*O*-(*tert*-butyldimethylsilyl)-2-deoxy-3,6-di-*O*-(*p*-methoxybenzyl)-D-glucopyranoside (1.135)
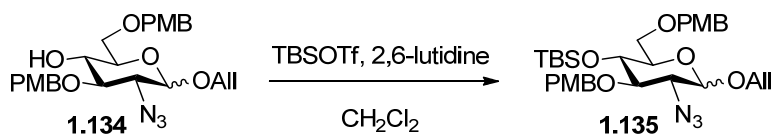
TBSOTf (0.53 mL, 2.3 mmol) was added dropwise to a solution of **1.134** (900 mg, 1.8 mmol) and 2,6-lutidine (0.30 mL, 2.6 mmol) in anhydrous CH_2Cl_2 (20 mL) stirring under Ar at 0 °C. After 2 h, the reaction was diluted with CH_2Cl_2, washed with saturated aqueous $NaHCO_3$ and brine, dried over Na_2SO_4, and concentrated in vacuum. The residue was purified by silica gel column chromatography to afford α,β-mixture **1.135** (920 mg, 85%) as a syrup. ^1H NMR (500 MHz, $CDCl_3$) of β anomer: δ 7.31-7.26 (m, 4 H), 6.90-6.87 (m, 4 H), 6.01-5.94 (m, 1 H), 5.36 (dd, *J* = 2.0, 17.5 Hz, 1 H), 5.24 (dd, *J* = 1.5, 10 Hz, 1 H), 4.83 (d, *J* = 10.5 Hz, 1 H), 4.65 (d, *J* = 10.5 Hz, 1 H), 4.60 (d, *J* = 12 Hz, 1 H), 4.46-4.41 (m, 2 H), 4.37 (d, *J* = 8.5 Hz, 1 H, 1-position), 4.17 (dd, *J* = 6.0, 13 Hz, 1 H), 3.82 (s, 3 H), 3.81 (s, 3 H), 3.73 (dd, *J* = 2.0, 11.0 Hz, 1 H), 3.56-3.51 (m, 2 H), 3.43-3.36 (m, 2 H), 3.20 (dd, *J* = 8.5, 9.5 Hz, 1 H), 0.86 (s, 9 H), 0.04 (s, 3 H), 0.00 (s, 3 H). ^{13}C NMR ($CDCl_3$, 125 MHz) of β anomer: δ 159.41, 159.32, 133.86, 130.61, 130.57, 129.45, 129.40, 117.84, 114.01, 113.93, 101.28, 83.25, 76.73, 74.97, 73.28, 71.28, 70.48, 69.18, 67.00, 55.53, 55.50, 26.17, 18.22, -3.42, -4.49. $[\alpha]_D^{25}$ of β anomer = +18° (*c* 1.0, $CHCl_3$). HR ESI MS: calcd. for $C_{31}H_{45}N_3O_7NaSi$ $[M+Na]^+$ *m/z*, 622.2924; found, 622.2927.

2-Azido-4-*O*-(*tert*-butyldimethylsilyl)-2-deoxy-3,6-di-*O*-(*p*-methoxybenzyl)-D-glucopyranose (1.136)
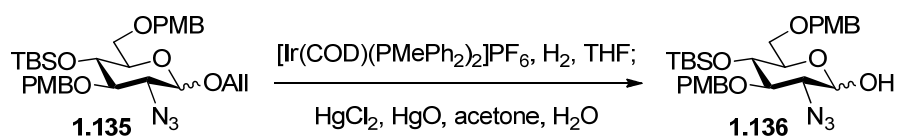
A solution of [Ir(COD)(PMePh$_2$)$_2$]PF$_6$ (72 mg, 80 µmol) in anhydrous THF (5 mL) was stirred under H$_2$ at rt until the color turned from red to colorless to pale yellow (15 min). After the H$_2$ atmosphere was exchanged with Ar, **1.135** (410 mg, 0.68 mmol, solution in 5 mL THF) was added slowly. TLC showed that isomerization was complete after stirring at rt for 1 h. The reaction was concentrated in vacuum, then dissolved in acetone/H$_2$O (9:1, 10 mL) and treated with HgCl$_2$ (950 mg, 3.5 mmol) and HgO (17 mg, 80 µmol). The mixture was stirred at rt under an Ar atmosphere for 15 min, then concentrated and purified by silica gel column chromatography to give hemiacetal **1.136** (323 mg, 85%) as a syrup. ^{1}H NMR (500 MHz, CDCl$_3$, all signals): δ 7.32-7.26 (m, 8 H), 6.90-6.87 (m, 8 H), 5.36 (d, *J* = 3.5 Hz, 1 H, 1-position of α-anomer), 4.81 (d, *J* = 10.5 Hz, 1 H), 4.79 (d, *J* = 10.5 Hz, 1 H), 4.66-4.58 (m, 4 H, includes 1-position of β-anomer), 4.42 (d, *J* = 12 Hz, 2 H), 4.07-4.04 (m, 1 H), 3.81 (s, 12 H), 3.77 (dd, *J* = 9.0, 10.5 Hz, 1 H), 3.68-3.64 (m, 2 H), 3.53 (t, *J* = 8.5 Hz, 1 H), 3.50-3.42 (m, 5 H), 3.35-3.30 (m, 2 H), 3.18 (dd, *J* = 8.0, 10 Hz, 1 H), 0.85 (s, 9 H), 0.82 (s, 9 H), -0.02 (s, 6 H), -0.03 (s, 3 H), -0.05 (s, 3 H). ^{13}C NMR (CDCl$_3$, 125 MHz), all signals: δ 159.62, 159.58, 159.31, 159.29, 130.51, 130.02, 129.91, 129.85, 129.78, 129.46, 129.34, 114.11, 114.07, 113.94, 113.90, 96.52, 92.28, 83.02, 80.13, 76.38, 75.10, 75.04, 73.34, 73.23, 72.08, 71.93, 71.42, 69.18, 69.12, 68.06, 64.68, 55.53, 55.50, 26.12, 26.09, 18.18, 18.15, -3.39, -3.44,

-4.43, -4.50. HR ESI MS: calcd. for $C_{28}H_{41}N_3O_7NaSi$ [M+Na]$^+$ *m/z*, 582.2611; found, 582.2604.

6-*O*-[2-Azido-4-*O*-(*tert*-butyldimethylsilyl)-2-deoxy-3,6-di-*O*-(*p*-methoxybenzyl)-α-D-glucopyranosyl]-1-*O*-allyl-2,3,4,5-tetra-*O*-(*p*-methoxybenzyl)-*myo*-inositol (1.138)
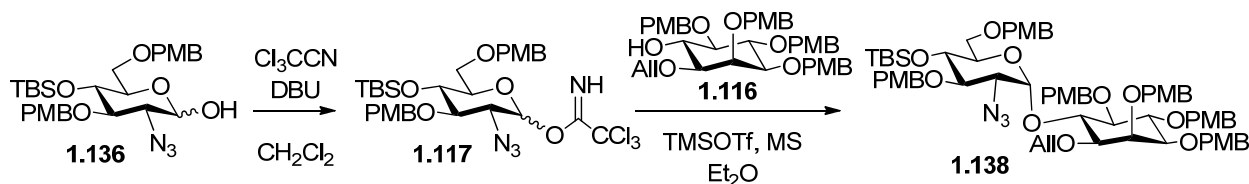
DBU (1 drop) was added to a solution of hemiacetal **1.136** (320 mg, 0.57 mmol) and trichloroacetonitrile (0.5 mL) in anhydrous CH_2Cl_2 (5 mL) stirring under an Ar atmosphere at 0 ºC. After 1 h, the reaction mixture was concentrated in vacuum and purified with a triethylamine-neutralized silica gel column to give **1.117** (335 mg, 83%). A mixture of the resulting trichloroacetimidate **1.117** (310 mg, 0.44 mmol), acceptor **1.116** (180 mg, 0.26 mmol), and MS 4 Å (100 mg) in anhydrous CH_2Cl_2 (5 mL) was stirred under an Ar atmosphere at rt for 1 h. After cooling to -10 ºC, TMSOTf (10 µl, 44 µmol) was added and the reaction was stirred for 10 min. Neutralization with triethylamine was followed by filtration through celite to remove MS, concentration in vacuum, and purification by silica gel column chromatography to give an α,β-mixture of the pseudodisaccharide as a syrup. Preparative HPLC (Waters Nova-Pak Silica 6 µm, 300 x 19 mm, eluent 20% EtOAc in hexanes, 10 mL/min, α-t_R = 16.1 min, β-t_R = 17.8 min) showed an α/β ratio of 1.2:1, and purification using this method afforded pure **1.138** (143 mg, 44%) as a white solid. Alternatively, the α,β-mixture can be taken directly to the next step and purified thereafter using silica gel column chromatography. ^{1}H NMR (500 MHz, CDCl$_3$): δ 7.38-7.22 (m, 10 H), 7.12-7.10 (m, 2 H), 6.92-6.83 (m, 10

H), 6.83-6.77 (m, 2 H), 6.00-5.92 (m, 1 H), 5.78 (d, J = 3.5 Hz, 1 H, 1-position), 5.30 (dd, J = 2.0, 17.5 Hz, 1 H), 5.20 (d, J = 1.5, 10.5 Hz, 1 H), 4.94 (d, J = 11.5 Hz, 1 H), 4.86 (d, J = 10 Hz, 1 H), 4.85 (d, J = 10.5 Hz, 1 H), 4.80-4.78 (m, 3 H), 4.74 (d, J = 10.5 Hz, 1 H), 4.67 (d, J = 10 Hz, 1 H), 4.62 (d, J = 11.5 Hz, 1 H), 4.57 (d, J = 11.5 Hz, 1 H), 4.43 (d, J = 11.5 Hz, 1 H), 4.35 (d, J = 11.5 Hz, 1 H), 4.28 (t, J = 9.5 Hz, 1 H), 4.09 (t, J = 9.5 Hz, 1 H), 4.03-3.99 (m, 4 H), 3.84 (s, 3 H), 3.83 (s, 3 H), 3.82 (s, 3 H), 3.81 (s, 3 H), 3.80 (s, 3 H), 3.79 (s, 3 H), 3.78 (t, J = 9.0 Hz, 1 H), 3.73 (t, J = 10.0 Hz, 1 H), 3.40 (t, J = 9.5 Hz, 1 H), 3.39-3.35 (m, 3 H), 3.33 (dd, J = 2.0, 11 Hz, 1 H), 3.22 (dd, J = 4.0, 10.5 Hz, 1 H), 0.80 (s, 9 H), 0.01 (s, 3 H), -0.03 (s, 3 H). ^{13}C NMR (CDCl$_3$, 125 MHz): δ 159.46, 159.33, 159.31, 159.19, 158.97, 134.64, 131.24, 131.20, 130.86, 130.81, 130.75, 129.90, 129.72, 129.46, 129.39, 129.15, 128.57, 117.11, 114.04, 113.92, 113.87, 113.81, 97.99, 82.22, 82.03, 81.31, 80.93, 80.39, 75.67, 75.63, 74.84, 74.29, 73.90, 73.07, 72.68, 72.59, 71.67, 70.97, 68.27, 64.22, 55.55, 55.54, 55.52, 26.33, 18.29, -3.49, -4.61. $[\alpha]_D^{25}$ = +51° (c 1.0, CHCl$_3$). HR ESI MS: calcd. for C$_{69}$H$_{87}$N$_3$O$_{16}$NaSi [M+Na]$^+$ m/z, 1264.5753; found, 1264.5693.

6-O-[2-Azido-4-O-($tert$-butyldimethylsilyl)-2-deoxy-3,6-di-O-(p-methoxybenzyl)-α-D-glucopyranosyl]-2,3,4,5-tetra-O-(p-methoxybenzyl)-myo-inositol (1.114)
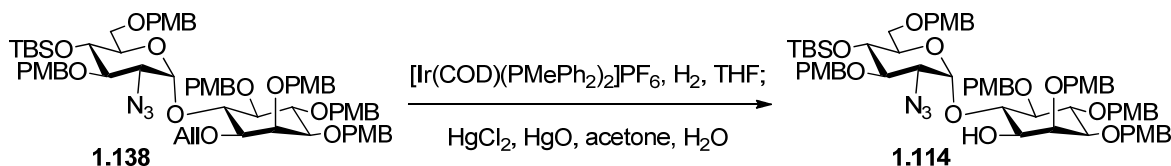
A solution of [Ir(COD)(PMePh$_2$)$_2$]PF$_6$ (6 mg, 7 µmol) in anhydrous THF (2.5 mL) was stirred under H$_2$ at rt until the color turned from red to colorless to pale yellow (10 min). After the H$_2$ atmosphere was exchanged with Ar, **1.138** (88 mg, 70 µmol, solution in 2.5

mL THF) was added slowly. TLC showed that isomerization was complete after stirring at rt for 1 h. The reaction was concentrated in vacuum, then dissolved in acetone/H_2O (9:1, 5 mL) and treated with $HgCl_2$ (95 mg, 0.35 mmol) and HgO (2 mg, 7 μmol). The mixture was stirred at rt under an Ar atmosphere for 5 min, then concentrated and purified by silica gel column chromatography to give pseudodisaccharide **1.114** (81 mg, 96%) as a syrup. ^{1}H NMR (500 MHz, $CDCl_3$): δ 7.33-7.28 (m, 8 H), 7.19-7.17 (m, 4 H), 6.90-6.80 (m, 12 H), 5.53 (d, J = 4.0 Hz, 1 H, 1-position), 4.96 (d, J = 11 Hz, 1 H), 4.91 (d, J = 10.5 Hz, 1 H), 4.87 (d, J = 10 Hz, 1 H), 4.80 (d, J = 11 Hz, 1 H), 4.76-4.62 (m, 6 H), 4.30 (s, 2 H), 4.04 (t, J = 9.5 Hz, 1 H), 3.97 (t, J = 9.0 Hz, 1 H), 3.97-3.95 (m, 1 H), 3.92-3.89 (m, 1 H), 3.83 (s, 3 H), 3.82 (s, 3 H), 3.81 (s, 6 H), 3.80 (s, 6 H), 3.77 (t, J = 8.5 Hz, 1 H), 3.72 (t, J = 9 Hz, 1 H), 3.63-3.60 (m, 1 H), 3.46-3.41 (m, 3 H), 3.38 (t, J = 9.5 Hz, 1 H), 3.27 (dd, J = 2.0, 10.5 Hz, 1 H), 3.17 (d, J = 7.0 Hz, 1 H), 0.85 (s, 9 H), 0.02 (s, 3 H), 0.00 (s, 3 H). ^{13}C NMR ($CDCl_3$, 125 MHz): δ 159.52, 159.36, 159.34, 159.20, 159.14, 131.21, 131.15, 130.93, 130.58, 130.52, 130.37, 129.95, 129.84, 129.61, 129.10, 129.04, 114.10, 113.97, 113.94, 113.91, 113.87, 98.15, 81.84, 81.36, 80.90, 80.83, 80.29, 77.12, 75.62, 74.99, 74.79, 74.60, 73.52, 73.02, 72.91, 72.51, 70.91, 68.14, 64.98, 55.53, 55.49, 26.28, 18.24, -3.44, -4.60. $[\alpha]_D^{25}$ = +10º (c 1.0, $CHCl_3$). HR ESI MS: calcd. for $C_{66}H_{83}N_3O_{16}NaSi$ [M+Na]$^+$ m/z, 1224.5440; found, 1224.5420.

Phenyl 2-*O*-allyl-3-*O*-(*p*-methoxybenzyl)-4,6-*O*-(*p*-methoxybenzylidene)-1-thio-α-D-mannopyranoside (1.161)
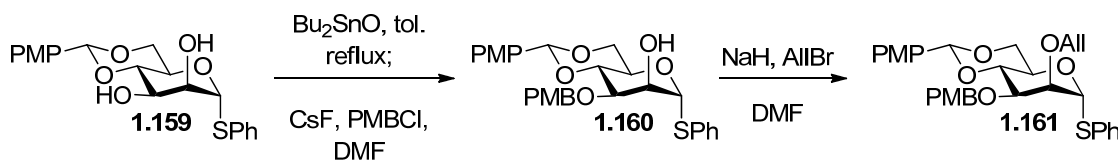
A mixture of **1.159**[145] (1.36 g, 3.48 mmol) and dibutyltin oxide (0.95 g, 3.8 mmol) in anhydrous toluene (50 mL) was refluxed with azeotropic removal of water using a Dean-Stark apparatus for 4 h. After cooling to rt and concentration in vacuum, the residue was dissolved in anhydrous DMF (20 mL) and cooled to 0 °C, after which cesium fluoride (1.22 g, 8.00 mmol) and *p*-methoxybenzyl chloride (1.0 mL, 7.3 mmol) were added to the solution. After stirring overnight under an Ar atmosphere at rt, the reaction mixture was filtered through celite into cold saturated aqueous $NaHCO_3$ and EtOAc. The organic layer was washed with brine, dried over Na_2SO_4, and concentrated in vacuum. The residue was purified by silica gel column chromatography to give **1.160** (a small scale NMR tube acetylation was performed to confirm the regiochemistry of the product), which was taken directly to the next step. To a solution of **1.160** in anhydrous DMF (30 mL) under Ar at 0 °C was added NaH (60% dispersion in mineral oil, 350 mg, 8.7 mmol). After stirring for 30 min, allyl bromide (0.73 mL, 8.7 mmol) was added dropwise and the reaction was stirred for 1 h. The reaction was quenched with MeOH and diluted with EtOAc. The organic layer was washed with brine, dried over Na_2SO_4, and concentrated in vacuum. The residue was purified by silica gel column chromatography to give **1.161** (1.3 g, 68%, 2 steps) as a syrup. ^{1}H NMR (500 MHz, $CDCl_3$): δ 7.46-7.44 (m, 4 H), 7.34-7.29 (m, 5 H), 6.93-6.89 (m, 4 H), 5.97-5.89 (m, 1 H), 5.60 (s, 1 H), 5.53 (d, *J* = 1.0 Hz, 1 H, 1-position), 5.30 (dd, *J* = 2.0, 17.5 Hz, 1 H), 5.21 (dd, *J* = 1.5, 10.5 Hz, 1 H), 4.81 (d,

J = 11.5 Hz, 1 H), 4.66 (d, *J* = 11.5 Hz, 1 H), 4.31-4.16 (m, 5 H), 3.96-3.93 (m, 2 H), 3.87 (t, *J* = 10 Hz, 1 H), 3.83 (s, 3 H), 3.83 (s, 3 H). ^{13}C NMR (125 MHz, CDCl$_3$): δ 160.21, 159.48, 134.81, 134.15, 131.73, 130.69, 130.39, 129.62, 129.37, 127.82, 127.65, 118.19, 114.02, 113.79, 101.74, 87.53, 79.22, 78.38, 75.97, 73.07, 72.77, 68.71, 65.67, 55.54. $[\alpha]_D^{25}$ = +154° (*c* 1.0, CHCl$_3$). HR ESI MS: calcd. for C$_{31}$H$_{34}$O$_7$NaS [M+Na]$^+$ *m/z*, 573.1923; found, 573.1925.

Phenyl 2-*O*-allyl-3,4-di-*O*-(*p*-methoxybenzyl)-1-thio-α-D-mannopyranoside (1.118)
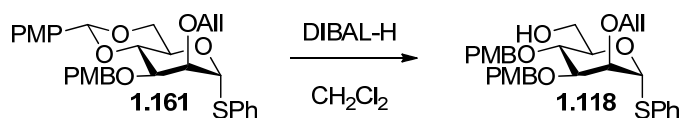
To a solution of **1.161** (550 mg, 1.0 mmol) in anhydrous CH$_2$Cl$_2$ (15 mL) stirring under Ar at 0 ºC was added DIBAL-H (1.0 M solution in toluene, 2.0 mL, 2.0 mmol) dropwise over 1 h. After stirring at 0 ºC for an additional hour, saturated aqueous Na-K-tartrate was added and the mixture was stirred vigorously for 2 h. After separation of the two phases, the organic layer was washed with brine, dried over Na$_2$SO$_4$, and concentrated in vacuum. The residue was purified by silica gel column chromatography to give **1.118** (471 mg, 85%) as a syrup. ^{1}H NMR (500 MHz, CDCl$_3$): δ 7.46-7.44 (m, 2 H), 7.36-7.26 (m, 7 H), 6.93-6.88 (m, 4 H), 5.97-5.89 (m, 1 H), 5.52 (d, *J* = 1.5 Hz, 1 H, 1-position), 5.30 (dd, *J* = 1.5, 17.5 Hz, 1 H), 5.22 (dd, *J* = 2.0, 10.5 Hz, 1 H), 4.88 (d, *J* = 10.5 Hz, 1 H), 4.68 (s, 2 H), 4.59 (d, *J* = 11 Hz, 1 H), 4.16 (d, *J* = 6.0 Hz, 2 H), 4.13-4.09 (m, 1 H), 3.95 (t, *J* = 9.5 Hz, 1 H), 3.92 (dd, *J* = 2.0, 3.0 Hz, 1 H), 3.88 (dd, *J* = 3.0, 9.5 Hz, 1 H), 3.84 (s, 3 H), 3.83-3.76 (m, 2 H), 3.82 (s, 3 H). ^{13}C NMR (125 MHz, CDCl$_3$): δ 159.60, 159.57, 134.87, 134.27, 132.02, 130.79, 130.47, 129.98, 129.85, 129.35, 127.86,

118.20, 114.14, 114.12, 86.34, 79.91, 76.65, 75.21, 74.80, 73.45, 72.29, 72.00, 62.51, 55.54. $[\alpha]_D^{25}$ = +18° (*c* 1.0, CHCl$_3$). HR ESI MS: calcd. for C$_{31}$H$_{36}$O$_7$NaS [M+Na]$^+$ *m/z*, 575.2079; found, 575.2063.

3,4,6-tri-*O*-(*p*-Methoxybenzyl)-1,2-O-(1-methoxyethylidene)-β-D-mannopyranoside (1.164)
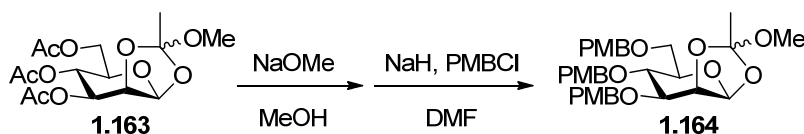
After a solution of **1.163**[141] (2.00 g, 5.52 mmol) in 15 mL of 0.05 M NaOMe in methanol was stirred at rt for 20 min, it was concentrated to afford a white powder (note: Neutralization with Amberlyst H$^+$ resin caused significant decomposition of the orthoester, so the reaction was taken directly to the next step). To the crude triol in anhydrous DMF (30 mL) stirring under Ar at 0 °C was slowly added NaH (60% dispersion in mineral oil, 1.10 g, 27.5 mmol). After stirring for 30 min, *p*-methoxybenzyl chloride (2.30 mL, 22.0 mmol) was added dropwise. The reaction was stirred for 3 h while warming to rt and then quenched with MeOH and diluted with EtOAc. The solution was washed with brine, dried over Na$_2$SO$_4$, and concentrated in vacuum. The residue was purified by silica gel column chromatography to give **1.164** (2.50 g, 76 %, 2 steps) as a syrup. ^{1}H NMR (500 MHz, CDCl$_3$): δ 7.32-7.30 (m, 2 H), 7.25-7.24 (m, 2 H), 7.14-7.12 (m, 2 H), 6.87-6.82 (m, 6 H), 5.32 (d, *J* = 2.5 Hz, 1 H, 1-position), 4.78 (d, *J* = 10.5 Hz, 1 H), 4.73 (d, *J* = 12 Hz, 1 H), 4.70 (d, *J* = 11.5 Hz, 1 H), 4.54-4.47 (m, 3 H), 4.34 (dd, *J* = 2.5, 4.0 Hz, 1 H), 3.83 (t, *J* = 9.5 Hz, 1 H), 3.80 (s, 6 H), 3.79 (s, 3 H), 3.68-3.65 (m, 3 H), 3.38 (dt, *J* = 3.5, 9.0 Hz, 1 H), 3.28 (s, 3 H), 1.72 (s, 3 H). ^{13}C NMR (125 MHz,

105

CDCl$_3$): δ 129.95, 129.86, 129.46, 114.13, 114.01, 113.94, 97.76, 78.83, 75.10, 74.44, 74.19, 73.23, 72.25, 68.90, 55.51, 49.98, 24.62. [α]$_D^{25}$ = +12° (*c* 1.0, CHCl$_3$). HR ESI MS: calcd. for C$_{33}$H$_{40}$O$_{10}$Na [M+Na]$^+$ *m/z*, 619.2519; found, 619.2524.

2-*O*-Acetyl-3,4,6-tri-*O*-(*p*-methoxybenzyl)-D-mannopyranose (1.165)
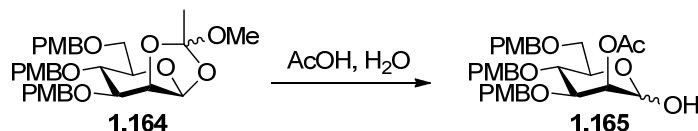
To a round bottom flask containing **1.164** (2.30 g, 3.85 mmol) was added AcOH/H$_2$O (1:1, 20 mL). The poorly soluble substrate went into solution as the reaction was stirred vigorously at rt over 3 h, after which the solution was diluted with CH$_2$Cl$_2$ and poured into a separatory funnel containing cold, saturated aqueous NaHCO$_3$. The aqueous phase was extracted with CH$_2$Cl$_2$ two additional times, and the combined organic layers were washed with saturated aqueous NaHCO$_3$ and brine, dried over Na$_2$SO$_4$, and concentrated in vacuum. The resulting residue was purified by silica gel column chromatography to give hemiacetal **1.165** (1.57 g, 70%) as a glassy syrup, while the minor product was identified as the regioisomer containing 1-*O*-acetyl and 2-OH functional groups. ^{1}H NMR (500 MHz, CDCl$_3$): δ 7.27-7.25 (m, 4 H), 7.05-7.03 (m, 2 H), 6.86-6.81 (m, 6 H), 5.35 (dd, *J* = 2.0, 3.0 Hz, 1 H), 5.20 (d, *J* = 2.0 Hz, 1 H, 1-position), 4.75 (d, *J* = 10.5 Hz, 1 H), 4.63 (d, *J* = 11 Hz, 1 H), 4.54 (d, *J* = 12 Hz, 1 H), 4.46 (d, *J* = 10 Hz, 1 H), 4.44 (d, *J* = 12 Hz, 1 H), 4.35 (d, *J* = 10.5 Hz, 1 H), 4.04-4.00 (m, 1 H), 3.99 (dd, *J* = 3.0, 9.0 Hz, 1 H), 3.80 (s, 3 H), 3.79 (s, 3 H), 3.78 (s, 3 H), 3.68 (t, *J* = 10 Hz, 1 H), 3.66-3.60 (m, 2 H), 3.37 (d, *J* = 3.5 Hz, 1 H), 2.14 (s, 3 H). ^{13}C NMR (125 MHz, CDCl$_3$): δ 170.74, 159.50, 159.44, 130.73, 130.37, 130.17, 129.96, 129.95, 129.76,

114.04, 113.99, 113.94, 92.75, 77.55, 74.96, 74.49, 73.24, 71.67, 71.41, 69.31, 69.03, 55.50, 55.48, 55.45, 21.40. HR ESI MS: calcd. for $C_{32}H_{38}O_{10}Na$ [M+Na]$^+$ *m/z*, 605.2363; found, 605.2392.

Allyl 6-*O*-(*p*-methoxytriphenylmethyl)-α-D-mannopyranoside (1.167)
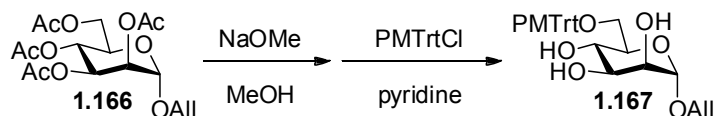
After a solution of allyl **1.166**[146] (2.45 g, 7.24 mmol) in 20 mL of 0.05 M NaOMe in methanol was stirred at rt for 30 min, it was neutralized to pH 6-7 using Amberlyst H$^+$ resin. The solution was filtered off and concentrated to afford a white powder, which was directly used for the next step. After the crude tetraol was dissolved in pyridine (30 mL), *p*-methoxytrityl chloride (5.60 g, 18.1 mmol) was added and the reaction was stirred at rt for 2 h, then concentrated in vacuum and purified by silica gel column chromatography to afford **1.167** (2.30 g, 66%, 2 steps) as a white foam. ^{1}H NMR (500 MHz, CDCl$_3$): δ 7.45-7.43 (m, 4 H), 7.28-7.33 (m, 6 H), 7.24-7.21 (m, 2 H), 6.83-6.84 (m, 2 H), 5.95-5.87 (m, 1 H), 5.30 (dd, *J* = 1.5, 17 Hz, 1 H), 5.21 (dd, *J* = 1.5, 10.8 Hz, 1 H), 4.86 (d, *J* = 1.5 Hz, 1 H, 1-position), 4.19 (dd, *J* = 5.5, 13.5 Hz, 1 H), 3.99 (dd, *J* = 6.5, 13 Hz, 1 H), 3.93 (dd, *J* = 1.5, 3.5 Hz, 1 H), 3.84-3.83 (m, 1 H), 3.79 (s, 3 H), 3.74-3.71 (m, 2 H), 3.43 (dd, *J* = 4.5, 9.5 Hz, 1 H), 3.39 (dd, *J* = 4.5, 9.5 Hz, 1 H). ^{13}C NMR (125 MHz, CDCl$_3$): δ 158.92, 144.37, 144.25, 135.39, 133.89, 130.57, 128.54, 128.20, 127.31, 117.84, 113.49, 98.86, 87.33, 71.86, 70.72, 70.58, 70.15, 65.05, 55.46. [α]$_D^{25}$ = +17° (*c* 1.0, CHCl$_3$). HR ESI MS: calcd. for $C_{29}H_{32}O_7Na$ [M+Na]$^+$ *m/z*, 515.2046; found, 515.2054.

Allyl 2,3,4-tri-*O*-(*p*-methoxybenzyl)-6-*O*-(*p*-methoxytriphenylmethyl)-α-D-mannopyranoside (1.168)
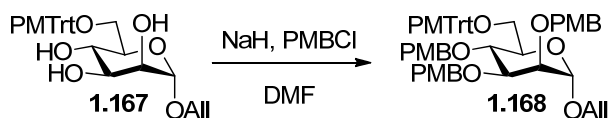
To a solution of **1.167** (2.10 g, 4.26 mmol) in anhydrous DMF (40 mL) stirring under Ar at 0 °C was slowly added NaH (60% dispersion in mineral oil, 756 mg, 18.9 mmol). After stirring for 30 min, *p*-methoxybenzyl chloride (1.97 mL, 18.9 mmol) was added dropwise. The reaction was stirred overnight at rt and then quenched with MeOH and diluted with EtOAc. The solution was washed with saturated aqueous NaHCO$_3$ and brine, dried over Na$_2$SO$_4$, and concentrated in vacuum. The residue was purified by silica gel column chromatography to give **1.168** (2.61 g, 73 %) as a white foam. ^{1}H NMR (500 MHz, CDCl$_3$): δ 7.52-7.51 (m, 4 H), 7.37-7.33 (m, 4 H), 7.30-7.20 (m, 8 H), 6.87-6.79 (m, 8 H), 6.71-6.70 (m, 2 H), 5.93-5.85 (m, 1 H), 5.25 (dd, *J* = 1.5, 17 Hz, 1 H), 5.17 (dd, *J* = 1.0, 10.5 Hz, 1 H), 4.92 (d, *J* = 1.5 Hz, 1 H, 1-position), 4.76 (d, *J* = 12 Hz, 1 H), 4.65-4.63 (m, 2 H), 4.59 (d, *J* = 12 Hz, 1 H), 4.56 (d, *J* = 11 Hz, 1 H), 4.24 (dd, *J* = 4.5, 12.5 Hz, 1 H), 4.18 (d, *J* = 10 Hz, 1 H), 3.99 (dd, *J* = 6.0, 13 Hz, 1 H), 3.94 (t, *J* = 9.5 Hz, 1 H), 3.87 (dd, *J* = 3.0, 9.5 Hz, 1 H), 3.81 (s, 3 H), 3.78-3.80 (m, 2 H), 3.78 (s, 3 H), 3.78 (s, 3 H), 3.77 (s, 3 H), 3.47 (dd, *J* = 1.5, 9.5 Hz, 1 H), 3.24 (dd, *J* = 5.5, 9.5 Hz, 1 H). ^{13}C NMR (125 MHz, CDCl$_3$): δ 159.30, 158.67, 145.02, 144.84, 136.08, 134.20, 131.09, 130.95, 130.79, 130.71, 130.07, 129.50, 129.44, 128.91, 128.83, 127.95, 126.89, 117.45, 113.97, 113.78, 113.24, 97.02, 86.13, 80.23, 75.32, 75.03, 74.93, 72.53, 72.23, 67.77, 63.12, 55.50, 55.48, 55.39. [α]$_D^{25}$ = +13° (*c* 1.0, CHCl$_3$). HR ESI MS: calcd. for C$_{53}$H$_{56}$O$_{10}$Na [M+Na]$^+$ *m/z*, 875.3771; found, 875.3762.

Allyl 2,3,4-tri-*O*-(*p*-methoxybenzyl)-α-D-mannopyranoside (1.169)
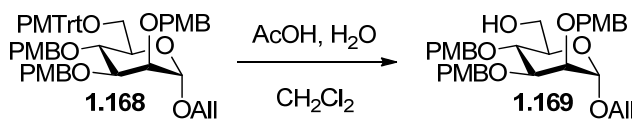
After a solution of **1.168** (2.40 g, 2.81 mmol) in AcOH/CH$_2$Cl$_2$/H$_2$O (15:4:1, 20 mL) was stirred at rt for 2.5 h, it was diluted with CH$_2$Cl$_2$ and poured into cold, saturated aqueous NaHCO$_3$. The organic layer was washed with saturated aqueous NaHCO$_3$ and brine, then dried over Na$_2$SO$_4$. After concentration in vacuum, the residue was purified by silica gel column chromatography to give **1.169** (1.53 g, 94%) as a syrup. ^{1}H NMR (500 MHz, CDCl$_3$): δ 7.29-7.28 (m, 4 H), 7.24-7.22 (m, 2 H), 6.88-6.85 (m, 6 H), 5.86-5.78 (m, 1 H), 5.20 (dd, *J* = 2.0, 17.5 Hz, 1 H), 5.15 (dd, *J* = 1.5, 10.5, 1 H), 4.85 (d, *J* = 10.5 Hz, 1 H), 4.79 (d, *J* = 1.5 Hz, 1 H, 1-position), 4.71 (d, *J* = 12 Hz, 1 H), 4.61 (d, *J* = 12, 1 H), 4.57-4.55 (m, 3 H), 4.10 (dd, *J* = 5.0, 13 Hz, 1 H), 3.91-3.87 (m, 3 H), 3.81 (s, 3 H), 3.80 (s, 3 H), 3.79 (s, 3 H), 3.74-3.79 (m, 3 H), 3.64-3.61 (m, 1 H). ^{13}C NMR (125 MHz, CDCl$_3$): δ 159.50, 159.39, 133.88, 130.91, 130.83, 130.53, 129.97, 129.75, 129.45, 117.49, 114.07, 114.01, 97.69, 80.16, 75.12, 74.90, 74.62, 72.81, 72.41, 72.15, 68.05, 62.70, 55.51. [α]$_D^{25}$ = +35° (*c* 1.0, CHCl$_3$). HR ESI MS: calcd. for C$_{33}$H$_{40}$O$_9$Na [M+Na]$^+$ *m/z*, 603.2570; found, 603.2549.

Allyl 6-*O*-(*tert*-butyldimethylsilyl)-2,3,4-tri-*O*-(*p*-methoxybenzyl)-α-D-mannopyranoside (1.170)
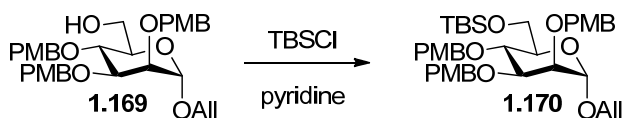
A solution of **1.169** (1.50 g, 2.58 mmol) and TBSCl (777 mg, 5.16 mmol) in pyridine (25 mL) was stirred under Ar overnight at rt. After concentration to remove most of the pyridine, the residue was dissolved in CH_2Cl_2 and poured into water. The aqueous layer was extracted twice with CH_2Cl_2 and the combined organic layers were washed with saturated aqueous $NaHCO_3$ and brine, then dried over Na_2SO_4 and concentrated in vacuum. The resulting residue was purified by silica gel column chromatography to obtain **1.170** (1.62 g, 88%) as a glassy syrup. ^{1}H NMR (500 MHz, CDCl$_3$): δ 7.29-7.27 (m, 4 H), 7.23-7.21 (m, 2 H), 6.87-6.84 (m, 6 H), 5.86-5.80 (m, 1 H), 5.20 (dd, *J* = 1.5, 17 Hz, 1 H), 5.13 (dd, *J* = 1.5, 10.5 Hz, 1 H), 4.83 (d, *J* = 10.5 Hz, 1 H), 4.66 (d, *J* = 12.5 Hz, 1 H), 4.59 (d, *J* = 12 Hz, 1 H), 4.56-4.52 (m, 3 H, includes 1-position), 4.12 (dd, *J* = 4.5, 13 Hz, 1 H), 3.91-3.80 (m, 4 H), 3.81 (s, 3 H), 3.80 (s, 3 H), 3.80 (s, 3 H), 3.79-3.77 (m, 1 H), 3.73 (dd, *J* = 2.0, 3.5 Hz, 1 H), 3.57 (ddd, *J* = 2.0, 5.0, 9.0 Hz, 1 H), 0.89 (s, 9 H), 0.064 (s, 3 H), 0.058 (s, 3 H). ^{13}C NMR (125 MHz, CDCl$_3$): δ 159.41, 159.35, 134.20, 131.20, 131.09, 130.78, 129.86, 129.58, 129.48, 117.24, 114.00, 113.95, 113.90, 97.01, 80.21, 74.96, 74.90, 74.79, 73.55, 72.34, 72.05, 67.66, 63.09, 55.50, 26.16, -4.90, -5.04. $[\alpha]_D^{25}$ = +23° (*c* 1.0, CHCl$_3$). HR ESI MS: calcd. for $C_{39}H_{54}O_9NaSi$ [M+Na]$^+$ *m/z*, 717.3435; found, 717.3434.

6-O-(tert-Butyldimethylsilyl)-2,3,4-tri-O-(p-methoxybenzyl)-D-mannopyranose (1.171)
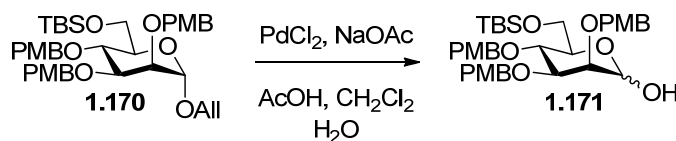
To a solution of **1.170** (491 mg, 0.707 mmol) in CH_2Cl_2/AcOH (1:1, 8 mL) was added H_2O (5 drops), sodium acetate (373 mg, 4.50 mmol), and palladium chloride (248 mg, 1.41 mmol). After stirring under Ar at rt for 5 h, the reaction was concentrated down to a volume of ~1 mL and diluted with EtOAc. After catalyst filtration through celite, the organic layer was washed with saturated aqueous $NaHCO_3$ and brine, then dried over Na_2SO_4 and concentrated in vacuum. The residue was purified by silica gel column chromatography to give an α,β-mixture of hemiacetal **1.171** (381 mg, 82%). ^1H NMR (500 MHz, $CDCl_3$, signals of major isomer): δ 7.32-7.22 (m, 6 H), 6.90-6.85 (m, 6 H), 5.19 (dd, J = 2.0, 3.5 Hz, 1 H, 1-position), 4.85 (d, J = 11 Hz, 1 H), 4.68 (d, J = 12 Hz, 1 H), 4.62-4.55 (m, 4 H), 3.94-3.92 (m, 1 H), 3.87-3.78 (m, 13 H), 3.74 (dd, J = 2.0, 3.0 Hz, 1 H), 3.37 (d, J = 3.0 Hz, 1 H), 0.90 (s, 9 H), 0.070 (s, 3 H), 0.061 (s, 3 H). ^{13}C NMR (125 MHz, $CDCl_3$, all signals): δ 164.46, 164.38, 136.23, 136.10, 135.90, 134.96, 134.81, 134.60, 119.15, 119.05, 119.01, 118.96, 98.68, 97.91, 87.79, 84.60, 81.62, 80.17, 80.10, 79.94, 79.88, 79.53, 79.28, 78.59, 77.86, 77.44, 77.23, 77.13, 68.51, 67.88, 60.57, 60.54, 26.27, 26.20, -4.85, -5.03. HR ESI MS: calcd. for $C_{36}H_{50}O_9NaSi$ [M+Na]$^+$ m/z, 677.3122; found, 677.3103.

Phenyl *O*-[3,4,6-tri-*O*-(*p*-methoxybenzyl)-α-D-mannopyranosyl]-(1→6)-2-*O*-allyl-3,4-di-*O*-(*p*-methoxybenzyl)-1-thio-α-D-mannopyranoside (1.173)
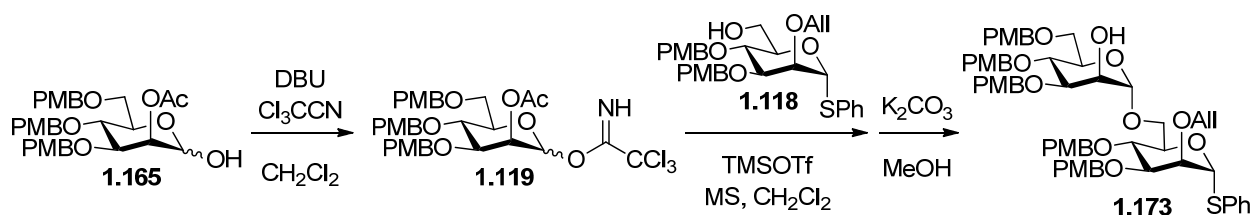
DBU (5 drops) was added to a solution of hemiacetal **1.171** (735 mg, 1.26 mmol) and trichloroacetonitrile (0.5 mL) in anhydrous CH_2Cl_2 (12 mL) stirring under an Ar atmosphere at 0 ºC. After 20 min, the reaction mixture was concentrated in vacuum and purified with a triethylamine-neutralized silica gel column to give **1.119** (706 mg, 77%). A mixture of the resulting trichloroacetimidate **1.119** (706 mg, 0.97 mmol), acceptor **1.118** (413 mg, 0.75 mmol), and MS 4 Å (150 mg) in anhydrous CH_2Cl_2 (10 mL) was stirred under an Ar atmosphere at rt for 1 h. After cooling to 0 ºC, TMSOTf (10 µl, 55 µmol) was added and the reaction was stirred for 5 min. Neutralization with triethylamine was followed by filtration through celite to remove MS, concentration in vacuum, and purification by silica gel column chromatography to give crude **1.172**, which was dissolved in anhydrous MeOH (10 mL) and treated with K_2CO_3 (to pH ~9). After stirring for 1 h, the reaction was neutralized by Amberlyst H^+ resin, filtered, and concentrated in vacuum. The residue was purified by silica gel column chromatography to afford α anomer **1.173** (530 mg, 66%, 2 steps) as a syrup. ^1H NMR (500 MHz, $CDCl_3$): δ 7.45-7.43 (m, 2 H), 7.35-7.33 (m, 2 H), 7.28-7.25 (m, 5 H), 7.20-7.19 (m, 2 H), 7.08-7.06 (m, 2 H), 6.92-6.90 (m, 2 H), 6.85-6.81 (m, 10 H), 5.97-5.89 (m, 1 H), 5.52 (d, *J* = 1.5 Hz, 1 H, Man-I 1-position), 5.31 (dd, *J* = 1.5, 17 Hz, 1 H), 5.20 (dd, *J* = 1.5, 10.5 Hz, 1 H), 4.99 (d, *J* = 1.5 Hz, 1 H, Man-II 1-position), 4.85 (d, *J* = 11 Hz, 1 H), 4.74 (d, *J* = 10

Hz, 1 H), 4.69-4.63 (m, 2 H), 4.61-4.54 (m, 3 H), 4.45 (d, *J* = 10.5 Hz, 1 H), 4.41 (d, *J* = 12 Hz, 1 H), 4.38 (d, *J* = 10 Hz, 1 H), 4.20-4.09 (m, 3 H), 4.05 (s, broad, 1 H), 3.93-3.86 (m, 3 H), 3.83 (s, 3 H), 3.81 (s, 3 H), 3.78 (s, 3 H), 3.77 (s, 3 H), 3.75 (s, 3 H), 3.84-3.75 (m, 3 H), 3.72-3.66 (m, 3 H), 3.59 (dd, *J* = 1.5, 10.5 Hz, 1 H), 2.41 (s, broad, 1 H). ^{13}C NMR (125 MHz, CDCl$_3$): δ 159.59, 159.57, 159.45, 159.38, 159.34, 135.02, 134.94, 131.15, 131.05, 130.80, 130.60, 130.44, 130.29, 129.90, 129.85, 129.81, 129.78, 129.75, 129.35, 127.43, 118.03, 114.16, 114.12, 114.03, 113.94, 113.84, 99.82, 85.96, 80.09, 79.64, 76.65, 75.11, 74.91, 74.65, 74.12, 73.15, 72.72, 72.13, 71.63, 71.51, 71.23, 68.61, 68.30, 66.71, 55.53, 55.51, 55.45. $[\alpha]_D^{25}$ = +78° (*c* 1.0, CHCl$_3$). HR ESI MS: calcd. for C$_{61}$H$_{70}$O$_{15}$NaS [M+Na]$^+$ *m/z*, 1097.4333; found, 1097.4349.

Phenyl [6-*O*-(*tert*-butyldimethylsilyl)-2,3,4-tri-*O*-(*p*-methoxybenzyl)-α-D-mannopyranosyl]-(1→2)-[3,4,6-tri-*O*-(*p*-methoxybenzyl)-α-D-mannopyranosyl]-(1→6)-2-*O*-allyl-3,4-di-*O*-(*p*-methoxybenzyl)-1-thio-α-D-mannopyranoside (1.115)
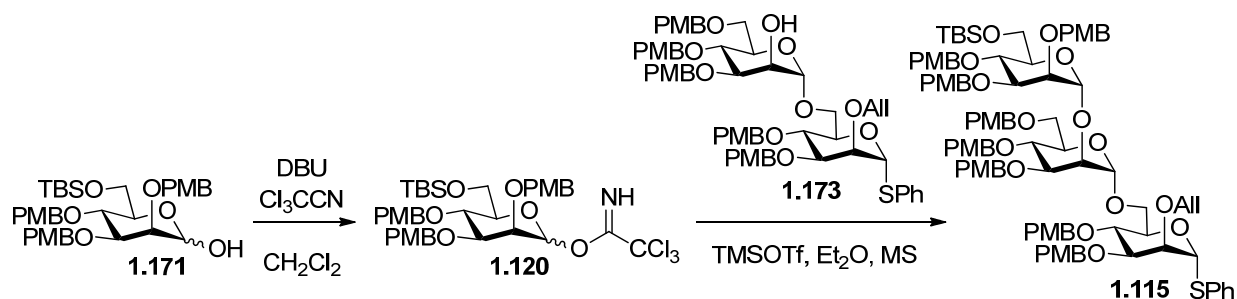
DBU (2 drops) was added to a solution of hemiacetal **1.171** (144 mg, 0.22 mmol) and trichloroacetonitrile (0.3 mL) in anhydrous CH$_2$Cl$_2$ (3 mL) stirring under an Ar atmosphere at 0 °C. After 1 h, the reaction mixture was concentrated in vacuum and purified with a triethylamine-neutralized silica gel column to give **1.120** (129 mg, 73%). A mixture of the resulting trichloroacetimidate **1.120** (129 mg, 0.16 mmol), acceptor

1.173 (121 mg, 0.11 mmol), and MS 4 Å (50 mg) in anhydrous Et_2O (5 mL) was stirred under an Ar atmosphere at rt for 1 h. After cooling to 0 ºC, TMSOTf (3 µl, 16 µmol) was added and the reaction was stirred for 5 min. Neutralization with triethylamine was followed by filtration through celite to remove MS, concentration in vacuum, and purification by silica gel column chromatography to give α anomer **1.115** (145 mg, 76%) as a syrup. ^{1}H NMR (500 MHz, $CDCl_3$) : δ 7.46-7.45 (m, 2 H), 7.34-7.32 (m, 2 H), 7.26-7.17 (m, 14 H), 7.15-7.10 (m, 3 H), 6.91-6.75 (m, 16 H), 5.95-5.87 (m, 1 H), 5.51 (d, J = 1.5 Hz, 1 H, Man-I 1-position), 5.30 (dd, J = 1.5, 17 Hz, 1 H), 5.23 (d, J = 1.0 Hz, 1 H, Man-III 1-position), 5.18 (dd, J = 1.0, 10 Hz, 1 H), 4.85 (d, J = 10.5 Hz, 1 H), 4.82 (d, J = 2.0 Hz, 1 H, Man-II 1-position), 4.82 (d, J = 10.5 Hz, 1 H), 4.77 (d, J = 10.5 Hz, 1 H), 4.66 (d, J = 11.5 Hz, 1 H), 4.63 (d, J = 11.5 Hz, 1 H), 4.60 (d, J = 12 Hz, 1 H), 4.55 (d, J = 10.5 Hz, 1 H), 4.51-4.47 (m, 2 H), 4.46 (d, J = 10.5 Hz, 1 H), 4.45 (d, J = 10.5 Hz, 1 H), 4.42-4.36 (m, 5 H), 4.22-4.15 (m, 2 H), 4.10-4.07 (m, 2 H), 3.96-3.91 (m, 3 H), 3.89-3.84 (m, 4 H), 3.83 (s, 3 H), 3.83-3.82 (m, 2 H), 3.81 (s, 3 H), 3.80 (s, 3 H), 3.79-3.77 (m, 1 H), 3.76 (s, 3 H), 3.75 (s, 3 H), 3.74 (s, 3 H), 3.74-3.72 (m, 2 H), 3.69 (s, 3 H), 3.68 (s, 3 H), 3.66-3.63 (m, 2 H), 3.62-3.57 (m, 2 H), 0.88 (s, 9 H), 0.05 (s, 3 H), 0.04 (s, 3 H). ^{13}C NMR (125 MHz, $CDCl_3$): δ 159.59, 159.45, 159.36, 159.32, 159.29, 159.09, 159.12, 159.15, 135.24, 134.94, 131.56, 131.27, 131.23, 131.07, 130.98, 130.89, 130.84, 130.64, 130.43, 129.89, 129.87, 129.81, 129.70, 129.61, 129.54, 129.38, 127.36, 118.05, 114.11, 114.05, 113.98, 113.93, 113.87, 113.84, 113.70, 99.50, 98.74, 86.16, 80.28, 80.08, 79.65, 76.65, 74.94, 74.85, 74.74, 74.69, 74.67, 74.59, 73.77, 73.08, 73.02, 72.46, 72.14, 72.08, 71.94, 71.66, 71.48, 69.14, 66.86, 62.93, 55.52, 55.48, 55.43, 55.41, 55.37, 55.32, 26.22, 18.59, -4.74, -4.98. The configurations of all three

anomeric positions were established as α by coupled ^{13}C NMR J_{CH} values (125 MHz): 99.50 (J_{CH} = 171 Hz, Man-II), 98.74 (J_{CH} = 171 Hz, Man-III), 86.16 (J_{CH} = 167 Hz, Man-I). $[\alpha]_D^{25}$ = +37° (c 1.0, CHCl$_3$). HR ESI MS: calcd. for $C_{97}H_{118}O_{23}NaSiS$ [M+Na]$^+$ m/z, 1733.7452; found, 1733.7410.

(2-Cyanoethoxy)-(diisopropylamino)-(2,3-di-O-oleoyl-sn-glycerol)-phosphine (1.179)
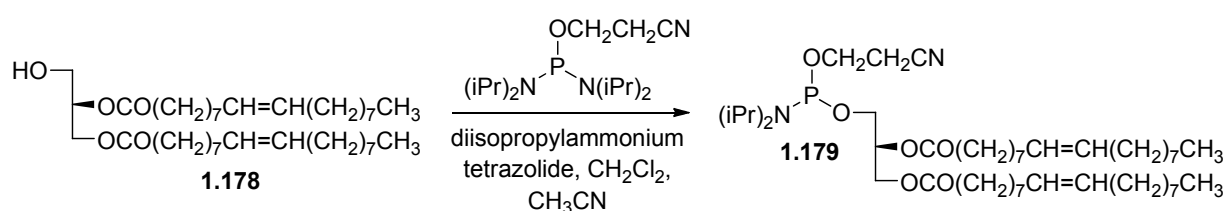
To a solution of known glycerolipid **1.178**[147] (516 mg, 0.83 mmol) and commercially available bis(diisopropylamino)(2-cyanoethoxy)phosphine (375 mg, 1.24 mmol) in anhydrous CH$_2$Cl$_2$/acetonitrile (2:1, 15 mL) was added diisopropylammonium tetrazolide (142 mg, 0.83 mmol). After the reaction stirred at rt under Ar for 1 h, it was diluted with CH$_2$Cl$_2$ and poured into saturated aqueous NaHCO$_3$. The aqueous layer was extracted 3x with CH$_2$Cl$_2$, after which the combined organic layers were dried over Na$_2$SO$_4$ and concentrated in vacuum. Purification using a triethylamine-neutralized silica gel column gave a 1:1 diastereomeric (originating at phosphorus) mixture of phosphoramidite **1.179** (585 mg, 85%) as a white solid. ^1H NMR (CDCl$_3$, 400 MHz): δ 5.38-5.29 (m, 4 H), 5.21-5.15 (m, 1 H), 4.37-4.29 (m, 1 H), 4.19-4.12 (m, 1 H), 3.87-3.54 (m, 6 H), 2.63 (t, J = 7.0 Hz, 2 H), 2.33-2.28 (m, 4 H), 2.02-1.98 (m, 8 H), 1.65-1.58 (m, 4 H), 1.34-1.24 (m, 32 H), 1.17 (t, J = 8.0 Hz, 12 H), 0.87 (t, J= 8.0 Hz, 6 H). ^{31}P NMR (CDCl$_3$, 160 MHz): δ 150.64, 150.48.

6-*O*-[2-Azido-2-deoxy-3,6-di-*O*-(*p*-methoxybenzyl)-α-D-glucopyranosyl]-1-*O*-[(2-cyanoethoxy)-(2,3-di-*O*-oleoyl-*sn*-glycerol)-phosphono]-2,3,4,5-tetra-*O*-(*p*-methoxybenzyl)-*myo*-inositol (4)
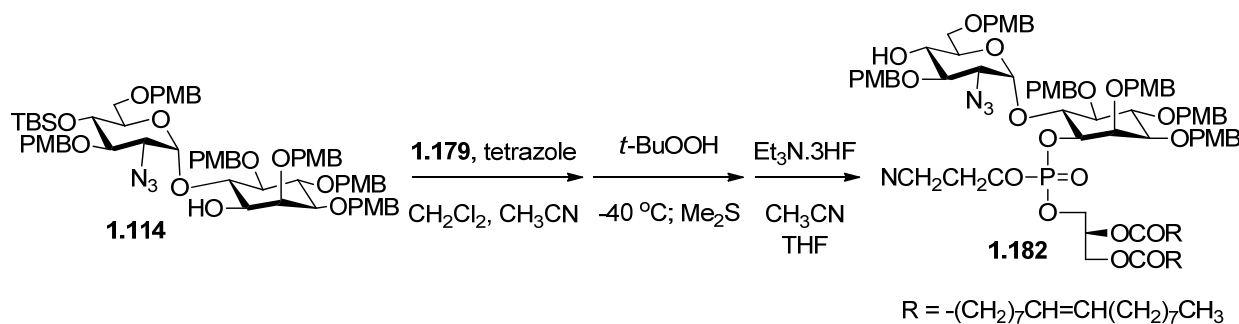
To a solution of pseudodisaccharide **1.114** (50 mg, 41.6 µmol) and tetrazole (0.45 M solution in acetonitrile, 0.92 mL, 0.416 mmol) stirring in anhydrous CH_2Cl_2-CH_3CN (3:1, 8 mL) under Ar at rt was slowly added a solution of freshly prepared phosphoramidite **1.179** (171 mg in 1 mL dry CH_2Cl_2, 0.208 mmol). After the reaction stirred at rt under Ar for 30 min, it was cooled to -40 ºC and treated with *tert*-butyl hydroperoxide (5.5 M solution in decane, 151 µl, 0.832 mmol). The solution stirred for 1 h at -40 ºC, then Me_2S (125 µl, 1.66 mmol) was added and stirring continued for 1 h at -40 ºC. The mixture was poured into saturated aqueous $NaHCO_3$ and extracted 3x with CH_2Cl_2. The combined organic layers were dried over Na_2SO_4 and concentrated in vacuum. Purification by silica gel column chromatography gave the desired intermediate (quickly characterized by MALDI-MS), which was then dissolved in anhydrous THF-CH_3CN (1:1, 4 mL) and treated with $Et_3N•3HF$ (1 mL) under Ar at rt. After stirring for 5 days at rt, the reaction was quenched by dropwise addition of saturated aqueous $NaHCO_3$. The mixture was extracted 3x with CH_2Cl_2, and the combined organic layer was dried over Na_2SO_4, concentrated in vacuum, and purified by silica gel column chromatography to give **1.182** (42 mg, 56%, 2 steps) as a ~1:1 mixture of diastereomers (originating at

phosphorus). Preparative HPLC (Waters Nova-Pak Silica 6 µm, 300 x 19 mm, eluent 30% acetone in hexanes, 10 mL/min, isomer 1-t_R = 14.3 min, isomer 2-t_R = 15.2 min) was used to separate the mixture, and isomer 1 was characterized and carried forward to complete the synthesis. ^{1}H NMR (500 MHz, CDCl$_3$, isomer 1): δ 7.36-7.34 (m, 2 H), 7.33-7.31 (m, 2 H), 7.29-7.27 (m, 2 H), 7.22-7.20 (m, 2 H), 7.15-7.13 (m, 4 H), 6.90-6.83 (m, 8 H), 6.80-6.76 (m, 4 H), 5.40 (d, J = 3.5 Hz, 1 H, 1-position), 5.38-5.31 (m, 4 H), 5.23 (pent, J = 5.5 Hz, 1 H), 4.94 (d, J = 10.5 Hz, 1 H), 4.92 (d, J = 11 Hz, 1 H), 4.86 (d, J = 10.5 Hz, 1 H), 4.83-4.78 (m, 2 H), 4.70-4.67 (m, 3 H), 4.62 (d, J = 10.5 Hz, 1 H), 4.61 (d, J = 11 Hz, 1 H), 4.43-4.32 (m, 5 H), 4.29-4.21 (m, 4 H), 4.17-4.12 (m, 1 H), 4.10 (dd, J = 6.0, 12 Hz, 1 H), 4.04-4.00 (m, 2 H), 3.82 (s, 3 H), 3.81 (s, 3 H), 3.80 (s, 3 H), 3.79 (s, 3 H), 3.78 (s, 3 H), 3.78-3.77 (m, 1 H), 3.76 (s, 3 H), 3.67 (dt, J = 3.0, 9.5 Hz, 1 H), 3.51 (dd, J = 2.0, 10 Hz, 1 H), 3.99 (t, J = 9.5 Hz, 1 H), 3.32-3.26 (m, 2 H), 3.18 (dd, J = 3.5, 10 Hz, 1 H), 2.84-2.73 (m, 2 H), 2.29 (t, J = 7.5 Hz, 4 H), 2.10 (d, J = 4.0 Hz, 1 H), 2.04-2.00 (m, 8 H), 1.61-1.56 (m, 4 H), 1.33-1.27 (m, 36 H), 0.89 (t, J = 6.5 Hz, 1 H). ^{13}C NMR (CDCl$_3$, 125 MHz): δ 173.38, 173.04, 159.69, 159.46, 159.41, 159.35, 159.29, 131.10, 130.98, 130.56, 130.53, 130.48, 130.24, 130.06, 129.96, 129.70, 129.53, 129.50, 129.29, 116.60, 114.22, 114.04, 113.96, 113.91, 113.88, 97.76, 81.48, 80.88, 80.86, 80.57, 78.56, 76.68, 75.68, 75.56, 75.11, 74.59, 74.52, 73.28, 72.78, 72.39, 69.97, 69.56, 69.51, 68.96, 66.39, 66.34, 62.71, 62.65, 62.61, 61.71, 55.51, 55.48, 34.31, 34.15, 32.14, 30.01, 29.99, 29.94, 29.77, 29.56, 29.48, 29.46, 29.41, 29.40, 29.34, 29.31, 27.47, 27.44, 25.03, 22.92, 19.91, 19.86, 14.36. ^{31}P NMR (CDCl$_3$, 160 MHz): δ -1.42. $[\alpha]_D^{25}$ = +24° (c 1.0, CHCl$_3$). HR ESI MS: calcd. for C$_{102}$H$_{143}$N$_4$O$_{23}$NaP [M+Na]$^+$ m/z, 1845.9778; found, 1845.9757.

Phenyl [6-*O*-(*tert*-butyldimethylsilyl)-2,3,4-tri-*O*-(*p*-methoxybenzyl)-α-D-mannopyranosyl]-(1→2)-[3,4,6-tri-*O*-(*p*-methoxybenzyl)-α-D-mannopyranosyl]-(1→6)-3,4-di-*O*-(*p*-methoxybenzyl)-1-thio-α-D-mannopyranoside (1.183)
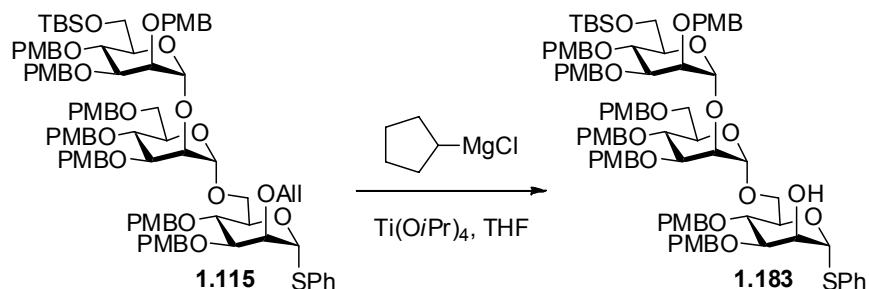
To a solution of **1.115** (56 mg, 32 µmol) in anhydrous THF (5 mL) was added titanium(IV) isopropoxide (25 mg in 0.5 mL hexanes, 80 µmol). Cyclopentylmagnesium chloride (2.0 M solution in THF, 160 µl) was added dropwise under an Ar atmosphere at rt. After 2 h, saturated aqueous Na-K-tartrate was poured into the reaction, which was stirred vigorously for 2 h. The mixture was extracted 3x with CH_2Cl_2, and then the combined organic layer was washed with brine, dried over Na_2SO_4, and concentrated in vacuum. The resulting residue was purified by silica gel column chromatography to obtain **1.183** (45 mg, 82%) as a syrup. ^{1}H NMR (500 MHz, CDCl$_3$): δ 7.44-7.43 (m, 2 H), 7.32-7.30 (m, 2 H), 7.26-7.18 (m, 14 H), 7.15-7.11 (m, 3 H), 6.91-6.90 (m, 2 H), 6.87-6.75 (m, 14 H), 5.53 (d, *J* = 1.0 Hz, 1 H, Man-I 1-position), 5.24 (d, *J* = 1.5 Hz, 1 H, Man-III 1-position), 4.83 (d, *J* = 2.0 Hz, 1 H), 4.82-4.80 (m, 2 H, includes Man-II 1-position), 4.77 (d, *J* = 10.5 Hz, 1 H), 4.65 (s, 2 H), 4.59 (d, *J* = 12 Hz, 1 H), 4.55 (d, *J* = 10.5 Hz, 1 H), 4.50-4.44 (m, 4 H), 4.41-4.37 (m, 5 H), 4.25-4.22 (m, 2 H), 4.07 (t, *J* = 2.0 Hz, 1 H), 3.95-3.84 (m, 6 H), 3.83 (s, 3 H), 3.81 (s, 3 H), 3.80 (s, 3 H), 3.82-3.79 (m, 2 H), 3.77 (s, 3 H), 3.76 (s, 3 H), 3.74 (s, 3 H), 3.74-3.72 (m, 3 H), 3.70 (s, 3 H), 3.68 (s, 3 H), 3.65-3.57 (m, 4 H), 2.72 (s, broad, 1 H), 0.88 (s, 9 H), 0.06 (s, 3 H), 0.05 (s, 3 H).

^{13}C NMR (125 MHz, CDCl$_3$): δ 159.78, 159.44, 159.33, 159.30, 159.20, 159.15, 131.50, 131.25, 131.16, 131.09, 130.91, 130.86, 130.65, 130.58, 129.96, 129.84, 129.81, 129.74, 129.64, 129.58, 129.56, 129.41, 127.42, 114.27, 114.05, 114.04, 113.94, 113.86, 113.84, 113.72, 99.54, 98.56, 87.57, 80.43, 79.96, 79.64, 74.98, 74.93, 74.85, 74.78, 74.59, 74.19, 73.74, 73.08, 72.89, 72.24, 72.10, 71.94, 71.52, 70.07, 69.15, 66.56, 62.94, 55.52, 55.49, 55.44, 55.41, 55.32, 29.95, 26.23, 18.61, -4.74, -4.97. [α]$_D^{25}$ = +58° (c 1.0, CHCl$_3$). HR ESI MS: calcd. for C$_{94}$H$_{114}$O$_{23}$NaSiS [M+Na]$^+$ m/z, 1693.7139; found, 1693.7136.

Phenyl [6-O-(tert-butyldimethylsilyl)-2,3,4-tri-O-(p-methoxybenzyl)-α-D-mannopyranosyl]-(1→2)-[3,4,6-tri-O-(p-methoxybenzyl)-α-D-mannopyranosyl]-(1→6)-3,4-di-O-(p-methoxybenzyl)-2-O-triethylsilyl-1-thio-α-D-mannopyranoside (1.184)
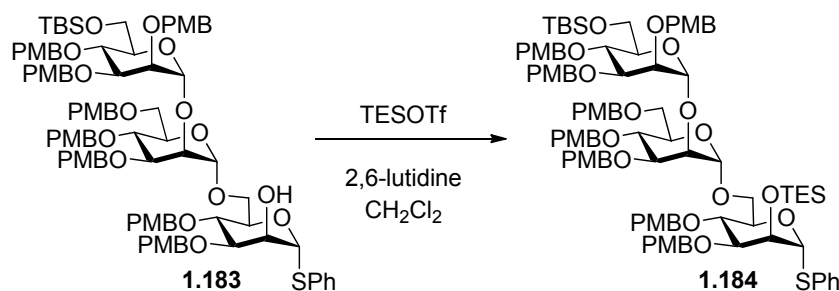
TESOTf (6.5 μl, 29 μmol) was added slowly to a solution of **1.183** (15.8 mg, 9.45 μmol) and 2,6-lutidine (4 μl, 33 μmol) in anhydrous CH$_2$Cl$_2$ (1 mL) stirring under Ar at 0 °C. After 2 h, saturated aqueous NaHCO$_3$ was added to the reaction, which was then extracted 3x with CH$_2$Cl$_2$. The combined organic layer was dried over Na$_2$SO$_4$, concentrated in vacuum, and purified by silica gel column chromatography to afford **1.184** (15.2 mg, 90%) as a syrup. ^{1}H NMR (500 MHz, CDCl$_3$): δ 7.46-7.44 (m, 2 H),

7.31-7.29 (m, 2 H), 7.26-7.15 (m, 14 H), 7.13-7.10 (m, 3 H), 6.88-6.84 (m, 4 H), 6.82-6.73 (m, 12 H), 5.31 (d, J = 2.0 Hz, 1 H, Man-I 1-position), 5.24 (d, J = 1.5 Hz, 1 H, Man-III 1-position), 4.83-4.80 (m, 3 H, includes Man-II 1-position), 4.76 (d, J = 10.5 Hz, 1 H), 4.68 (d, J = 11 Hz, 1 H), 4.60 (d, J = 11.5 Hz, 1 H), 4.59 (d, J = 11 Hz, 1 H), 4.54 (d, J = 10.5 Hz, 1 H), 4.48 (s, 2 H), 4.45 (d, J = 10 Hz, 1 H), 4.40-4.33 (m, 5 H), 4.28 (t, J = 2.0 Hz, 1 H), 4.19 (ddd, J = 1.0, 3.0, 9.0 Hz, 1 H), 4.07 (t, J = 2.5 Hz, 1 H), 3.92 (t, J = 9.5 Hz, 1 H), 3.91-3.84 (m, 4 H), 3.82 (s, 3 H), 3.81 (s, 3 H), 3.79 (s, 3 H), 3.80-3.77 (m, 2 H), 3.75-3.71 (m, 12 H), 3.70 (s, 3 H), 3.66 (s, 3 H), 3.68-3.63 (m, 3 H), 3.58 (dd, J = 2.0, 11 Hz, 1 H), 3.55 (dd, J = 1.5, 11.5 Hz, 1 H), 0.94 (t, J = 8.0 Hz, 9 H), 0.88 (s, 9 H), 0.60 (dq, J = 2.0, 8.0 Hz, 6 H), 0.06 (s, 3 H), 0.05 (s, 3 H). ^{13}C NMR (125 MHz, CDCl$_3$): δ 159.43, 159.40, 159.31, 159.29, 159.19, 159.16, 159.15, 135.24, 131.54, 131.34, 131.27, 131.26, 130.97, 130.88, 130.81, 130.69, 130.59, 129.76, 129.73, 129.57, 129.53, 129.36, 127.30, 114.03, 113.94, 113.85, 113.82, 113.69, 99.33, 98.73, 89.70, 80.68, 80.44, 79.66, 74.91, 74.85, 74.76, 74.65, 74.62, 74.54, 73.79, 73.06, 72.99, 72.45, 72.20, 72.13, 72.08, 71.91, 71.47, 71.45, 68.98, 67.01, 62.95, 55.50, 55.48, 55.47, 55.45, 55.42, 55.39, 55.29, 29.94, 26.21, 18.59, 7.12, 5.26, -4.76, -4.99. $[\alpha]_D^{25}$ = +28° (c 1.0, CHCl$_3$). HR ESI MS: calcd. for C$_{100}$H$_{128}$O$_{23}$NaSi$_2$S [M+Na]$^+$ m/z, 1807.8003; found, 1807.7996.

[6-*O*-(*tert*-Butyldimethylsilyl)-2,3,4-tri-*O*-(*p*-methoxybenzyl)-α-D-mannopyranosyl]-(1→2)-[3,4,6-tri-*O*-(*p*-methoxybenzyl)-α-D-mannopyranosyl]-(1→6)-3,4-di-*O*-(*p*-methoxybenzyl)-2-*O*-triethylsilyl-D-mannopyranose (1.185)
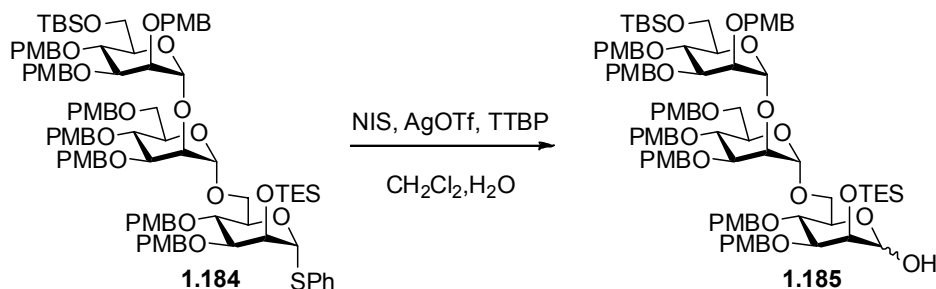
To a mixture of **1.184** (15.0 mg, 8.4 µmol), 2,4,6-tri-*tert*-butylpyrimidine (8.3 mg, 33.6 µmol), and *N*-iodosuccinimide (3.8 mg, 16.8 µmol) in wet CH_2Cl_2 (1 mL) at 0 ºC was added silver triflate (4.3 mg, 16.8 µmol). After stirring for 30 min, saturated aqueous $Na_2S_2O_3$ was added and the mixture was stirred for an additional 30 min while warming to rt. The reaction was extracted 3x with CH_2Cl_2, and the combined organic layer was dried over Na_2SO_4, concentrated in vacuum, and purified by silica gel column chromatography to afford hemiacetal **1.185** (10.5 mg, 74%) as a syrup. ^{1}H NMR (500 MHz, $CDCl_3$): δ 7.28-7.16 (m, 14 H), 7.09-7.08 (m, 2 H), 6.86-6.76 (m, 16 H), 5.17 (s, broad, 1 H, Man-III 1-position), 4.90 (s, broad, 1 H), 4.83-4.81 (m 2 H), 4.78-4.76 (d, *J* = 11 Hz, 1 H), 4.68-4.63 (m, 2 H), 4.58-4.49 (m, 5 H), 4.48-4.34 (m, 8 H), 4.08 (t, *J* = 1.0 Hz, 1 H), 3.99 (t, *J* = 1.0 Hz, 1 H), 3.95-3.90 (m, 2 H), 3.87-3.83 (m, 5 H), 3.82-3.80 (m, 6 H), 3.79-3.77 (m, 4 H), 3.76-3.74 (m, 8 H), 3.74 (s, 3 H), 3.73 (s, 3 H), 3.71 (s, 3 H), 3.69-3.63 (m, 5 H), 3.61-3.56 (m, 4 H), 0.96-0.87 (m, 18 H), 0.61-0.56 (dq, J = 1.5, 7.5 Hz, 6 H), 0.02 (s, 3 H), 0.01 (s, 3 H). ^{13}C NMR ($CDCl_3$, 125 MHz): δ 159.49, 159.43, 159.41, 159.34, 159.26, 159.20, 131.22, 131.12, 130.92, 130.87, 130.73, 130.59, 129.92, 129.75, 129.59, 129.51, 129.50, 114.06, 113.95, 113.89, 113.85, 113.75, 99.32,

97.96, 95.25, 80.07, 79.62, 75.29, 75.08, 74.89, 74.78, 74.47, 73.58, 73.10, 72.69, 72.33, 72.13, 72.11, 72.06, 71.68, 70.43, 69.67, 68.59, 63.09, 55.49, 55.45, 55.43, 55.37, 31.85, 29.96, 26.25, 22.91, 18.67, 14.37, 11.68, 7.16, 5.24, -4.75, -4.92. HR ESI MS: calcd. for $C_{94}H_{124}O_{24}NaSi_2$ [M+Na]$^+$ m/z, 1715.7919; found, 1715.7977.

6-O-{[6-O-($tert$-Butyldimethylsilyl)-2,3,4-tri-O-(p-methoxybenzyl)-α-D-mannopyranosyl]-(1→2)-[3,4,6-tri-O-(p-methoxybenzyl)-α-D-mannopyranosyl]-(1→6)-[3,4-di-O-(p-methoxybenzyl)-2-O-triethylsilyl-α-D-mannopyranosyl]-(1→4)-[2-azido-2-deoxy-3,6-di-O-(p-methoxybenzyl)-α-D-glucopyranosyl]}-1-O-[(2-cyanoethoxy)-(2,3-di-O-oleoyl-sn-glycerol)-phosphono]-2,3,4,5-tetra-O-(p-methoxybenzyl)-myo-inositol (1.187)
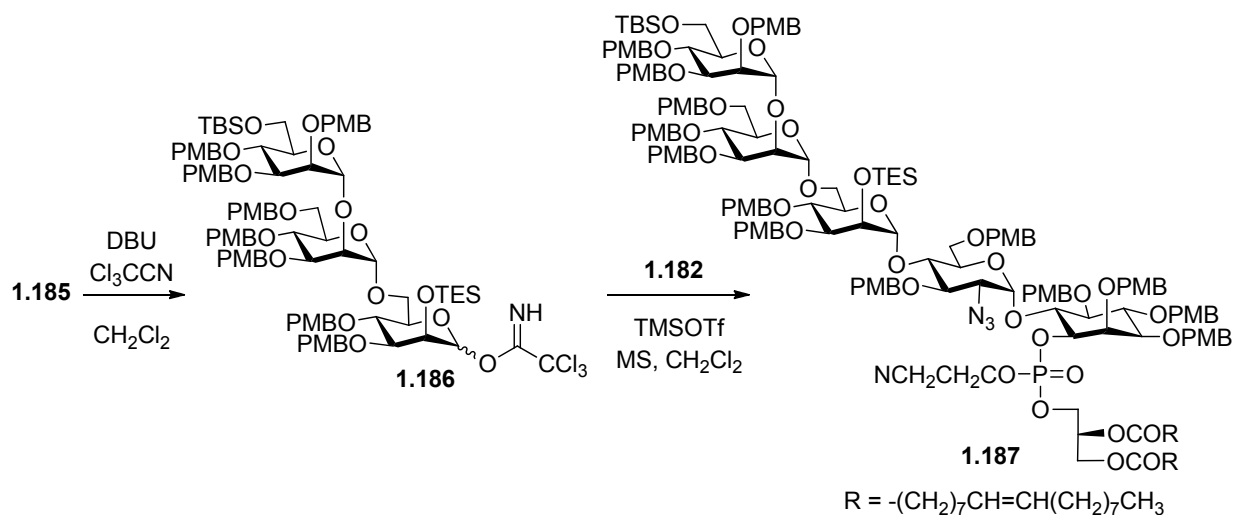
DBU (1 drop) was added to a solution of hemiacetal **1.185** (52 mg, 31 µmol) and trichloroacetonitrile (0.5 mL) in anhydrous CH_2Cl_2 (5 mL) stirring under an Ar atmosphere at 0 ºC. After 1 h, the reaction mixture was concentrated in vacuum and purified with a triethylamine-neutralized silica gel column to give **1.186** (49 mg, 88%). A mixture of the resulting trichloroacetimidate **1.186** (33.3 mg, 18.0 µmol), acceptor **1.182**

(11.0 mg, 6.0 µmol), and MS 4 Å (10 mg) in anhydrous CH_2Cl_2 (400 µl) was stirred under an Ar atmosphere at rt for 1 h. After cooling to 0 ºC, TMSOTf (0.36 M solution in anhydrous CH_2Cl_2, 10 µl) was added and the reaction was stirred for 10 min. Saturated aqueous $NaHCO_3$ and CH_2Cl_2 were then added, and the resulting mixture was passed through celite to remove MS. After extraction of the aqueous layer with CH_2Cl_2 3x, the combined organic phase was dried over Na_2SO_4, concentrated in vacuum, and purified by silica gel column chromatography to give α-pseudopentasaccharide **1.187** (11.5 mg, 64%) as a syrup. ^{1}H NMR (500 MHz, $CDCl_3$, resolved signals): δ 7.31-7.04 (m, 28 H), 6.89-6.70 (m, 28 H), 5.43 (d, J = 3.5 Hz, 1 H, GlcN$_3$ 1-position), 5.40-5.34 (m, 4 H), 5.21 (m, 2 H, includes Man-III 1-position, glyceride CH), 4.91 (d, J = 11.5 Hz, 1 H), 4.86-4.84 (m, 2 H), 4.81-4.72 (m, 6 H, includes Man-II 1-position), 4.70 (d, J = 9.5 Hz, 1 H), 4.65 (d, J = 12 Hz, 1 H), 4.60-4.53 (m, 4 H), 4.04 (s, broad, 1 H), 3.55 (dd, J = 4.0, 11 Hz, 1 H), 3.49 (dd, J = 2.0, 12.5 Hz, 1 H), 3.40-3.34 (m, 2 H), 3.21 (dd, J = 4.0, 10 Hz, 1 H), 2.76-2.68 (m, 2 H), 2.28 (t, J = 7.5 Hz, 4 H), 2.06-1.98 (m, 8 H), 0.49-0.40 (m, 6 H), 0.05 (s, 3 H), 0.04 (s, 3 H). ^{13}C NMR ($CDCl_3$, 125 MHz): δ 173.35, 173.00, 159.42, 159.39, 159.37, 159.33, 159.25, 159.19, 159.17, 159.15, 159.13, 159.09, 131.67, 131.32, 131.28, 131.13, 131.06, 130.96, 130.90, 130.77, 130.70, 130.61, 130.52, 130.42, 130.24, 129.95, 129.70, 129.66, 129.57, 129.47, 129.23, 129.07, 116.56, 114.10, 114.03, 113.90, 113.82, 113.79, 113.64, 99.84, 98.79, 97.76, 81.39, 80.71, 80.66, 80.56, 79.65, 79.00, 76.66, 75.53, 75.39, 75.05, 74.83, 74.79, 74.70, 74.60, 74.38, 73.72, 73.34, 73.09, 72.93, 72.79, 72.51, 72.36, 72.20, 72.10, 71.82, 71.24, 70.54, 69.59, 69.54, 69.02, 68.65, 68.40, 67.30, 66.55, 66.36, 66.33, 66.11, 64.56, 63.23, 62.64, 61.72, 55.49, 55.44, 55.33, 55.30, 55.25, 55.22, 34.30, 34.14, 32.14, 30.00, 29.97,

29.94, 29.76, 29.56, 29.54, 29.45, 29.40, 29.34, 29.29, 27.46, 27.43, 26.20, 25.02, 22.91, 19.84, 19.78, 18.56, 14.34, 7.17, 5.17, -4.74, -5.03. ^{31}P NMR (CDCl$_3$, 160 MHz): δ -1.31. $[\alpha]_D^{25}$ = +10° (*c* 0.5, CHCl$_3$). HR ESI MS: calcd. for C$_{196}$H$_{265}$N$_4$O$_{46}$NaSi$_2$P [M+Na]$^+$ *m/z*, 3520.7694; found, 3520.7732. Note: One of the mannose 1-*O*-positions was suppressed in the NMR spectra for this compound, but was present after the next transformation (see information for compound **1.188** below).

6-*O*-{[2,3,4-tri-*O*-(*p*-methoxybenzyl)-α-D-mannopyranosyl]-(1→2)-[3,4,6-tri-*O*-(*p*-methoxybenzyl)-α-D-mannopyranosyl]-(1→6)-[3,4-di-*O*-(*p*-methoxybenzyl)-α-D-mannopyranosyl]-(1→4)-[2-azido-2-deoxy-3,6-di-*O*-(*p*-methoxybenzyl)-α-D-glucopyranosyl]} -1-*O*-[(2-cyanoethoxy)-(2,3-di-*O*-oleoyl-*sn*-glycerol)-phosphono]-2,3,4,5-tetra-*O*-(*p*-methoxybenzyl)-*myo*-inositol (1.188)

R = -(CH$_2$)$_7$CH=CH(CH$_2$)$_7$CH$_3$
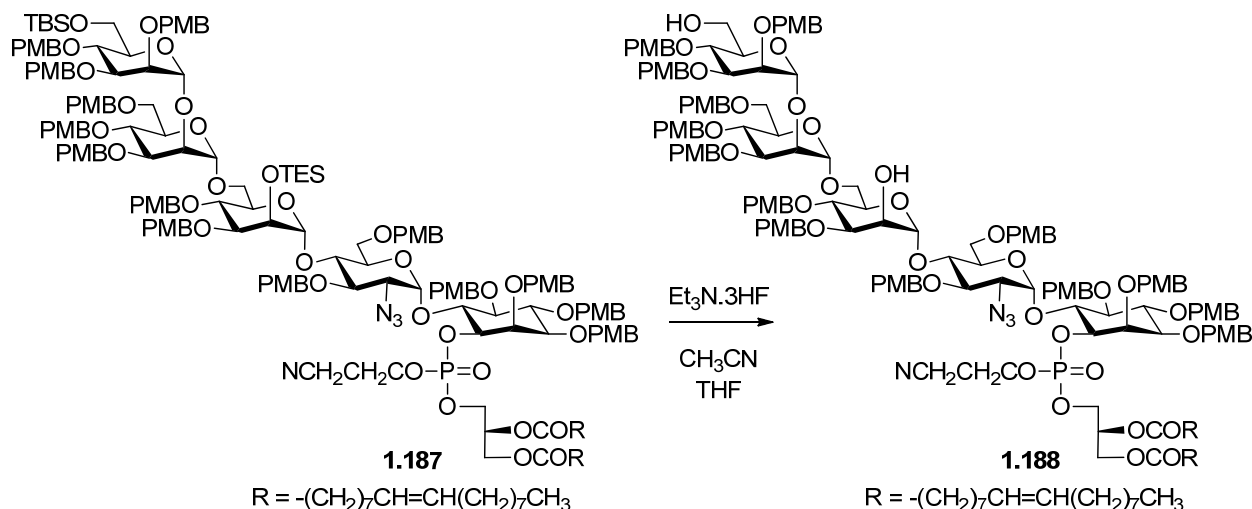
Compound **1.187** (6.0 mg, 1.7 μmol) was dissolved in anhydrous THF-CH$_3$CN (1:1, 600 μl) and treated with Et$_3$N•3HF (300 μl) under Ar at rt (TLC showed that selectivity for removal of the primary TBS ether was not substantial). After stirring overnight at rt, the reaction was quenched by dropwise addition of saturated aqueous NaHCO$_3$. The

aqueous layer was extracted 3x with CH_2Cl_2, and the combined organic layer was dried over Na_2SO_4, concentrated in vacuum, and purified by silica gel column chromatography to give **1.188** (4.0 mg, 70%). ^1H NMR (500 MHz, $CDCl_3$, resolved signals): δ 7.34-7.09 (m, 28 H), 6.89-6.71 (m, 28 H), 5.40 (d, J = 4.0 Hz, 1 H, $GlcN_3$ 1-position), 5.32-5.38 (m, 4 H), 5.23-5.25 (m, 2 H, includes Man-III 1-*O*-position, glyceride CH), 5.15 (s, 1 H, Man-I 1 position), 4.98 (s, 1 H, Man-II 1 position), 4.92 (d, J = 11 Hz, 1 H), 4.90 (d, J = 9 Hz, 1 H), 4.84-4.74 (m, 5 H), 4.69-4.60 (m, 5 H), 3.54-3.48 (m, 4 H), 3.38 (t, J = 9.5 Hz, 1 H), 3.27 (d, J = 10 Hz, 1 H), 3.18-3.16 (m, 2 H), 2.82-2.72 (m, 2 H), 2.29 (t, J = 7.5 Hz, 4 H), 2.06-1.98 (m, 8 H). ^{13}C NMR ($CDCl_3$, 125 MHz): δ 173.34, 172.99, 159.63, 159.47, 159.45, 159.42, 159.39, 159.37, 159.21, 159.15, 131.16, 131.07, 131.06, 131.04, 130.97, 130.70, 130.66, 130.56, 130.49, 130.36, 130.23, 130.11, 129.94, 129.86, 129.78, 129.73, 129.70, 129.67, 129.51, 129.41, 129.25, 129.17, 116.55, 114.17, 114.09, 114.06, 114.05, 113.93, 113.88, 113.84, 113.82, 101.80, 99.63, 99.51, 97.92, 81.44, 80.74, 80.62, 79.50, 79.43, 76.65, 75.56, 75.22, 75.17, 75.08, 74.93, 74.82, 74.71, 74.19, 74.13, 73.63, 73.16, 72.94, 72.89, 72.78, 72.44, 72.03, 71.96, 71.90, 71.71, 70.04, 69.54, 69.19, 68.88, 68.40, 66.41, 65.50, 63.20, 62.69, 61.73, 55.49, 55.46, 55.42, 55.40, 55.37, 55.32, 55.27, 55.23, 34.31, 34.15, 32.13, 30.00, 29.93, 29.75, 29.55, 29.54, 29.45, 29.40, 29.34, 29.30, 27.46, 27.43, 25.03, 22.91, 19.90, 19.83, 14.33. Configurations of anomeric positions were established as α by coupled ^{13}C NMR J_{CH} values (125 MHz): 101.80 (J_{CH} = 176 Hz, Man-1), 99.66 (J_{CH} = 175 Hz, Man-1), 99.54 (J_{CH} = 170 Hz, Man-1), 97.90 (J_{CH} = 177 Hz, $GlcN_3$-1). ^{31}P NMR ($CDCl_3$, 160 MHz): δ -1.27. HR ESI MS: calcd. for $C_{184}H_{237}N_4O_{46}NaP$ [M+Na]$^+$ *m/z*, 3292.5964; found, 3292.6030.

(2-Cyanoethoxy)-[2-(9-fluorenylmethoxycarbonylamino)ethoxy]-

(diisopropylamino)-phosphine (1.189)
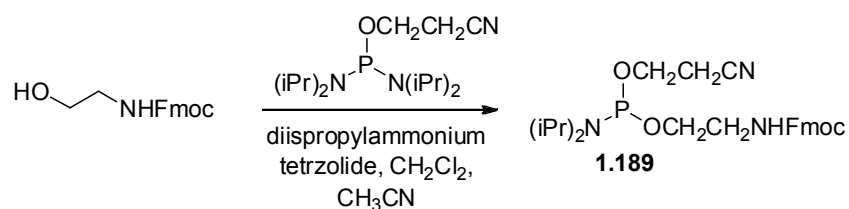
To a solution of *N*-Fmoc-ethanolamine (38 mg, 132 μmol) and commercially available

bis(diisopropylamino)(2-cyanoethoxy)phosphine (84 μl, 264 μmol) in anhydrous CH_2Cl_2-

CH_3CN (2:1, 3 mL) was added diisopropylammonium tetrazolide (24 mg, 135 μmol).

After the reaction stirred at rt under Ar for 1 h, it was diluted with CH_2Cl_2 and poured into

saturated aqueous $NaHCO_3$. The aqueous layer was extracted 3x with CH_2Cl_2, after

which the combined organic layers were dried over Na_2SO_4 and concentrated in

vacuum. Purification using a triethylamine-neutralized silica gel column gave

phosphoramidite **1.189** (59 mg, 92%) as a white solid. ^{1}H NMR ($CDCl_3$, 400

MHz): δ 7.78 (m, 2 H), 7.62-7.61 (m, 2 H), 7.43-7.40 (m, 2 H), 7.34-7.31 (m, 2 H), 5.27

(s, broad, 1 H), 4.42 (d, *J* = 7.0 Hz, 2 H), 4.24 (t, *J* = 7.0 Hz, 1 H), 3.90-3.84 (m, 1 H),

3.82-3.58 (m, 5 H), 3.44 (q, *J* = 5.0 Hz, 2 H), 2.61 (t, *J* = 6.5 Hz, 2 H), 1.20 (t, *J* = 8.0 Hz,

12 H). ^{13}C NMR ($CDCl_3$, 125 MHz): δ 156.65, 144.21, 141.55, 127.92, 127.28, 125.30,

120.21, 117.90, 66.91, 63.06, 62.93, 58.69, 58.53, 47.79, 43.41, 43.31, 42.41, 24.92,

24.87, 24.81, 20.64, 20.58. ^{31}P NMR ($CDCl_3$, 160 MHz): δ 149.65.

6-*O*-{[6-*O*-[(2-cyanoethoxy)-[2-(9-fluorenylmethoxycarbonylamino)ethyl]-phosphono]-2,3,4-tri-*O*-(*p*-methoxybenzyl)-α-D-mannopyranosyl]-(1→2)-[3,4,6-tri-*O*-(*p*-methoxybenzyl)-α-D-mannopyranosyl]-(1→6)-[3,4-di-*O*-(*p*-methoxybenzyl)-α-D-mannopyranosyl]-(1→4)-[2-azido-2-deoxy-3,6-di-*O*-(*p*-methoxybenzyl)-α-D-glucopyranosyl]}-1-*O*-[(2-cyanoethoxy)-(2,3-di-*O*-oleoyl-*sn*-glycerol)-phosphono]-2,3,4,5-tetra-*O*-(*p*-methoxybenzyl)-*myo*-inositol (1.190)
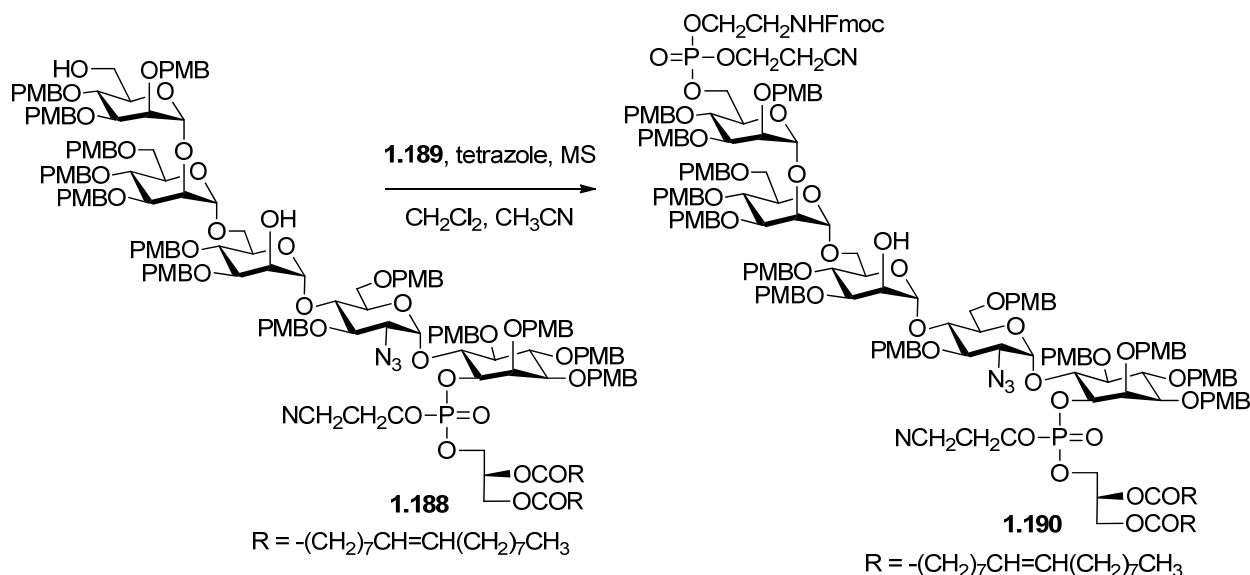
To a solution of pseudopentasaccharide diol **1.188** (2.70 mg, 0.82 µmol) stirring in anhydrous CH$_2$Cl$_2$-CH$_3$CN (3:1, 1 mL) under Ar at rt was added a solution of freshly prepared phosphoramidite **1.189** (4.0 mg in 200 µl dry CH$_2$Cl$_2$, 8.2 µmol) and tetrazole (0.45 M solution in acetonitrile, 36 µl, 16.4 µmol). After stirring at rt under Ar for 1 h, TLC showed conversion to one major spot with a small amount of starting material remaining. The reaction was quenched by cooling to -40 °C and adding *tert*-butyl hydroperoxide (5.5 M solution in decane, 6 µl, 32.8 µmol). The solution stirred for 1 h at -40 °C, then Me$_2$S (4.9 µl, 65.6 µmol) was added and stirring continued for 1 h at -40 °C. After passage through celite to remove MS, the mixture was poured into saturated aqueous

NaHCO$_3$ and extracted 3x with CH$_2$Cl$_2$. The combined organic layers were dried over Na$_2$SO$_4$ and concentrated in vacuum. Purification by silica gel column chromatography afforded unreacted starting material (0.49 mg) and crude **1.188**. The latter was further purified with a Sephadex LH-20 size exclusion column (CHCl$_3$/MeOH 5:1) to provide **1.190** as a diastereomeric mixture (1.51 mg, 50%, 61% based on recovered starting material). ^{1}H NMR (500 MHz, CDCl$_3$, resolved signals): δ 7.66-7.65 (m, 2 H), 7.50-7.49 (m, 2 H), 5.31 (s, 1 H, GlcN$_3$ 1-position), 5.27 (s, 4 H), 5.14 (m, 2 H, includes Man-III 1-position, glyceride CH), 4.94 (s, 1 H, Man-I 1-position), 4.90 (s, 1 H, Man-II 1-position), 2.66 (m, 2 H), 2.19 (m, 4 H), 1.93 (m, 8 H). ^{31}P NMR (CDCl$_3$, 160 MHz): δ -1.48, -2.27. HR ESI MS: calcd. for C$_{204}$H$_{264}$N$_8$O$_{51}$P$_2$ [M+2NH$_4$]$^{2+}$ *m/z*, 1851.8893; found, 1851.8940. MALDI TOF MS (positive mode): calcd. for C$_{204}$H$_{256}$N$_6$O$_{51}$NaP$_2$ [M+Na]$^+$ *m/z*, 3690.7; found, 3690.9. Regiochemistry was established by comparing the chemical shifts of the Man-I 2-*O*-position protons from the starting material (**1.188**) and the product, which was aided by COSY NMR spectroscopy. The analysis suggested that the Man-I 2-*O*-position proton did not shift downfield, as would be expected if that site had been phosphorylated.

6-*O*-{[6-*O*-[(2-Aminoethyl)-phosphono]-α-D-mannopyranosyl]-(1→2)-(α-D-mannopyranosyl)-(1→6)-(α-D-mannopyranosyl)-(1→4)-(2-amino-2-deoxy-α-D-glucopyranosyl)}-1-*O*-[(2,3-di-*O*-oleoyl-*sn*-glycerol)-phosphono]-*myo*-inositol (1.109)
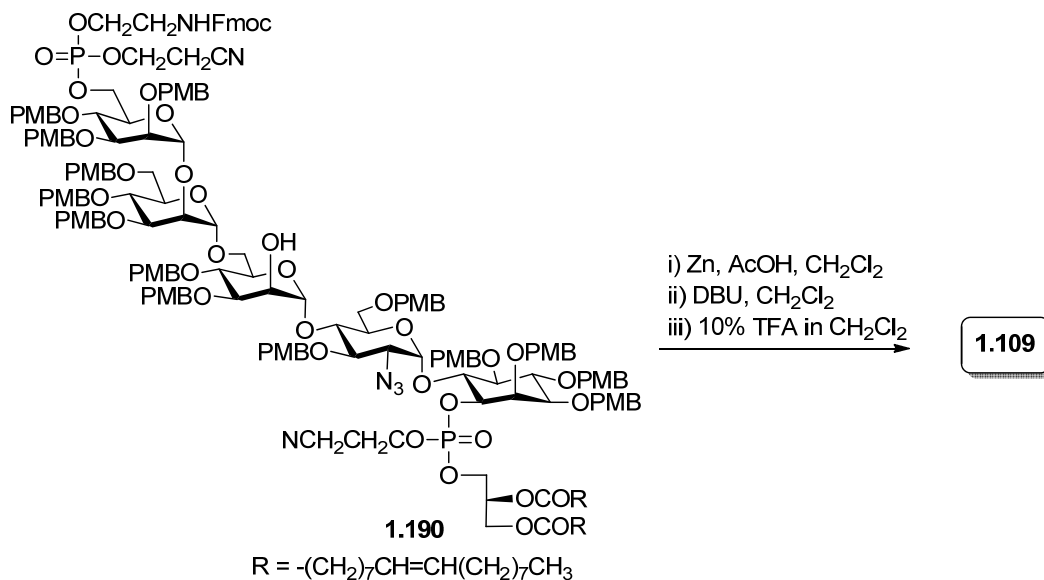
To a solution of **1.190** (1.28 mg, 0.35 µmol) in CH_2Cl_2 (400 µl) was added acetic acid (1 drop) and zinc powder (1 mg). After stirring for 2 h, MALDI TOF MS showed complete reduction of the azide [MALDI TOF MS (positive mode): calcd. for $C_{206}H_{258}N_4O_{51}NaP_2$ $[M+Na]^+$ *m/z*, 3664.7; found, 3664.7]. The mixture was filtered and condensed in vacuum to remove acetic acid, and the resulting residue was re-dissolved in CH_2Cl_2 (300 µl) and treated with DBU (1 µl). The solution stirred for 1 h, after which MALDI TOF MS confirmed removal of the Fmoc and cyanoethyl protecting groups [MALDI TOF MS (positive mode): calcd. for $C_{183}H_{240}N_2O_{49}Na_3P_2$ $[M-2H+3Na]^+$ *m/z*, 3380.6; found, 3380.9]. Then, 20% TFA in CH_2Cl_2 (300 µl) was added directly to the reaction, giving a final concentration of ~10% TFA. After stirring for 30 min, the reaction was co-evaporated with toluene 5 times. Purification of the crude product by Sephadex LH-20

size exclusion chromatography (CHCl$_3$/MeOH/H$_2$O 3:3:1) gave **1.109** (0.46 mg, 81%).

^{1}H NMR (500 MHz, CDCl$_3$/CD$_3$OD/D$_2$O 3:3:1, anomeric region): δ 5.28 (1 H, GlcNH$_2$-1),

5.25 (4 H, lipid sp^2-CH), 5.18 (1 H, glyceride CH), 5.09 (1 H, Man-1), 5.00 (1 H, Man-1),

4.88 (1 H, Man-1). ^{31}P NMR (CDCl$_3$, 160 MHz): δ 4.29, 3.63. MALDI TOF MS (negative

mode): calcd. for C$_{71}$H$_{129}$N$_2$O$_{35}$P$_2$ [M-H]$^-$ *m/z*, 1631.8; found, 1632.1. MALDI TOF MS

(positive mode): calcd. for C$_{71}$H$_{128}$N$_2$O$_{35}$Na$_3$P$_2$ [M-2H+3Na]$^+$ *m/z*, 1699.8; found, 1700.4.

6-*O*-{[6-*O*-[(2-Aminoethyl)-phosphono]-α-D-mannopyranosyl]-(1→2)-(α-D-mannopyranosyl)-(1→6)-[2-*O*-[(2-aminoethyl)-phosphono]-α-D-mannopyranosyl]-(1→4)-(2-amino-2-deoxy-α-D-glucopyranosyl)}-1-*O*-[(2,3-di-*O*-oleoyl-*sn*-glycerol)-phosphono]-*myo*-inositol (1.110)
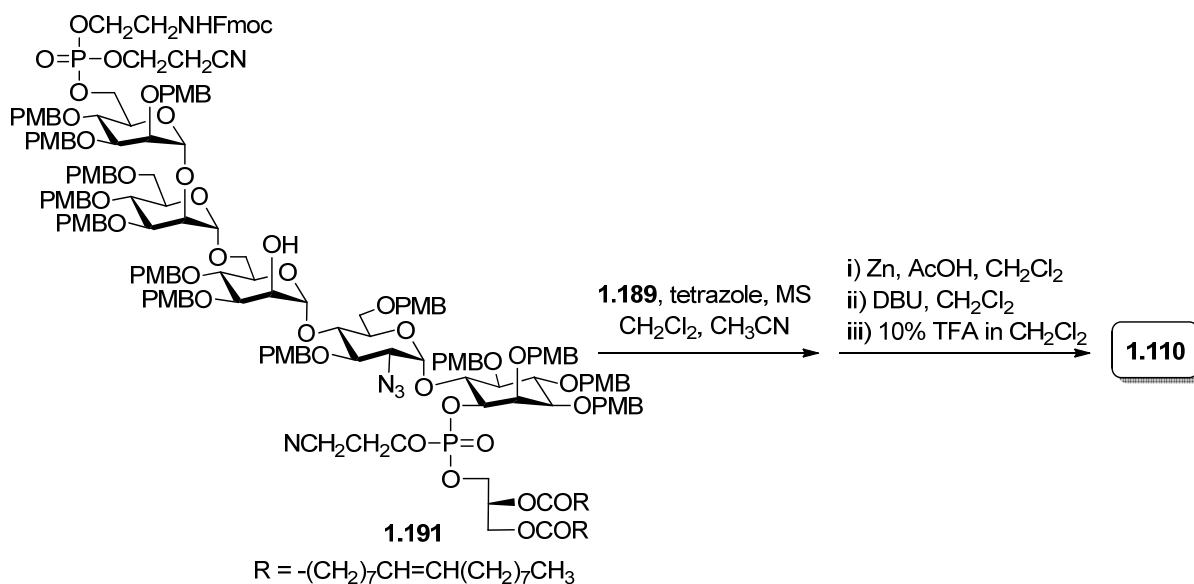
A mixture of **1.191** (microscale quantity sufficient for characterization by MALDI TOF

MS), freshly prepared phosphoramidite **1.189** (3.0 mg, 6.2 µmol, large excess), and MS

4 Å (5 mg) was stirred in anhydrous CH$_2$Cl$_2$ (200 µl) under Ar at rt for 1 h. Tetrazole

(0.45 M solution in acetonitrile, 28 µl, 12.4 µmol) was added and the reaction stirred

overnight at rt. The mixture was cooled to -40 ºC and treated with *tert*-butyl hydroperoxide (5.5 M solution in decane, 4.5 µl, 24.8 µmol). The solution stirred for 1 h at -40 ºC, then Me$_2$S (3.7 µl, 49.6 µmol) was added and stirring continued for 1 h at -40 ºC. After passage through celite to remove MS, saturated aqueous NaHCO$_3$ was added and then the mixture was extracted 3x with CH$_2$Cl$_2$. The combined organic layers were dried over Na$_2$SO$_4$ and concentrated in vacuum. The crude material was passed through a Sephadex LH-20 size exclusion column (CHCl$_3$/MeOH 5:1) to provide the diphosphorylated GPI intermediate, which was taken directly to the three-step global deprotection. To a solution of the intermediate in CH$_2$Cl$_2$ (200 µl) was added acetic acid (1 drop) and zinc powder (1 mg). After stirring for 2 h, the mixture was filtered and condensed in vacuum to remove acetic acid, and the resulting residue was re-dissolved in CH$_2$Cl$_2$ (150 µl) and treated with DBU (1 µl). The solution stirred for 1 h, then 20% TFA in CH$_2$Cl$_2$ (150 µl) was added directly to the reaction, giving a final concentration of ~10% TFA. After stirring for 30 min, the reaction was co-evaporated with toluene 5 times to give **1.110** (isolated yield not obtained). MALDI TOF MS (negative mode): calcd. for C$_{73}$H$_{135}$N$_3$O$_{38}$P [M-H]$^-$ *m/z*, 1754.8; found, 1755.0.

(2-Cyanoethoxy)-(diisopropylamino)-(2,3-di-*O*-stearyl-*sn*-glycerol)-phosphine (1.192)
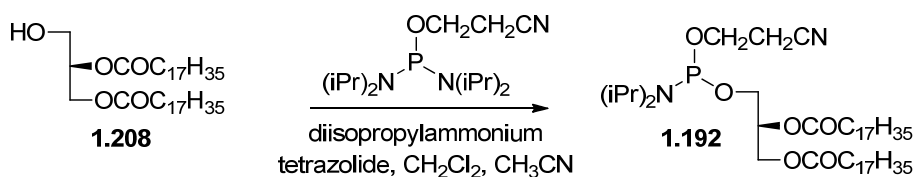
To a solution of known glycerolipid **1.208**[156] (1.04 g, 1.66 mmol) and commercially available bis(diisopropylamino)(2-cyanoethoxy)phosphine (970 mg, 0.32 mmol) in

anhydrous CH_2Cl_2/acetonitrile (3:1, 12 mL) was added diisopropylammonium tetrazolide (266 mg, 1.66 mmol). After the reaction stirred at rt under Ar for 1 h, it was diluted with CH_2Cl_2 and poured into saturated aqueous $NaHCO_3$. The aqueous layer was extracted 3x with CH_2Cl_2, after which the combined organic layers were dried over Na_2SO_4 and concentrated in vacuum. Purification using a triethylamine-neutralized silica gel column gave a 1:1 diastereomeric (originating at phosphorus) mixture of phosphoramidite **1.192** (1.25 g, 90%) as a white solid. ^1H NMR (CDCl$_3$, 400 MHz): δ 5.21-5.16 (m, 1 H), 4.37-4.30 (m, 1 H), 4.20-4.13 (m, 1 H), 3.89-3.48 (m, 6 H), 2.63 (t, J = 6.4 Hz, 2 H), 2.33-2.28 (m, 4 H), 1.65-1.58 (m, 4 H), 1.34-1.24 (m, 56 H), 1.17 (t, J = 7.2 Hz, 12 H), 0.87 (t, J= 7.2 Hz, 6 H). ^{31}P NMR (CDCl$_3$, 160 MHz): δ 150.64, 150.48.

6-*O*-[2-Azido-2-deoxy-3,6-di-*O*-(*p*-methoxybenzyl)-α-D-glucopyranosyl]-1-*O*-[(2-cyanoethoxy)-(2,3-di-*O*-stearyl-*sn*-glycerol)-phosphono]-2,3,4,5-tetra-*O*-(*p*-methoxybenzyl)-*myo*-inositol (1.195)
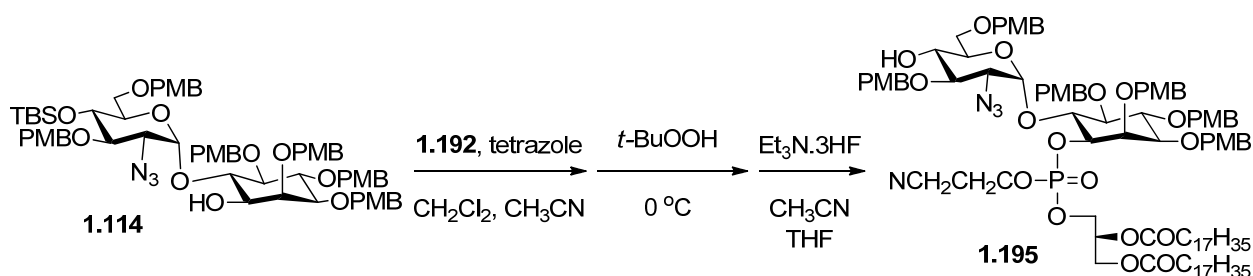
To a solution of pseudodisaccharide **1.114** (150 mg, 125 µmol) and tetrazole (0.45 M solution in acetonitrile, 1.66 mL, 0.75 mmol) stirring in anhydrous CH_2Cl_2-CH_3CN (3:1, 8 mL) under Ar at rt was slowly added a solution of freshly prepared phosphoramidite **1.192** (326 mg in 1 mL dry CH_2Cl_2, 375 µmol). After the reaction stirred at rt under Ar for 20 min, it was cooled to 0 °C and treated with *tert*-butyl hydroperoxide (5.5 M solution in

decane, 151 µl, 0.832 mmol). The solution stirred for 1 h at while warming to rt, then diluted with CH_2Cl_2. The mixture was poured into saturated aqueous $NaHCO_3$ and extracted 3x with CH_2Cl_2. The combined organic layers were dried over Na_2SO_4 and concentrated in vacuum. Purification by silica gel column chromatography gave the desired intermediate (quickly characterized by MALDI-MS), which was then dissolved in anhydrous THF-CH_3CN (1:1, 4 mL) and treated with $Et_3N•3HF$ (2 mL) under Ar at rt. After stirring for 7 days at rt, the reaction was quenched by dropwise addition of saturated aqueous $NaHCO_3$. The mixture was extracted 3x with CH_2Cl_2, and the combined organic layer was dried over Na_2SO_4, concentrated in vacuum, and purified by silica gel column chromatography to give **1.195** (124 mg, 54%, 2 steps) as a ~1:1 mixture of diastereomers (originating at phosphorus). Preparative HPLC (Waters Nova-Pak Silica 6 µm, 300 x 19 mm, eluent 30% acetone in hexanes, 10 mL/min, isomer 1-t_R = 18.4 min, isomer 2-t_R = 19.6 min) was used to separate the mixture, and isomer 1 was characterized and carried forward to complete the synthesis. ^{1}H NMR (500 MHz, CDCl$_3$, isomer 1): δ 7.36-7.34 (m, 2 H), 7.33-7.31 (m, 2 H), 7.29-7.27 (m, 2 H), 7.22-7.20 (m, 2 H), 7.15-7.13 (m, 4 H), 6.90-6.83 (m, 8 H), 6.80-6.76 (m, 4 H), 5.40 (d, J = 4.0 Hz, 1 H, 1-position), 5.23 (pent, J = 5.5 Hz, 1 H), 4.94 (d, J = 10.5 Hz, 1 H), 4.92 (d, J = 11 Hz, 1 H), 4.86 (d, J = 10 Hz, 1 H), 4.83-4.78 (m, 2 H), 4.70-4.67 (m, 3 H), 4.62 (d, J = 10.5 Hz, 1 H), 4.61 (d, J = 11 Hz, 1 H), 4.43-4.32 (m, 5 H), 4.29-4.21 (m, 4 H), 4.17-4.12 (m, 1 H), 4.10 (dd, J = 6.0, 12 Hz, 1 H), 4.04-4.00 (m, 2 H), 3.82 (s, 3 H), 3.81 (s, 3 H), 3.80 (s, 3 H), 3.79 (s, 3 H), 3.78 (s, 3 H), 3.78-3.77 (m, 1 H), 3.76 (s, 3 H), 3.67 (dt, J = 3.0, 10 Hz, 1 H), 3.51 (dd, J = 1.5, 9.5 Hz, 1 H), 3.40 (t, J = 9.0 Hz, 1 H), 3.33-3.26 (m, 2 H), 3.18 (dd, J = 3.5, 10.5 Hz, 1 H), 2.84-2.73 (m, 2 H), 2.29 (t, J = 7.5 Hz, 4 H), 2.09

(d, *J* = 4.0 Hz, 1 H), 1.61-1.56 (m, 4 H), 1.32-1.26 (m, 56 H), 0.89 (t, *J* = 6.5 Hz, 1 H). ^{13}C NMR (CDCl$_3$, 125 MHz): δ 173.41, 173.06, 159.69, 159.43, 159.41, 159.35, 159.29, 131.11, 130.98, 130.57, 130.52, 130.49, 130.24, 130.06, 129.70, 129.53, 129.50, 129.29, 116.60, 114.21, 114.04, 113.96, 113.90, 113.88, 97.77, 81.48, 80.86, 80.57, 78.57, 76.67, 75.69, 75.57, 75.11, 74.59, 73.28, 72.78, 72.40, 69.96, 69.56, 69.53, 68.97, 66.37, 66.35, 62.70, 62.64, 62.62, 61.71, 55.50, 55.47, 55.45, 34.33, 34.18, 32.16, 29.96, 29.93, 29.92, 29.90, 29.78, 29.76, 29.61, 29.58, 29.56, 29.38, 29.35, 25.05, 22.93, 14.36. ^{31}P NMR (CDCl$_3$, 160 MHz): δ -1.42. $[\alpha]_D^{25}$ = +26° (*c* 1.0, CHCl$_3$). HR ESI MS: calcd. for C$_{102}$H$_{147}$N$_4$O$_{23}$NaP [M+Na]$^+$ *m/z*, 1850.0091; found, 1850.0048.

[6-*O*-(*tert*-Butyldimethylsilyl)-2,3,4-tri-*O*-(*p*-methoxybenzyl)-α-D-mannopyranosyl]-(1→2)-[3,4,6-tri-*O*-(*p*-methoxybenzyl)-α-D-mannopyranosyl]-(1→6)-2-*O*-allyl-3,4-di-*O*-(*p*-methoxybenzyl)-D-mannopyranose (1.209)
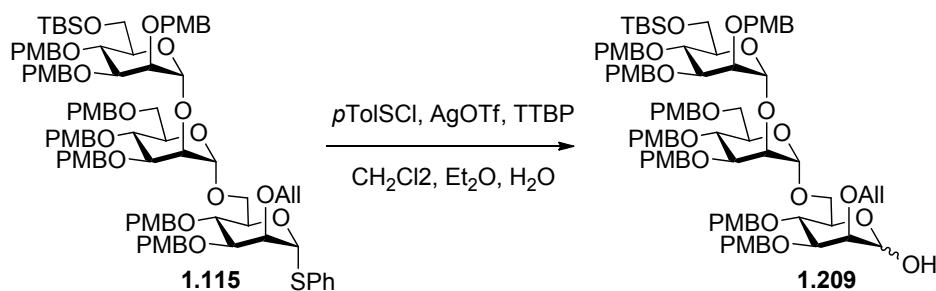
To a solution of **1.115** (85 mg, 49.6 μmol) and 2,4,6-tri-*tert*-butylpyrimidine (62 mg, 248 μmol) in CH$_2$Cl$_2$ (2.0 mL) at -60 °C was added silver triflate (51 mg in 1.0 mL Et$_2$O, 199 μmol). Then, *p*TolSCl (12 μl, 59.5 μmol) was added directly to the mixture to pre-activate the substrate. After stirring for 1 min, acetone-H$_2$O (10:1, 105 μl) was added and the reaction was warmed to rt gradually and stirred for 2 h. After quenching with triethylamine and concentration in vacuum, the resulting residue was redissolved in

CH$_2$Cl$_2$ and filtered to remove solids. The filtrate was then washed with water, dried over Na2SO4, concentrated, and purified by silica gel column chromatography to afford unreacted starting material **1.115** (15 mg) and hemiacetal **1.209** (40 mg, 50% yield, 68% BRSM). The desired product, an anomeric mixture, was quickly characterized by ^{1}H NMR and HR ESI MS (see Appendix A for spectra). HR ESI MS: calcd. for C$_{91}$H$_{114}$O$_{24}$NaSi [M+Na]$^+$ *m/z*, 1641.7367; found, 1641.7310. We thank Prof. Xuefei Huang of Michigan State University for providing *p*-TolSCl.

6-*O*-{[2,3,4-tri-*O*-(*p*-methoxybenzyl)-α-D-mannopyranosyl]-(1→2)-[3,4,6-tri-*O*-(*p*-methoxybenzyl)-α-D-mannopyranosyl]-(1→6)-[2-*O*-allyl-3,4-di-*O*-(*p*-methoxybenzyl)-α-D-mannopyranosyl]-(1→4)-[2-azido-2-deoxy-3,6-di-*O*-(*p*-methoxybenzyl)-α-D-glucopyranosyl]}-1-*O*-[(2-cyanoethoxy)-(2,3-di-*O*-oleoyl-*sn*-glycerol)-phosphono]-2,3,4,5-tetra-*O*-(*p*-methoxybenzyl)-*myo*-inositol (1.198)
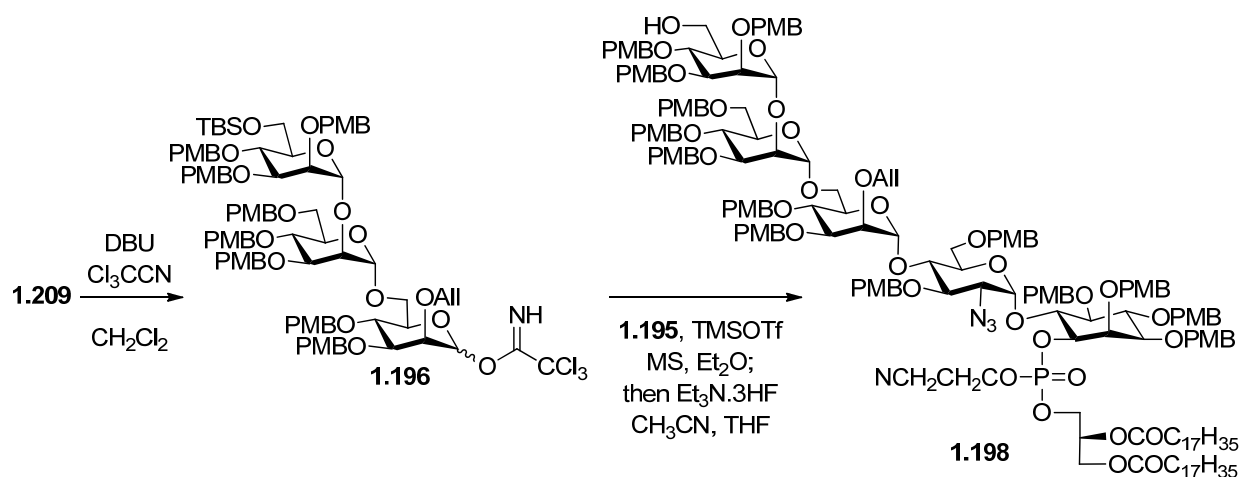
DBU (1 drop) was added to a solution of hemiacetal **1.209** (36 mg, 22.2 μmol) and trichloroacetonitrile (0.25 mL) in anhydrous CH$_2$Cl$_2$ (2 mL) stirring under an Ar atmosphere at 0 °C. After 1 h, the reaction mixture was concentrated in vacuum and purified with a triethylamine-neutralized silica gel column to give **1.196** (36 mg, 92%). A

mixture of the resulting trichloroacetimidate **1.196** (36 mg, 20.4 μmol), acceptor **1.195** (23 mg, 12.6 μmol), and MS 4 Å (10 mg) in anhydrous Et_2O (0.5 mL) was stirred under an Ar atmosphere at rt for 1 h. After cooling to 0 ºC, TMSOTf (0.5 μl, 0.1 equiv) was added and the reaction was stirred for 5 min. Saturated aqueous $NaHCO_3$ and Et_2O were then added, and the resulting mixture was passed through celite to remove MS. After extraction of the aqueous layer with Et_2O 3x, the combined organic phase was dried over Na_2SO_4, concentrated in vacuum, and taken directly to the next step. Thus, crude intermediate **1.197** was dissolved in anhydrous THF-CH_3CN (1:1, 2 mL) and treated with $Et_3N•3HF$ (0.5 mL) under Ar at rt. After stirring overnight, the reaction was quenched by dropwise addition of saturated aqueous $NaHCO_3$. The aqueous layer was extracted 3x with Et_2O, and the combined organic layer was dried over Na_2SO_4, concentrated in vacuum, and purified by silica gel column chromatography to give **1.198** (35 mg, 83%, 2 steps) as a syrup. ^1H NMR (500 MHz, $CDCl_3$, resolved signals): δ 5.67-5.75 (m, 1 H), 5.42 (d, J = 4.0 Hz, 1 H, $GlcN_3$ 1-position), 5.23 (pent, J = 4.5 Hz, 1 H), 5.20 (s, 1 H, Man-III 1-position), 5.13 (dd, J = 2.0, 17.5 Hz, 1 H), 5.08 (d, J = 1.5 Hz, 1 H, Man-I 1-position), 4.99 (dd, J = 2.0, 10.5 Hz, 1 H), 4.94-4.89 (m, 4 H), 4.85-4.79 (m, 5 H, includes Man-II 1-position), 4.74 (d, J = 10.5 Hz, 1 H), 4.69-4.59 (m, 8 H), 4.55-4.47 (m, 9 H), 4.45-4.40 (m, 8 H), 4.37-4.21 (m, 14 H), 4.15-4.09 (m, 4 H), 4.07-4.04 (m, 1 H), 4.01 (t, J = 9.0 Hz, 1 H), 3.92 (t, J = 9.5 Hz, 1 H), 3.87-3.84 (m, 5 H), 3.53-3.48 (m, 4 H), 3.42-3.37 (m, 6 H), 3.33-3.31 (m, 1 H), 3.25 (dd, J = 3.5, 11 Hz, 1 H), 3.20 (dd, J = 3.5, 10 Hz, 1 H), 2.80-2.70 (m, 2 H), 2.82 (t, J = 8.0 Hz, 4 H), 1.60-1.54 (m, 4 H), 1.31-1.25 (m, 56 H), 0.89 (t, J = 7.0 Hz, 6 H). ^{13}C NMR ($CDCl_3$, 125 MHz): δ 173.40, 173.05, 159.43, 159.37, 159.32, 159.29, 159.23, 159.13, 135.49, 131.15, 131.06, 130.99,

130.93, 130.73, 130.59, 130.49, 130.32, 130.18, 129.77, 129.72, 129.622, 129.52, 129.41, 129.28, 129.25, 129.15, 128.77, 116.58, 116.47, 114.10, 114.07, 114.04, 113.98, 113.93, 113.83, 101.09, 99.79 (2 overlapping signals confirmed by HMQC), 97.94, 81.42, 80.76, 80.62, 79.82, 79.85, 79.51, 79.26, 76.61, 76.26, 75.60, 75.25, 75.21, 75.09, 74.99, 74.83, 74.78, 74.62, 74.57, 74.25, 73.48, 73.12, 73.09, 73.00, 72.78, 72.35, 72.05, 72.02, 71.94, 71.86, 71.65, 70.16, 69.58, 69.42, 69.09, 68.47, 66.40, 62.96, 62.67, 62.64, 62.54, 61.72, 55.46, 55.33, 55.31, 55.26, 55.23, 34.33, 34.18, 32.17, 29.96, 29.91, 29.77, 29.61, 29.58, 29.56, 29.38, 29.35, 25.05, 22.93, 19.89, 19.83, 14.36. Configurations of anomeric positions were established as α by coupled ^{13}C NMR J_{CH} values (125 MHz): 101.09 (J_{CH} = 167 Hz, Man-1), 99.79 (J_{CH} = 174 Hz, Man-1), 99.79 (J_{CH} = 174 Hz, Man-1), 97.94 (J_{CH} = 177 Hz, GlcN$_3$-1). ^{31}P NMR (CDCl$_3$, 160 MHz): δ -1.38. $[α]_D^{25}$ = +32° (c 1.0, CHCl$_3$). HR ESI MS: calcd. for $C_{187}H_{245}N_4O_{46}NaP$ [M+Na]$^+$ m/z, 3336.6590; found, 3336.6597.

6-*O*-{[6-*O*-[(2-cyanoethoxy)-[2-(9-fluorenylmethoxycarbonylamino)ethyl]-phosphono]-2,3,4-tri-*O*-(*p*-methoxybenzyl)-α-D-mannopyranosyl]-(1→2)-[3,4,6-tri-*O*-(*p*-methoxybenzyl)-α-D-mannopyranosyl]-(1→6)-[2-*O*-allyl-3,4-di-*O*-(*p*-methoxybenzyl)-α-D-mannopyranosyl]-(1→4)-[2-azido-2-deoxy-3,6-di-*O*-(*p*-methoxybenzyl)-α-D-glucopyranosyl]}-1-*O*-[(2-cyanoethoxy)-(2,3-di-*O*-stearyl-*sn*-glycerol)-phosphono]-2,3,4,5-tetra-*O*-(*p*-methoxybenzyl)-*myo*-inositol (1.199)
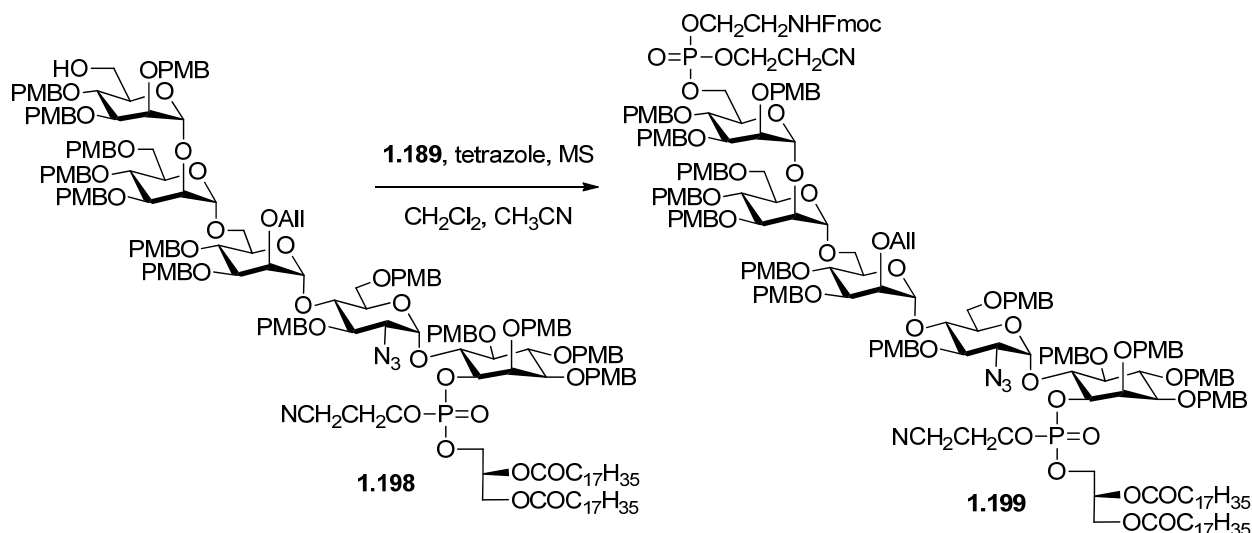
To a solution of pseudopentasaccharide alcohol **1.198** (32 mg, 9.7 µmol) stirring in anhydrous CH_2Cl_2 (1 mL) under Ar at rt was added a solution of freshly prepared phosphoramidite **1.189** (23 mg in dry CH_2Cl_2, 48 µmol) and tetrazole (0.45 M solution in acetonitrile, 216 µl, 97 µmol). After stirring at rt under Ar for 1 h, the reaction was cooled to -40 ºC and treated with *tert*-butyl hydroperoxide (5.5 M solution in decane, 53 µl, 291 µmol). The solution stirred for 1 h at -40 ºC, then Me_2S (43 µl, 582 µmol) was added and stirring continued for 1 h at -40 ºC. The mixture was poured into saturated aqueous $NaHCO_3$ and extracted 3x with CH_2Cl_2. The combined organic layers were dried over Na_2SO_4 and concentrated in vacuum. Purification by silica gel column chromatography afforded **1.199** as a ~1:1 diastereomeric mixture (29 mg, 81%). Preparative HPLC

(Waters Nova-Pak Silica 6 µm, 300 x 19 mm, eluent 35% acetone in hexanes, 10 mL/min, isomer 1-t_R = 14.6 min, isomer 2-t_R = 15.7 min) was used to separate the mixture facilitate characterization. ^{1}H NMR (500 MHz, CDCl$_3$, isomer 1): δ 7.74 (d, J = 7.5 Hz, 2 H), 7.58 (d, J = 7.0 Hz, 1 H), 7.39-7.36 (m, 2 H), 7.32-7.28 (m), 7.11 (m), 7.06-7.04 (m, 2 H), 6.88-6.72 (m), 5.75-5.67 (m, 1 H), 5.53 (t, J = 7.0 Hz, 1 H), 5.42 (d, J = 3.5 Hz, 1 H, GlcN$_3$ 1-position), 5.23 (pent, J = 4.5 Hz, 1 H), 5.20 (s, 1 H, Man-III 1-position), 5.15-5.12 (m, 5 H, includes Man-I 1-position), 5.00 (d, J = 10.5 Hz, 1 H), 4.93-4.89 (m, 2 H), 4.86-4.77 (m, 5 H, includes Man-II 1-position), 4.73 (d, J = 10.5 Hz, 1 H), 4.69-4.56 (m, 8 H), 4.52-4.47 (m, 6 H), 4.45-4.36 (m, 9 H), 4.33-4.21 (m, 17 H), 4.19-4.05 (m, 8 H), 3.02-4.93 (m, 3 H), 3.91-3.86 (m, 7 H), 3.82 (s, 3 H), 3.80-3.79 (m, 3 H), 3.78 (s, 3 H), 3.77 (s, 3 H), 3.76 (s, 6 H), 3.74 (s, 12 H), 3.73 (s, 3 H), 3.72-3.69 (m, 4 H), 3.65 (s, 3 H), 3.64 (s, 3 H), 3.62 (s, 3 H), 3.59-3.49 (m, 5 H), 3.45 (s, 1 H), 3.41 (s, 3 H), 3.39-3.37 (m, 3 H), 3.34-3.32 (m, 2 H), 3.27 (dd, J = 4.0, 10.5 Hz, 1 H), 3.22 (dd, J = 3.5, 10 Hz, 1 H), 2.77-2.69 (m, 2 H), 2.27 (m), 2.05 (m), 1.32-1.22 (m), 0.89 (t, J = 6.5 Hz, 6 H). ^{13}C NMR (CDCl$_3$, 125 MHz): δ 173.40, 173.05, 159.45, 159.38, 159.32, 159.26, 159.20, 156.62, 144.21, 141.49, 135.47, 135.44, 131.19, 131.09, 131.04, 130.94, 130.89, 130.81, 130.67, 130.63, 130.52, 130.49, 130.36, 130.17, 129.84, 129.77, 129.72, 129.64, 129.61, 129.52, 129.48, 129.27, 128.77, 127.88, 127.32, 125.43, 125.27, 120.13, 117.19, 116.65, 116.44, 114.10, 114.07, 114.04, 113.99, 113.92, 113.87, 113.80, 113.78, 100.95, 99.67, 99.56, 97.92, 81.43, 80.61, 79.85, 79.57, 77.73, 76.65, 76.25, 75.57, 75.08, 75.02, 74.92, 74.81, 74.79, 74.59, 74.49, 74.25, 73.44, 73.11, 73.08, 72.79, 72.56, 72.43, 72.16, 71.99, 71.94, 71.86, 71.37, 71.34, 70.09, 69.59, 69.55, 68.96, 68.56, 68.48, 68.21, 67.36, 67.28, 67.10, 66.68, 66.39, 66.35,

63.00, 62.71, 62.68, 62.32, 62.28, 61.74, 55.45, 55.34, 55.30, 55.27, 55.24, 47.39, 41.54, 34.33, 34.18, 32.44, 32.17, 29.95, 29.91, 29.77, 29.60, 29.55, 29.38, 29.3426.63, 25.85, 25.05, 23.66, 22.93, 19.88, 19.83, 19.36, 19.31, 14.35. ^{31}P NMR (CDCl$_3$, 160 MHz): δ -0.32, -1.25. [α]$_D^{25}$ = +6º (*c* 0.25, CHCl$_3$). HR ESI MS: calcd. for C$_{207}$H$_{268}$N$_7$O$_{51}$NaP$_2$ [M+NH$_4$]$^+$ *m/z*, 3729.8068; found, 3729.7986.

6-*O*-{[6-*O*-[(2-cyanoethoxy)-[2-(9-fluorenylmethoxycarbonylamino)ethyl]-phosphono]-2,3,4-tri-*O*-(*p*-methoxybenzyl)-α-D-mannopyranosyl]-(1→2)-[3,4,6-tri-*O*-(*p*-methoxybenzyl)-α-D-mannopyranosyl]-(1→6)-[3,4-di-*O*-(*p*-methoxybenzyl)-α-D-mannopyranosyl]-(1→4)-[2-azido-2-deoxy-3,6-di-*O*-(*p*-methoxybenzyl)-α-D-glucopyranosyl]}-1-*O*-[(2-cyanoethoxy)-(2,3-di-*O*-stearyl-*sn*-glycerol)-phosphono]-2,3,4,5-tetra-*O*-(*p*-methoxybenzyl)-*myo*-inositol (1.200)
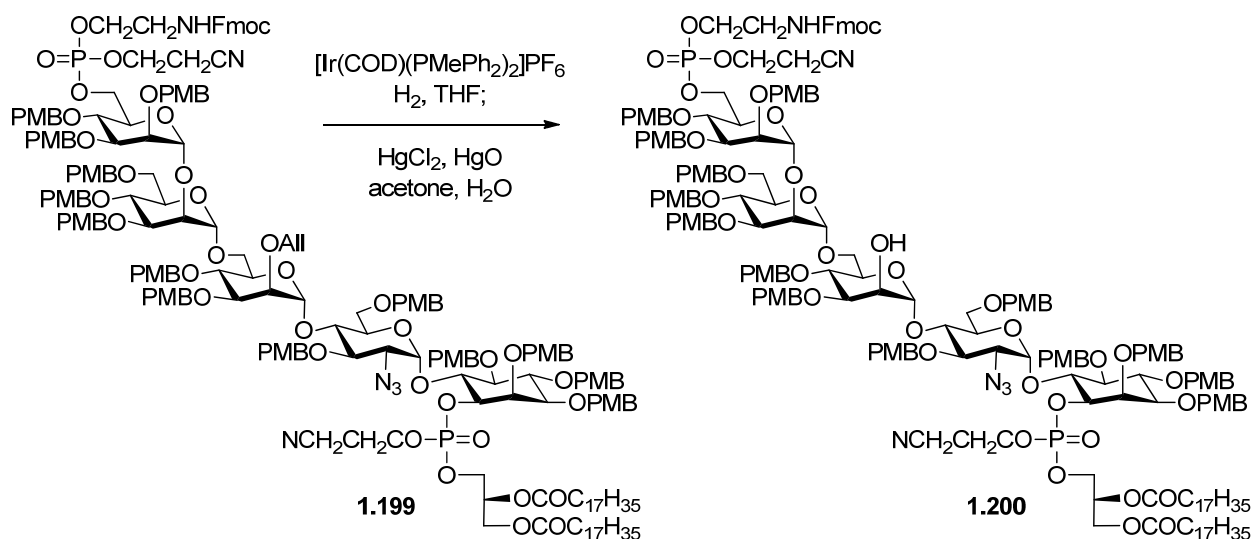
A solution of [Ir(COD)(PMePh$_2$)$_2$]PF$_6$ (9.0 mg, 11 μmol) in anhydrous THF (0.5 mL) was stirred under H$_2$ at rt until the color turned from red to colorless to pale yellow (10 min). After the H$_2$ atmosphere was exchanged with Ar, **1.99** (27 mg, 7.3 μmol, solution in 0.5 mL THF) was added slowly. After 2 h, the reaction was concentrated in vacuum, then

dissolved in acetone/H_2O (9:1, 1 mL) and treated with $HgCl_2$ (6 mg, 22 µmol) and HgO (0.2 mg, 0.7 µmol). Note: The isomerization reaction cannot be monitored by TLC; we took small aliquots of the reaction forward to treatment with Hg(II), then checked MALDI MS to determine if the isomerization was proceeding. The mixture was stirred at rt under an Ar atmosphere for 2 h, then concentrated and purified by silica gel column chromatography to give **1.200** (24 mg, 90%), which was taken directly to the next step after characterization by mass spectrometry. MALDI TOF MS (positive mode): calcd. for $C_{204}H_{260}N_6O_{51}NaP_2$ [M+Na]$^+$ *m/z*, 3694.7; found, 3695.0.

6-*O*-{[6-*O*-[(2-cyanoethoxy)-[2-(9-fluorenylmethoxycarbonylamino)ethyl]-phosphono]-2,3,4-tri-*O*-(*p*-methoxybenzyl)-α-D-mannopyranosyl]-(1→2)-[3,4,6-tri-*O*-(*p*-methoxybenzyl)-α-D-mannopyranosyl]-(1→6)-[3,4-di-*O*-(*p*-methoxybenzyl)-2-*O*-succinyl-α-D-mannopyranosyl]-(1→4)-[2-azido-2-deoxy-3,6-di-*O*-(*p*-methoxybenzyl)-α-D-glucopyranosyl]}-1-*O*-[(2-cyanoethoxy)-(2,3-di-*O*-stearyl-*sn*-glycerol)-phosphono]-2,3,4,5-tetra-*O*-(*p*-methoxybenzyl)-*myo*-inositol (1.201)
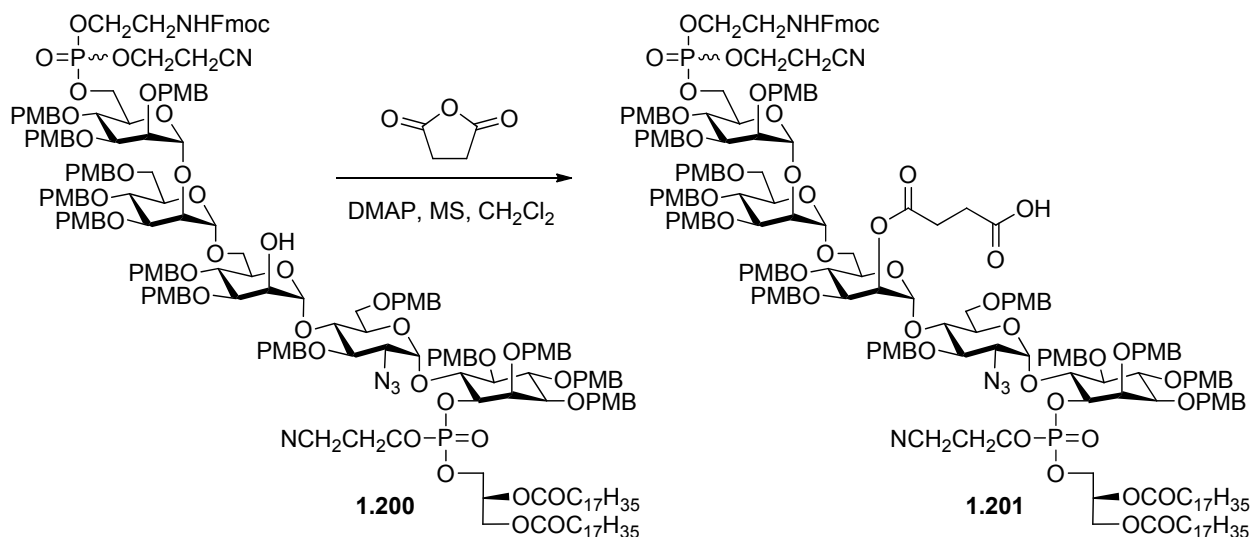
To a mixture of **1.200** (12 mg, 3.2 µmol) and molecular sieves (~10 mg) in CH_2Cl_2 were added succinic anhydride (3.2 mg, 32 µmol) and DMAP (4.0 mg, 32 µmol) at rt under Ar. After stirring for 6 h, additional succinic anhydride (3.2 mg, 32 µmol) and DMAP (4.0 mg, 32 µmol) were added. The reaction was stirred overnight, treated with AcOH, concentrated, and purified by silica gel column chromatography to afford **1.201** (8.1 mg, 67%). ^{1}H NMR (500 MHz, CDCl$_3$, mixture of 2 diastereomers from previous phosphorylation reaction): See Appendix A. ^{31}P NMR (CDCl$_3$, 160 MHz): δ -2.05, -2.36. MALDI TOF MS (positive mode): calcd. for $C_{208}H_{264}N_6O_{54}Na_1P_2$ [M+Na]$^+$ *m/z*, 3794.7; found, 3794.1.

6-*O*-{[6-*O*-[(2-cyanoethoxy)-[2-(9-fluorenylmethoxycarbonylamino)ethyl]-phosphono]-2,3,4-tri-*O*-(*p*-methoxybenzyl)-α-D-mannopyranosyl]-(1→2)-[3,4,6-tri-*O*-(*p*-methoxybenzyl)-α-D-mannopyranosyl]-(1→6)-[3,4-di-*O*-(*p*-methoxybenzyl)-2-*O*-propargylsuccinamide-α-D-mannopyranosyl]-(1→4)-[2-azido-2-deoxy-3,6-di-*O*-(*p*-methoxybenzyl)-α-D-glucopyranosyl]}-1-*O*-[(2-cyanoethoxy)-(2,3-di-*O*-stearyl-*sn*-glycerol)-phosphono]-2,3,4,5-tetra-*O*-(*p*-methoxybenzyl)-*myo*-inositol (1.202)
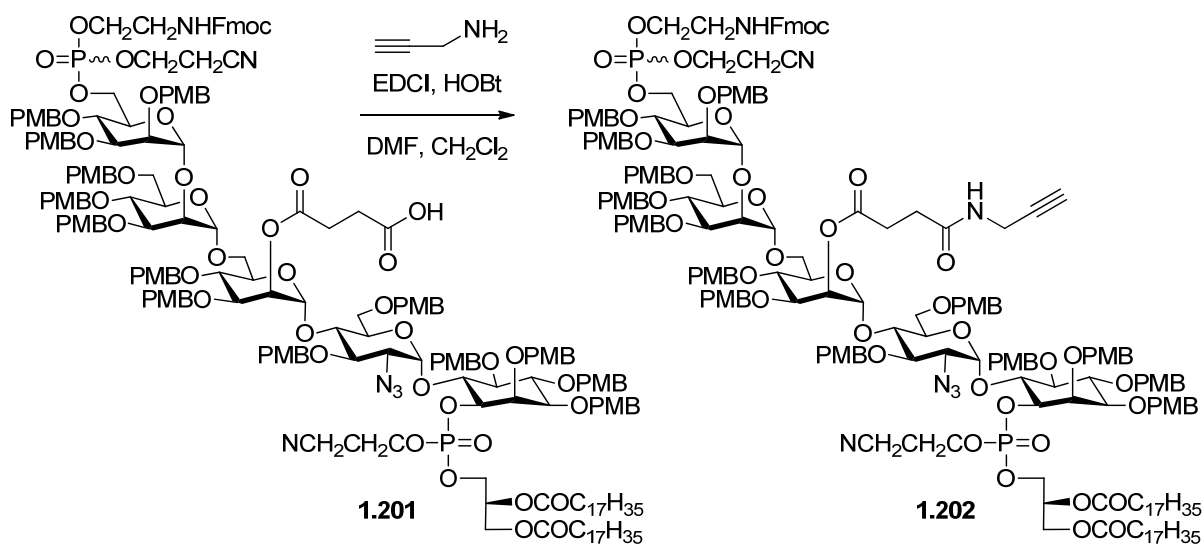
To a solution of **1.201** (2.0 mg, 0.53 µmol) in CH_2Cl_2 stirring under an Ar atmosphere at rt was added HOBt (solution in CH_2Cl_2/DMF, total 0.17 mg, 1.2 µmol) and EDCI (solution in CH_2Cl_2, total 0.23 mg, 1.2 µmol). After stirring for 15 min, propargylamine (solution in CH_2Cl_2, total 0.05 mg, 0.83 µmol) was added. The reaction was stirred overnight, treated with 1 drop AcOH, concentrated, and purified by silica gel column chromatography to afford **1.202** (1.5 mg, 75%). ^{1}H NMR (500 MHz, CDCl$_3$, mixture of 2 diastereomers): See Appendix A. HR ESI MS: calcd. for $C_{211}H_{267}N_7O_{53}Na_2P_2$ [M+2Na]$^{2+}$ *m/z*, 1927.3944; found, 1927.3900.

6-*O*-{[6-*O*-[(2-Aminoethyl)-phosphono]-α-D-mannopyranosyl]-(1→2)-(α-D-mannopyranosyl)-(1→6)-(2-*O*-propargylsuccinamide-α-D-mannopyranosyl)-(1→4)-(2-amino-2-deoxy-α-D-glucopyranosyl)}-1-*O*-[(2,3-di-*O*-stearyl-*sn*-glycerol)-phosphono]-*myo*-inositol (1.111)
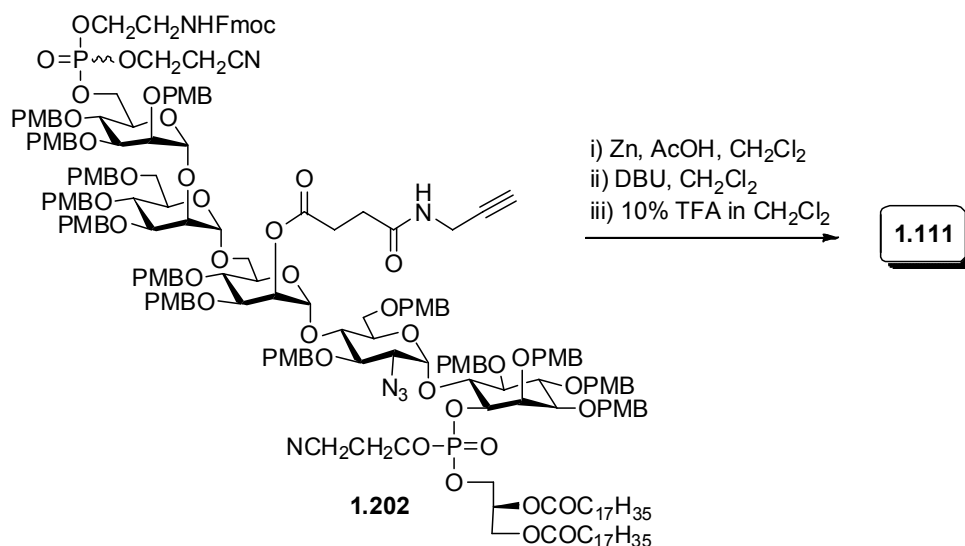
To a solution of **1.202** (1.02 mg, 0.26 µmol) in CH_2Cl_2 (250 µl) was added acetic acid (1 drop) and zinc powder (1 mg). After stirring for 1 h, MALDI TOF MS showed complete reduction of the azide [MALDI TOF MS (positive mode): calcd. for $C_{211}H_{269}N_5O_{53}NaP_2$ [M+Na]$^+$ *m/z*, 3805.8; found, 3805.2]. The mixture was filtered and condensed in vacuum to remove acetic acid, and the resulting residue was re-dissolved in CH_2Cl_2 (250 µl) and treated with DBU (1 µl). The solution stirred for 1 h, after which MALDI TOF MS confirmed removal of the Fmoc and cyanoethyl protecting groups [MALDI TOF MS (positive mode): calcd. for $C_{190}H_{251}N_2O_{51}Na_3P_2$ [M-2H+3Na]$^+$ *m/z*, 3521.6; found, 3522.2]. Then, 20% TFA in CH_2Cl_2 (250 µl) was added directly to the reaction, giving a final concentration of ~10% TFA. After stirring for 30 min, the reaction was co-evaporated with toluene 5 times. Purification of the crude product by Sephadex LH-20 size exclusion chromatography ($CHCl_3$/MeOH/H_2O 3:3:1) gave **1.111** (0.40 mg, 85%).

^{1}H NMR (500 MHz, CDCl$_3$/CD$_3$OD/D$_2$O 3:3:1, anomeric region): δ 5.39 (1 H, GlcNH$_2$-1), 5.35 (2 H), 5.27 (1 H, glyceride CH), 5.18 (1 H, Man-1), 5.11 (1 H, Man-1), 4.97 (1 H, Man-1). ^{31}P NMR (CDCl$_3$, 160 MHz): δ -0.38, -0.35. MALDI TOF MS (positive mode): calcd. for C$_{78}$H$_{139}$N$_3$O$_{37}$Na$_3$P$_2$ [M-2H+3Na]$^+$ *m/z*, 1840.8; found, 1841.4.

6-*O*-{[6-*O*-[(2-cyanoethoxy)-[2-(9-fluorenylmethoxycarbonylamino)ethyl]-phosphono]-2,3,4-tri-*O*-(*p*-methoxybenzyl)-α-D-mannopyranosyl]-(1→2)-[3,4,6-tri-*O*-(*p*-methoxybenzyl)-α-D-mannopyranosyl]-(1→6)-[3,4-di-*O*-(*p*-methoxybenzyl)-2-*O*-biotinylsuccinamide-α-D-mannopyranosyl]-(1→4)-[2-azido-2-deoxy-3,6-di-*O*-(*p*-methoxybenzyl)-α-D-glucopyranosyl]}-1-*O*-[(2-cyanoethoxy)-(2,3-di-*O*-stearyl-*sn*-glycerol)-phosphono]-2,3,4,5-tetra-*O*-(*p*-methoxybenzyl)-*myo*-inositol (1.204)

To a solution of **1.201** (1.8 mg, 0.48 µmol) in CH$_2$Cl$_2$ stirring under an Ar atmosphere at rt was added HOBt (solution in CH$_2$Cl$_2$/DMF, total 0.13 mg, 0.96 µmol) and EDCI

(solution in CH_2Cl_2, total 0.18 mg, 0.96 µmol). After stirring for 15 min, PEG_3-biotin-amine (solution in CH_2Cl_2, total 0.25 mg, 0.63 µmol) was added. The reaction was stirred overnight, treated with 1 drop AcOH, concentrated, and purified by silica gel column chromatography to afford **1.204** (1.4 mg, 70%). MALDI TOF MS: calcd. for $C_{226}H_{296}N_{10}O_{58}NaP_2S$ $[M+Na]^+$ m/z, 4195.0; found, 4195.1.

6-*O*-{[6-*O*-[(2-Aminoethyl)-phosphono]-α-D-mannopyranosyl]-(1→2)-(α-D-mannopyranosyl)-(1→6)-(2-*O*-biotinylsuccinamide-α-D-mannopyranosyl)-(1→4)-(2-amino-2-deoxy-α-D-glucopyranosyl)}-1-*O*-[(2,3-di-*O*-stearyl-*sn*-glycerol)-phosphono]-*myo*-inositol (1.112)
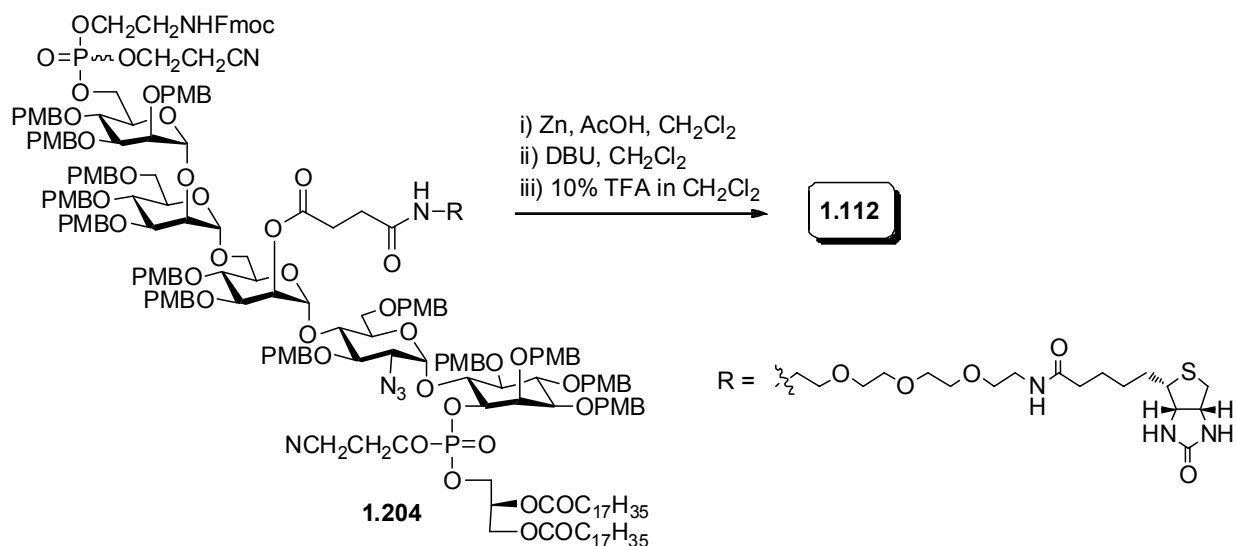
To a solution of **1.204** (0.53 mg, 0.13 µmol) in CH_2Cl_2 (250 µl) was added acetic acid (1 drop) and zinc powder (1 mg). After stirring for 1 h, MALDI TOF MS showed complete reduction of the azide [MALDI TOF MS (positive mode): calcd. for $C_{226}H_{298}N_8O_{58}NaP_2S$ $[M+Na]^+$ m/z, 4169.0; found, 4169.1]. The mixture was filtered and condensed in vacuum to remove acetic acid, and the resulting residue was re-dissolved in CH_2Cl_2 (250 µl) and treated with DBU (1 µl). The solution stirred for 1 h, after which MALDI TOF

MS confirmed removal of the Fmoc and cyanoethyl protecting groups [MALDI TOF MS (positive mode): calcd. for $C_{205}H_{280}N_6O_{56}Na_3P_2S$ [M-2H+3Na]$^+$ *m/z*, 3884.8; found, 3884.7]. Then, 20% TFA in CH_2Cl_2 (250 µl) was added directly to the reaction, giving a final concentration of ~10% TFA. After stirring for 30 min, the reaction was co-evaporated with toluene 5 times. Purification of the crude product by Sephadex LH-20 size exclusion chromatography ($CHCl_3$/MeOH/H_2O 3:3:1) gave **1.112**. MALDI TOF MS (positive mode): calcd. for $C_{93}H_{171}N_6O_{42}P_2$ [M+H]$^+$ *m/z*, 2138.0; found, 2138.5. Also observed in the MALDI TOF MS spectrum (in Appendix A) are several other species corresponding to the desired compound with varying phosphate counterions. The isolated yield of this target could not be calculated due to decomposition of the 2-*O*-ester bond (see section 1.4), although the initial MALDI TOF MS analysis showed a virtually quantitative reaction.

1.5 References

(1)   Ferguson, M. A. J.; Williams, A. F. Cell-surface anchoring of proteins via glycosyl-phosphatidylinositol structures. *Annu. Rev. Biochem.* **1988**, *57*, 121.

(2)   Singer, S. J.; Nicolson, G. L. The fluid mosaic model of the structure of cell membranes. *Science* **1972**, *175*, 720.

(3)   Ferguson, M. A. J.; Homans, S. W.; Dwek, R. A.; Rademacher, T. W. Glycosyl-phosphatidylinositol moiety that anchors Trypanosoma brucei variant surface glycoprotein to the membrane. *Science* **1988**, *239*, 753.

(4)   McConville, M. J.; Ferguson, M. A. J. The structure, biosynthesis and function of glycosylated phosphatidylinositols in the parasitic protozoa and higher eukaryotes. *Biochem. J.* **1993**, *294*, 305.

(5)   Ferguson, M. A. J.; Brimacombe, J. S.; Cottaz, S.; Field, R. A.; Güther, L. S.; Homans, S. W.; McConville, M. J.; Mehlert, A.; Milne, K. G.; Ralton, J. E.; Roy, Y. A.; Schneider, P.; Zitzmann, N. Glycosyl-phosphatidylinositol molecules of the parasite and the host. *Parasitology* **1994**, *108*, S45.

(6)   Englund, P. T. The Structure and Biosynthesis of Glycosyl Phosphatidylinositol Protein Anchors. *Annu. Rev. Biochem.* **1993**, *62*, 121.

(7)   Udenfriend, S.; Kodukula, K. How glycosyl-phosphatidylinositol-anchored membrane proteins are made. *Annu. Rev. Biochem.* **1995**, *64*, 563.

(8)   He, H. T.; Finne, J.; Goridis, C. Biosynthesis, membrane association, and release of N-CAM-120, a phosphatidylinositol-linked form of the neural cell adhesion molecule. *J. Cell Biol.* **1987**, *105*, 2489.

(9)   Eardley, D. D.; Koshland, M. E. Glycosylphosphatidylinositol: a candidate system for interleukin-2 signal transduction. *Science* **1991**, *251*, 78.

(10)   Robinson, P. J.; Millrain, M.; Antoniou, J.; Simpson, E.; Mellor, A. L. A glycophospholipid anchor is required for Qa-2-mediated T cell activation. *Nature* **1989**, *342*, 85.

(11)   Cross, G. A. M. Cellular and Genetic Aspects of Antigenic Variation in Trypanosomes. *Annu. Rev. Immunol.* **1990**, *8*, 83.

(12)   Hwa, K. Glycosyl phosphatidylinositol-linked glycoconjugates: structure, biosynthesis, and function. *Adv. Exp. Med. Biology* **2001**, *491*, 207.

(13)   Paulick, M. G.; Bertozzi, C. R. The glycosylphosphatidylinositol anchor: A complex membrane-anchoring structure for proteins. *Biochemistry* **2008**, *47*, 6991.

(14)   Ferguson, M. A. The structure, biosynthesis and functions of glycosylphosphatidylinositol anchors, and the contributions of trypanosome research. *J. Cell. Sci.* **1999**, *112*, 2799.

(15)   Eisenhaber, B.; Bork, P.; Eisenhaber, F. Post-translational GPI lipid anchor modification of proteins in kingdoms of life: analysis of protein sequence data from complete genomes. *Protein Eng.* **2001**, *14*, 17.

(16)   Sefton, B. M.; Buss, J. E. The covalent modification of eukaryotic proteins with lipid. *J. Cell Biol.* **1987**, *104*, 1449.

(17)   Charollais, J.; Van Der Goot, F. G. Palmitoylation of membrane proteins. *Mol. Membr. Biol.* **2009**, *26*, 55.

(18) Johnson, D. R.; Bhatnagar, R. S.; Knoll, L. J.; Gordon, J. I. Genetic and biochemical studies of protein N-myristoylation. *Annu. Rev. Biochem.* **1994**, *63*, 869.

(19) Low, M. G.; Finean, J. B. Release of alkaline phosphatase from membranes by a phosphatidylinositol-specific phospholipase C. *Biochem. J.* **1977**, *167*, 281.

(20) Low, M. G.; Finean, J. B. Specific release of plasma membrane enzymes by a phosphatidylinositol-specific phospholipase C. *Biochim. Biophys. Acta* **1978**, *508*, 565.

(21) Low, M. G.; Zilversmit, D. B. Role of phosphatidylinositol in attachment of alkaline phosphatase to membranes. *Biochemistry* **1980**, *19*, 3913.

(22) Ikezawa, H.; Yamanegi, M.; Taguchi, R.; Miyashita, T.; Ohyabu, T. Studies on phosphatidylinositol phosphodiesterase (phospholipase C type) of Bacillus cereus: I. Purification, properties and phosphatase-releasing activity. *Biochim. Biophys. Acta* **1976**, *450*, 154.

(23) Taguchi, R.; Asahi, Y.; Ikezawa, H. Ectoenzyme release from rat liver and kidney by phosphatidylinositol-specific phospholipase C. *J. Biochem.* **1980**, *97*, 911.

(24) Slein, M. W.; Logan, G. F. Mechanism of action of the toxin of Bacillus anthracis I. Effect in vivo on some blood serum components. *J. Bacteriol.* **1960**, *80*, 77.

(25) Slein, M. W.; Logan, G. F. Mechanism of action of the toxin of Bacillus anthracis II. Alkaline phosphatasemia produced by culture *J. Bacteriol.* **1962**, *83*, 359.

(26) Slein, M. W.; Logan, G. F. Partial purification and properties of two phospholipases of Bacillus cereus. *J. Bacteriol.* **1963**, *85*, 369.

(27) Slein, M. W.; Logan, G. F. Characterization of the phospholipases of Bacillus cereus and their effects on erythrocytes, bone, and kidney cells. *J. Bacteriol.* **1965**, *90*, 69.

(28) Low, M. G. Biochemistry of the glycosyl-phosphatidylinositol membrane protein anchors. *Biochem. J.* **1987**, *244*, 1.

(29) Futerman, A. H.; Low, M. G.; Ackermann, K. E.; Sherman, W. R.; Silman, I. Identification of covalently bound inositol in the hydrophobic membrane-anchoring domain of acetylcholinesterase. *Biochem. Biophys. Res. Commun.* **1985**, *129*, 312.

(30) Roberts, W. L.; Rosenberry, T. L. Identification of covalently attached fatty acids in the hydrophobic membrane-binding domain of human erythrocyte acetylcholinesterase. *Biochem. Biophys. Res. Commun.* **1985**, *133*, 621.

(31) Campbell, D. G.; Gagnon, J.; Reid, K. B. M.; Williams, A. F. Rat brain Thy-1 glycoprotein. The amino acid sequence, disulphide bonds and an unusual hydrophobic region. *Biochem. J.* **1981**, *195*, 15.

(32) Tse, A. G. D.; Barclay, A. N.; Watts, A.; Williams, A. F. A glycophospholipid tail at the carboxyl terminus of the Thy-1 glycoprotein of neurons and thymocytes. *Science* **1985**, *230*, 1003.

(33) Holder, A. A. Carbohydrate is linked through ethanolamine to the C-terminal amino acid of Trypanosoma brucei variant surface glycoprotein. *Biochem. J.* **1983**, *209*, 261.

(34)   Holder, A. A. Characterisation of the cross-reacting carbohydrate groups on two variant surface glycoproteins of Trypanosoma brucei. *Mol. Biochem. Parasitol.* **1983**, *7*, 331.

(35)   Ferguson, M. A.; Haldar, K.; Cross, G. A. Trypanosoma brucei variant surface glycoprotein has a sn-1,2-dimyristyl glycerol membrane anchor at its COOH terminus. *J. Biol. Chem.* **1985**, *260*, 4963.

(36)   Ferguson, M. A.; Low, M. G.; Cross, G. A. Glycosyl-sn-1,2-dimyristylphosphatidylinositol is covalently linked to Trypanosoma brucei variant surface glycoprotein. *J. Biol. Chem.* **1985**, *260*, 14547.

(37)   Parthasarathy, R.; Eisenberg, F. The inositol phospholipids: a stereochemical view of biological activity. *Biochem. J.* **1986**, *235*, 313.

(38)   Ikezawa, H. Glycosylphosphatidylinositol (GPI)-Anchored Proteins. *Biol. Pharm. Bull.* **2002**, *25*, 409.

(39)   Almeida, I. C.; Camargo, M. M.; Procópio, D. O.; Silva, L. S.; Mehlert, A.; Travassos, L. R.; Gazzinelli, R. T.; Ferguson, M. A. J. Highly purified glycosylphosphatidylinositols from Trypanosoma cruzi are potent proinflammatory agents. *EMBO J.* **2000**, *19*, 1476.

(40)   Tiede, A.; Bastisch, I.; Schubert, J.; Orlean, P.; Schmidt, R. E. Biosynthesis of glycosylphosphatidylinositols in mammals and unicellular microbes. *Biol. Chem.* **1999**, *380*, 503.

(41)   Masterson, W. J.; Doering, T. L.; Hart, G. W.; Englund, P. T. A novel pathway for glycan assembly: Biosynthesis of the glycosyl-phosphatidylinositol anchor of the trypanosome variant surface glycoprotein. *Cell* **1989**, *56*, 793.

(42) Menon, A. K.; Schwarz, R. T.; Mayor, S.; Cross, G. A. Cell-free synthesis of glycosyl-phosphatidylinositol precursors for the glycolipid membrane anchor of Trypanosoma brucei variant surface glycoproteins. Structural characterization of putative biosynthetic intermediates. *J. Biol. Chem.* **1990**, *265*, 9033.

(43) Stevens, V. L.; Zhang, H. Coenzyme A dependence of glycosylphosphatidylinositol biosynthesis in a mammalian cell-free system. *J. Biol. Chem.* **1994**, *269*, 31397.

(44) Güther, M. L.; Ferguson, M. A. The role of inositol acylation and inositol deacylation in GPI biosynthesis in Trypanosoma brucei. *EMBO J.* **1995**, *14*, 3080.

(45) M L Güther, W. J. M., and M A Ferguson The effects of phenylmethylsulfonyl fluoride on inositol-acylation and fatty acid remodeling in African trypanosomes. *J. Biol. Chem.* **1994**, *269*, 18694.

(46) Hong, Y.; Nagamune, K.; Morita, Y. S.; Nakatani, F.; Ashida, H.; Maeda, Y.; Kinoshita, T. Removal or maintenance of inositol-linked acyl chain in glycosylphosphatidylinositol is critical in Trypanosome life cycle. *J. Biol. Chem.* **2006**, *281*, 11595.

(47) Ikezawa, H. GPI-anchored proteins. *Biol. Pharm. Bull.* **2002**, *25*, 409.

(48) Kinoshita, T.; Inoue, N. Dissecting and manipulating the pathway for glycosylphos-phatidylinositol-anchor biosynthesis. *Curr. Opin. Chem. Biol.* **2000**, *4*, 632.

(49) Takeda, J.; Kinoshita, T. GPI-anchor biosynthesis. *Trends Biochem. Sci.* **1995**, *20*, 367.

(50)   Amthauer, R.; Kodukula, K.; Gerber, L.; Udenfriend, S. Evidence that the putative COOH-terminal signal transamidase involved in glycosylphosphatidylinositol protein synthesis is present in the endoplasmic reticulum. *PNAS* **1993**, *90*, 3973.

(51)   Chen, R.; Knez, J. J.; Merrick, W. C.; Medof, M. E. Comparative efficiencies of C-terminal signals of native glycophosphatidylinositol (GPI)-anchored proproteins in conferring GPI-anchoring. *J. Cell. Biochem.* **2002**, *84*, 68.

(52)   Cross, G. A. M. Identification, purification and properties of clone-specific glycoprotein antigens constituting the surface coat of Trypanosoma brucei. *Parasitology* **1975**, *71*, 393.

(53)   Caras, I. W.; Weddell, G. N.; Davitz, M. A.; Nussenzweig, V.; Martin, D. W., Jr. Signal for attachment of a phospholipid membrane anchor in decay accelerating factor. *Science* **1987**, *238*, 1280.

(54)   Xia, M. Q.; Tone, M.; Packman, L.; Hale, G.; Waldmann, H. Characterization of the CAMPATH-1 (CDw52) antigen: biochemical analysis and cDNA cloning reveal an unusually small peptide backbone. *Eur. J. Immunol.* **1991**, *21*, 1677.

(55)   Tanaka, S.; Maeda, Y.; Tashima, Y.; Kinoshita, T. Inositol deacylation of glycosylphosphatidylinositol-anchored proteins Is mediated by mammalian PGAP1 and yeast Bst1p. *J. Biol. Chem.* **2004**, *279*, 14256.

(56)   Fujita, M.; Yoko-o, T.; Jigami, Y. Inositol deacylation by Bst1p is required for the quality control of glycosylphosphatidylinositol-anchored proteins. *Mol. Biol. Cell* **2006**, *17*, 834.

(57)   Deeg, M. A.; Humphrey, D. R.; Yang, S. H.; Ferguson, T. R.; Reinhold, V. N.; Rosenberry, T. L. Glycan components in the glycoinositol phospholipid anchor of

human erythrocyte acetylcholinesterase. Novel fragments produced by trifluoroacetic acid. *J. Biol. Chem.* **1992**, *267*, 18573.

(58)   Roberts, W. L.; Santikarn, S.; Reinhold, V. N.; Rosenberry, T. L. Structural characterization of the glycoinositol phospholipid membrane anchor of human erythrocyte acetylcholinesterase by fast atom bombardment mass spectrometry. *J. Biol. Chem.* **1988**, *263*, 18776.

(59)   Treumann, A.; Lifely, M. R.; Schneider, P.; Ferguson, M. A. J. Primary structure of CD52 *J. Biol. Chem.* **1995**, *270*, 6088.

(60)   Field, M. C.; Menon, A. K.; Cross, G. A. M. A glycosylphosphatidylinositol protein anchor from procyclic stage Trypanosoma brucei: lipid structure and biosynthesis. *EMBO J.* **1991**, *10*, 2731.

(61)   Ferguson, M. A. J.; Murray, P.; Rutherford, H.; McConville, M. J. A simple purification of procyclic acidic repetitive protein and demonstration of a sialylated glycosyl-phosphatidylinositol membrane anchor. *Biochem. J.* **1993**, *291*, 51.

(62)   Abuin, G.; Cuoto, A. S.; de Lederkremer, R. M.; Casal, O. L.; Galli, C.; Colli, W.; Alves, M. J. M. Trypanosoma cruzi:The Tc-85 Surface Glycoprotein Shed by Trypomastigotes Bears a Modified Glycosylphosphatidylinositol Anchor. *Exp. Parasitol.* **1996**, *82*, 290.

(63)   Gerold, P.; Schofield, L.; Blackman, M. J.; Holder, A. A.; Schwarz, R. T. Structural analysis of the glycosyl-phosphatidylinositol membrane anchor of the merozoite surface proteins-1 and -2 of Plasmodium falciparum. *Mol. Biochem. Parasitol.* **1996**, *75*, 131.

(64) Luhrs, C. A.; Slomiany, B. L. A human membrane-associated folate binding protein is anchored by a glycosyl-phosphatidylinositol tail. *J. Biol. Chem.* **1989**, *264*, 21446.

(65) Mayor, S.; Menon, A. K.; Cross, G. A. M. Glycolipid precursors for the membrane anchor of Trypanosoma brucei variant surface glycoproteins. II. Lipid structures of phosphatidylinositol-specific phospholipase C sensitive and resistant glycolipids. *J. Biol. Chem.* **1990**, *265*, 6174.

(66) Walter, E. I.; Roberts, W. L.; Rosenberry, T. L.; Ratnoff, W. D.; Medof, M. E. Structural basis for variations in the sensitivity of human decay accelerating factor to phosphatidylinositol-specific phospholipase C cleavage. *Immunol.* **1990**, *144*, 1030.

(67) Ralton, J. E.; McConville, M. J. Delineation of three pathways of glycosylphosphatidylinositol biosynthesis in Leishmania mexicana : Precursors from different pathways are assembled on distinct pools of phosphatidylinositol and undergo fatty acid remodeling. *J. Biol. Chem.* **1998**, *273*, 4245.

(68) Reggiori, F.; Canivenc-Gansel, E.; Conzelmann, A. Lipid remodeling leads to the introduction and exchange of defined ceramides on GPI proteins in the ER and Golgi of Saccharomyces cerevisiae. *EMBO J.* **1997**, *16*, 3506.

(69) Masterson, W. J.; Raper, J.; Doering, T. L.; Hart, G. W.; Englund, P. T. Fatty acid remodeling: A novel reaction sequence in the biosynthesis of trypanosome glycosyl phosphatidylinositol membrane anchors. *Cell* **1990**, *62*, 73.

(70) Mayor, S.; Riezman, H. Sorting GPI-anchored proteins. *Nature Rev. Mol. Cell Biol.* **2004**, *5*, 110.

(71)   Trotter, J.; Klein, C.; Kramer, E. GPI-anchored proteins and glycosphingolipid-rich rafts: Platforms for adhesion and signaling. *Neuroscientist* **2000**, *6*, 271.

(72)   Brown, D. A.; Rose, J. K. Sorting of GPI-anchored proteins to glycolipid-enriched membrane subdomains during transport to the apical cell surface. *Cell* **1992**, *68*, 533.

(73)   Montecucco, C.; Papini, E.; Schiavo, G. Bacterial protein toxins penetrate cells via a four-step mechanism. *FEBS Lett.* **1994**, *346*, 92.

(74)   Braun, V.; Focareta, T. Pore-forming bacterial protein hemolysins (cytolysins) *Crit. Rev. Microbiol.* **1991**, *18*, 115.

(75)   Low, M.; Saltiel, A. Structural and functional roles of glycosyl-phosphatidylinositol in membranes. *Science* **1988**, *239*, 268.

(76)   Low, M. G. Glycosyl-phosphatidylinositol: a versatile anchor for cell surface proteins. *FASEB J.* **1989**, *3*, 1600.

(77)   Barboni, E.; Rivero, B.; George, A.; Martin, S.; Renoup, D.; Hounsell, E.; Barber, P.; Morris, R. The glycophosphatidylinositol anchor affects the conformation of Thy-1 protein. *J. Cell. Sci.* **1995**, *108*, 487.

(78)   Homans, S. W.; Edge, C. J.; Ferguson, M. A. J.; Dwek, R. A.; Rademacher, T. W. Solution structure of the glycosylphosphatidylinositol membrane anchor glycan of Trypanosoma brucei variant surface glycoprotein. *Biochemistry* **1989**, *28*, 2881.

(79)   Rademacher, T. W.; Edge, C. J.; Dwek, R. A. Dropping anchor with the lipophosphoglycans. *Curr. Biol.* **1991**, *1*, 41.

(80)   Lehto, M. T.; Sharom, F. J. Proximity of the protein moiety of a GPI-anchored protein to the membrane surface: A FRET study. *Biochemistry* **2002**, *41*, 8368.

(81)   Jones, D. R.; Varela-Nieto, I. The role of glycosyl–phosphatidylinositol in signal transduction. *Int. J. Biochem. Cell Biol.* **1997**, *30*, 313.

(82)   Gaulton, G. N.; Pratt, J. C. Glycosylated phosphatidylinositol molecules as second messengers. *Seminars Immunol.* **1994**, *6*, 97.

(83) Field, M. C. Is there evidence for phospho-oligosaccharides as insulin mediators? *Glycobiology* **1997**, *7*, 161.

(84)   Taguchi, R.; Hamakawa, N.; Harada-Nishida, M.; Fukui, T.; Nojima, K.; Ikezawa, H. Microheterogeneity in glycosylphosphatidylinositol anchor structures of bovine liver 5'-nucleotidase. *Biochemistry* **1994**, *33*, 1017.

(85)   Murakata, C.; Ogawa, T. A total synthesis of GPI anchor of trypanosoma brucei. *Tetrahdron Lett.* **1991**, *32*, 671.

(86)   Murakata, C.; Ogawa, T. Stereoselective total synthesis of the glycosyl phosphatidylinositol (GPI) anchor of *Trypanosoma brucei*. *Carbohydr. Res.* **1992**, *235*, 95.

(87)   Baeschlin, D. K.; Chaperon, A. R.; Charbonneau, V.; Green, L. G.; Ley, S. V.; Lücking, U.; Walther, E. Rapid assembly of oligosaccharides: Total synthesis of a glycosylphosphatidylinositol anchor of Trypanosoma brucei. *Angew. Chem. Int. Ed. Engl.* **1998**, *37*, 3423.

(88)   Baeschlin, D. K.; Chaperon, A. R.; Green, L. G.; Hahn, M. G.; Ince, S. J.; Ley, S. V. 1,2-Diacetals in synthesis: Total synthesis of a glycosylphosphatidylinositol anchor of Trypanosoma brucei. *Chem. Eur. J.* **2000**, *6*, 172.

(89)   Campbell, A. S.; Fraser-Reid, B. First synthesis of a fully phosphorylated GPI membrane anchor: Rat brain Thy-1. *J. Am. Chem. Soc.* **1995**, *117*, 10387.

(90)   Udodong, U. E.; Madsen, R.; Roberts, C.; Fraser-Reid, B. A ready, convergent synthesis of the heptasaccharide GPI membrane anchor of rat brain Thy-1 glycoprotein. *J. Am. Chem. Soc.* **1993**, *115*, 7886.

(91)   Pekari, K.; Schmidt, R. R. A variable concept for the preparation of branched glycosyl phosphatidyl inositol anchors. *J. Org. Chem.* **2003**, *68*, 1295.

(92)   Mayer, T. G.; Kratzer, B.; Schmidt, R. R. Synthesis of a GPI anchor of yeast (*Saccharomyces cerevisae*). *Angew. Chem. Int. Ed. Engl.* **1994**, *33*, 2177.

(93)   Mayer, T. G.; Schmidt, R. R. Glycosyl phosphatidylinositol (GPI) anchor synthesis based on versatile building blocks - total synthesis of a GPI anchor of yeast. *Eur. J. Org. Chem.* **1999**, 1153.

(94)   Pekari, K.; Tailler, D.; Weingart, R.; Schmidt, R. R. Synthesis of the fully phosphorylated GPI anchor pseudohexasaccharide of Toxoplasma gondii. *J. Org. Chem.* **2001**, *66*, 7432.

(95)   Lu, J.; Jayaprakash, K. N.; Fraser-Reid, B. First synthesis of a malarial prototype: a fully lipidated and phosphorylated GPI membrane anchor. *Tetrahdron Lett.* **2004**, *45*, 879.

(96)   Hewitt, M. C.; Snyder, D. A.; Seeberger, P. H. Rapid synthesis of a glycosylphosphatidylinositol-based malaria vaccine using automated solid-phase oligosaccharide synthesis. *J. Am. Chem. Soc.* **2002**, *124*, 13434.

(97)   Schofield, L.; Hewitt, M. C.; Evans, K.; Siomos, M.-A.; Seeberger, P. H. Synthetic GPI as a candidate anti-toxic vaccine in a model of malaria. *Nature* **2002**, *418*, 785.

(98) Wu, X.; Guo, Z. Convergent synthesis of a fully phosphorylated GPI anchor of the CD52 antigen. *Org. Lett.* **2007**, *9*, 4311.

(99) Xue, J.; Guo, Z. Convergent synthesis of a GPI containing an acylated inositol. *J. Am. Chem. Soc.* **2003**, *125*, 16334.

(100) Xue, J.; Shao, N.; Guo, Z. First total synthesis of a GPI-anchored peptide. *J. Org. Chem.* **2003**, *68*, 4020.

(101) Yashunsky, D. V.; Borodkin, V. S.; Ferguson, M. A. J.; Nikolaev, A. V. The Chemical Synthesis of Bioactive Glycosylphosphatidylinositols from Trypanosoma cruzi Containing an Unsaturated Fatty Acid in the Lipid. *Angew. Chem. Int. Ed. Engl.* **2005**, *45*, 468.

(102) Gigg, R.; Gigg, J. In *Glycopeptides and related compounds: synthesis, analysis, and applications*; Large, D. G., Warren, C. D., Eds.; Marcel Dekker, Inc.: New York, 1997, p 327.

(103) Guo, Z.; Bishop, L. Chemical synthesis of GPIs and GPI-anchored glycopeptides. *Eur. J. Org. Chem.* **2004**, 3585.

(104) Sureshan, K. M.; Shashidhar, M. S.; Praveen, T.; Das, T. Regioselective protection and deprotection of inositol hydroxyl groups. *Chem. Rev.* **2003**, *103*, 4477.

(105) Garegg, P. J.; Iverson, T.; Johansson, R.; Lindberg, B. Synthesis of some mono-O-benzyl- and penta-O-methyl-myo-inositols. *Carbohydr. Res.* **1984**, *130*, 322.

(106) Martín-Lomas, M.; Khiar, N.; García, S.; Koessler, J.-L.; Nieto, P. M.; Rademacher, T. W. Inositolphosphoglycan mediators structurally related to

glycosyl phosphatidylinositol anchors: Synthesis, structure and biological activity. *Chem. Eur. J.* **2000**, *6*, 3608.

(107) Murakata, C.; Ogawa, T. Synthetic study on glycophosphatidyl inositol (GPI) anchor of trypanosoma brucei: Glycoheptaosyl core. *Tetrahdron Lett.* **1990**, *31*, 2439.

(108) Gou, D.-M.; Liu, Y.-C.; Chen, C.-S. An efficient chemoenzymic access to optically active *myo*-inositol polyphosphates. *Carbohydr. Res.* **1992**, *234*, 51.

(109) Xue, J.; Guo, Z. Convergent synthesis of an inner core GPI of sperm CD52. *Bioorg. Med. Chem. Lett.* **2002**, *12*, 2015.

(110) Jia, Z. J.; Olsson, L.; Fraser-Reid, B. *J. Chem. Soc., Perkin Trans. 1* **1990**, 631.

(111) Conrad, R. M.; Grogan, J. M. Stereoselective synthesis of myo-inositol via ring-closing metathesis: A building block for glycosylphosphatidylinositol (GPI) anchor synthesis. *Org. Lett.* **2002**, *4*, 1359.

(112) Hori, H.; Nishida, Y.; Ohrui, H.; Meguro, H. Regioselective de-O-benzylation with Lewis acids. *J. Org. Chem.* **1989**, *54*, 1346.

(113) Grundler, G.; Schmidt, R. R. Glycosylimidate, 13. Anwendung des trichloracetimidat-verfahrens auf 2-azidoglucose- und 2-azidogalactose-derivate. *Leibigs Ann. Chem.* **1984**, 1826.

(114) Crossman, A.; Brimacombe, J. S.; Ferguson, M. A. J. Parasite glycoconjugates. Part 7.1 Synthesis of further substrate analogues of early intermediates in the biosynthetic pathway of glycosylphosphatidylinositol membrane anchors. *J. Chem. Soc., Perkin Trans. 1* **1997**, 2769.

(115) Cottaz, S.; Brimacombe, J. S.; Ferguson, M. A. J. Parasite glycoconjugates. Part 1. The synthesis of some early and related intermediates in the biosynthetic pathway of glycosyl-phosphatidylinositol membrane anchors. *J. Chem. Soc., Perkin Trans. 1* **1993**, 2945.

(116) Garegg, P. J.; Konradsson, P.; Oscarson, S.; Ruda, K. Synthesis of part of a proposed insulin second messenger glycosylinositol phosphate and the inner core of glycosylphosphatidylinositol anchors. *Tetrahdron* **1997**, *53*, 17727.

(117) Alper, P. B.; Hung, S.-C.; Wong, C.-H. Metal catalyzed diazo transfer for the synthesis of azides from amines. *Tetrahedron Lett.* **1996**, *37*, 6029.

(118) Lemieux, R. U.; Hendriks, K. B.; Stick, R. V. Halide ion catalyzed glycosidation reactions. Syntheses of .alpha.-linked disaccharides. *J. Am. Chem. Soc.* **1976**, *97*, 4056.

(119) Madsen, R.; Udodong, U. E.; Roberts, C.; Mootoo, D. R.; Konradsson, P.; Fraser-Reid, B. Studies related to synthesis of glycophosphatidylinositol membrane-bound protein anchors. 6. Convergent assembly of subunits. *J. Am. Chem. Soc.* **1995**, *117*, 1554.

(120) Verduyn, R.; Elie, C. J. J.; Dreef, C. E.; Marel, G. A. v. d.; van Boom, J. H. Synthesis of a highly unsaturated fatty acid moiety of lipo-oligosaccharides determining host-specificity in Rhizobium. *Recl. Trav. Chim. Pays-Bas.* **1990**, *109*.

(121) Cottaz, S.; Brimacombe, J. S.; Ferguson, M. A. J. Synthesis of a partially protected 1D-6-O-(2-azido-2-deoxy-.alpha.-D-glucopyranosyl)-myo-inositol: a useful precursor of glycosylphosphatidylinositols and related compounds. *Carbohydr. Res.* **1995**, *270*, 85.

(122) Frick, W.; Bauer, A.; Bauer, J.; Wied, S.; Müller, G. Structure−activity relationship of synthetic phosphoinositolglycans mimicking metabolic insulin action. *J. Am. Chem. Soc.* **1998**, *37*, 13421.

(123) Bannwarth, W.; Trzeciak, A. A simple and effective chemical phosphorylation procedure for biomolecules. *Helv. Chim. Acta* **1987**, *70*, 175.

(124) Campbell, A. S.; Fraser-Reid, B. Support studies for installing the phosphodiester residues of the Thy-1 glycoprotein membrane anchor. *Bioorg. Med. Chem.* **1994**, *2*, 1209.

(125) Nikolaev, A. V.; Ivanova, I. A.; Shibaev, V. N. The stepwise synthesis of oligo(glycosyl phosphates) via glycosyl hydrogenphosphonates. The chemical synthesis of oligomeric fragments from Hansenula capsulata Y-1842 exophosphomannan and from Escherichia coli K51 capsular antigen. *Carbohydr. Res.* **1993**, *242*, 91.

(126) Hewitt, M. C.; Snyder, D. A.; Seeberger, P. H. Rapid Synthesis of a Glycosylphosphatidylinositol-Based Malaria Vaccine Using Automated Solid-Phase Oligosaccharide Synthesis. *J. Am. Chem. Soc.* **2002**, *124*, 13434.

(127) Reichardt, N.-C.; Martín-Lomas, M. A Practical Solid-Phase Synthesis of Glycosylphosphatidylinositol Precursors. *Angew. Chem. Int. Ed. Engl.* **2003**, *42*, 4674.

(128) Yashunsky, D. V.; Borodkin, V. S.; Ferguson, M. A. J.; Nikolaev, A. V. The chemical synthesis of bioactive glycosylphosphatidylinositols from Trypanosoma cruzi containing an unsaturated fatty acid in the lipid. *Angew. Chem. Int. Ed. Engl.* **2006**, *45*, 468.

(129) Kolb, H. C.; Finn, M. G.; Sharpless, B. Click chemistry: Diverse chemical function from a few good reactions. *Angew. Chem. Int. Ed. Engl.* **2001**, *40*, 2004.

(130) Dawson, P.; Muir, T.; Clark-Lewis, I.; Kent, S. Synthesis of proteins by native chemical ligation. *Science* **1994**, *266*, 776.

(131) Mootoo, D. R.; Konradsson, P.; Udodong, U.; Fraser-Reid, B. Armed and disarmed n-pentenyl glycosides in saccharide couplings leading to oligosaccharides. *J. Am. Chem. Soc.* **1988**, *110*, 5583.

(132) Xue, J.; Liu, P.; Pan, Y.; Guo, Z. A total synthesis of OSW-1. *J. Org. Chem.* **2008**, *73*, 157.

(133) Hsu, T.-L.; Hanson, S. R.; Kishikawa, K.; Wang, S.-K.; Sawa, M.; Wong, C.-H. Alkynyl sugar analogs for the labeling and visualization of glycoconjugates in cells. *Proc. Natl. Acad. Sci. U.S.A.* **2007**, *104*, 2614.

(134) Green, N. M. Avidin. 1. The use of [14C]biotin for kinetic studies and for assay. *Biochem. J.* **1963**, *89*, 585.

(135) Schmidt, R. R.; Michel, J. Facile synthesis of alpha- and beta-o-Glycosyl Imidates; preparation of glycosides and disaccharides. *Angew. Chem. Int. Ed. Engl.* **1980**, *19*, 731.

(136) Lee, J.; Cha, J. K. Selective cleavage of allyl ethers. *Tetrahedron Lett.* **1996**, *37*, 3663.

(137) Oltvoort, J. J., Van Boeckel, C. A. A., De Koning, J. H., Van Boom, J. H. Use of the cationic iridium complex 1,5-cyclooctadiene-bis[methyldiphenylphosphine]-iridium hexafluorophosphate in carbohydrate chemistry: Smooth isomerization of allyl ethers to 1-propenyl ethers *Synthesis* **1981**, 305.

(138) Sim, M. M.; Kondo, H.; Wong, C. H. Synthesis of dibenzyl glycosyl phosphites using dibenzyl N,N-diethylphosphoramidite as phosphitylating reagent: an effective route to glycosyl phosphates, nucleotides, and glycosides. *J. Am. Chem. Soc.* **1993**, *115*, 2260.

(139) Sharkey, P. F.; Eby, R.; Schuerch, C. Chemical synthesis of alpha(1→2)-d-glucopyranan. *Carbohydr. Res.* **1981**, *96*, 223.

(140) Crich, D.; Banerjee, A. Stereocontrolled synthesis of the d- and l-glycero-beta-d-manno-heptopyranosides and their 6-deoxy analogues. Synthesis of Methyl alpha-l-rhamno-pyranosyl-(1-3)-d-glycero-beta-d-manno-heptopyranosyl- (1-3)-6-deoxy-glycero-beta-d-manno-heptopyranosyl-(1-4)-alpha-l- rhamno-pyranoside, a tetrasaccharide subunit of the lipopolysaccharide from Plesimonas shigelloides. *J. Am. Chem. Soc.* **2006**, *128*, 8078.

(141) Garegg, P. J.; Maron, L. Improved synthesis of 3,4,6-tri-O-benzyl-alpha-D-mannopyranosides. *Acta Chem. Scand., Ser. B* **1979**, *B33*, 39.

(142) Crich, D.; Sun, S. Direct chemical synthesis of β-mannopyranosides and other glycosides via glycosyl triflates *Tetrahedron* **1998**, *54*, 8321.

(143) Crich, D.; Cai, W. Chemistry of 4,6-*O*-benzylidene-D-glycopyranosyl triflates: Contrasting behavior between the gluco and manno series *J. Org. Chem.* **1999**, *64*, 4926.

(144) Pozsgay, V.; Coxon, B. Stereoselective preparation of alkyl glycosides of 2-acetamido-2-deoxy-alpha-D-glucopyranose by nonclassical halide-ion catalysis and synthesis and NMR spectroscopy of alpha-D-GalpNAc-OMe. *Carbohydr. Res.* **1995**, *277*, 171.

(145) Crich, D.; Banerjee, A. Stereocontrolled Synthesis of the D- and L-glycero-β-D-manno-heptopyranosides and their 6-deoxy analogues. Synthesis of methyl α-L-rhamno-pyranosyl-(1→3)-D-glycero-β-D-manno-heptopyranosyl- (1→3)-6-deoxy-glycero-β-D-manno-heptopyranosyl-(1→4)-α-L- rhamno-pyranoside, a tetrasaccharide subunit of the lipopolysaccharide from Plesimonas shigelloides. *J. Am. Chem. Soc.* **2006**, *128*, 8078.

(146) Mori, T.; Hatano, K.; Matsuoka, K.; Esumi, Y.; Toone, E. J.; Terunuma, D. Synthesis of carbosilane dendrimers having peripheral mannose and mannobiose. *Tetrahedron* **2005**, *61*, 2751.

(147) Pfeiffer, F. R.; Miao, C. K.; Weisbach, J. A. *J. Org. Chem.* **1970**, *35*, 221.

CHAPTER 2

**SYNTHESIS AND STRUCTURAL STUDIES OF
CD52 PEPTIDES AND GLYCOPEPTIDES**

2.1 Introduction

According to a 1999 analysis of the SWISS-PROT protein database, over half of all proteins may be glycosylated.[1] The two primary modes of protein glycosylation are *N*- and *O*-glycosylation, which occur at asparagine (Asn) and serine (Ser)/threonine (Thr) residues, respectively. The cellular functions of *N*-linked glycosylation in euokaryotes have been extensively studied and include molecular recognition, immune response, modulation of protein function, protein folding, and protein stabilization.[2] The *N*-glycan, an oligosaccharide that is covalently linked to asparagine in the consensus sequence Asn-X-Ser/Thr (where X is any amino acid except proline), has the ability to affect protein structure and, consequently, activity.[3-5] This observation has provided the impetus to design studies that combine synthesis and spectroscopic analysis to probe the effects of *N*-glycosylation on protein conformation and function.[5-10] Such studies require access to pure and structurally defined samples, a task made challenging by microheterogeneity in biosynthetic glycoproteins, which generally exist as complex mixtures of glycoforms. However, advances in carbohydrate and peptide synthesis have enabled chemists to obtain sufficient quantities of homogeneous glycopeptides and small glycoproteins for comparative structural analyses.[11-13] The following introductory sections will include brief overviews of the process of *N*-glycosylation, its effects on protein structure, its role in the bioactivity of the CD52 antigen, and synthetic methods for obtaining glycosylated peptides/proteins for structural studies. Finally, our work in this area involving the CD52 antigen will be discussed in detail.

2.1.1 Protein *N*-Glycosylation

Asparagine glycosylation is a ubiquitous co-translational protein modification that occurs in eukaryotic and some prokaryotic systems, and is characterized by the attachment of an oligosaccharide to Asn through a β-glycosylamide linkage.[14] As mentioned above, *N*-glycosylation may only occur at the consensus tripeptide sequence Asn-X-Ser/Thr (where X is any amino acid except proline). However, the presence of this motif does not necessitate that the site will be glycosylated, for reasons that remain unclear.

N-glycans can be separated into three general classes that include high-mannose-type, hybrid-type, and complex-type structures, each of which can be attained through a common biosynthetic pathway (Figure 2.1).[15] *N*-glycosylation is initiated by the oligosaccharyl transferase-mediated attachment of a dolichol-linked tetradecasaccharide ($Glc_3Man_9GlcNAc_2$, Figure 2.2) to the Asn amide nitrogen of a growing polypeptide chain during protein synthesis. This oligosaccharide then undergoes enzymatic modification in the ER, including glucose trimming by glucosidases I and II, a process that plays a vital role in protein folding and quality control.[16] After the protein has been correctly folded, additional mannose trimming/modification occurs to form high-mannose type structures. In mammals, high-mannose type structures may then be converted to hybrid-type or complex-type *N*-glycans by subsequent addition/trimming of sugars such as glucose, galactose, fucose, sialic acid, and others. Primitive unicellular organisms do not contain the biosynthetic tools necessary to form hybrid- or complex-type glycans, but utilize the early stages of the *N*-glycosylation process to aid in protein folding.
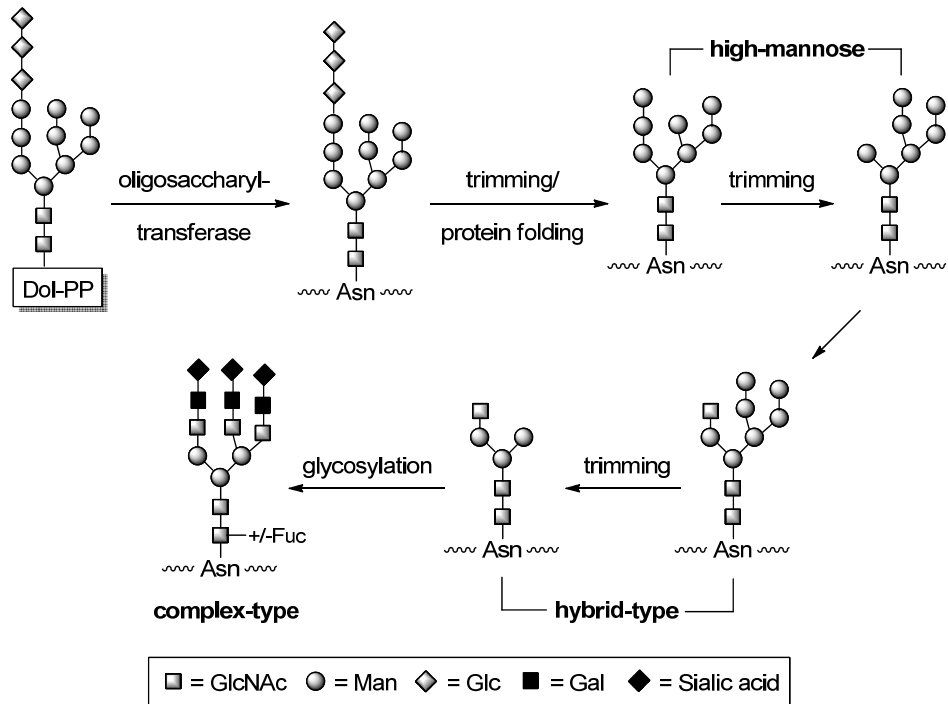
Figure 2.1. The *N*-glycosylation pathway
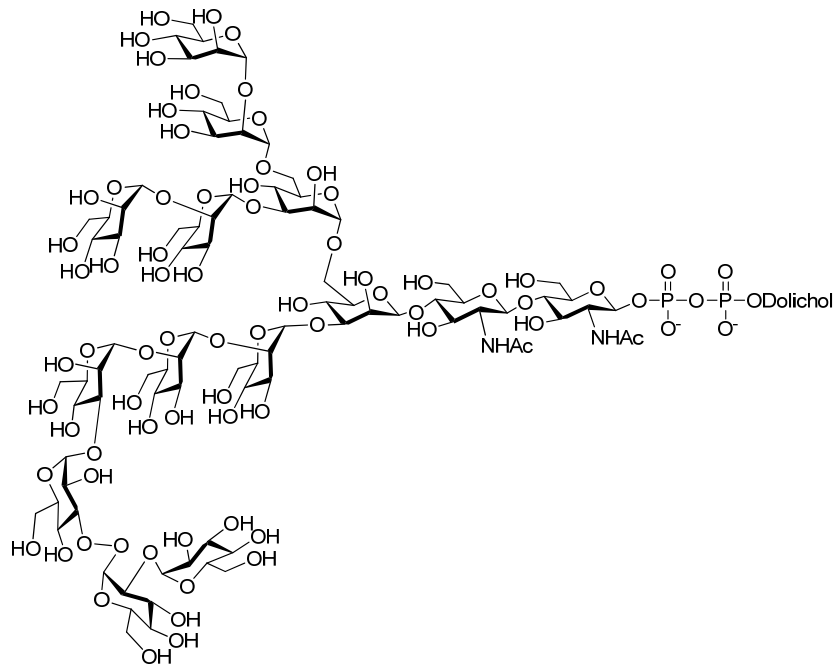
Figure 2.2. The Glc$_3$Man$_9$GlcNAc$_2$ tetradecasaccharide *N*-glycan donor

2.1.2 Effects of *N*-Glycosylation on Protein Structure

Protein glycosylation is the most prevalent co- and post-translational modification, and understanding its effects on protein structure and function is crucial to the study of biological systems. Glycoproteins are expressed throughout the cell and are involved in many diverse and vital functions, but their structural analysis – specifically, determining what structural implications glycosylation has on the 3D structure of a protein – is quite complicated for several reasons.

The first roadblock to glycopeptide/glycoprotein characterization is accessing a sufficient amount of pure sample, which, depending on the analytical technique, can range from microgram to milligram quantities. In the vast majority of cases, these molecules cannot be isolated from natural sources in a sufficient quantity, and thus researchers have turned to expression systems and chemical synthesis/semi-synthesis. Although the former technique is useful for obtaining large quantities of sample, it does not produce natively glycosylated proteins. In addition, expressed glycoproteins are usually formed as complex heterogeneous mixtures due to the phenomenon of microheterogeneity. Therefore, chemical synthesis (covered in section 2.1.4) and semi-synthesis, although costly and time-consuming, have become the best route to pure and structurally well-defined glycopeptides and small glycoproteins.

Even after an acceptably pure sample is available in sufficient quantity, structural analysis can be a daunting prospect. X-ray crystallography, the powerful standard for protein structure determination, is a difficult task due to the flexible and dynamic nature of carbohydrates. In fact, even though well over half of proteins are estimated to be glycosylated,[17] only 3% of structures in the Protein Data Bank[18] contain glycoprotein

chains.[10] Furthermore, most of this small fraction of solved structures required some type of glycan modification or truncation to achieve acceptable crystal formation. As a result, the glycan and peptide chain are analyzed separately for most glycoproteins, and thus no truly accurate representation of the 3D structure can be generated. To overcome these limitations, NMR spectroscopy has become the primary tool for the analysis of glycosylated proteins. The techniques used for this purpose, which have been reviewed in detail,[10] mostly rely on 2D NMR spectroscopy, specifically nuclear Overhauser effect correlation spectroscopy (NOESY), in combination with molecular modeling and other methods. Circular dichroism (CD) is another method that is useful for identifying common protein structural motifs such as the α-helix or β-sheet, and is also useful for quickly contrasting conformational changes in related peptide/protein derivatives.

Several hallmark examples demonstrate how these techniques have been used to determine glycoprotein structure and how covalently linked carbohydrates can affect structure and function. While very few glycoproteins have been characterized by X-ray crystallography, the simian immunodeficiency virus (SIV, closely related to HIV) envelope glycoprotein gp120, which enlists *N*-glycans to assist in virus attachment to host cells and to evade immune detection, was characterized with its glycans intact.[19-20] This important achievement has helped scientists to rationally design carbohydrate-based vaccine candidates for HIV that have shown some promise.[21] In the case of the human T-cell specific surface glycoprotein CD2, which is a key component of immune stimulation, NMR structural determination was enabled by expressing a sample that was uniformly ^{15}N-isotopically labeled.[22] These studies led to the conclusion that the *N*-

glycan in CD2 was responsible for stabilizing the protein, which could unfold or aggregate without carbohydrate present.

More pertinent to our research was work done by Imperiali and co-workers, in which synthetic peptides and glycopeptides were analyzed by NMR spectroscopy to determine what effect *N*-glycans had on the secondary/tertiary structure of a relatively small peptide.[6-7] Their molecule of interest was a short peptide sequence from the influenza A virus envelope glycoprotein hemagglutinin (HA), which is involved in host cell recognition and infection.[21] The authors synthesized a non-glycosylated nonapeptide as well as a glycosylated version carrying an *N*-linked chitobiose disaccharide [β-D-GlcNAc(1→4)β-D-GlcNAc] group, which is present in the core of all *N*-linked glycans. By determining the structures of these synthetic compounds using 2D NMR spectroscopy, it was discovered that a conformational switch occurred upon glycosylation of the peptide. In fact, the free peptide exhibited an "Asx" turn conformation that is important for the *N*-glycosylation process, whereas the glycopeptide exhibited a Type I β-turn conformation, which is present in the natively folded HA glycoprotein. Therefore, *N*-glycosylation triggered a structural change from an open conformation to a more compact conformation in the HA model system.

2.1.3 Structure and Function of the Human CD52 Antigen

Our interest in the effect of *N*-glycosylation on protein structure lies in the human CD52 antigen, a GPI-anchored glycopeptide that is expressed on lymophocyte and sperm cells.[23-25] Although both lymphocyte and sperm CD52 share an identical 12 amino acid peptide, structural variations in their GPI anchor and *N*-linked glycan lead to

distinct biological functions, with the former playing a role in the human immune system and the latter being involved in the human reproductive process.[24,26] Lymphocyte CD52 antibodies have been used to treat immune-related diseases such as leukaemia,[27] whereas sperm CD52-specific antibodies have been isolated from infertile women and suggest the potential for immunocontraceptive development.[28-29]

Structurally, the two forms of CD52 have the same remarkably short peptide and exhibit one *N*-glycosylation site at the Asn^3 residue, to which complex-type glycans are linked (Figure 2.3).[24-25] Interestingly, the makeup of the *N*-linked glycans is one of the main structural differences between the two forms. For example, bi- and tri-antennary *N*-glycans, peripheral fucosylation, and the α(2→3)-linkage of sialic acid residues are unique features of sperm CD52 and are therefore termed "male-specific modifications" of the antigen.[26] In addition, certain modifications of the CD52 GPI anchor have been observed. For instance, lymphocyte CD52 bears an additional α–mannose unit at the Man-III 2-*O*-position and its phospholipid is composed of a diacylglycerolipid, which is in contrast to the monoalkylglycerolipid found in sperm CD52.[26] The structural differences of the *N*-glycans/GPI between sperm and lymphocyte CD52 seem to have a critical influence on their bioactivity. Sperm CD52-specific antibodies bind to the *N*-glycan of the antigen and may inhibit sperm-egg binding.[28-29] Lymphocyte CD52 antibodies, however, recognize a sequence of the peptide chain,[27] suggesting a possible difference in peptide structure between the two forms of CD52 and therefore the potential for conformational change induced by *N*-glycosylation or GPI anchoring.
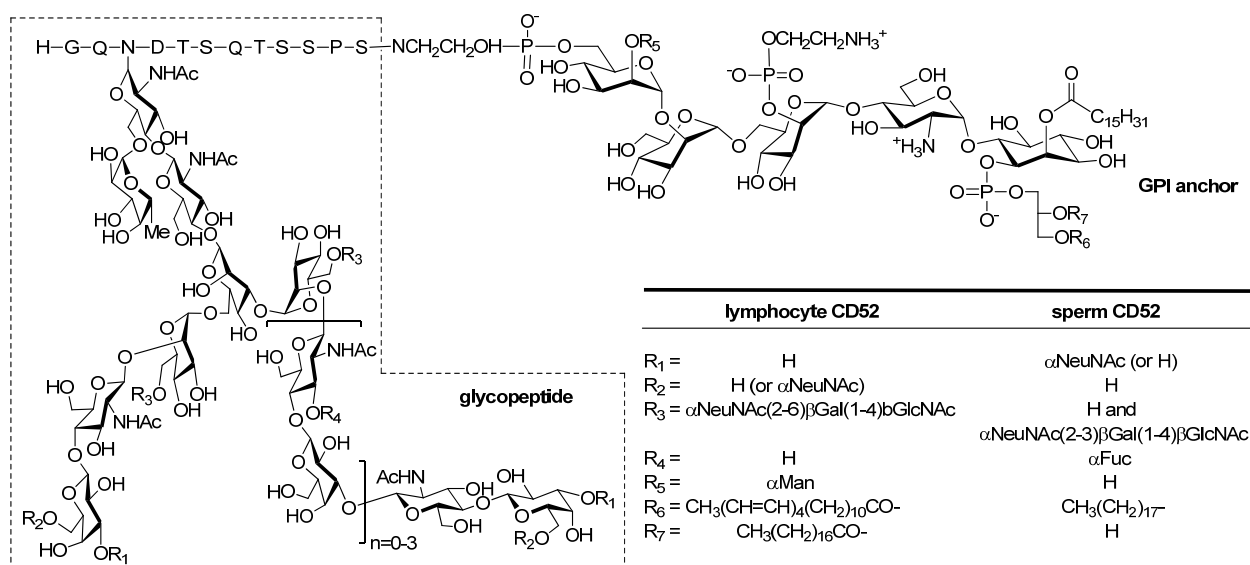
Figure 2.3. Structural comparison of lymphocyte and sperm CD52

The figure includes a table:

	lymphocyte CD52	sperm CD52
$R_1 =$	H	αNeuNAc (or H)
$R_2 =$	H (or αNeuNAc)	H
$R_3 =$	αNeuNAc(2-6)βGal(1-4)bGlcNAc	H and αNeuNAc(2-3)βGal(1-4)βGlcNAc
$R_4 =$	H	αFuc
$R_5 =$	αMan	H
$R_6 =$	$CH_3(CH=CH)_4(CH_2)_{10}CO-$	$CH_3(CH_2)_{17}-$
$R_7 =$	$CH_3(CH_2)_{16}CO-$	H

2.1.4 Chemical Synthesis of *N*-Linked Glycopeptides

As a result of advances in peptide and carbohydrate synthesis, the preparation of glycopeptides and even some small glycoproteins is now a fairly straightforward process. While the preparation of glycopeptides/glycoproteins using various strategies has been reviewed extensively elsewhere,[11,30] this section will briefly focus on methods for the chemical synthesis of *N*-linked glycopeptides, which are the topic of this research. Although chemical synthesis of *N*-linked glycopeptides is relatively costly and laborious, it is currently the best option available for accessing significant quantities of homogeneous and structurally well-defined samples.

Synthesis of an *N*-linked glycopeptide almost universally begins with the preparation of a custom glycosylated asparagine derivative that can subsequently be used in peptide chain elongation to eventually form the desired structure (Scheme 2.1). First, a glycosyl amine carrying the desired suitably protected *N*-glycan must be

prepared, usually by reduction of a glycosyl azide that was synthesized using conventional regio/stereoselective oligosaccharide techniques. Alternatively, treatment of unprotected *N*-acetylglucosamine reducing sugars with saturated ammonium bicarbonate is useful for converting oligosaccharides obtained from natural sources directly in glycosyl amines. The newly formed glycosyl amine is then reacted with a protected aspartic acid derivative in the presence of a coupling reagent (e.g. EDCI/HOBt) to effect a condensation reaction, thus forming a glycosyl asparagine building block that can be subjected to peptide chain elongation and eventually global deprotection to afford the desired glycopeptide.
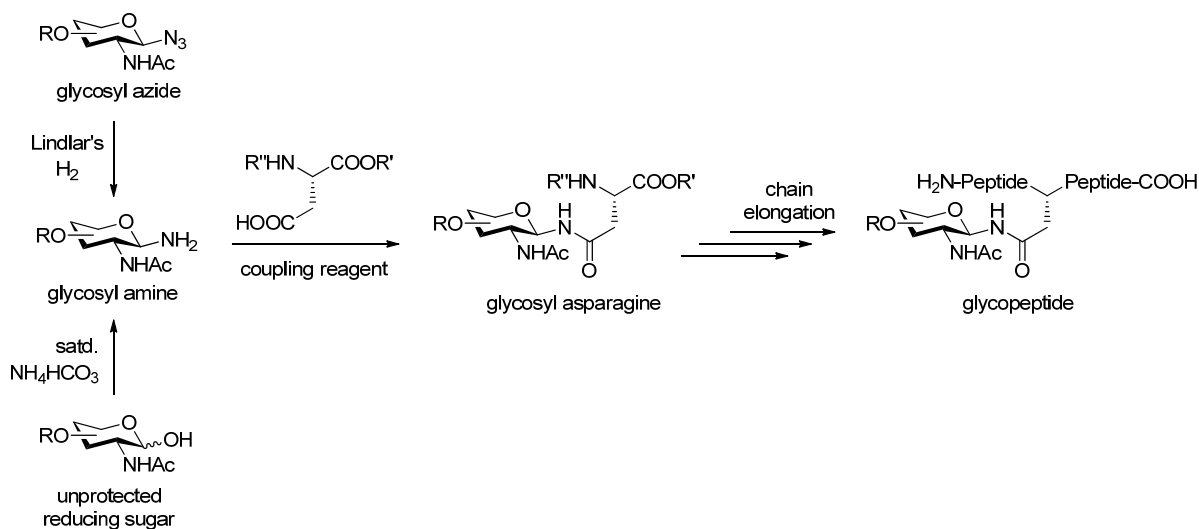
Scheme 2.1. Glycosyl amine formation and application to glycopeptide synthesis

Several strategies have been developed for applying a protected glycosyl asparagine building block to peptide chain elongation. Perhaps the most obvious is solution phase synthesis, in which the glycosyl asparagine can be elaborated at the *C*- and/or *N*-terminus by cycles of selective deprotection/coupling or by convergent

coupling to a larger peptide fragment. Kunz, a pioneer in the field, employed this methodology in conjunction with a divergent-convergent assembly in the synthesis of a divalent Lewis[x] antigen (Scheme 2.2).[31] Through a series of solution phase reactions, per-*O*-acetyl-protected glycosyl asparagine derivative **2.1** was diverted to intermediates **2.2** and **2.3**, which were set up for coupling with EDCI and HOBt. The resulting fully protected glycopeptide **2.4**, which contained two *N*-glycans, was then elongated at the *C*-terminus and deprotected to give the divalent glycopeptide **2.5**. While successful, the solution phase strategy requires purification at each step, thus increasing lab work and cost while decreasing the overall efficiency of a synthesis dramatically.
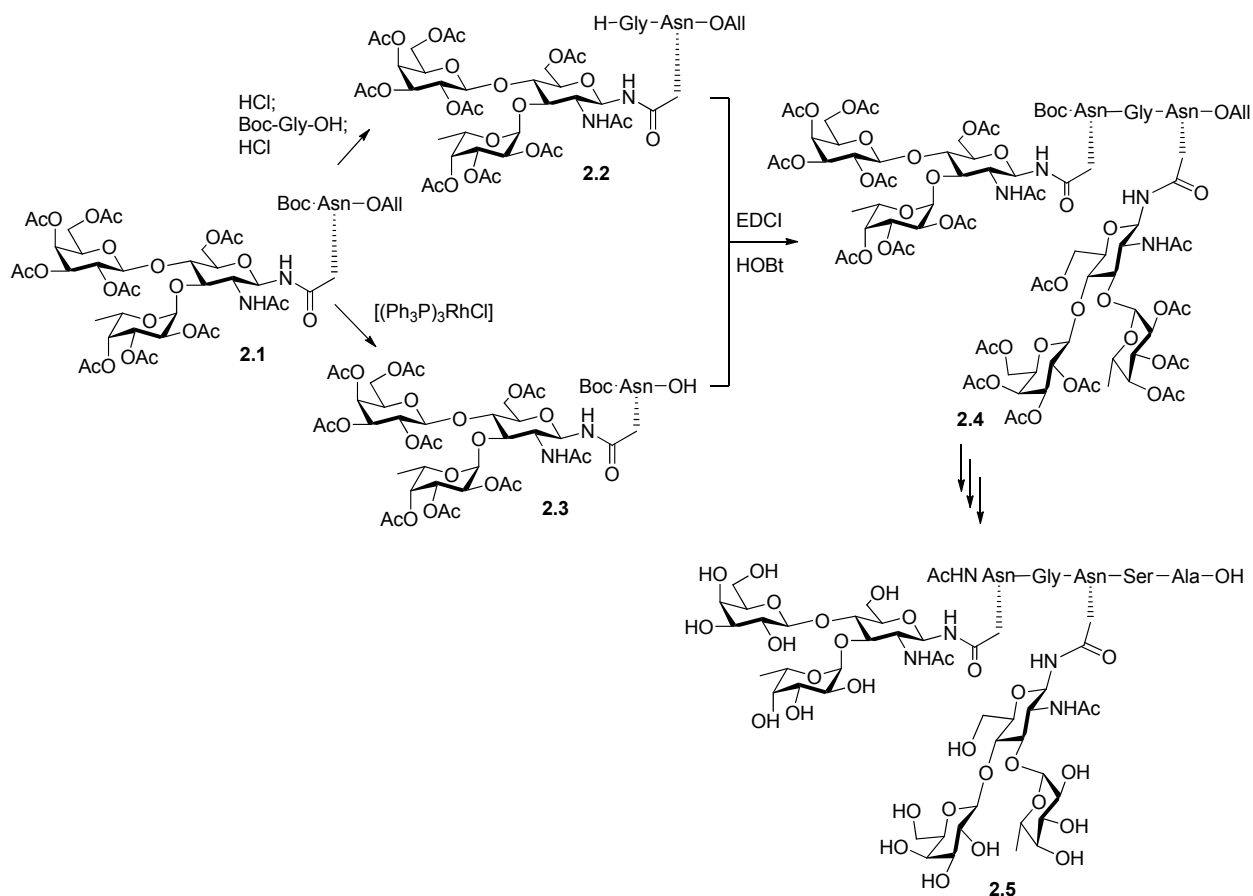
Scheme 2.2. Kunz's solution phase synthesis of a divalent Lewis[x] antigen

A major development in the area of glycopeptide synthesis was the application of the solid phase peptide synthesis (SPPS) strategy, which was originally developed by Merrifield in the 1960s.[32] SPPS involves the stepwise elongation of a growing peptide chain that is anchored at the *C*-terminus carboxyl group to insoluble polymeric beads via a cleavable linker. Thus, the desired product remains attached to the solid support throughout the process, allowing impurities to be easily washed away after each step. SPPS has become the clear standard for peptide and glycopeptide synthesis due to its speed, ease of use, high yields, availability on automated synthesizers, and the ability to prepare relatively large peptide fragments (maximum ~50-70 amino acid residues, depending on the sequence). SPPS can be easily adapted to glycopeptide synthesis by employing custom glycosyl asparagine building blocks in place of standard amino acids at the desired position. In addition, SPPS offers a substantial degree of flexibility so that any target glycopeptide, regardless of protecting/functional groups used, should be accessible. For example, The *N*-protecting group can be either Boc, which is removed with TFA, or Fmoc, which is removed with the relatively weak base piperidine. For glycopeptide SPPS, Fmoc protection is typically used so that glycosidic bonds are not repeatedly subjected to the acidic conditions required for Boc removal. In addition, the available linkers, which bridge the peptide chain and the solid support, are chemically diverse, so that the peptide may be cleaved from the resin under various conditions. For instance, linkers exist that are cleaved under strongly acidic conditions (95% TFA, example: Wang resin), weakly acidic conditions (1% TFA or AcOH, example: 2-chlorotrityl resin), or neutral conditions (palladium catalysis, example: HYCRAM resin). Because the incorporation of glycans to the SPPS process incurs various

considerations about sterics, protecting group tactics, and functional group lability, the flexibility of SPPS is very useful in planning a synthesis. Scheme 2.3 depicts a standard glycopeptide synthesis using Fmoc-SPPS. Starting from a pre-loaded resin, the desired number of Fmoc-SPPS cycles involving Fmoc deprotection and amino acid coupling are carried out to give solid-supported peptide **2.7**. Then, using a minimal amount of the valuable glycosyl asparagine building block **2.8**, the *N*-glycan is added to the desired position of the growing peptide chain to give an intermediate of type **2.9**. Additional cycles of Fmoc-SPPS are then carried out to form the remainder of the peptide, after which cleavage from the resin, global deprotection, and HPLC purification provided the desired glycopeptide **2.10**.
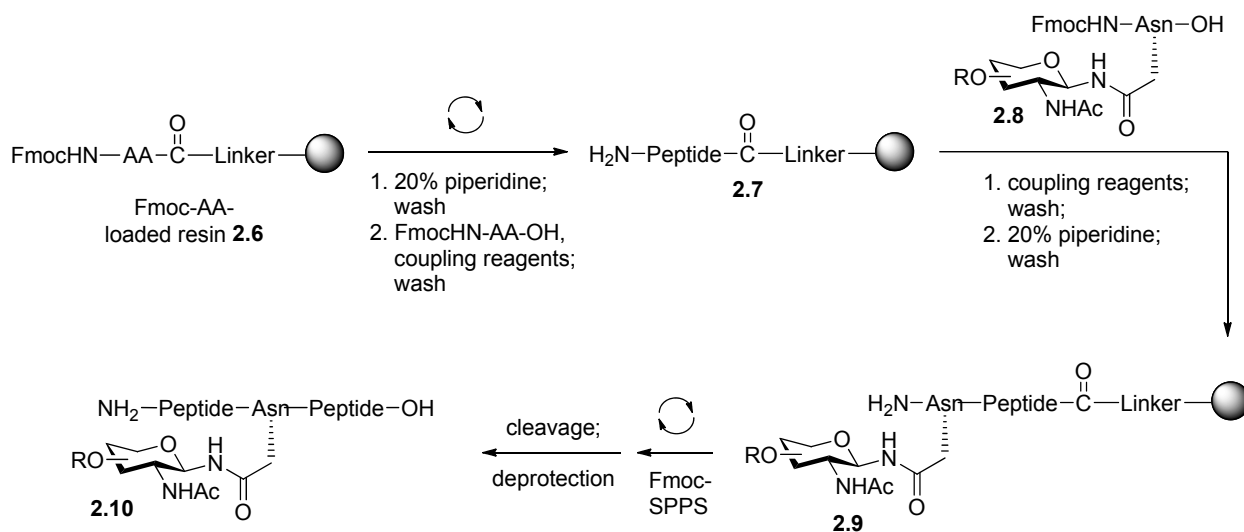
Scheme 2.3. A typical glycopeptide synthesis using Fmoc-SPPS

In addition to the solution and solid phase synthesis methods described above, our group previously developed a third option specifically for application to glycopeptide synthesis called "solution phase synthesis with solid phase work-up."[33-34] In this method,

glycosyl asparagines using unprotected oligosaccharide chains were employed in peptide coupling reactions. The polar *N*-glycans acted as phase tags, such that work-up of the reaction mixtures by addition of cold diethyl ether precipitated the desired product out of the NMP solution in excellent yield and purity. Like SPPS, this strategy negated the need for intermediate purification. Moreover, final deprotection of the glycan, which can sometimes be problematic for certain structures, was bypassed. Using this method, Guo synthesized several targets, including hydrogenation-sensitive glycopeptide **2.11** (tyrosine residues can be affected) and tetravalent glycopeptide **2.12** bearing four vicinal oligosaccharide chains (Figure 2.4). Although not widely applied, this method is a viable alternative to solution phase synthesis and SPPS.

2.11

2.12
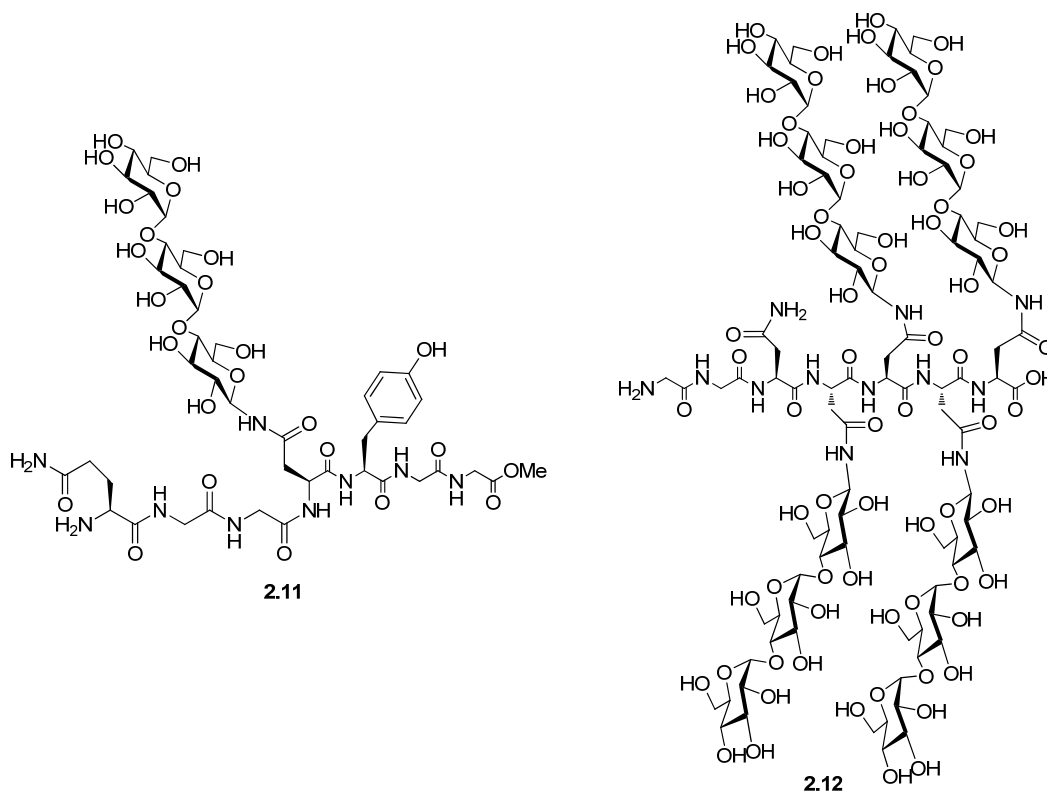
Figure 2.4. Glycopeptides synthesized using Guo's "solution phase synthesis with solid phase work-up" method

2.2 Results and Discussion

2.2.1 Background and Project Design

As laid out in section 2.1.3, the CD52 antigen exists in two distinct functional forms, sperm and lymphocyte CD52, despite the fact that both species have an identical primary amino acid sequence. As a result, it is possible that variations in the *N*-glycan or GPI anchor or both induce conformational changes in the peptide that lead to contrasting biological functions. I felt that this presented an excellent opportunity for probing the effects of glycosylation on peptide structure in a serviceable model system.

To explore this interesting question, I set out to compare the structures of non-glycosylated CD52 peptides to their glycosylated counterparts to determine what effect a model *N*-glycan might have on the conformation of the CD52 peptide backbone. For this purpose, I prepared the natural and *N*-terminal acetylated CD52 peptides **2.13** and **2.14** (Figure 2.5), as well as glycopeptides **2.15** and **2.16**-**2.17**, which contained a
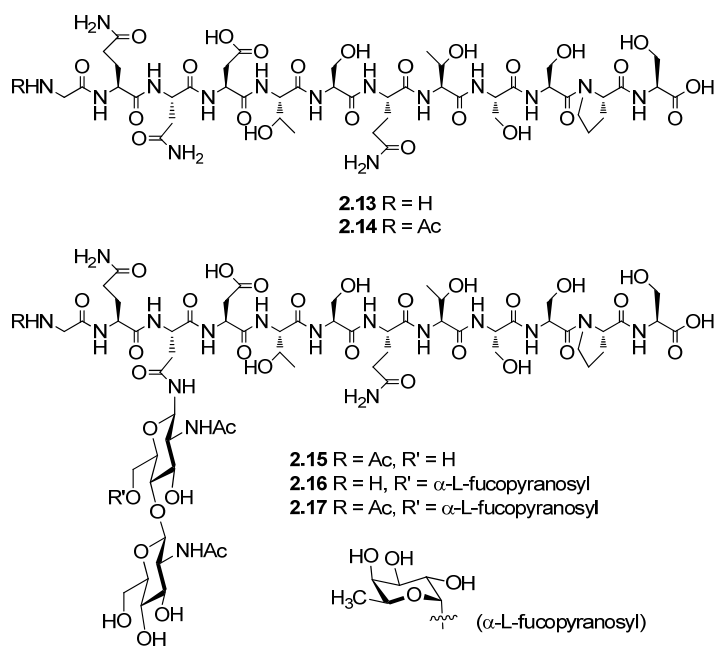
Figure 2.5. Target CD52 peptides and glycopeptides

disaccharide β-D-GlcNAc(1→4)-β-D-GlcNAc and a fucose-containing branched trisaccharide β-D-GlcNAc(1→4)[α-L-Fuc(1→6)]-β-D-GlcNAc, respectively, using Fmoc-SPPS. Next, CD was used to examine the solution structures of the synthetic targets and determine whether CD52 can form any specific secondary/tertiary structure and whether Asn-*N*-glycosylation or *N*-terminal acetylation could result in any significant secondary/tertiary structure changes.

2.2.2 Synthesis of Peptides 2.13 and 2.14

The straightforward preparation of peptides **2.13** and **2.14** was carried out using standard Fmoc-SPPS on an automatic peptide synthesizer. Commercially available Ser-loaded resin and Fmoc-protected amino acids were used to synthesize the target peptide on a 0.1 mmol scale (84% yield based on weight). A portion of the resin-bound peptide was *N*-acetylated, and another portion was left unaltered at the *N*-terminus. Concomitant release of the peptides from the solid support and deprotection of the amino acid side chains was accomplished using a 95% TFA aqueous solution containing 2.5% triethylsilane. Purification of the products by reverse phase (RP)-HPLC gave the desired peptides **2.13** and **2.14**. All spectroscopic data gathered for **2.13** were in agreement with previously reported values,[35] and **2.14** was positively characterized using NMR spectroscopy and MS.

2.2.3 Synthesis of Glycopeptides 2.15-2.17

The most widely adopted method for glycopeptide synthesis is solid phase synthesis. However, due to the acid lability of *O*-glycosidic bonds, particularly the fucosidic linkage,[36] and the potential for strong base-induced β-elimination or amino

acid epimerization,[37] care must be taken in the selection of protecting groups and overall synthetic strategy. Thus, partially or fully benzyl-protected oligosaccharide-asparagine conjugates were used in the target syntheses to facilitate late-stage deprotection under mild conditions, and measures were taken to ensure that acid sensitive functionalities would remain intact throughout each synthesis.

The primary challenge of synthesizing **2.16** and **2.17** is the α-fucosidic linkage, which is particularly acid sensitive when it is fully benzylated.[36] Although acyl-protected fucosides are more stable to acidic conditions,[38] protection of the 2-*O*-position by an acyl group, which has the neighboring group participation effect, must be avoided to achieve α–fucosylation. Our group developed the "solution-phase synthesis with solid-phase workup" strategy, which employs unprotected carbohydrate and peptide building blocks,[33-34] to address the problem in an earlier synthesis of **2.17**.[39] During this study, it was observed that an unprotected fucoside intermediate could withstand treatment with 20% TFA, which is strong enough to deprotect peptide side chains. Based on these results, our group developed a strategy for solid phase glycopeptide synthesis that is compatible with all glycosidic bonds.[40-41] I therefore made use of the 2-chlorotrityl resin, a hyper acid sensitive support that can release fully protected peptides upon treatment with 10% acetic acid, as the solid phase support in my synthesis of the target compounds.

Perbenzylated disaccharide-Asn conjugate **2.24** was chosen as the glycosyl amino acid to be employed in Fmoc-SPPS en route to glycopeptide **2.15** (Scheme 2.4). Starting from D-glucosamine hydrochloride, reported methods were used to arrive at **2.18**,[42-43] which was deacetylated and then benzylated to afford thioglycoside **2.19**.

Glycosylation of acceptor **2.20**[44] by donor **2.19** was promoted by NIS and TfOH to give disaccharide **2.21** in 75% yield. After phthalimide removal and subsequent *N*-acetylation to afford **2.22**, Lindlar's catalyst was used to reduce the anomeric azide under a H_2 atmosphere to give a glycosyl amine, which immediately underwent amide bond formation using the active ester Fmoc-Asp(OBt)-OtBu to furnish **2.23**. Finally, treatment of the product with 20% TFA to remove the *C*-terminal *tert*-butyl ester protecting group resulted in the desired disaccharide-Asn conjugate **2.24**.
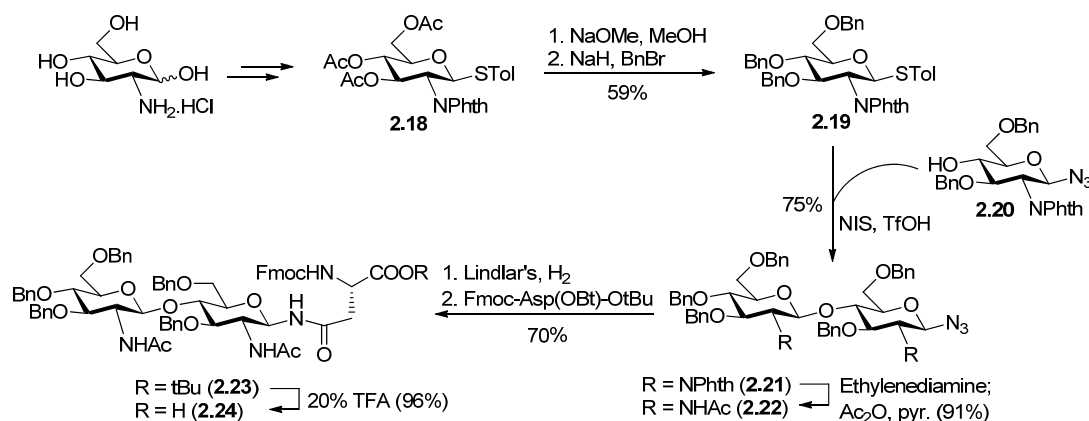
Scheme 2.4. Synthesis of disaccharide-Asn conjugate **2.24**

With glycosyl amino acid **2.24** in hand, solid phase construction of glycopeptide **2.15** commenced (Scheme 2.5). The preparation of resin-linked nonapeptide **2.25** was carried out on an automated peptide synthesizer using standard Fmoc-SPPS chemistry starting from Ser-loaded 2-chlorotrityl resin. Coupling of the reactive benzotriazole (Bt) ester of **2.24** with peptide **2.25** was completed manually. In this case, only 1.5 equivalents of the valuable intermediate **2.24** were used in the synthesis. The mixture of **2.25** and the active ester of **2.24** was shaken under an Ar atmosphere overnight to give

2.26. The subsequent peptide chain elongation and *N*-terminal acetylation followed to afford resin-bound glycopeptide **2.27**. Release of the glycopeptide from the solid support was achieved with 10% acetic acid. Finally, the resultant glycopeptide was deprotected in two steps, including palladium-catalyzed *N*-glycan debenzylation and the amino acid side chain deprotection using 20% TFA to produce the target glycopeptide **2.15**, which was purified by RP-HPLC.
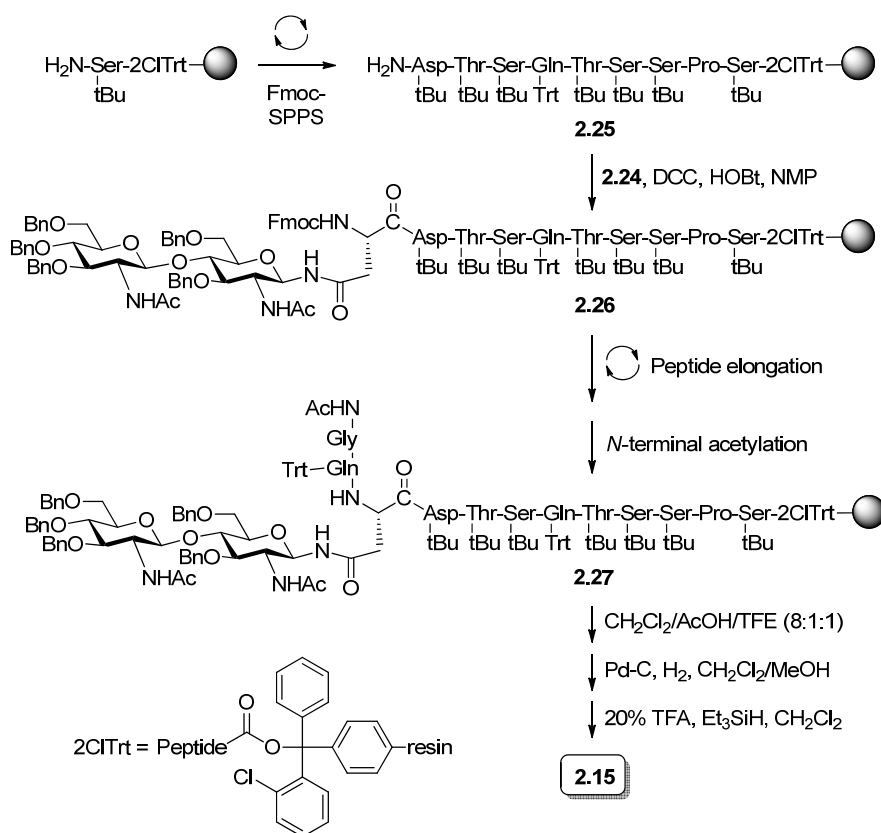
Scheme 2.5. Solid phase synthesis of glycopeptide **2.15**

Partially benzylated trisaccharide-Asn conjugate **2.36** was chosen as the glycosylated asparagine to be employed in Fmoc-SPPS en route to glycopeptides **2.16** and **2.17** (Scheme 2.6). Previous studies suggested that the remaining free hydroxyl

groups in **2.26** would remain inert during the peptide elongation process.[33] Glycosyl azide **2.34** was previously prepared by Shao et al,[39] while a slightly shorter pathway leading to **2.34** was developed in the work presented herein. Starting from D-glucosamine, *p*-methoxy benzylidene acetal **2.28**[45] was synthesized in four steps. 3-*O*-Benzylation of this intermediate followed by regioselective acetal ring opening gave glycosyl acceptor **2.29** in 71% yield over two steps. The resultant PMB group on the 6-O-position could be easily and selectively removed later under mild conditions.
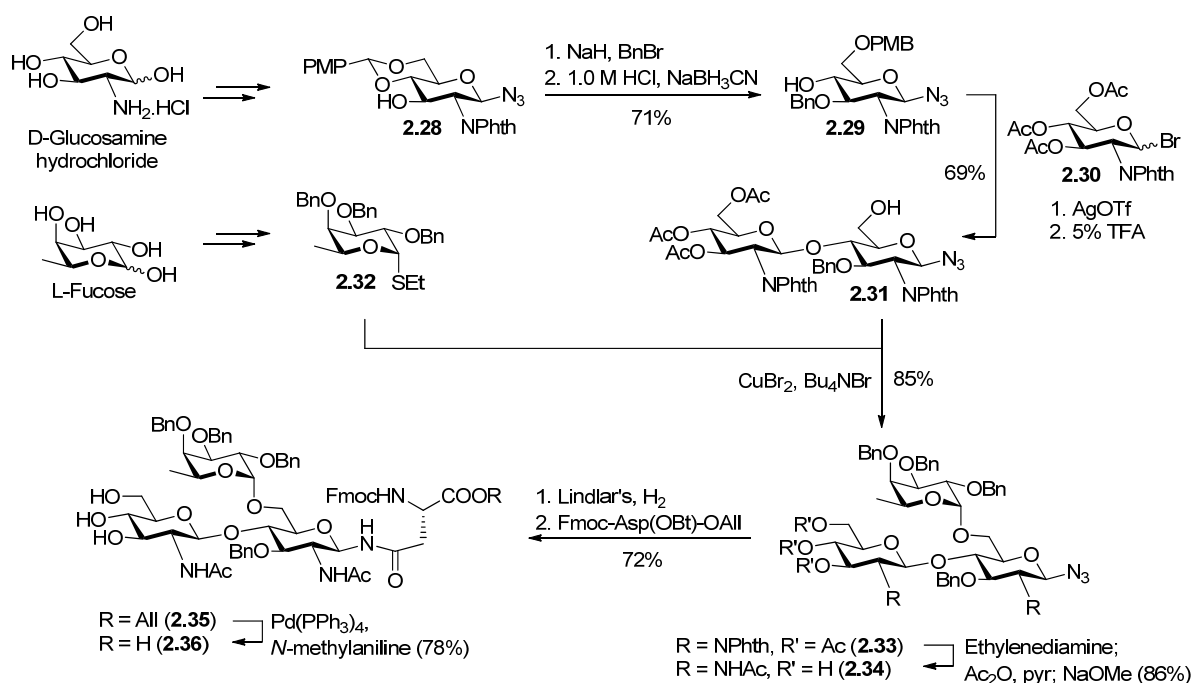
Scheme 2.6. Synthesis of trisaccharide-Asn conjugate **2.36**

Alcohol **2.29** underwent glycosylation with glycosyl bromide **2.30**[46] in the presence of AgOTf. The disaccharide product contained a small quantity of an inseparable impurity, so full characterization of the product was completed after acidic removal of the PMB group, which proceeded to give β-disaccharide **2.31** in 69% over

two steps. The resulting alcohol **2.31** was fucosylated by **2.32**[47] stereoselectively according to the conditions (CuBr$_2$/Bu$_4$NBr) set forth by Lemieux et al.[48] The transformation from **2.33** to **2.34** was achieved in a 3 step sequence, including removal of the *N*-phthalimido and *O*-acetyl groups, acetylation, and then *O*-deacetylation. *O*-Deacetylation at this stage was preferential due to potential complications in late-stage basic deprotection, and, as mentioned above, the free hydroxyl groups would remain inert throughout the remainder of the synthesis. Next, Lindlar's catalyst and a H$_2$ atmosphere were employed to reduce the anomeric azide and produce a glycosyl amine, which underwent amide bond formation with the active ester Fmoc-Asp(OBt)-OAll to furnish **2.35**. In contrast to the previous trisaccharide-Asn conjugate,[39] in which the carboxylic group was protected by a *tert*-butyl group, an allyl group was used to protect the carboxylic group in **2.35**. The allyl ester could be deprotected without acid, thus allowing fucose to remain benzylated. Indeed, treatment of **2.35** with Pd(PPh$_3$)$_4$ and *N*-methylaniline resulted in the desired trisaccharide-Asn conjugate **2.36**, which was subsequently used in Fmoc-SPPS.

Fmoc-SPPS construction of glycopeptides **2.16** and **2.17** (Scheme 2.7) began with the manual coupling of the benzotriazole active ester of glycosyl-Asn conjugate **2.36** to the 2-chlorotrityl-resin anchored nonapeptide **2.25**. The resulting glycodecapeptide **2.37** was then elongated at the *N*-terminus by manual Fmoc-SPPS to give fully protected, resin-bound glycopeptide **2.38**. Both the natural and *N*-terminal acetylated trisaccharide glycopeptides, **2.16** and **2.17**, were accessible from **2.38**. Glycopeptide **2.16** was obtained via cleavage of **2.38** from the solid support followed by palladium catalyzed *N*-glycan debenzylation and TFA-mediated side chain deprotection

as described above. Care was taken during debenzylation of to use aldehyde-free solvents to prevent *N*-terminal methylation via reductive amination. After the benzyl protecting groups were removed, the fucosidic linkage became stable to 20% TFA treatment, which was used to achieve amino acid side chain deprotection. Glycopeptide **2.17** was afforded by first carrying out solid phase *N*-terminal acetylation, then completing the same protocols of glycopeptide release and global deprotection described for **2.16**. Purification by RP-HPLC gave the desired glycopeptides **2.16** and **2.17**. Characterization of **2.16** was carried out using NMR and MS, while all spectroscopic data gathered for **2.17** were in agreement with previously reported values.[39]
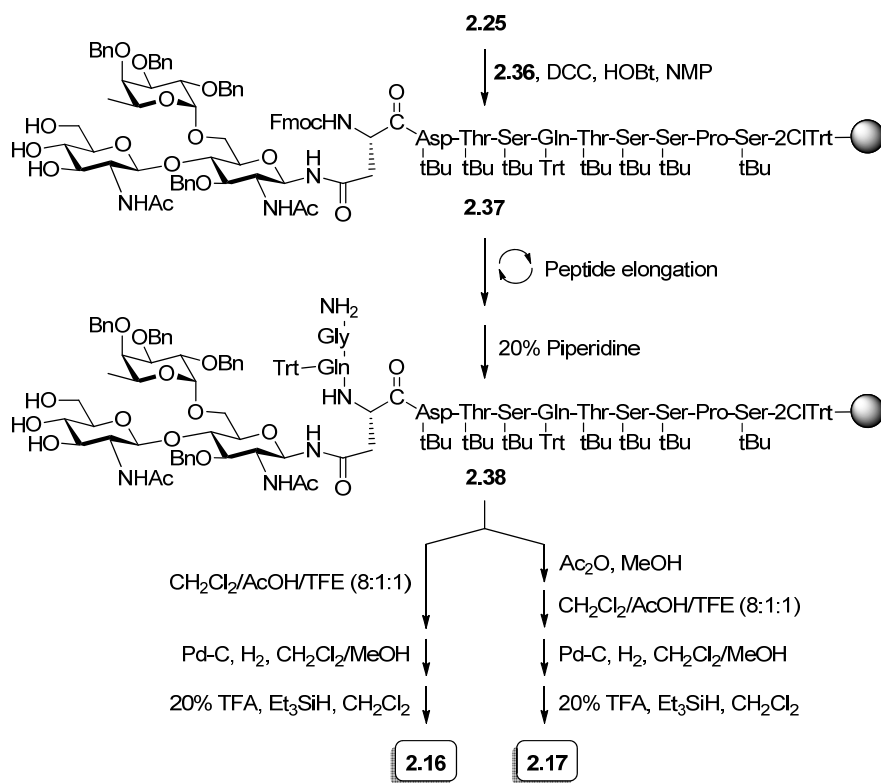
Scheme 2.7. Solid phase synthesis of glycopeptides **2.16** and **2.17**.

2.2.4 CD Structural Studies

CD studies were performed by Yu-Cheng Chang. The aqueous solution conformations of the synthetic CD52 peptides and glycopeptides **2.13**-**2.17** were studied using CD spectroscopy, which has previously been used to probe the effects of glycosylation on peptide structure.[49-51] The CD spectra of **2.13**, **2.14**, **2.15**, **2.16**, and **2.17** are very similar with peak minima at 196, 201, 201, 198, and 200 nm, respectively (Figure 2.6). These features are suggestive of random coil conformations for all derivatives as clearly described in the literature.[49,52] It was thus concluded that, in this case, neither *N*-glycosylation nor *N*-terminal acetylation led to any noticeable ordered secondary conformation of the CD52 peptide backbone, and thus further conformational studied by NMR spectroscopy were not pursued.
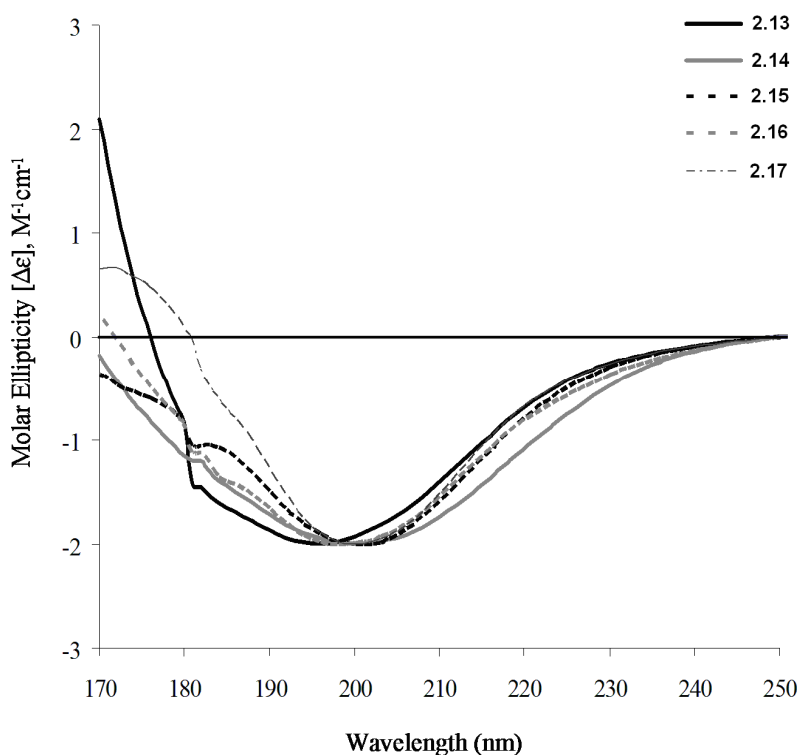
Figure 2.6. CD spectra of **2.13-2.17** in H_2O at room temperature

2.3 Conclusions

The free peptide of the human CD52 antigen and four *N*-terminal acetylated or Asn-glycosylated derivatives or both (**2.13**-**2.17**) were synthesized by SPPS. Benzylated glycosyl asparagine conjugates were employed as building blocks in the solid phase synthesis of glycopeptides. To avoid strong acid treatment that may affect the α-fucosidic bond, 2-chlorotrityl resin, which is particularly acid-labile, was used as the solid phase support so that the glycopeptides could be released under mildly acidic conditions compatible with all glycosidic linkages. CD structural studies of the synthetic peptides and glycopeptides led us to conclude that neither *N*-glycosylation nor *N*-terminal acetylation had a noticeable influence on the random coil conformation of the CD52 peptide, even though the fucose-containing branched trisaccharide is relatively sterically hindered. I believe that this is probably a result of the unique structure and properties of the CD52 peptide, as it is extremely short and hydrophilic. However, the conformation of the CD52 antigen when it contains larger, natural *N*-glycans or when it is GPI-anchored onto the cell surface is still unknown.

2.4 Future Work

This work focused on the synthesis and structural comparison of several CD52 derivatives containing highly truncated *N*-glycans. Although Imperiali and co-workers observed a conformational change by addition of a simple disaccharide,[6-7] in our case glycosylation with model carbohydrates did not incur any changes according to CD. Thus, one potential future pathway for this work would be to synthesize CD52 glycopeptides bearing more natural *N*-glycans, as shown in Figure 2.3, although the

complexity of the synthetic work would increase by multitudes. Another possible future project would involve structural analysis of GPI-anchored CD52 peptides and glycopeptides to determine whether attachment of a GPI anchor induces conformational changes. Again, synthesis would be a demanding task for such a project, although our group has extensive experience in GPI synthesis. Finally, the target molecules of this research could be analyzed in detail by 2D NMR to determine whether any subtle change in conformation was imparted by glycosylation, which would require a heavy investment of time and resources.

2.5 Experimental

General Methods

^{1}H NMR spectra were recorded at 400 or 500 MHz with chemical shifts reported in ppm (δ) downfield from tetramethylsilane (TMS) or relative to $CHCl_3$ (7.26 ppm) unless otherwise noted. The coupling constants (J) are reported in hertz (Hz). Thin layer chromatography (TLC) was performed on silica gel GF_{254} plates with detection by UV or charring with a 5% H_2SO_4 in EtOH solution. Molecular sieves 4 Å (4 Å MS) were dried in high vacuum at 170-180 ^{o}C for 6-10 h immediately before use. Anhydrous solvents were obtained from a solvent purification system, while commercial anhydrous reagents were used without further purification. Automated peptide synthesis was carried out on an Applied Biosystems 433A peptide synthesizer using fresh reagents and solvents purchased from Applied Biosystems. 2,5-Dihydroxybenzoic acid (DHB) was used as the MALDI TOF MS matrix, and samples were dissolved in either H_2O-CH_3CN (1:1) containing 1% TFA or CH_2Cl_2-MeOH (1:1) for unprotected and fully protected compounds, respectively.

Preparation of Compounds

CD52 Peptide 2.14
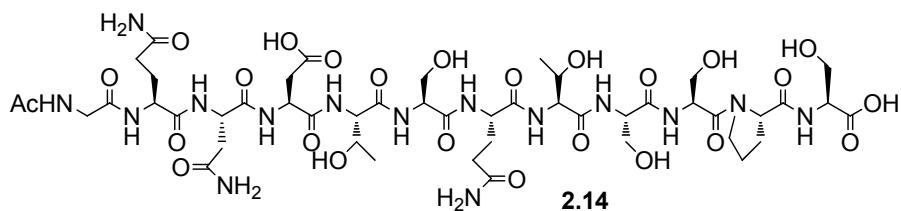
The resin-bound, fully protected precursor of CD52 peptide **2.13**[35] was subjected to acetylation conditions (pyr-Ac$_2$O 2:1) for 4 h. After the resin was washed thoroughly and filtered, the desired *N*-terminal acetylated peptide **2.14** was released by treatment with 95% aqueous TFA containing 2.5% Et$_3$SiH as the cation scavenger. After precipitation by cold ether and lyophilization, **2.14** was purified by RP-HPLC (Supelco Discovery C18, 250 x 10 mm, eluent 5% CH$_3$CN in H$_2$O, 2 mL/min, R_t = 14.9 min). ^{1}H NMR (500 MHz, D$_2$O, DHO at δ 4.79 as reference): δ 4.72 (t, *J* = 7.0 Hz, 1 H), 4.54-4.43 (m, 4 H), 4.41-4.39 (m, 3 H), 4.35-4.31 (m, 2 H), 4.25 (dd, *J* = 5.0, 6.5 Hz, 1 H), 3.73-3.94 (m, 11 H), 2.95 (dd, *J* = 6.5, 17 Hz, 1 H), 2.87 (dd, *J* = 6.0, 15.5 Hz, 1 H), 2.85 (dd, *J* = 7.0, 17.0 Hz, 1 H), 2.77 (dd, *J* = 8.0, 15.5 Hz, 1 H), 2.40-2.29 (m, 5 H), 2.21-2.08 (m, 2 H), 2.07 (s, 3 H), 2.05-1.96 (m, 5 H), 1.22 (d, *J* = 2.0 Hz, 3 H), 1.20 (d, *J* = 1.5 Hz, 3 H). ESI MS: [M+Na]$^+$ calcd for C$_{47}$H$_{75}$N$_{15}$O$_{25}$Na, 1272.4932; found: *m/z* 1272.4956.

***p*-Methylphenyl 3,4,6-tri-*O*-benzyl-2-deoxy-2-phthalimido-1-thio-β-D-glucopyranoside (2.19)**
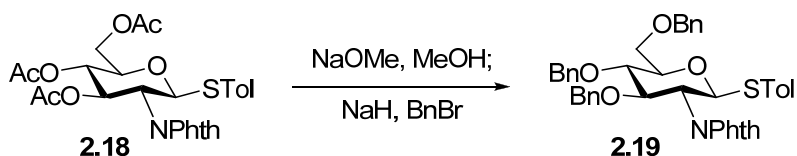
After **2.18** (5.00 g, 9.23 mmol) was treated with NaOMe in methanol (0.05 M, 40 mL) at rt for 2 h, the solution was neutralized to pH 6-7 by amberlyst H$^+$ resin. After filtration of the resin, the filtrate was concentrated to afford a white powder that was directly used for the next step. To a solution of the triol intermediate (3.00 g, 7.22 mmol) in DMF (60 mL) was added tetrabutylammonium iodide (TBAI, 300 mg, 0.76 mmol) and benzyl bromide (5.71 mL, 45.9 mmol). The solution was cooled to 0 °C and then NaH (60% dispersion in mineral oil, 1.6 g, 40.0 mmol) was added slowly. The reaction mixture was stirred at 0 °C for 1 h and then stirred at rt overnight. The reaction was quenched with aqueous NH$_4$Cl and extracted with CH$_2$Cl$_2$. The organic phase was washed with aqueous NH$_4$Cl and brine, then dried over Na$_2$SO$_4$ and filtered. The solvent was evaporated and the crude product was purified by silica gel chromatography to give **2.19** as white foam (2.9 g, 59%). ^{1}H NMR (400 MHz, CDCl$_3$): δ 7.90-7.60 (m, 4 H), 7.42-7.26 (m, 10 H), 7.04-6.82 (m, 5 H), 5.51 (d, 1 H), 4.76-4.90 (m, 2 H), 4.74-4.56 (m, 3 H), 4.50-4.36 (m, 2 H), 4.26 (t, 1 H), 3.90-3.66 (m, 4 H), 2.29 (s, 3 H). ESI MS: [M+Na]$^+$ calcd for C$_{42}$H$_{39}$NO$_6$NaS, 708.2; found: *m/z* 708.4.

O-(-3,4,6-tri-O-Benzyl-2-deoxy-2-phthalimido-β-D-glucopyranosyl)-(1→4)-3,6-di-O-benzyl-2-deoxy-2-phthalimido-β-D-glucopyranosyl Azide (2.21)
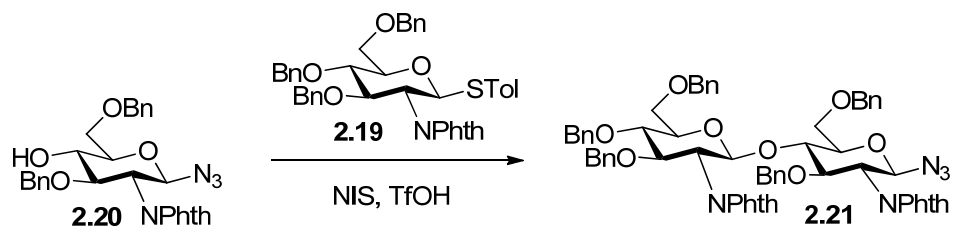
To a solution of **2.19** (1.0 g, 1.46 mmol) and **2.20** (514 mg, 1.00 mmol) in anhydrous CH_2Cl_2 (50 mL) was added 4 Å MS under an Ar atmosphere. The reaction was cooled to -30 °C, and NIS (520 mg, 2.31 mmol) was added. TfOH (41 μL, 0.46 mmol) was then added dropwise over a 5 min period. The reaction mixture was stirred for 20 min, and was then filtered through celite. The filtrate was washed with aqueous $NaHCO_3$, $Na_2S_2O_3$, and brine solution. The organic layer was dried over Na_2SO_4, filtered, and concentrated to give yellowish oil. Silica gel chromatography yielded **2.21** (800 mg, 75%) of as clear syrup. NMR data were consistent with literature-reported values.[53] MALDI TOF MS: $[M-N_2+Na]^+$ calcd for $C_{63}H_{57}N_3O_{12}Na$, 1070.4; found: m/z 1070.2; $[M+Na]^+$ calcd for $C_{63}H_{57}N_5O_{12}Na$, 1098.4; found: m/z 1098.2.

O-(2-Acetamido-3,4,6-tri-O-benzyl-2-deoxy-β-D-glucopyranosyl)-(1→4)-2-acetamido-3,6-di-O-benzyl-2-deoxy-β-D-glucopyranosyl Azide (2.22)
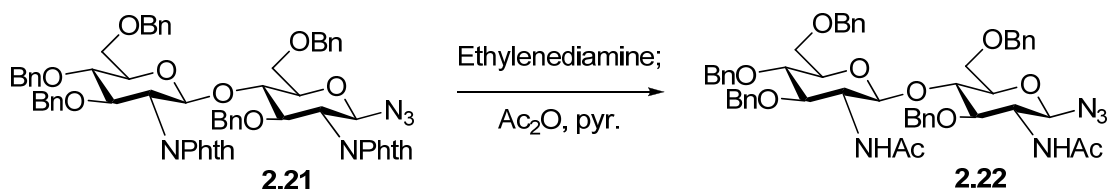
After a mixture of **2.21** (200 mg, 0.19 mmol), ethylenediamine (1 mL), and 1-butanol (5 mL) was stirred at 90 °C overnight, it was concentrated to dryness under vacuum. The

resulting residue was dissolved in Ac$_2$O/pyridine (1:2, 3 mL) and stirred overnight at rt. After the reaction mixture was diluted with EtOAc (50 mL), the solution was washed with saturated NaHCO$_3$ and brine, dried over Na$_2$SO$_4$, filtered, and concentrated under vacuum. The residue was purified by silica gel chromatography to give **2.22** as white foam (156 mg, 91%). NMR data were consistent with literature-reported values.[53] MALDI TOFMS: [M-N$_2$+Na]$^+$ calcd for C$_{51}$H$_{57}$N$_3$O$_{10}$Na, 894.4; found: *m/z* 895.0; [M+Na]$^+$ calcd for C$_{51}$H$_{57}$N$_5$O$_{10}$Na, 922.4; found: *m/z* 922.8.

N^α-(9-Fluorenylmethoxycarbonyl)-N^γ-[2-acetamido-3,4,6-tri-*O*-benzyl-2-deoxy-β-D-glucopyranosyl)-(1→4)-2-acetamido-3,6-di-*O*-benzyl-2-deoxy-β-D-glucopyranosyl]-L-asparagine *tert*-Butyl Ester (2.23)

To a solution of Fmoc-Asp-OtBu in CH$_2$Cl$_2$ (10 mL) and NMP (1 mL) was subsequently added HOBt and DCC. The mixture was stirred at rt for 1 h to give the active ester. Meanwhile, a mixture of **2.22** and Lindlar's catalyst in CH$_2$Cl$_2$/MeOH was stirred at rt for 2.5 h under an H$_2$ atmosphere. After filtration through celite and concentration in vacuum, the resulting residue was dissolved in CH$_2$Cl$_2$ (2 mL), and then the freshly prepared active ester solution was added (precipitated DCU was filtered off before addition). The mixture was stirred at rt overnight, concentrated, and purified directly by silica gel chromatography to give **2.23** as white foam (70%). ^{1}H NMR (500 MHz, CD$_3$OD-CDCl$_3$ 1:5): δ 7.71 (d, 2 H, *J* = 8.0 Hz), 7.56 (d, 2 H, *J* = 7.5 Hz), 7.40-7.06 (m,

32 H), 4.79-4.67 (m, 4 H), 4.61-4.53 (m, 3 H), 4.51 (d, 1 H, *J* = 10.5 Hz), 4.42 (t, 1 H, *J* = 5 Hz), 4.40-4.31 (m, 5 H), 4.23 (t, 1 H, *J* = 7.5 Hz), 4.16 (t, 1 H, *J* = 7.0 Hz), 4.04 (t, 1 H, *J* = 7.0 Hz), 3.96 (t, 1 H, *J* = 8.5 Hz), 3.84 (t, 1 H, *J* = 10.0 Hz), 3.64-3.49 (m, 7 H), 3.49-3.41 (m, 2 H), 3.28-3.23 (m, 1 H), 2.77 (ddd, 2 H, *J* =16 Hz, 3.5 Hz), 1.78 (s, 3 H), 1.73 (s, 3 H), 1.37 (s, 9 H). MALDI TOF MS: [M +Na]$^+$ calcd for $C_{74}H_{82}N_4O_{15}Na$, 1289.6; found: *m/z* 1289.9.

N^α-(9-Fluorenylmethoxycarbonyl)-N^γ-[2-acetamido-3,4,6-tri-*O*-benzyl-2-deoxy-β-D-glucopyranosyl)-(1→4)-2-acetamido-3,6-di-*O*-benzyl-2-deoxy-β-D-glucopyranosyl]-L-asparagine (2.24)
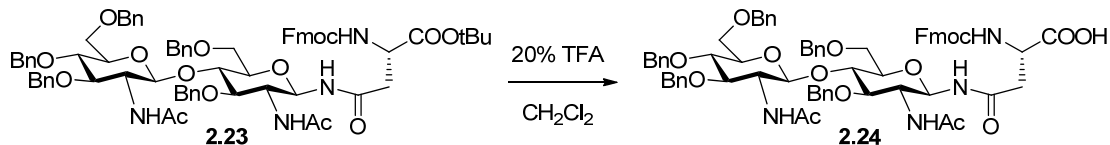
To a solution of **2.23** (55 mg, 43 μmol) in CH_2Cl_2 (4 mL) was added triethylsilane (0.25 mL) and TFA (1 mL). After the mixture was stirred for 2.5 h at rt, Et$_3$N was added to quench the reaction, which was then concentrated and subjected to silica gel chromatography to give **2.24** as white foam (50 mg, 96%). ^{1}H NMR (400 MHz, CD$_3$OD-CDCl$_3$ 1:5): δ 7.76 (d, *J* = 7.2 Hz, 2 H), 7.63 (d, *J* = 7.2 Hz, 2 H), 7.37-7.16 (m, 32 H), 5.71 (d, *J* = 2.4 Hz, 1 H), 4.78-4.52 (m, 9H), 4.49-4.44 (4 H), 4.39-4.31 (m, 2 H), 4.26-4.16 (m, 3 H), 3.93-3.73 (m, 6 H), 3.66-3.53 (m, 5 H), 3.37 (s, broad, 1 H), 2.86 (dd, *J* = 5.6, 16.4 Hz, 1 H), 2.76 (dd, *J* = 7.2, 15.2 Hz, 1 H), 2.04 (s, 3 H), 1.86 (s, 3 H). MALDI TOF MS: [M+Na]$^+$ calcd for $C_{70}H_{74}N_4O_{15}Na$, 1233.5; found: *m/z* 1233.4.

Resin-Bound Glycopeptide 2.25
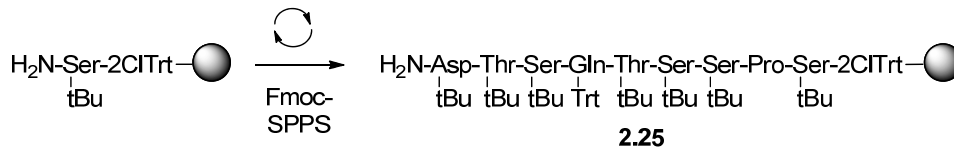
Ser-loaded 2-chlorotrityl resin (417 mg, 0.25 mmol) was subjected to eight cycles of Fmoc-SPPS on an automated peptide synthesizer to prepare resin-bound nonapeptide **2.25** (661 mg, 93% by weight) using HBTU-DIEA as the condensation reagent and 20% piperidine as the deprotection reagent. The product was then used in the SPPS construction of glycopeptides **2.15**, **2.16**, and **2.17**.

CD52 Glycopeptide 2.15
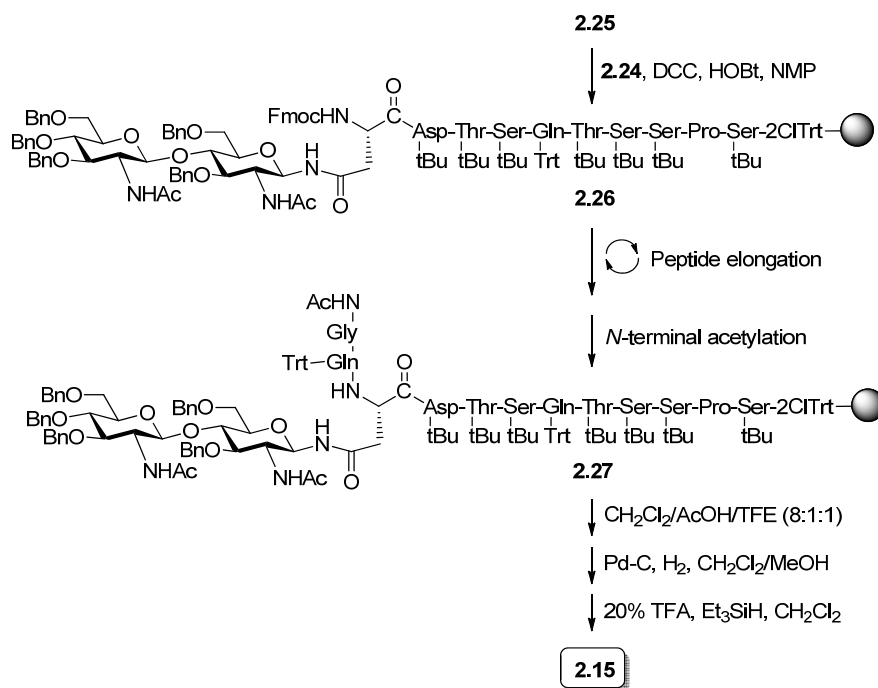
A solution of glycosyl amino acid **2.24** (37 mg, 30 μmol), HOBt (8 mg, 60 μmol), and DCC (12 mg, 60 μmol) in NMP (1 mL) was stirred at rt for 1 h and then transferred to a SPPS vessel containing resin-bound nonapeptide **2.25** (56 mg, 20 μmol). The mixture

was shaken at rt overnight under an Ar atmosphere, after which the resin was filtered off and washed thoroughly with NMP to give solid supported glycopeptide **2.26**. After Fmoc removal with 20% piperidine in NMP, the resin was subjected to two manual Fmoc-SPPS cycles using the benzotriazole active esters of Fmoc-Gln(Trt)-OH and Fmoc-Gly-OH to afford the desired peptide sequence. After final Fmoc deprotection and *N*-terminal acetylation of half of the sample with Ac_2O to give **2.27**, the resin was treated with CH_2Cl_2/AcOH/TFE (8:1:1) at rt for 2 h to release the glycopeptide. The resin was filtered off and the cleavage mixture was diluted with hexanes and concentrated under vacuum to give a white solid (13 mg, 42% based on **2.25**). To the resulting fully protected glycopeptide (13 mg, 4 µmol) was added solvent CH_2Cl_2-MeOH (1:1, 1 mL), 10% Pd/C (13 mg), and a H_2 atmosphere. After MALDI MS showed complete reaction, the catalyst was filtered off and the solvent was evaporated to get the debenzylated product (8 mg, 78% based on previous step), which was treated with 20% TFA in CH_2Cl_2 (1 mL) at rt for 2.5 h. After co-evaporation with toluene and thorough washing of the residue with diethyl ether, the product **2.15** was lyophilized and then purified by RP-HPLC (Supelco Discovery C18, 250 x 10 mm, eluent 2.0% *i*-PrOH in H_2O, 2 mL/min, R_t = 16.1 min, 2.2 mg, 42% based on previous yield given). ^{1}H NMR (500 MHz, D_2O, DHO at δ 4.79 as reference): δ 5.05 (d, *J* = 10.0 Hz, 1 H), 4.69 (t, *J* = 7.0 Hz, 1 H), 4.61 (d, *J* = 8.0 Hz, 1 H), 4.55 (t, *J* = 5.0 Hz, 1 H), 4.51 (t, *J* = 5.0 Hz, 1 H), 4.47-4.40 (m, 4 H), 4.37-4.32 (m, 2 H), 4.28-4.26 (m, 2 H), 4.01-3.81 (m, 15 H), 3.78-3.74 (m, 4 H), 3.69-3.64 (m, 2 H), 3.60-3.55 (m, 2 H), 3.52-3.49 (m, 2 H), 2.89 (dd, *J* = 6.0, 16. Hz, 1 H), 2.77 (dd, *J* = 7.5, 15.0 Hz, 2 H), 2.69 (dd, *J* = 6.5, 16.0 Hz, 1 H), 2.42-2.30 (m, 5 H), 2.22-2.11 (m, 2 H), 2.08 (s, 6 H), 2.06-2.04 (m, 2 H), 2.02 (s, 3 H), 2.01-1.99 (m, 2 H),

1.24 (s, 3 H), 1.23 (s, 3 H). ESI MS: [M+2H]$^{2+}$ calcd for $C_{63}H_{103}N_{17}O_{35}$, 828.8401; found: *m/z* 828.8364.

3-*O*-Benzyl-2-deoxy-6-*O*-(*para*-methoxybenzyl)-2-phthalimido-β-D-glucopyranosyl Azide (2.29)
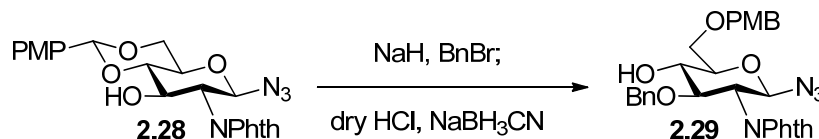
To a solution of **2.28** (2.20 g, 4.86 mmol) in DMF (15 mL) at 0 ºC was added NaH (60% dispersion in mineral oil, 1.24 g, 7.27 mmol). After stirring for 30 min, benzyl bromide (0.86 mL, 7.27 mmol) was added to the reaction mixture, which was stirred at rt overnight. After quenching excess NaH with MeOH, the reaction was concentrated under vacuum to remove most of the DMF, then diluted with EtOAc and washed with saturated NaHCO$_3$, brine, dried over Na$_2$SO$_4$, and concentrated under vacuum. Purification by silica gel chromatography gave the benzylated intermediate (2.11 g, 3.9 mmol, 80%), which was then dissolved in THF and cooled to 0 ºC. To this solution was added MS 4 Å (1.0 g), NaBH$_3$CN (2.4 g, 39 mmol), and 1.0 M HCl in dry Et$_2$O (to pH 1-2). After 1 h, MS were filtered off, and the filtrate was diluted with EtOAc. The organic layer was washed with cold NaHCO$_3$ and brine, then dried over Na$_2$SO$_4$, filtered, and concentrated under vacuum. Silica gel chromatography gave **2.29** as colorless syrup (1.9 g, 89%). ^{1}H NMR (500 MHz, CDCl$_3$): δ 7.83-7.71 (m, 4 H), 7.29 (d, *J* = 8.5 Hz, 2 H), 7.04-6.89 (m, 7 H), 5.36 (d, *J* = 9.5 Hz, 1 H), 4.75 (d, *J* = 12.0 Hz, 1 H), 4.59 (d, *J* = 12.0 Hz, 1 H), 4.53 (d, *J* = 11.5 Hz, 2 H), 4.26 (dd, *J* = 8.5, 10.5 Hz, 1 H), 4.08 (dd, *J* = 9.5,

10.5 Hz, 1 H), 3.85-3.81 (m, 2 H), 3.82 (s, 3 H) 3.79-3.70 (m, 2 H). ESI MS: [M+Na]$^+$ calcd for C$_{29}$H$_{28}$N$_4$O$_7$Na, 567.1832; found: *m/z* 567.1856.

O-(2-Deoxy-2-acetamido-β-D-glucopyranosyl)-(1→4)-[O-2,3,4-tri-O-benzyl-α-fucopyranosyl)-(1→6)]-3-O-benzyl-2-deoxy-2-acetamido-β-D-glucopyranosyl Azide (2.31)
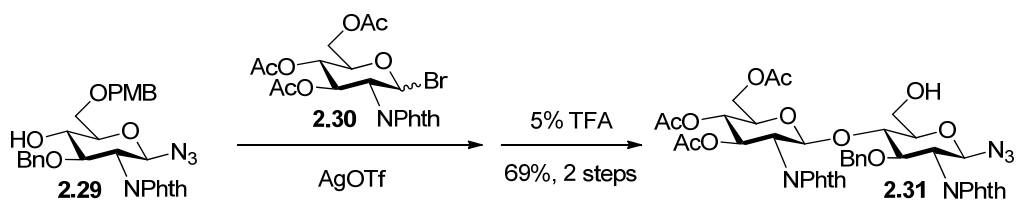
To a solution of 2,3,4-tri-O-acetyl-2-deoxy-2-phthalimido-β-D-glucopyranosyl acetate (75 mg, 0.15 mmol) in CH$_2$Cl$_2$ (2 mL) was added 33% HBr in HOAc (100 µL) at 0 °C. After being stirred at rt for 5 h, the reaction mixture was washed with saturated aqueous NaHCO$_3$ and brine, dried over Na$_2$SO$_4$, and concentrated under vacuum to give glycosyl bromide **2.30** as syrup that was directly used in the glycosylation reaction. After a mixture of **2.30** (all product acquired from bromination), **2.29** (40 mg, 0.07 mmol), and MS 4 Å (50 mg) in dry CH$_2$Cl$_2$ (2 mL) was stirred at rt for 1 h, it was cooled to -50 °C. To this mixture was added AgOTf (38 mg, 0.15 mmol). The reaction was then warmed to rt and stirred for 3 h, at which point the MS were filtered off, and the resulting filtrate was washed with NaHCO$_3$ and brine, then dried over Na$_2$SO$_4$ and concentrated under vacuum. The residue was not fully separable by silica gel chromatography, as another compound co-eluted with the desired disaccharide. Thus, to a solution of the intermediate in CH$_2$Cl$_2$ (4 mL) was added TFA (0.2 mL) and Et$_3$SiH (0.5 mL). After the reaction stirred for 2.5 h, it was quenched with Et$_3$N, concentrated, and purified by silica

gel chromatography to give pure **2.31** (43 mg, 69% yield over two steps). Spectroscopic

data of **2.31** were identical to literature-reported values.[39]

N^{α}-(9-Fluorenylmethoxycarbonyl)-N^{γ}-[2-acetamido-3,4,6-tri-*O*-benzyl-2-deoxy-β-D-glucopyranosyl)-(1→4)-[*O*-2,3,4-tri-*O*-benzyl-α-fucopyranosyl)-(1→6)]-3-*O*-benzyl-2-deoxy-2-acetamido-β-D-glucopyranosyl]-L-asparagine Allyl Ester (2.35)
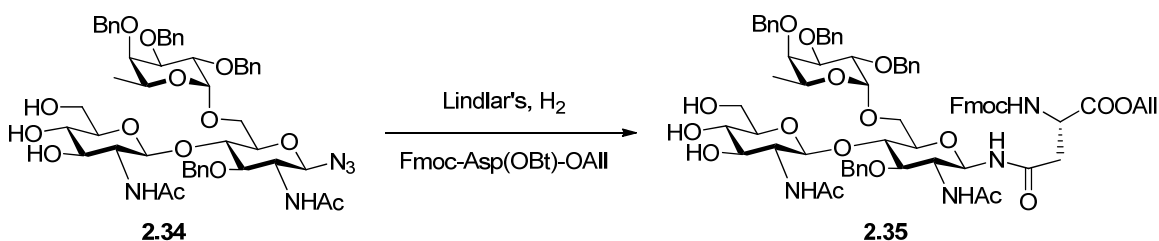
Glycosyl azide **2.34** (127 mg, 0.133 mmol) was dissolved in a mixture of CH_2Cl_2 (1 mL)

and MeOH (3 mL). Lindlar's catalyst (127 mg) was then added and the reaction was

stirred under a H_2 atmosphere at rt for 3 h. After filtration of the catalyst by silica gel, the

reaction was concentrated under vacuum to give the glycosyl amine intermediate.

Meanwhile, to a solution of Fmoc-Asp(OH)-OAll (79 mg, 0.20 mmol) in CH_2Cl_2 (3 mL)

and NMP (0.1 mL) was added DCC (49 mg, 0.24 mmol) and HOBt (32 mg, 0.24 mmol).

After stirring for 1 h, DCU was filtered off and the active ester solution was directly

transferred to a solution of the glycosyl amine in CH_2Cl_2 (1 mL). The reaction was stirred

at rt under an Ar atmosphere overnight, then concentrated and purified by silica gel

chromatography to give the glycosyl-Asn conjugate **2.35** (122 mg, 72%). ^{1}H NMR (400

MHz, $CDCl_3$-CD_3OD 3:1): δ 7.56 (d, *J* = 8.0 Hz, 2 H), 7.40 (d, *J* = 7.2 Hz, 2 H), 7.21-

7.05 (m, 24 H), 5.72-5.65 (m, 1 H), 5.11 (d, *J* = 16.8 Hz, 1 H), 5.02 (d, *J* = 10.4 Hz, 1 H),

4.77 (d, *J* = 11.6 Hz, 1 H), 4.72 (d, *J* = 11.2 Hz, 1 H), 4.68-4.55 (m, 4 H), 4.44-4.40 (m, 6

H), 4.23 (dd, *J* = 7.6, 10.8 Hz, 1 H), 4.04-3.99 (m, 2 H), 3.87-3.84 (m, 2 H), 3.74 (dd, *J* =

3.2, 9.6 Hz, 1 H), 3.71-3.66 (m, 4 H), 3.62-3.56 (m, 5 H), 3.35-3.27 (m, 4 H), 3.13-3.07 (m, 4 H), 2.62 (dd, J = 6.0, 16.4 Hz, 1 H) 2.49 (dd, J = 4.0, 16.4 Hz, 1 H), 1.77 (s, 3 H), 1.67 (s, 3 H), 0.95 (d, J = 6.4 Hz, 3 H). ESI MS: $[M+Na]^+$ calcd for $C_{72}H_{82}N_4O_{19}Na$, 1329.5414; found: m/z 1329.5471.

N^α-(9-Fluorenylmethoxycarbonyl)-N^γ-[2-acetamido-3,4,6-tri-O-benzyl-2-deoxy-β-D-glucopyranosyl)-(1→4)-[O-2,3,4-tri-O-benzyl-α-fucopyranosyl)-(1→6)]-3-O-benzyl-2-deoxy-2-acetamido-β-D-glucopyranosyl]-L-asparagine (2.36)
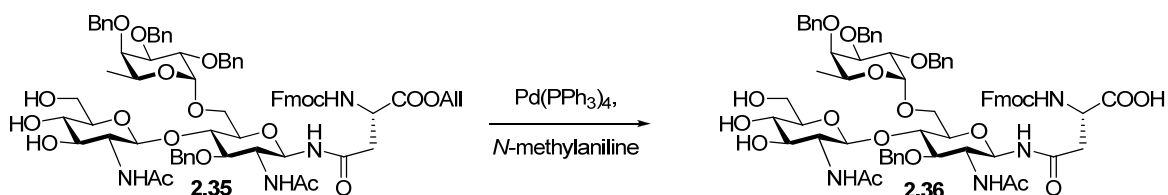
To a solution of **2.35** (77 mg, 0.058 mmol) in CH_2Cl_2/MeOH (1:1, 2 mL) was added *N*-methylaniline (100 μL) and Pd(PPh$_3$)$_4$ (12 mg, 0.01 mmol). The reaction mixture was stirred overnight at rt, then concentrated under vacuum and purified by silica gel chromatography to give **2.36** (57 mg, 78%). ^{1}H NMR (500 MHz, CD$_3$OD, δ 4.78 as reference): δ 7.69 (d, J = 7.2 Hz, 2 H), 7.55-7.52 (m, 2 H), 7.29-7.15 (m, 24 H), 4.98 (d, J = 11.6 Hz, 1 H), 4.90 (d, J = 10.0 Hz, 1 H), 4.84 (d, J = 2.4 Hz, 1 H), 4.71-4.66 (m, 4 H), 4.61 (d, J = 8.8 Hz, 1H), 4.54 (d, J = 10.4 Hz, 1 H), 4.47 (d, J = 11.2 Hz, 1 H), 4.24-4.23 (m, 3 H), 4.11 (t, J = 6.4 Hz, 1 H), 4.01 (d, J = 5.6 Hz, 1 H), 3.90-3.81 (m, 4 H), 3.78-3.68 (m, 5 H), 3.53 (t, J = 9.6 Hz, 1 H), 3.47-3.42 (m, 2 H), 3.38 (t, J = 9.8 Hz, 1 H), 3.31-3.28 (m, 3 H), 3.19-1.17 (m, 1 H), 2.65 (s, broad, 2 H), 1.91 (s, 3 H), 1.84 (s, 3 H), 1.05 (d, J = 5.6 Hz, 3 H). ESI MS: $[M+Na]^+$ calcd for $C_{69}H_{78}N_4O_{19}Na$, 1289.5116; found: m/z 1289.5158.

CD52 Glycopeptide 2.16
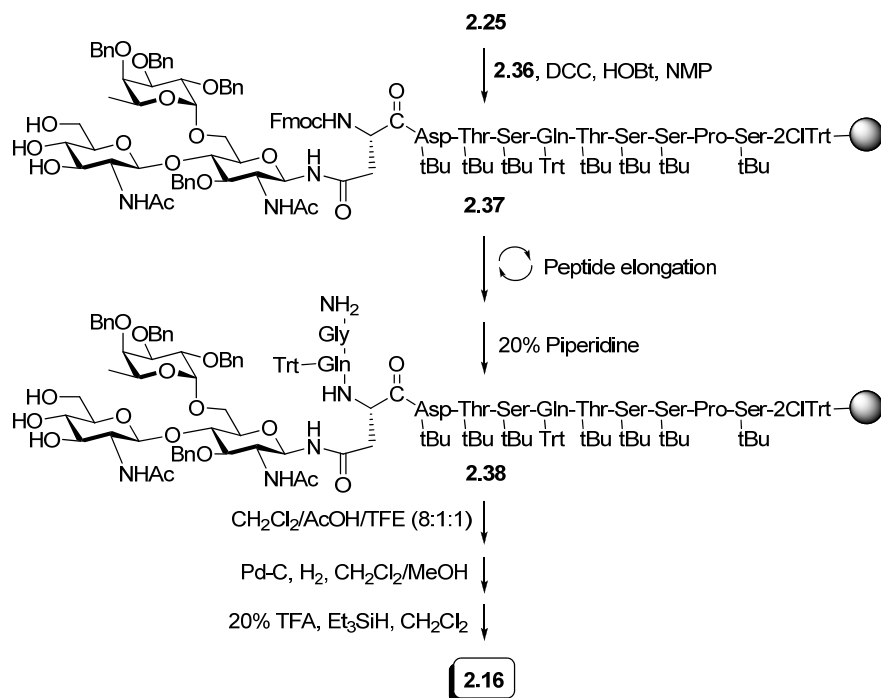
A solution of glycosyl amino acid **2.36** (51 mg, 40 µmol), HOBt (12 mg, 90 µmol), and DCC (18 mg, 90 µmol) in NMP (1 mL) was stirred at rt for 1 h and then transferred to a SPPS vessel containing resin-bound nonapeptide **2.25** (56 mg, 20 µmol). The mixture was shaken at rt overnight under an Ar atmosphere, after which the resin was filtered off and washed thoroughly with NMP to give resin supported glycopeptide **2.37**. After Fmoc removal with 20% piperidine in NMP, the resin was subjected to two manual Fmoc-SPPS cycles using the benzotriazole active esters of Fmoc-Gln(Trt)-OH and Fmoc-Gly-OH to give the desired peptide sequence. After final Fmoc deprotection to give **2.38**, half of the resin was treated with CH_2Cl_2/AcOH/TFE (8:1:1) at rt for 2 h to release the glycopeptide. The resin was filtered off and the cleavage mixture was diluted with hexanes and concentrated under vacuum to give a white solid (13 mg, 43% based on **2.25**). To the resulting fully protected glycopeptide (13 mg, 4.3 µmol) was added

CH$_2$Cl$_2$-MeOH (1:1, 1 mL), 10% Pd/C (13 mg), and a H$_2$ atmosphere (MeOH used in the debenzylation was refluxed with NaBH$_4$ for several hours and then distilled to reduce any formaldehyde present and thus prevent *N*-methylation via reductive amination). After MALDI MS showed complete reaction, the catalyst was filtered off and the solvent was evaporated to get the debenzylated product (10 mg, 87% based on previous step), which was treated with 20% TFA in CH$_2$Cl$_2$ (1 mL) at rt for 2.5 h. After co-evaporation with toluene and thorough washing of the residue with diethyl ether, the product **2.16** was lyophilized and then purified by RP-HPLC (Supelco Discovery C18, 250 x 10 mm, eluent 1.5% *i*-PrOH in H$_2$O, 2 mL/min, R_t = 17.9 min, 2.1 mg, 31% based on previous yield given). ^{1}H NMR (500 MHz, D$_2$O, DHO at δ 4.79 as reference): δ 5.05 (d, *J* = 10.0 Hz, 1 H), 4.90 (d, *J* = 4.0 Hz, 1 H), 4.67 (d, *J* = 8.5 Hz, 1 H), 4.54 (t, *J* = 5.5 Hz, 1 H), 4.53-4.51 (m, 1 H), 4.49-4.44 (m, 2 H), 4.43-4.40 (m, 2 H), 4.37-4.32 (m, 2 H), 4.27 (t, *J* = 6.0 Hz, 1 H), 4.14 (dd, *J* = 6.5, 13.0 Hz, 1 H), 3.95-3.86 (m, 11 H), 3.85-3.74 (m, 8 H), 3.70-3.68 (m, 2 H), 3.57 (t, *J* = 8.5 Hz, 1 H), 3.53-3.46 (m, 2 H), 2.90 (dd, *J* = 5.0, 16.5 Hz, 1 H), 2.86-2.77 (m, 3 H), 2.42-2.37 (m, 4 H), 2.35-2.32 (m, 1 H), 2.21-2.17 (m, 1 H), 2.12-2.10 (m, 1 H), 2.09 (s, 3 H), 2.08-2.04 (m, 2 H), 2.03 (s, 3 H), 2.02-2.00 (m, 2 H), 1.24-1.20 (m, 9 H). MALDI TOF MS: [M+Na]$^+$ calcd for C$_{67}$H$_{109}$N$_{17}$O$_{38}$Na, 1782.7; found: *m/z* 1782.6.

CD52 Glycopeptide 2.17
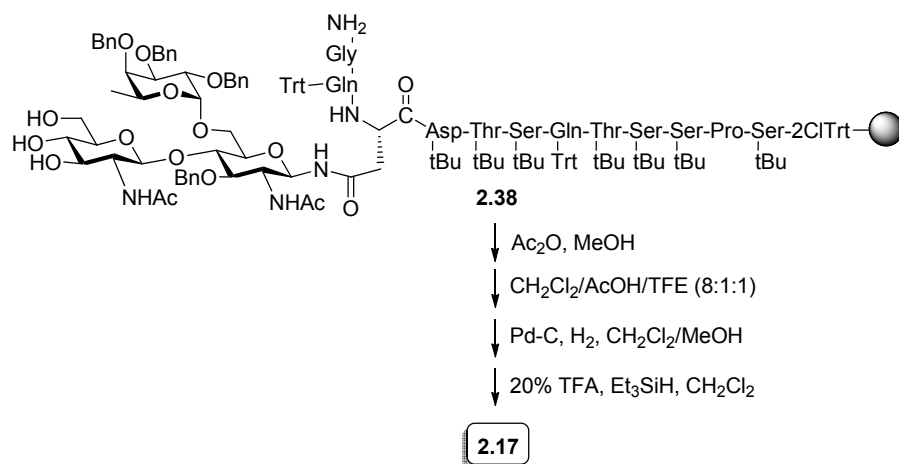
2.17 was prepared according to the procedure described for the synthesis of **2.16**. The half of resin-bound glycopeptide **2.38** (10 µmol) remaining from the synthesis of **2.16** was treated with Ac₂O-MeOH (1:2, 1 mL) at rt for 4 h. The resin was then treated with CH₂Cl₂/AcOH/TFE (8:1:1) at rt for 2 h to release the glycopeptide. The resin was filtered off and the cleavage mixture was diluted with hexanes and concentrated under vacuum to give a white solid (12 mg, 40% based on **2.25**). The remaining deprotection steps were carried out according to the protocol described for **2.16** to arrive at **2.17**, which was purified by RP-HPLC (Supelco Discovery C18, 250 x 10 mm, eluent 1.5% *i*-PrOH in H₂O, 2 mL/min, R_t = 17.9 min, 1.9 mg, 28% based on previous yield given). Spectroscopic data of **2.17** were consistent with literature-reported values.[39]

Circular Dichroism Spectroscopy

CD spectra of all derivatives were recorded on a Chirascan circular dichroism spectrometer equipped with a water bath to control the temperature at 25 °C. The solutions of **2.13**, **2.14**, **2.15**, **2.16**, and **2.17** were prepared from dry samples in ddH₂O to give concentrations of 6.6×10^{-2}, 3.2×10^{-2}, 1.6×10^{-2}, 4.2×10^{-2}, and 1.8×10^{-2} mM,

respectively. The molar ellipticity was normalized using the equation $\varepsilon=\theta/(32.98 \times C)$, in which θ is the CD absorbance of each peptide analog. The molar ellipticities of **2.13**, **2.14**, **2.15**, **2.16**, and **2.17** were normalized from concentrations of 6.6×10^{-2}, 3.2×10^{-2}, 8.0×10^{-2}, 6.2×10^{-2}, and 9.2×10^{-2} mM, respectively. Each curve represents the average of five scans.

2.5 References

(1)   Apweiler, R.; Hermjakob, H.; Sharon, N. On the frequency of protein glycosylation, as deduced from analysis of the SWISS-PROT database. *Biochim. Biophys. Acta* **1999**, *1473*, 4.

(2)   Varki, A. Biological roles of oligosaccharides: All of the theories are correct. *Glycobiology* **1993**, *3*, 97.

(3)   Helenius, A.; Aebi, M. Intracellular functions of N-linked glycans. *Science* **2001**, *291*, 2364.

(4)   O'Connor, S. E.; Imperiali, B. Modulation of protein structure and function by asparagine-linked glycosylation. *Chem. Biol.* **1996**, *3*, 803.

(5)   Pratt, M.; Bertozzi, C. Synthetic glycopeptides and glycoproteins as tools for biology. *Chem. Soc. Rev.* **2005**, *34*, 58.

(6)   O'Connor, S. E.; Imperiali, B. Conformational switching by asparagine-linked glycosylation. *J. Am. Chem. Soc.* **1997**, *119*, 2295.

(7)   O'Connor, S. E.; Imperiali, B. A molecular basis for glycosylation-induced conformational switching. *Chem. Biol.* **1998**, *5*, 427.

(8)   Bosques, C. J.; Tschampel, S. M.; Woods, R. J.; Imperiali, B. Effects of glycosylation on peptide conformation: A synergistic experimental and computational study. *J. Am. Chem. Soc.* **2004**, *126*, 8421.

(9)   O'Connor, S. E.; Imperiali, B. Effect of N-linked glycosylation on glycopeptide and glycoprotein structure. *Curr. Opin. Chem. Biol.* **1999**, *3*, 643.

(10)   Meyer, B.; Möller, H. Conformation of glycopeptides and glycoproteins. *Top. Curr. Chem.* **2007**, *267*, 187.

(11) Buskas, T.; Ingale, S.; Boons, G.-J. Glycopeptides as versatile tools for glycobiology. *Glycobiology* **2006**, *16*, 113R.

(12) Seitz, O. Glycopeptide synthesis and the effects of glycosylation on protein structure and activity. *ChemBioChem* **2000**, *1*, 214.

(13) Guo, Z.; Shao, N. Glycopeptide and glycoprotein synthesis involving unprotected carbohydrate building blocks. *Med. Res. Rev.* **2005**, *25*, 655.

(14) Weerapana, E.; Imperiali, B. Asparagine-linked protein glycosylation: From eukaryotic to prokaryotic systems. *Glycobiology* **2006**, *16*, 91R.

(15) Kornfeld, R.; Kornfeld, S. Assembly of asparagine-linked oligosaccharides. *Annu. Rev. Biochem* **1985**, *54*, 631.

(16) Ruddock, L. W.; Molinari, M. N-glycan processing in ER quality control. *J. Cell. Sci.* **2006**, *119*, 4373.

(17) Apweiler, R.; Hermjakob, H.; Sharon, N. On the frequency of protein glycosylation, as deduced from analysis of the SWISS-PROT database. *Biochim. Biophys. Acta* **1999**, *1473*, 4.

(18) Berman, H. M.; Westbrook, J.; Feng, Z.; Gilliland, G.; Bhat, T. N.; Weissig, H.; Shindyalov, I. N.; Bourne, P. E. The Protein Data Bank. *Nucleic Acids Res.* **2000**, *28*, 235.

(19) Chen, B.; Vogan, E. M.; Gong, H.; Skehel, J. J.; Wiley, D. C.; Harrison, S. C. Determining the structure of an unliganded and fully glycosylated SIV gp120 envelope glycoprotein. *Structure* **2005**, *13*, 197.

(20) Chen, B.; Vogan, E. M.; Gong, H.; Skehel, J. J.; Wiley, D. C.; Harrison, S. C. Structure of an unliganded simian immunodeficiency virus gp120 core. *Nature* **2005**, *433*, 834.

(21) Swarts, B. M.; Guo, Z. In *Carbohydrate-based vaccines and immunotherapies*; Guo, Z., Boons, G.-J., Eds.; John Wiley & Sons, Inc.: Hoboken, 2009, p 167.

(22) Wyss, D. F.; Choi, J. S.; Li, J.; Knoppers, M. H.; Willis, K. J.; Arulanandam, A. R.; Smolyar, A.; Reinherz, E. L.; Wagner, G. Conformation and function of the N-linked glycan in the adhesion domain of human CD2. *Science* **1995**, *269*, 1273.

(23) Hale, G.; Xia, M. Q.; Tighe, H. P.; Dyer, M. J.; Waldmann, H. The CAMPATH-1 antigen (CDw52). *Tissue Antigens* **1990**, *35*, 118.

(24) Treumann, A.; Lifely, M. R.; Schneider, P.; Ferguson, M. A. J. Primary structure of CD52 *J. Biol. Chem.* **1995**, *270*, 6088.

(25) Xia, M. Q.; Hale, G.; Lifely, M. R.; Ferguson, M. A.; Campbell, D.; Packman, L.; Waldmann, H. Structure of the CAMPATH-1 antigen, a glycosylphosphatidylinositol-anchored glycoprotein which is an exceptionally good target for complement lysis. *Biochem. J.* **1993**, *293*, 633.

(26) Schröter, S.; Derr, P.; Conradt, H. S.; Nimtz, M.; Hale, G.; Kirchhoff, C. Male-specific modification of human CD52. *J. Biol. Chem.* **1999**, *274*, 29862

(27) James, L. C.; Hale, G.; Waldman, H.; Bloomer, A. C. 1.9 Å structure of the therapeutic antibody CAMPATH-1H fab in complex with a synthetic peptide antigen. *J. Mol. Biol.* **1999**, *289*, 293.

(28) Tsuji, Y.; Clausen, H.; Nudelman, E.; Kaizu, T.; Hakomori, S.-I.; Isojima, S. Human sperm carbohydrate antigens defined by an antisperm human

monoclonal antibody derived from an infertile woman bearing antisperm antibodies in her serum. *J. Exp. Med.* **1988**, *168*, 343.

(29) Diekman, A. B.; Norton, E. J.; Klotz, K. L.; Westbrook, V. A.; Shibahara, H.; Naaby-Hansen, S.; Flickinger, C. J.; Herr, J. C. N-linked glycan of a sperm CD52 glycoform associated with human infertility *FASEB J.* **1999**, *13*, 1303.

(30) *Glycopeptides and related compounds: Synthesis, analysis, and applications*; Large, D. G.; Warren, C. D., Eds.; Marcel Dekker, Inc.: New York, 1997.

(31) Bruch, K. v. d.; Kunz, H. *Angew. Chem. Int. Ed.* **1994**, *33*, 101.

(32) Merrifield, R. B. Solid phase peptide synthesis. I. The synthesis of a tetrapeptide. *J. Am. Chem. Soc.* **1963**, *85*, 2149.

(33) Wen, S.; Guo, Z. Unprotected oligosaccharides as phase tags: Solution-phase synthesis of glycopeptides with solid-phase workups. *Org. Lett.* **2001**, *3*, 3773.

(34) Xue, J.; Guo, Z. Efficient synthesis of complex glycopeptides based on unprotected oligosaccharides. *J. Org. Chem.* **2003**, *68*, 2713.

(35) Guo, Z.; Nakahara, Y.; Nakahara, Y.; Ogawa, T. Solid-phase synthesis of CD52 glycopeptide and an efficient route to Asn-core pentasaccharide conjugate. *Bioorgan. Med. Chem.* **1997**, *5*, 1917.

(36) Kunz, H.; Unverzagt, C. Protecting-group-dependent stability of intersaccharide bonds - synthesis of a fucosyl-chitobiose glycopeptide. *Angew. Chem., Int. Ed. Engl.* **1988**, *27*, 1697.

(37) Sjölin, P.; Elofsson, M.; Kihlberg, J. Removal of acyl protective groups from glycopeptides: Base does not epimerize peptide stereocenters, and beta-elimination Is slow. *J. Org. Chem.* **1996**, *61*, 560.

(38) Bruch, K. v. d.; Kunz, H. Synthesis of N-glycopeptide clusters with Lewisx antigen side chains and their coupling to carrier proteins. *Angew. Chem., Int. Ed. Engl.* **1994**, *33*, 101.

(39) Shao, N.; Xue, J.; Guo, Z. Chemical synthesis of CD52 glycopeptides containing the acid-labile fucosyl linkage. *J. Org. Chem.* **2003**, *68*, 9003.

(40) Shao, N.; Guo, Z. A facile synthesis of the fucosylated N-linked glycan core and its application to solid-phase synthesis of CD52 glycopeptide. *Pol. J. Chem.* **2005**, *79*, 297.

(41) Shao, N.; Xue, J.; Guo, Z. Chemical synthesis of a skeleton structure of sperm CD52 - A GPI-anchored glycopeptide. *Angew. Chem. Int. Ed.* **2004**, *43*, 1569.

(42) Ogawa, T.; Beppu, K. Synthesis of 3-O-(2-acetamido-2-deoxy-3-O-β--galactopyranosyl-β--galactopyranosyl)-1,2-di-O-tetradecyl-sn-glycerol. *Carbohydr. Res* **1982**, *101*, 271.

(43) Hansen, S. G.; Skrydstrup, T. Studies directed to the synthesis of oligochitosans - preparation of building blocks and their evaluation in glycosylation studies. *Eur. J. Org. Chem.* **2007**, 3392.

(44) Matsuo, I.; Nakahara, Y.; Ito, Y.; Nukada, T.; Nakahara, Y.; Ogawa, T. Synthesis of a glycopeptide carrying a N-linked core pentasaccharide. *Bioorg. Med. Chem.* **1995**, *3*, 1455.

(45) Söderman, P.; Larsson, E. A.; Widmalm, G. Synthesis of the trifucosylated N-linked hexasaccharide of a glycoprotein from haemonchus contortus. *Eur. J. Org. Chem.* **2002**, 1614.

(46)   Lemieux, R. U.; Takeda, T.; Chung, B. Y. Synthesis of 2-Amino-2-deoxy-β-D-glucopyranosides. *ACS Symp. Ser.* **1976**, *39*, 90.

(47)   Peters, T.; Weimar, T. Improved synthesis of -L-Fuc(14)--D-GlcNAc and -L-Fuc(16)--D-GlcNAc building blocks: A convergent strategy employing 4-O6-O acetyl migration; NOE data of the protected -1,4-linked disaccharide. *Liebigs Ann. Chem.* **1991**, 237.

(48)   Lemieux, R. U.; Hendriks, K. B.; Stick, R. V.; James, K. Halide ion catalyzed glycosidation reactions. Synthesis of alpha-linked disaccharides. *J. Am. Chem. Soc.* **1975**, *97*, 4056.

(49)   Urge, L.; Jackson, D. C.; Gorbics, L.; Wroblewski, K.; Graczyk, G.; Otvos, L. Synthesis and conformational analysis of N-glycopeptides that contain extended sugar chains. *Tetrahedron* **1994**, *50*, 2373.

(50)   Horvat, Š.; Otvos, L.; Urge, L.; Horvat, J.; Čudić, M.; Varga-Defterdarović, L. Circular dichroism study of the carbohydrate-modified opiod peptides. *Spectrochim. Acta A* **1999**, *55*, 2347.

(51)   Biondi, L.; Filira, F.; Gobbo, M.; Rocchi, R. Conformational investigations on glycosylated asparagine-oligopeptides of increasing chain length. *J. Peptide Sci.* **2002**, *7*, 80.

(52)   Gratzer, W. B.; Cowburn, D. A. Optical activity of biopolymers. *Nature* **1969**, *222*, 426.

(53)   Kerékgyárto, J.; Agoston, K.; Batta, G.; Kamerling, J. P.; Vliegenthart, J. F. G. Synthesis of fully and partially benzylated glycosyl azides *via* thioalkyl glycosides

as precursors for the preparation of N-glycopeptides. *Tetrahedron Lett.* **1998**, *39*, 7189.

Appendix A: Selected Characterization Data From Chapter 1
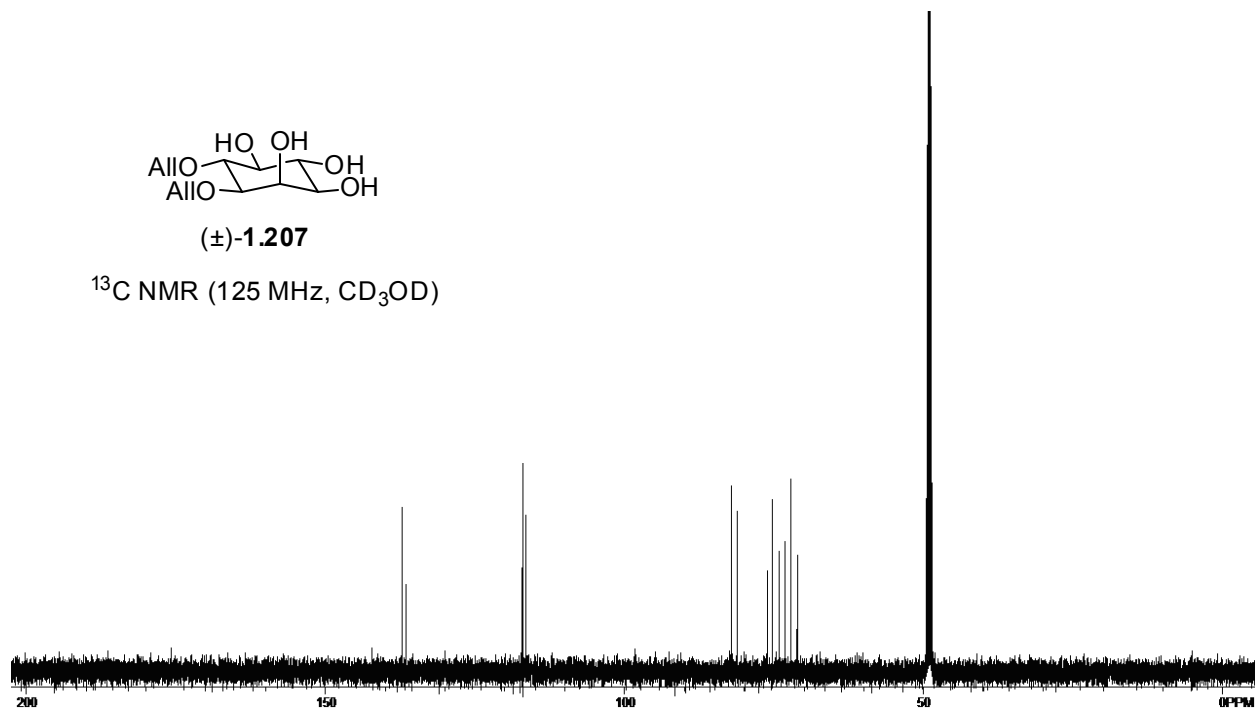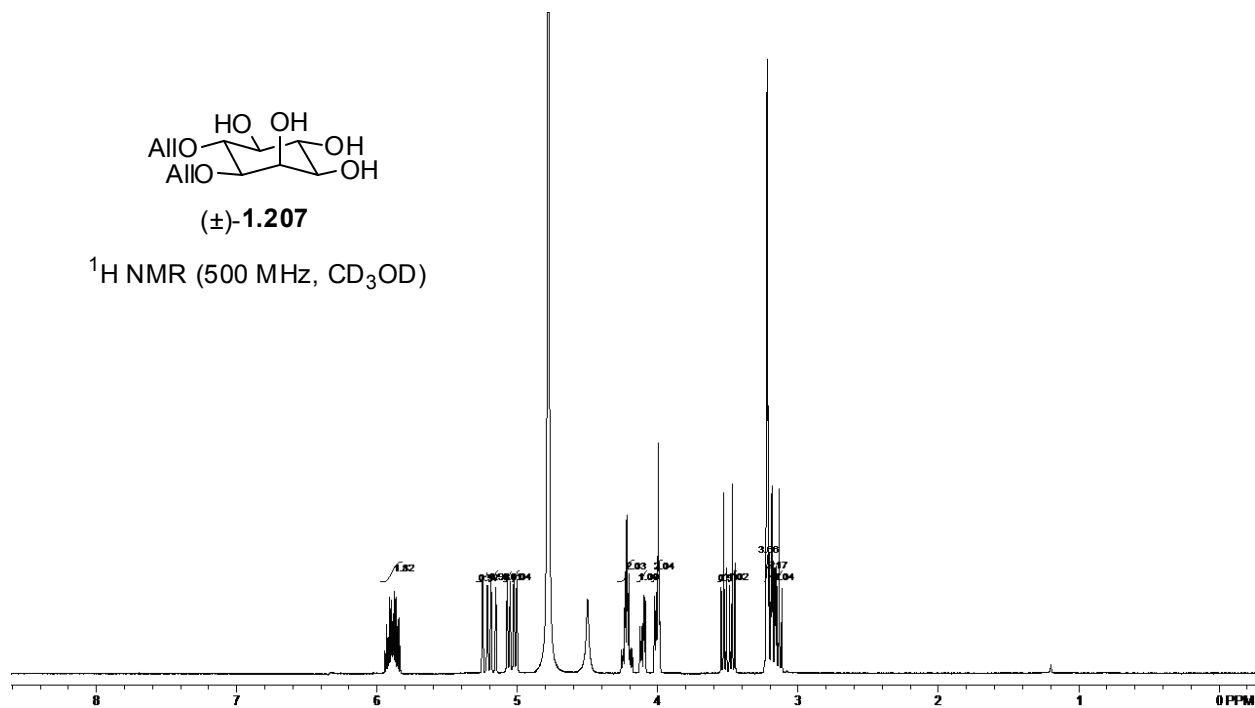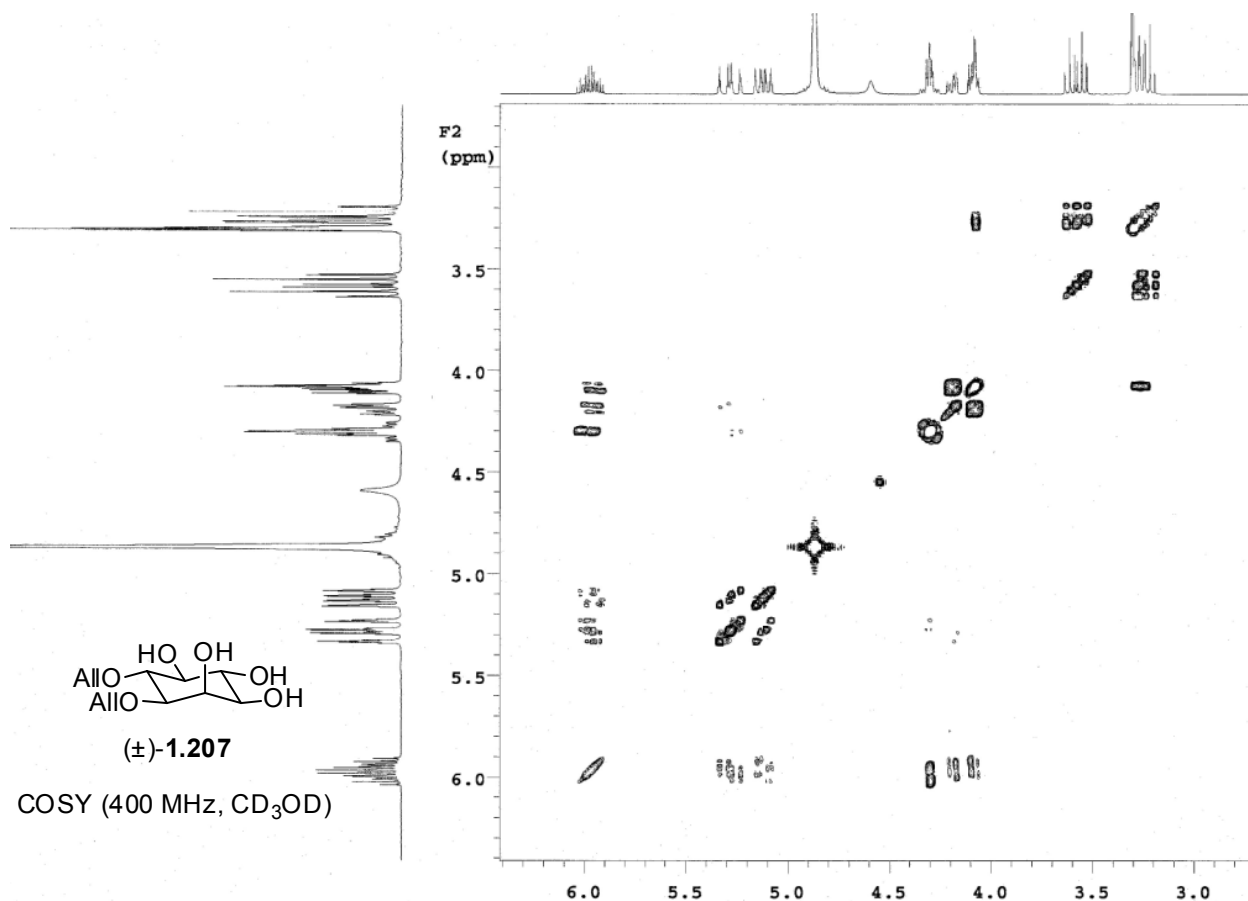
(±)-**1.207**

^{1}H NMR (500 MHz, CD$_3$OD)

(±)-**1.207**

^{13}C NMR (125 MHz, CD$_3$OD)

F2
(ppm)

HO OH
AllO
AllO OH
OH

(±)-**1.207**

COSY (400 MHz, CD₃OD)

Single Mass Analysis
Tolerance = 5.0 PPM / DBE: min = -1.5, max = 50.0
Element prediction: Off
Number of isotope peaks used for i-FIT = 3

Monoisotopic Mass, Even Electron Ions
397 formula(e) evaluated with 2 results within limits (up to 50 best isotopic matches for each mass)
Elements Used:
C: 0-500   H: 0-1000   N: 0-5   O: 0-10   23Na: 0-1
Guo- Ben Swarts BMS-V1-97 mw260 LCT0100 in meoh 1uL
Shay 2008-07b.pro
2008_0822_0100_13 14 (0.301) Cm (12:17-1:8x2.000)

HO OH
AllO
AllO OH
OH

(±)-**1.207**
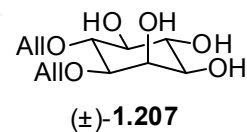
HR ESI MS

LCT Premier 22-Aug-2008 14:34:37
1: TOF MS ES+
1.43e+004
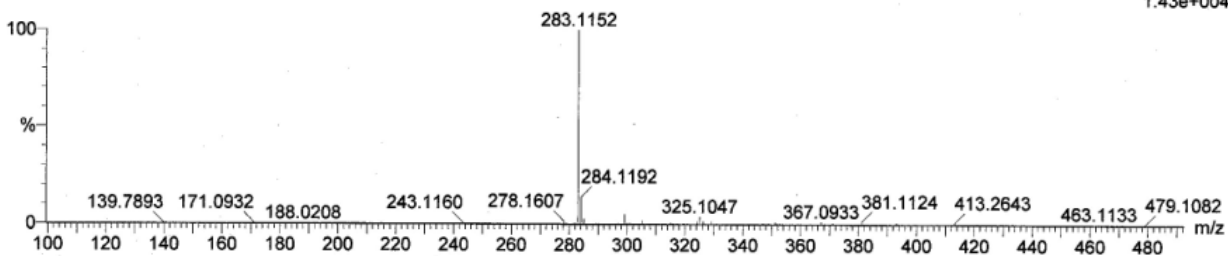
Mass	Calc. Mass	mDa	PPM	DBE	i-FIT	i-FIT (Norm)	Formula
Minimum:				-1.5			
Maximum:		2.0	5.0	50.0			
283.1152	283.1158	-0.6	-2.1	2.5	142.3	0.0	C12 H20 O6 23Na
	283.1141	1.1	3.9	1.5	147.4	5.1	C9 H19 N2 O8
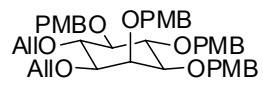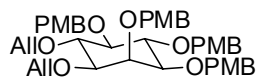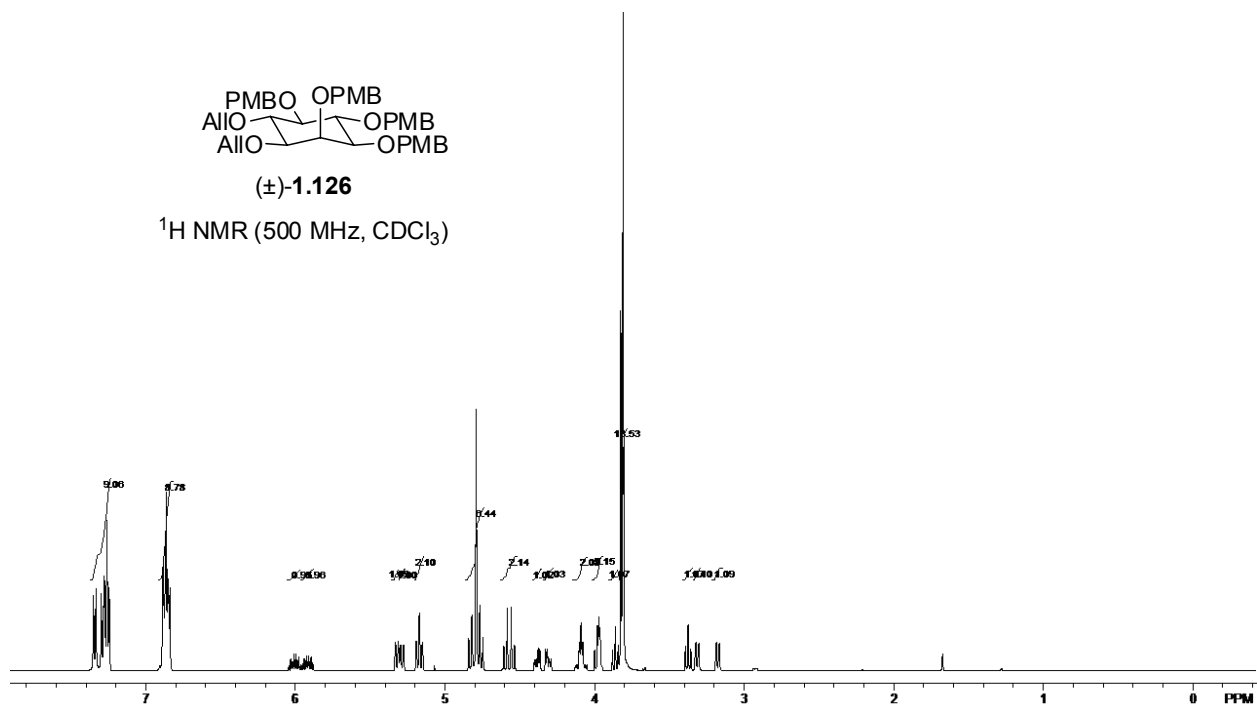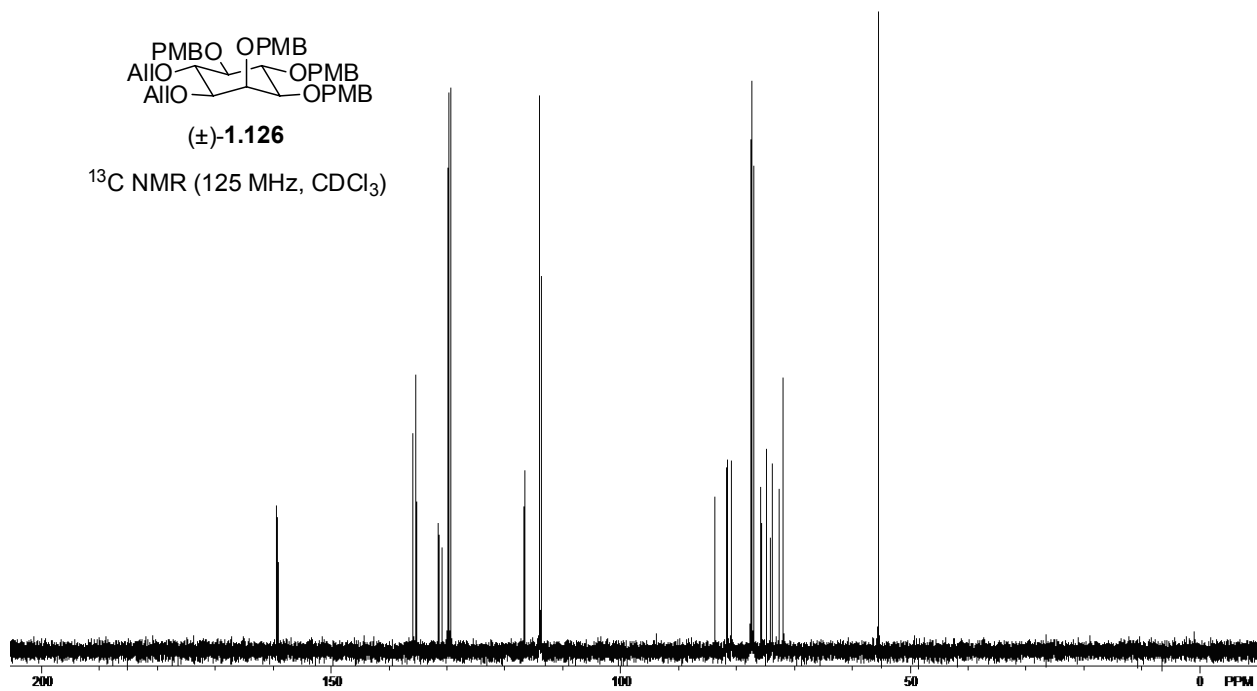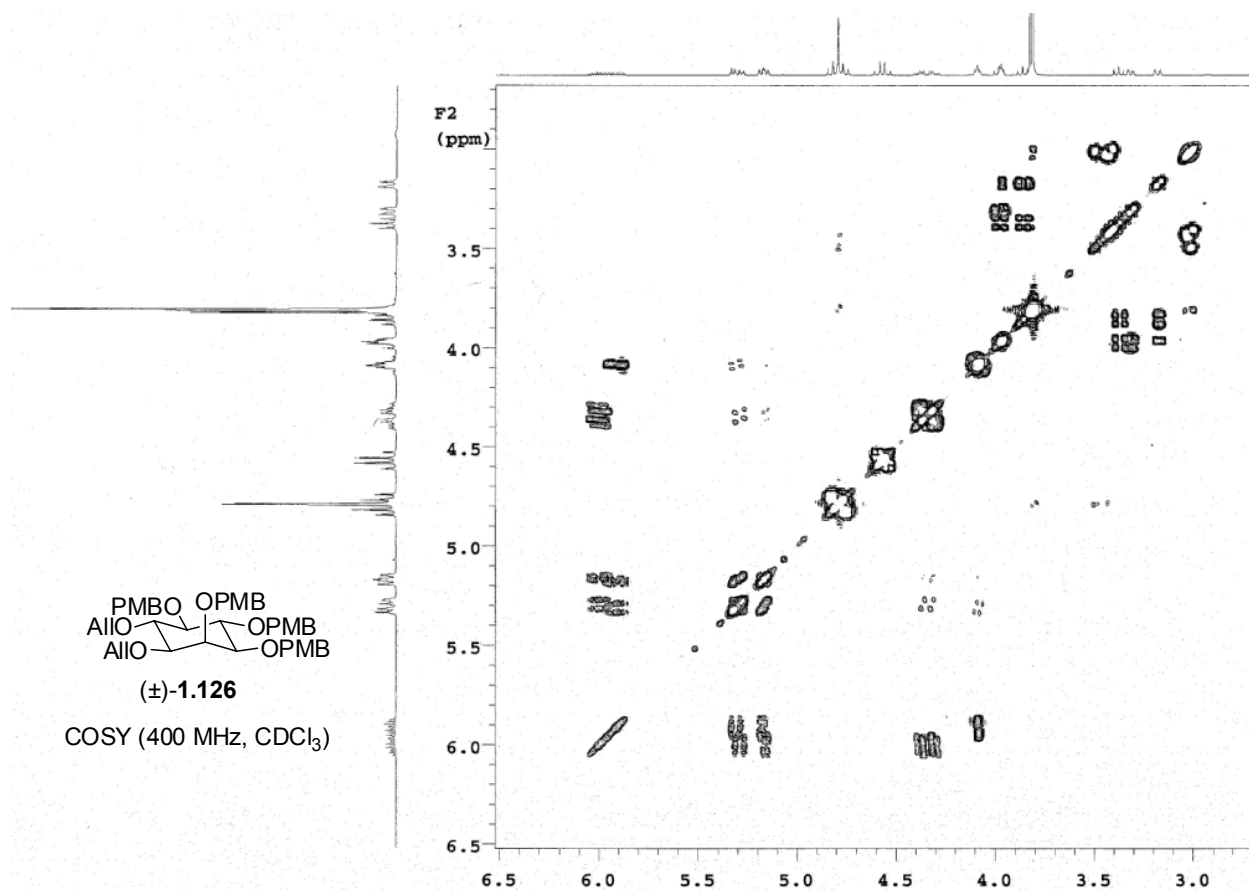
PMBO OPMB
AllO OPMB
AllO OPMB

(±)-**1.126**

^{1}H NMR (500 MHz, CDCl$_3$)

PMBO OPMB
AllO OPMB
AllO OPMB

(±)-**1.126**

^{13}C NMR (125 MHz, CDCl$_3$)

F2
(ppm)

PMBO OPMB
AllO—OPMB
AllO—OPMB

(±)-**1.126**

COSY (400 MHz, CDCl₃)

Single Mass Analysis

Tolerance = 5.0 PPM / DBE: min = -1.5, max = 50.0
Element prediction: Off
Number of isotope peaks used for i-FIT = 3

Monoisotopic Mass, Even Electron Ions
393 formula(e) evaluated with 3 results within limits (all results (up to 1000) for each mass)
Elements Used:
C: 0-500   H: 0-1000   N: 0-1   O: 0-10   23Na: 0-1
Guo- Ben Swarts BMS-V-98 LCT0269 mw740 0.5uL meoh
Shay 2008-07b.pro
2009_0109_0269 11 (0.230) Cm (9:11-2:7x2.000)

PMBO OPMB
AllO—OPMB
AllO—OPMB
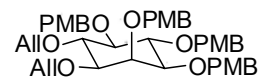
(±)-**1.126**

HR ESI MS

LCT Premier 09-Jan-2009 14:05:00
1: TOF MS ES+
1.82e+004

763.3448

764.3478

765.3510

758.3890   766.3531   779.3181   786.4276 793.3508   m/z

714.8138   725.8076 731.8267

720.0   730.0   740.0   750.0   760.0   770.0   780.0   790.0
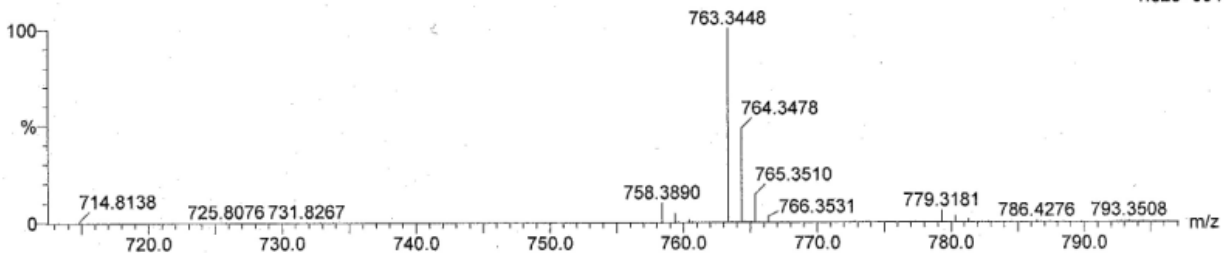
| | | | Minimum: | | -1.5 | | | |
| | | | Maximum: | 5.0 | 5.0 | 50.0 | | |

Mass	Calc. Mass	mDa	PPM	DBE	i-FIT	i-FIT (Norm)	Formula
763.3448	763.3458	-1.0	-1.3	18.5	84.0	0.0	C44 H52 O10 23Na
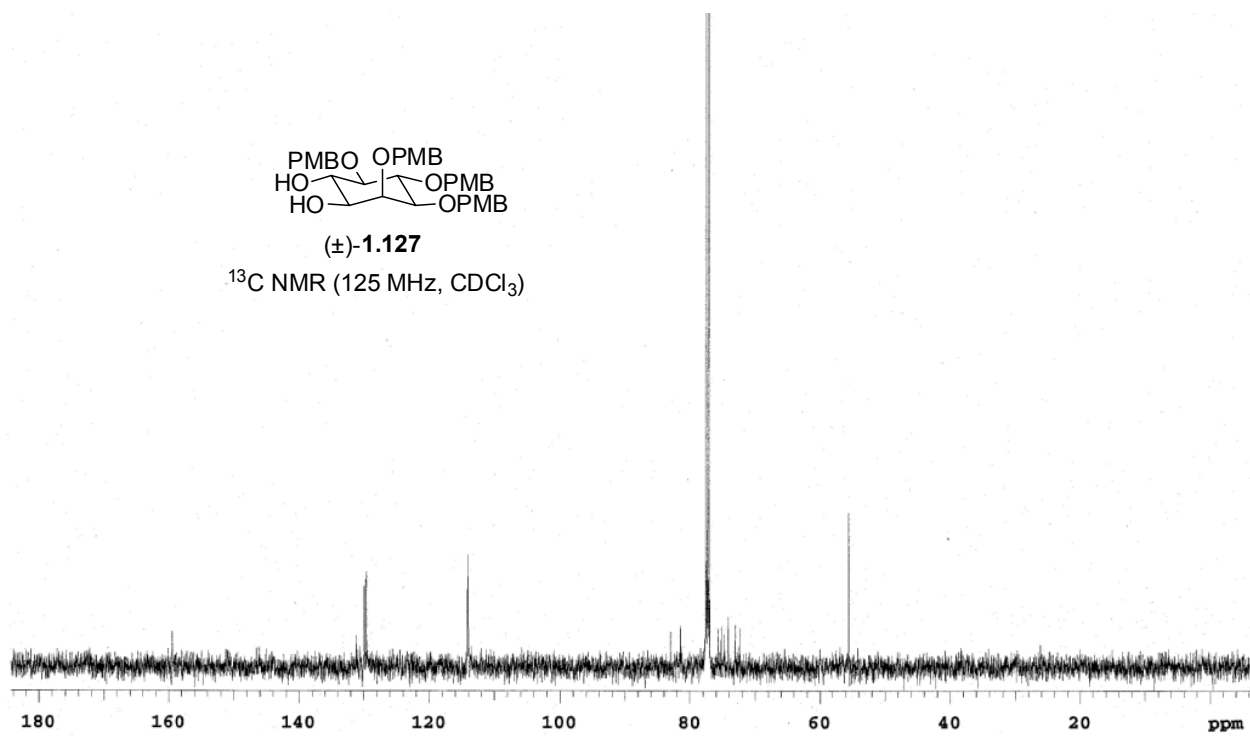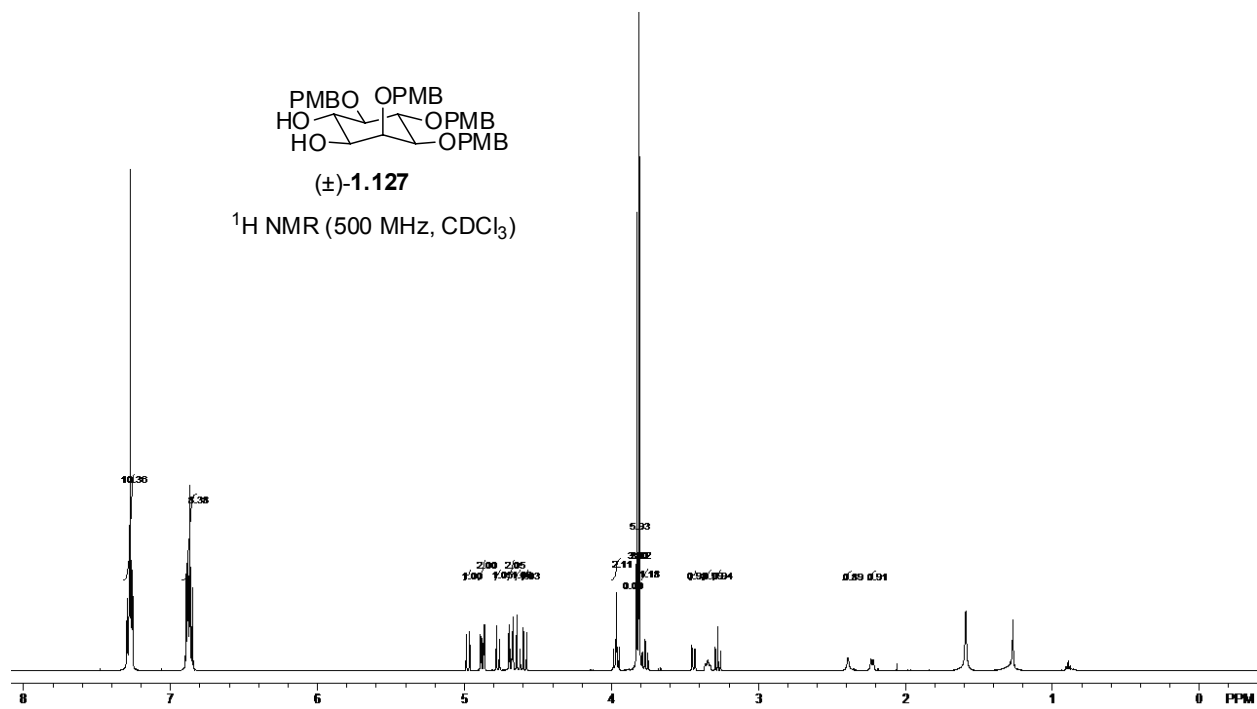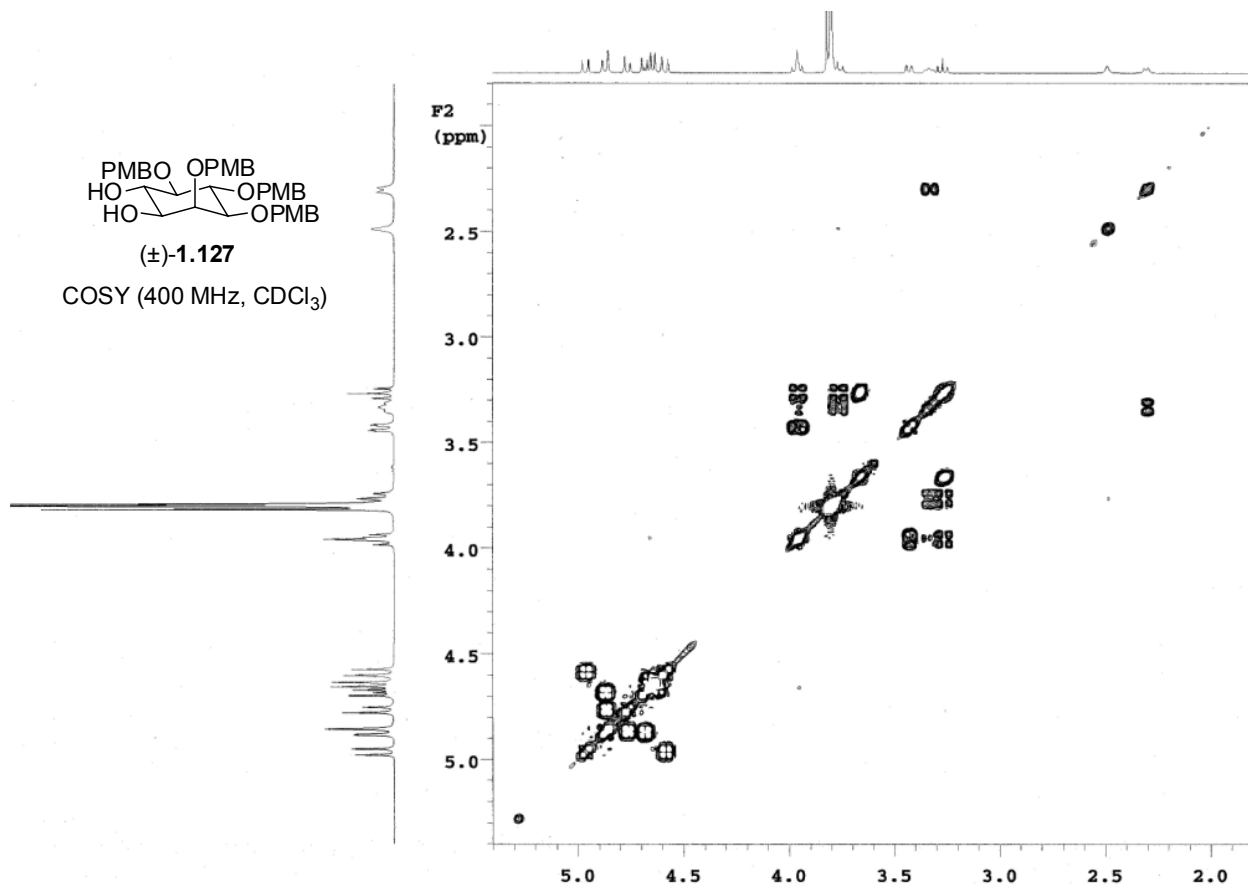
PMBO OPMB
HO OPMB
HO OPMB

(±)-**1.127**

^{1}H NMR (500 MHz, CDCl$_3$)

PMBO OPMB
HO OPMB
HO OPMB

(±)-**1.127**

^{13}C NMR (125 MHz, CDCl$_3$)

PMBO OPMB
HO—⟮ ⟯—OPMB
HO—⟮ ⟯—OPMB

(±)-**1.127**

COSY (400 MHz, CDCl₃)

PMBO OPMB
HO—⟮ ⟯—OPMB
HO—⟮ ⟯—OPMB

(±)-**1.127**

HR ESI MS

Single Mass Analysis
Tolerance = 6.0 PPM / DBE: min = -1.5, max = 50.0
Element prediction: Off
Number of isotope peaks used for i-FIT = 3

Monoisotopic Mass, Even Electron Ions
178 formula(e) evaluated with 3 results within limits (up to 50 best isotopic matches for each mass)
Elements Used:
C: 0-500   H: 0-1000   O: 0-10   23Na: 0-1

Guo; Ben Swarts BMS-V1-05 mw660 LCT0039 2uL meoh 3cm stk
DOPH   LCT Premier
2008_0725_0039_14 12 (0.247) Cm (11:12-1:5x1.200)

15:43:09 25-Jul-2008

1: TOF MS ES+
2.54e+003
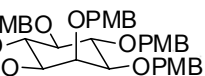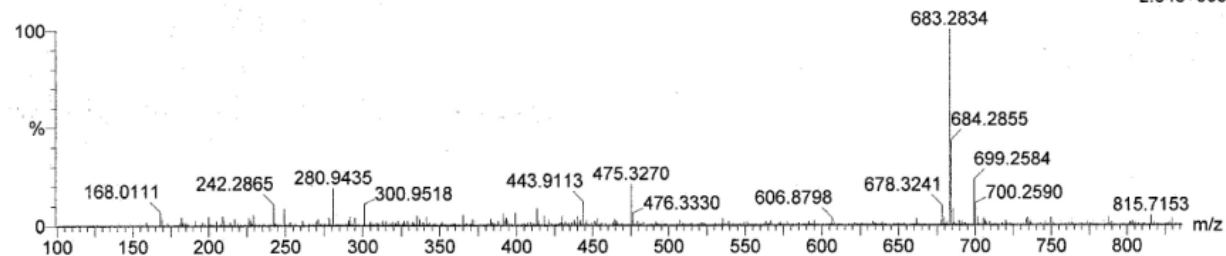
Minimum:			-1.5				
Maximum:	100.0	6.0	50.0				
Mass	Calc. Mass	mDa	PPM	DBE	i-FIT	i-FIT (Norm)	Formula
683.2834	683.2832	0.2	0.3	16.5	89.2	0.1	C38 H44 O10 23Na
	683.2856	-2.2	-3.2	19.5	91.7	2.7	C40 H43 O10
	683.2797	3.7	5.4	28.5	94.1	5.1	C47 H39 O5

PMBO OPMB
HO OPMB
AllO OPMB

(±)-**1.128**

¹H NMR (500 MHz, CDCl₃)

PMBO OPMB
HO OPMB
AllO OPMB

(±)-**1.128**

¹³C NMR (125 MHz, CDCl₃)

PMBO OPMB
HO—OPMB
AllO—OPMB

(±)-**1.128**
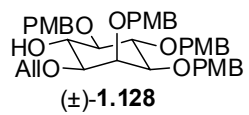
COSY (500 MHz, CDCl$_3$)
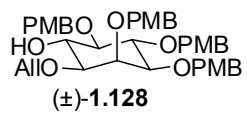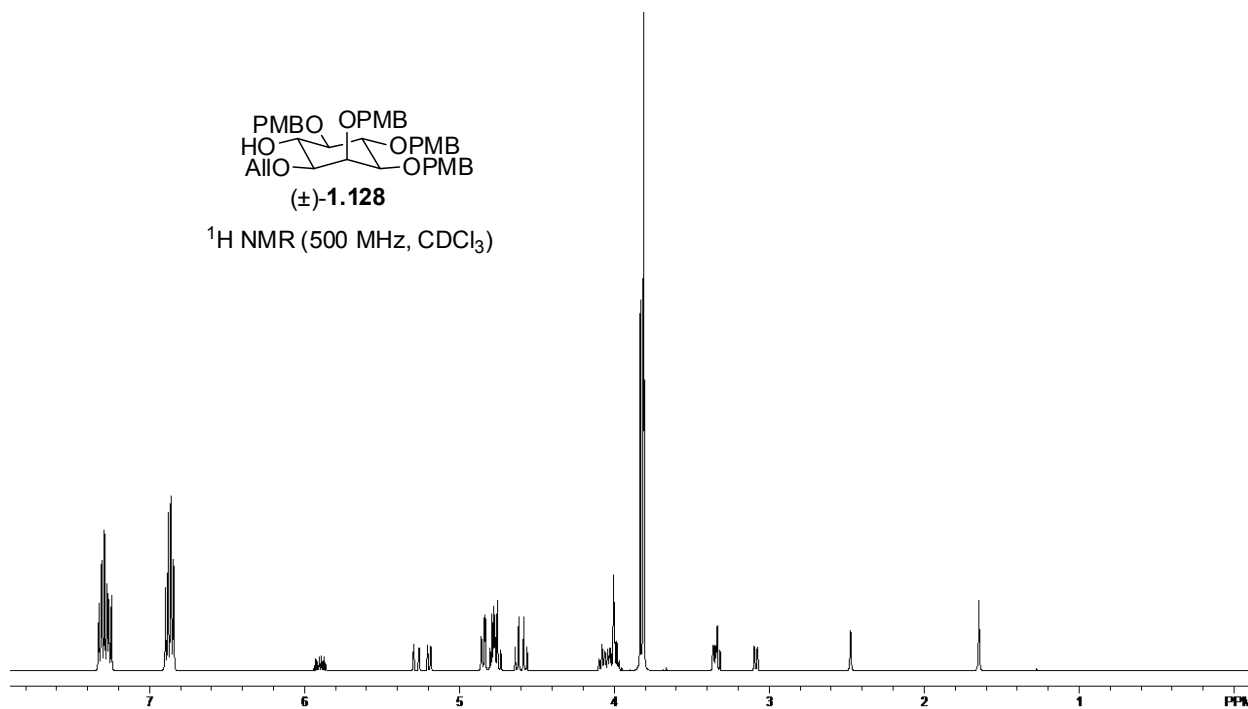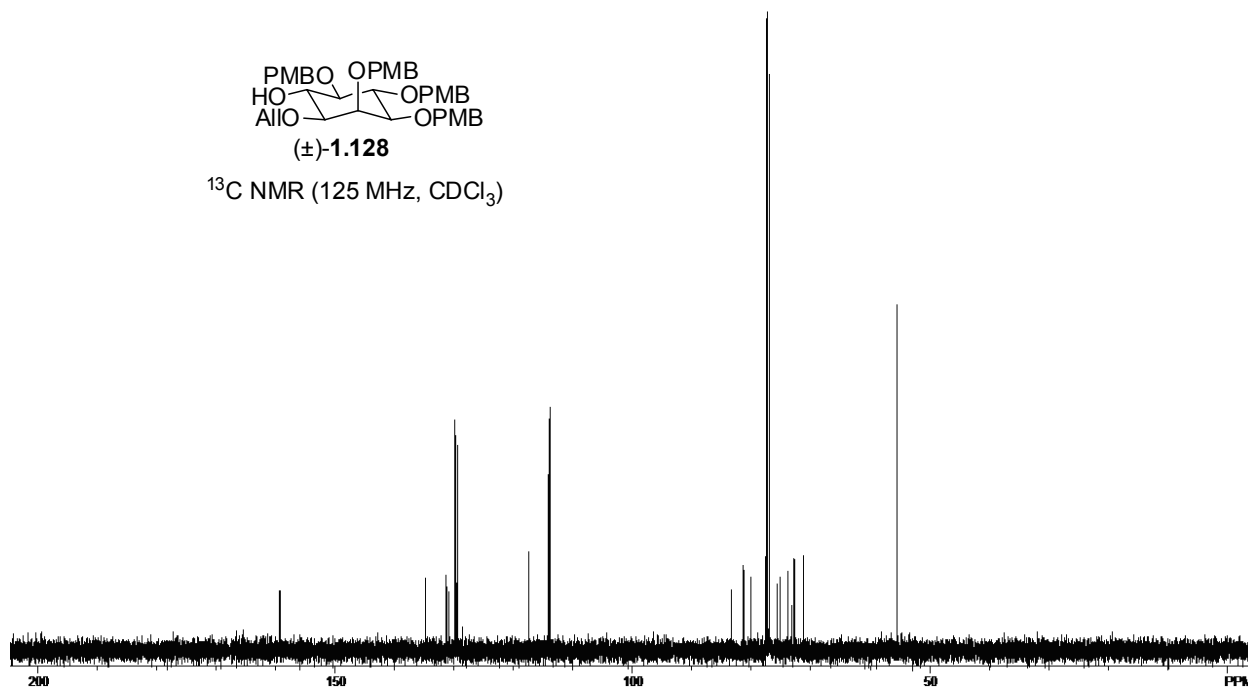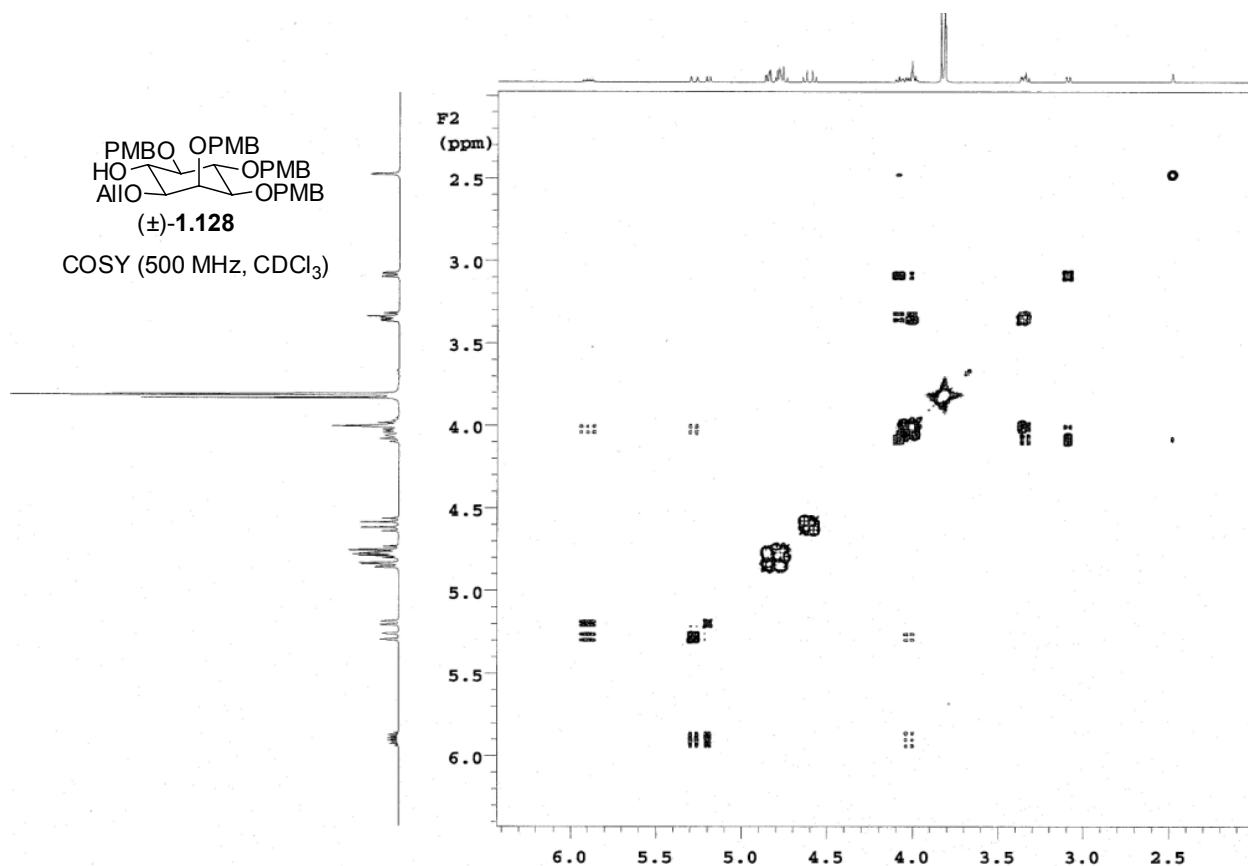
Single Mass Analysis
Tolerance = 10.0 PPM / DBE: min = -1.5, max = 60.0
Element prediction: Off
Number of isotope peaks used for i-FIT = 3

Monoisotopic Mass, Even Electron Ions
258 formula(e) evaluated with 5 results within limits (up to 50 best isotopic matches for each mass)
Elements Used:
C: 0-80   H: 0-200   O: 0-15   23Na: 0-1
guo- Ben Swarts BMS-VI-28-A mw700 LCT0111 10pg/ul meoh 0.1ul 1ul stk
Shay 2008-07b.pro
2008_0822_0111_30 13 (0.300) Cm (10:15-1:7x2.000)

PMBO OPMB
HO—OPMB
AllO—OPMB

(±)-**1.128**
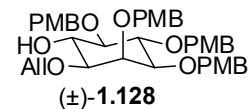
HR ESI MS

LCT Premier 22-Aug-2008 16:58:39
1: TOF MS ES+
4.43e+003
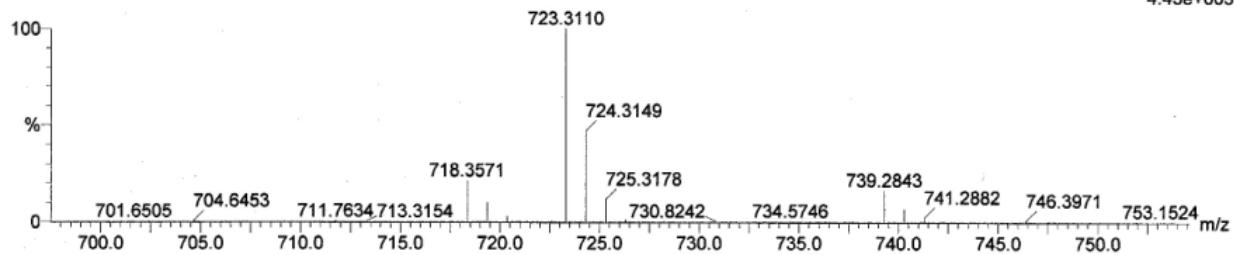
Minimum:				-1.5						
Maximum:		8.0	10.0	60.0						

Mass	Calc. Mass	mDa	PPM	DBE	i-FIT	i-FIT (Norm)	Formula			
723.3110	723.3145	-3.5	-4.8	17.5	122.2	0.0	C41	H48	O10	23Na
	723.3169	-5.9	-8.2	20.5	125.9	3.7	C43	H47	O10	
	723.3086	2.4	3.3	26.5	126.8	4.6	C48	H44	O5	23Na
	723.3110	0.0	0.0	29.5	127.2	5.0	C50	H43	O5	
	723.3052	5.8	8.0	38.5	131.7	9.5	C57	H39		

HPLC chromatogram for purification of (±)-**9**

Conditions: Waters Nova-Pak Silica 6 μm, 300 x 19 mm eluent 33% EtOAc in hexanes, 10 ml/min

(±)-**1.128**
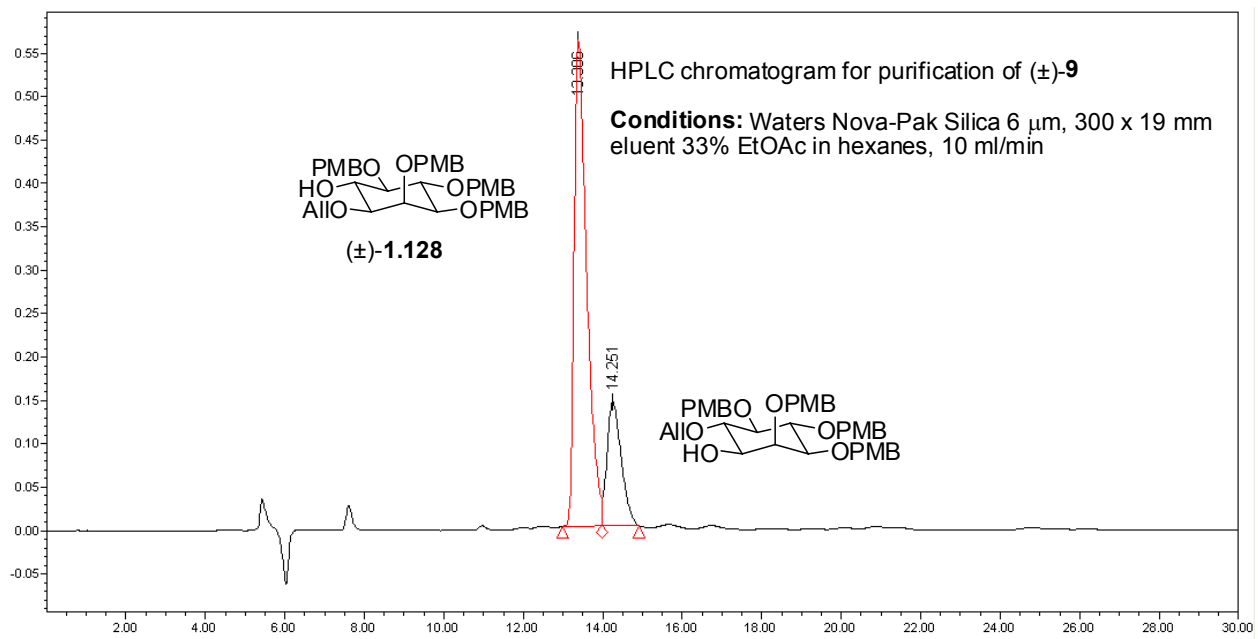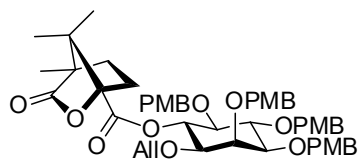
(-)-**1.129**

^{1}H NMR (500 MHz, CDCl$_3$)
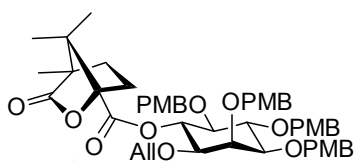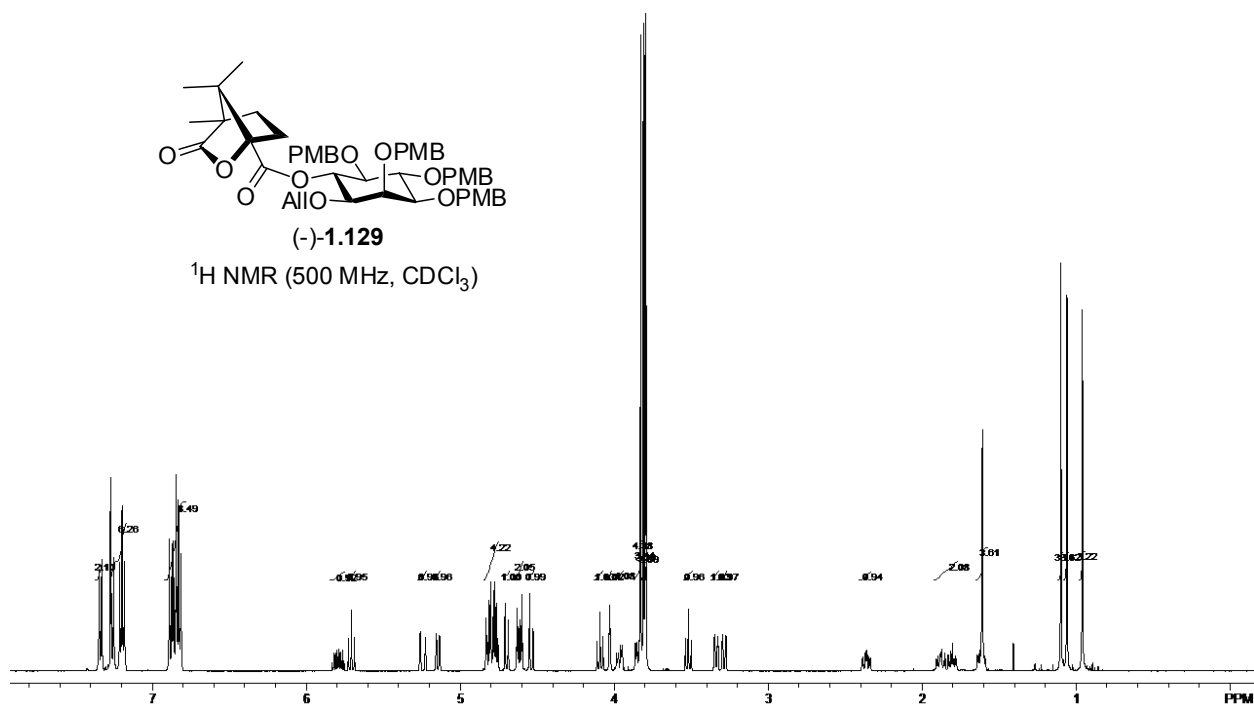
(-)-**1.129**

^{13}C NMR (125 MHz, CDCl$_3$)
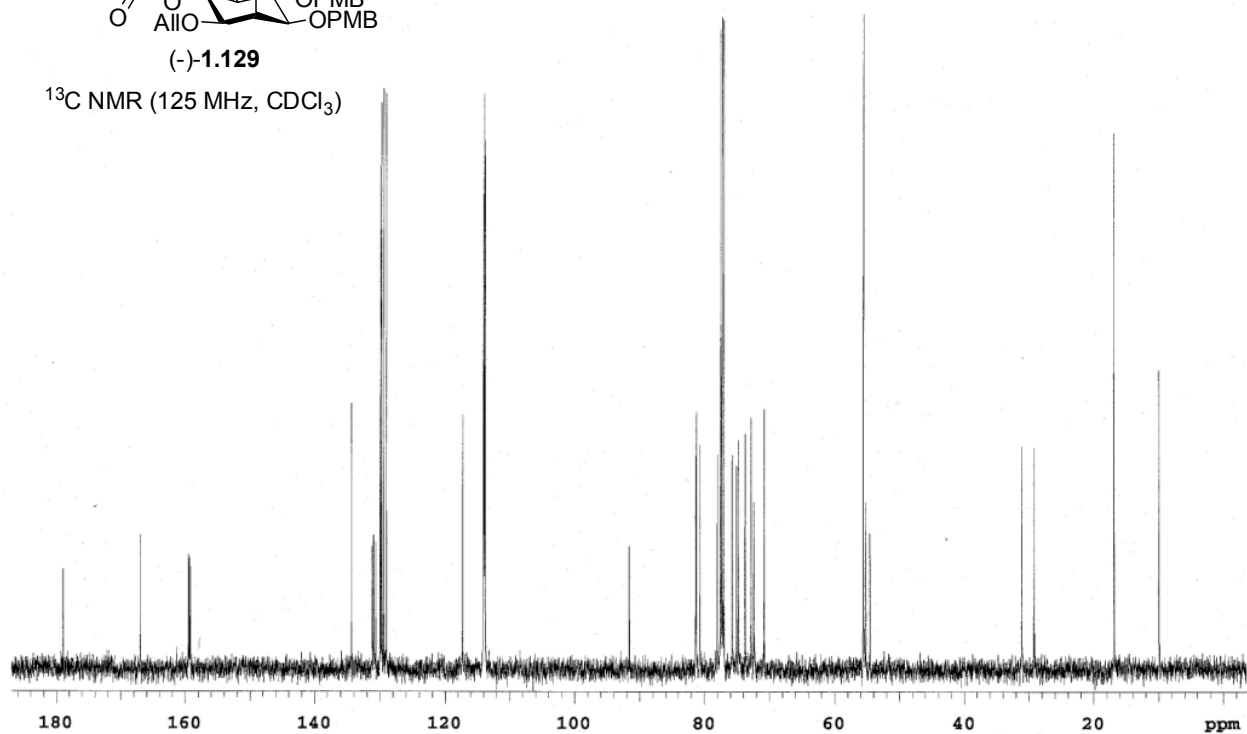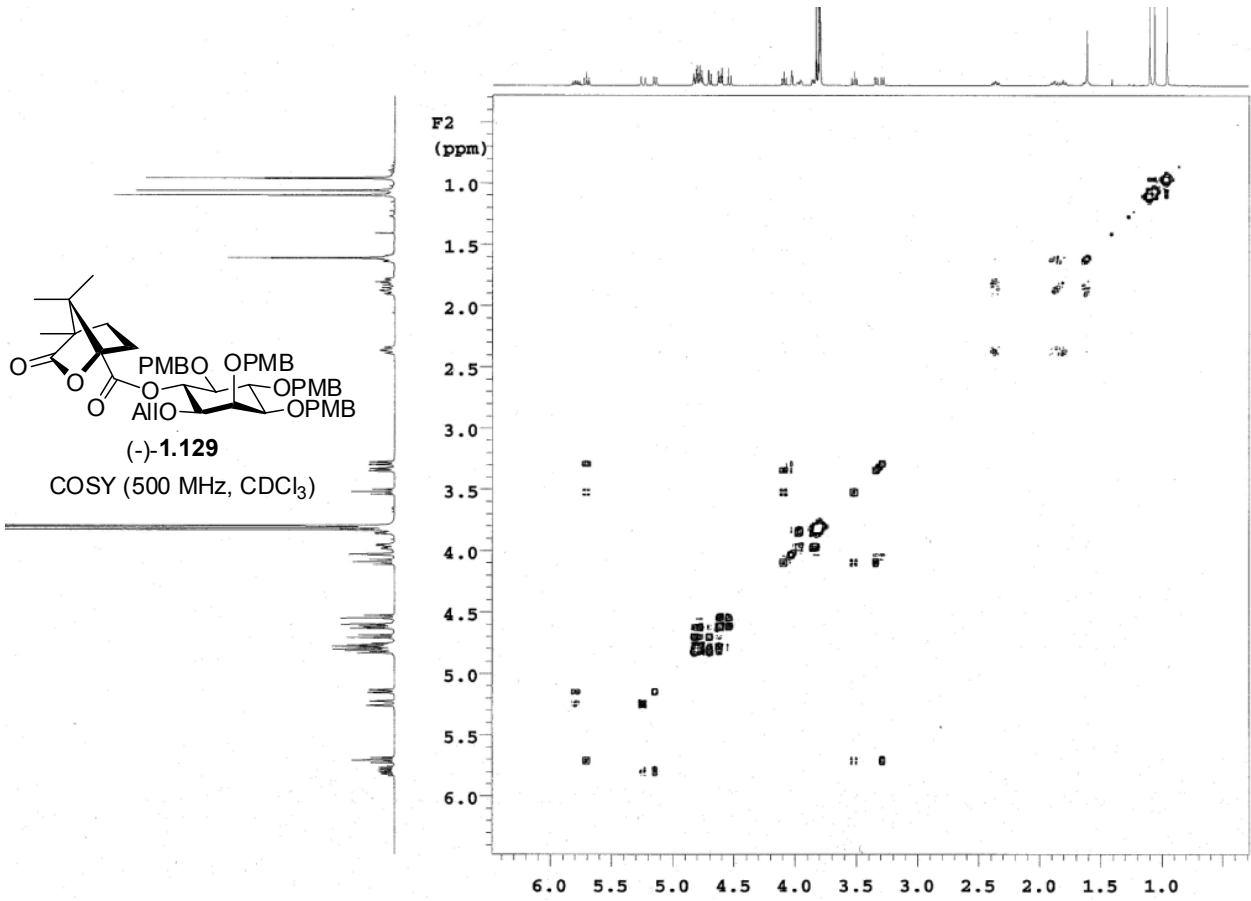
(-)-**1.129**

COSY (500 MHz, CDCl$_3$)

Single Mass Analysis
Tolerance = 5.0 PPM / DBE: min = -1.5, max = 60.0
Element prediction: Off
Number of isotope peaks used for i-FIT = 3

Monoisotopic Mass, Even Electron Ions
276 formula(e) evaluated with 3 results within limits (up to 50 best isotopic matches for each mass)
Elements Used:
C: 0-113   H: 0-116   O: 0-13   23Na: 0-1
guo- Ben Swarts BMS-VI-41 mw880 LCT0106 10pg/ul meoh 1ul 1ul stk
Shay 2008-07b.pro
2008_0822_0106_22 11 (0.230) Cm (9:11-2:6x2.000)
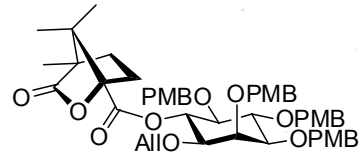
(-)-**1.129**

HR ESI MS

LCT Premier 22-Aug-2008 16:15:10
1: TOF MS ES+
1.73e+003
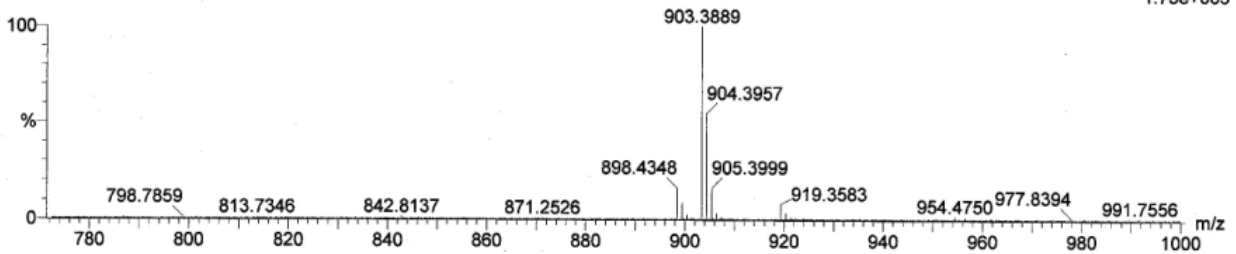
Mass	Calc. Mass	mDa	PPM	DBE	i-FIT	i-FIT (Norm)	Formula			
903.3889	903.3932	-4.3	-4.8	21.5	87.6	0.1	C51	H60	O13	23Na
	903.3897	-0.8	-0.9	33.5	90.9	3.3	C60	H55	O8	
	903.3873	1.6	1.8	30.5	91.2	3.6	C58	H56	O8	23Na
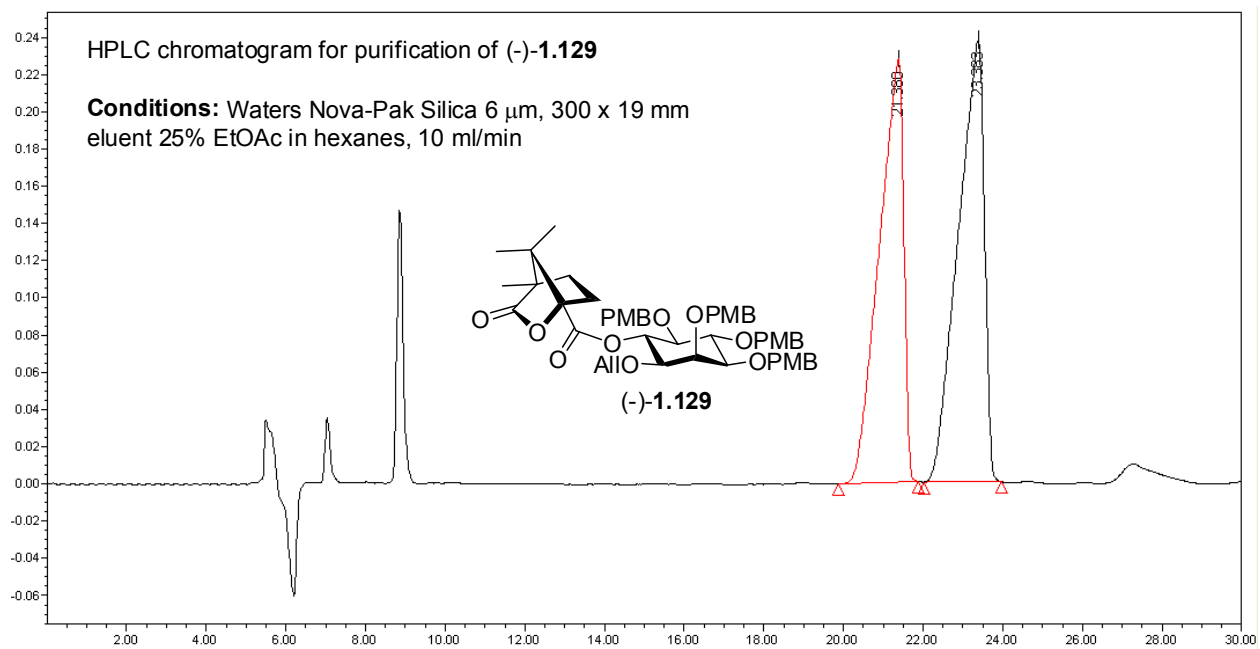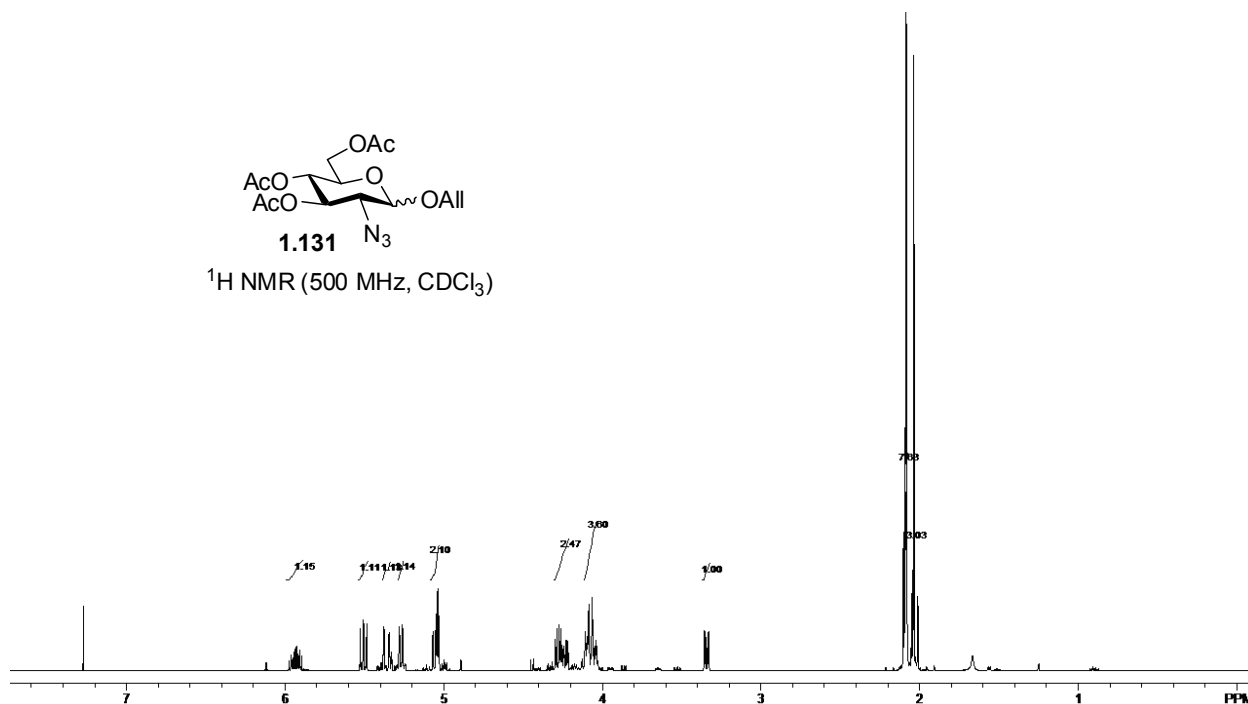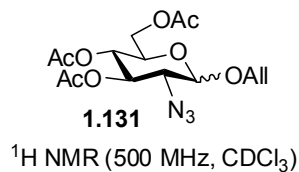
Minimum: -1.5
Maximum: 8.0   5.0   60.0

HPLC chromatogram for purification of (-)-**1.129**

Conditions: Waters Nova-Pak Silica 6 μm, 300 x 19 mm
eluent 25% EtOAc in hexanes, 10 ml/min

(-)-**1.129**

1.131

^{1}H NMR (500 MHz, CDCl$_3$)

Single Mass Analysis
Tolerance = 5.0 PPM / DBE: min = -1.5, max = 50.0
Element prediction: Off
Number of isotope peaks used for i-FIT = 3

Monoisotopic Mass, Even Electron Ions
412 formula(e) evaluated with 3 results within limits (up to 50 best isotopic matches for each mass)
Elements Used:
C: 0-500   H: 0-1000   N: 0-4   O: 0-8   23Na: 0-1
Guo- Ben Swarts BMS-VI-75 LCT0221 mw371 5uL meoh
Shay 2008-07b.pro
2008_1125_0221_01 15 (0.318) Cm (12:20-(4:8+30:37)x3.000)

1.131

HR ESI MS
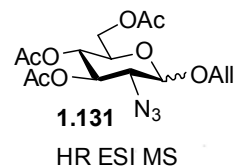
LCT Premier 25-Nov-2008 09:46:03
1: TOF MS ES+
3.28e+004
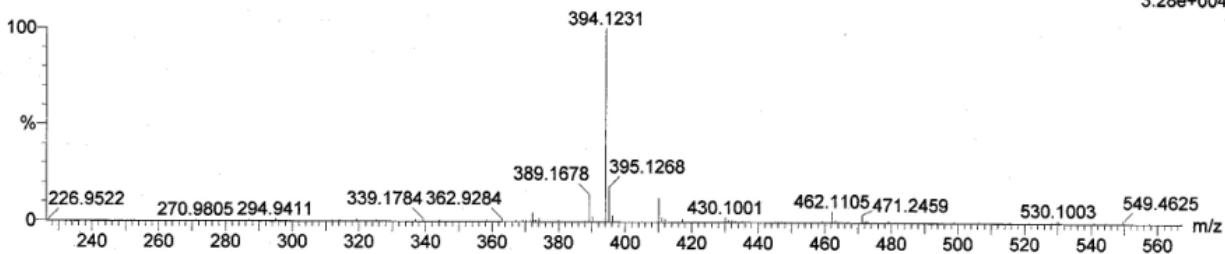
Minimum:				-1.5				
Maximum:		5.0	5.0	50.0				
Mass	Calc. Mass	mDa	PPM	DBE	i-FIT	i-FIT (Norm)	Formula	
394.1231	394.1226	0.5	1.3	6.5	18.0	0.0	C15 H21 N3 O8 23Na	←
	394.1250	-1.9	-4.8	9.5	25.2	7.2	C17 H20 N3 O8	
	394.1232	-0.1	-0.3	22.5	29.5	11.4	C29 H16 N O	
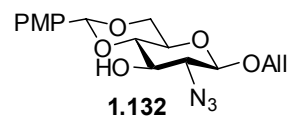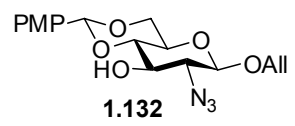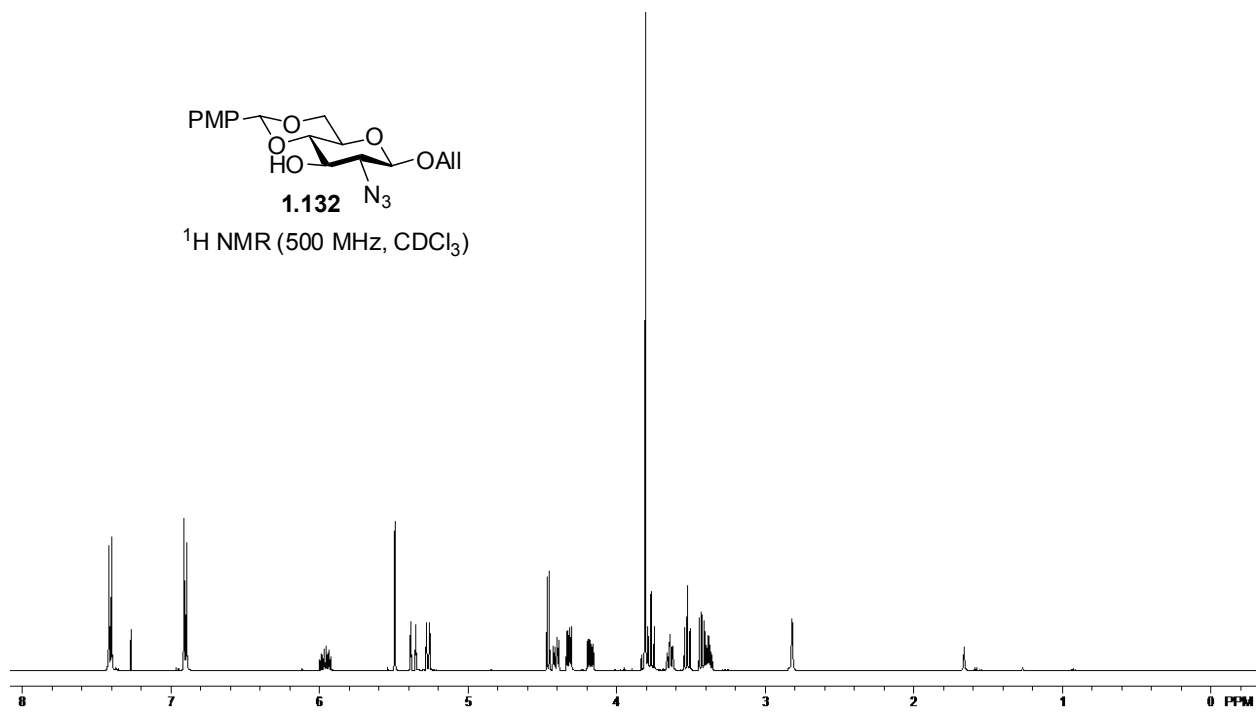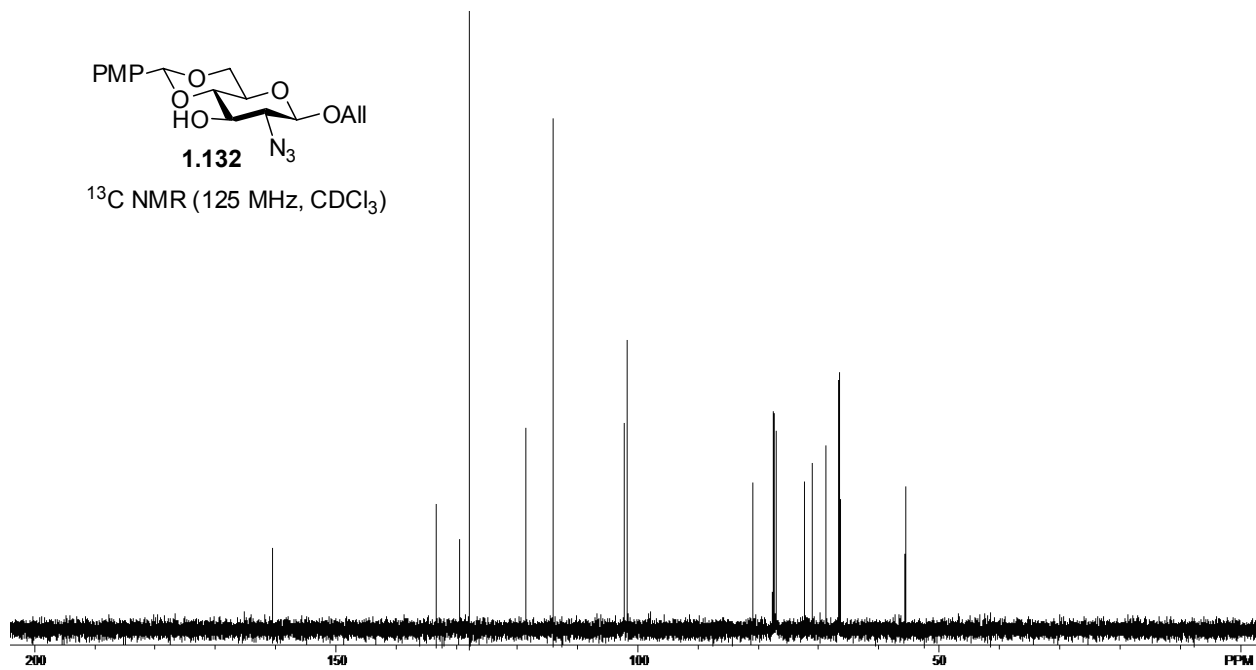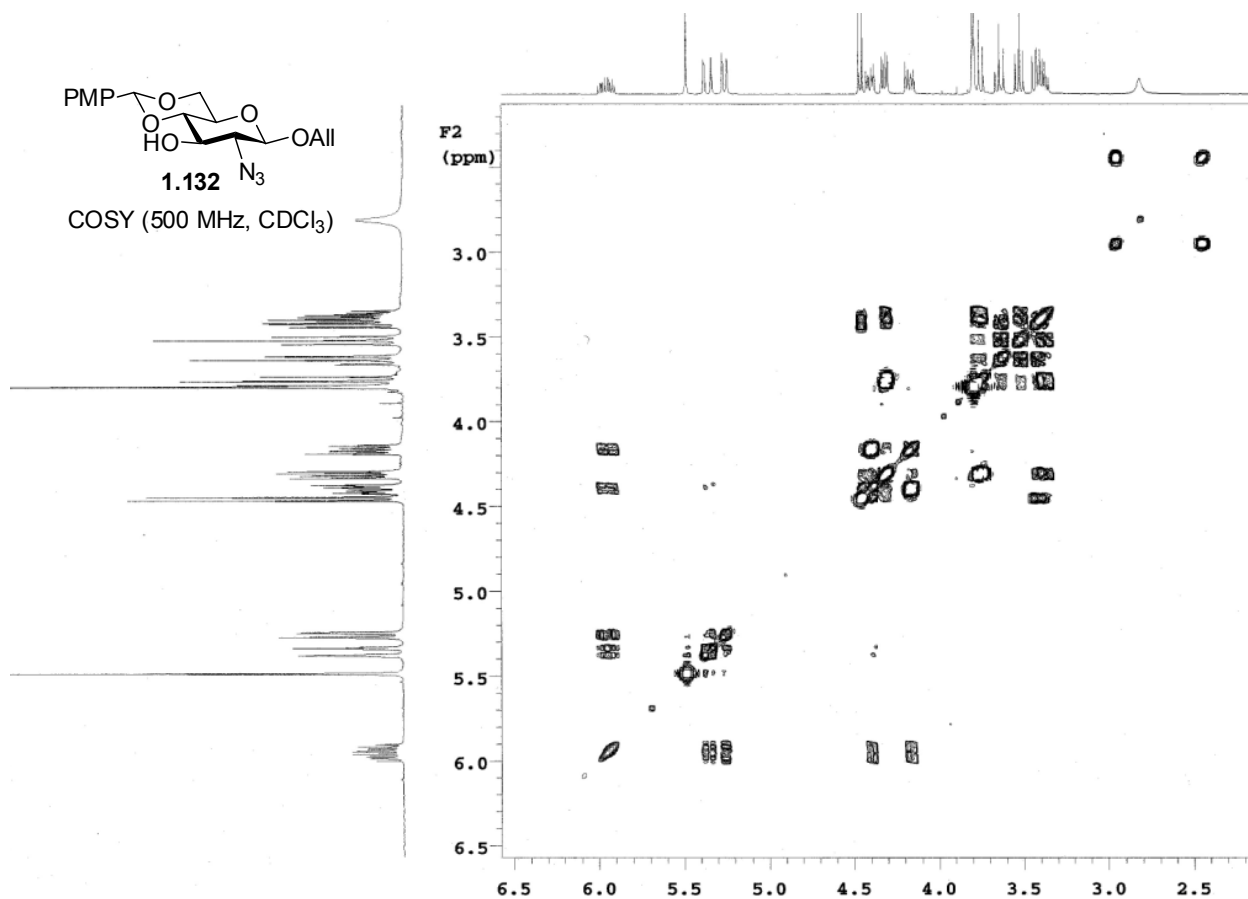
PMP—O
O
HO
1.132 N₃
OAll

¹H NMR (500 MHz, CDCl₃)

PMP—O
O
HO
1.132 N₃
OAll

¹³C NMR (125 MHz, CDCl₃)

PMP–O
HO
1.132 N₃
OAll

COSY (500 MHz, CDCl₃)

F2 (ppm)

Single Mass Analysis
Tolerance = 5.0 PPM / DBE: min = -1.5, max = 50.0
Element prediction: Off
Number of isotope peaks used for i-FIT = 3

Monoisotopic Mass, Even Electron Ions
310 formula(e) evaluated with 2 results within limits (up to 50 best isotopic matches for each mass)
Elements Used:
C: 0-500   H: 0-1000   N: 0-4   O: 0-6   23Na: 0-1
Guo- Ben Swarts BMS-VI-83 LCT0230 mw363 0.5uL meoh
Shay 2008-07b.pro
2008_1202_0230_03 18 (0.388) Cm (18:19-(2:4+28:32)x2.000)

PMP–O
HO
1.132 N₃
OAll

HR ESI MS
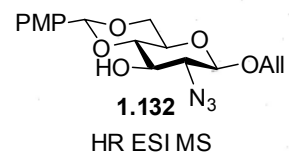
LCT Premier 02-Dec-2008 09:58:40
1: TOF MS ES+
5.42e+003
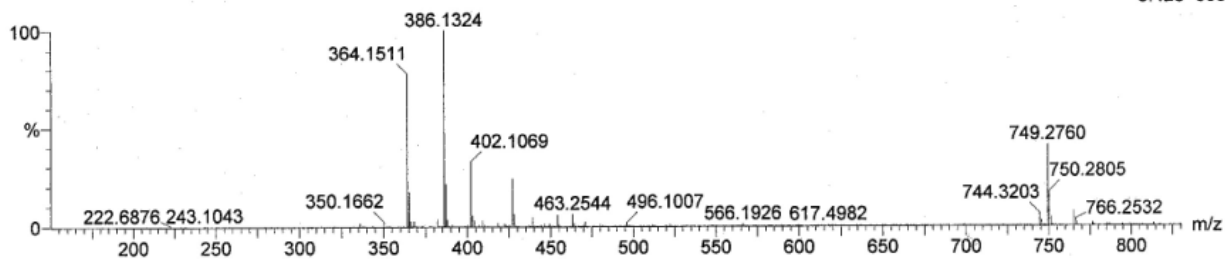
Minimum:			-1.5	
Maximum:	5.0	5.0	50.0	

Mass	Calc. Mass	mDa	PPM	DBE	i-FIT	i-FIT (Norm)	Formula
364.1511	364.1509	0.2	0.5	8.5	45.9	0.3	C17 H22 N3 O6
	364.1525	-1.4	-3.8	9.5	47.0	1.4	C20 H23 N O4 23Na
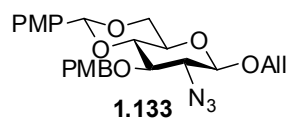
1.133
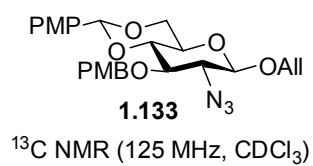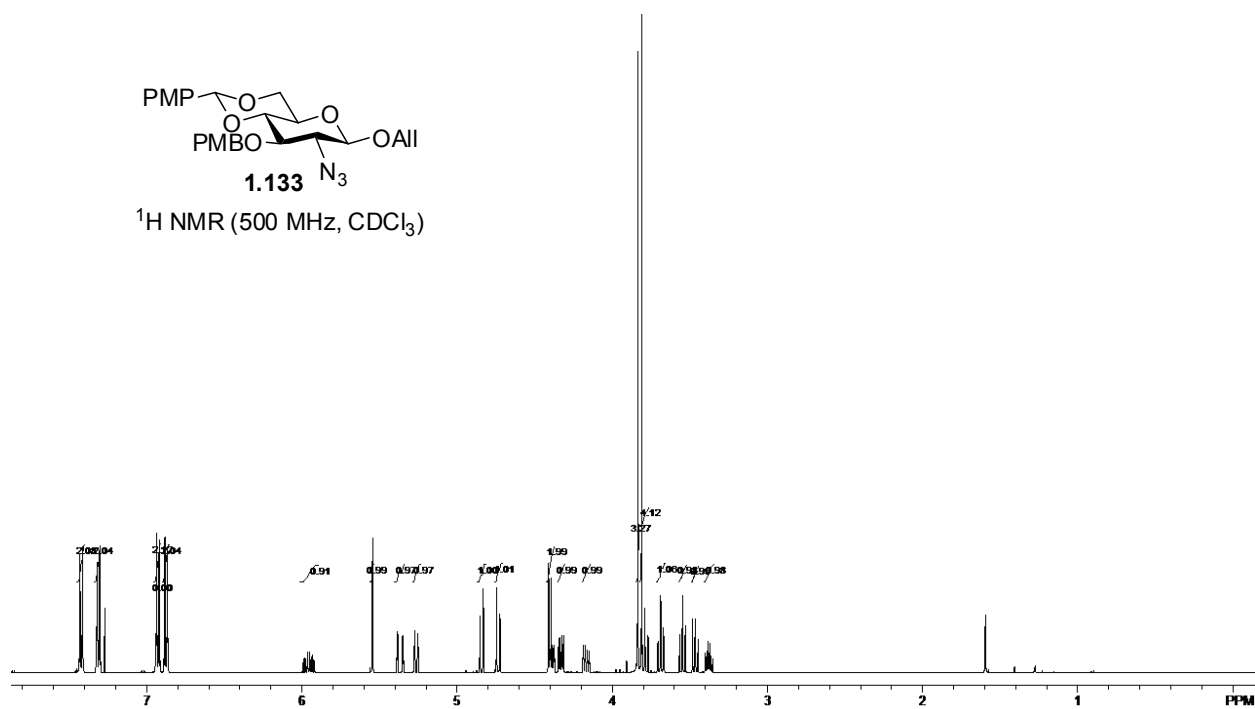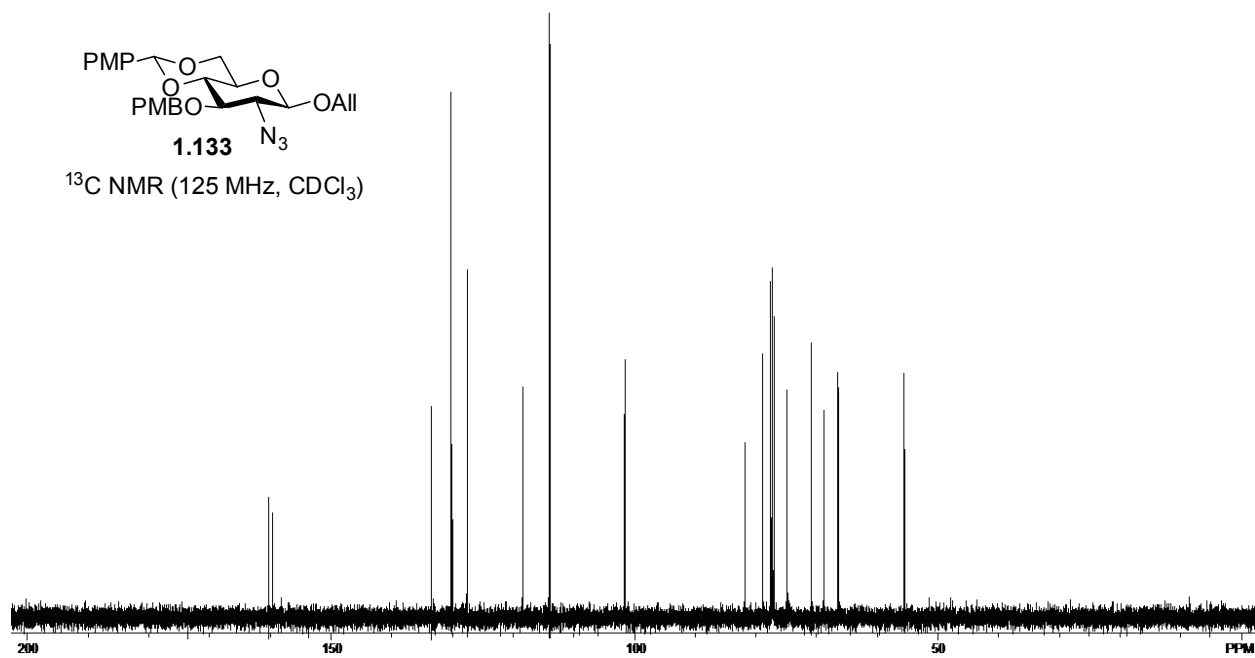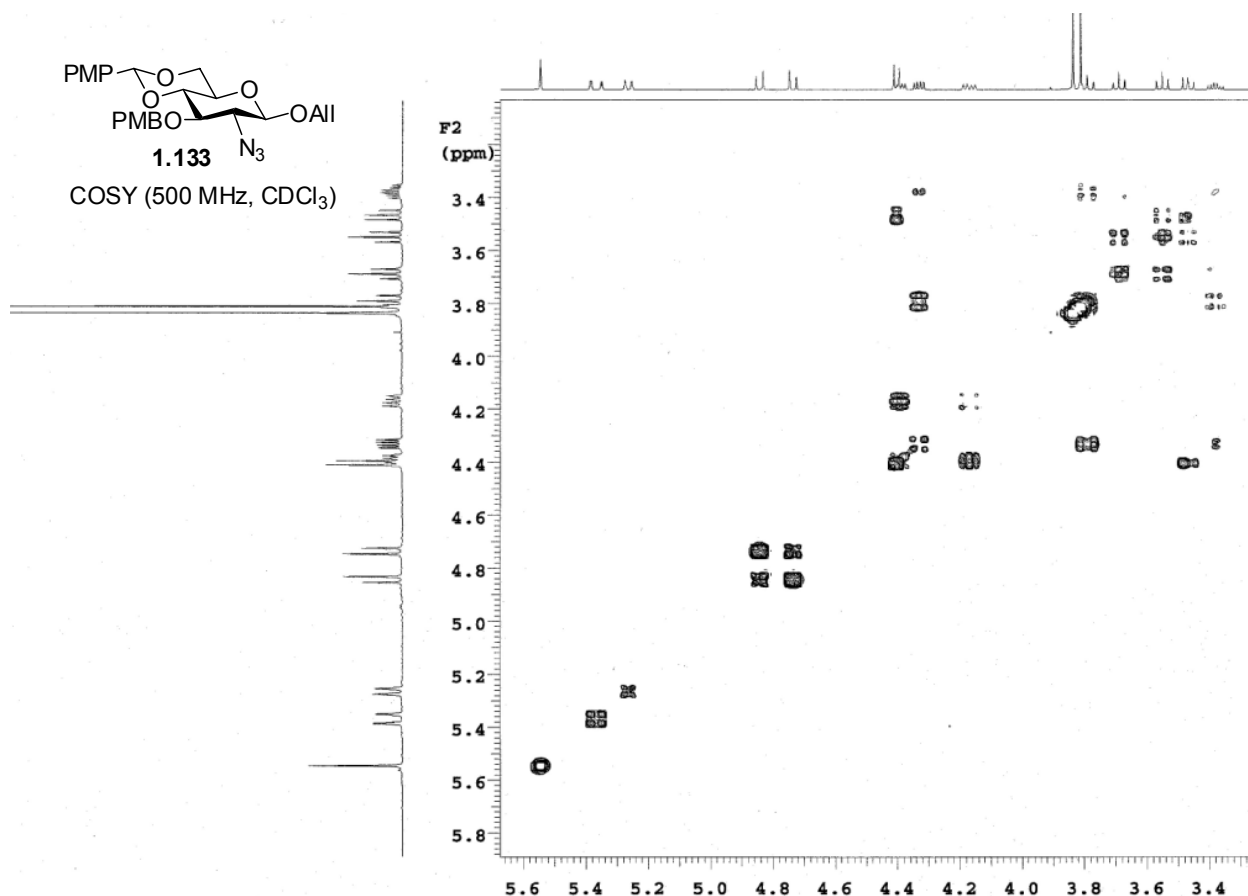
^{1}H NMR (500 MHz, CDCl$_3$)

1.133

^{13}C NMR (125 MHz, CDCl$_3$)

PMP, PMBO — **1.133** — OAll, N₃

COSY (500 MHz, CDCl₃)

F2 (ppm)

Single Mass Analysis
Tolerance = 5.0 PPM / DBE: min = -1.5, max = 100.0
Element prediction: Off
Number of isotope peaks used for i-FIT = 3

Monoisotopic Mass, Even Electron Ions
602 formula(e) evaluated with 2 results within limits (up to 50 closest results for each mass)
Elements Used:
C: 0-40   H: 0-83   N: 0-4   O: 0-10   23Na: 0-1
Guo, Ben Swarts, BMS-VI-84 LCT0229 mw483 0.5uL meoh
Shay 2008-07b.pro
2008_1202_0229_02 11 (0.229) Cm (9:11-1:6x5.000)

PMP, PMBO — **1.133** — OAll, N₃

HR ESI MS
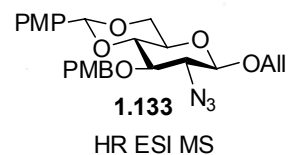
LCT Premier 02-Dec-2008 09:55:50
1: TOF MS ES+
4.11e+003
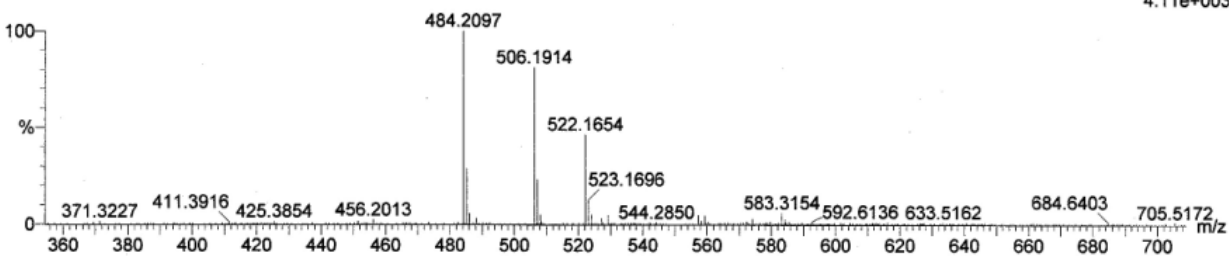
Mass	Calc. Mass	mDa	PPM	DBE	i-FIT	i-FIT (Norm)	Formula
Minimum:				-1.5			
Maximum:		5.0	5.0	100.0			
484.2097	484.2100	-0.3	-0.6	13.5	28.9	2.3	C28 H31 N O5 23Na
	484.2084	1.3	2.7	12.5	26.7	0.1	C25 H30 N3 O7
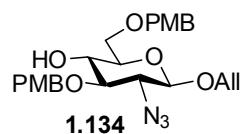
^{1}H NMR (500 MHz, CDCl$_3$)
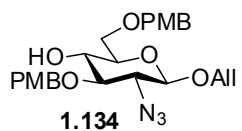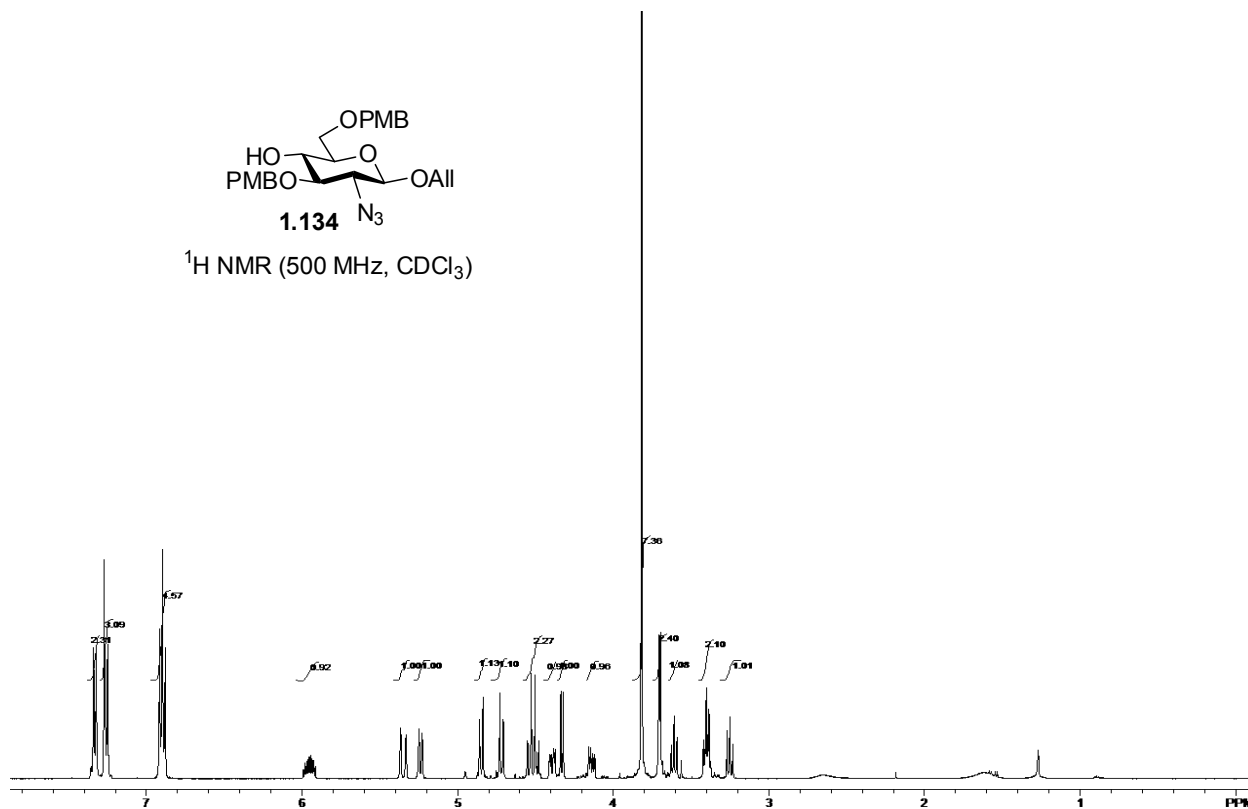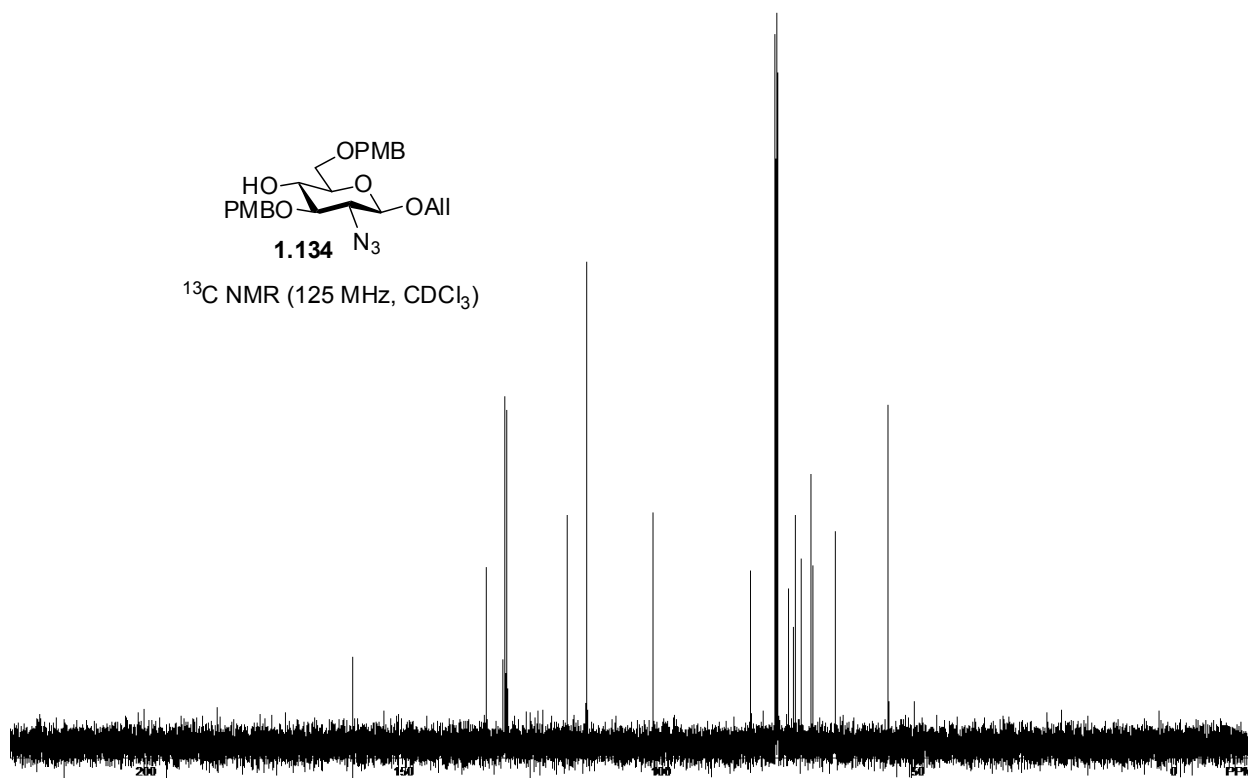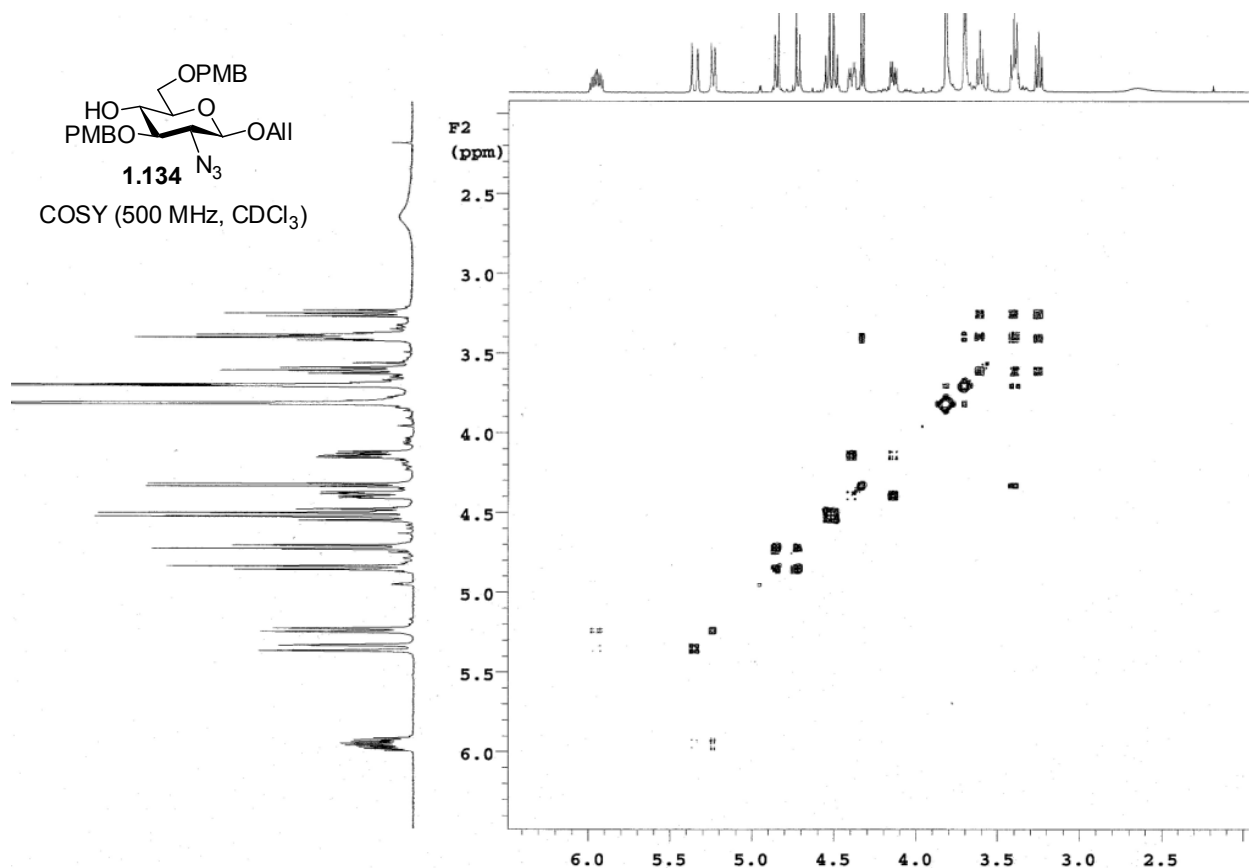
^{13}C NMR (125 MHz, CDCl$_3$)

OPMB

HO

PMBO

OAll

1.134 N₃

COSY (500 MHz, CDCl₃)

F2
(ppm)

2.5

3.0

3.5

4.0

4.5

5.0

5.5

6.0

6.0   5.5   5.0   4.5   4.0   3.5   3.0   2.5

Single Mass Analysis
Tolerance = 5.0 PPM / DBE: min = -1.5, max = 50.0
Element prediction: Off
Number of isotope peaks used for i-FIT = 3

Monoisotopic Mass, Even Electron Ions
483 formula(e) evaluated with 4 results within limits (up to 50 best isotopic matches for each mass)
Elements Used:
C: 0-500   H: 0-1000   N: 0-4   O: 0-7   23Na: 0-1
Guo- Ben Swarts BMS-VI-70-A mw485 LCT0160 1uL meoh
Shay 2008-07b.pro
2008_1002_0160_01 20 (0.423) Cm (20:23-39:46x2.000)

OPMB

HO

PMBO

OAll

1.134 N₃

HR ESI MS
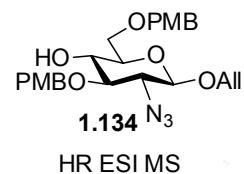
LCT Premier 02-Oct-2008 11:27:50
1: TOF MS ES+
1.22e+004
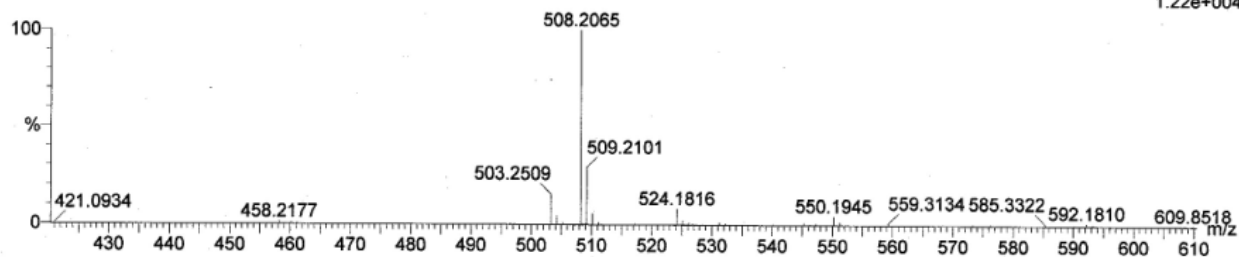
Minimum:				-1.5			
Maximum:		5.0	5.0	50.0			
Mass	Calc. Mass	mDa	PPM	DBE	i-FIT	i-FIT (Norm)	Formula
508.2065	508.2060	0.5	1.0	11.5	35.5	0.0	C25 H31 N3 O7 ← 23Na
	508.2084	-1.9	-3.7	14.5	40.9	5.4	C27 H30 N3 O7
	508.2065	0.0	0.0	27.5	45.1	9.5	C39 H26 N
	508.2041	2.4	4.7	24.5	47.5	11.9	C37 H27 N 23Na

1.135

OPMB
TBSO
PMBO
OAll
N₃

¹H NMR (500 MHz, CDCl₃)

1.135

OPMB
TBSO
PMBO
OAll
N₃

¹³C NMR (125 MHz, CDCl₃)

OPMB
TBSO—O
PMBO—OAll
1.135 N₃
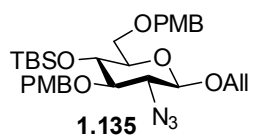
COSY (500 MHz, CDCl₃)
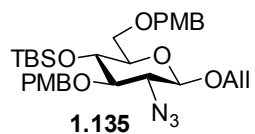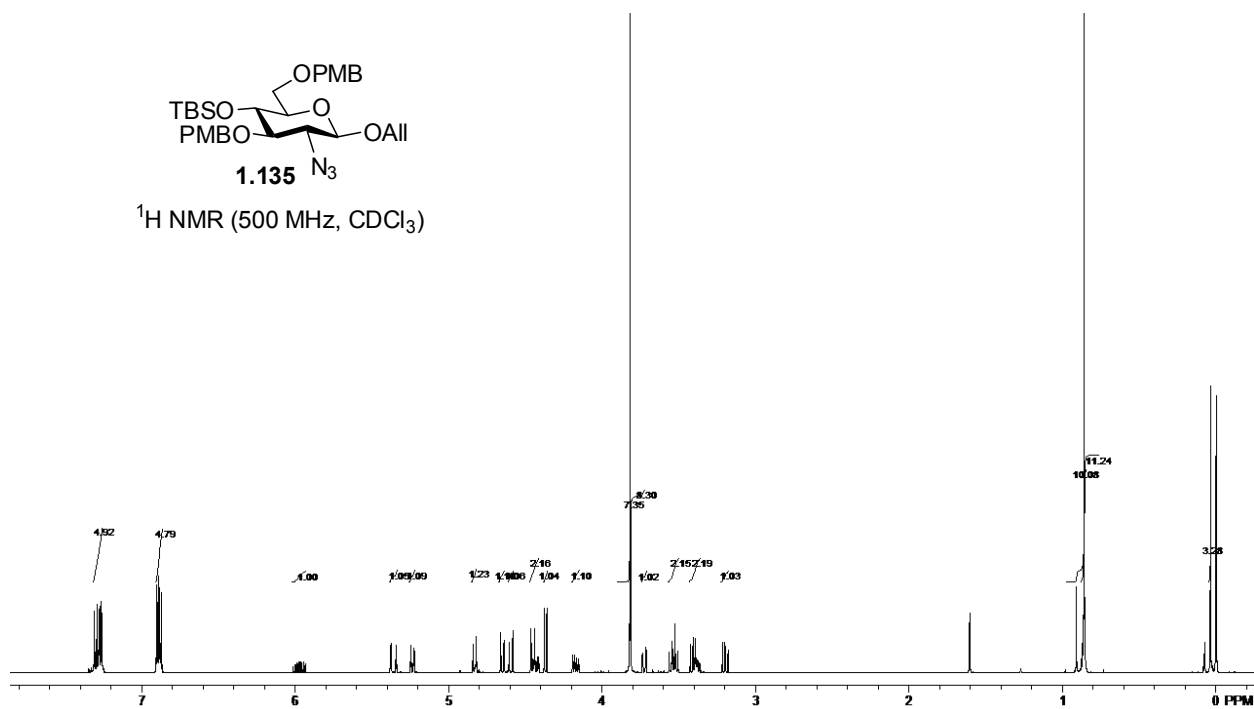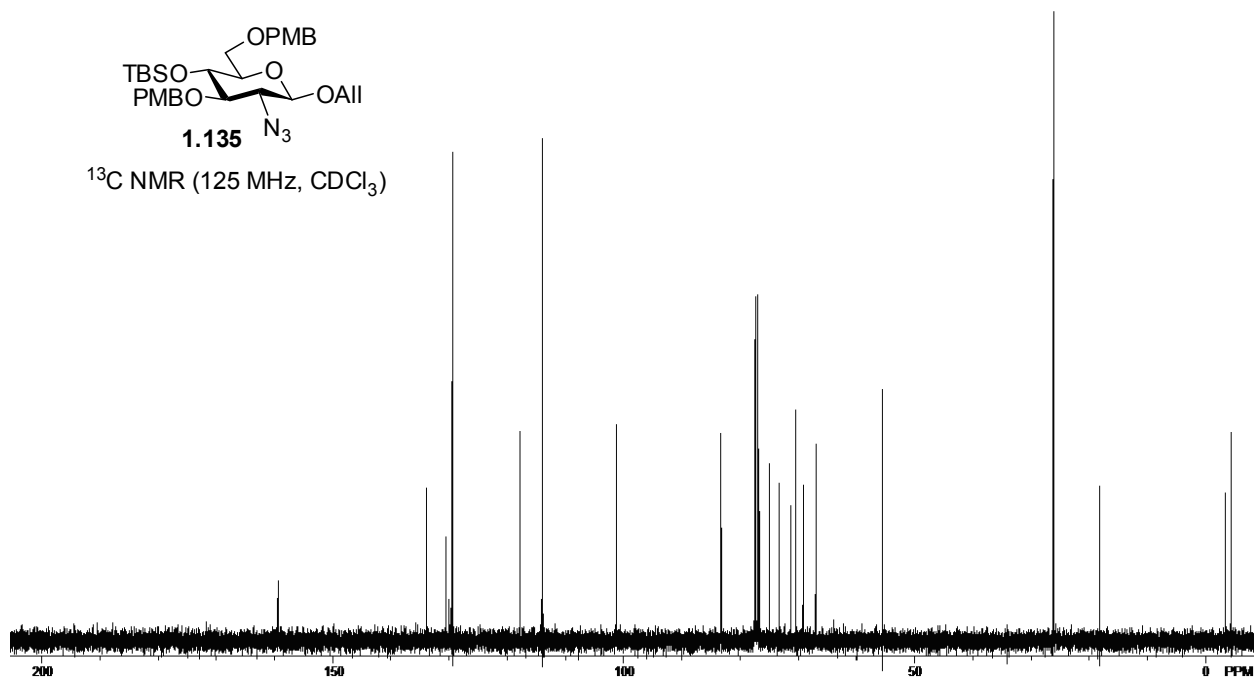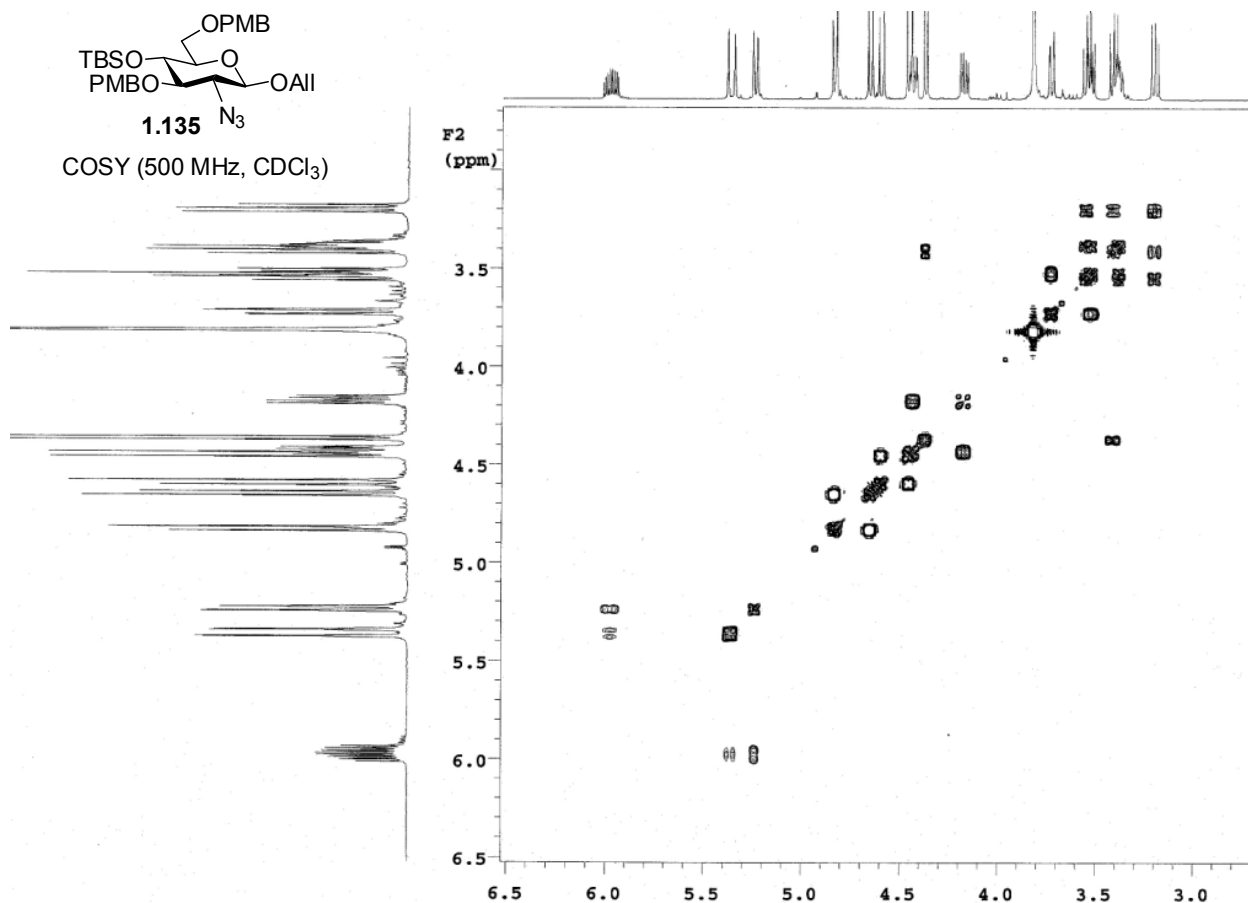
Single Mass Analysis
Tolerance = 1.0 PPM / DBE: min = -1.5, max = 50.0
Element prediction: Off
Number of isotope peaks used for i-FIT = 3

Monoisotopic Mass, Even Electron Ions
256 formula(e) evaluated with 1 results within limits (up to 50 best isotopic matches for each mass)
Elements Used:
C: 0-40 H: 0-50 N: 0-3 O: 0-7 Na: 0-1 Si: 0-1
Guo-Ben Swarts IBMS-VI-73 mw599 LCT0164 1uL meoh RF150
Shay 2008-07b.pro
2008_1007_0164_05 14 (0.300) Cm (11:17-33:43x2.000)

OPMB
TBSO—O
PMBO—OAll
1.135 N₃

HR ESI MS
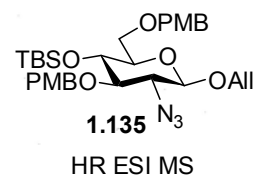
LCT Premier 07-Oct-2008 2::6::3
1: TOF MS ES+
3.50e+004
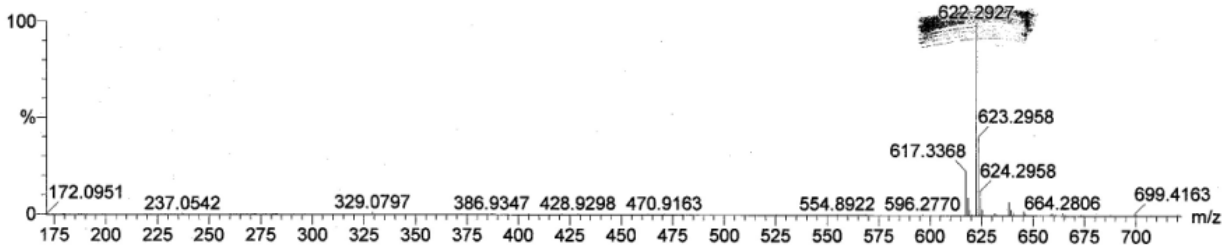
Minimum:				-1.5			
Maximum:		5.0	1.0	50.0			
Mass	Calc. Mass	mDa	PPM	DBE	i-FIT	i-FIT (Norm)	Formula
622.2927	622.2924	0.3	0.5	11.5	39.3	0.0	C31 H45 N3 O7 Na Si

1.136

^{1}H NMR (500 MHz, CDCl$_3$)

1.136

^{13}C NMR (125 MHz, CDCl$_3$)

1.136
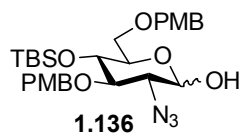
COSY (500 MHz, CDCl$_3$)
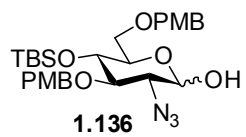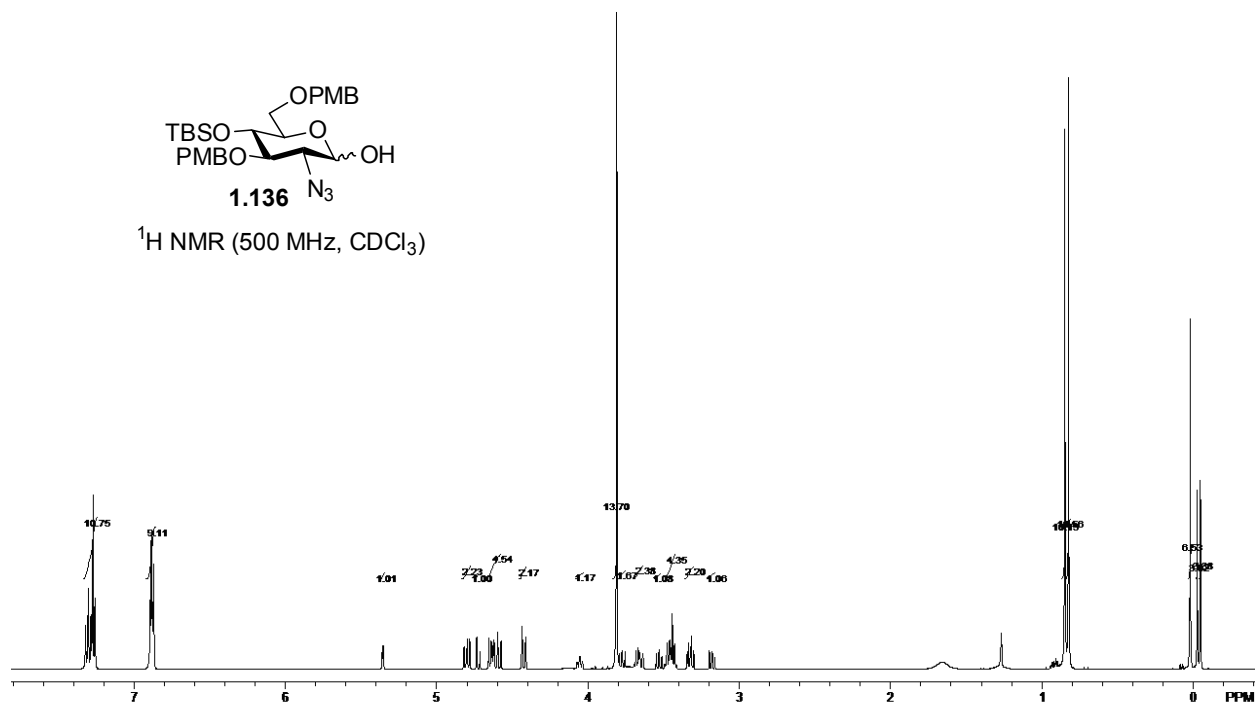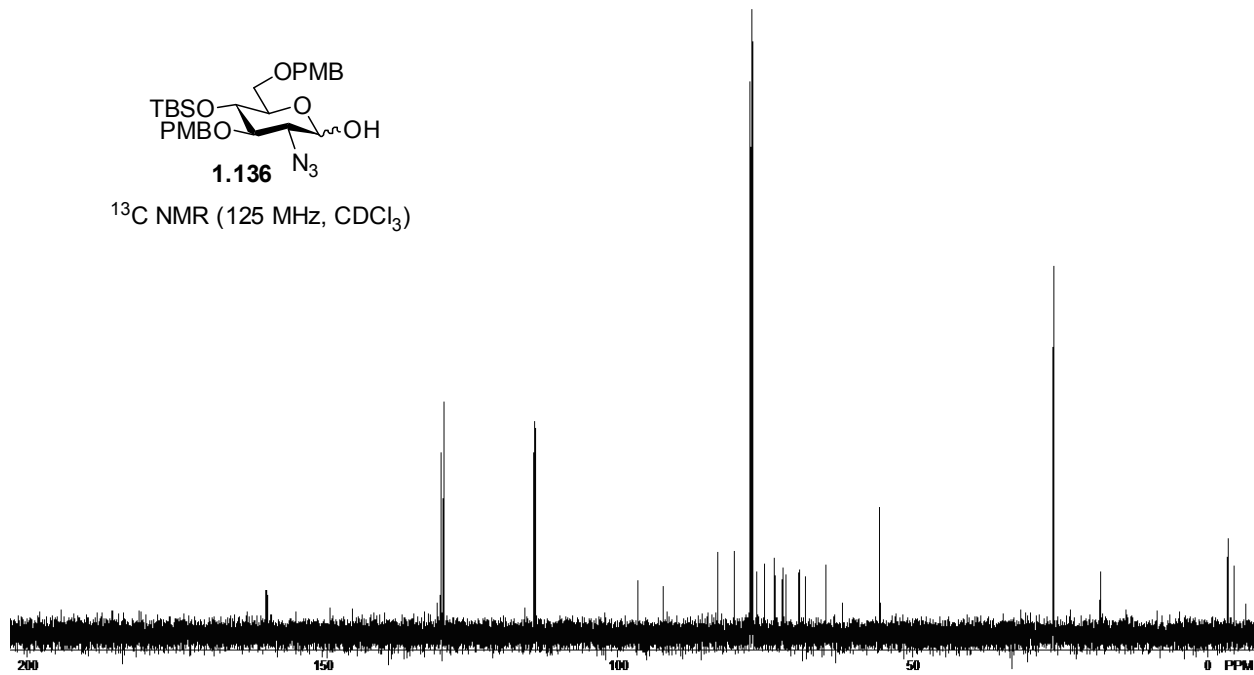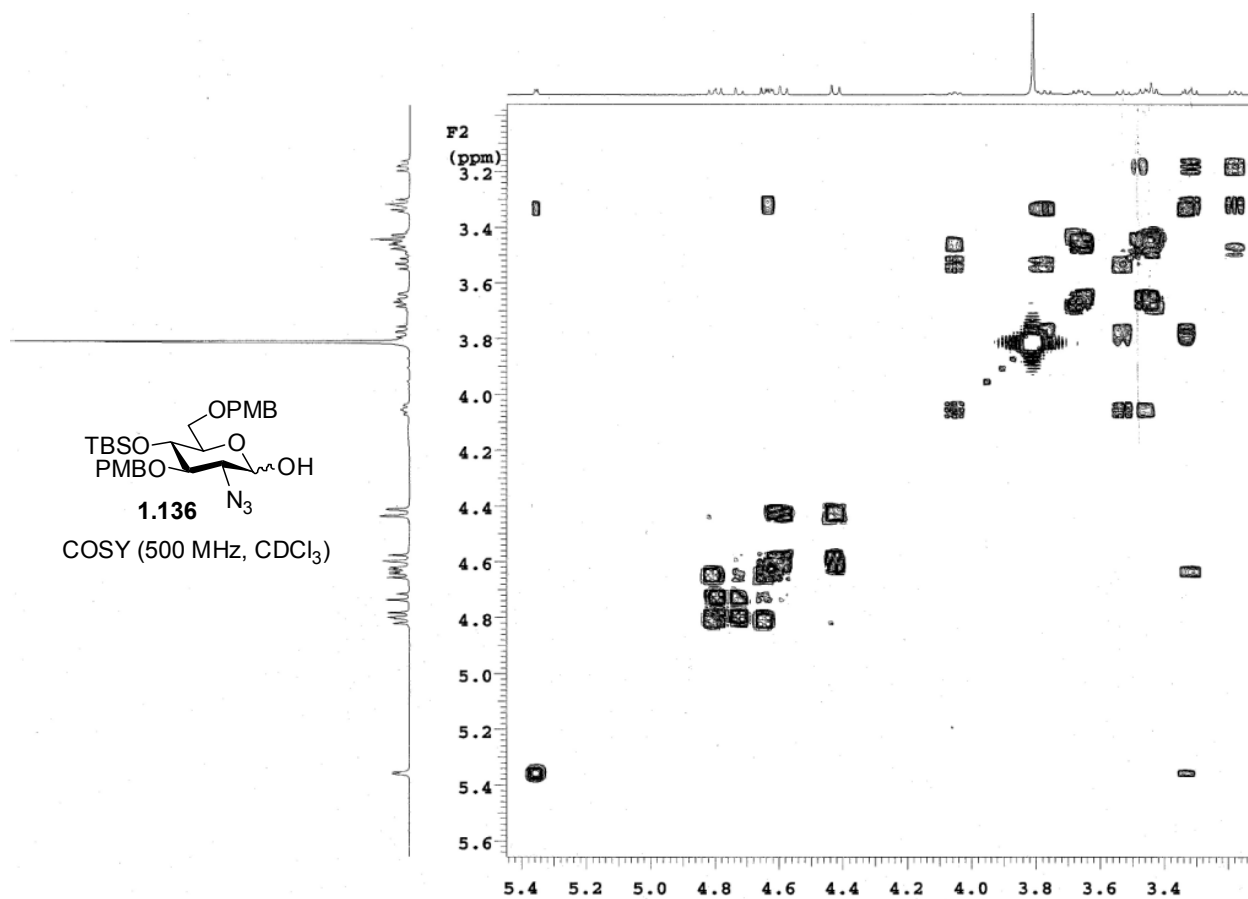
Single Mass Analysis

Tolerance = 5.0 mDa   /   DBE: min = -1.5, max = 50.0
Element prediction: Off
Number of isotope peaks used for i-FIT = 3

Monoisotopic Mass, Even Electron Ions
1331 formula(e) evaluated with 11 results within limits (up to 50 best isotopic matches for each mass)
Elements Used:
C: 0-50   H: 0-100   N: 0-3   O: 0-12   Na: 0-1   Si: 0-1

1.136

HR ESI MS
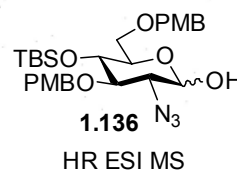
Ben Swarts   BMS-VI-90
Shay 2008-07b.pro
2008_1125_0235 14 (0.300) Cm (11:17-(1:6+25:32)x3.000)

LCT Premier 05-Dec-2008 15:16:55
1: TOF MS ES+
6.30e+004
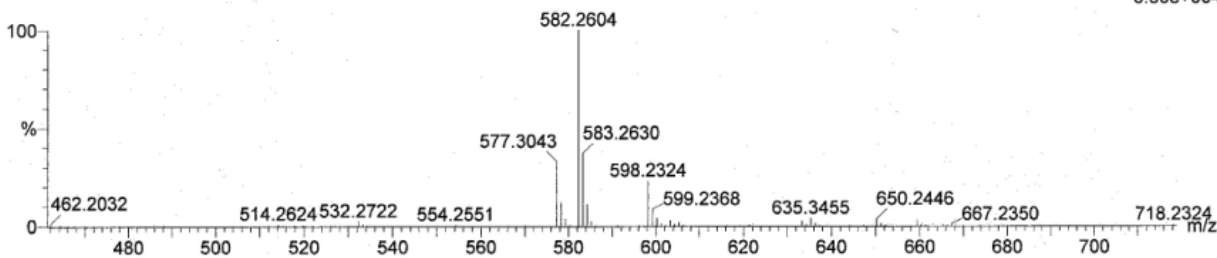
Minimum:				-1.5			
Maximum:		5.0	10.0	50.0			
Mass	Calc. Mass	mDa	PPM	DBE	i-FIT	i-FIT (Norm)	Formula
582.2604	582.2611	-0.7	-1.2	10.5	22.9	0.0	C28 H41 N3 O7 ←
							Na Si
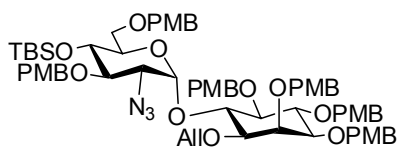
1.138

^{1}H NMR (500 MHz, CDCl$_3$)
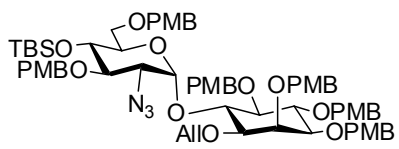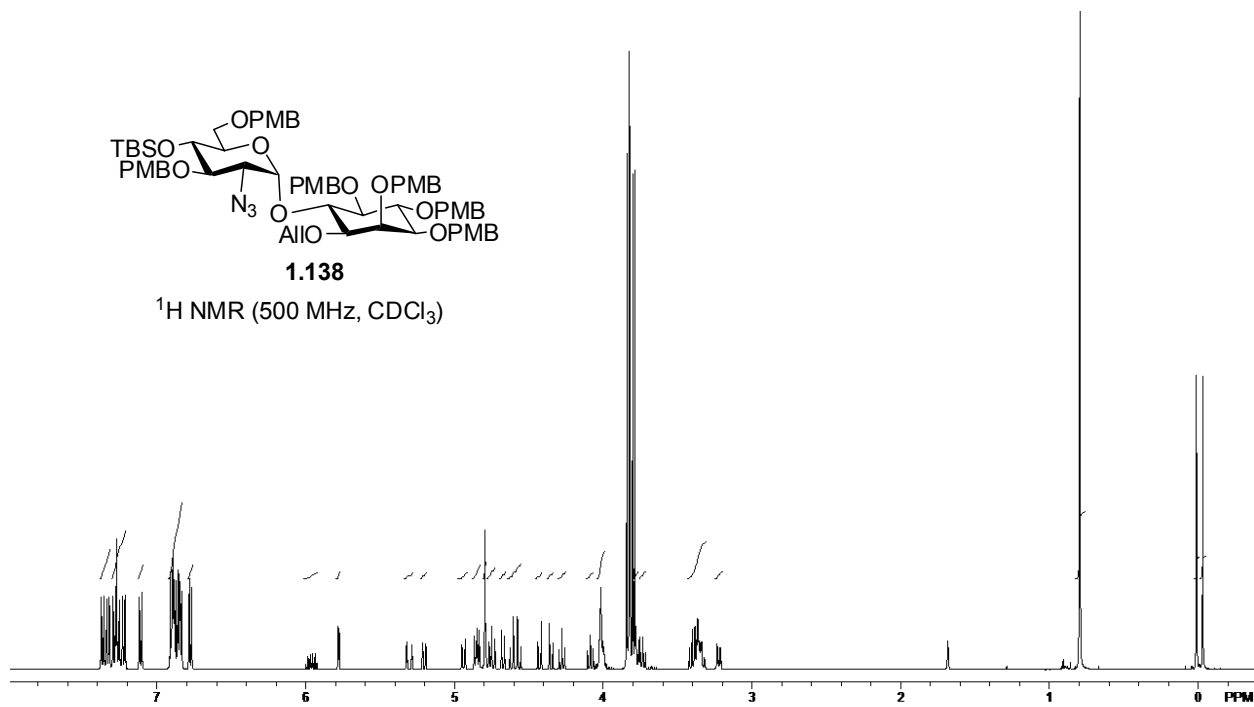
1.138

^{13}C NMR (125 MHz, CDCl$_3$)
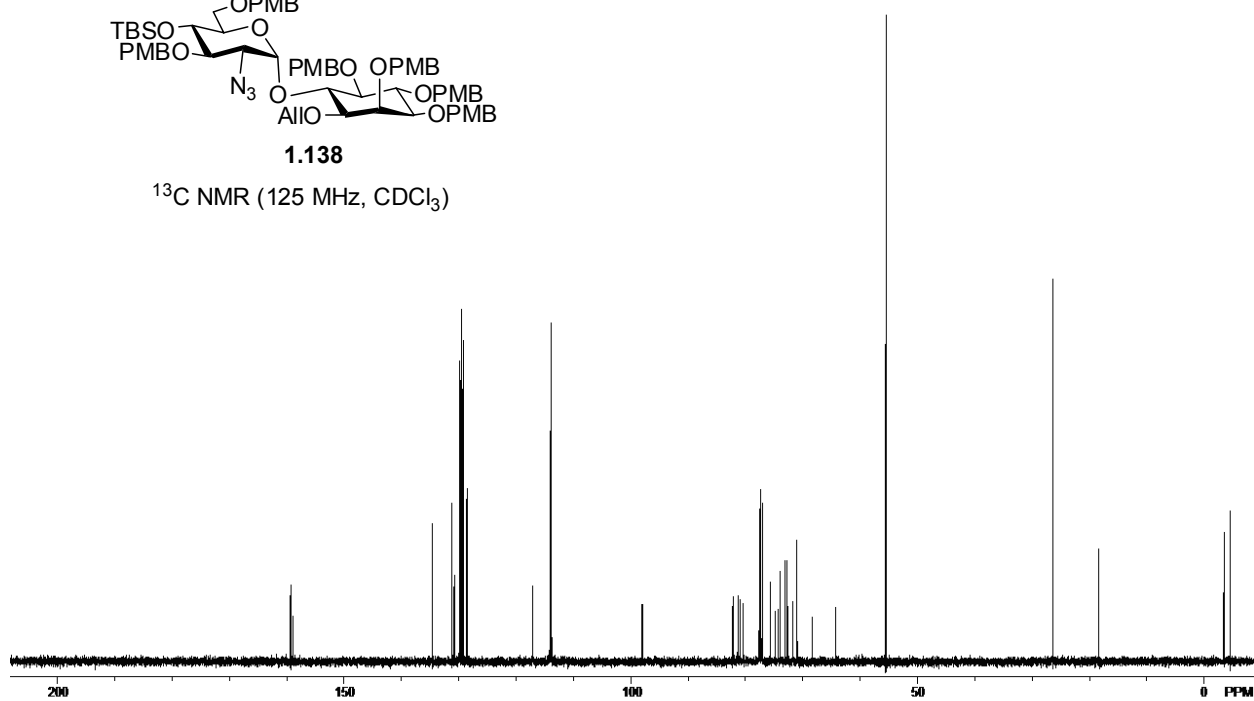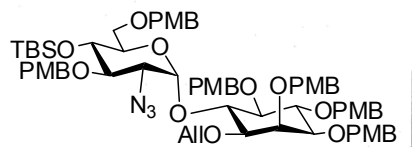
1.138

COSY (500 MHz, CDCl₃)
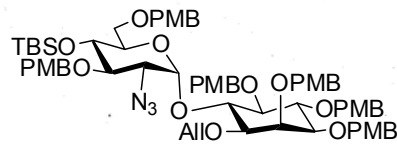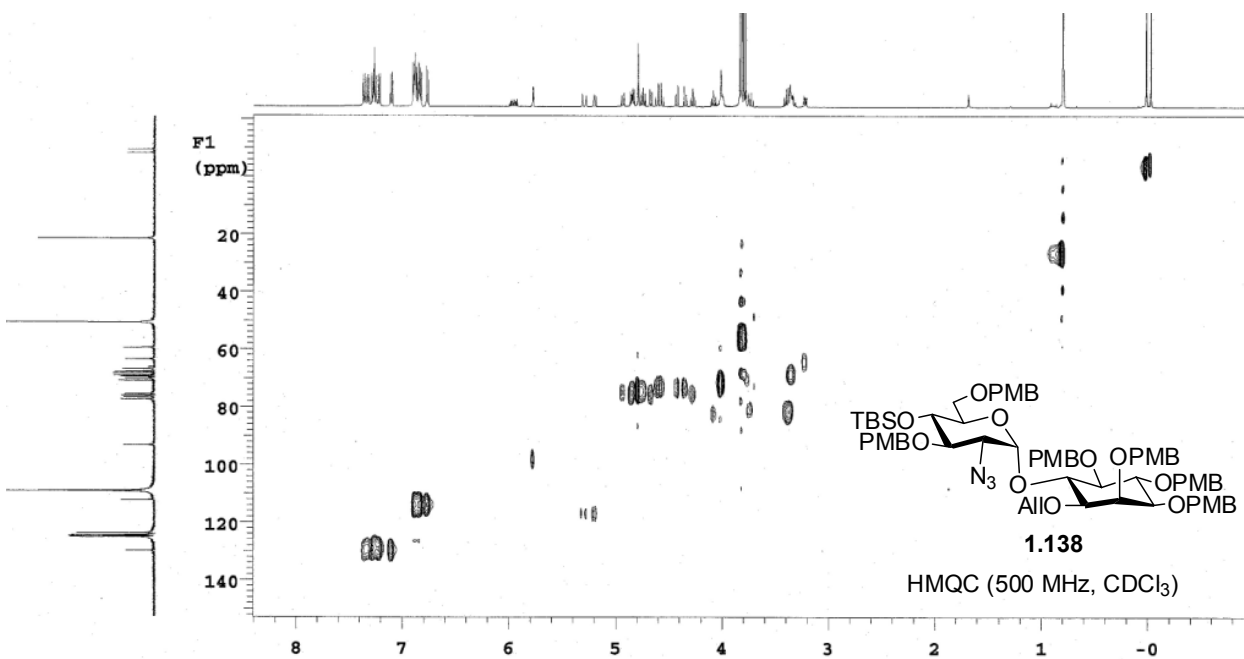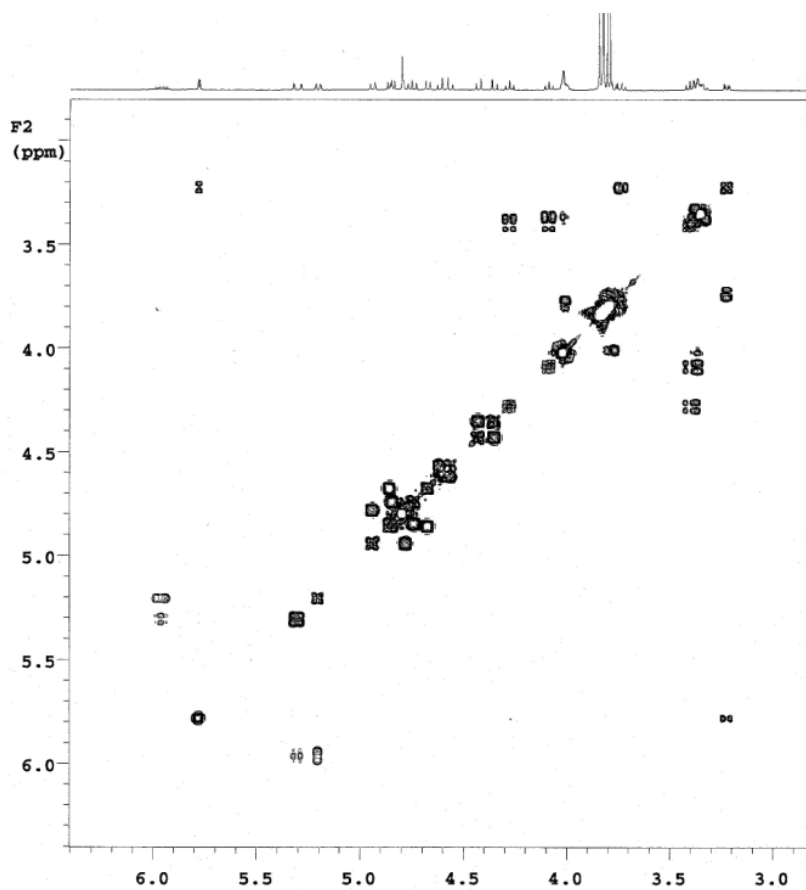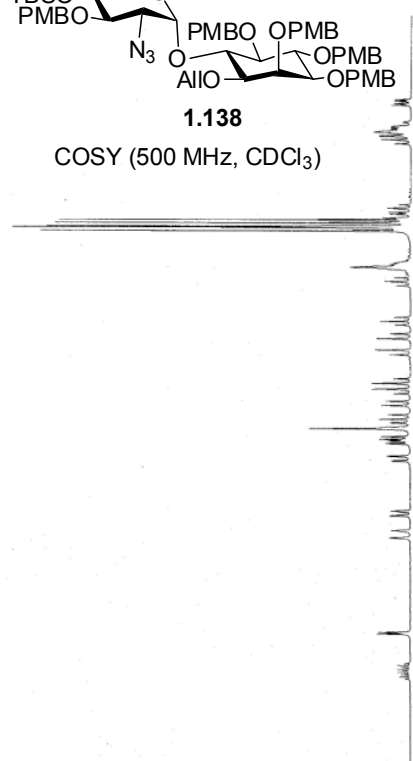
1.138

HMQC (500 MHz, CDCl₃)

Single Mass Analysis
Tolerance = 12.0 PPM / DBE: min = -1.5, max = 50.0
Element prediction: Off
Number of isotope peaks used for i-FIT = 3

Monoisotopic Mass, Even Electron Ions
335 formula(e) evaluated with 1 results within limits (up to 50 best isotopic matches for each mass)
Elements Used:
C: 0-70 H: 0-1000 N: 0-3 O: 0-16 23Na: 0-1 Si: 0-1
Guo- Ben Swarts BMS-VI-51 mw1241 LCT0140 0.5uL meoh added
Shay 2008-07b.pro
2008_0909_0140_12 17 (0.334) Cm (17:18-33:35x1.200)
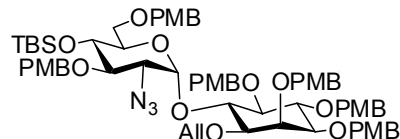
1.138

HR ESI MS

LCT Premier 09-Sep-2008 15:39:47
1: TOF MS ES+
1.80e+002
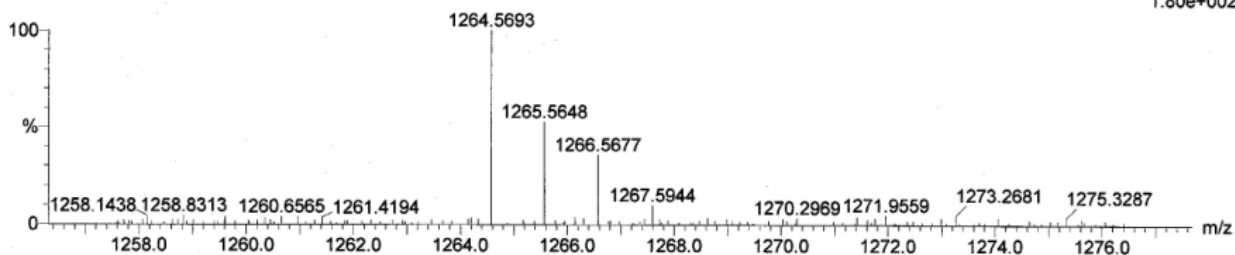
Minimum:				-1.5			
Maximum:		5.0	12.0	50.0			
Mass	Calc. Mass	mDa	PPM	DBE	i-FIT	i-FIT (Norm)	Formula
1264.5693	1264.5753	-6.0	-4.7	28.5	56.6	0.0	C69 H87 N3 O16
							23Na Si
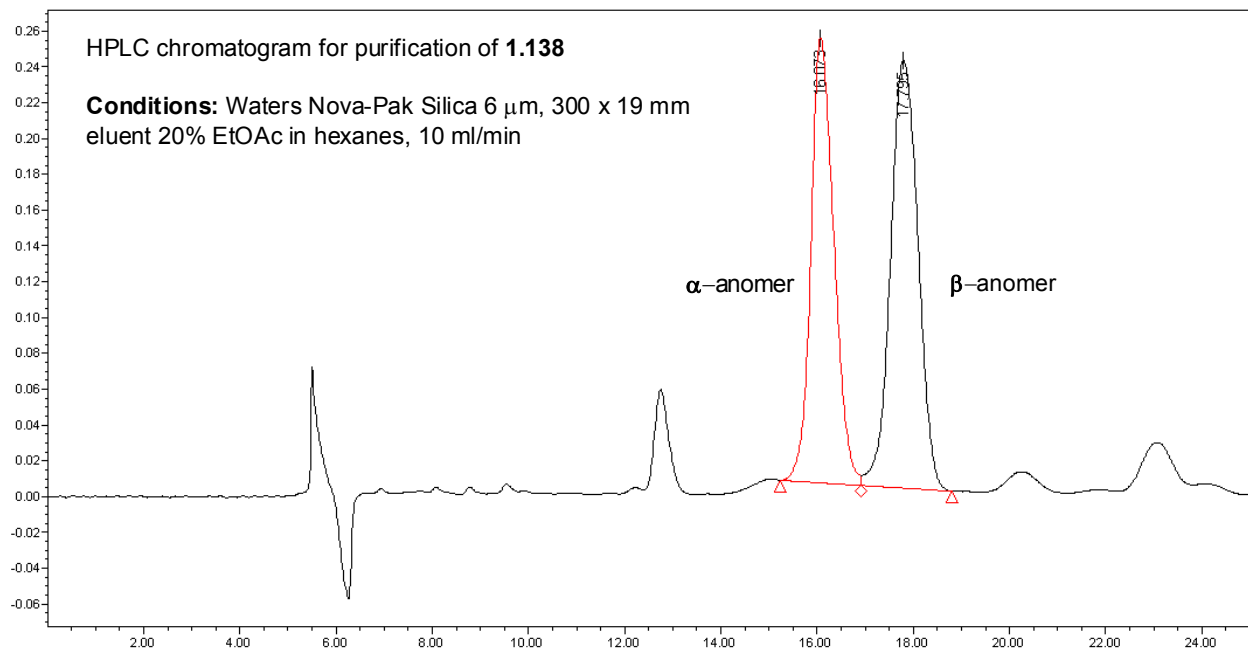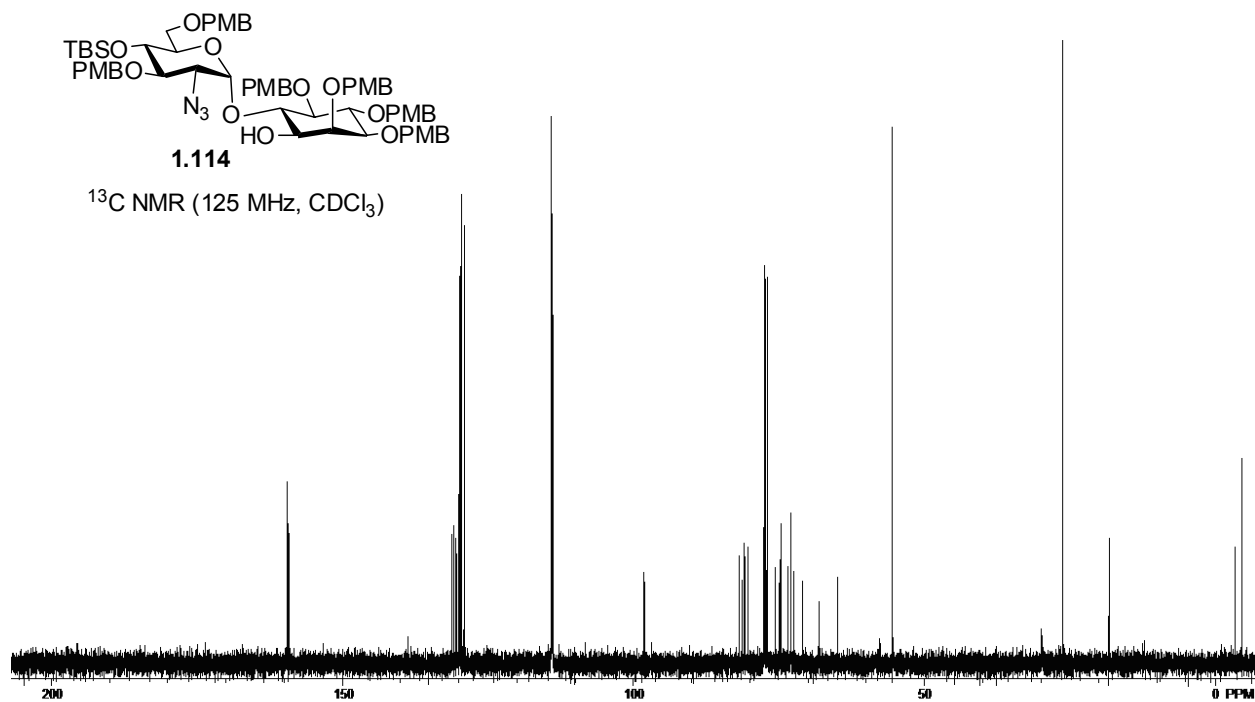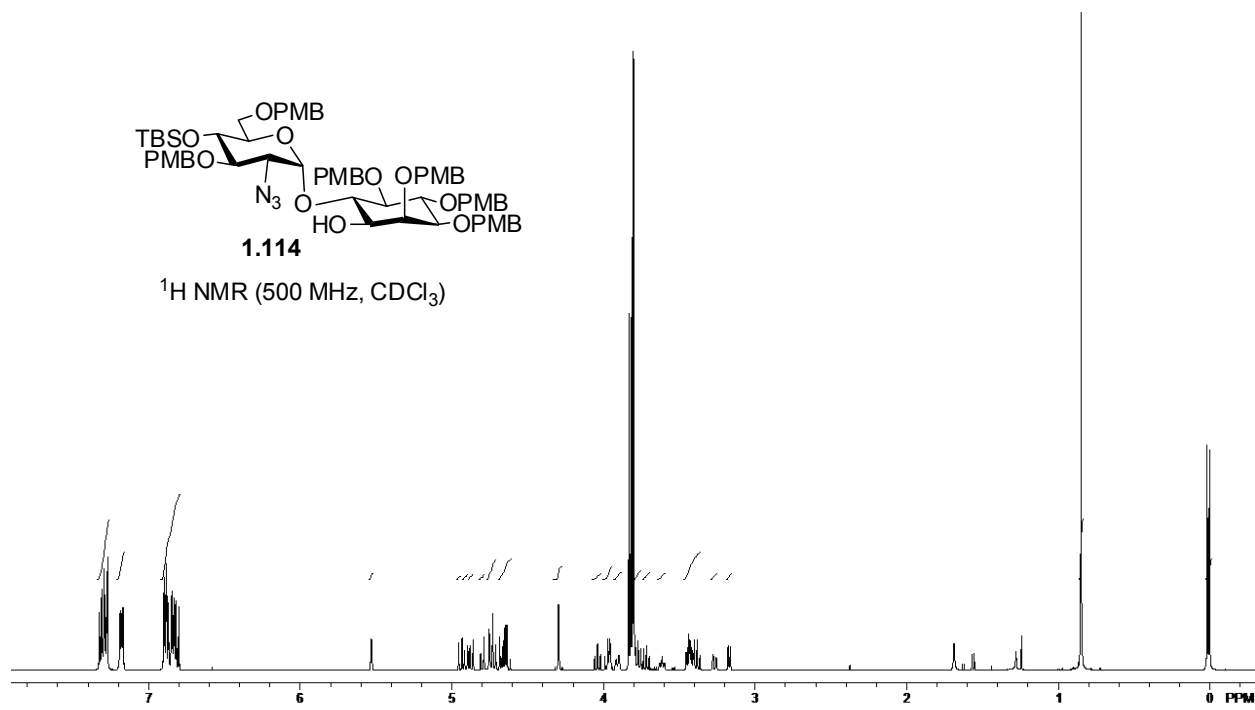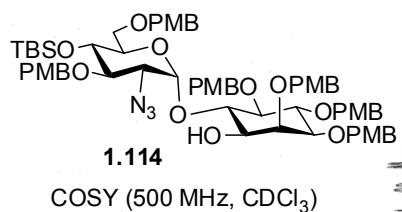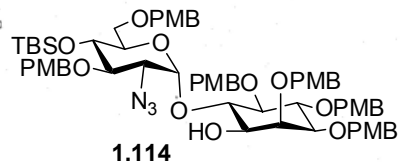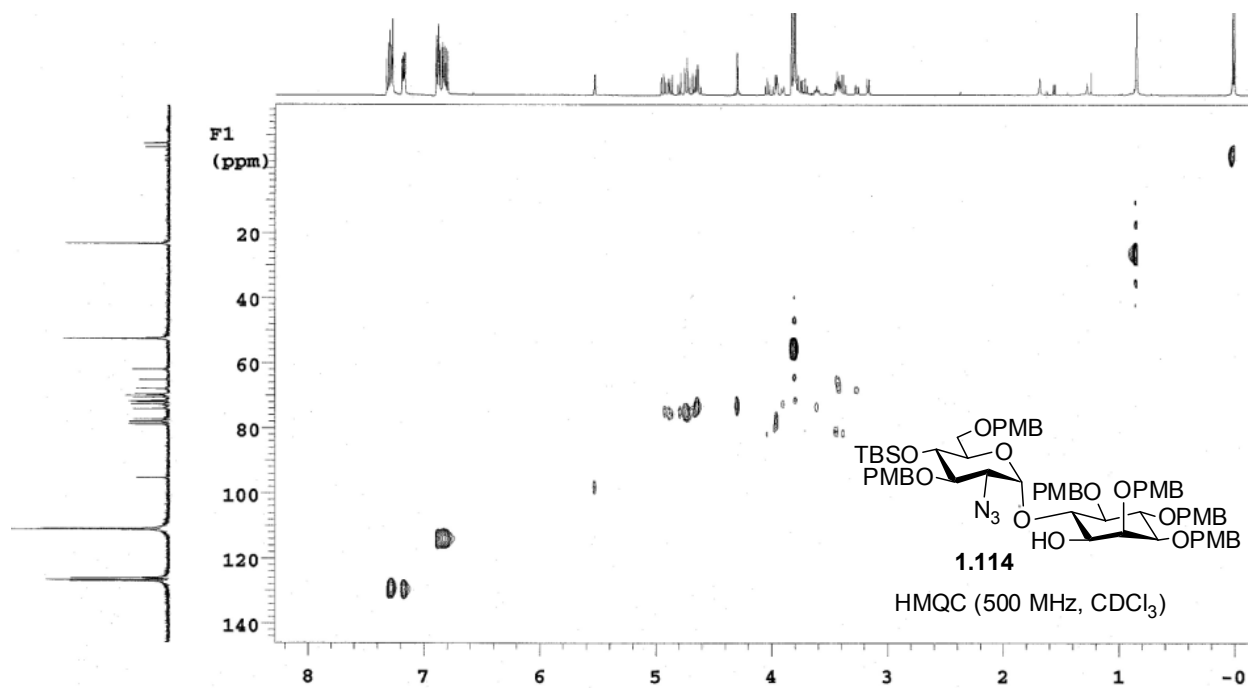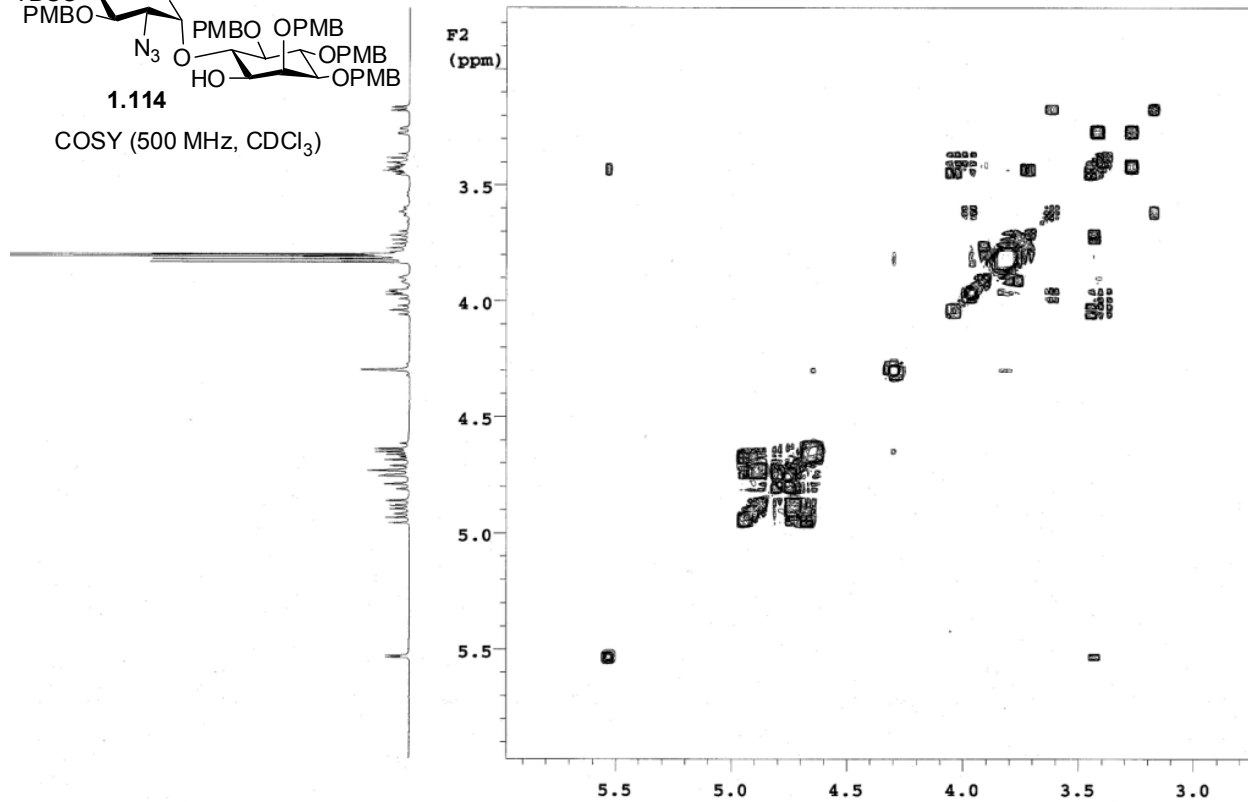
HPLC chromatogram for purification of **1.138**

Conditions: Waters Nova-Pak Silica 6 μm, 300 x 19 mm
eluent 20% EtOAc in hexanes, 10 ml/min

α–anomer   β–anomer

TBSO—
PMBO—
OPMB
O
N₃
O
HO—
PMBO OPMB
OPMB
OPMB
1.114

^{1}H NMR (500 MHz, CDCl$_3$)

TBSO—
PMBO—
OPMB
O
N₃
O
HO—
PMBO OPMB
OPMB
OPMB
1.114

^{13}C NMR (125 MHz, CDCl$_3$)

1.114

COSY (500 MHz, CDCl$_3$)

F2
(ppm)

1.114

HMQC (500 MHz, CDCl$_3$)

F1
(ppm)

Single Mass Analysis
Tolerance = 5.0 PPM / DBE: min = -1.5, max = 50.0
Element prediction: Off
Number of isotope peaks used for i-FIT = 3

Monoisotopic Mass, Even Electron Ions
5564 formula(e) evaluated with 20 results within limits (up to 50 best isotopic matches for each mass)
Elements Used:
C: 0-500   H: 0-1000   N: 0-5   O: 0-16   Na: 0-1   Si: 0-1
Guo- Ben Swarts BMS-VI-93 LCT0245 mw1201.5 0.5uL meoh
Shay 2008-07b.pro
2008_1125_0245 15 (0.300) Cm (13:18-(5:9+30:35)x5.000)
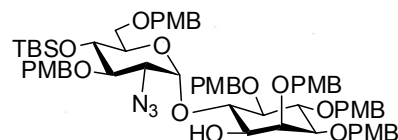
1.114

HR ESI MS

LCT Premier 10-Dec-2008 16:04:30
1: TOF MS ES+
1.80e+003
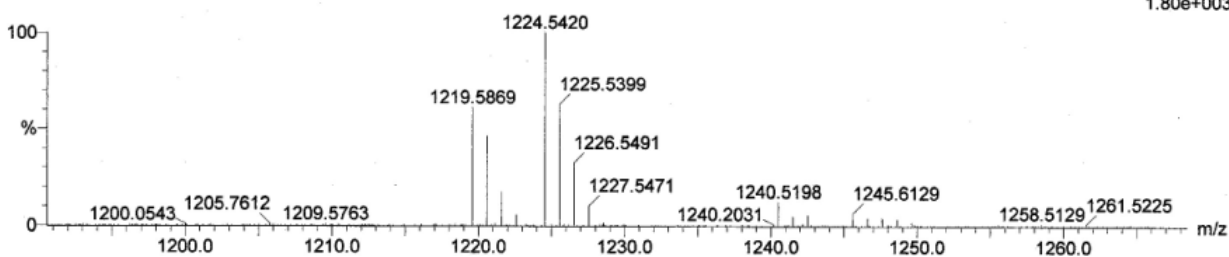
Mass	Calc. Mass	mDa	PPM	DBE	i-FIT	i-FIT (Norm)	Formula
Minimum:				-1.5			
Maximum:		5.0	5.0	50.0			
1224.5420	1224.5409	1.1	0.9	32.5	64.0	1.2	C70 H79 N3 O15 Na
	1224.5433	-1.3	-1.1	35.5	64.8	2.1	C72 H78 N3 O15
	1224.5440	-2.0	-1.6	27.5	64.9	2.1	C66 H83 N3 O16 Na Si
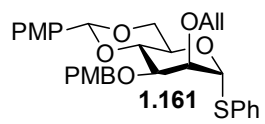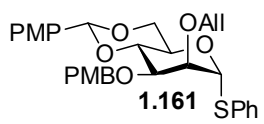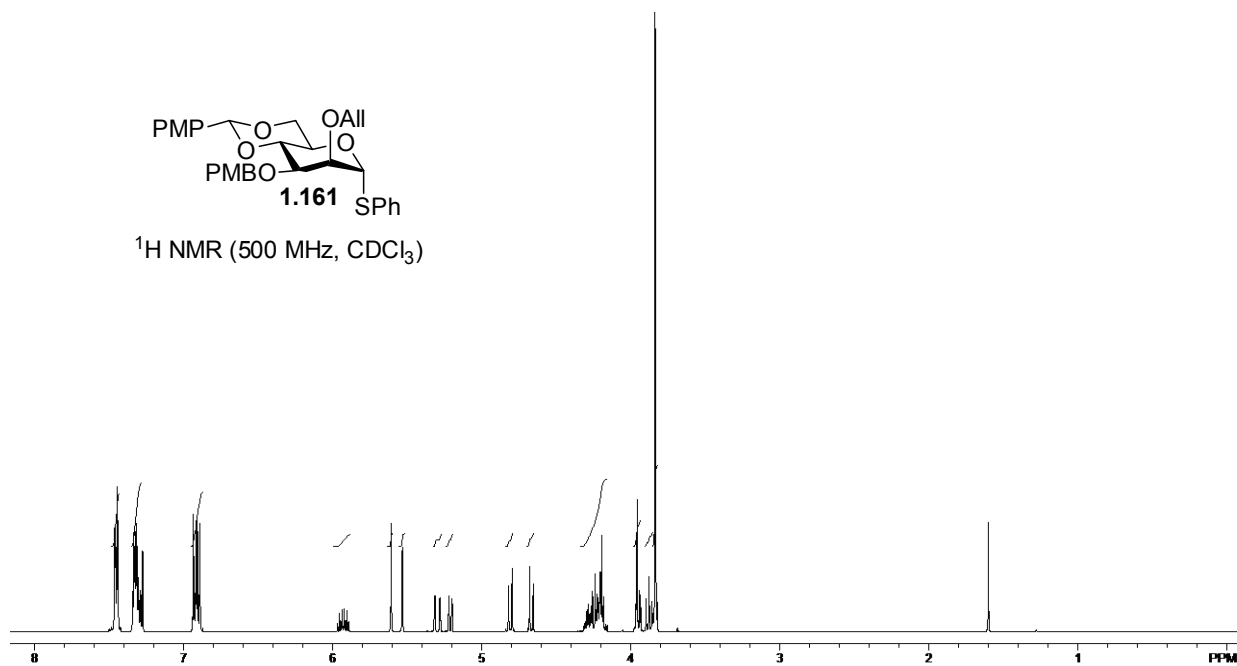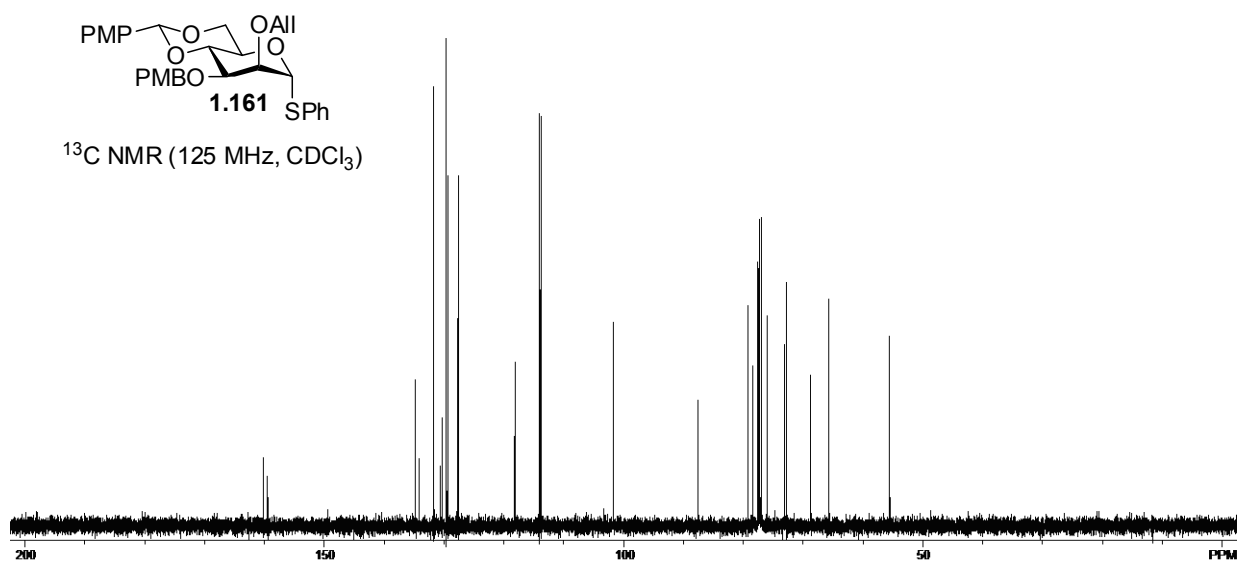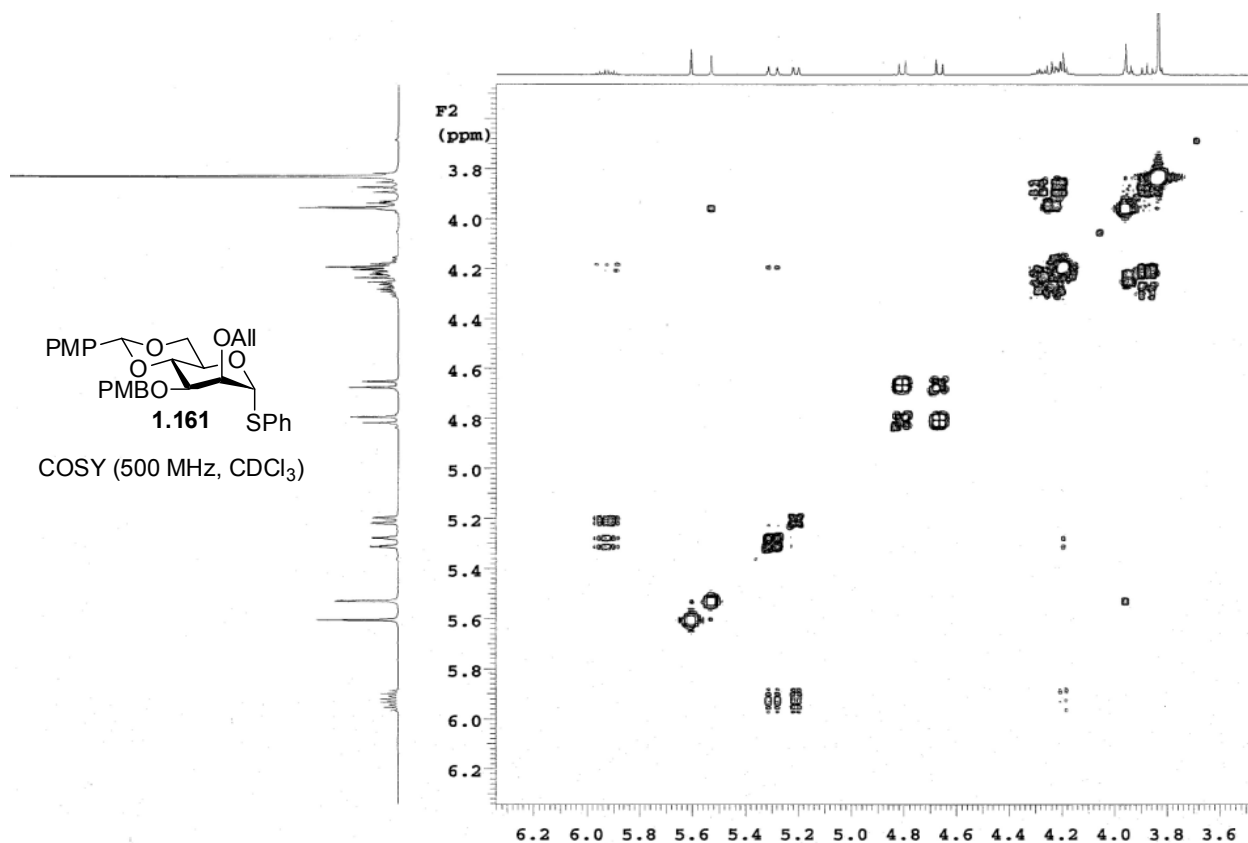
PMP—O—OAll
O
PMBO
1.161 SPh

^{1}H NMR (500 MHz, CDCl$_3$)

PMP—O—OAll
O
PMBO
1.161 SPh

^{13}C NMR (125 MHz, CDCl$_3$)

COSY (500 MHz, CDCl₃)

PMP, PMBO, OAll, SPh structure labeled **1.161**

Single Mass Analysis
Tolerance = 5.0 PPM / DBE: min = -1.5, max = 100.0
Element prediction: Off
Number of isotope peaks used for i-FIT = 3

Monoisotopic Mass, Even Electron Ions
265 formula(e) evaluated with 4 results within limits (up to 50 closest results for each mass)
Elements Used:
C: 25-40   H: 20-50   N: 0-4   O: 0-10   23Na: 0-1   S: 1-1
Ben Swarts   BMS-VII-68
Lew 2008-07b.pro
2009_0318_0336 13 (0.284) Cm (11:16-(3:8+24:36)x10.000)

HR ESI MS
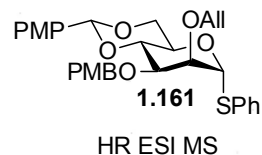
LCT Premier 18-Mar-2009 13:45:16
1: TOF MS ES+
3.61e+004
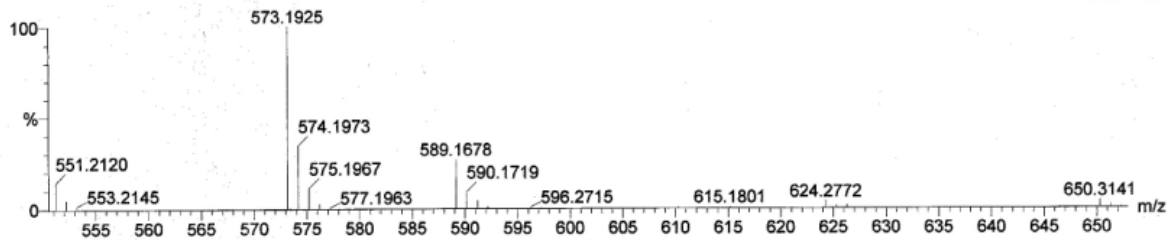

```
Minimum:                        -1.5
Maximum:        5.0     5.0     100.0

Mass        Calc. Mass   mDa    PPM     DBE     i-FIT   i-FIT (Norm)  Formula

573.1925    573.1923     0.2    0.3     14.5    25.5    0.9           C31  H34  O7   23Na  S
            573.1936     -1.1   -1.9    19.5    27.6    3.1           C32  H30  N4   O3
                                                                      23Na  S
            573.1907     1.8    3.1     13.5    25.2    0.6           C28  H33  N2   O9   S
            573.1947     -2.2   -3.8    17.5    28.0    3.4           C33  H33  O7   S
```
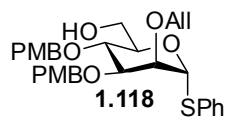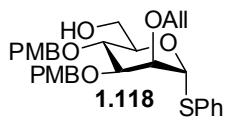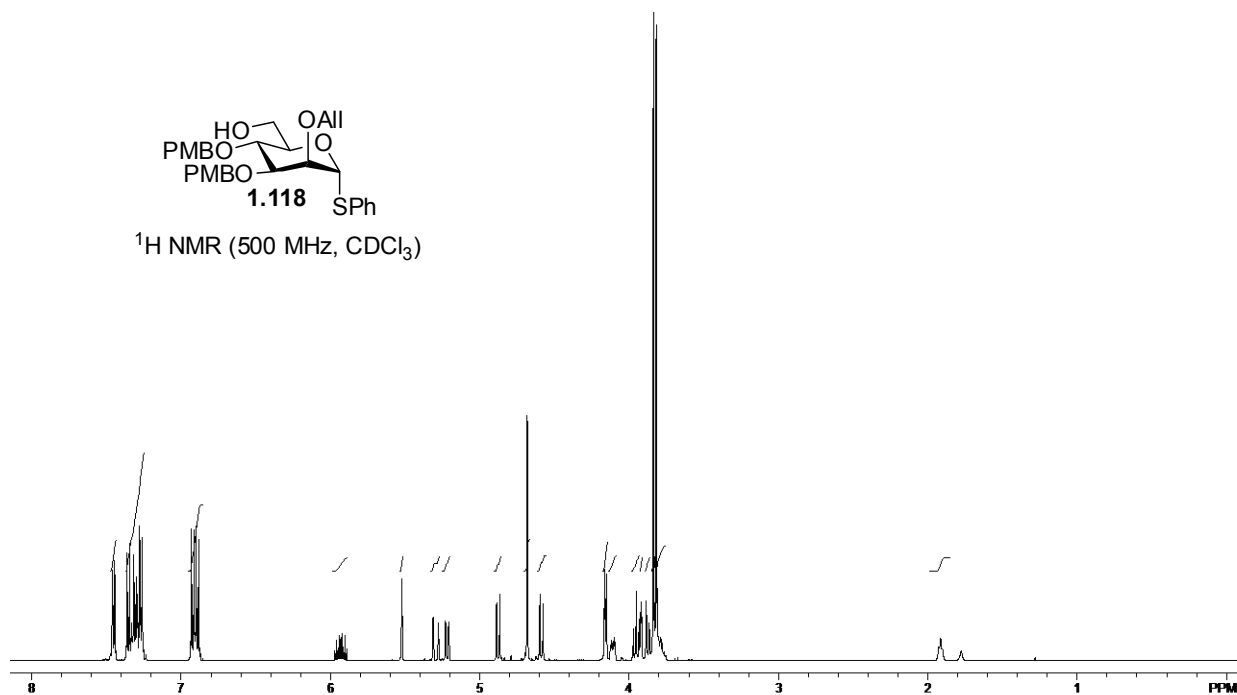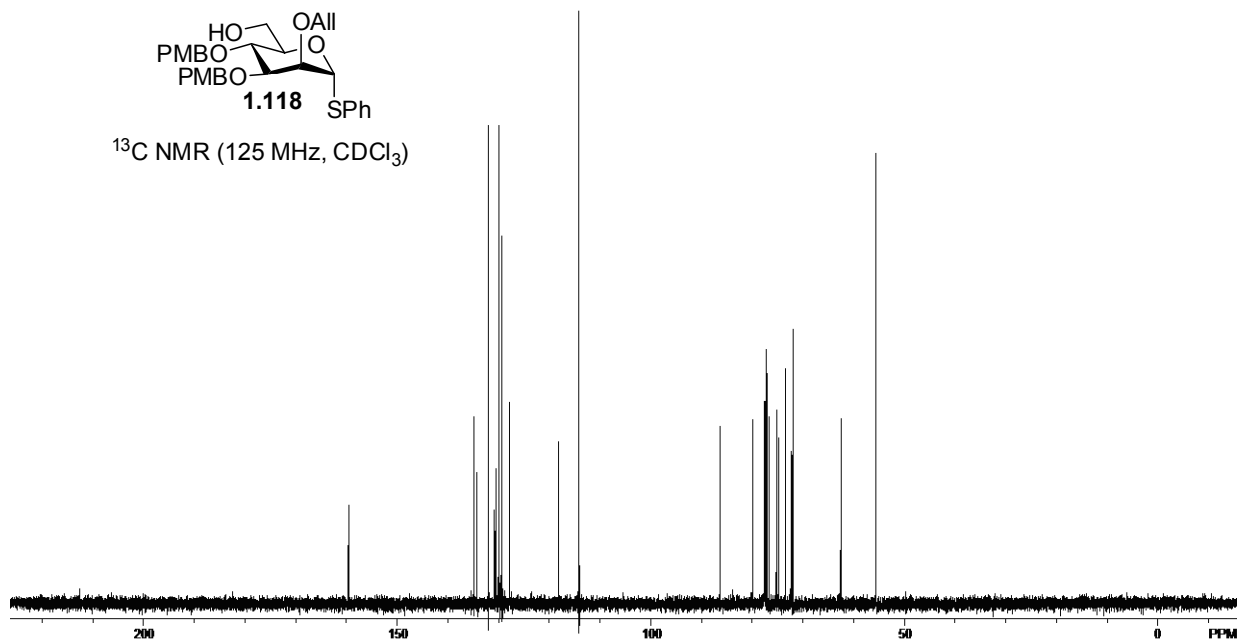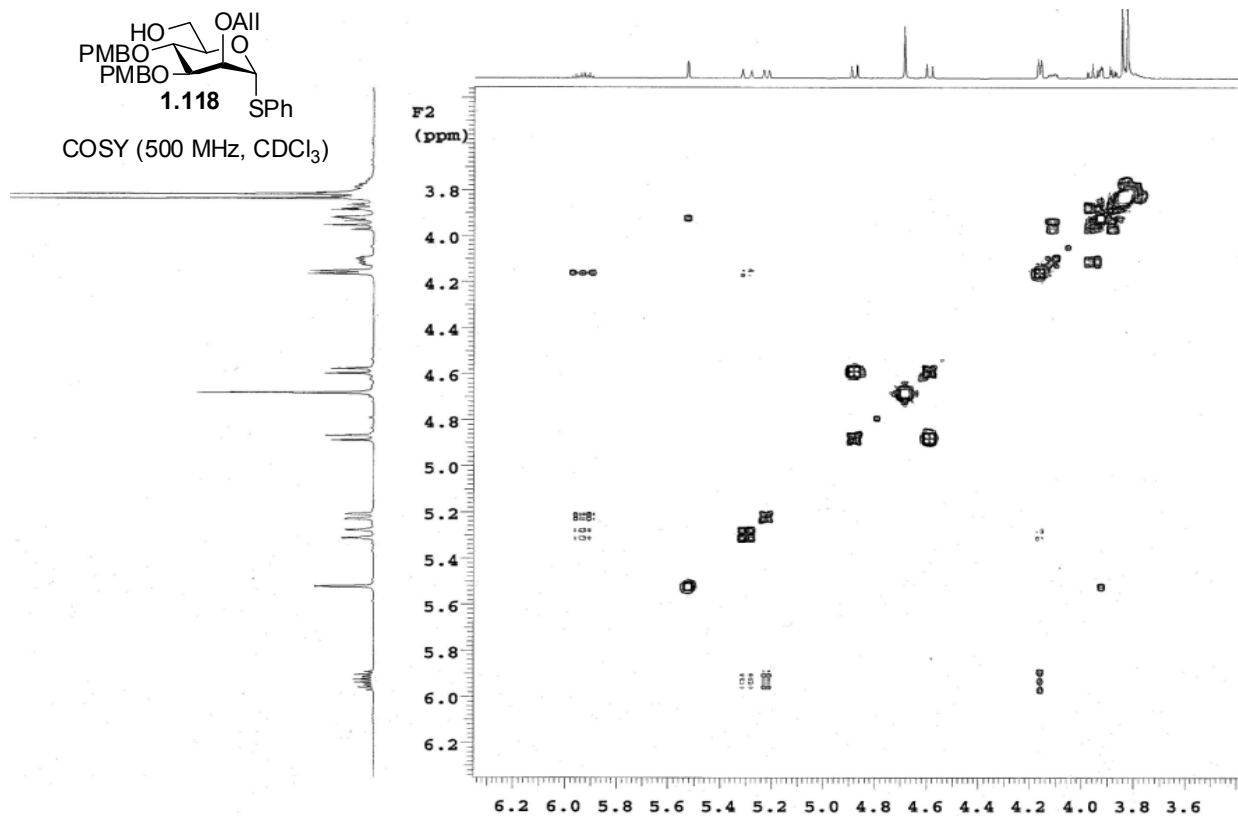
HO OAll
PMBO
PMBO
1.118 SPh

^{1}H NMR (500 MHz, CDCl$_3$)

HO OAll
PMBO
PMBO
1.118 SPh

^{13}C NMR (125 MHz, CDCl$_3$)

1.118

COSY (500 MHz, CDCl$_3$)

Single Mass Analysis
Tolerance = 5.0 PPM / DBE: min = -1.5, max = 50.0
Element prediction: Off
Number of isotope peaks used for i-FIT = 3

Monoisotopic Mass, Even Electron Ions
1127 formula(e) evaluated with 6 results within limits (up to 50 best isotopic matches for each mass)
Elements Used:
C: 0-500 H: 0-1000 N: 0-3 O: 0-10 23Na: 0-1 S: 0-1
Guo; Ben Swarts BMS-VIII-76
Lew 2008-07b.pro
2009_0325_0355 18 (0.389) Cm (18:21-2:7x2.000)

1.118

HR ESI MS
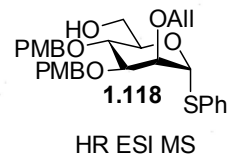
LCT Premier 25-Mar-2009 10:25:09
1: TOF MS ES+
2.00e+003
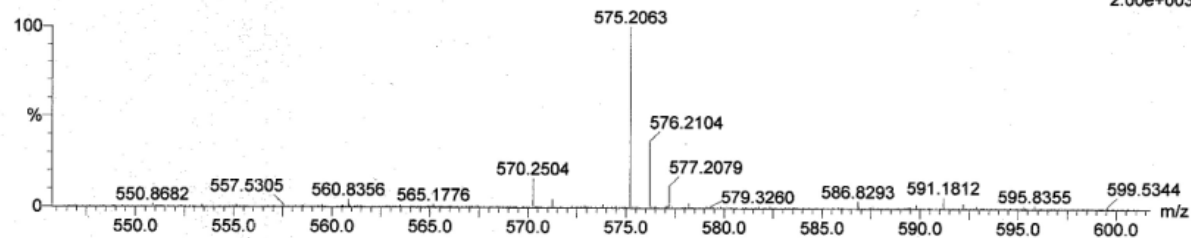
Mass	Calc. Mass	mDa	PPM	DBE	i-FIT	i-FIT (Norm)	Formula
575.2063	575.2063	0.0	0.0	12.5	79.2	0.7	C28 H35 N2 O9 S
	575.2079	-1.6	-2.8	13.5	79.3	0.7	C31 H36 O7 23Na S
	575.2039	2.4	4.2	9.5	83.3	4.7	C26 H36 N2 O9 23Na S
	575.2070	-0.7	-1.2	21.5	85.0	6.4	C36 H31 O7
	575.2046	1.7	3.0	18.5	85.2	6.7	C34 H32 O7 23Na
	575.2045	1.8	3.1	25.5	85.2	6.7	C40 H31 O2 S
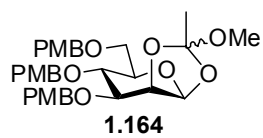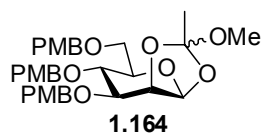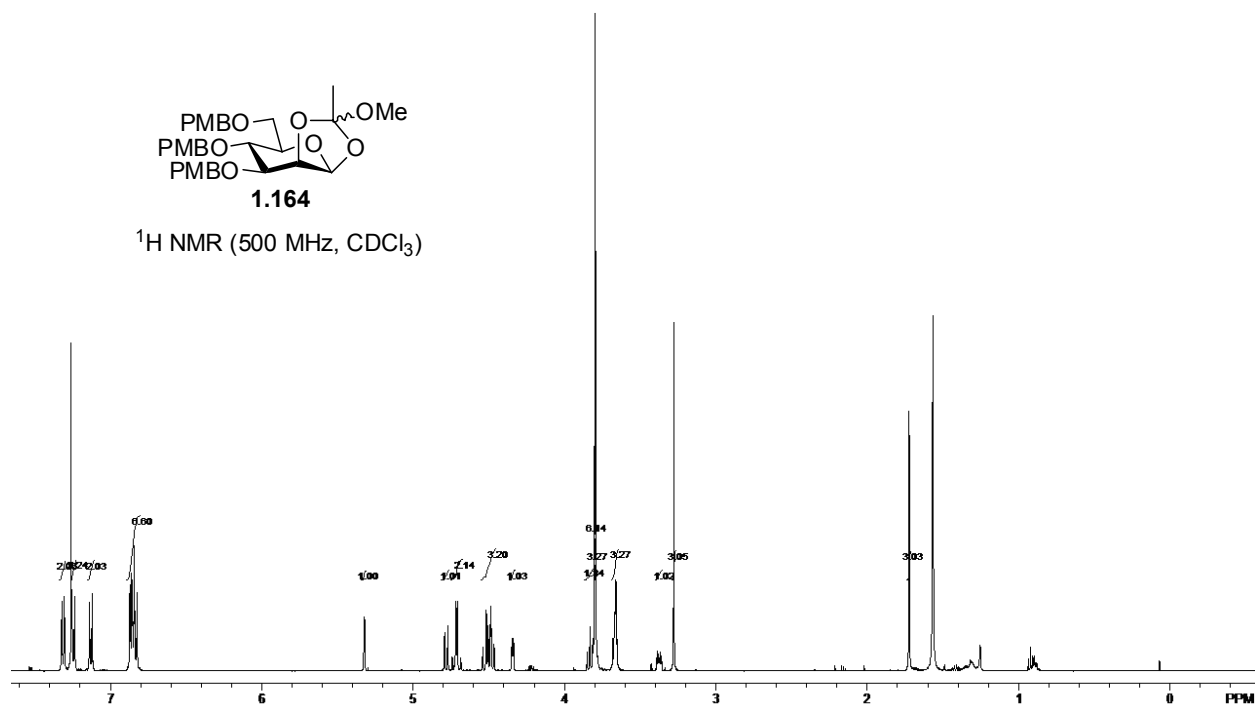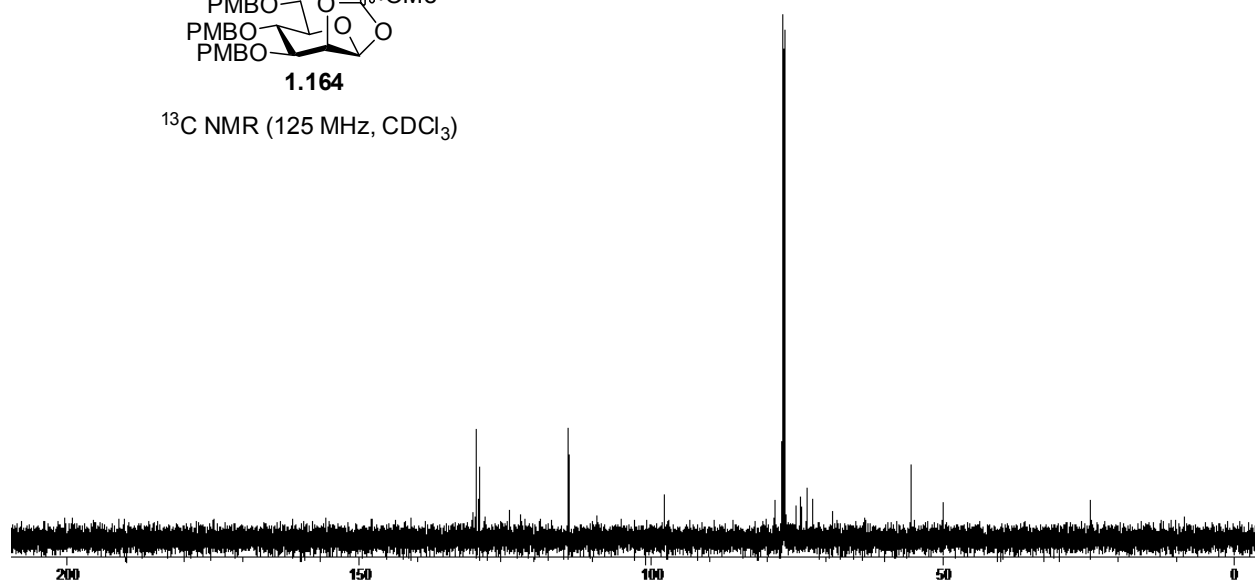
Minimum: -1.5
Maximum: 5.0   5.0   50.0

PMBO, PMBO, PMBO, OMe

1.164

^{1}H NMR (500 MHz, CDCl$_3$)

PMBO, PMBO, PMBO, OMe

1.164

^{13}C NMR (125 MHz, CDCl$_3$)

Single Mass Analysis
Tolerance = 5.0 PPM / DBE: min = -1.5, max = 50.0
Element prediction: Off
Number of isotope peaks used for i-FIT = 3

Monoisotopic Mass, Even Electron Ions
334 formula(e) evaluated with 2 results within limits (up to 50 best isotopic matches for each mass)
Elements Used:
C: 0-500   H: 0-1000   O: 0-30   Na: 0-1
Guo; Ben Swarts BMS-V-22 mw596 LCT0017 10pg/ul meoh 1cm stk inj3ul pluno
OA-FIA-1min DOP   LCT Premier

2008_0703_0017_11 16 (0.311) Cm (12:19-34:45)
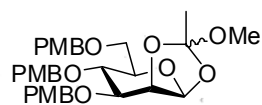
1.164

HR ESI MS

12:28:28 03-Jul-2008
16129 pushes/sec
1: TOF MS ES+
5.21e+004

M Na

619.2524

620.2570

605.2370
621.2584

243.9442 311.9320 328.9224 345.9121 396.9088 464.8973 489.8934 506.8851 574.8717 689.1618 m/z

260 280 300 320 340 360 380 400 420 440 460 480 500 520 540 560 580 600 620 640 660 680
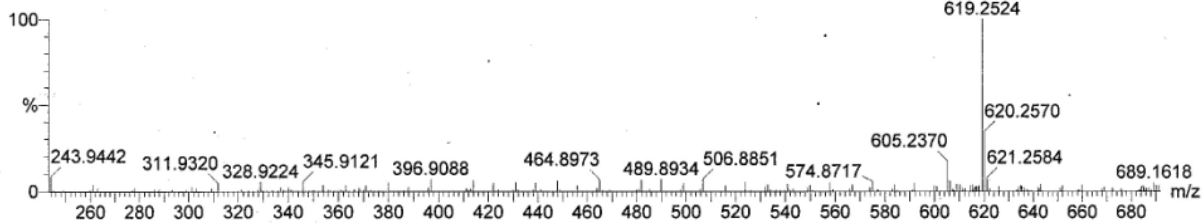
			Minimum:	-1.5		
			Maximum:	6.0	5.0	50.0

Mass	Calc. Mass	mDa	PPM	DBE	i-FIT	Formula
619.2524	619.2519	0.5	0.8	13.5	106.5	C33 H40 O10 Na
	619.2543	-1.9	-3.1	16.5	270.3	C35 H39 O10
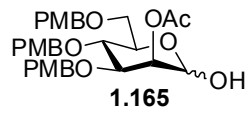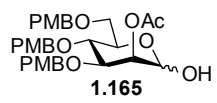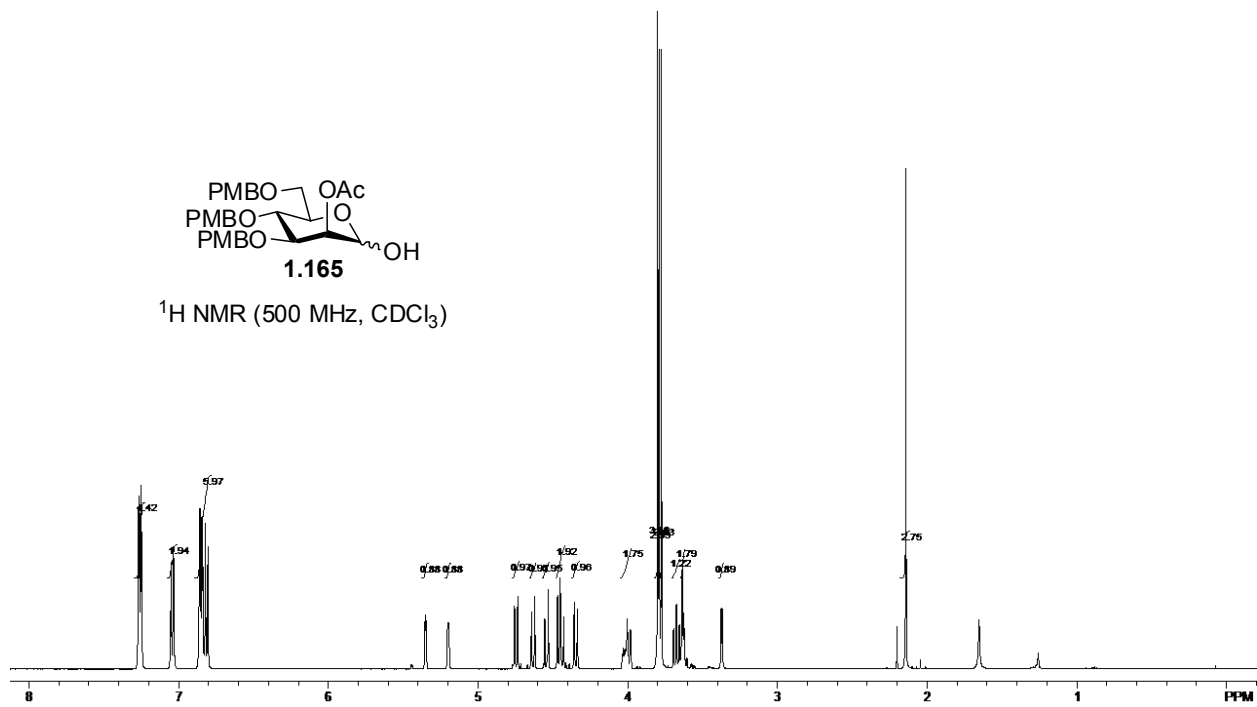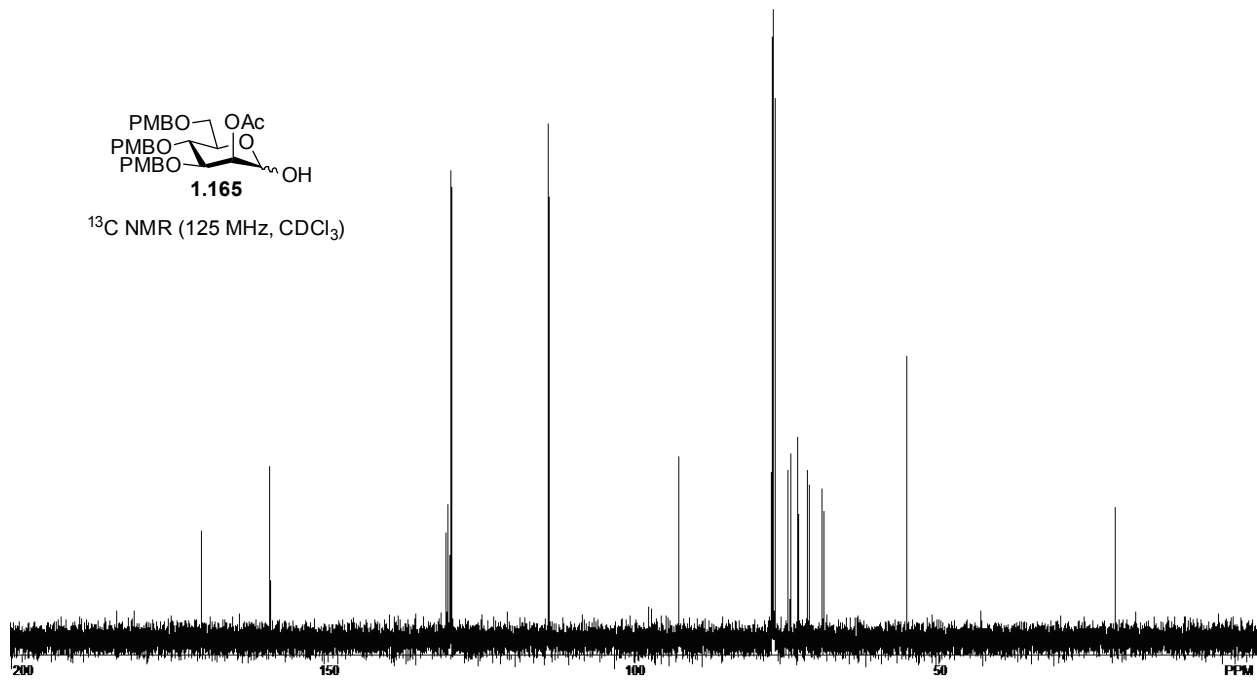
PMBO OAc
PMBO O
PMBO OH
1.165

^{1}H NMR (500 MHz, CDCl$_3$)

PMBO OAc
PMBO O
PMBO OH
1.165

^{13}C NMR (125 MHz, CDCl$_3$)

Single Mass Analysis
Tolerance = 5.0 PPM / DBE: min = -1.5, max = 50.0
Element prediction: Off
Number of isotope peaks used for i-FIT = 3

Monoisotopic Mass, Even Electron Ions
314 formula(e) evaluated with 3 results within limits (up to 50 best isotopic matches for each mass)
Elements Used:
C: 0-500   H: 0-1000   O: 0-30   Na: 0-1
Guo; Ben Swarts BMS-V-24 mw582 LCT0019 10pg/ul meoh 1cm stk inj3ul pluno
OA-FIA-1min DOP   LCT Premier

2008_0703_0019_13 16 (0.311) Cm (13:18-29:39)
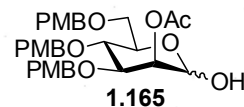
HR ESI MS

14:13:13 03-Jul-2008
16129 pushes/sec
1: TOF MS ES+
2.18e+004

1.165
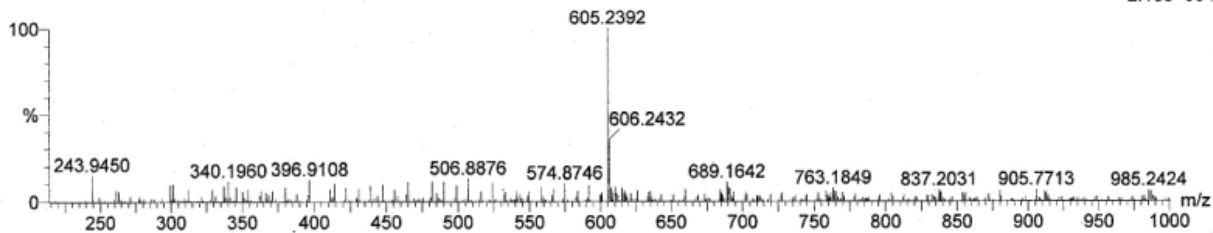
Minimum: -1.5
Maximum: 6.0   5.0   50.0

Mass	Calc. Mass	mDa	PPM	DBE	i-FIT	Formula			
605.2392	605.2363	2.9	4.8	13.5	9.8	C32	H38	O10	Na
	605.2387	0.5	0.8	16.5	45.0	C34	H37	O10	
	605.2421	-2.9	-4.8	4.5	102.6	C25	H42	O15	Na

PMTrtO⎯OH
HO⎯⎯O
HO⎯⎯
1.167 OAll

^{1}H NMR (500 MHz, CDCl$_3$)

PMTrtO⎯OH
HO⎯⎯O
HO⎯⎯
1.167 OAll
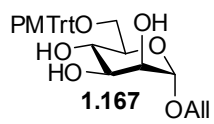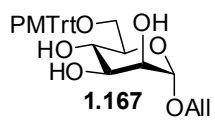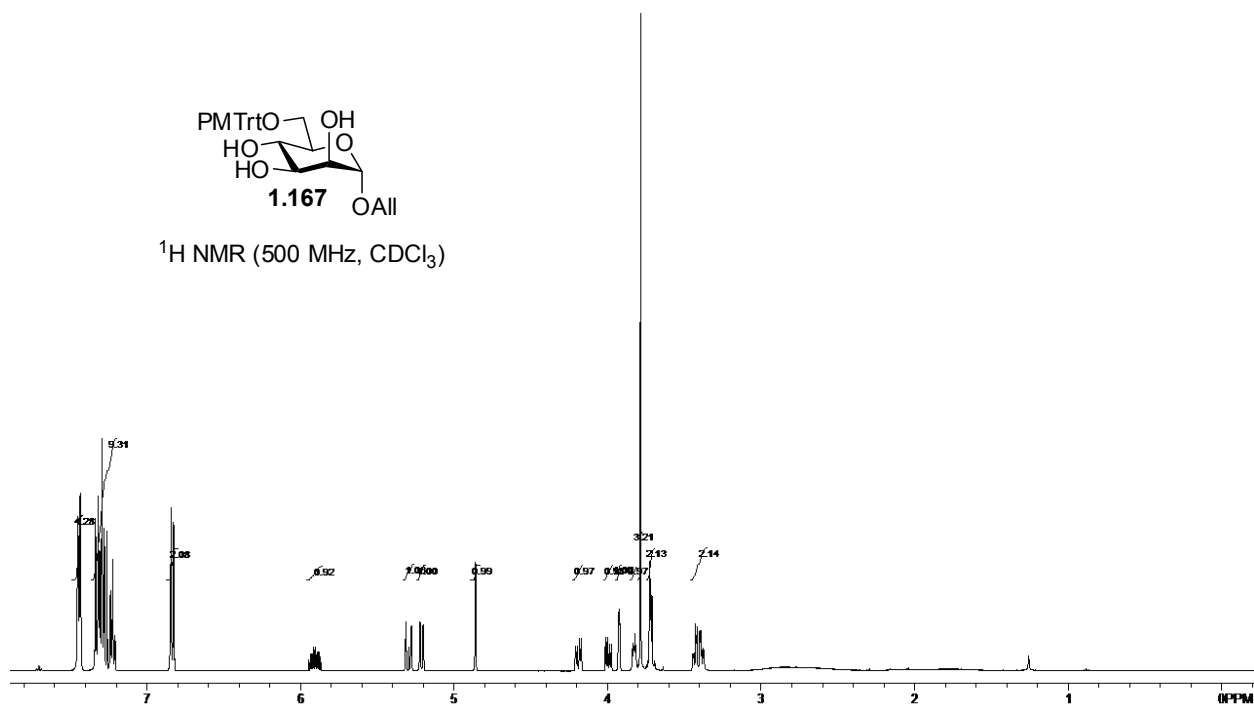
^{13}C NMR (125 MHz, CDCl$_3$)
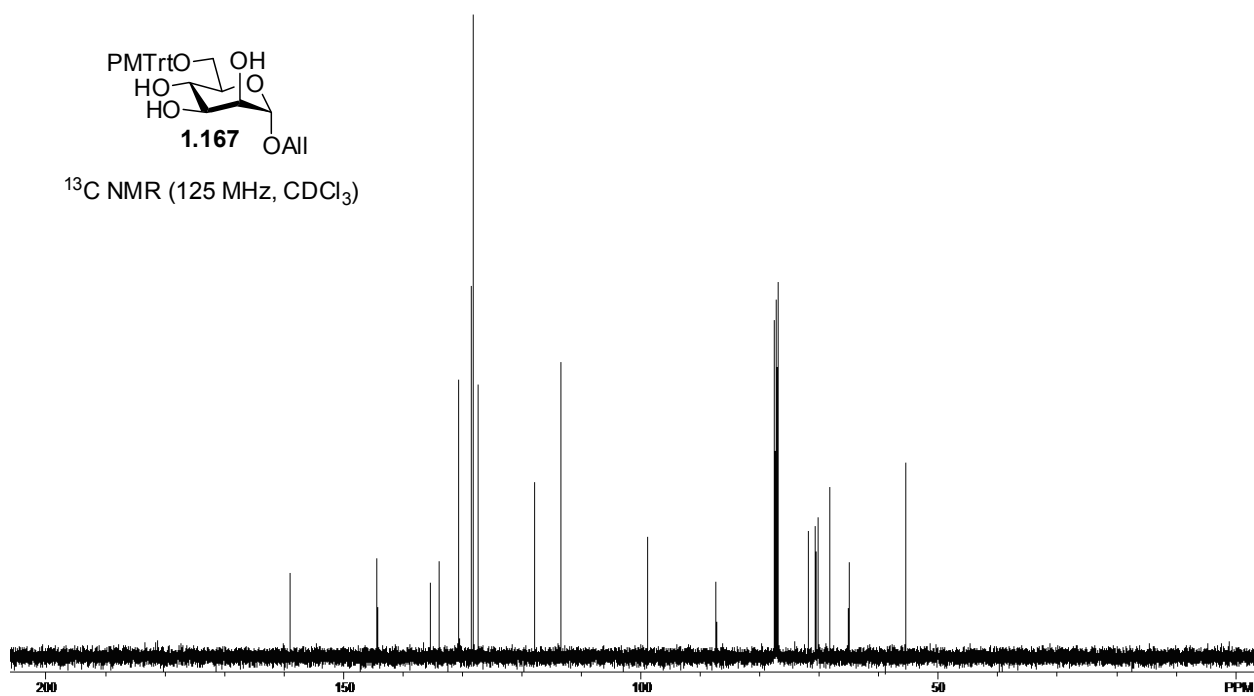
1H CDCl3 BMS-V-56 400 MHz 18mg
Pulse Sequence: gtncosy
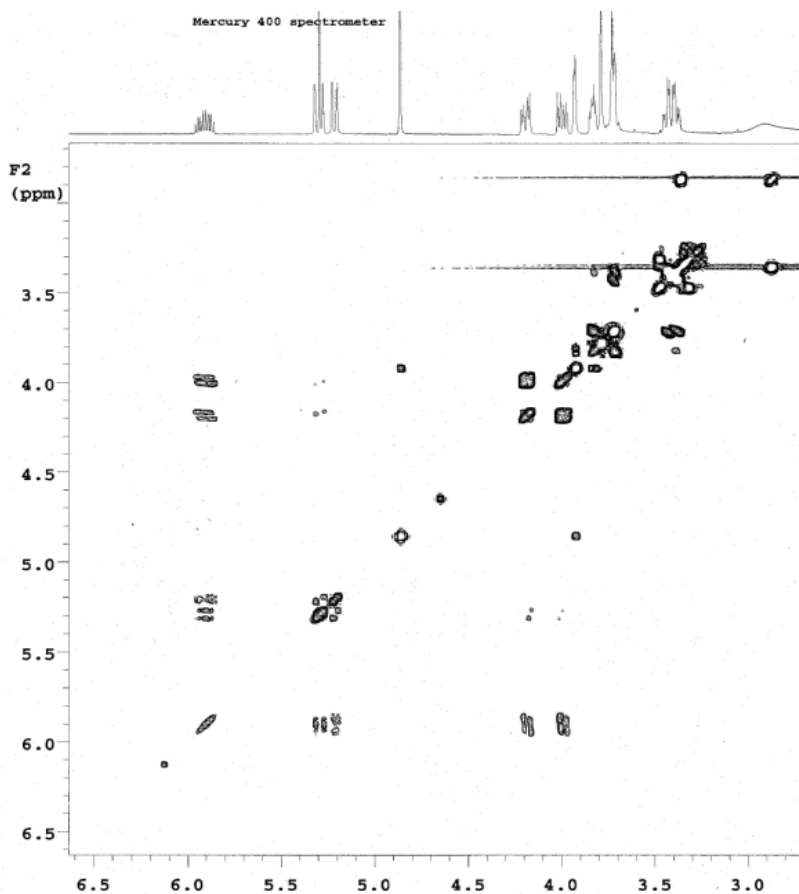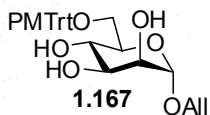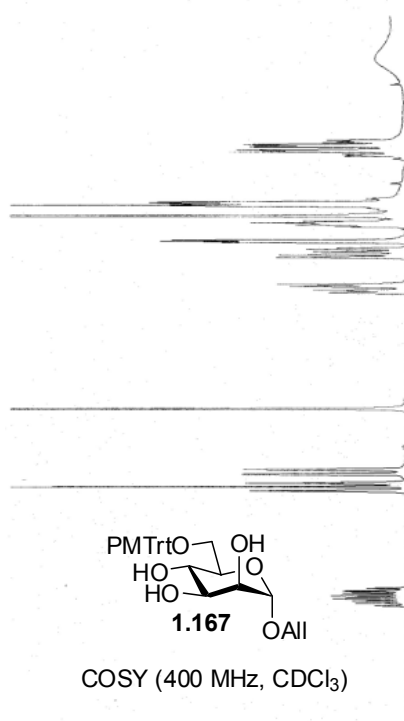
Mercury 400 spectrometer

F2
(ppm)

COSY (400 MHz, CDCl₃)

Single Mass Analysis
Tolerance = 5.0 PPM / DBE: min = -1.5, max = 50.0
Element prediction: Off
Number of isotope peaks used for i-FIT = 3

Monoisotopic Mass, Even Electron Ions
259 formula(e) evaluated with 2 results within limits (up to 50 best isotopic matches for each mass)
Elements Used:
C: 0-500   H: 0-1000   O: 0-30   Na: 0-1
Guo; Ben Swarts BMS-V-56 mw492 LCT0015 10pg/ul meoh 1cm stk inj3ul pluno
OA-FIA-1min DOP   LCT Premier

2008_0703_0015_09 16 (0.311) Cm (11:21-31:49)
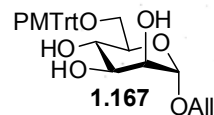
HR ESI MS

11:43:06 03-Jul-2008
16129 pushes/sec
1: TOF MS ES+
1.18e+004

MNa^+
515.2054
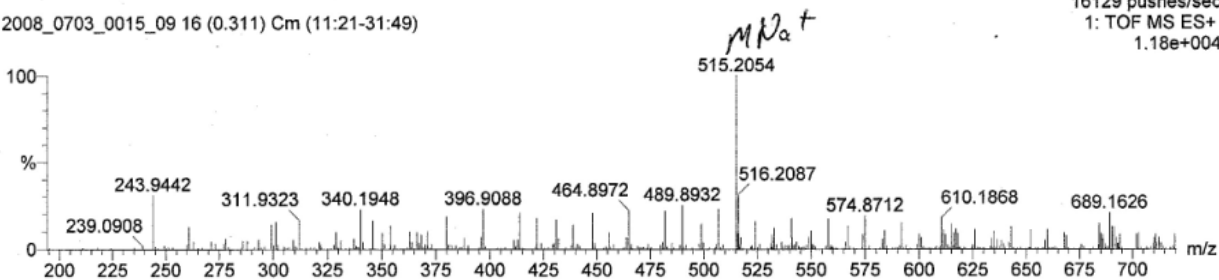
Mass	Calc. Mass	mDa	PPM	DBE	i-FIT	Formula	
515.2054	515.2046	0.8	1.6	13.5	5.3	C29 H32 O7	Na
	515.2070	-1.6	-3.1	16.5	27.1	C31 H31 O7	
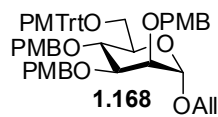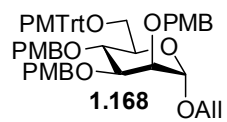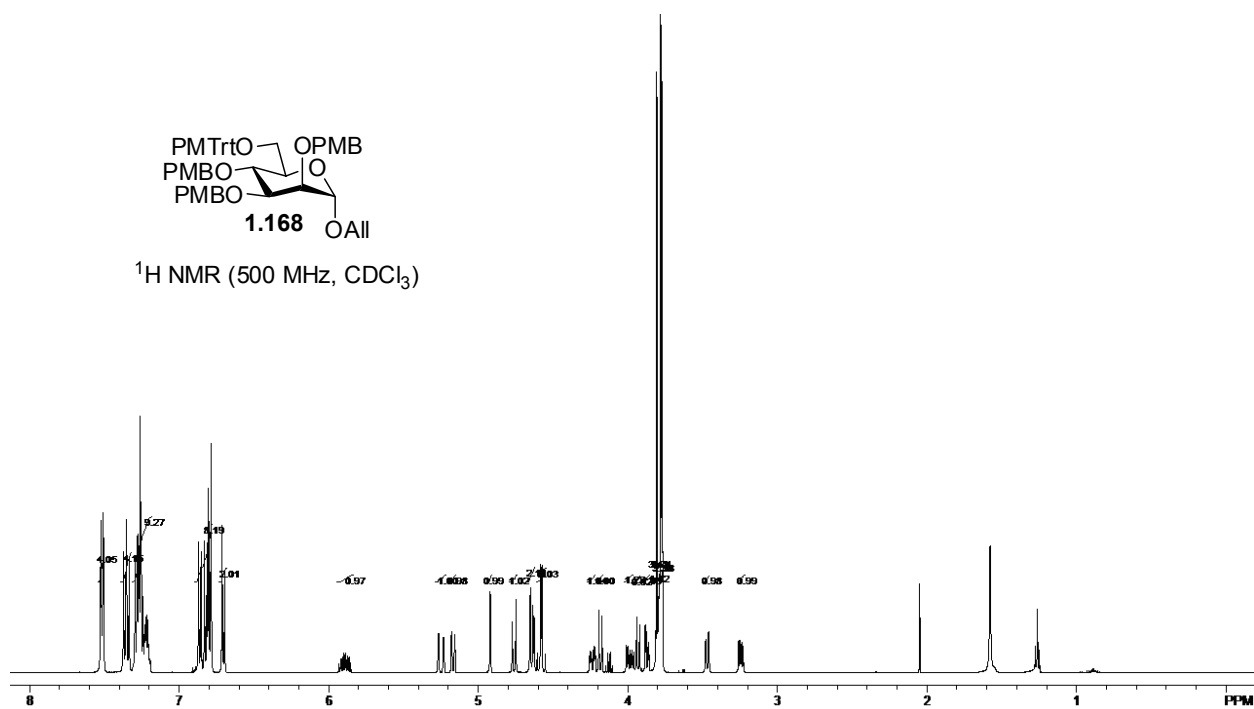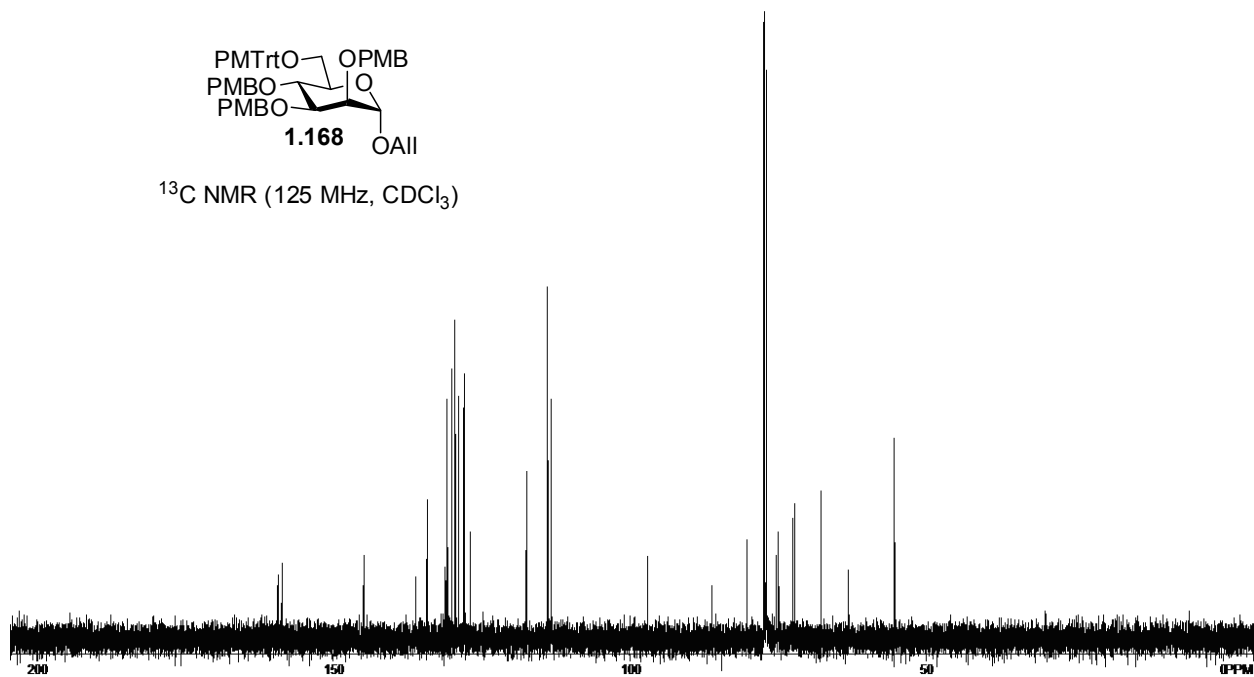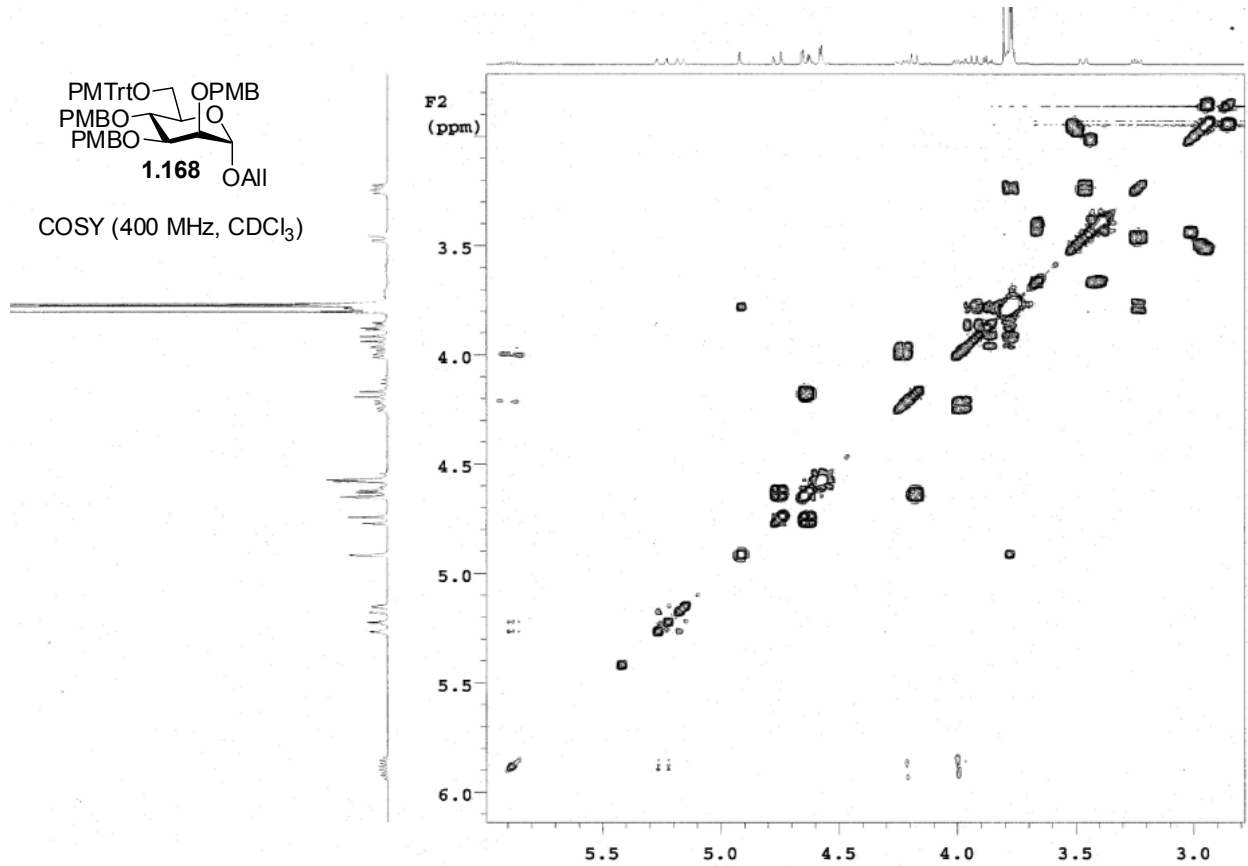
Minimum: -1.5
Maximum: 6.0 5.0 50.0

PMTrtO⟍ ⟍OPMB
PMBO⟍ ⟍O
PMBO⟍
1.168 ⟍OAll

^{1}H NMR (500 MHz, CDCl$_3$)

PMTrtO⟍ ⟍OPMB
PMBO⟍ ⟍O
PMBO⟍
1.168 ⟍OAll

^{13}C NMR (125 MHz, CDCl$_3$)

PMTrtO — OPMB
PMBO
PMBO
1.168 OAll

COSY (400 MHz, CDCl$_3$)

F2
(ppm)

3.5

4.0

4.5

5.0

5.5

6.0

5.5   5.0   4.5   4.0   3.5   3.0

Single Mass Analysis
Tolerance = 5.0 PPM / DBE: min = -1.5, max = 50.0
Element prediction: Off
Number of isotope peaks used for i-FIT = 3

PMTrtO — OPMB
PMBO
PMBO
1.168 OAll

HR ESI MS

Monoisotopic Mass, Even Electron Ions
525 formula(e) evaluated with 5 results within limits (up to 50 best isotopic matches for each mass)
Elements Used:
C: 0-500   H: 0-1000   O: 0-30   Na: 0-1
Guo; Ben Swarts BMS-V-63 mw852 LCT0020 10pg/ul meoh 1cm stk inj3ul pluno
OA-FIA-1min DOP   LCT Premier

2008_0703_0020_17 16 (0.311) Cm (11:21-32:45)
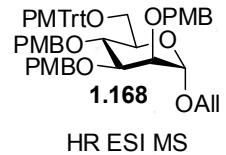
14:54:19 03-Jul-2008
16129 pushes/sec
1: TOF MS ES+
2.72e+004

m put 875.3762

100

876.3804

%

877.3842

273.1295

928.4627

274.1328 335.1259   421.2341 441.2996   563.4638   650.8665   755.3209   828.7160
0   m/z
300   350   400   450   500   550   600   650   700   750   800   850   900   950
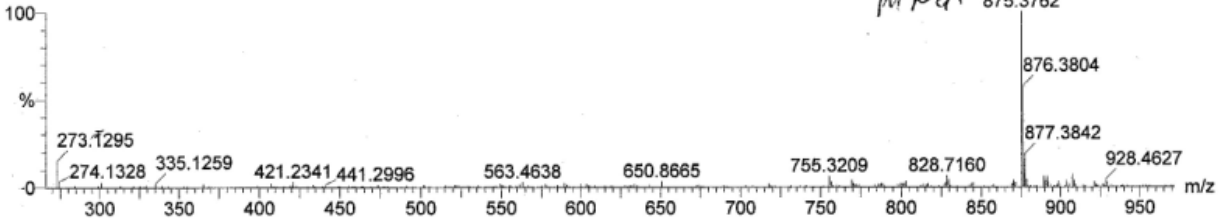
Minimum: -1.5
Maximum: 6.0   5.0   50.0

Mass   Calc. Mass   mDa   PPM   DBE   i-FIT   Formula

875.3762   875.3771   -0.9   -1.0   25.5   19.8   C53 H56 O10   Na
            875.3795   -3.3   -3.8   28.5   65.9   C55 H55 O10
            875.3737   2.5   2.9   37.5   340.0   C62 H51 O5
            875.3760   0.2   0.2   6.5   456.7   C37 H63 O23
            875.3736   2.6   3.0   3.5   641.4   C35 H64 O23   Na
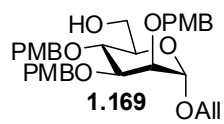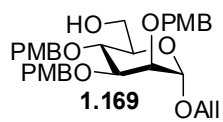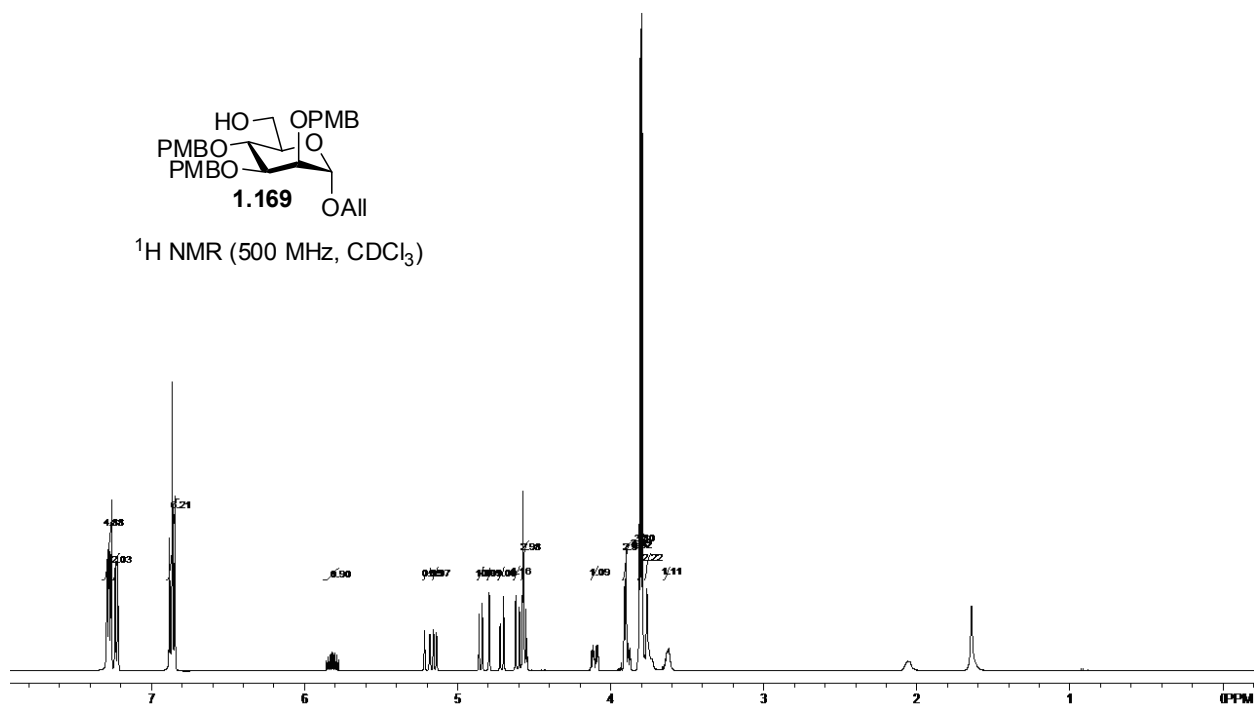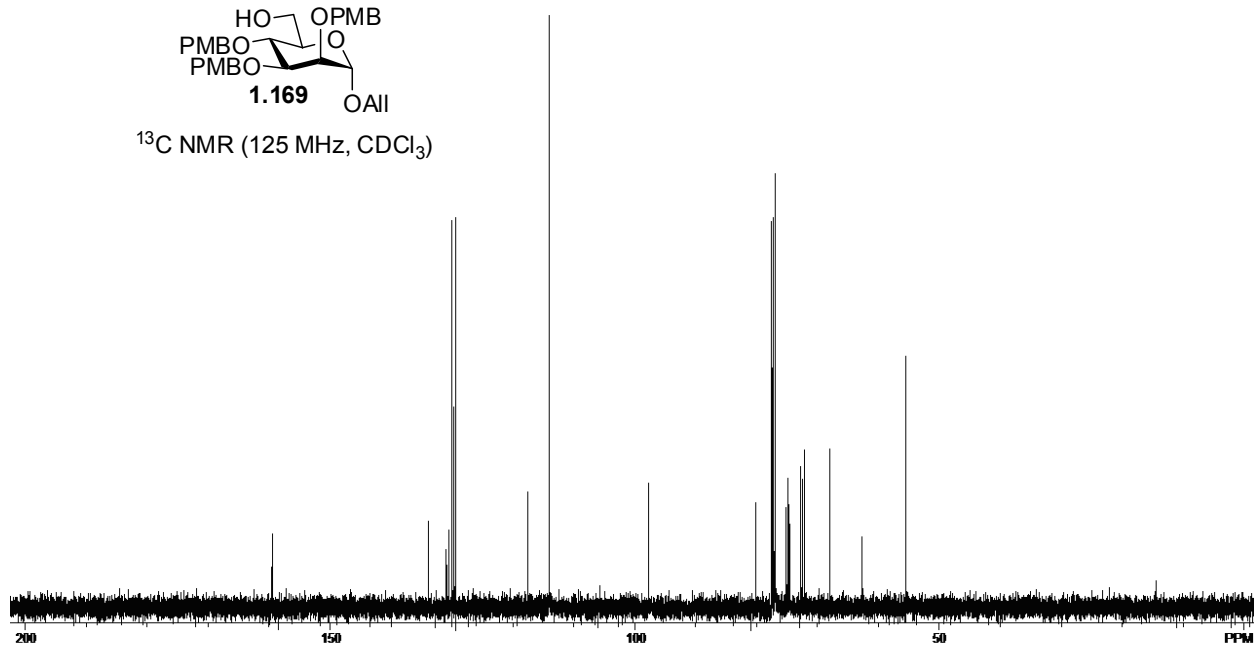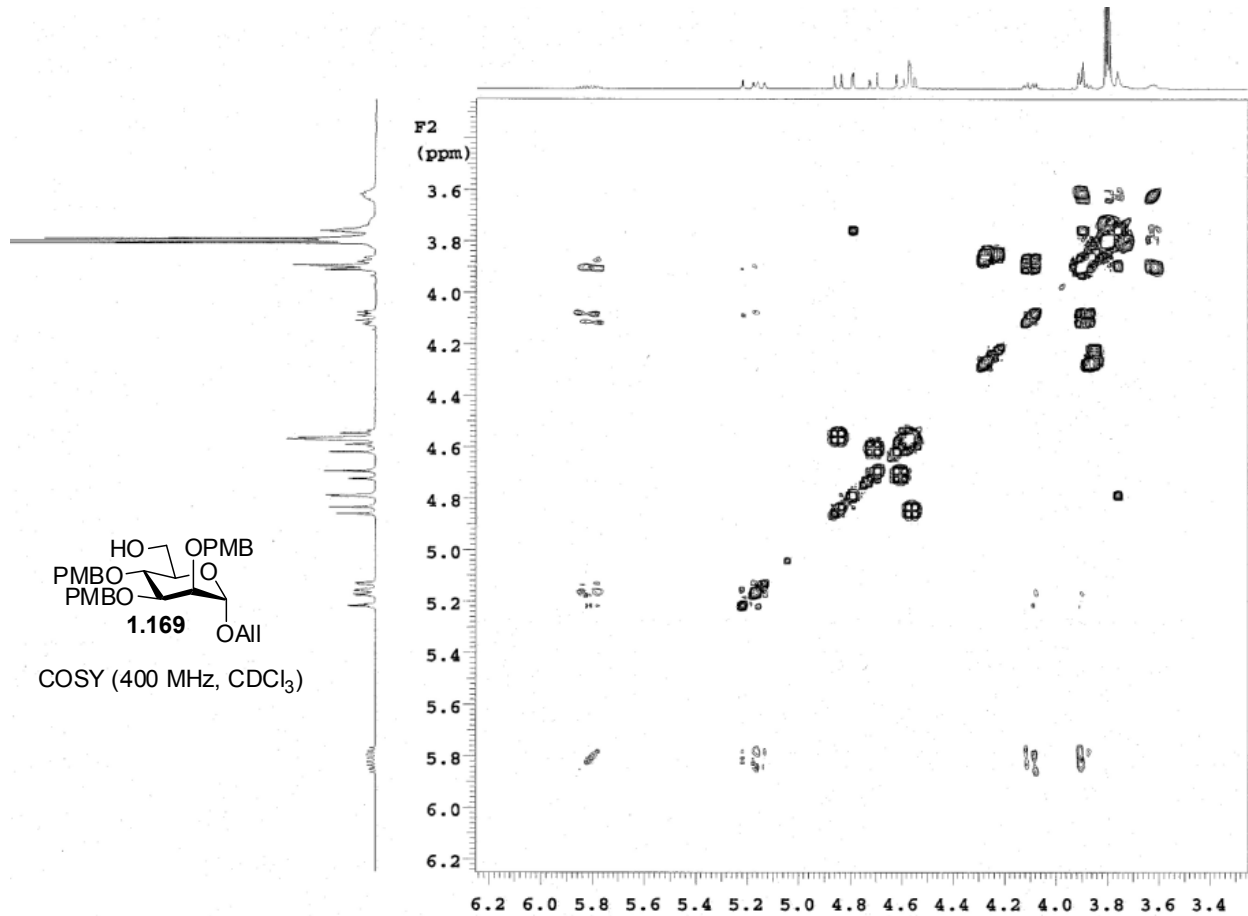
HO OPMB
PMBO
PMBO
1.169 OAll

O

^{1}H NMR (500 MHz, CDCl$_3$)

HO OPMB
PMBO
PMBO
1.169 OAll

O

^{13}C NMR (125 MHz, CDCl$_3$)

F2
(ppm)

3.6
3.8
4.0
4.2
4.4
4.6
4.8
5.0
5.2
5.4
5.6
5.8
6.0
6.2

6.2 6.0 5.8 5.6 5.4 5.2 5.0 4.8 4.6 4.4 4.2 4.0 3.8 3.6 3.4

1.169

COSY (400 MHz, CDCl$_3$)

Single Mass Analysis
Tolerance = 5.0 PPM / DBE: min = -1.5, max = 50.0
Element prediction: Off
Number of isotope peaks used for i-FIT = 3

Monoisotopic Mass, Even Electron Ions
323 formula(e) evaluated with 2 results within limits (up to 50 best isotopic matches for each mass)
Elements Used:
C: 0-500   H: 0-1000   O: 0-30   Na: 0-1
Guo; Ben Swarts BMS-V-70A mw580 LCT0016 10pg/ul meoh 1cm stk inj3ul pluno
OA-FIA-1min DOP   LCT Premier

2008_0703_0016_10 16 (0.311) Cm (12:20-34:46)

1.169

HR ESI MS
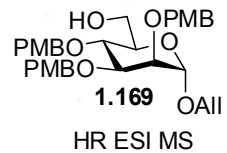
11:55:08 03-Jul-2008
16129 pushes/sec
1: TOF MS ES+
7.28e+004

mNa+

100%
%
0

603.2549
604.2584
605.2627
598.3007
506.8830
481.8840
413.8966
396.9079
340.1957
311.9313
243.9431
656.3427
m/z

260 280 300 320 340 360 380 400 420 440 460 480 500 520 540 560 580 600 620 640
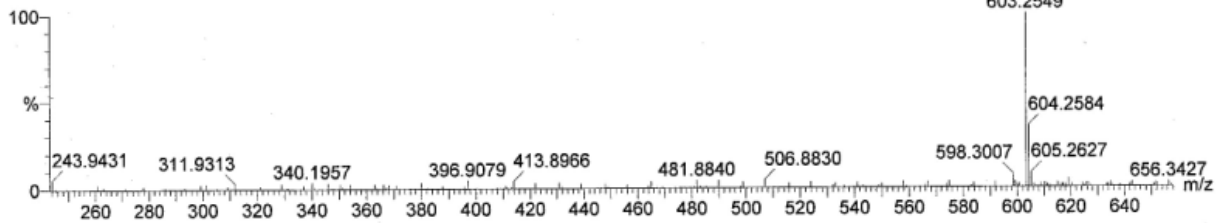
Minimum: -1.5
Maximum: 6.0   5.0   50.0

Mass	Calc. Mass	mDa	PPM	DBE	i-FIT	Formula		
603.2549	603.2570	-2.1	-3.5	13.5	72.8	C33	H40	O9 Na
	603.2535	1.4	2.3	25.5	1273.3	C42	H35	O4
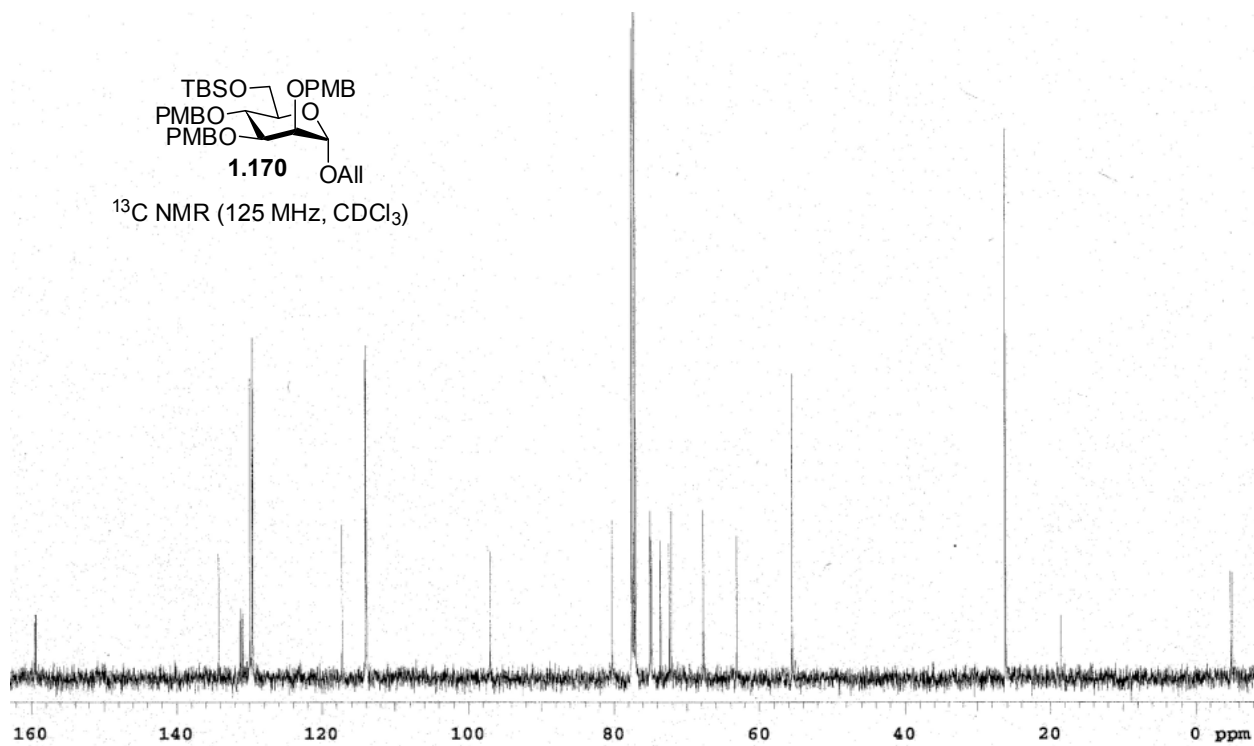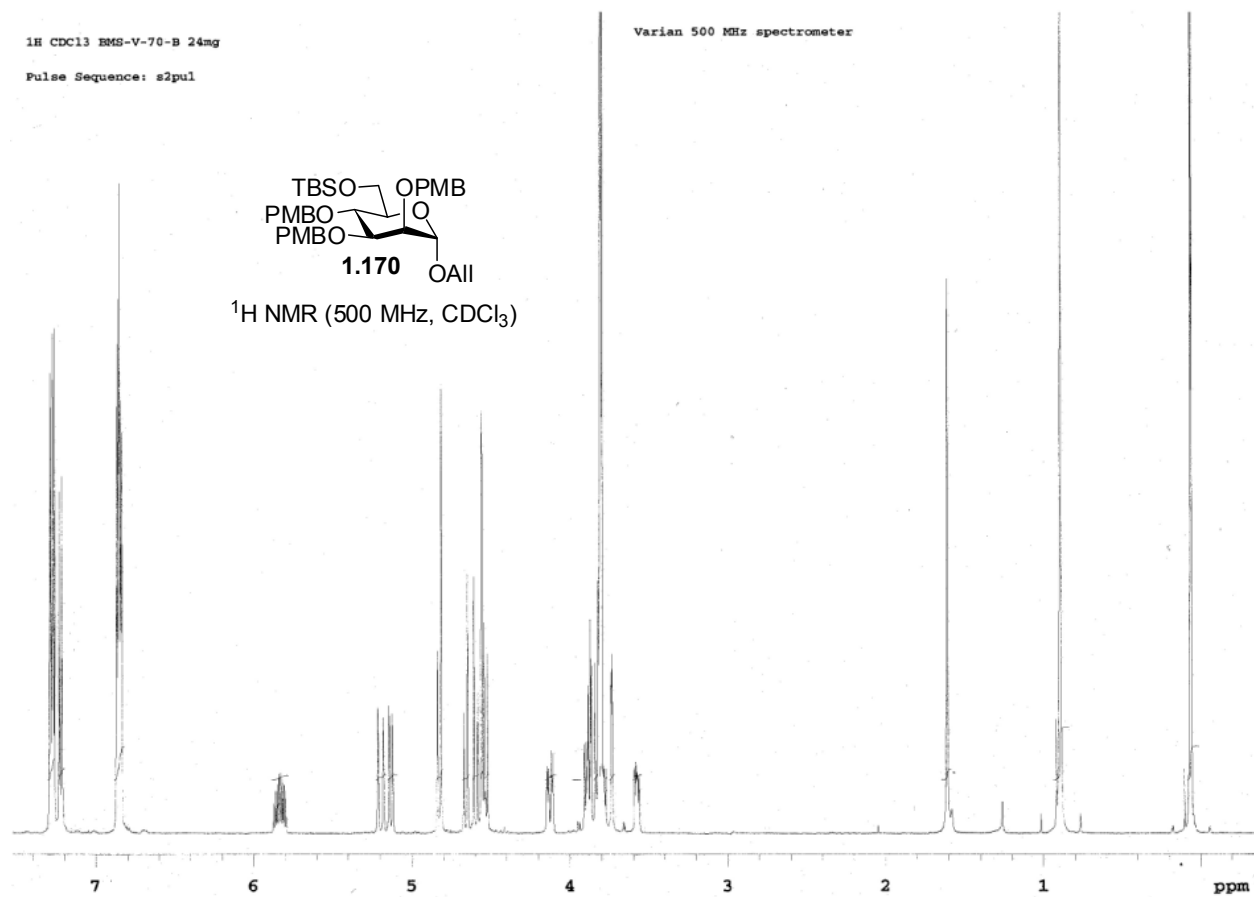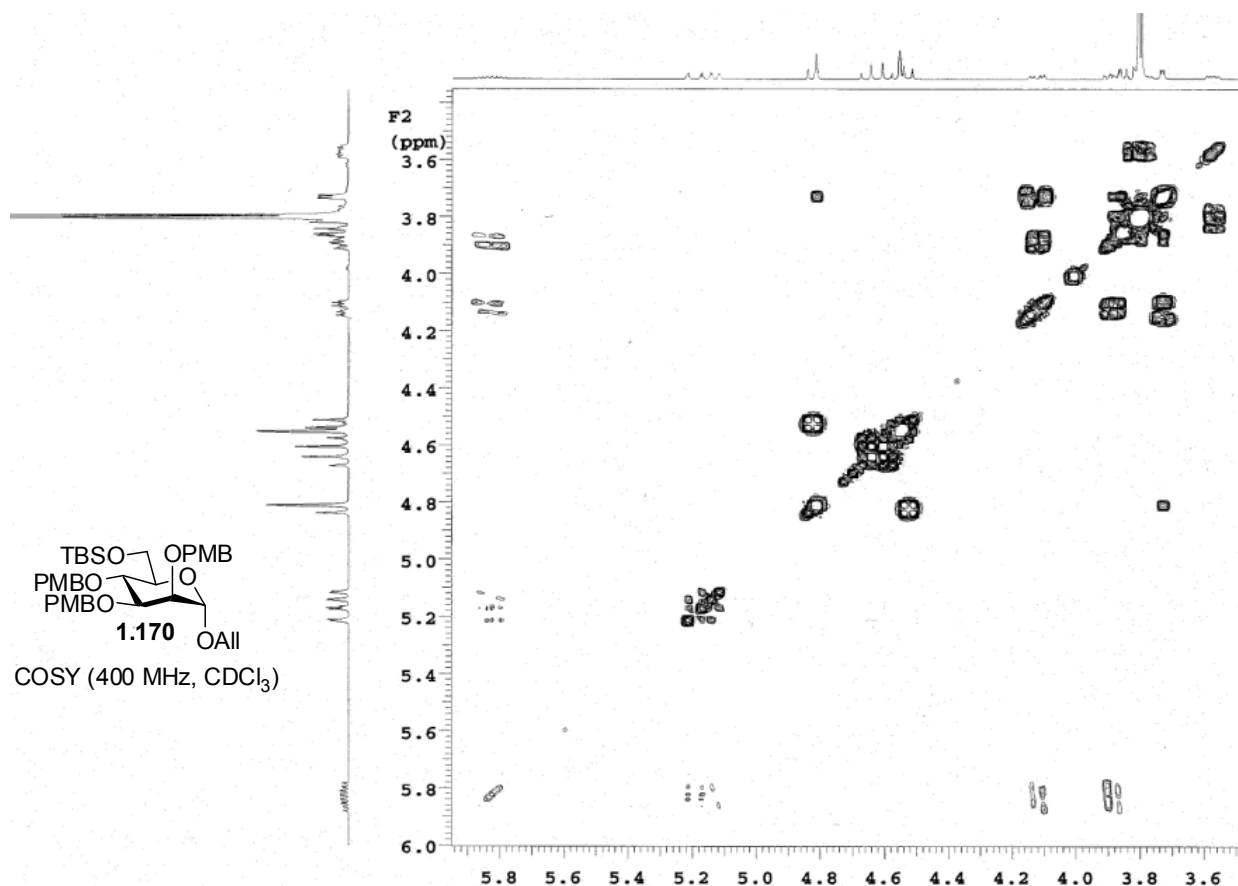
1H NMR (500 MHz, CDCl₃)

13C NMR (125 MHz, CDCl₃)

F2
(ppm)
3.6
3.8
4.0
4.2
4.4
4.6
4.8
5.0
5.2
5.4
5.6
5.8
6.0

5.8 5.6 5.4 5.2 5.0 4.8 4.6 4.4 4.2 4.0 3.8 3.6

1.170

TBSO—OPMB
PMBO
PMBO
OAll

COSY (400 MHz, CDCl₃)

Single Mass Analysis
Tolerance = 5.0 PPM / DBE: min = -1.5, max = 50.0
Element prediction: Off
Number of isotope peaks used for i-FIT = 3

Monoisotopic Mass, Even Electron Ions
785 formula(e) evaluated with 6 results within limits (up to 50 best isotopic matches for each mass)
Elements Used:
C: 0-500   H: 0-1000   O: 0-30   Na: 0-1   Si: 0-1

TBSO—OPMB
PMBO
PMBO
1.170 OAll
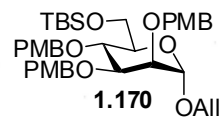
HR ESI MS

Guo; Ben Swarts BMS-V-70-B mw694 LCT0018 10pg/ul meoh 1cm stk inj3ul pluno
OA-FIA-1min DOP   LCT Premier

2008_0703_0018_12 16 (0.311) Cm (13:18-25:35)

14:03:00 03-Jul-2008
16129 pushes/sec
1: TOF MS ES+
1.40e+004

m Na⁺

717.3434
718.3461
719.3470
689.1605
243.9437 345.9112 396.9080 506.8853 574.8708 837.1989 911.2187 985.2373
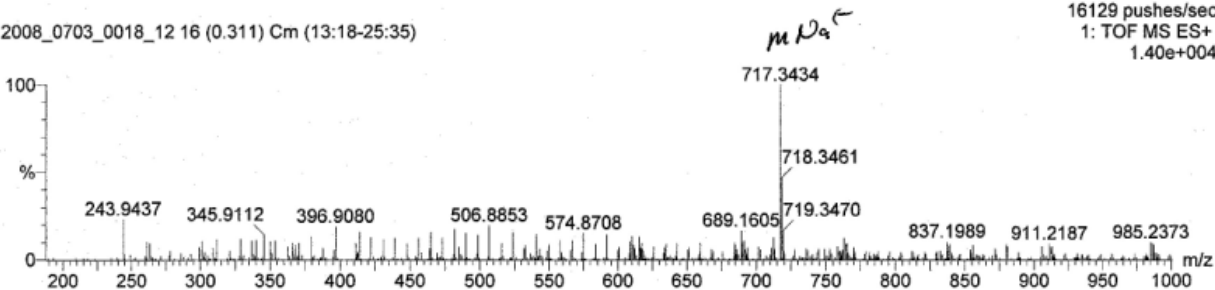
Minimum:			-1.5					
Maximum:	6.0	5.0	50.0					

Mass	Calc. Mass	mDa	PPM	DBE	i-FIT	Formula		
717.3434	717.3435	-0.1	-0.1	13.5	8.2	C39	H54 O9	Na Si
	717.3459	-2.5	-3.5	16.5	28.1	C41	H53 O9	Si
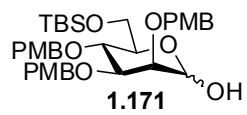
1.171
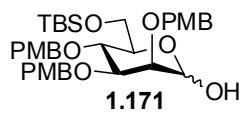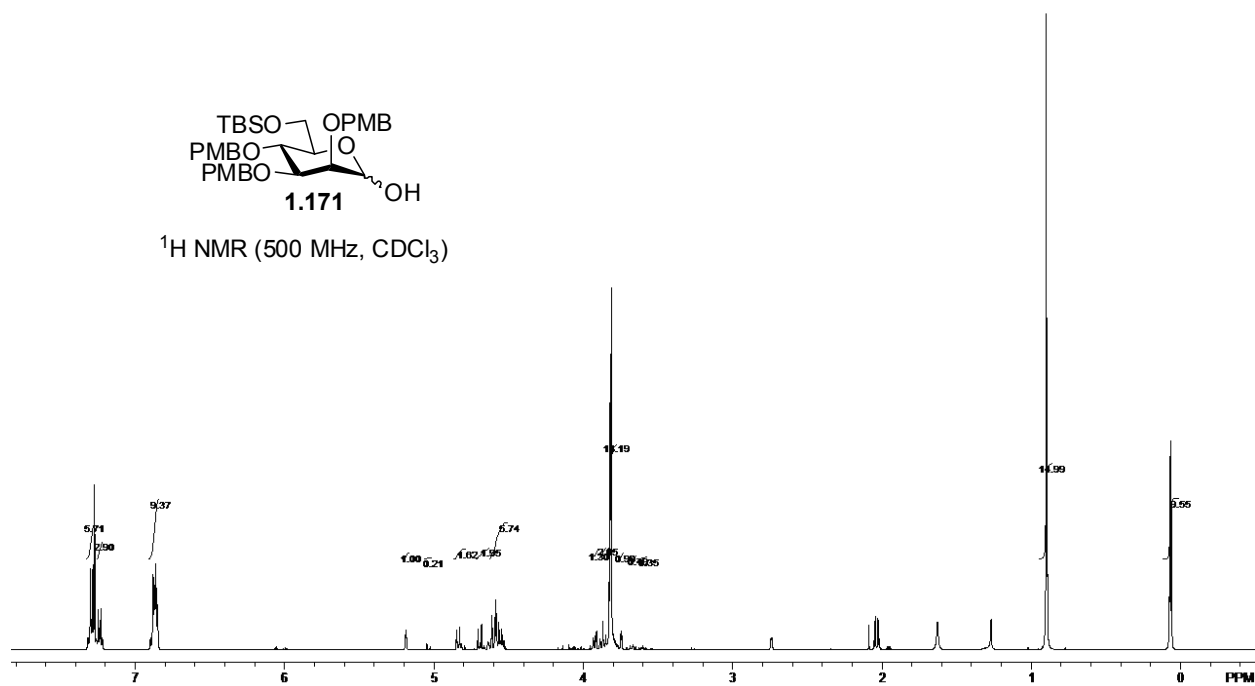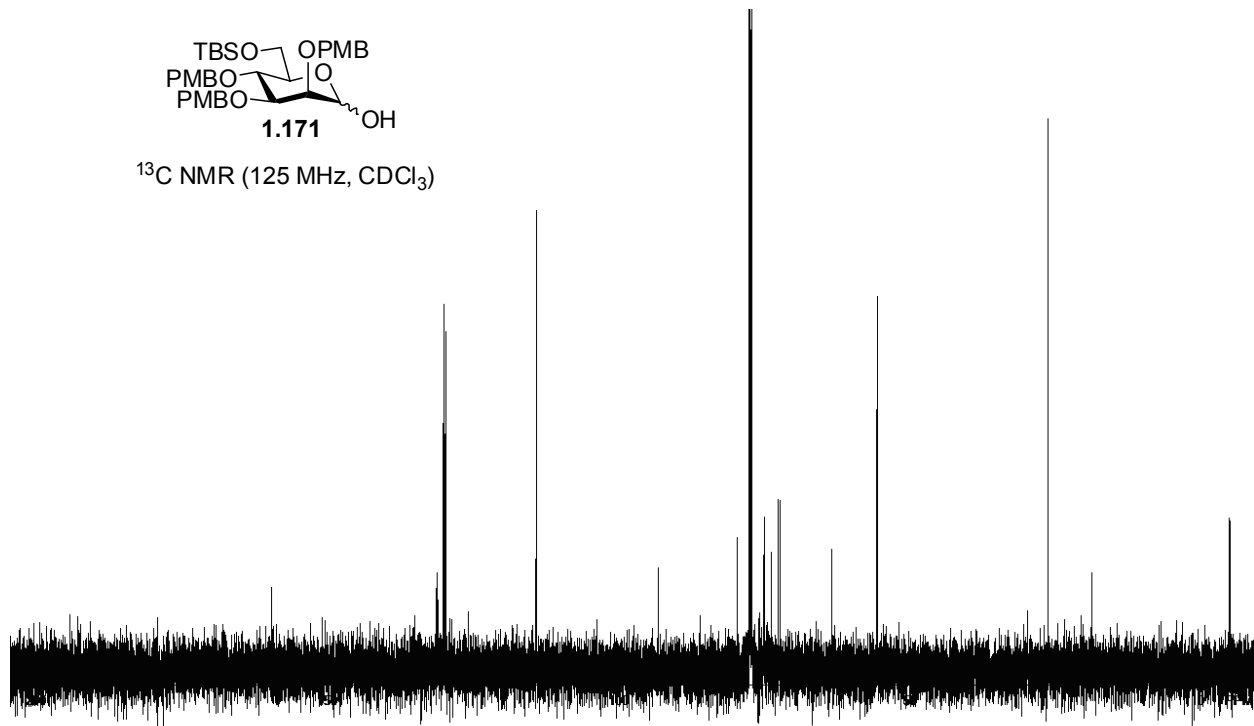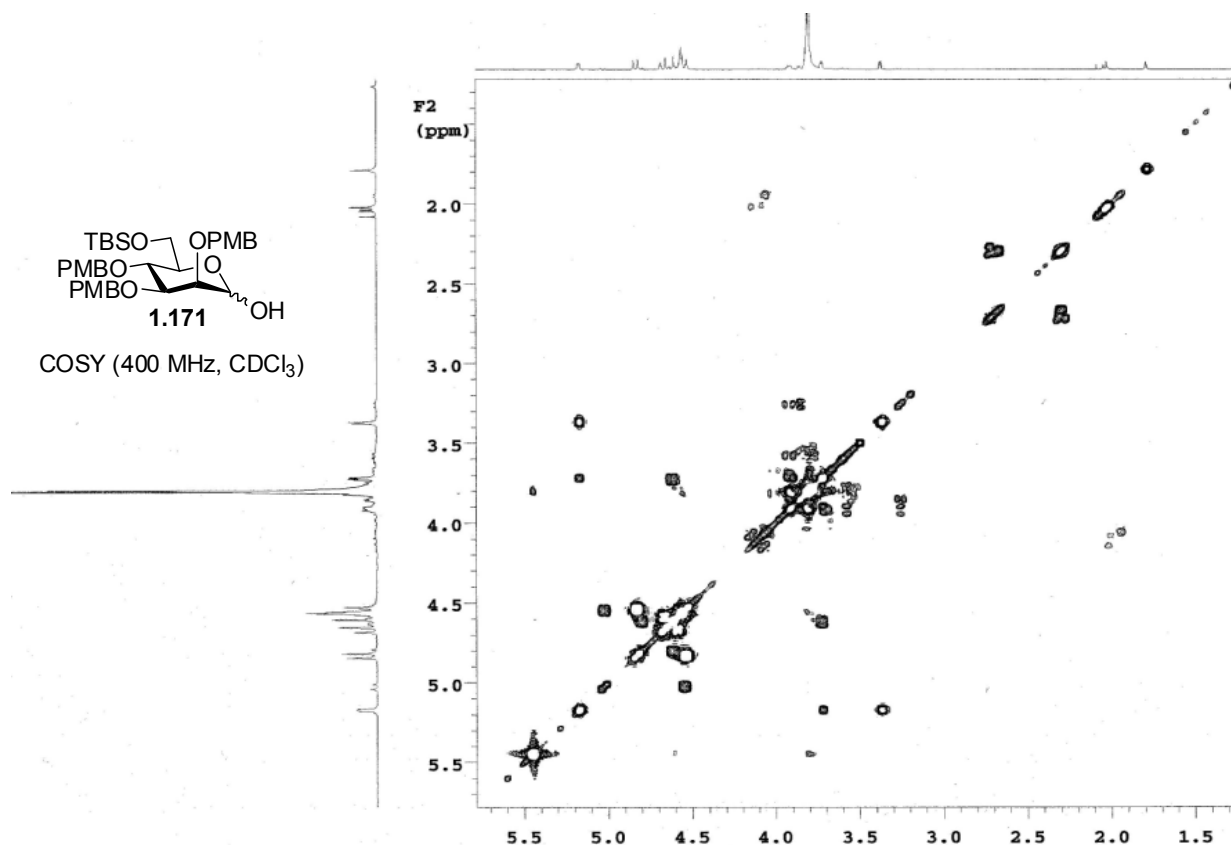
^{1}H NMR (500 MHz, CDCl$_3$)

1.171

^{13}C NMR (125 MHz, CDCl$_3$)

TBSO OPMB
PMBO
PMBO
1.171 OH

COSY (400 MHz, CDCl₃)

Single Mass Analysis

Tolerance = 5.0 PPM / DBE: min = -1.5, max = 50.0
Element prediction: Off
Number of isotope peaks used for i-FIT = 3

Monoisotopic Mass, Even Electron Ions
314 formula(e) evaluated with 4 results within limits (up to 50 best isotopic matches for each mass)
Elements Used:
C: 0-500 H: 0-1000 O: 0-9 23Na: 0-1 Si: 0-1

Guo- Ben Swarts BMS-V1-09mw654 LCT0093 in meoh 1uL 3x stk
Shay 2008-07b.pro
2008_0822_0093_01 14 (0.300) Cm (13:16-(3:7+35:42)x10.000)

TBSO OPMB
PMBO
PMBO
1.171 OH
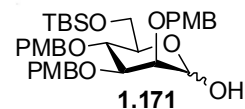
HR ESI MS

LCT Premier 22-Aug-2008 11:36:35
1: TOF MS ES+
6.04e+003
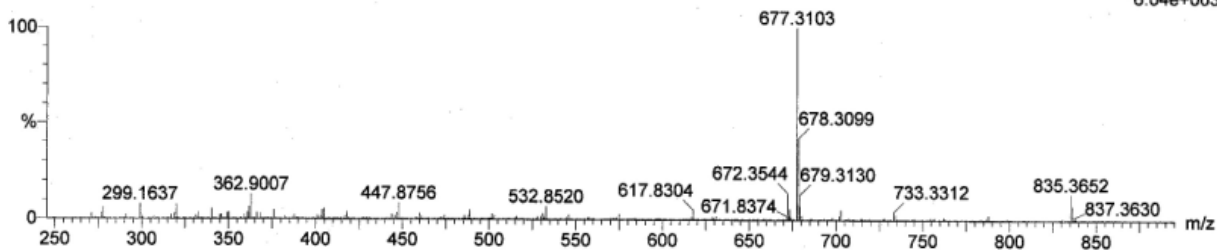
Minimum:				-1.5						
Maximum:		5.0	5.0	50.0						
Mass	Calc. Mass	mDa	PPM	DBE	i-FIT	i-FIT (Norm)	Formula			
677.3103	677.3090	1.3	1.9	17.5	31.9	0.4	C40	H46	O8	23Na
	677.3122	-1.9	-2.8	12.5	33.1	1.7	C36	H50	O9	23Na
							Si			
	677.3114	-1.1	-1.6	20.5	33.3	1.9	C42	H45	O8	
	677.3087	1.6	2.4	24.5	36.0	4.6	C45	H45	O4	Si
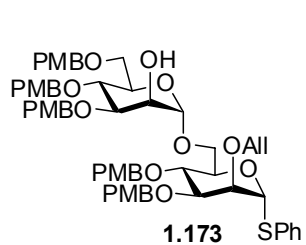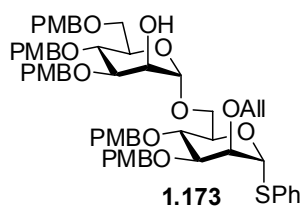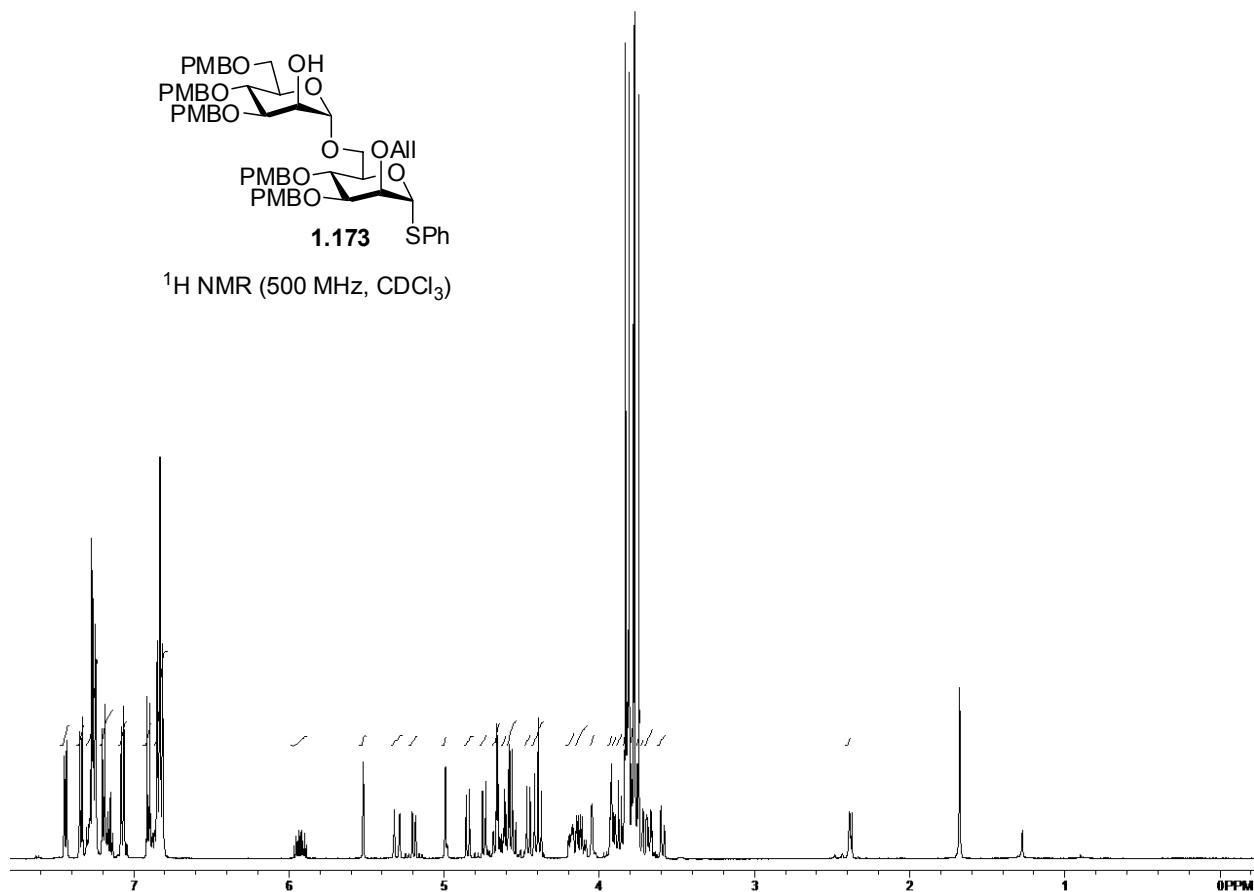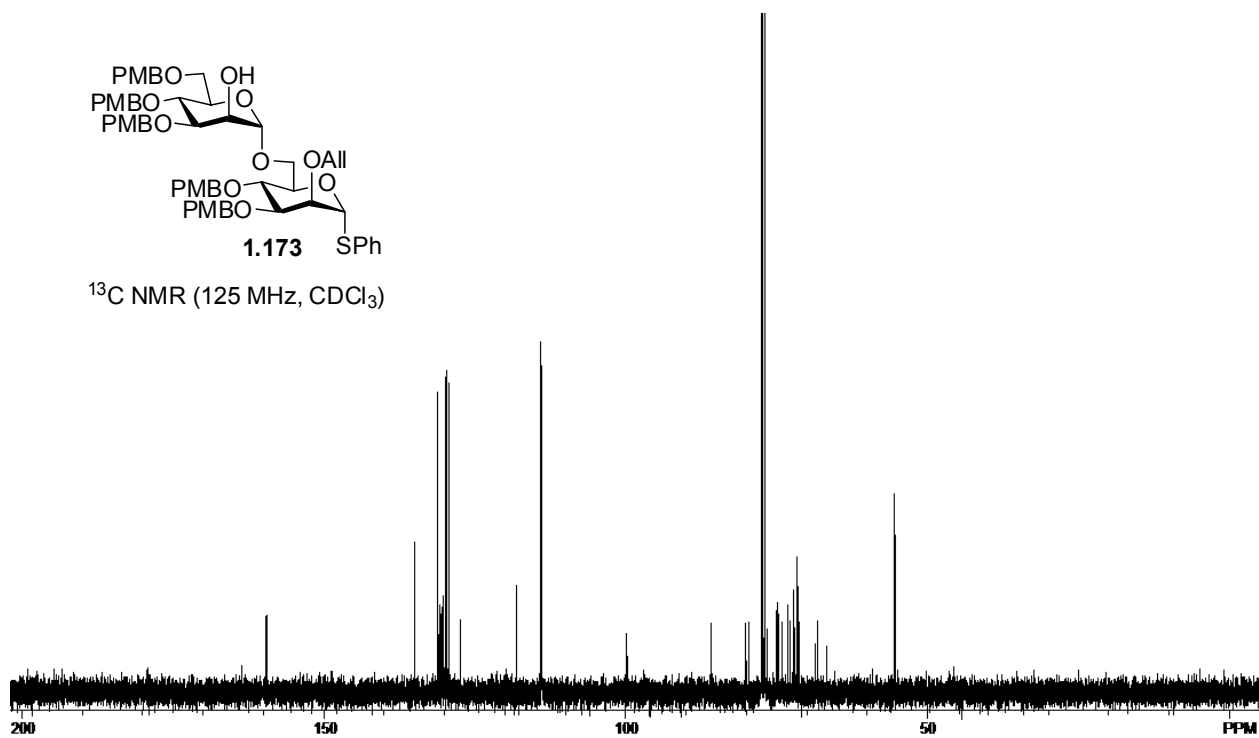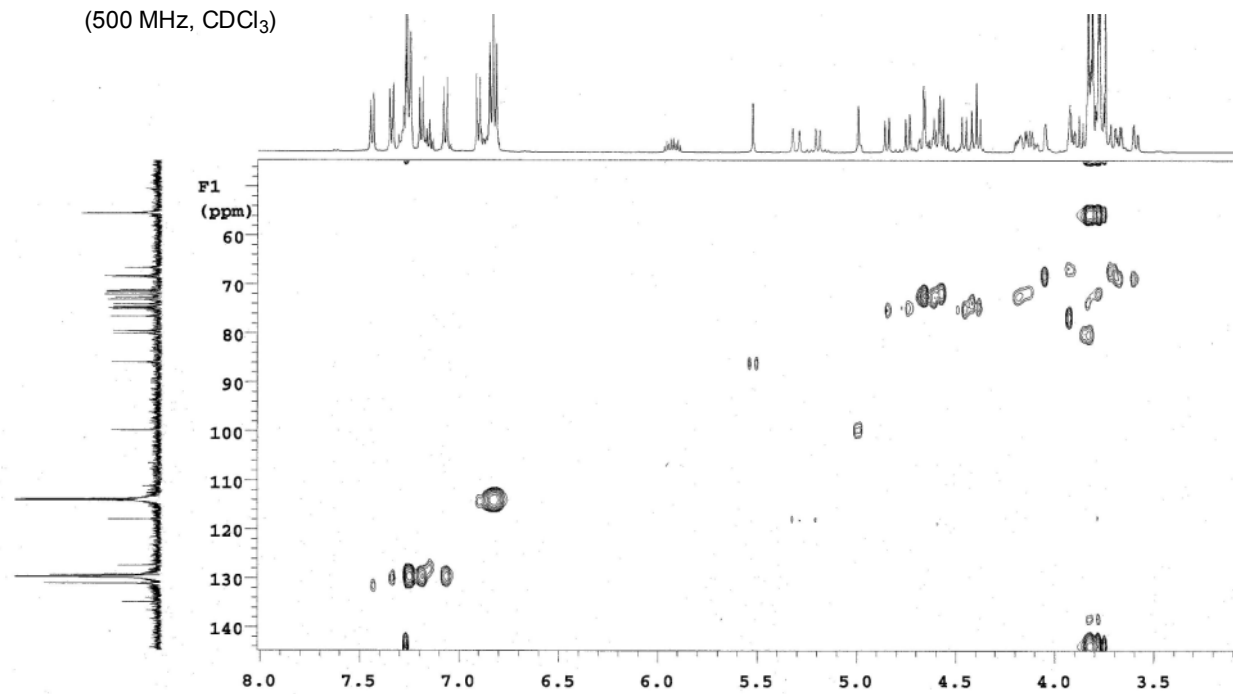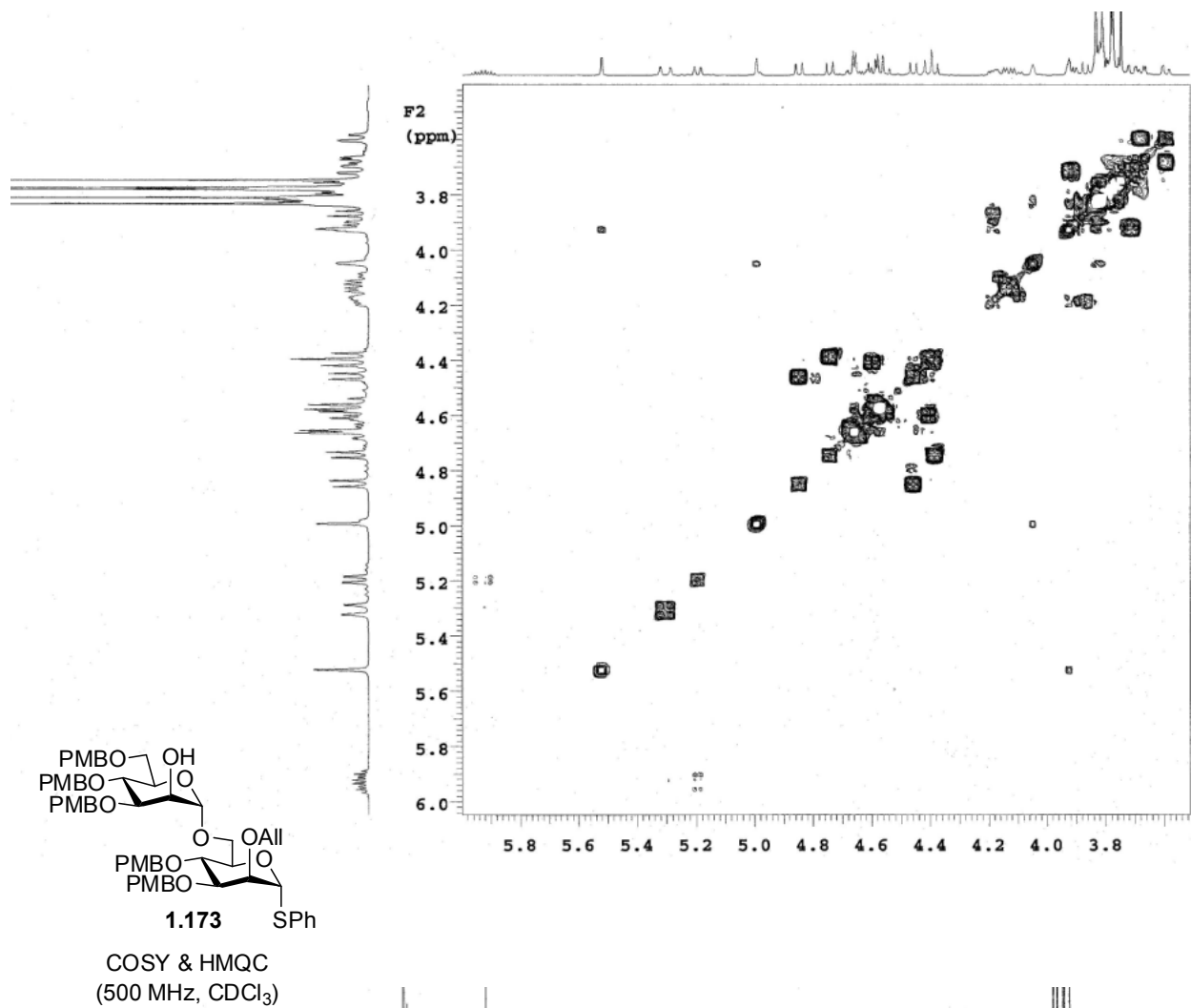
PMBO OH
PMBO O
PMBO
O OAll
PMBO O
PMBO
1.173 SPh

^{1}H NMR (500 MHz, CDCl$_3$)

PMBO OH
PMBO O
PMBO
O OAll
PMBO O
PMBO
1.173 SPh

^{13}C NMR (125 MHz, CDCl$_3$)

PMBO—OH
PMBO
PMBO
O
O—OAll
PMBO
PMBO
O
1.173   SPh

COSY & HMQC
(500 MHz, CDCl₃)

1.173

HR ESI MS

Single Mass Analysis
Tolerance = 5.0 PPM / DBE: min = -1.5, max = 50.0
Element prediction: Off
Number of isotope peaks used for i-FIT = 3

Monoisotopic Mass, Even Electron Ions
50 formula(e) evaluated with 6 results within limits (up to 50 best isotopic matches for each mass)
Elements Used:
C: 50-70 H: 60-80 O: 14-18 23Na: 0-1 S: 0-2
BEN SWARTS   BMS-VII-80
2008-07b.pro
2009_0330_0366 14 (0.283) Cm (11:17-(1:6+29:34)x2.000)
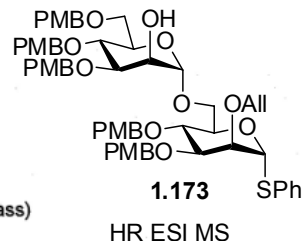
LCT Premier 30-Mar-2009 11:36:51
1: TOF MS ES+
1.33e+003
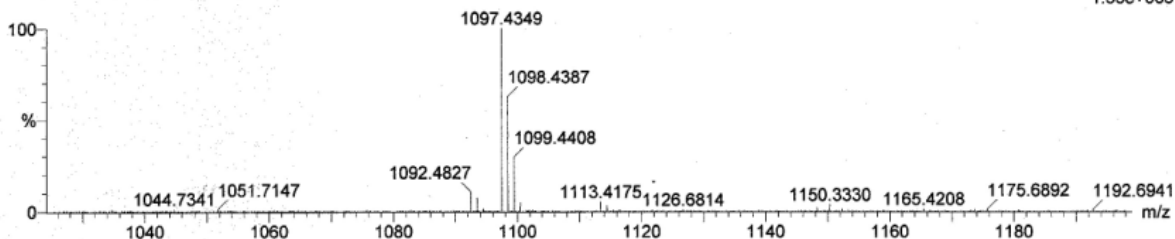
| Minimum: | | | | -1.5 | | | |
| Maximum: | | 5.0 | 5.0 | 50.0 | | | |

Mass	Calc. Mass	mDa	PPM	DBE	i-FIT	i-FIT (Norm)	Formula
1097.4349	1097.4333	1.6	1.5	26.5	49.5	1.0	C61 H70 O15 23Na S
	1097.4367	-1.8	-1.6	21.5	49.8	1.2	C58 H74 O15 23Na S2
	1097.4357	-0.8	-0.7	29.5	50.0	1.5	C63 H69 O15 S
	1097.4323	2.6	2.4	34.5	51.4	2.9	C66 H65 O15
	1097.4391	-4.2	-3.8	24.5	52.0	3.5	C60 H73 O15 S2
	1097.4299	5.0	4.6	31.5	52.7	4.1	C64 H66 O15 23Na
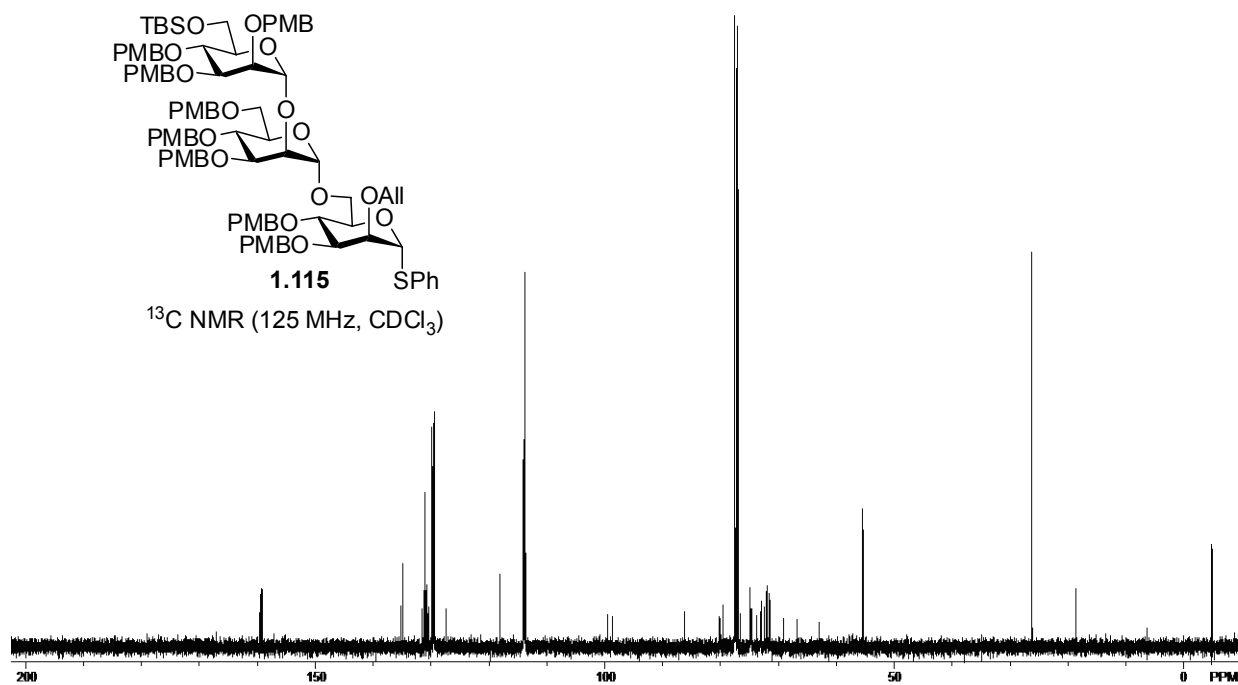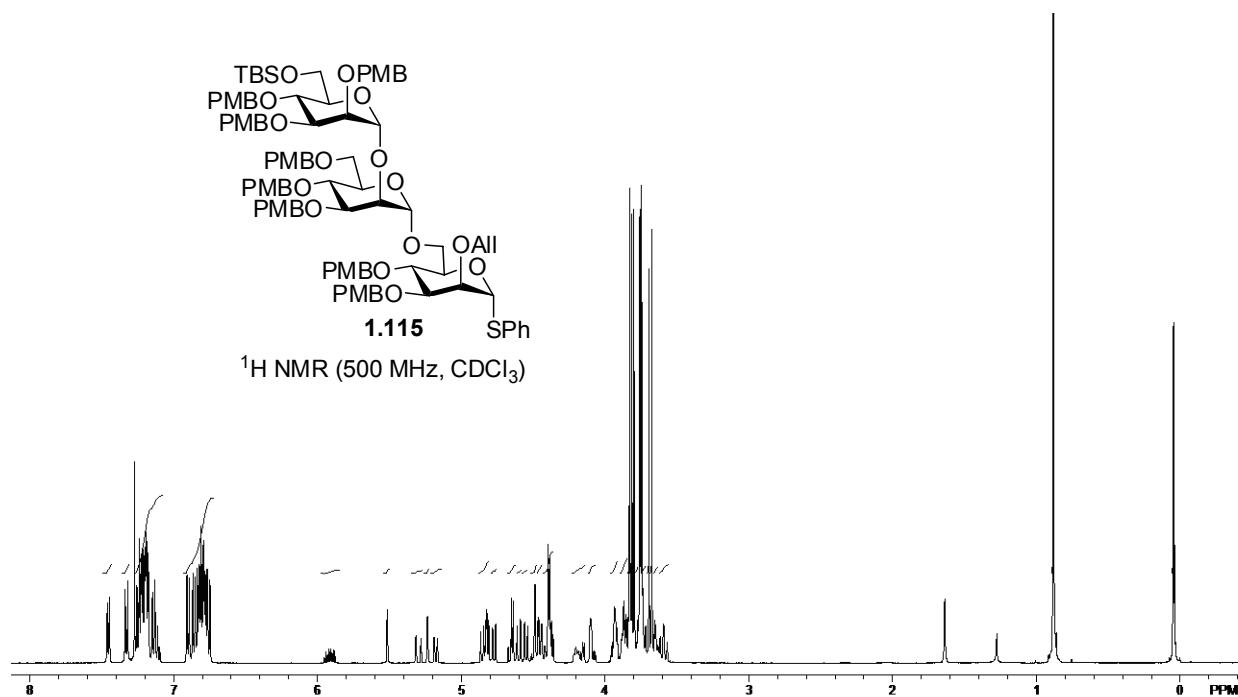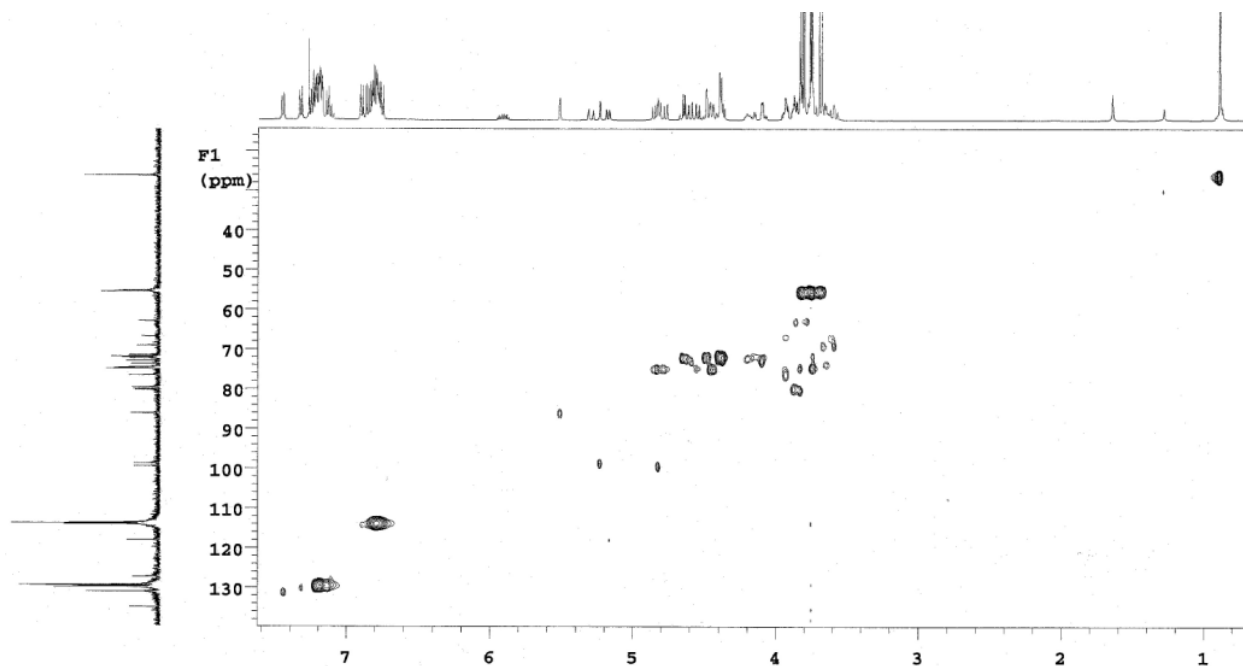
TBSO OPMB
PMBO
PMBO
O
PMBO
PMBO
O
PMBO
O OAll
PMBO
PMBO
O
1.115 SPh

^{1}H NMR (500 MHz, CDCl$_3$)

TBSO OPMB
PMBO
PMBO
O
PMBO
O
PMBO
PMBO
O
O OAll
PMBO
PMBO
O
1.115 SPh

^{13}C NMR (125 MHz, CDCl$_3$)

1.115

Coupled ^{13}C NMR
anomeric region
(125 MHz, CDCl$_3$)

100.174
99.404
98.804
98.038
86.827
85.494

1.115

COSY (500 MHz, CDCl$_3$)

F1
(ppm)

Single Mass Analysis
Tolerance = 5.0 PPM / DBE: min = -1.5, max = 50.0
Element prediction: Off
Number of isotope peaks used for i-FIT = 3

Monoisotopic Mass, Even Electron Ions
96 formula(e) evaluated with 11 results within limits (up to 50 best isotopic matches for each mass)
Elements Used:
C: 90-110   H: 110-125   O: 20-25   23Na: 0-1   S: 0-2   Si: 0-1

BEN SWARTS   BMS-VII-801
2008-07b.pro
2009_0330_0367 14 (0.284) Cm (10:20-(1:8+29:39)x2.000)

1.115
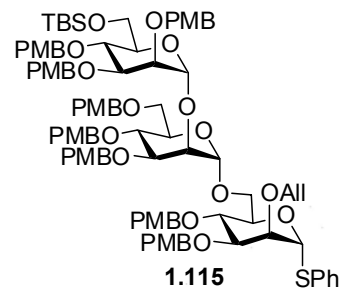
HMQC (500 MHz, CDCl₃)
& HR ESI MS

LCT Premier 30-Mar-2009 11:49:4
1: TOF MS ES+
8.22e+00
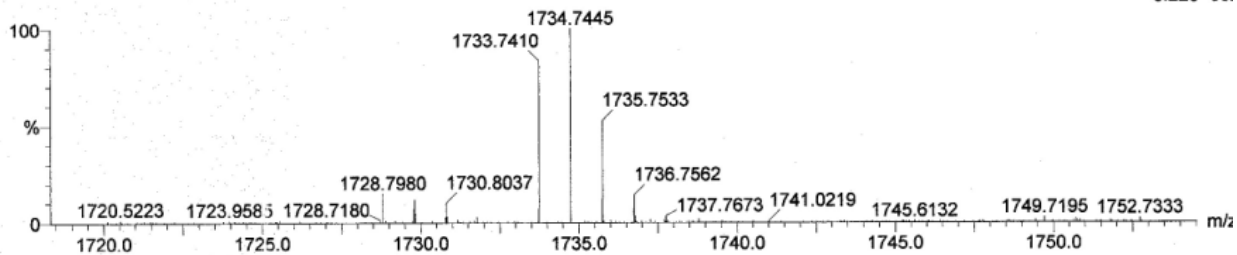
Minimum:				-1.5						
Maximum:		5.0	5.0	50.0						
Mass	Calc. Mass	mDa	PPM	DBE	i-FIT	i-FIT (Norm)	Formula			
1733.7410	1733.7485	-7.5	-4.3	34.5	62.0	4.5	C94	H122	O23	23Na
							S2	Si		
	1733.7325	8.5	4.9	38.5	62.5	5.0	C96	H117	O25	S2
	1733.7452	-4.2	-2.4	39.5	60.5	2.9	C97	H118	O23	23Na
							S	Si		
	1733.7454	-4.4	-2.5	39.5	60.3	2.8	C98	H118	O22	23Na
							S2			
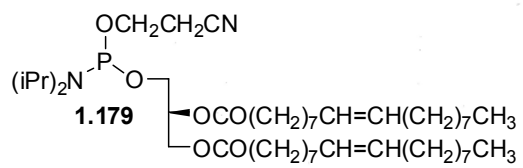
OCH$_2$CH$_2$CN

(iPr)$_2$N—P—O

1.179

OCO(CH$_2$)$_7$CH=CH(CH$_2$)$_7$CH$_3$
OCO(CH$_2$)$_7$CH=CH(CH$_2$)$_7$CH$_3$

^{1}H NMR (400 MHz, CDCl$_3$)

1.182

R = -(CH₂)₇CH=CH(CH₂)₇CH₃
¹H NMR (500 MHz, CDCl₃)

1.182

R = -(CH₂)₇CH=CH(CH₂)₇CH₃
¹³C NMR (125 MHz, CDCl₃)

HO
PMBO
OPMB
N₃
PMBO OPMB
OPMB
OPMB
OPMB
NCH₂CH₂CO-P=O
O
OCOR
OCOR

1.182

R = -(CH₂)₇CH=CH(CH₂)₇CH₃
COSY & HMQC (500 MHz, CDCl₃)
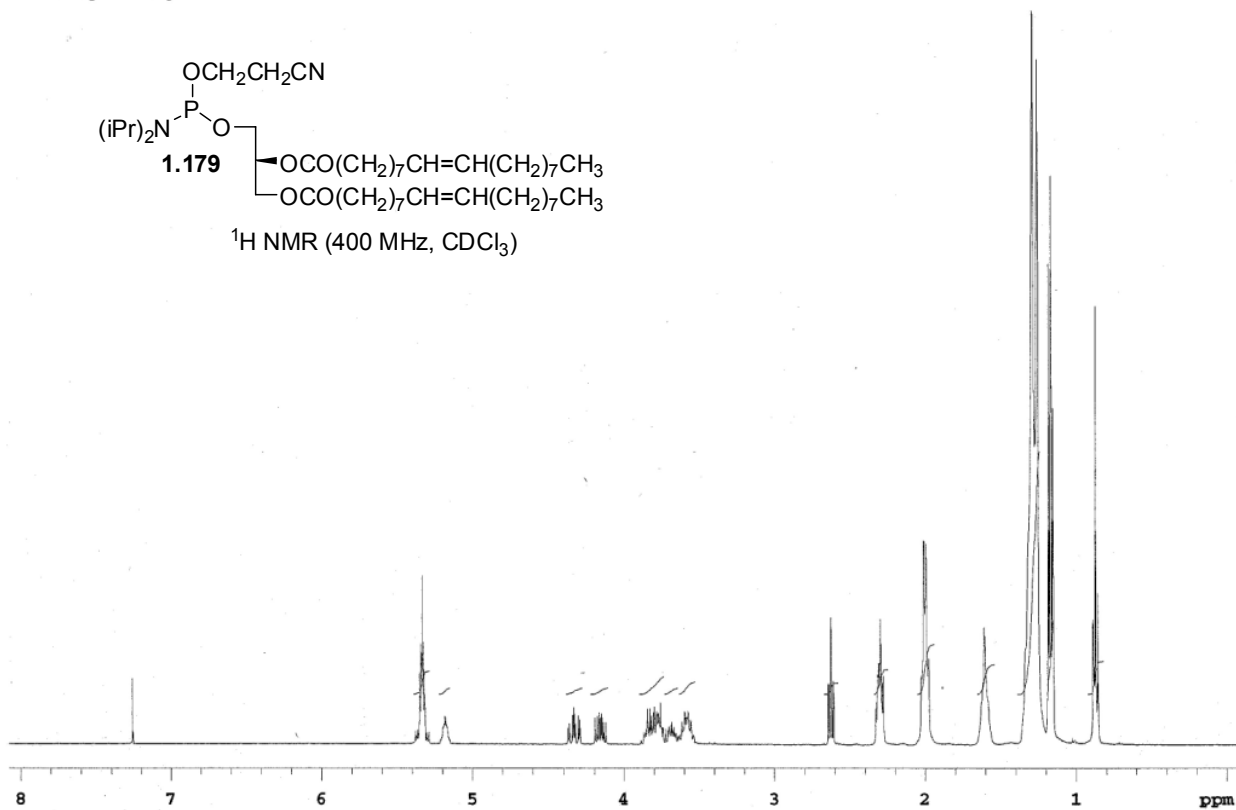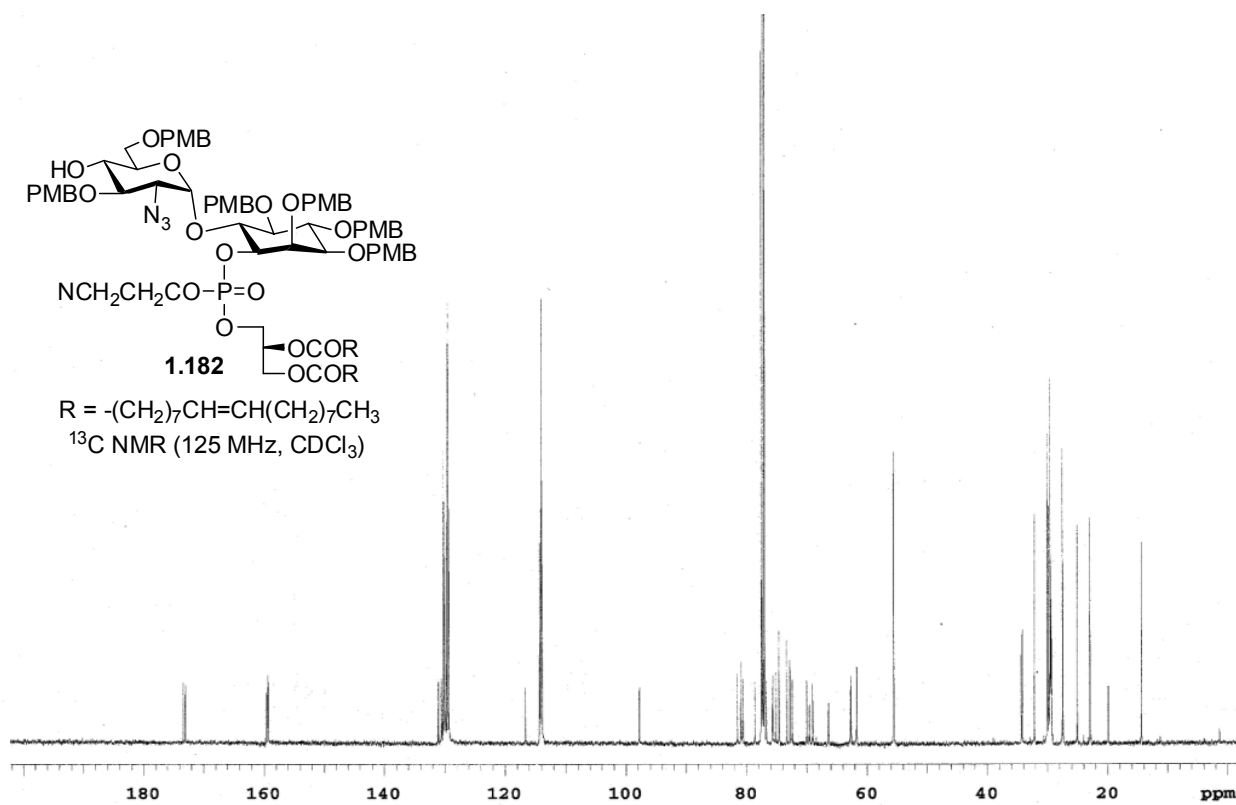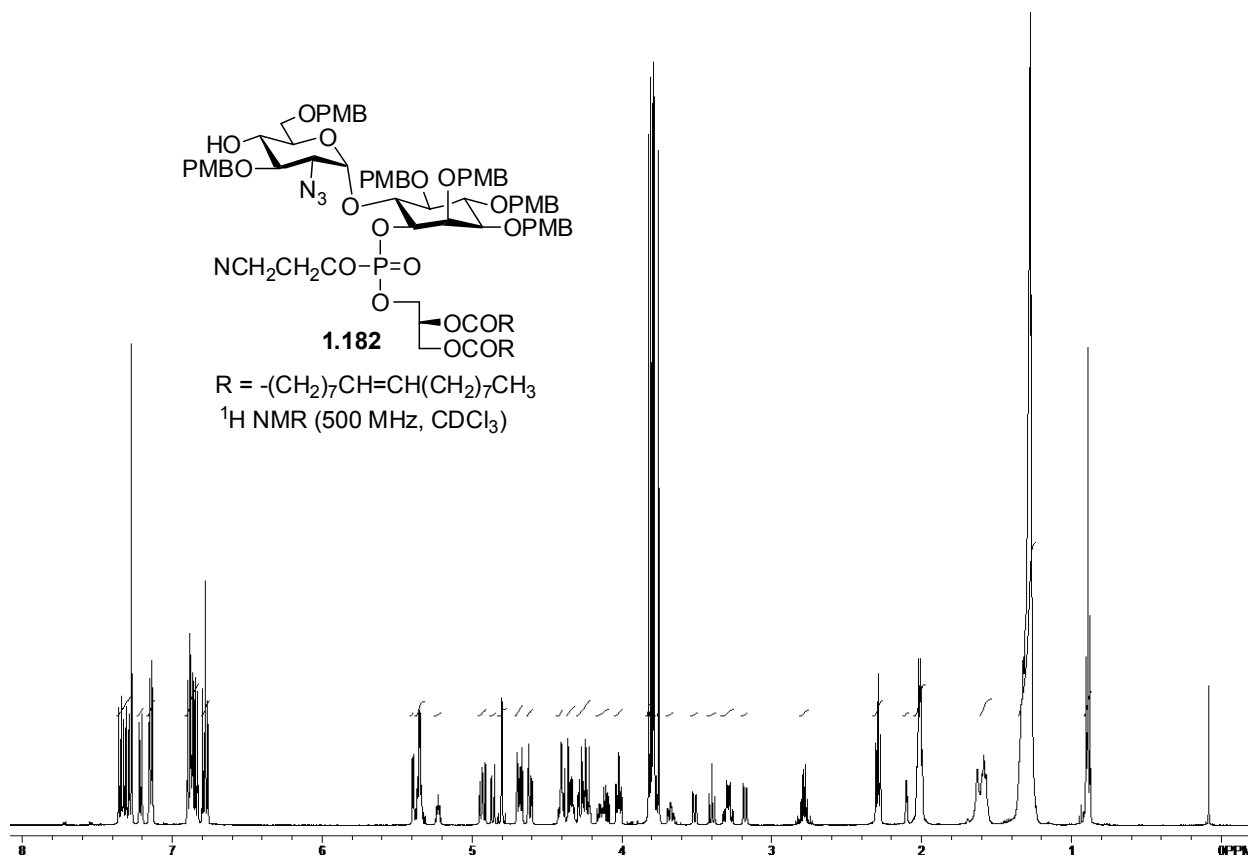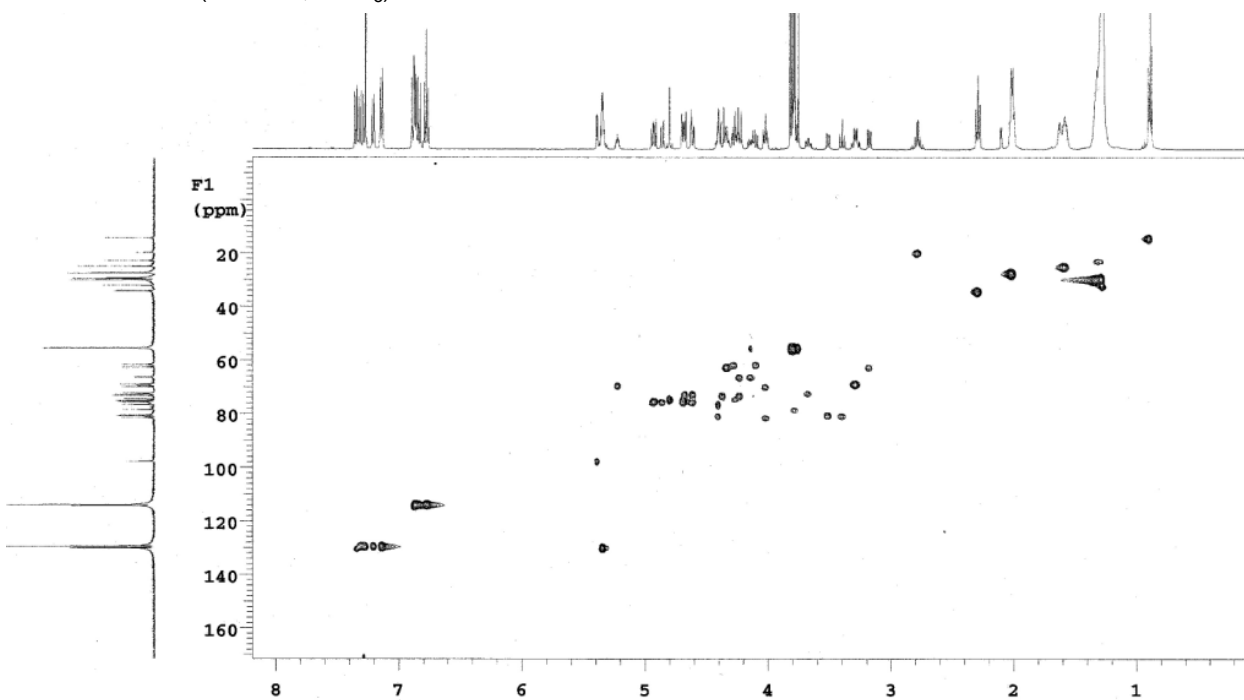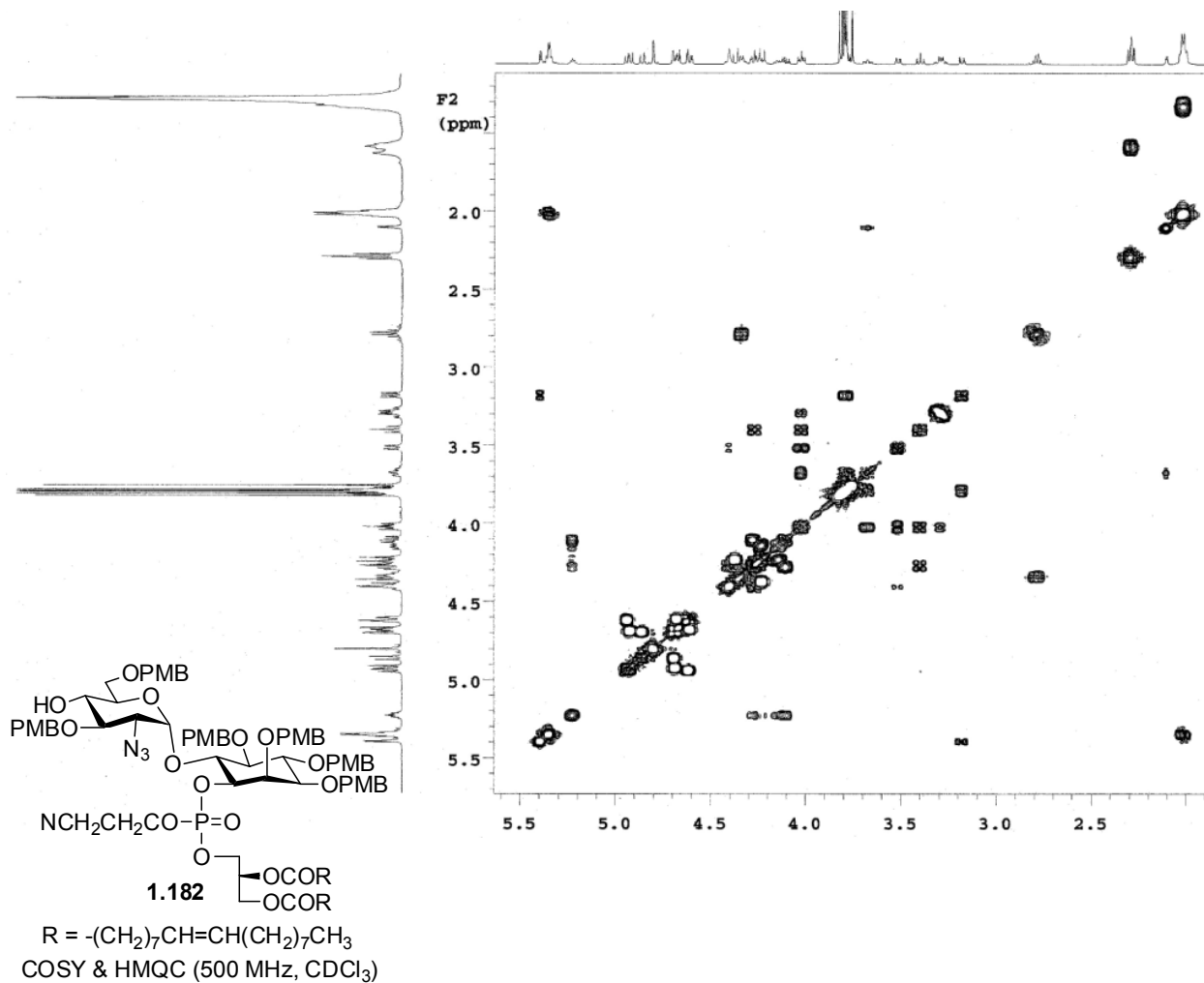
Single Mass Analysis
Tolerance = 5.0 PPM   /   DBE: min = -1.5, max = 50.0
Element prediction: Off
Number of isotope peaks used for i-FIT = 3

Monoisotopic Mass, Even Electron Ions
5877 formula(e) evaluated with 31 results within limits (all results (up to 1000) for each mass)
Elements Used:
C: 0-125   H: 0-175   N: 0-6   O: 0-25   Na: 0-1   P: 0-1

BEN SWARTS   BSM-VII-158
2008-07b.pro   LCT Premier 05-Oct-2009 13:35:29
2009_1005_0628 15 (0.301) Cm (13:18)   1: TOF MS ES+
                                                                                    4.12e+003
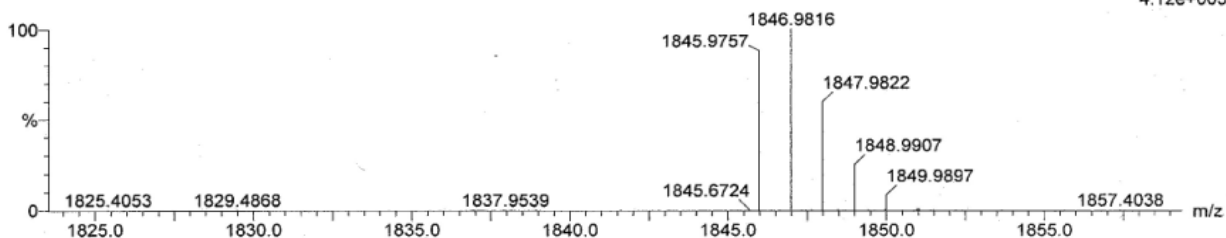
Minimum:				-1.5			
Maximum:		5.0	5.0	50.0			

Mass	Calc. Mass	mDa	PPM	DBE	i-FIT	i-FIT (Norm)	Formula
1845.9757	1845.9760	-0.3	-0.2	46.5	49.7	7.2	C114 H139 N2 O16 Na P
	1845.9754	0.3	0.2	49.5	50.4	7.9	C117 H137 O19
	1845.9762	-0.5	-0.3	38.5	46.8	4.3	C104 H138 N6 O22 Na
	1845.9762	-0.5	-0.3	32.5	43.6	1.1	C99 H142 N6 O25 P
	1845.9744	1.3	0.7	45.5	49.4	6.9	C111 H138 N4 O18 P
	1845.9738	1.9	1.0	29.5	43.1	0.6	C97 H143 N6 O25 Na P
	1845.9778	-2.1	-1.1	33.5	45.2	2.7	C102 H143 N4 O23 Na P

HPLC chromatogram for separation of diastereomers of **1.182**

Conditions: Waters Nova-Pak Silica 6 μm, 300 x 19 mm
eluent 30% acetone in hexanes, 10 ml/min

1.182

R = -(CH$_2$)$_7$CH=CH(CH$_2$)$_7$CH$_3$

HR ESI MS (above)
and HPLC

TBSO OPMB
PMBO
PMBO
O

PMBO
PMBO
PMBO
O

PMBO
PMBO
OH
O

SPh

1.183

^{1}H NMR (500 MHz, CDCl$_3$)

TBSO OPMB
PMBO
PMBO
O

PMBO
PMBO
PMBO
O

PMBO
PMBO
OH
O

SPh

1.183

^{13}C NMR (125 MHz, CDCl$_3$)

F2
(ppm)

3.6
3.8
4.0
4.2
4.4
4.6
4.8
5.0
5.2
5.4
5.6
5.8

5.6 5.4 5.2 5.0 4.8 4.6 4.4 4.2 4.0 3.8 3.6

1.183

COSY & HMQC
(500 MHz, CDCl₃)

19	6963.202	55.435	15.5
20	6958.549	55.398	17.7
21	6948.780	55.320	13.1
22	3295.044	26.232	31.4

F1
(ppm)

40
50
60
70
80
90
100
110
120
130

7 6 5 4 3 2 1

Single Mass Analysis
Tolerance = 5.0 PPM / DBE: min = -1.5, max = 50.0
Element prediction: Off
Number of isotope peaks used for i-FIT = 3

Monoisotopic Mass, Even Electron Ions
717 formula(e) evaluated with 24 results within limits (up to 50 closest results for each mass)
Elements Used:
C: 85-110   H: 100-160   O: 18-25   23Na: 0-1   Si: 0-2   S: 0-2
BEN SWARTS   BSM-VII-157
2008-07b.pro
2009_0625_0472a 14 (0.284) Cm (12:20-(1:8+30:36)x100.000)

1.183 SPh
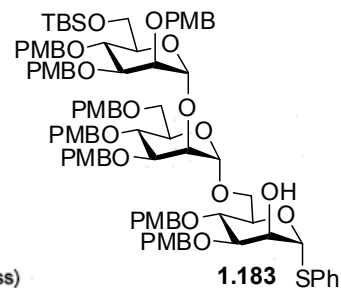
HR ESI MS

LCT Premier 26-Jun-2009 15:26:40
1: TOF MS ES+
2.50e+003
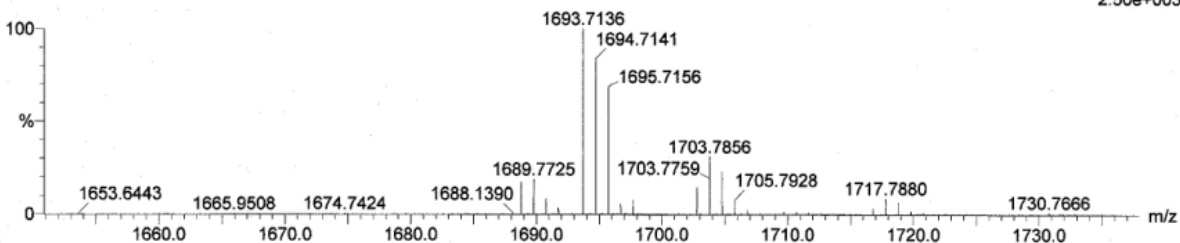
Minimum:				-1.5			
Maximum:		5.0	5.0	50.0			
Mass	Calc. Mass	mDa	PPM	DBE	i-FIT	i-FIT (Norm)	Formula
1693.7136	1693.7136	0.0	0.0	38.5	68.1	2.7	C93 H114 O24 23Na Si2
	1693.7135	0.1	0.1	45.5	68.6	3.2	C99 H113 O19 Si2 S
	1693.7138	-0.2	-0.1	45.5	68.4	3.0	C100 H113 O18 Si S2
	1693.7139	-0.3	-0.2	38.5	67.9	2.5	C94 H114 O23 23Na Si S
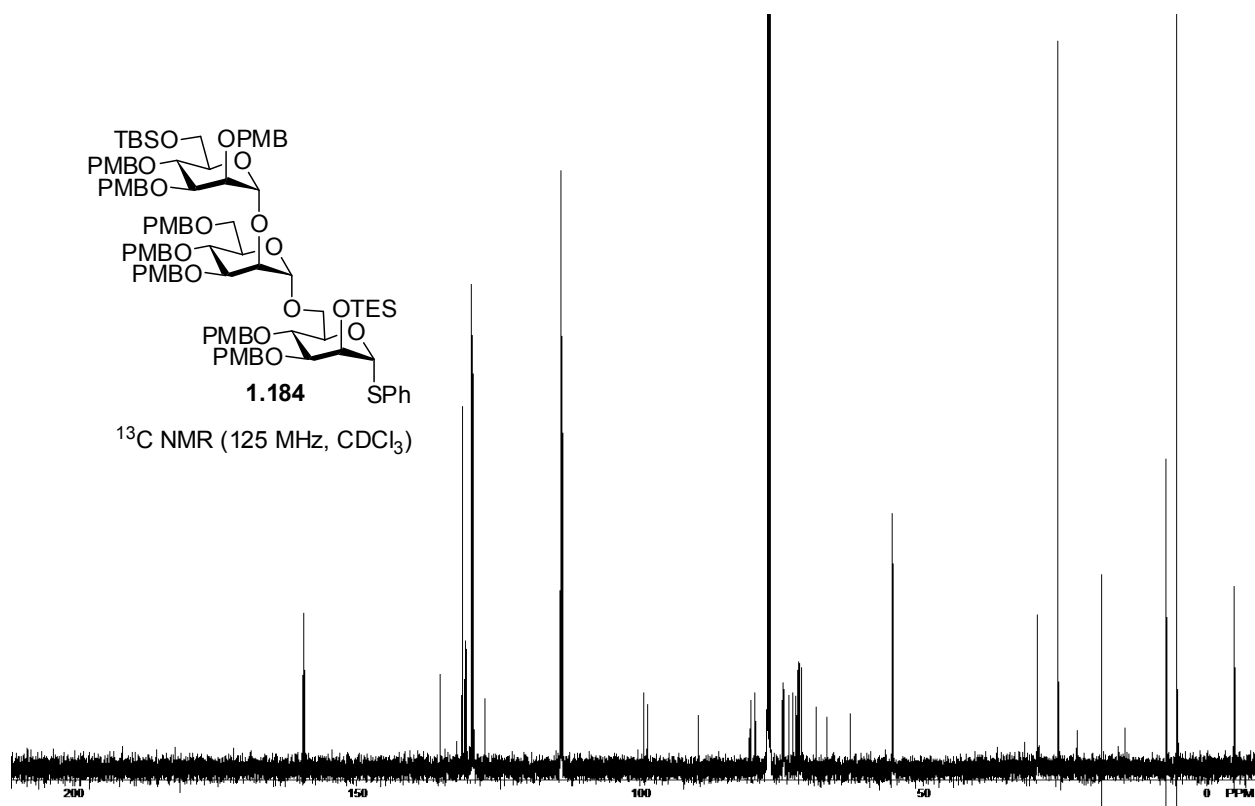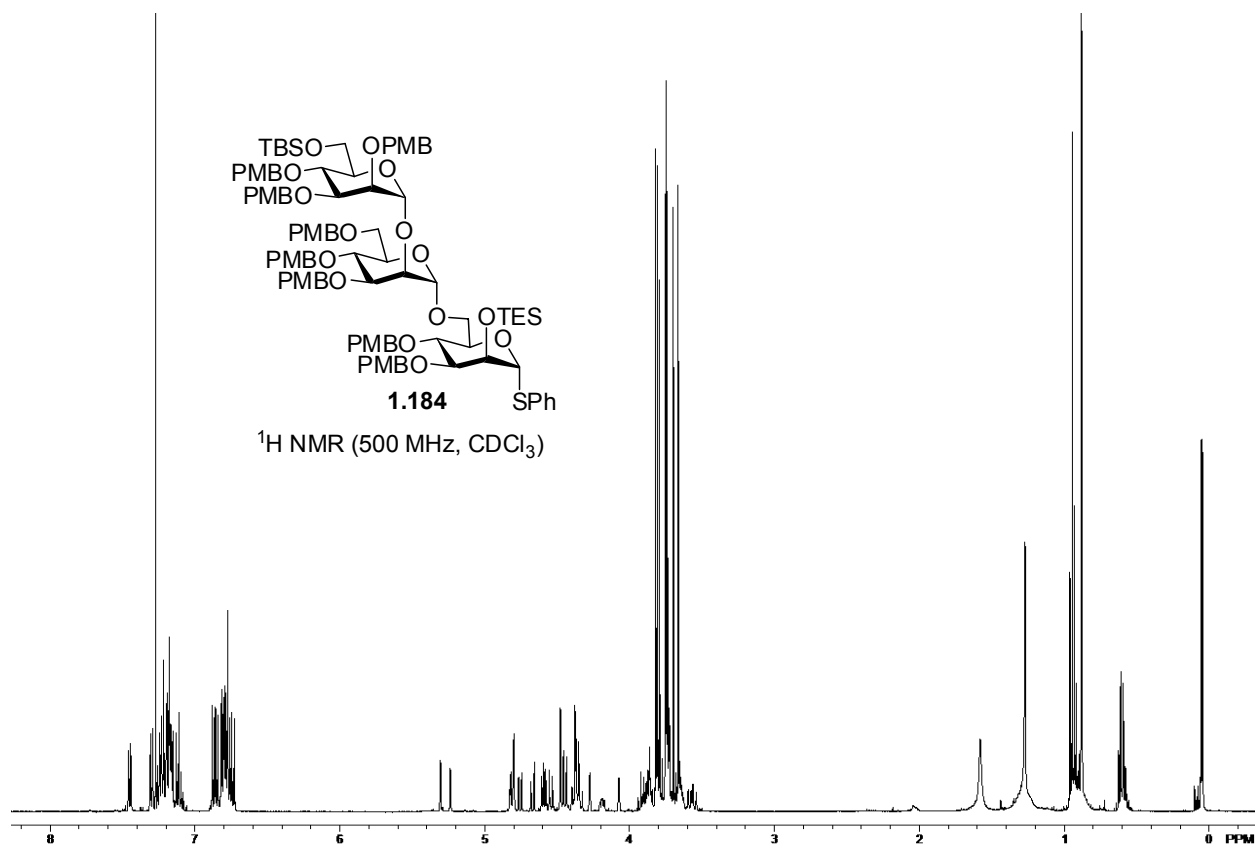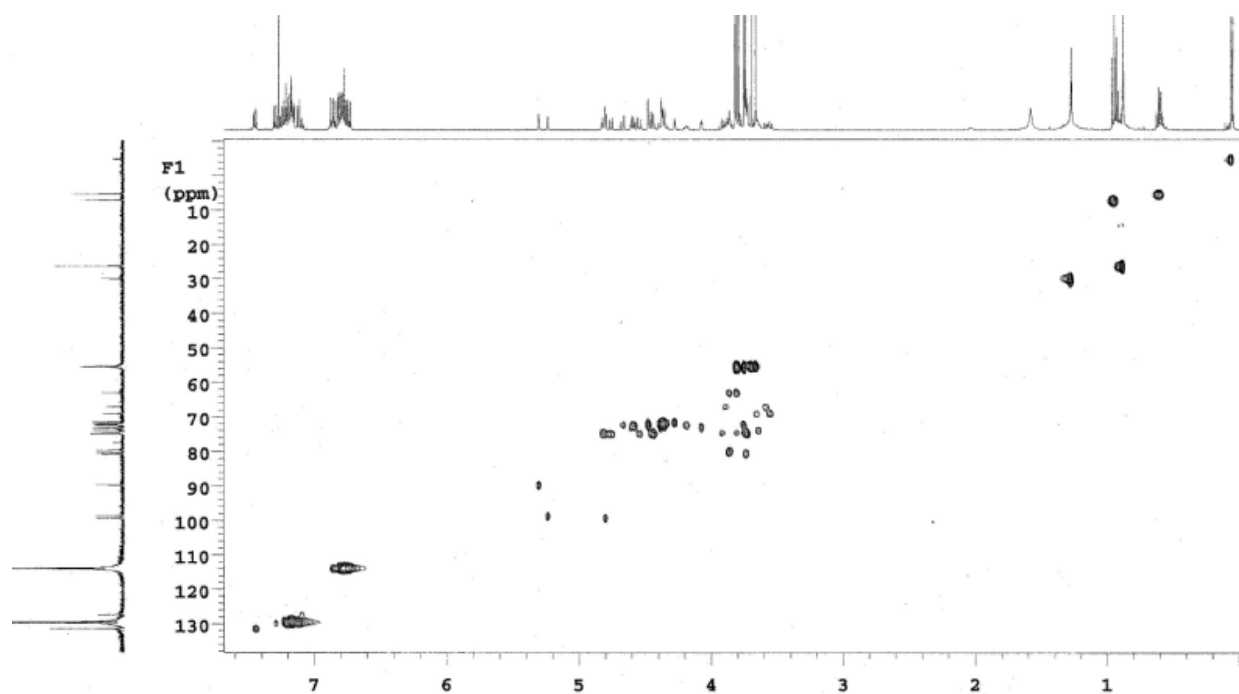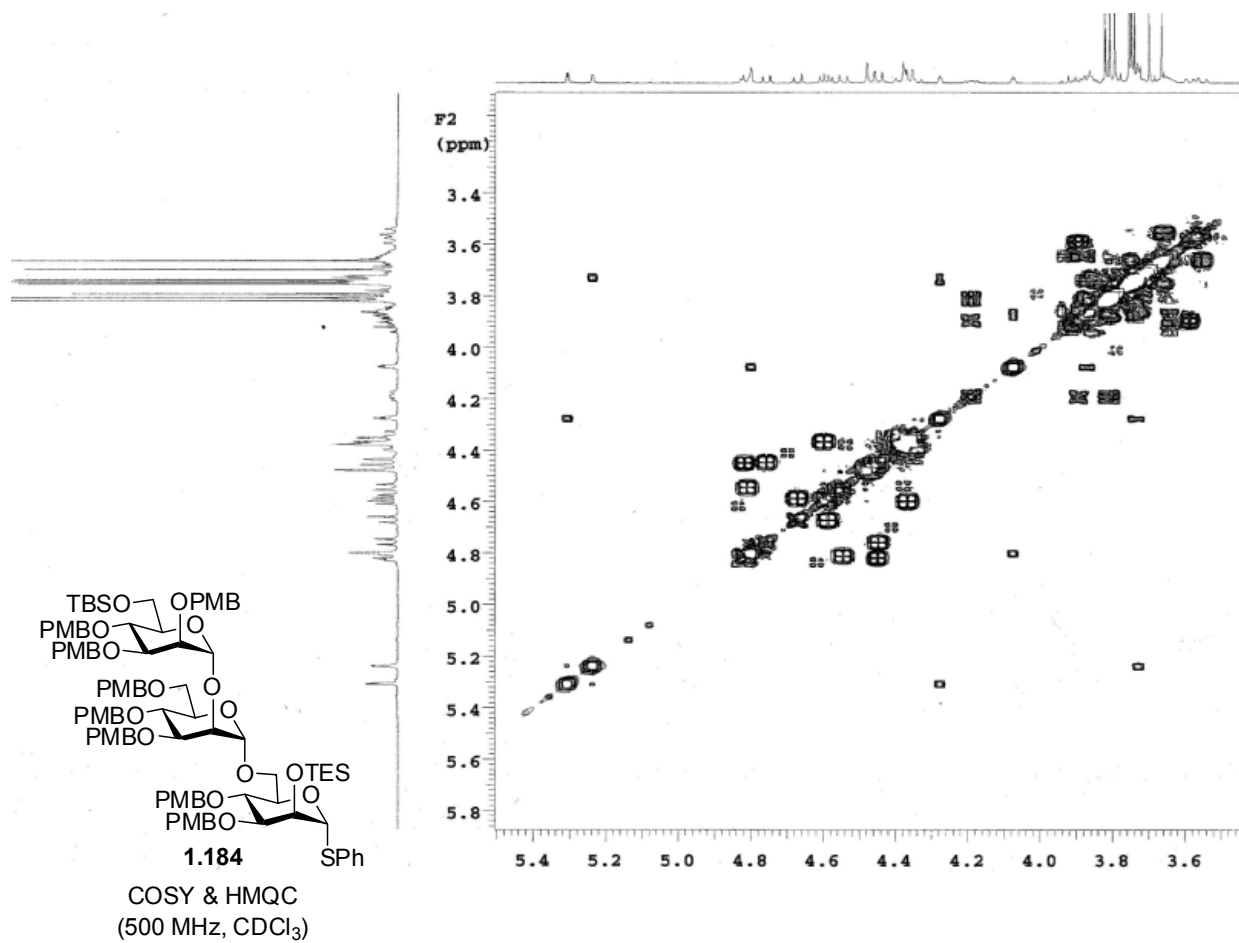
TBSO OPMB
PMBO
PMBO
O

PMBO
PMBO
PMBO
O

O OTES
PMBO
PMBO
O
1.184 SPh

¹H NMR (500 MHz, CDCl₃)

TBSO OPMB
PMBO
PMBO
O

PMBO
PMBO
PMBO
O

O OTES
PMBO
PMBO
O
1.184 SPh

¹³C NMR (125 MHz, CDCl₃)

F2
(ppm)

3.4
3.6
3.8
4.0
4.2
4.4
4.6
4.8
5.0
5.2
5.4
5.6
5.8

5.4 5.2 5.0 4.8 4.6 4.4 4.2 4.0 3.8 3.6

1.184

COSY & HMQC
(500 MHz, CDCl₃)

F1
(ppm)
10
20
30
40
50
60
70
80
90
100
110
120
130

7 6 5 4 3 2 1

Single Mass Analysis
Tolerance = 5.0 PPM / DBE: min = -1.5, max = 50.0
Element prediction: Off
Number of isotope peaks used for i-FIT = 3

Monoisotopic Mass, Even Electron Ions
24209 formula(e) evaluated with 69 results within limits (all results (up to 1000) for each mass)
Elements Used:
C: 0-120   H: 0-175   N: 0-5   O: 0-25   Na: 0-1   Si: 0-2   S: 0-2
BEN SWARTS   BSM-VIII-34
2008-07b.pro
2009_1002_0625 16 (0.318) Cm (11:27-(1:7+34:46))

1.184

HR ESI MS
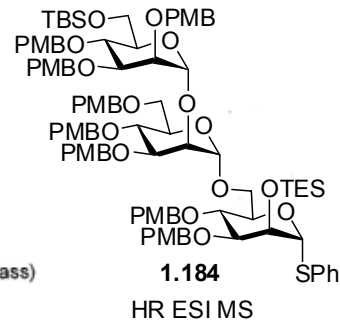
LCT Premier 02-Oct-2009 10:51:38
1: TOF MS ES+
2.39e+005

100- ⌐   1808.8010

                                     1809.8153

%   1810.8146

                                          1811.8163
        1778.7772   1805.8040   1824.7947   1862.8229 1866.3395   1883.8157
0 ───┬────────┬────────┬────────┬────────┬────────┬────────┬────────┬────────┬────────┬────────┬── m/z
    1780   1790   1800   1810   1820   1830   1840   1850   1860   1870   1880
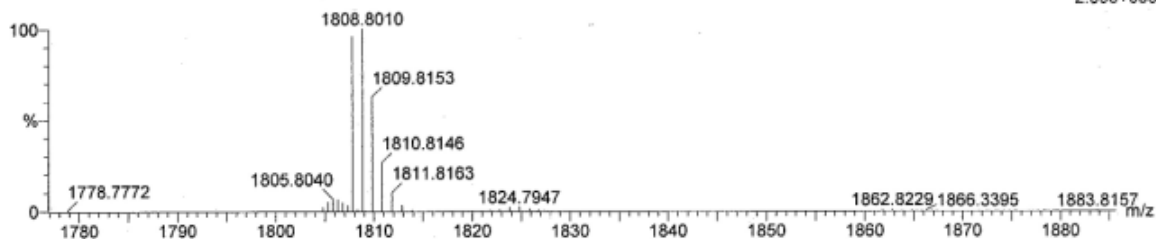
Minimum: -1.5
Maximum: 5.0   5.0   50.0

Mass	Calc. Mass	mDa	PPM	DBE	i-FIT	i-FIT (Norm)	Formula
1807.7996	1807.7996	0.0	0.0	46.5	62.5	5.1	C106 H123 O22 Si S
	1807.7997	-0.1	-0.1	29.5	62.7	5.2	C92 H132 N2 O25 Na Si2 S2
	1807.7994	0.2	0.1	46.5	62.9	5.4	C105 H123 O23 Si2
	1807.7998	-0.2	-0.1	46.5	62.1	4.7	C107 H123 O21 S2
	1807.7992	0.4	0.2	47.5	64.2	6.7	C105 H124 N4 O14 Na Si2 S2
	1807.8002	-0.6	-0.3	45.5	64.2	6.8	C106 H127 O18 Si2 S2
	1807.7990	0.6	0.3	37.5	62.2	4.8	C98 H127 N2 O24 Si S2
	1807.8003	-0.7	-0.4	38.5	62.9	5.4	C100 H128 O23 Na Si2 S

1.185

^{1}H NMR (500 MHz, CDCl$_3$)

1.185

^{13}C NMR (125 MHz, CDCl$_3$)

Single Mass Analysis
Tolerance = 5.0 PPM / DBE: min = -1.5, max = 50.0
Element prediction: Off
Number of isotope peaks used for i-FIT = 3

Monoisotopic Mass, Even Electron Ions
674 formula(e) evaluated with 3 results within limits (all results (up to 1000) for each mass)
Elements Used:
C: 0-100   H: 0-175   N: 0-1   O: 0-25   Na: 0-1   Si: 0-2
BEN SWARTS   BSM-VIII-35
2008-07b.pro
2009_1005_0627 16 (0.317) Cm (13:21-(1:9+35:45))

1.185

HR ESI MS

LCT Premier 05-Oct-2009 12:07:34
1: TOF MS ES+
3.25e+004

| Minimum: | | | -1.5 | | | |
| Maximum: | 5.0 | 5.0 | 50.0 | | | |

Mass	Calc. Mass	mDa	PPM	DBE	i-FIT	i-FIT (Norm)	Formula			
1715.7977	1715.7943	3.4	2.0	37.5	46.6	1.2	C96	H123	O24	Si2
	1715.7919	5.8	3.4	34.5	46.8	1.4	C94	H124	O24	Na Si2

GPI **1.187**
^{1}H NMR (500 MHz, CDCl$_3$)

GPI **1.187**
^{13}C NMR (125 MHz, CDCl$_3$)

GPI **1.187**
COSY (500 MHz, CDCl$_3$)

GPI **1.187**
HMQC (500 MHz, CDCl$_3$)

3142.922	25.021	-12.7
1802.660	14.351	15.1
902.020	7.181	14.8
648.017	5.159	-13.6

Single Mass Analysis
Tolerance = 5.0 PPM   /   DBE: min = -1.5, max = 100.0
Element prediction: Off
Number of isotope peaks used for i-FIT = 5

Monoisotopic Mass, Even Electron Ions
1824 formula(e) evaluated with 16 results within limits (all results (up to 1000) for each mass)
Elements Used:
C: 0-200   H: 0-300   N: 3-5   O: 0-50   23Na: 0-1   Si: 1-2   P: 0-1
BEN SWARTS   BSM-VIII-41 Cone 60
2008-07b.pro
2009_1026_0668a 17 (0.334) Cm (12:25-(1:8+39:46))

LCT Premier 26-Oct-2009 1?:4ɔ.47
1: TOF MS ES+
1.29e+003
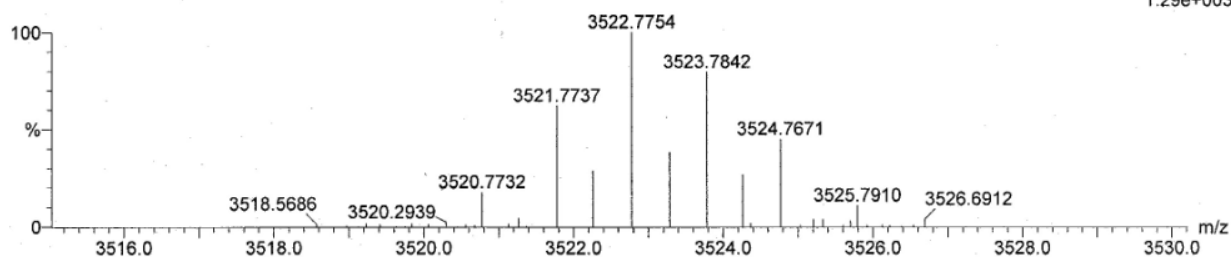
				DBE	i-FIT	i-FIT (Norm)	Formula
Minimum:				-1.5			
Maximum:		5.0	5.0	100.0			
Mass	Calc. Mass	mDa	PPM	DBE	i-FIT	i-FIT (Norm)	Formula
3520.7732	3520.7718	1.4	0.4	71.5	96.9	1.7	C198 H264 N4 O46 Si2 P
	3520.7694	3.8	1.1	68.5	97.0	1.8	C196 H265 N4 O46 23Na Si2 P

GPI **1.188**
^{1}H NMR (500 MHz, CDCl$_3$)

GPI **1.188**
^{13}C NMR (125 MHz, CDCl$_3$)
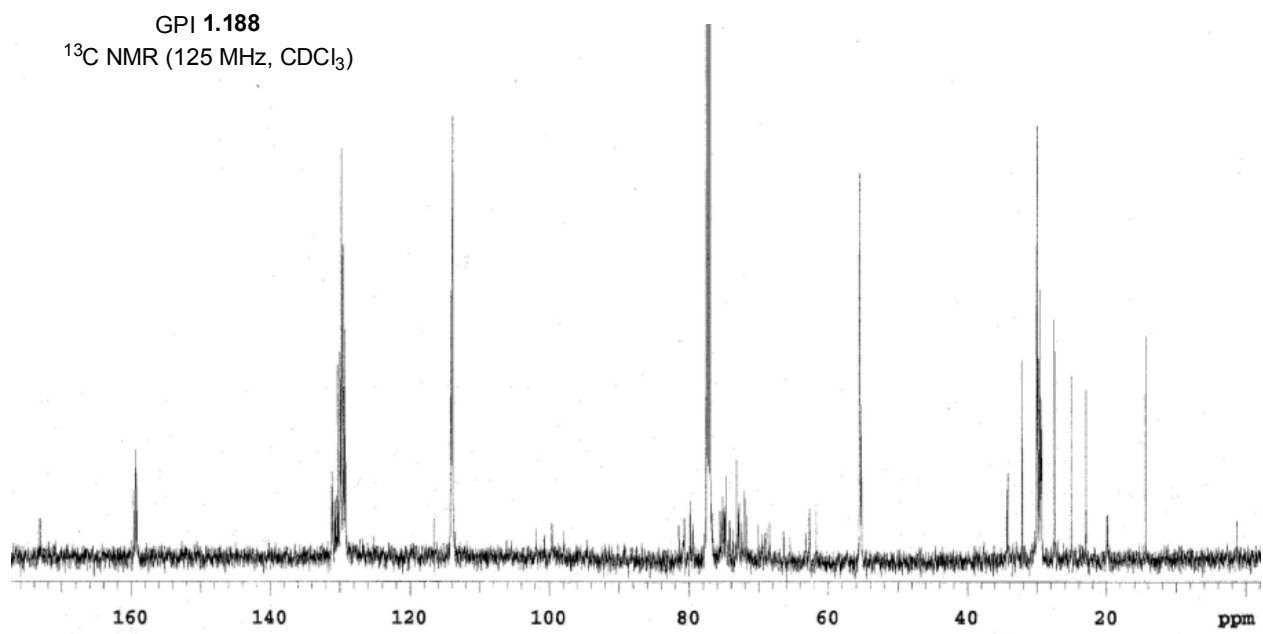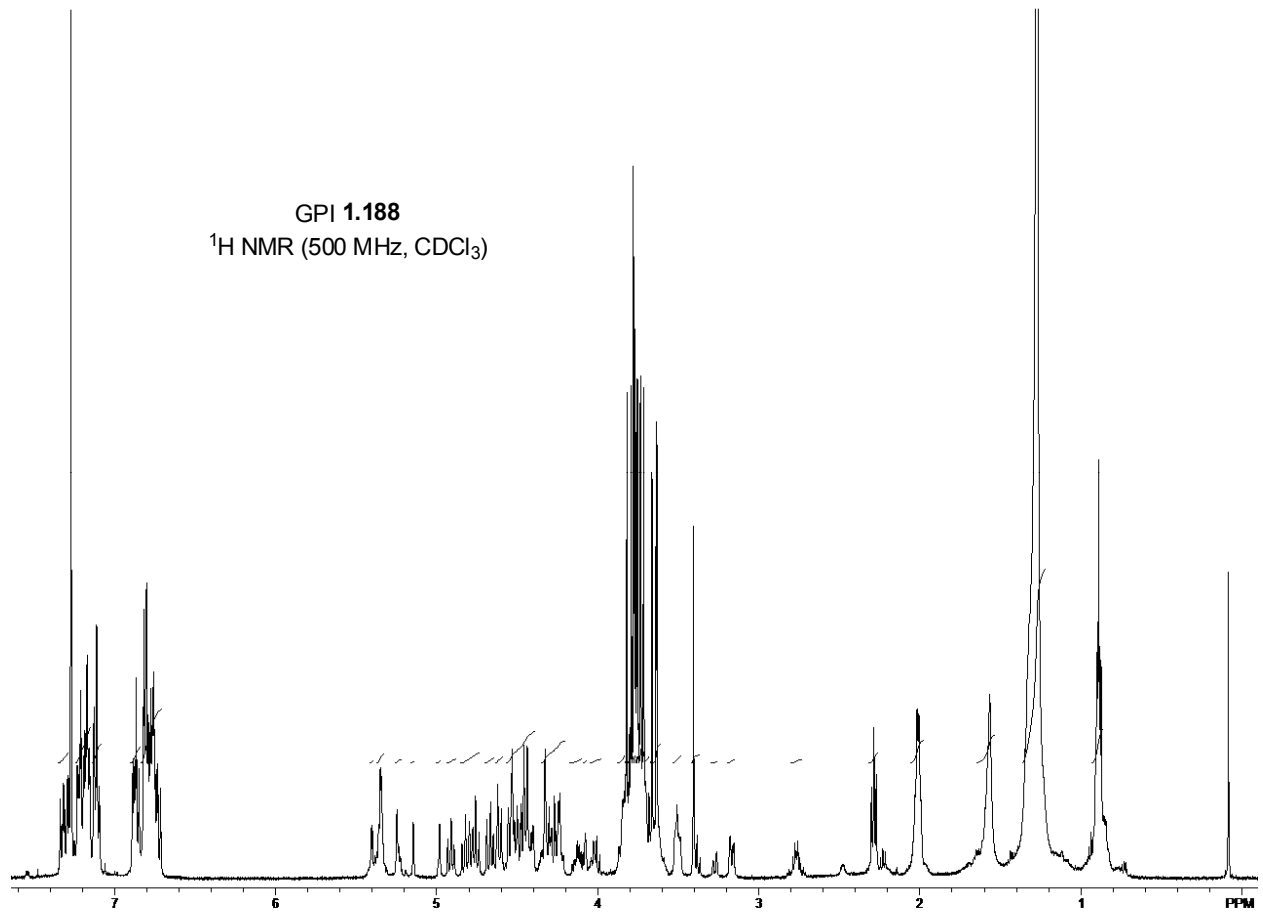
GPI **1.188**
^{13}C NMR (125 MHz, CDCl$_3$)
Anomeric region expansion

GPI **1.188**
COSY (500 MHz, CDCl$_3$)

GPI **1.188**
HMQC (500 MHz, CDCl₃)
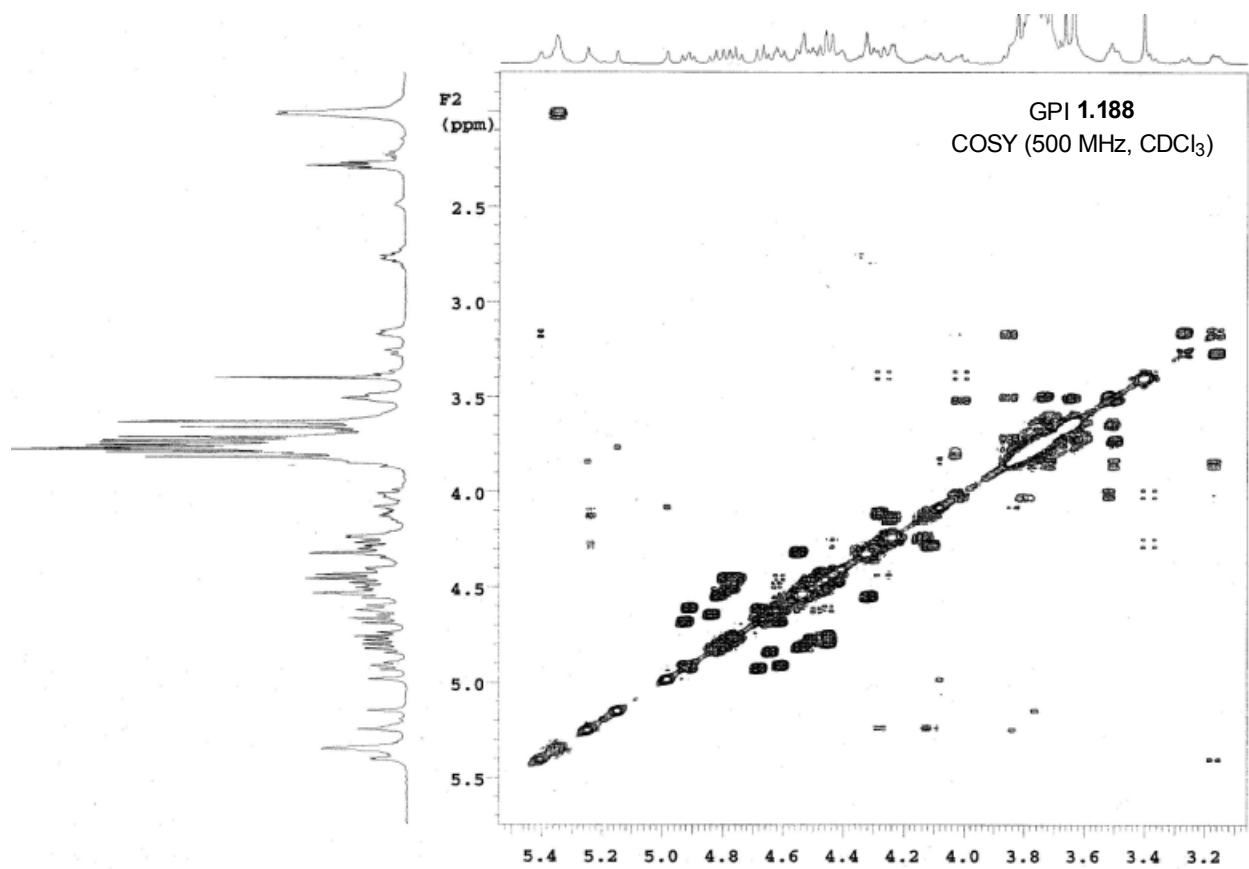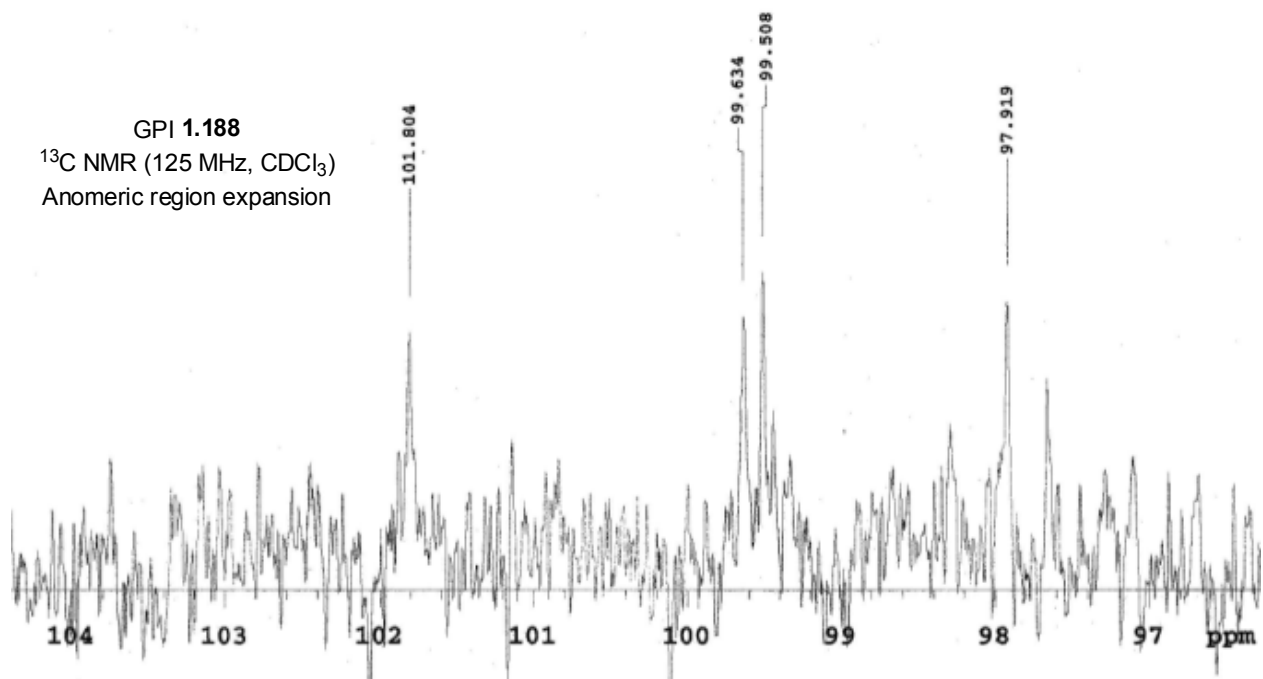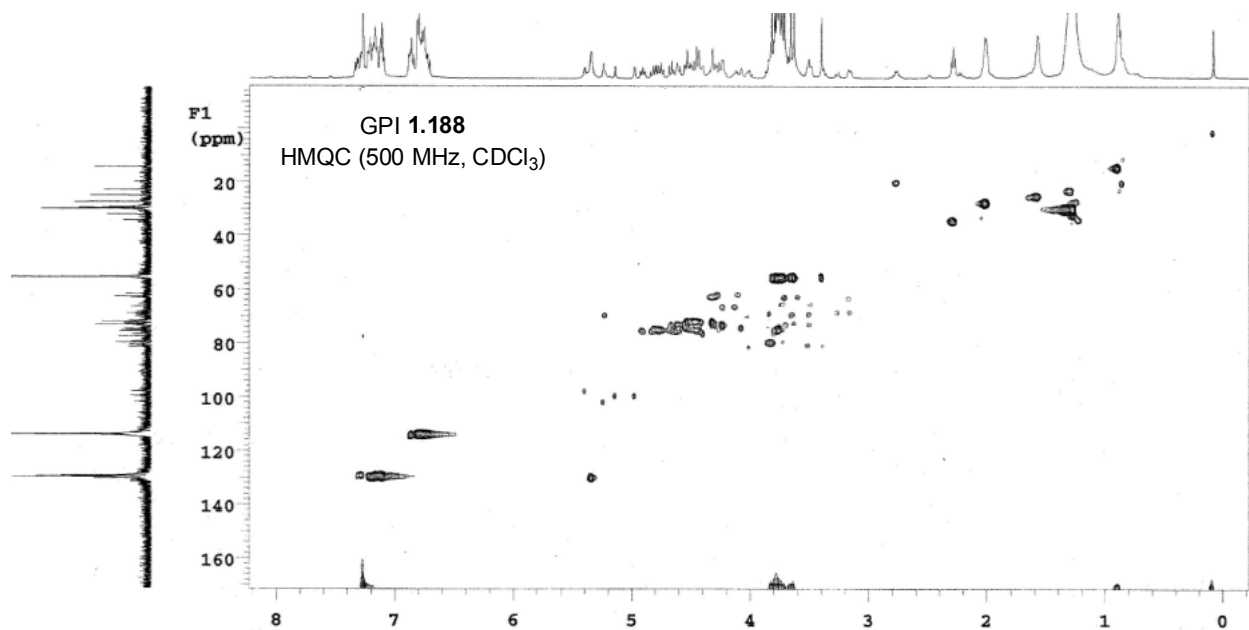
7	12820.623	102.067	-20.0
8	12787.593	101.804	27.3
9	12707.577	101.167	-15.3
10	12704.321	101.141	14.9
11	12575.459	100.115	-18.4
12	12514.982	99.634	30.4
13	12499.165	99.508	34.7
14	12299.591	97.919	30.3
15	12267.026	97.660	22.1
16	11812.054	94.038	-15.9
17	11507.343	91.612	17.4
18	11469.196	91.308	-15.5
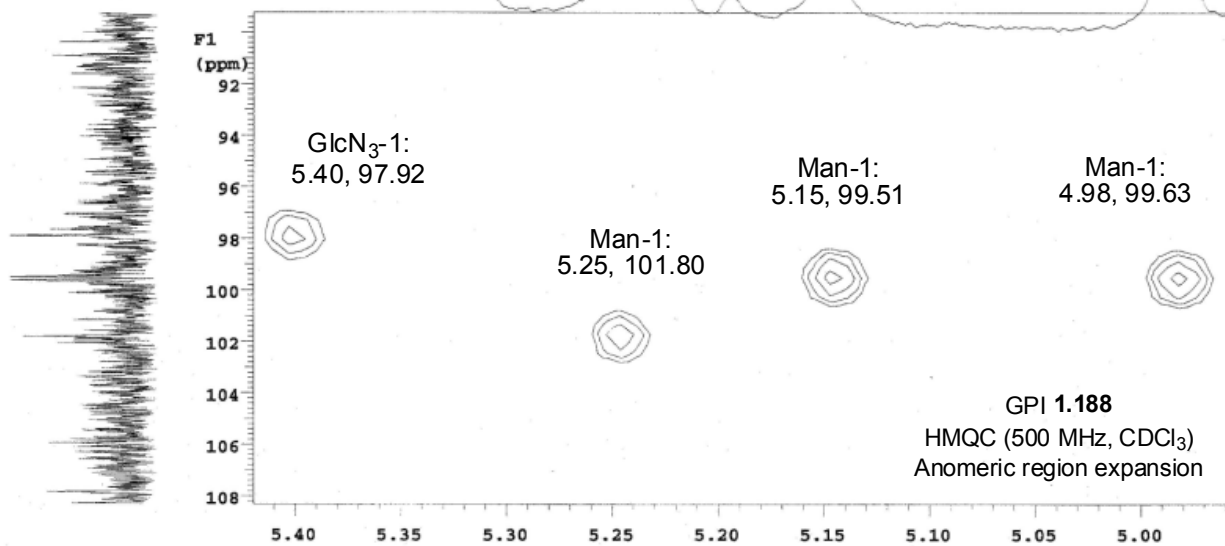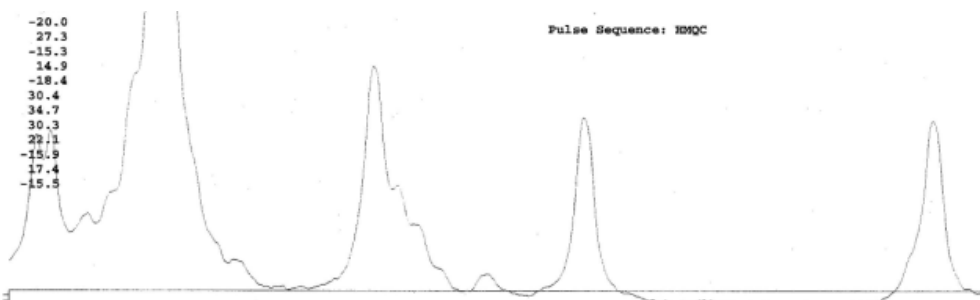
Pulse Sequence: HMQC

GlcN₃-1:
5.40, 97.92

Man-1:
5.25, 101.80

Man-1:
5.15, 99.51

Man-1:
4.98, 99.63

GPI **1.188**
HMQC (500 MHz, CDCl₃)
Anomeric region expansion

Single Mass Analysis
Tolerance = 5.0 PPM   /   DBE: min = -1.5, max = 100.0
Element prediction: Off
Number of isotope peaks used for i-FIT = 5

Monoisotopic Mass, Even Electron Ions
9473 formula(e) evaluated with 131 results within limits (all results (up to 1000) for each mass)
Elements Used:
C: 0-200   H: 0-250   N: 0-10   O: 0-50   23Na: 0-1   P: 0-1

BEN SWARTS   BSM-VIII-44 Cone 60
2008-07b.pro   LCT Premier 09-Nov-2009 14:52:42
2009_1106_0688_05 17 (0.334) Cm (16:21)   1: TOF MS ES+
                                                                        1.14e+003
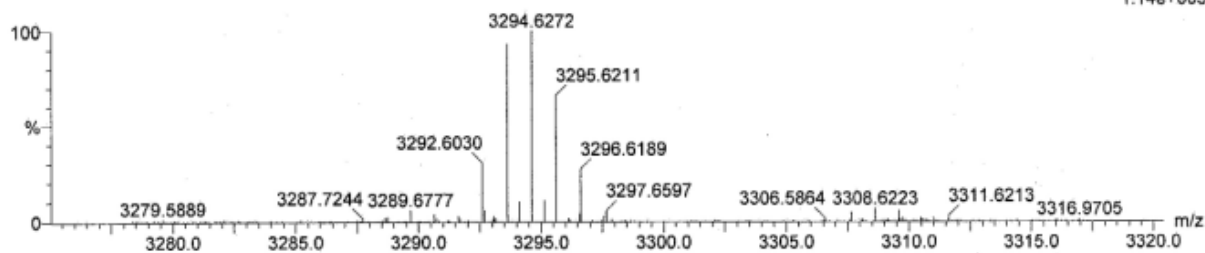
| Minimum: | | | | -1.5 | | | |
| Maximum: | | 5.0 | 5.0 | 100.0 | | | |

Mass	Calc. Mass	mDa	PPM	DBE	i-FIT	i-FIT (Norm)	Formula
							P
	3292.6189	-15.9	-4.8	68.5	94.2	3.6	C182 H237 N8 O44
							23Na P
	3292.6044	-1.4	-0.4	72.5	95.3	4.8	C182 H231 N10 O46
	3292.6063	-3.3	-1.0	63.5	94.9	4.4	C182 H241 N2 O49
							23Na P
	3292.6159	-12.9	-3.9	68.5	94.2	3.7	C183 H236 N6 O47
							23Na
	3292.6077	-4.7	-1.4	68.5	94.7	4.2	C183 H237 N6 O45
							23Na P
	3292.5932	9.8	3.0	72.5	97.5	7.0	C183 H231 N8 O47
	3292.5951	7.9	2.4	63.5	97.0	6.5	C183 H241 O50
							23Na P
	3292.6172	-14.2	-4.3	73.5	94.2	3.7	C184 H232 N10 O43
							23Na
	3292.6087	-5.7	-1.7	66.5	94.7	4.1	C184 H240 N2 O49
							P
	3292.5964	6.6	2.0	68.5	96.8	6.3	C184 H237 N4 O46
							23Na P

OCH$_2$CH$_2$CN

(iPr)$_2$N—P—OCH$_2$CH$_2$NHFmoc

1.189

^{1}H NMR (500 MHz, CDCl$_3$)

OCH$_2$CH$_2$CN

(iPr)$_2$N—P—OCH$_2$CH$_2$NHFmoc

1.189

^{13}C NMR (125 MHz, CDCl$_3$)

GPI **1.190**
^{1}H NMR (500 MHz, CDCl$_3$)
diasteromeric mixture
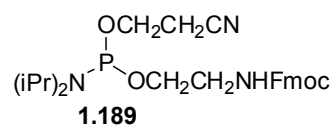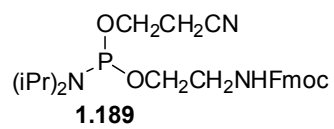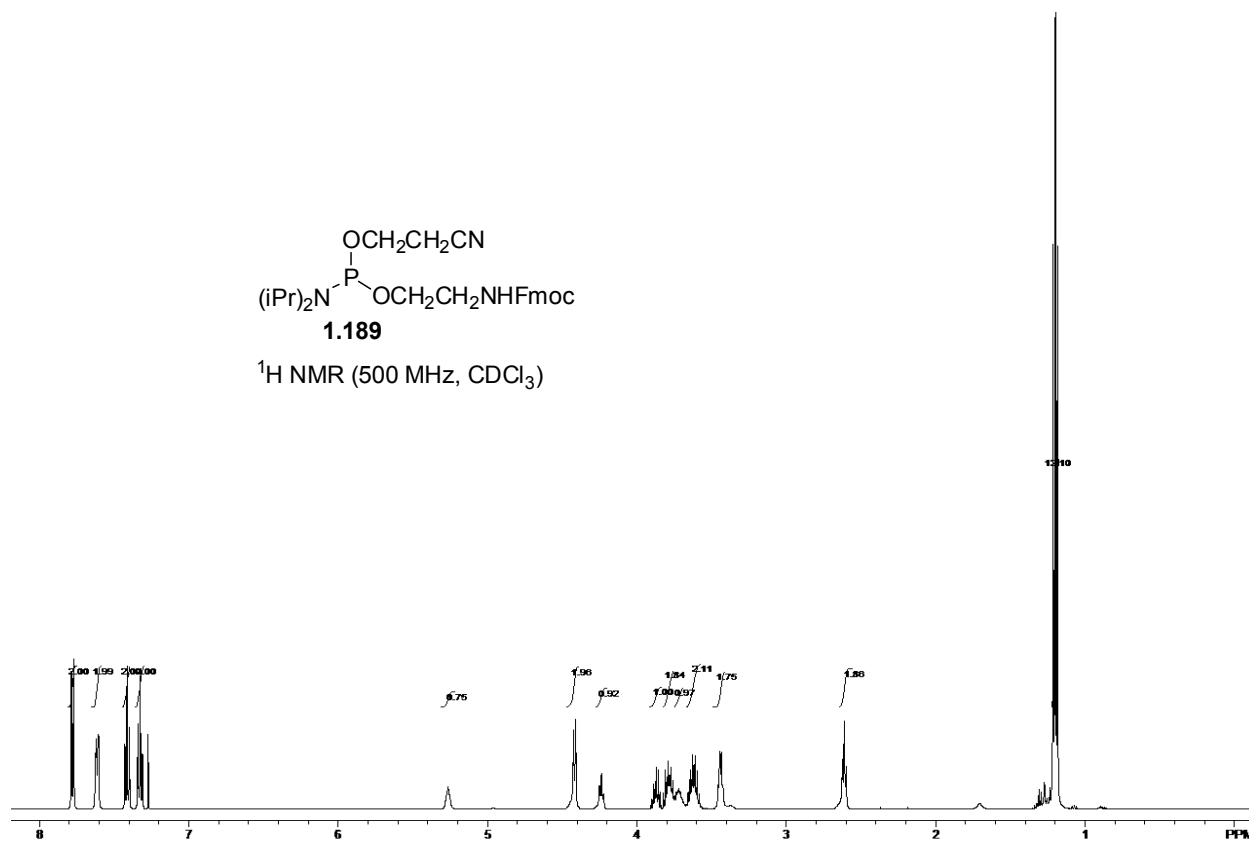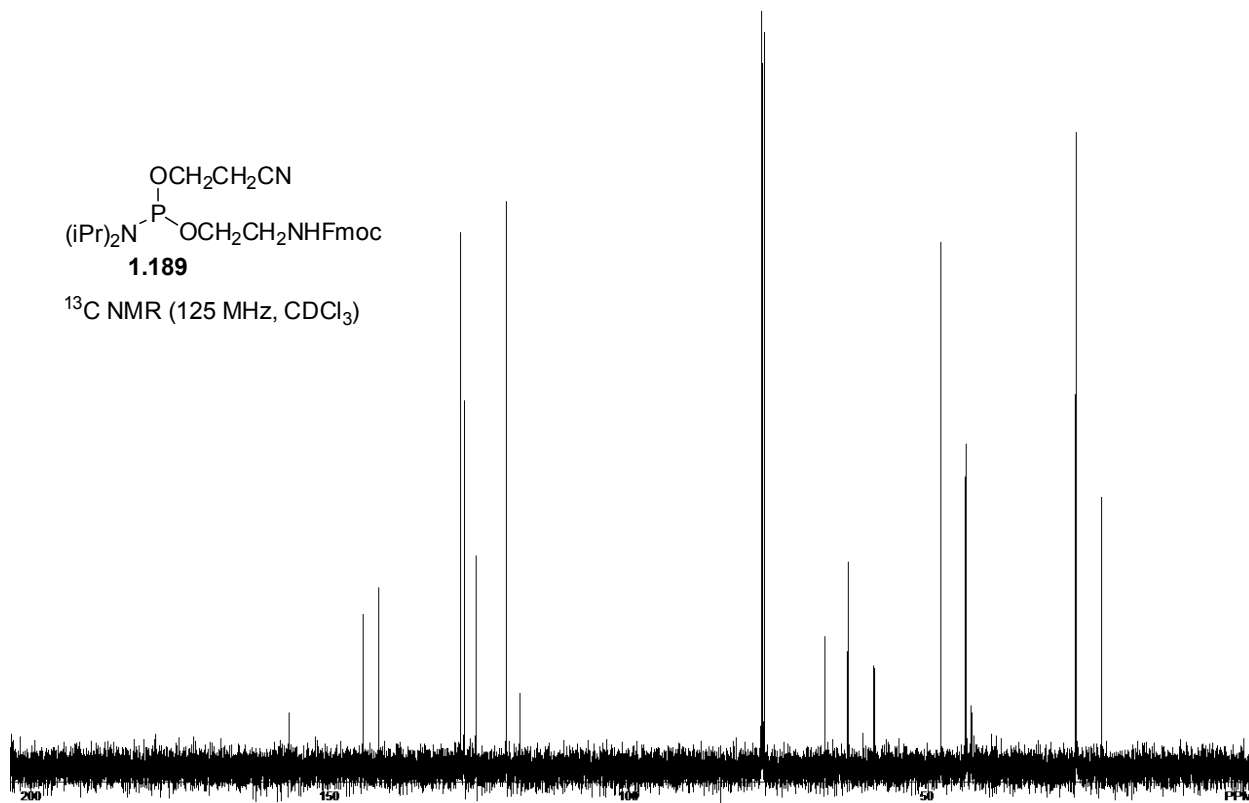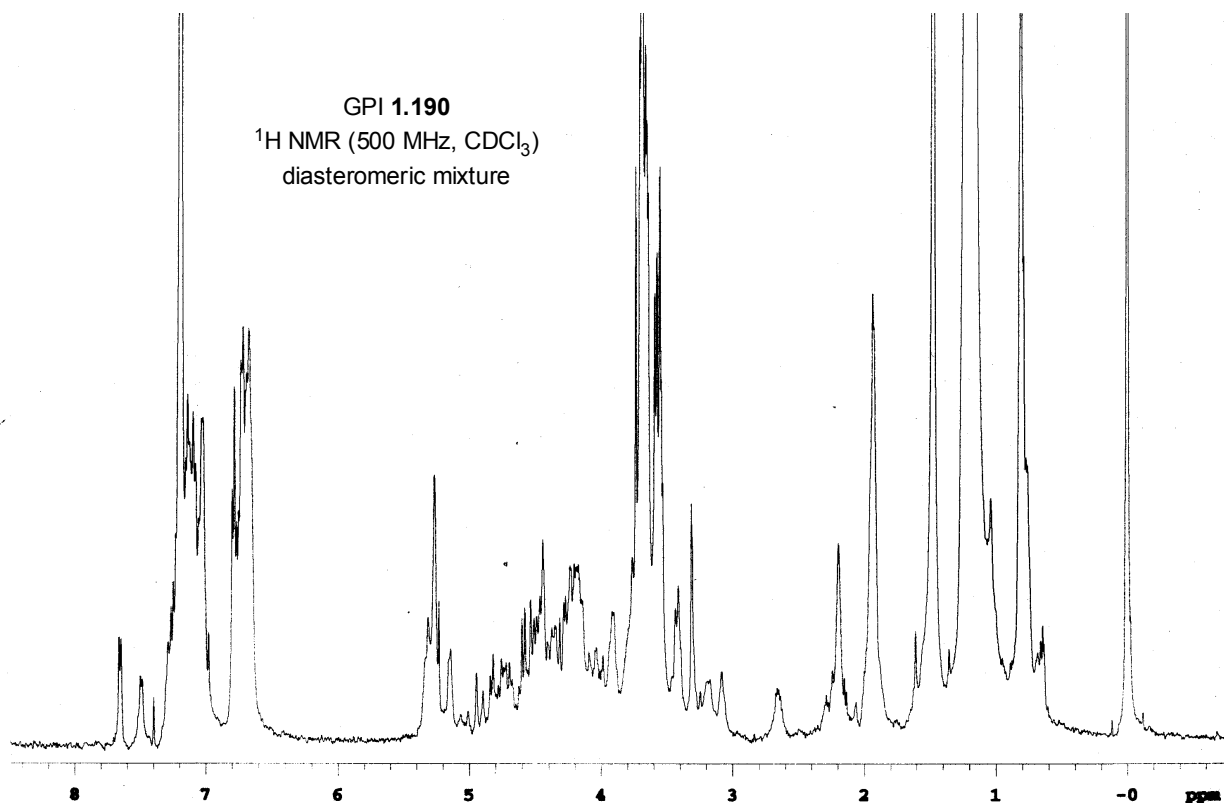
Guo; Ben Swarts bms-VIII-47 lct0713 mw3667.7 10uLmecl2 +meoh 1ul inj rf250 cv100 +AmAc
2008-07b.pro　　　　　　　　　　　　　　　　　**LCT Premier 25-Nov-2009 15:04:22**
2009_1125_0713d 17 (0.335) Cm (10:39-1:8x4.000)　　　　　　1: TOF MS ES+
　　　　　　　　　　　　　　　　　　　　　　　　　　　　4.10e3

GPI **1.190**
HR ESI MS
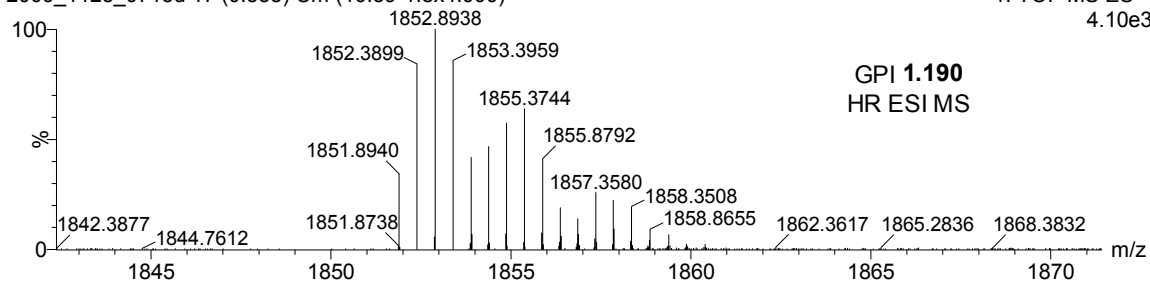
Doubly charged species: calcd. For C$_{204}$H$_{264}$N$_8$O$_{51}$P$_2$ [M+2NH$_4$]$^{2+}$ m/z, 1851.8893; found, 1851.8940.

Mass: 1851.8940
Calculated mass: 1851.8893
ppm error: +2.8ppm

Comment 1   BMS-VIII-47C
Comment 2   DHB Positive

GPI **1.190**
MALDI TOF MS

m/z	SN	Intens.	Area	Res.
3690.934	5.1	8.00	2	26326

GPI **1.109**
^{1}H NMR (500 MHz,
CDCl$_3$/CD$_3$OD/D$_2$O 3:3:1)
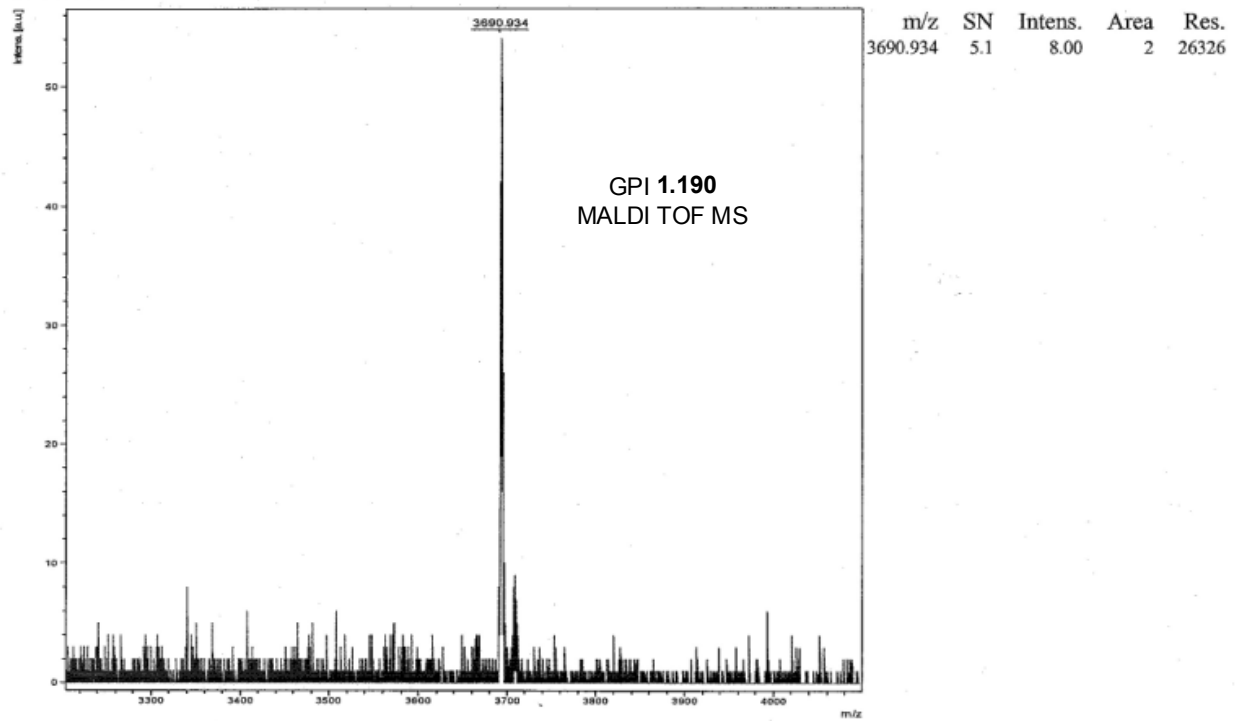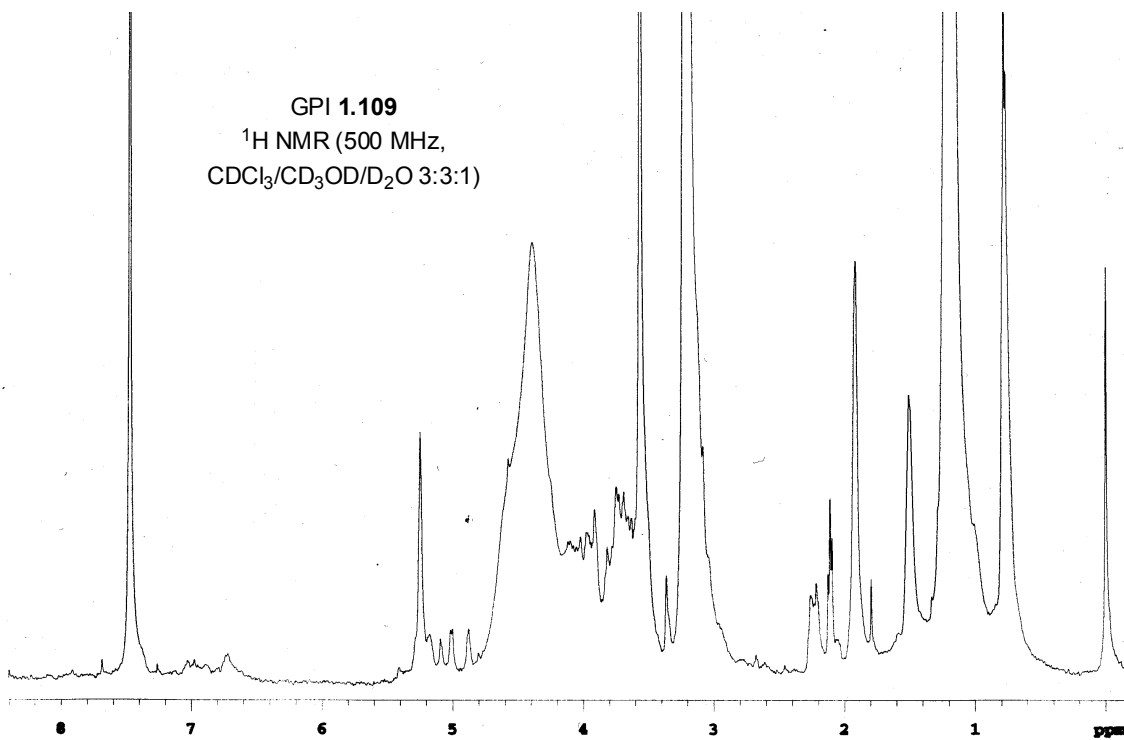
Comment 1   BMS-VIII-48 Final Product Negative Mode Sum
Comment 2   DHB Neg

GPI **1.109**
MALDI TOF MS
(negative mode)
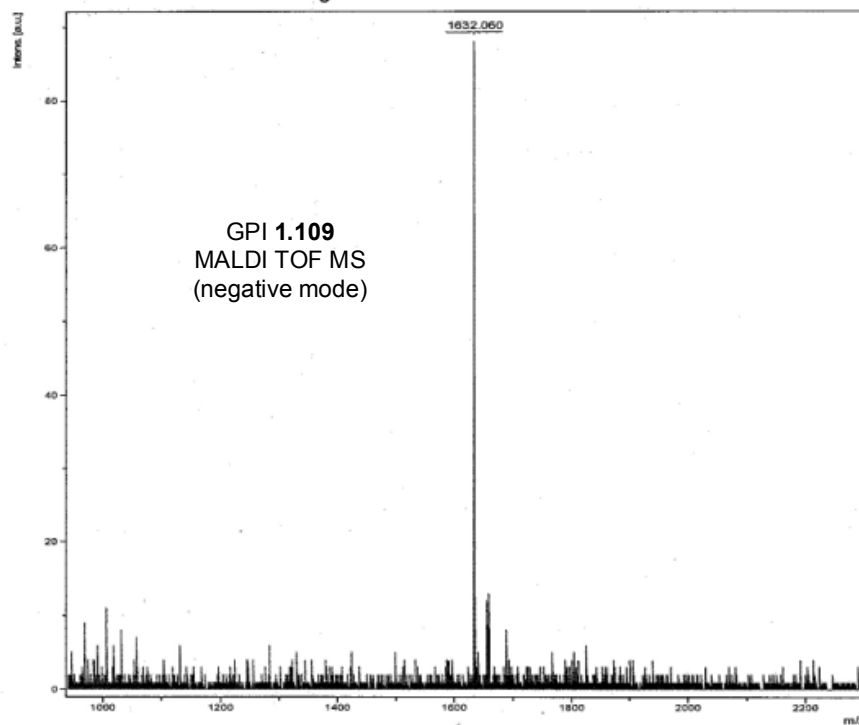
m/z	SN	Intens.	Area	Res.
1632.060	94.8	88.00	21	7531
1654.041	11.8	11.00	2	12666
1658.007	14.0	13.00	2	38846

Expansion

GPI **1.109**
MALDI TOF MS
(positive mode)

m/z	SN	Intens.	Area	Res.
1700.445	7.8	78.23	115	3460

Expansion

289
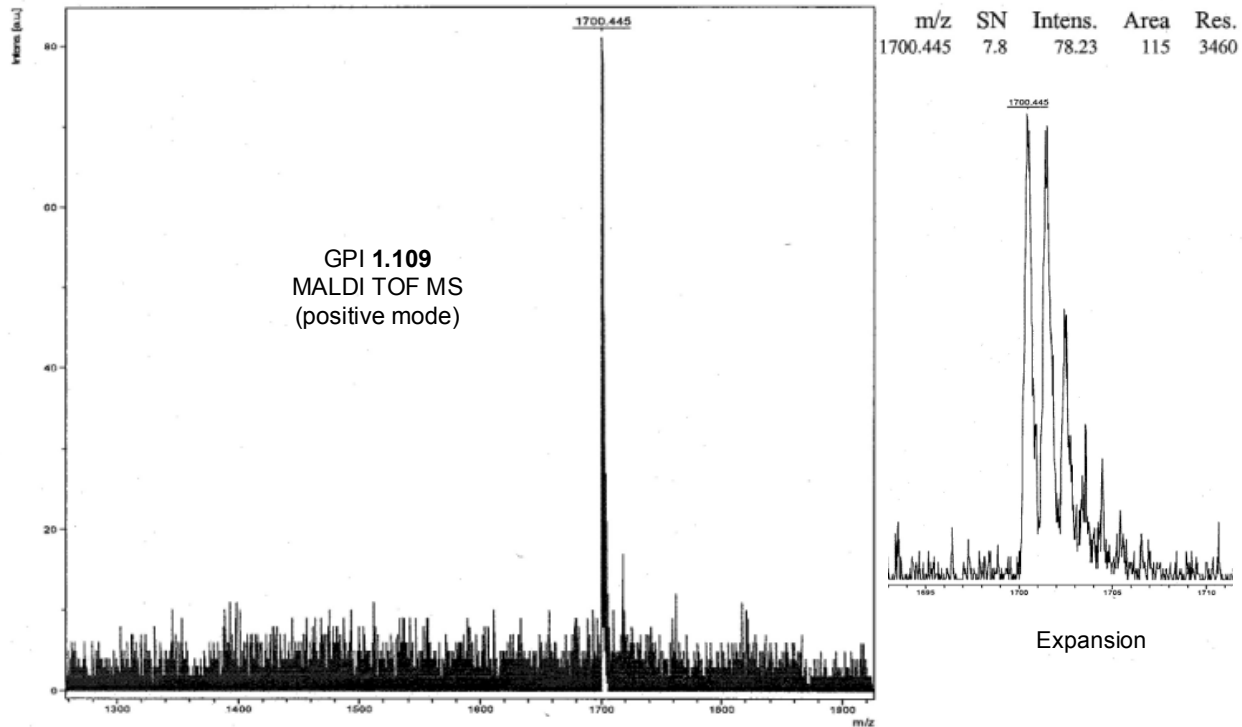
Comment 1   Fully Phosphorylated GPI w Unsatd Lipids
Comment 2   DHB Negative
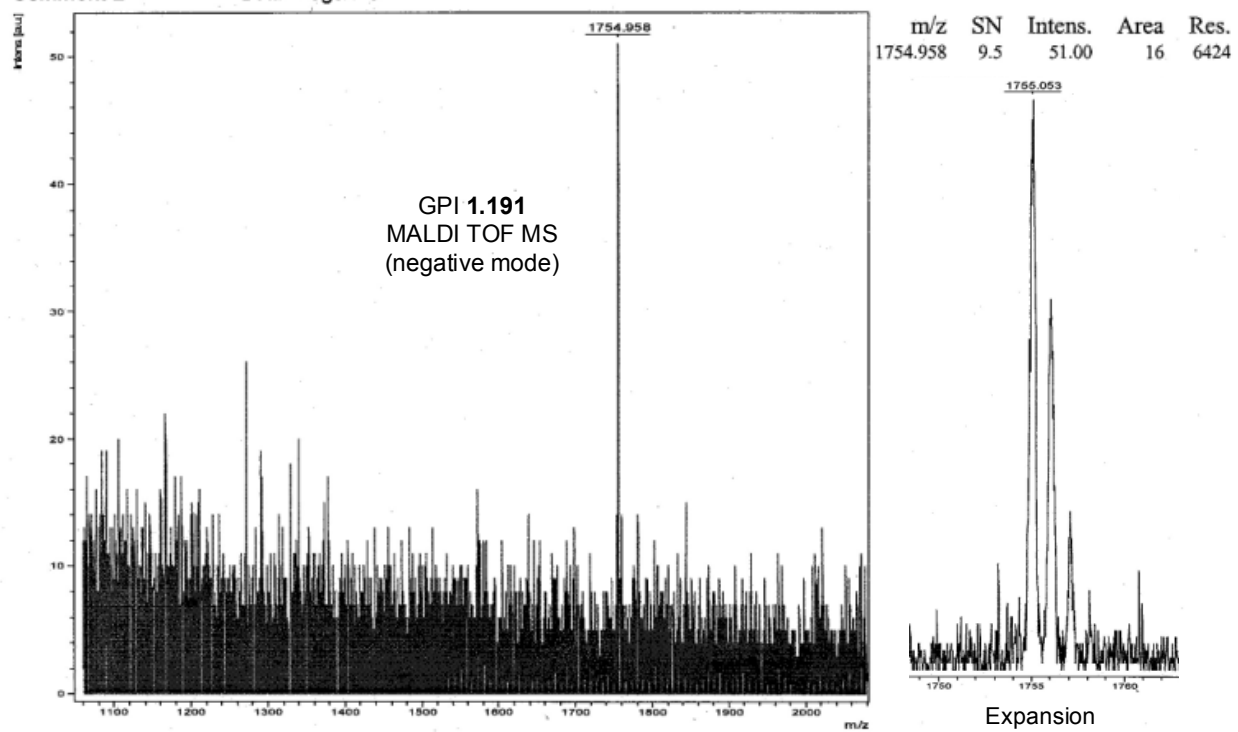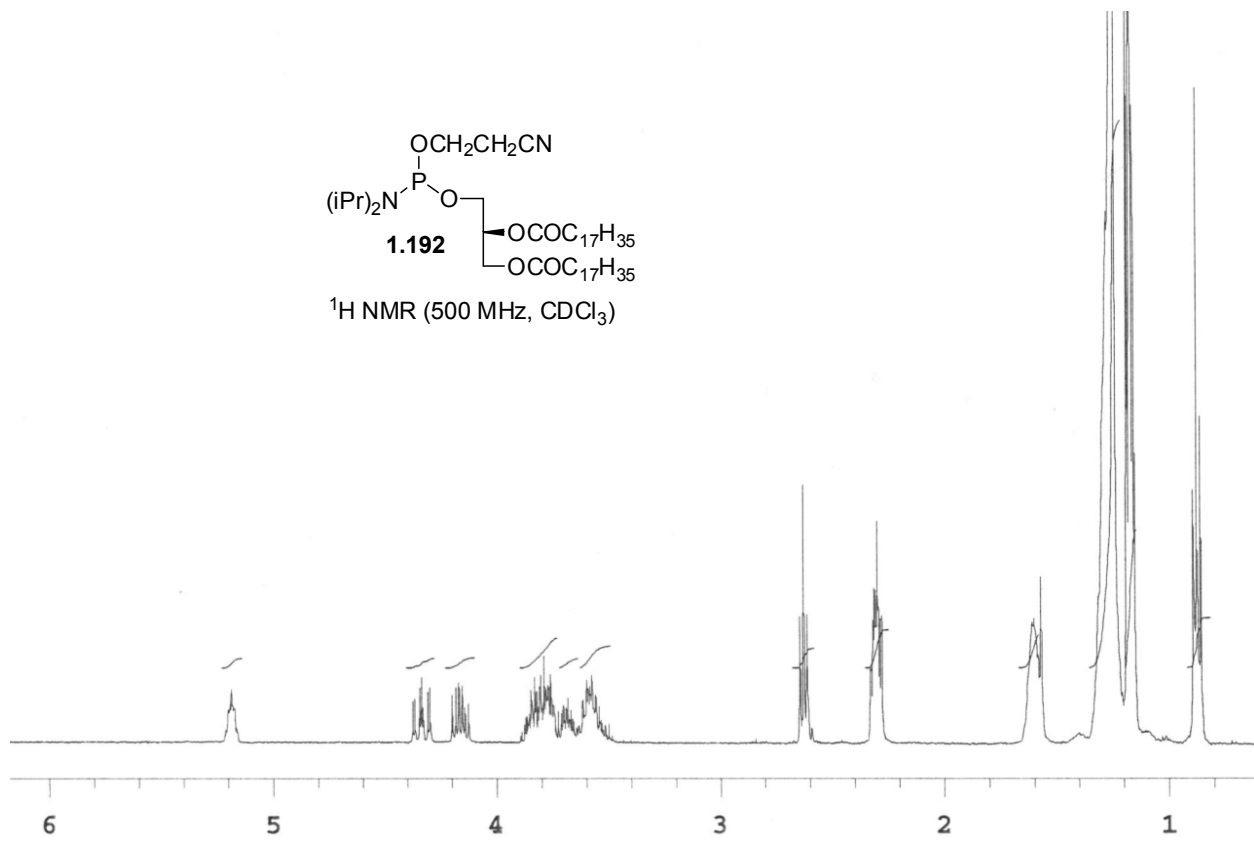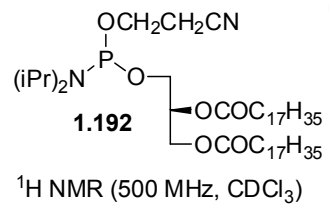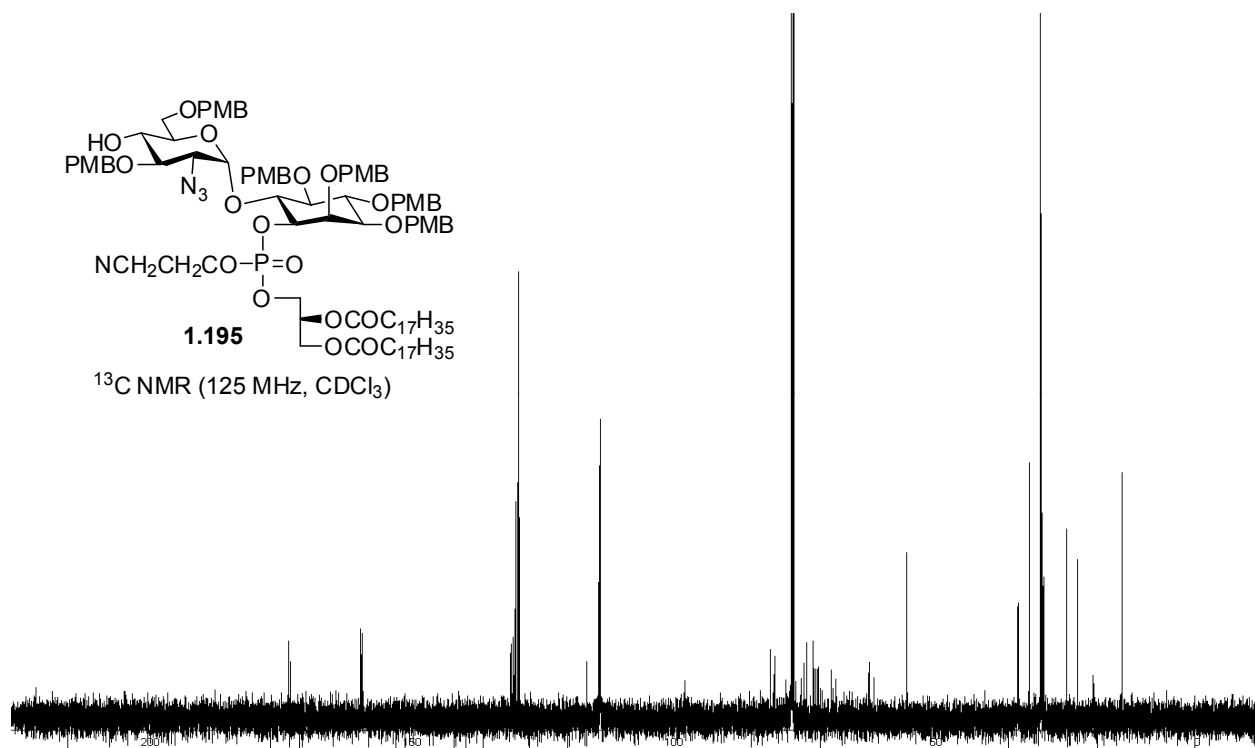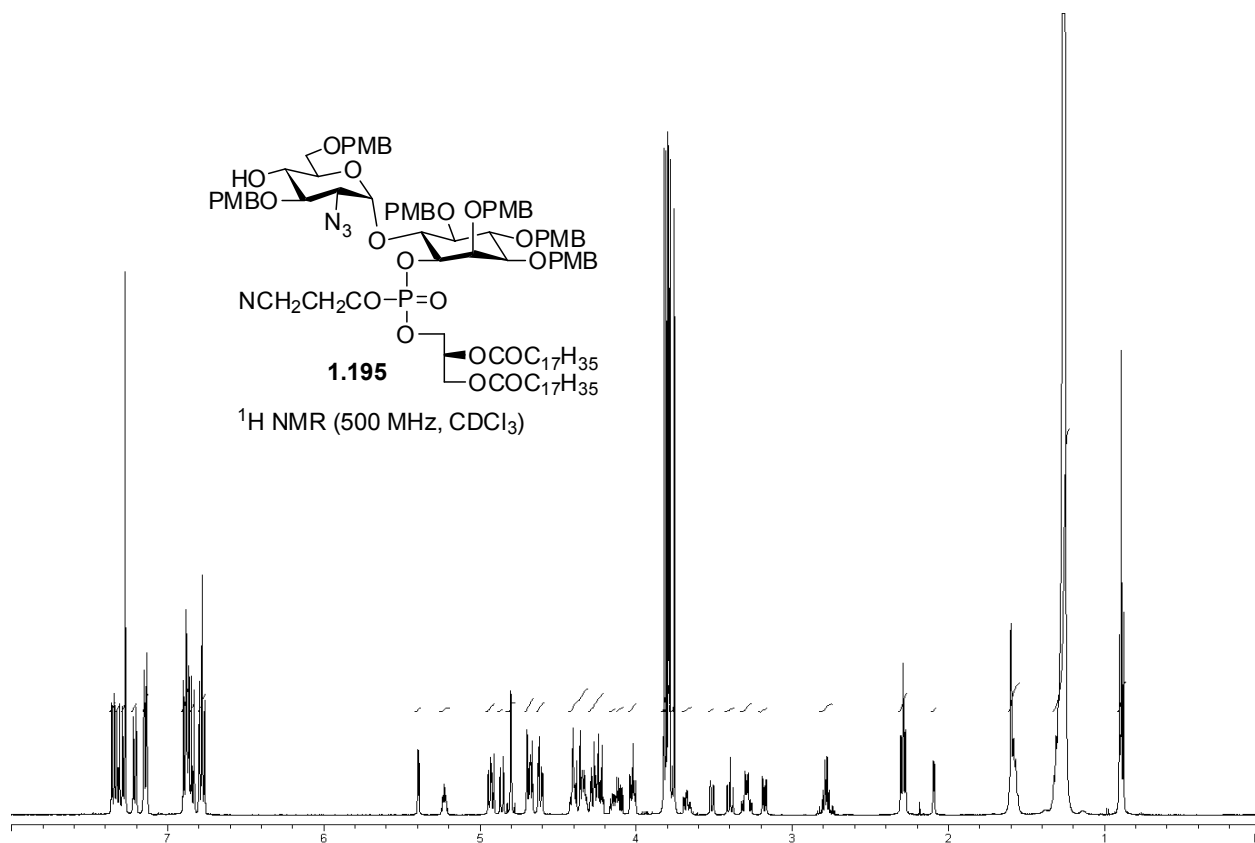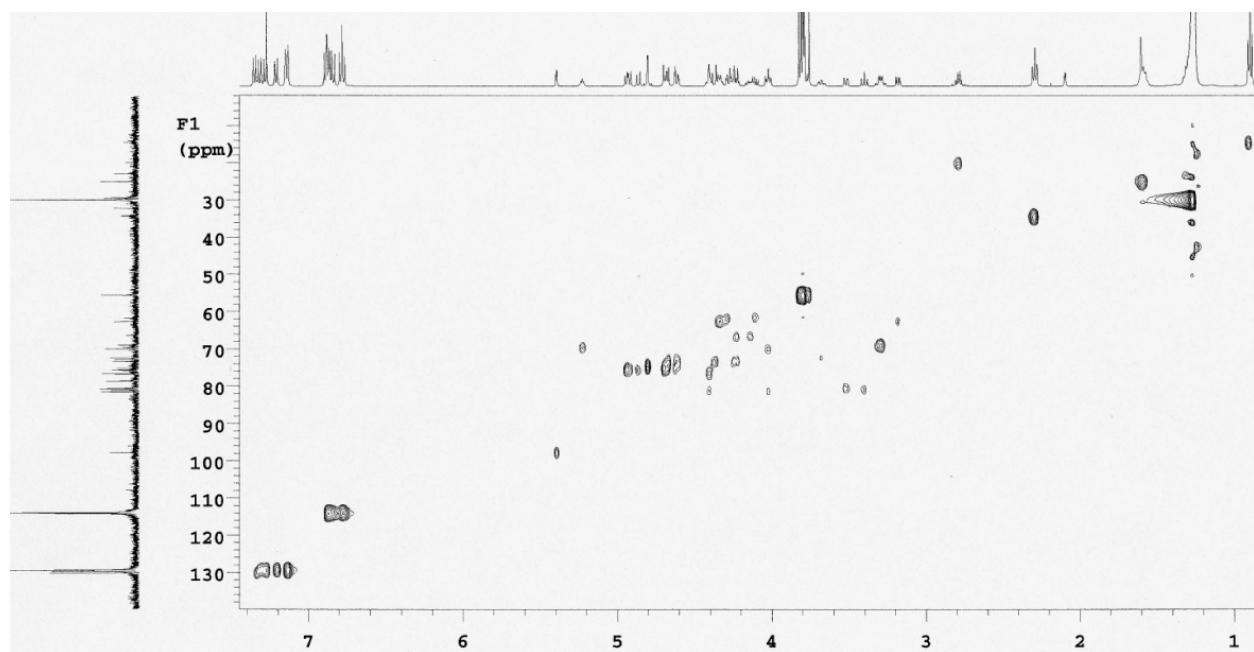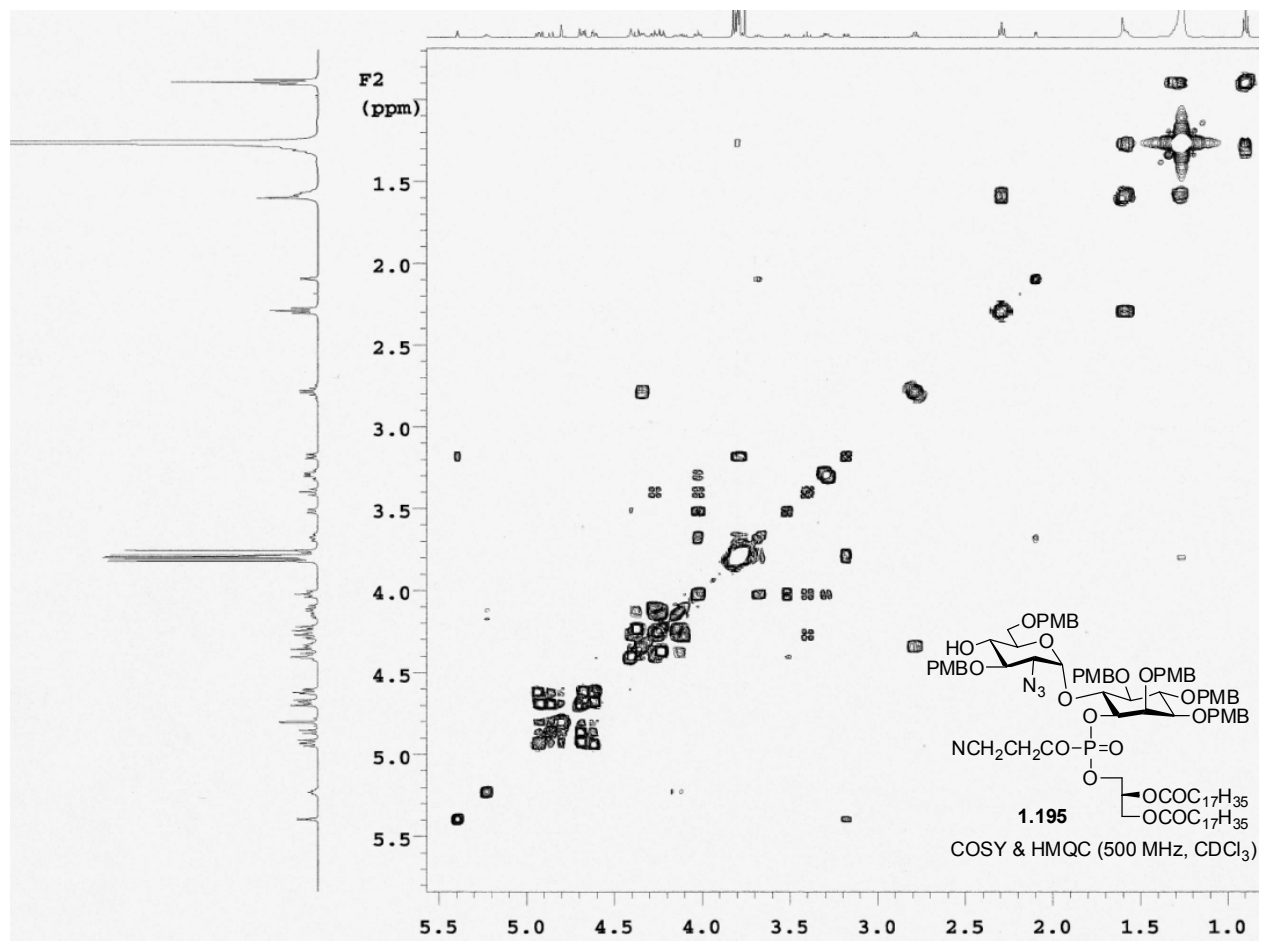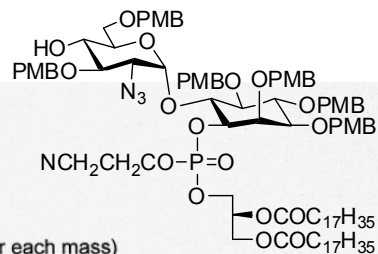
GPI **1.191**
MALDI TOF MS
(negative mode)

m/z	SN	Intens.	Area	Res.
1754.958	9.5	51.00	16	6424

Expansion

OCH₂CH₂CN

(iPr)₂N–P–O–

1.192

◄OCOC₁₇H₃₅

OCOC₁₇H₃₅

¹H NMR (500 MHz, CDCl₃)

1.195

^{1}H NMR (500 MHz, CDCl$_3$)

1.195

^{13}C NMR (125 MHz, CDCl$_3$)

F2 (ppm)

COSY & HMQC (500 MHz, CDCl₃)

1.195

F1 (ppm)

Single Mass Analysis
Tolerance = 5.0 PPM / DBE: min = -1.5, max = 100.0
Element prediction: Off
Number of isotope peaks used for i-FIT = 3

Monoisotopic Mass, Even Electron Ions
12591 formula(e) evaluated with 68 results within limits (up to 50 best isotopic matches for each mass)
Elements Used:
C: 0-500   H: 0-1000   N: 0-5   O: 0-25   23Na: 0-1   P: 0-1

BEN SWARTS   BMS-VII-122-A
2008-07b.pro
2009_0508_0423 9 (0.158) Cm (7:13-(1:3+19:26)x2.000)

1.195
HR ESI MS

LCT Premier 13-May-2009 13:49:09
1: TOF MS ES+
2.16e+003
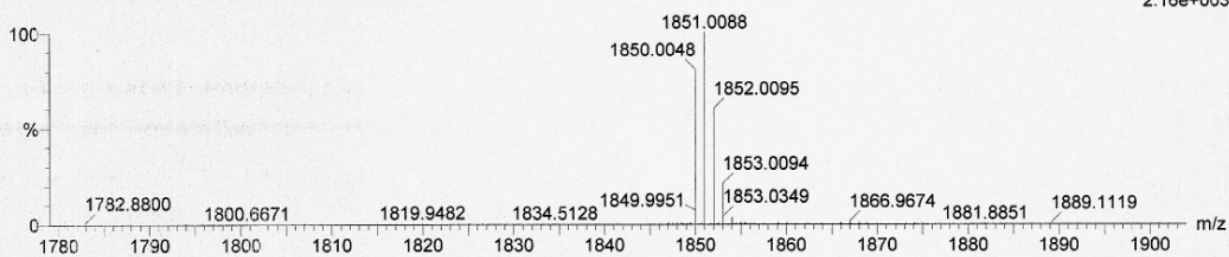
Mass	Calc. Mass	mDa	PPM	DBE	i-FIT	i-FIT (Norm)	Formula
		Minimum:		-1.5			
		Maximum:	5.0	5.0	100.0		
1850.0048	1850.0091	-4.3	-2.3	31.5	37.9	2.0	C102 H147 N4 O23 23Na P
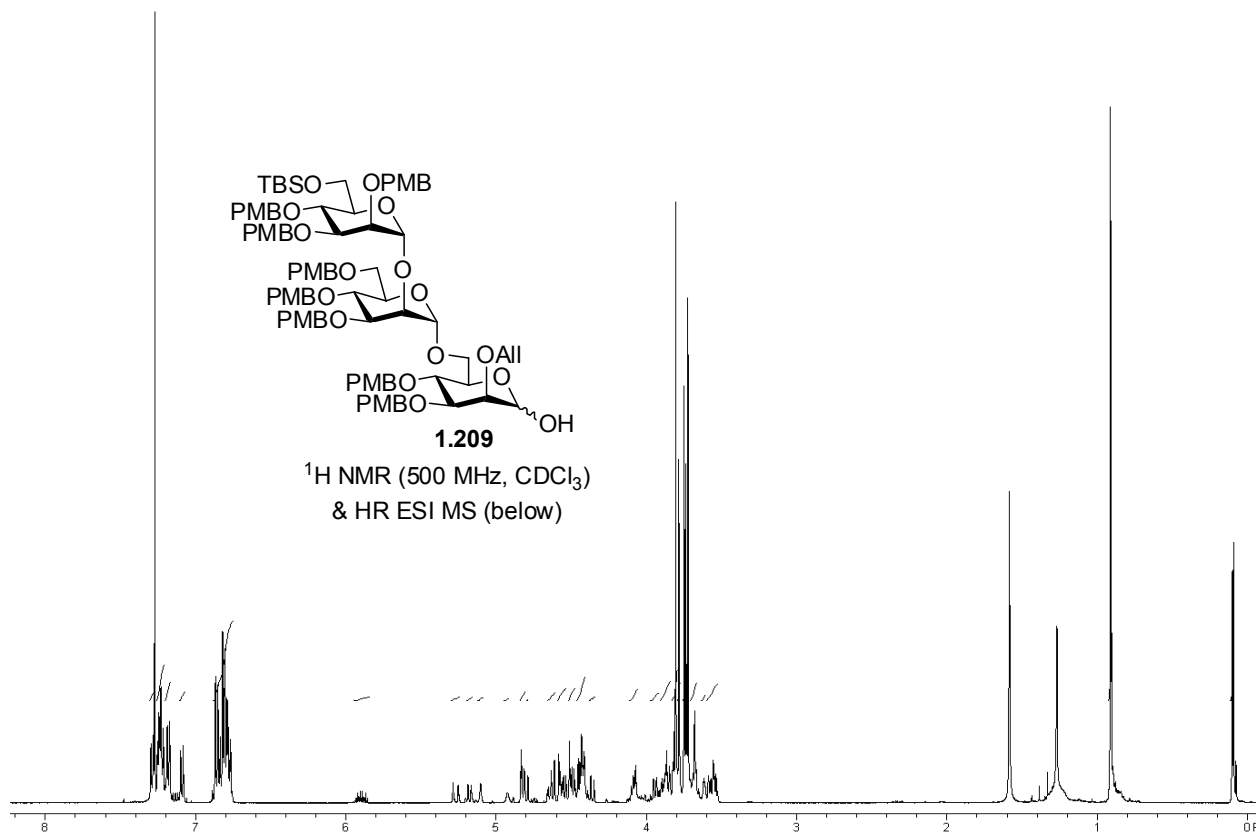
1.209

^{1}H NMR (500 MHz, CDCl$_3$)
& HR ESI MS (below)

Single Mass Analysis

Tolerance = 5.0 PPM / DBE: min = -1.5, max = 100.0
Element prediction: Off
Number of isotope peaks used for i-FIT = 3

Monoisotopic Mass, Even Electron Ions
11082 formula(e) evaluated with 65 results within limits (up to 50 best isotopic matches for each mass)
Elements Used:
C: 0-500   H: 0-1000   N: 0-5   O: 0-25   23Na: 0-1   Si: 0-1

BEN SWARTS   BMS-VII-83
2008-07b.pro
2009_0508_0424 15 (0.300) Cm (11:20-(1:8+23:30)x2.000)

LCT Premier 13-May-2009 14:07:37
1: TOF MS ES+
6.23e+002
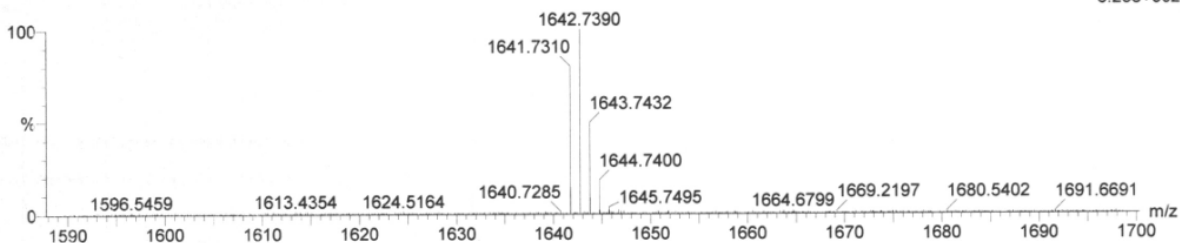
Minimum:				-1.5			
Maximum:		5.0	5.0	100.0			
Mass	Calc. Mass	mDa	PPM	DBE	i-FIT	i-FIT (Norm)	Formula
1641.7310	1641.7295	1.5	0.9	36.5	85.0	3.6	C90 H110 N2 O25 23Na
	1641.7252	5.8	3.5	39.5	86.9	5.6	C90 H109 N4 O23 Si
	1641.7367	-5.7	-3.5	35.5	84.6	3.2	C91 H114 O24 23Na Si
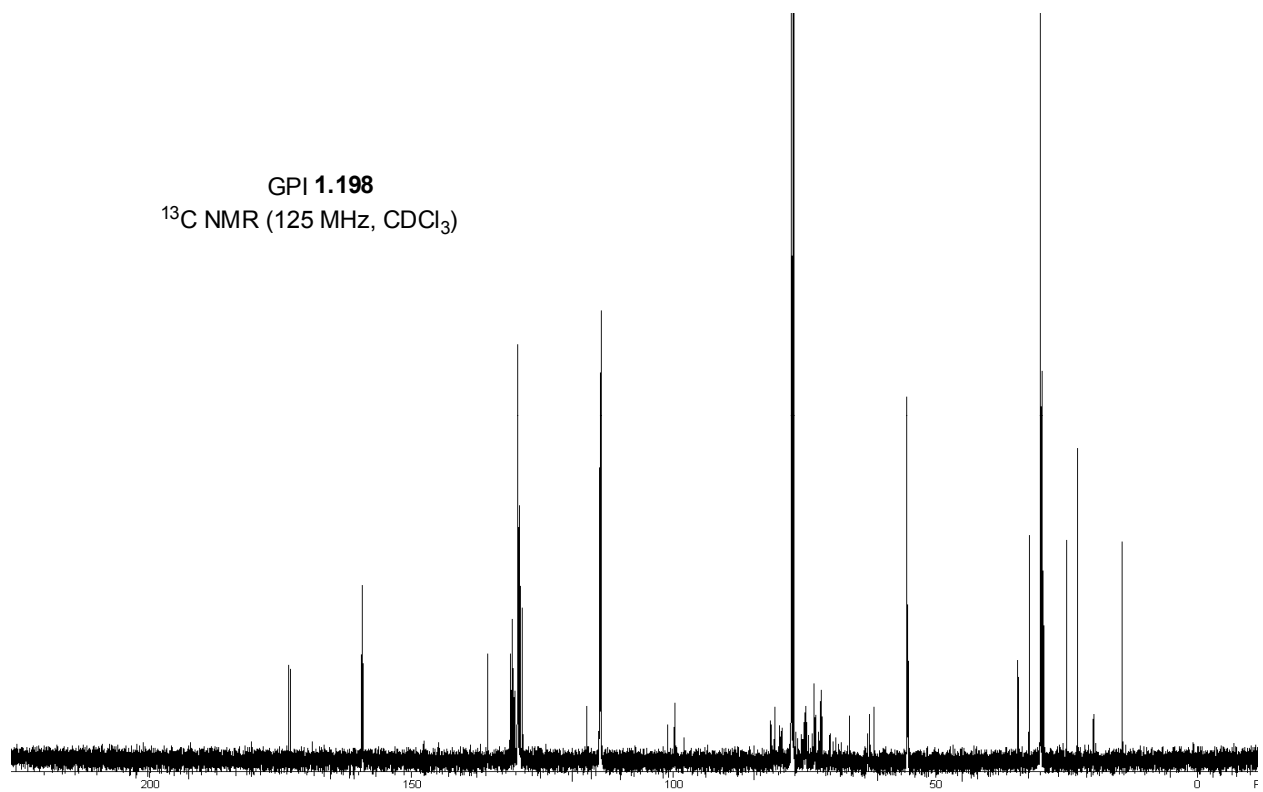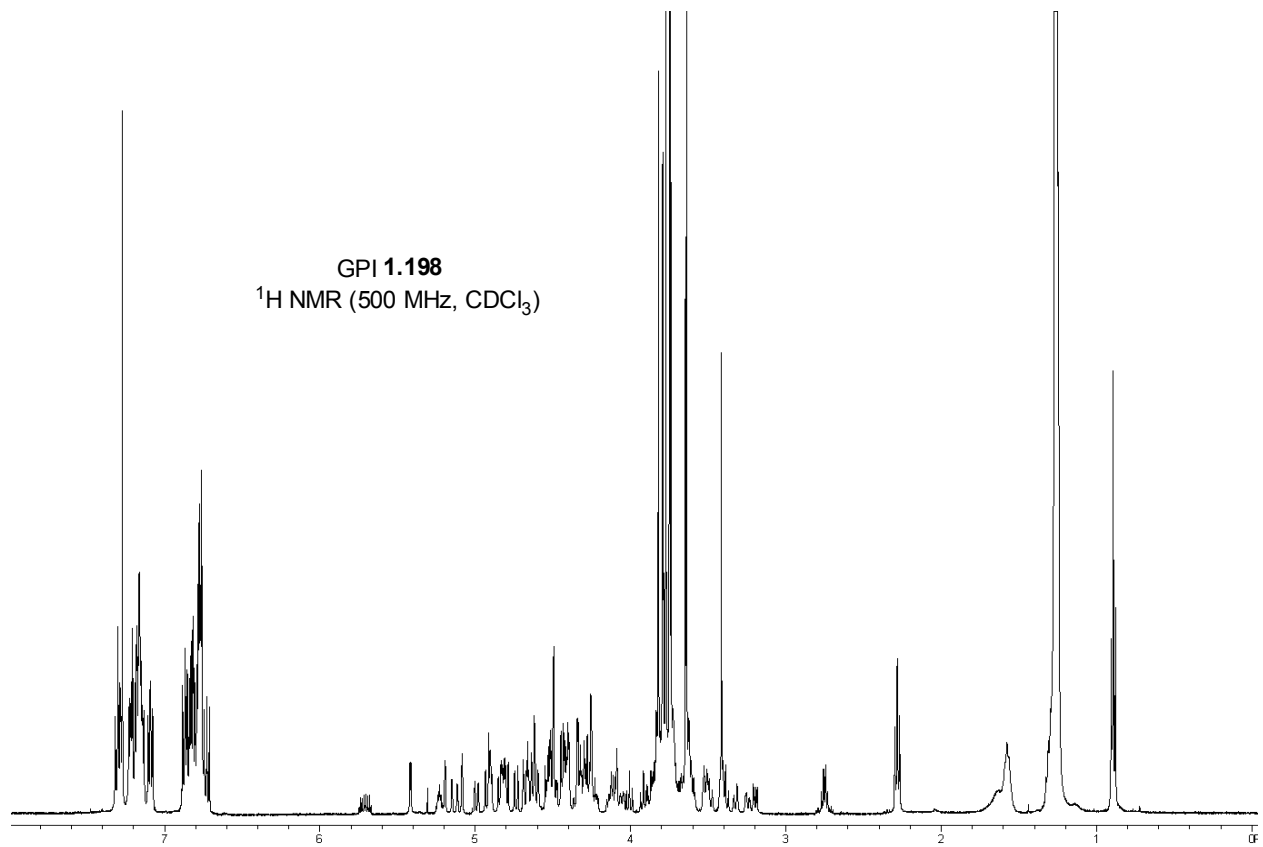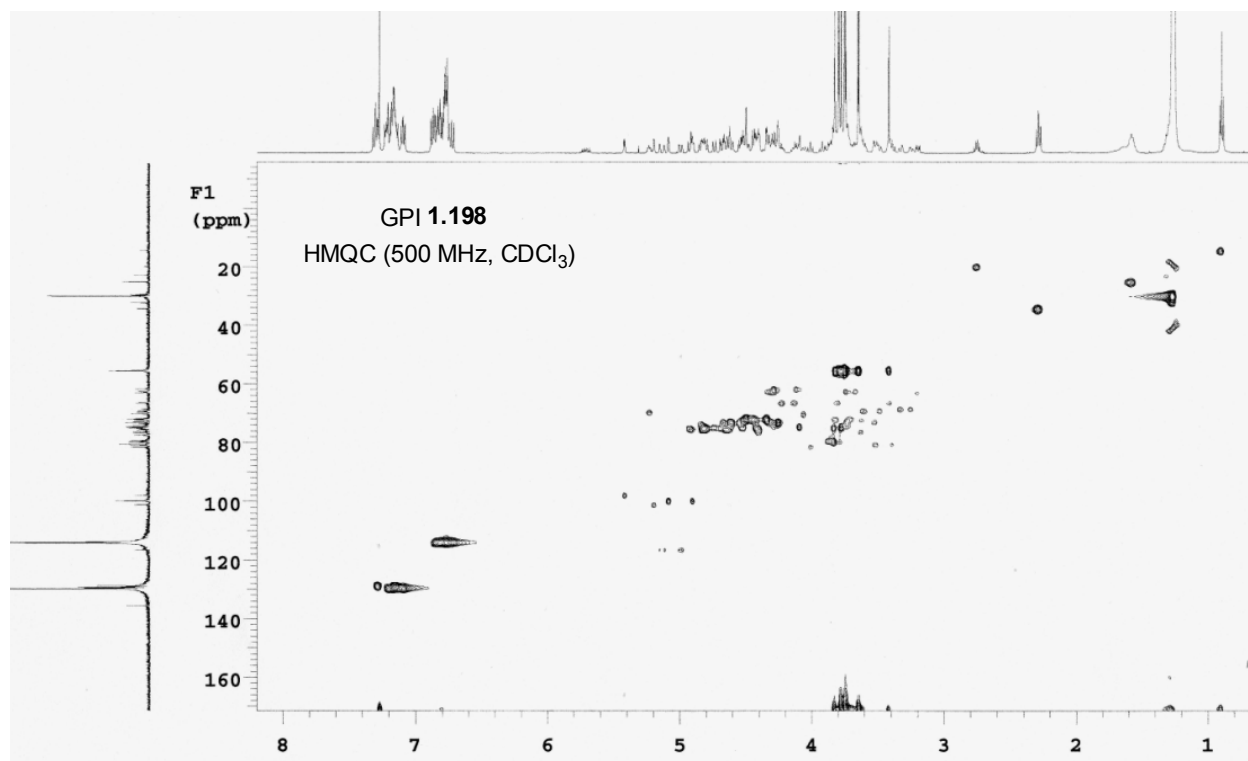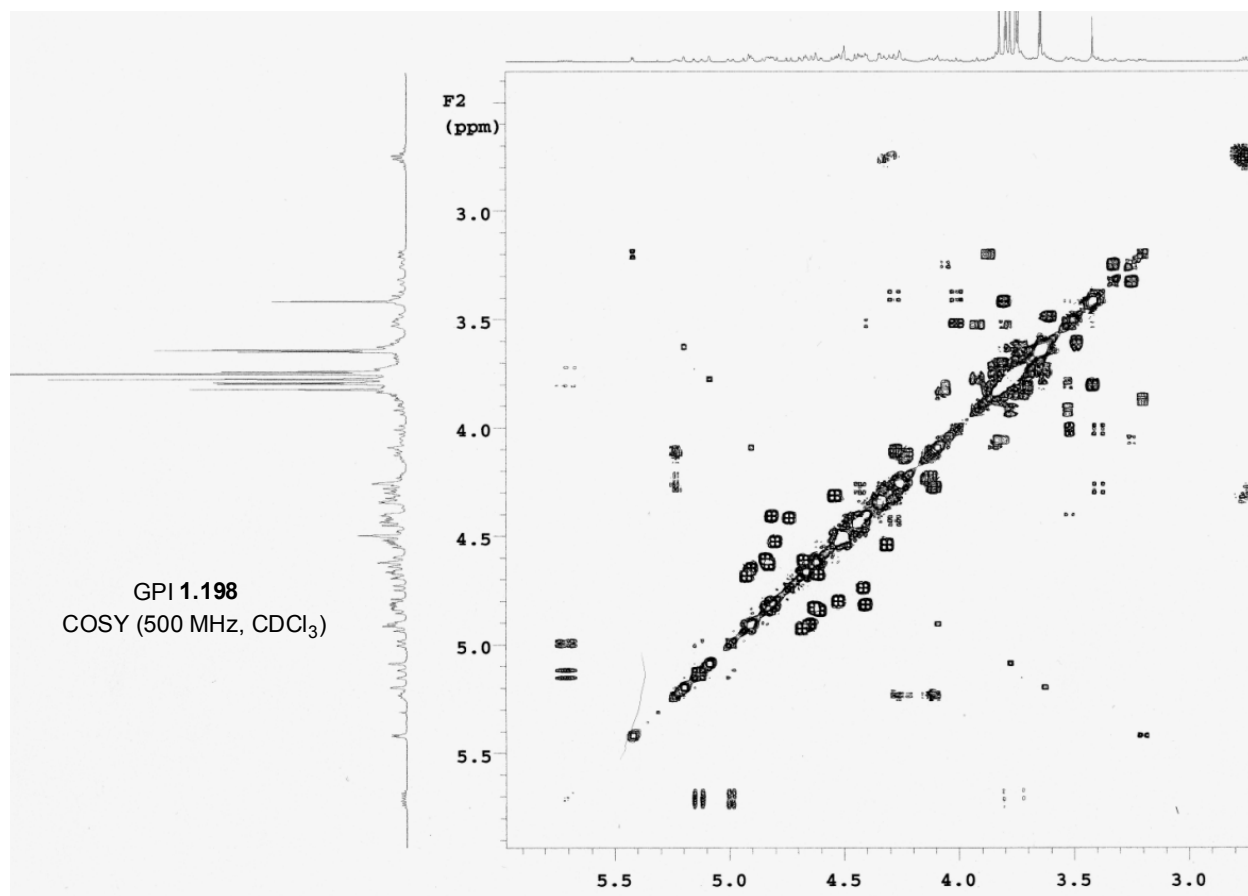
GPI **1.198**
^{1}H NMR (500 MHz, CDCl$_3$)

GPI **1.198**
^{13}C NMR (125 MHz, CDCl$_3$)

GPI **1.198**
COSY (500 MHz, CDCl$_3$)

GPI **1.198**
HMQC (500 MHz, CDCl$_3$)

Single Mass Analysis
Tolerance = 5.0 PPM / DBE: min = -1.5, max = 150.0
Element prediction: Off
Number of isotope peaks used for i-FIT = 3

GPI **1.198**
HR ESI MS

Monoisotopic Mass, Even Electron Ions
356 formula(e) evaluated with 17 results within limits (up to 50 best isotopic matches for each mass)
Elements Used:
C: 180-196   H: 230-260   N: 3-5   O: 40-52   23Na: 0-1   P: 0-1
BEN SWARTS   BSM-VII-119
2008-07b.pro
2009_0518_0436a 19 (0.389) Cm ((17+19:20+22:24)-(4:6+36:43)x2.000)

LCT Premier 18-May-2009 15:03:15
1: TOF MS ES+
8.55e+002
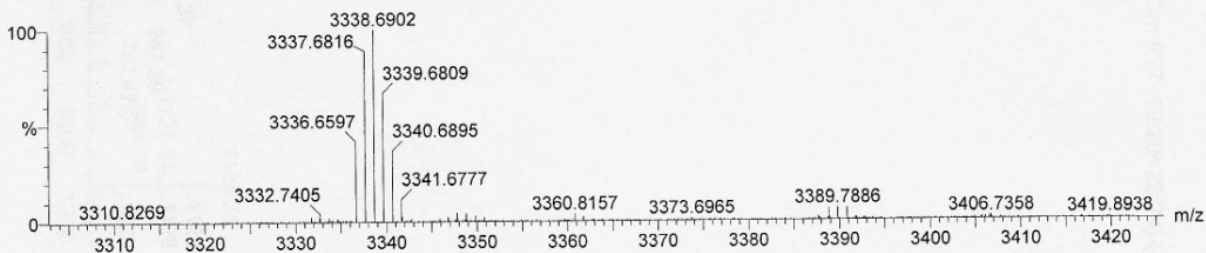
Mass	Calc. Mass	mDa	PPM	DBE	i-FIT	i-FIT (Norm)	Formula
Minimum:				-1.5			
Maximum:		5.0	5.0	150.0			
3336.6597	3336.6590	0.7	0.2	67.5	15.2	3.0	C187 H245 N4 O46 23Na P
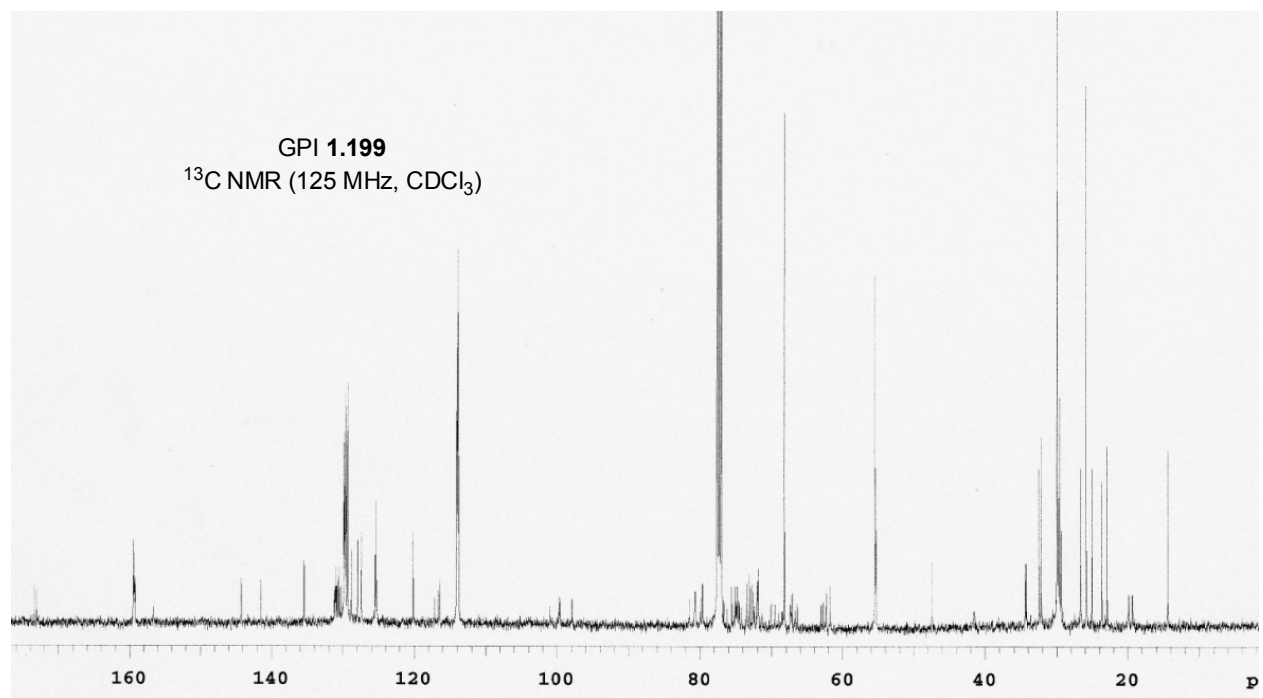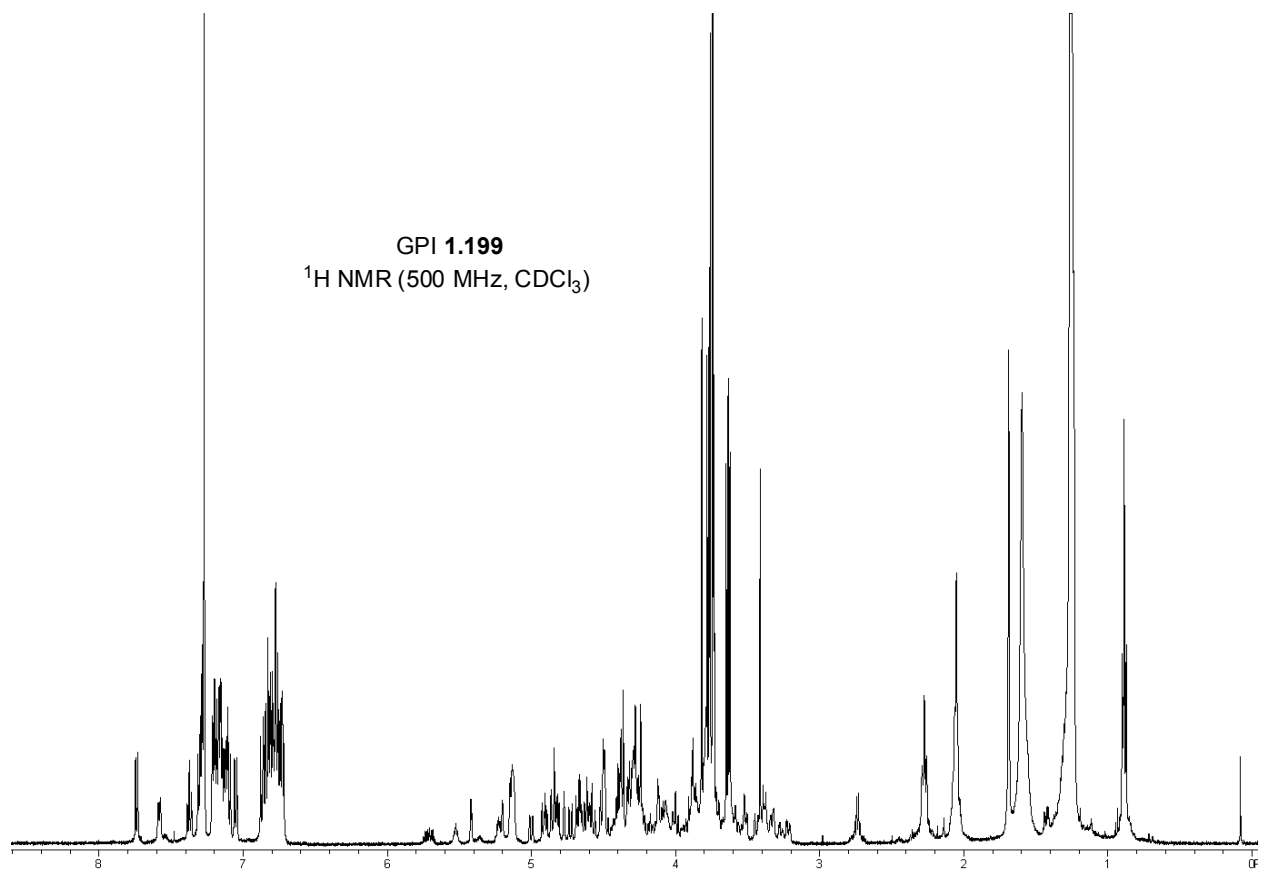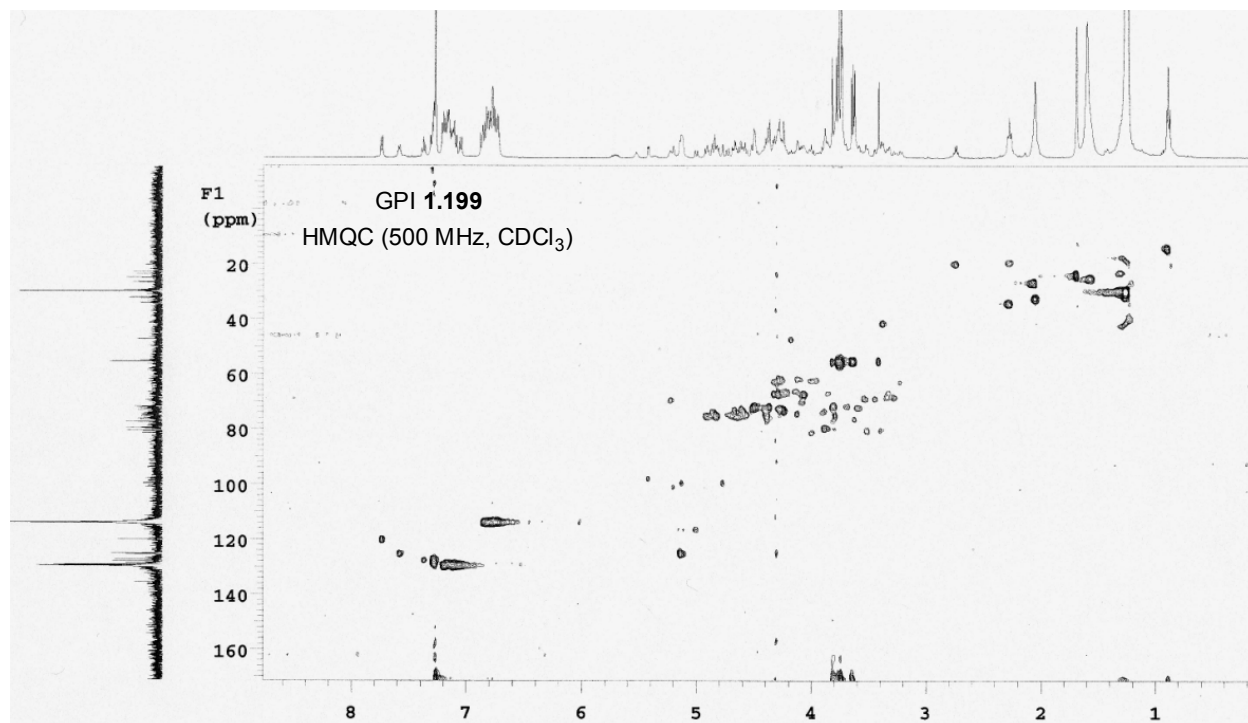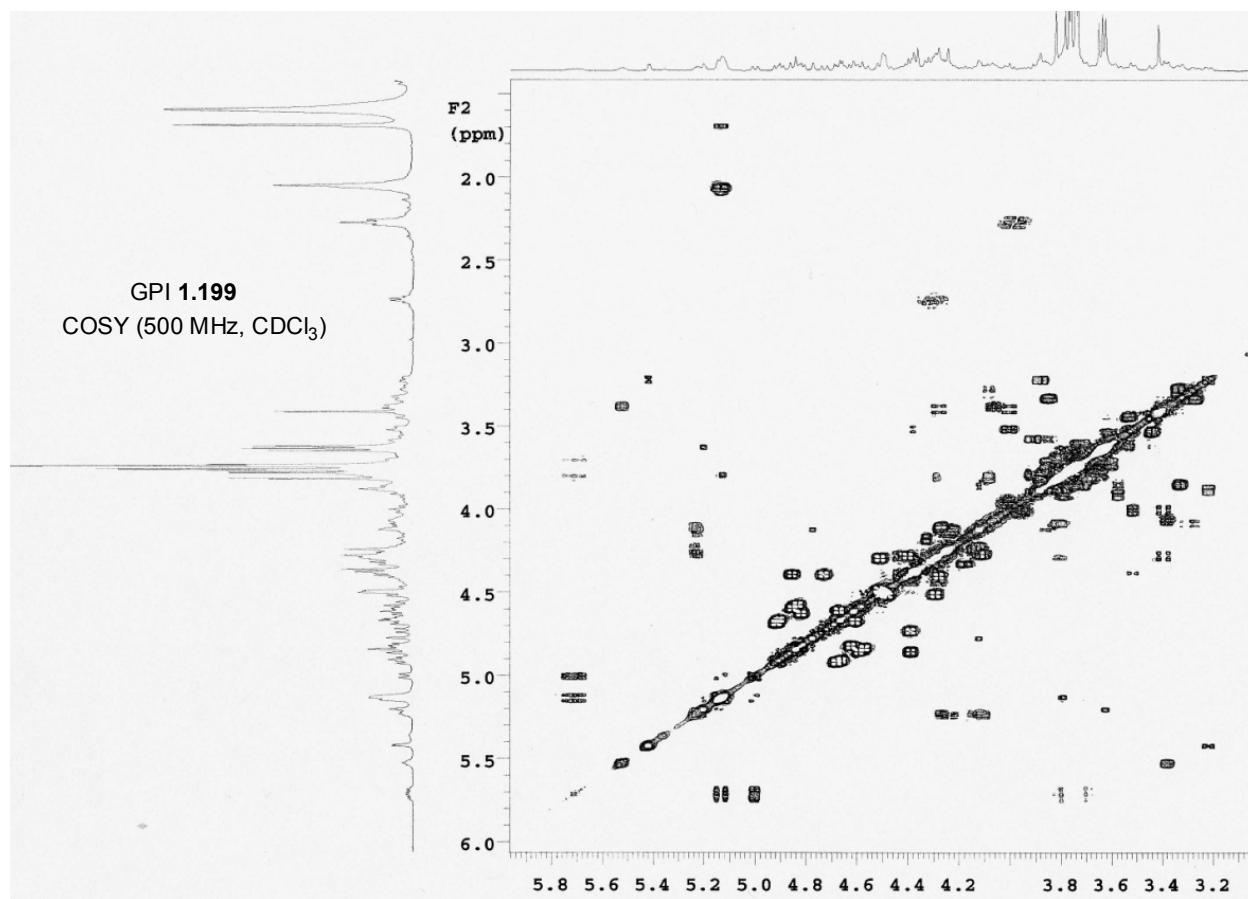
GPI **1.199**
^{1}H NMR (500 MHz, CDCl$_3$)

GPI **1.199**
^{13}C NMR (125 MHz, CDCl$_3$)

GPI **1.199**
COSY (500 MHz, CDCl$_3$)

GPI **1.199**
HMQC (500 MHz, CDCl$_3$)

Single Mass Analysis
Tolerance = 5.0 PPM / DBE: min = -1.5, max = 150.0
Element prediction: Off
Number of isotope peaks used for i-FIT = 3

Monoisotopic Mass, Odd and Even Electron Ions
1022 formula(e) evaluated with 78 results within limits (up to 50 best isotopic matches for each mass)
Elements Used:
C: 190-220   H: 230-270   N: 0-8   O: 40-60   23Na: 0-1   P: 2-2
BEN SWARTS   BSM-VII-132
2008-07b.pro
2009_0528_0445b 15 (0.300) Cm (12:22-(3:7+35:44)x2.000)

LCT Premier 28-May-2009 13:57:35
1: TOF MS ES+
3.54e+002
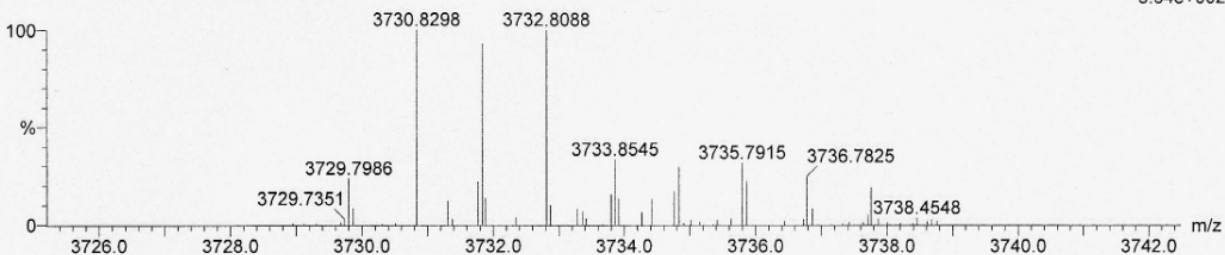
Mass	Calc. Mass	mDa	PPM	DBE	i-FIT	i-FIT (Norm)	Formula		
Minimum:				-1.5					
Maximum:		5.0	5.0	150.0					
3729.7986	3729.8001	-1.5	-0.4	70.0	59.8	5.2	C199 H270 N8 O56 P2		
	3729.8154	-16.8	-4.5	74.0	57.8	3.1	C203 H270 N8 O53 P2		
	3729.8041	-5.5	-1.5	74.0	59.2	4.5	C204 H270 N6 O54 P2		
	3729.8044	-5.8	-1.6	75.5	59.1	4.4	C205 H269 N7 O51 23Na P2		
	3729.7929	5.7	1.5	74.0	60.6	5.9	C205 H270 N4 O55 P2		
	3729.7932	5.4	1.4	75.5	60.6	5.9	C206 H269 N5 O52 23Na P2		
	3729.7942	4.4	1.2	79.0	60.4	5.7	C206 H266 N8 O51 P2		
	3729.8068	-8.2	-2.2	78.5	58.7	4.0	C207 H268 N7 O51 P2		

GPI **1.201**
^{1}H NMR (500 MHz, CDCl$_3$)
mixture of 2 diastereomers

| Comment 1 | BMS_VII_Succinylation Product |
| Comment 2 | DHB Positive |

GPI **1.201**
MALDI TOF MS

m/z	SN	Intens.	Area	Res.
3794.089	69.5	77.02	199	6583

3794.089

3794.089

3767.073

GPI **1.202**
^{1}H NMR (500 MHz, CDCl$_3$)
mixture of 2 diastereomers
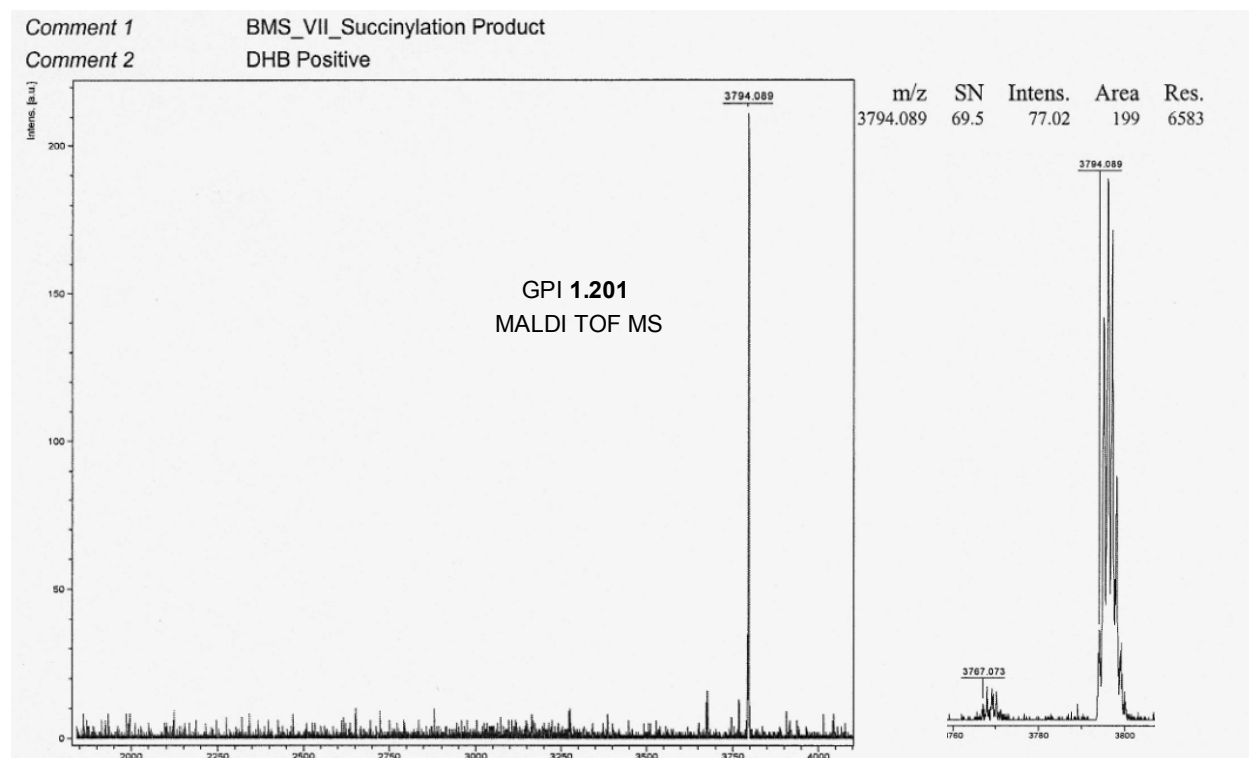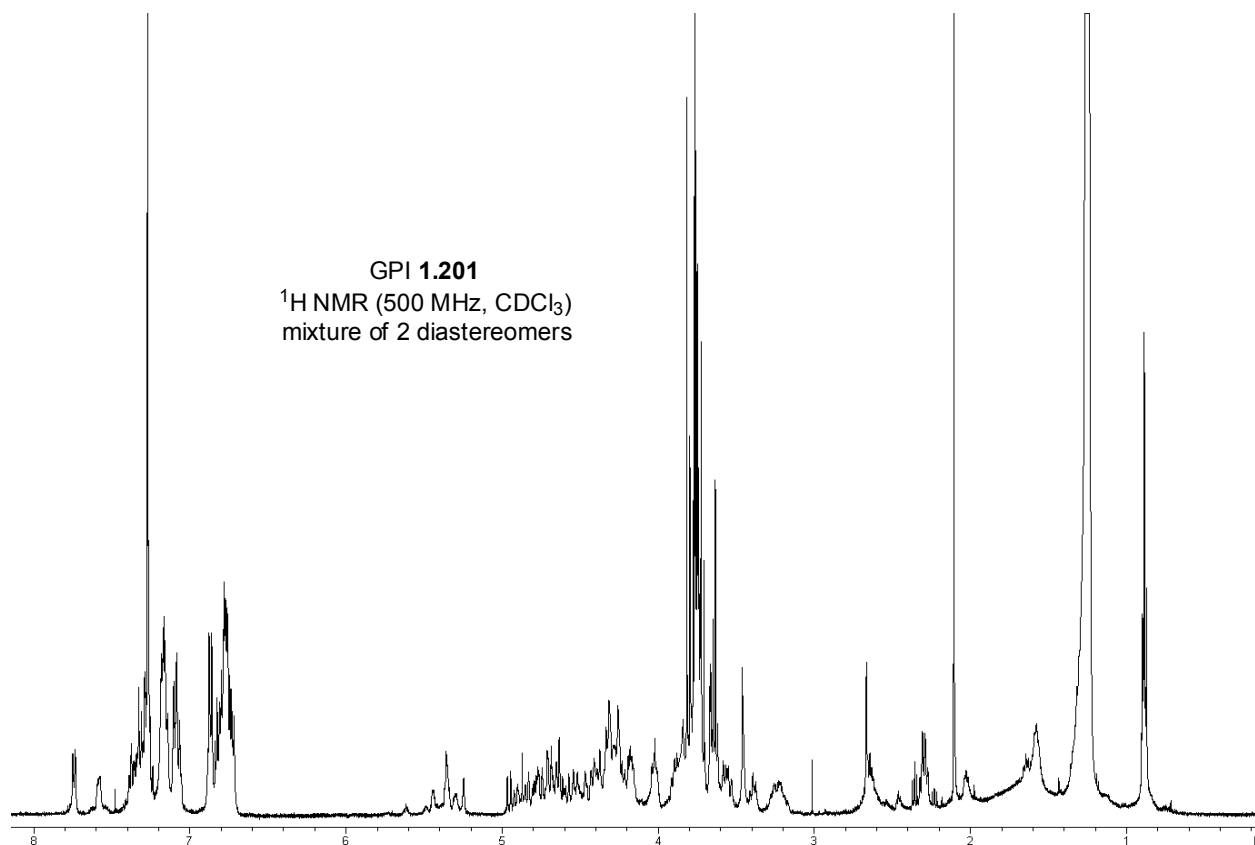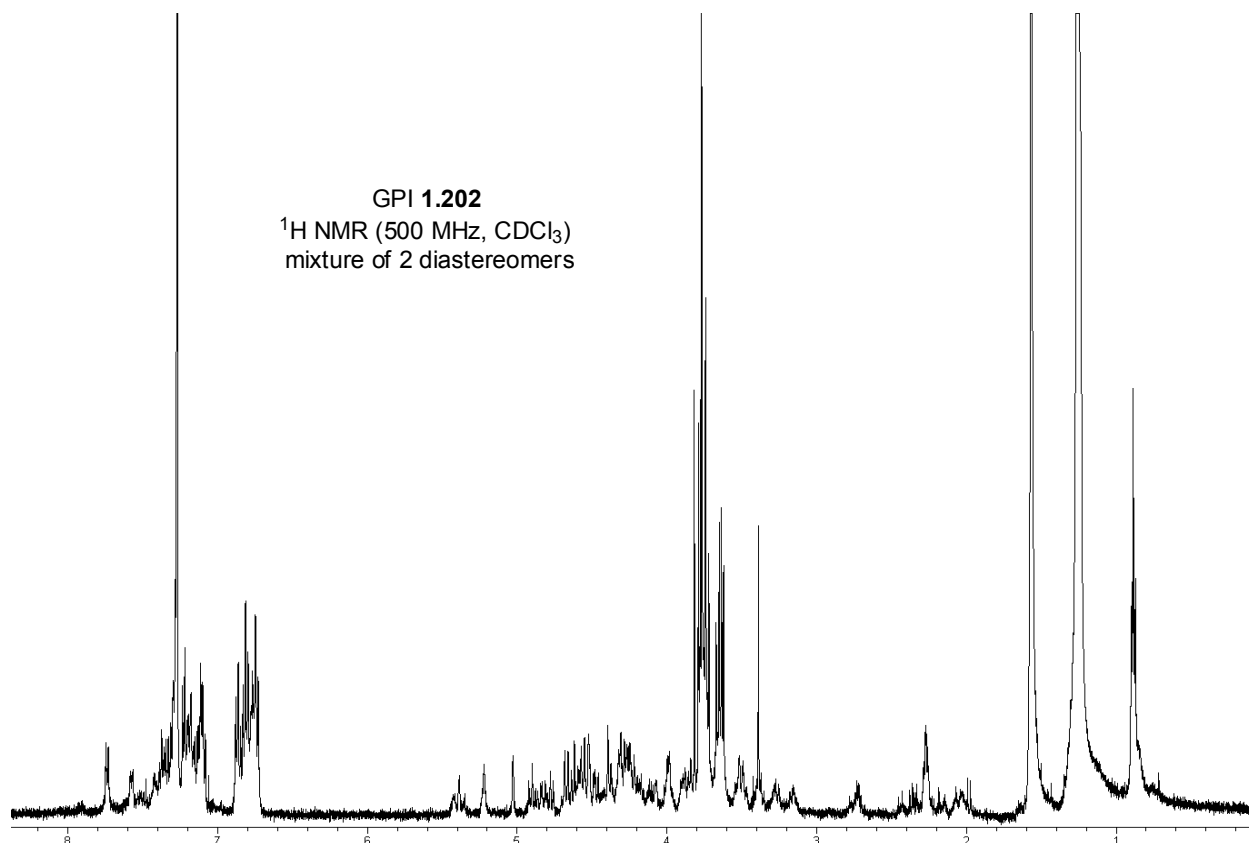
Single Mass Analysis
Tolerance = 5.0 PPM / DBE: min = 0.0, max = 100.0
Element prediction: Off
Number of isotope peaks used for i-FIT = 3

GPI **1.202**
HR ESI MS

Monoisotopic Mass, Odd and Even Electron Ions
196 formula(e) evaluated with 50 results within limits (all results (up to 1000) for each mass)
Elements Used:
C: 205-215   H: 260-270   N: 0-10   O: 45-60   23Na: 0-2   P: 2-2
2009_0819_0543a 14 (0.283) Cm (11:21)
LCT Premier 19-Aug-2009 14:46:26   BEN SWARTS   BSM-VII-186
1: TOF MS ES+
                                                                                          1.23e+003
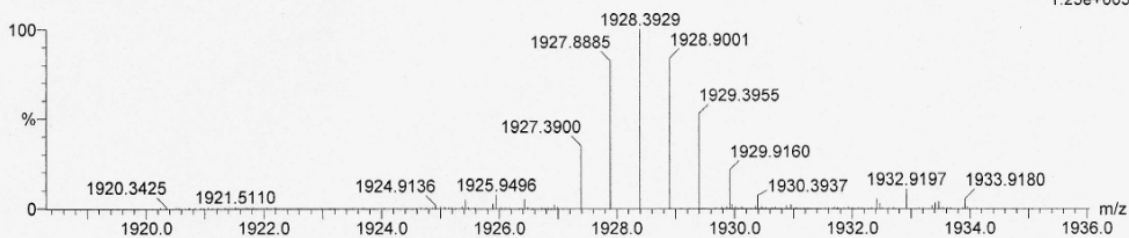
		0.0					
Minimum:			0.0				
Maximum:	5.0	5.0	100.0				

Mass	Calc. Mass	mDa	PPM	DBE	i-FIT	i-FIT (Norm)	Formula
	3854.7796	0.4	0.1	82.0	-1.$	n/a	C210 H267 N9 O52 23Na2 P2
	3854.7806	-0.6	-0.2	80.0	-1.$	n/a	C211 H270 N5 O56 23Na P2
	3854.7694	10.6	2.7	85.5	-1.$	n/a	C211 H264 N10 O52 23Na P2
3854.7800	3854.7683	11.7	3.0	82.0	-1.$	n/a	C211 H267 N7 O53 23Na2 P2

GPI **1.111**
^{1}H NMR (500 MHz,
CDCl$_3$/CD$_3$OD/D$_2$O 3:3:1)

GPI **1.111**
COSY NMR (500 MHz,
CDCl$_3$/CD$_3$OD/D$_2$O 3:3:1)

GPI **1.111**
HMQC NMR (500 MHz, CDCl$_3$/CD$_3$OD/D$_2$O 3:3:1)

Comment 1   BMS-VIII-02 GPI-Alkyne Target Molecule
Comment 2   DHB Positive

m/z	SN	Intens.	Area	Res.
1841.420	23.7	45.00	20	4548

GPI **1.111**
MALDI TOF MS
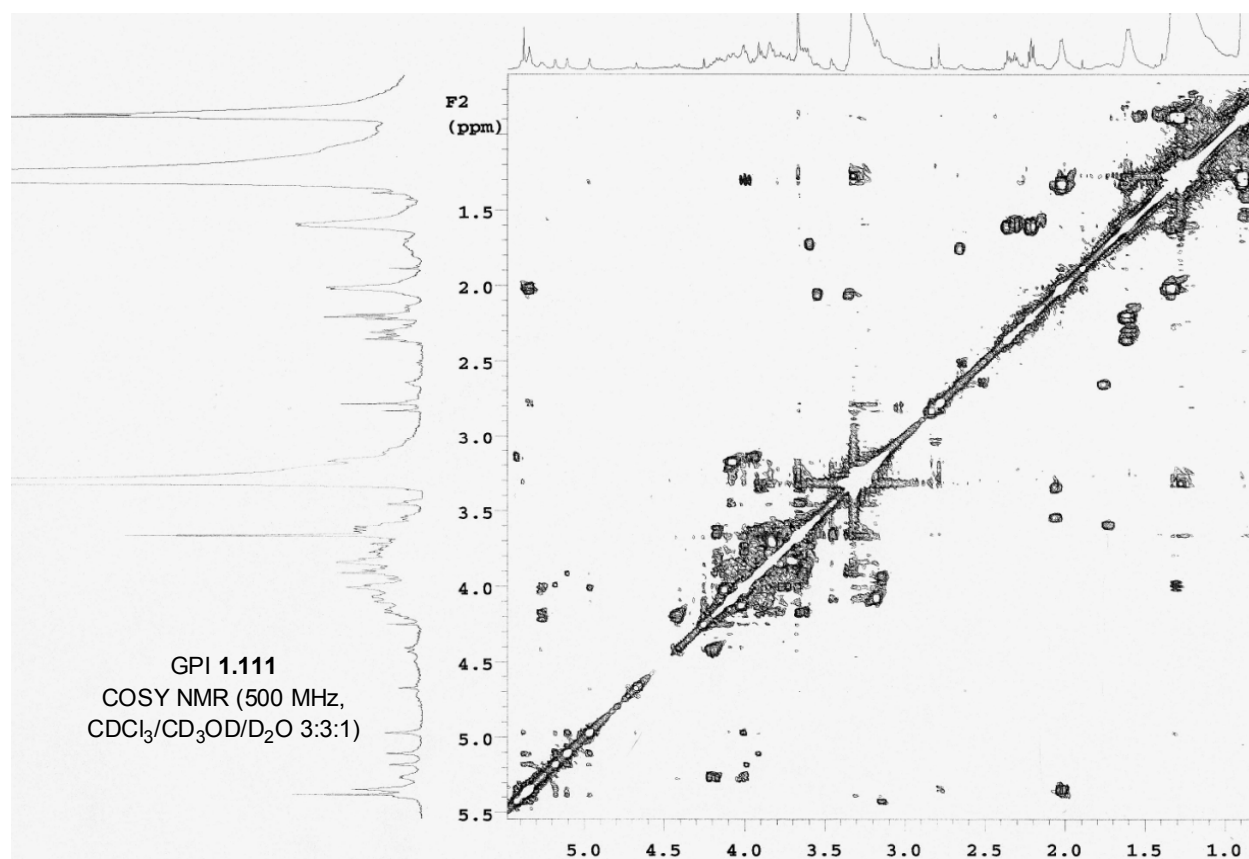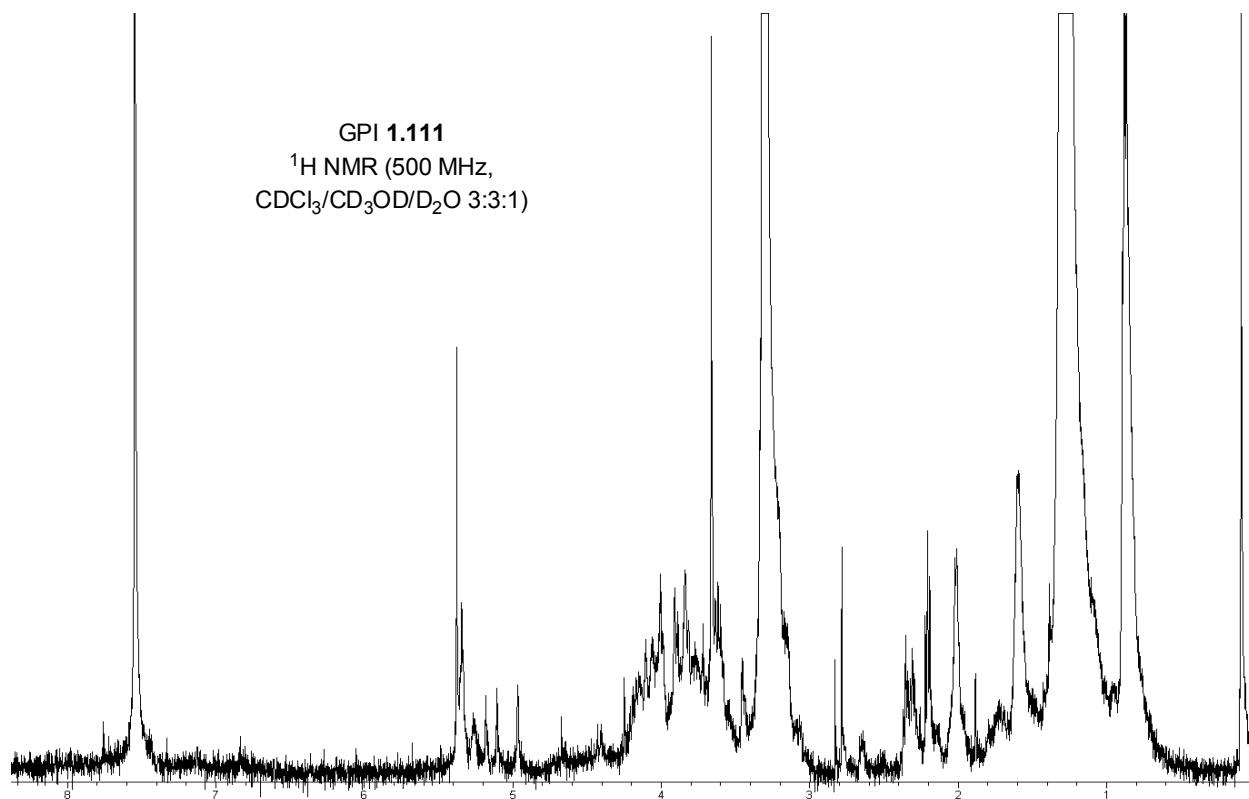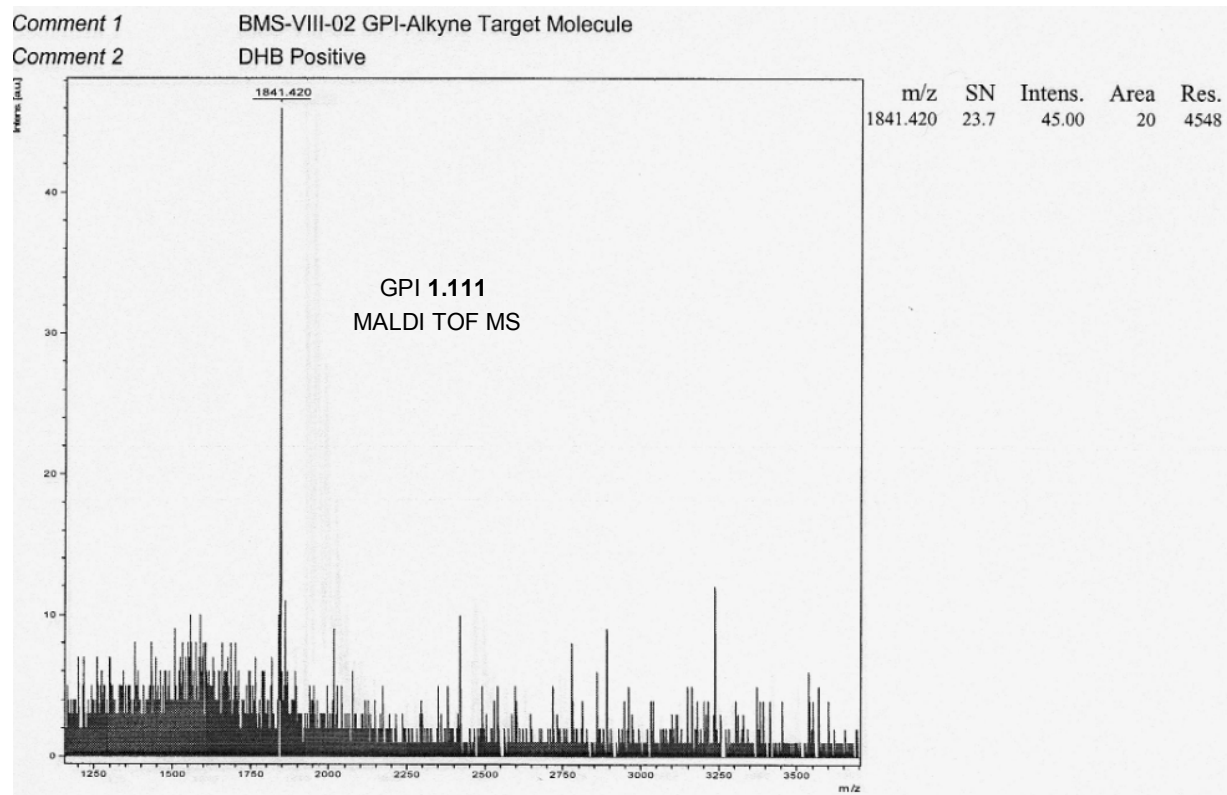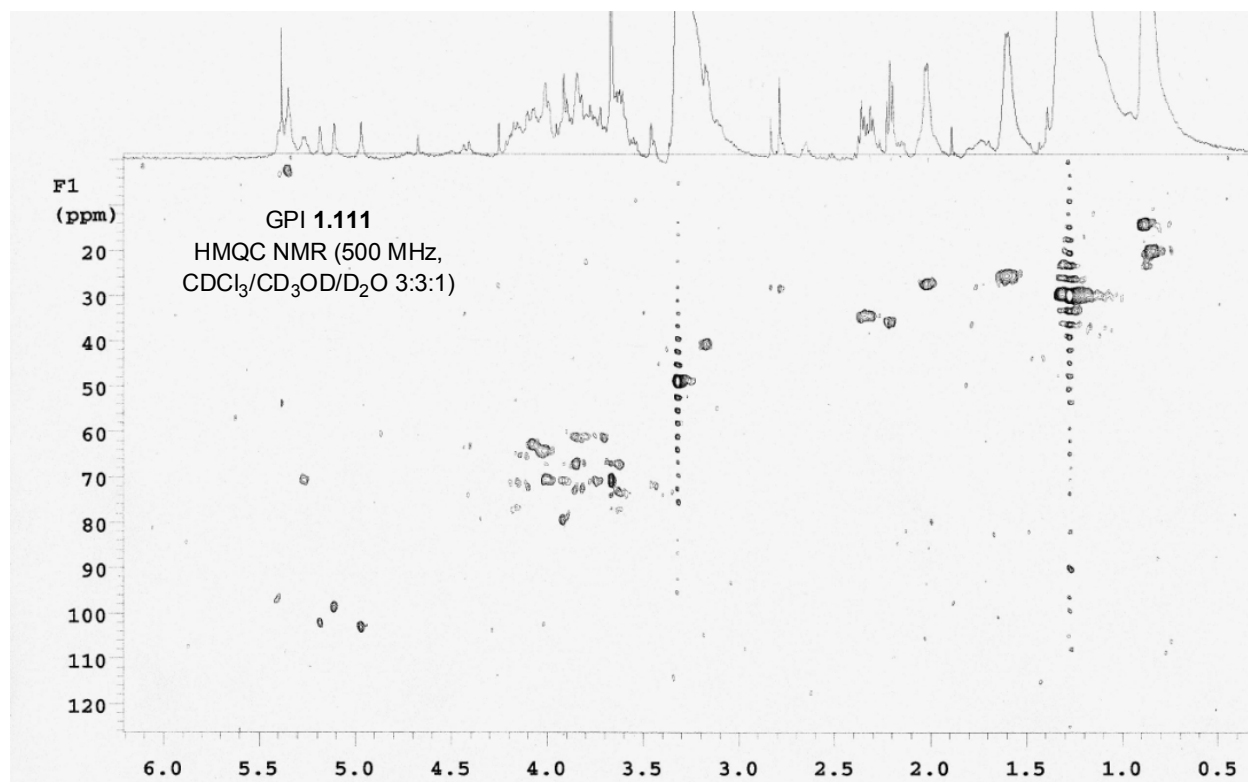
Comment 1   BMS-GPI-Biotin-Protected
Comment 2   DHB Positive
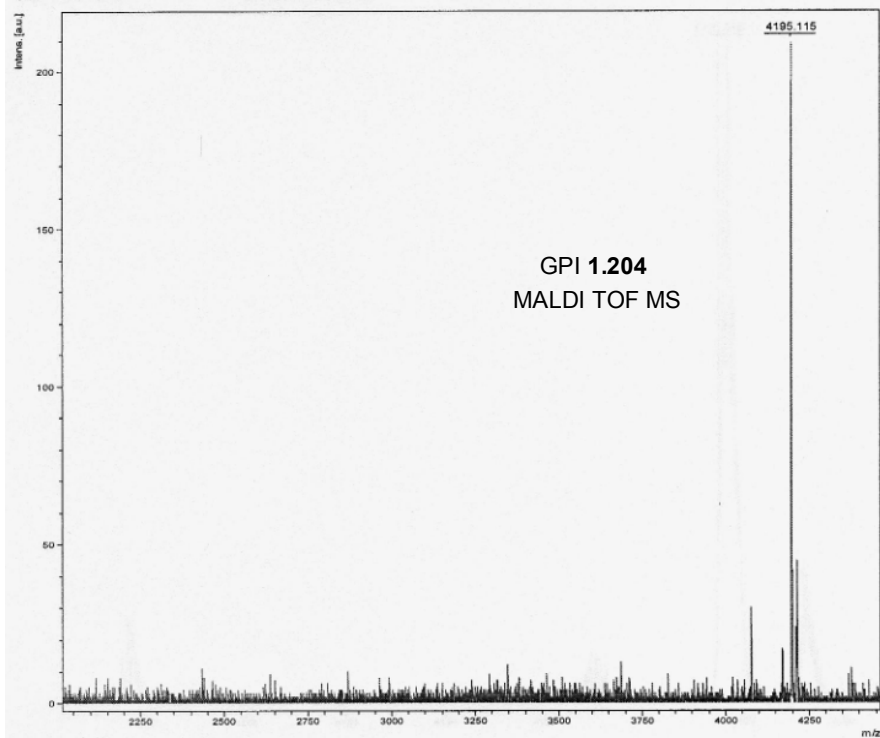
m/z	SN	Intens.	Area	Res.
4195.115	32.6	57.29	213	4808

GPI **1.204**
MALDI TOF MS

Comment 1   BMS-VIII-GPI-Biotin-Purified Positive
Comment 2   DHB Positive Mode
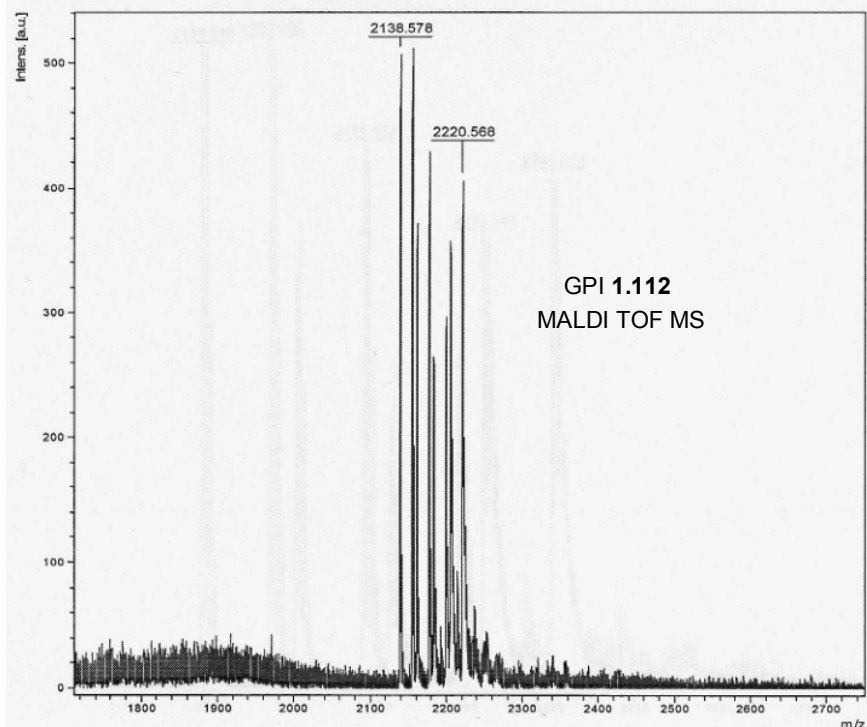
m/z	SN	Intens.	Area	Res.
2138.578	56.0	451.00	210	5224
2154.556	54.9	442.00	206	5071
2160.570	41.1	331.00	173	4727
2176.582	43.7	352.00	180	4549
2182.544	27.2	219.00	122	4438
2198.543	33.3	268.00	138	4444
2204.582	38.4	309.00	208	3267
2220.568	40.1	323.00	205	3343

GPI **1.112**
MALDI TOF MS

Appendix B: Selected Characterization Data From Chapter 2
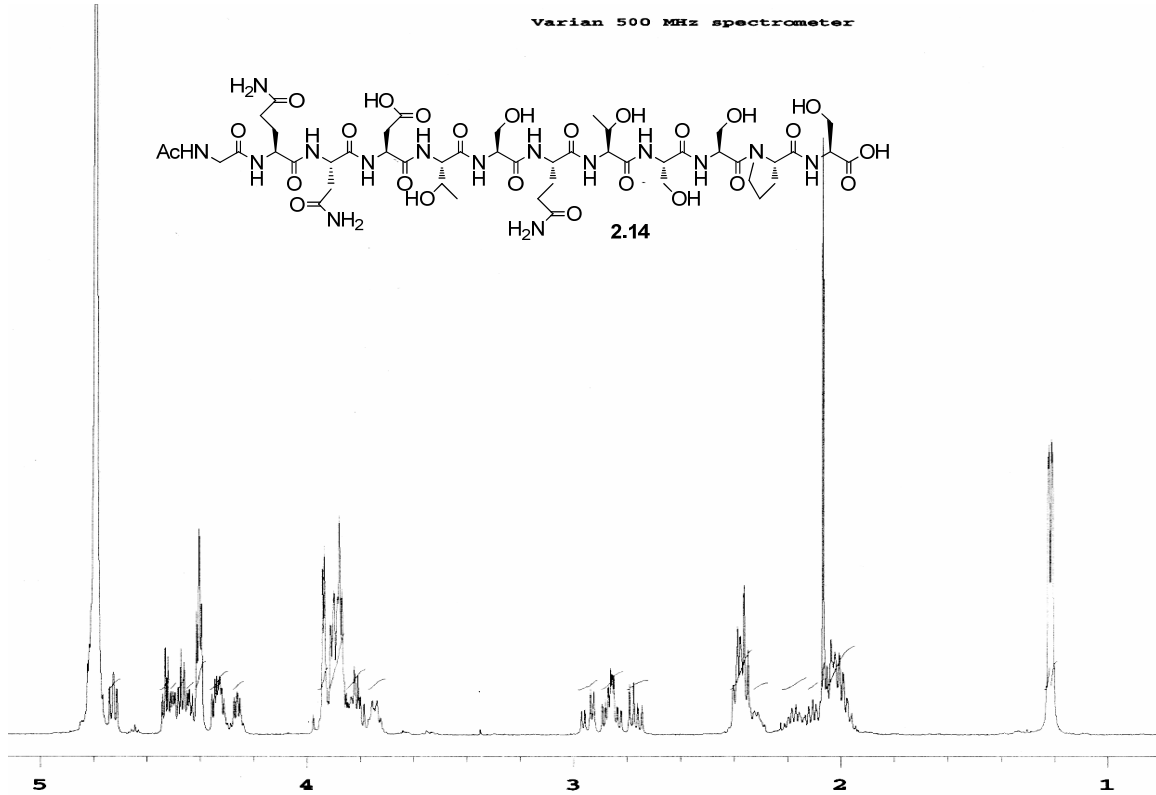
Varian 500 MHz spectrometer

2.14

Elemental Composition Report   **Page 1**

Single Mass Analysis
Tolerance = 6.0 PPM / DBE: min = -1.5, max = 50.0
Element prediction: Off
Number of isotope peaks used for i-FIT = 3

Monoisotopic Mass, Even Electron Ions
842 formula(e) evaluated with 2 results within limits (up to 50 best isotopic matches for each mass)
Elements Used:
C: 0-50   H: 0-100   N: 0-15   O: 0-25   23Na: 0-1
Guo- Ben Swarts CPS2-NHAc mw1249 LCT0074 2uL meoh 1cm stk
Shay 2008-07b.pro   LCT Premier
2008_0813_0074_09 14 (0.301) Cm (12:17-1:7x2.000)

15:08:57 13-Aug-2008

1: TOF MS ES+
4.11e+002
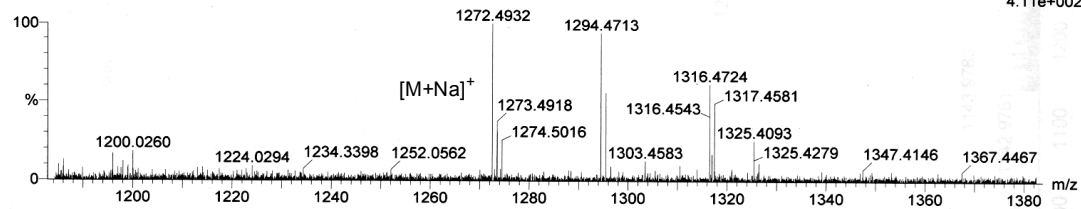

```
Minimum:                        -1.5
Maximum:            5.0   6.0   50.0

Mass        Calc. Mass   mDa   PPM   DBE    i-FIT   i-FIT (Norm)  Formula

1272.4932   1272.4956    -2.4  -1.9  17.5   160.6   0.3           C47  H75  N15  O25
                                                                  23Na
            1272.4980    -4.8  -3.8  20.5   161.5   1.3           C49  H74  N15  O25
```

Heteronuclear polarization transfer experiment

C13 AND DEPT SPECTRA

CH AND CH3 CARBONS

CH2 CARBONS

2.14

CH CARBONS

INDE
1
2
3
4
5
6
7
8
9
10
11
2
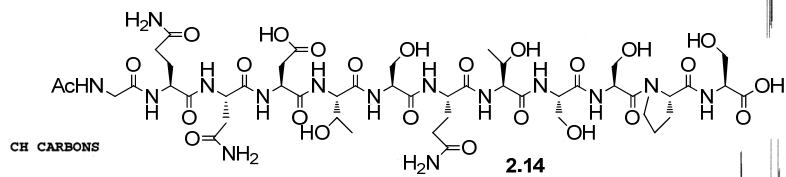
INDE
1
2
3
4
5
6
7
8
9
10
11
12
13
14
15
16
17
18
19
20
21
22
23
24

ALL CARBONS
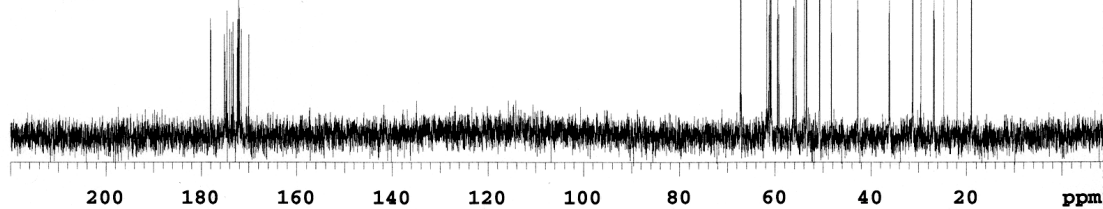
200 180 160 140 120 100 80 60 40 20 ppm

Mercury 400 spectrometer
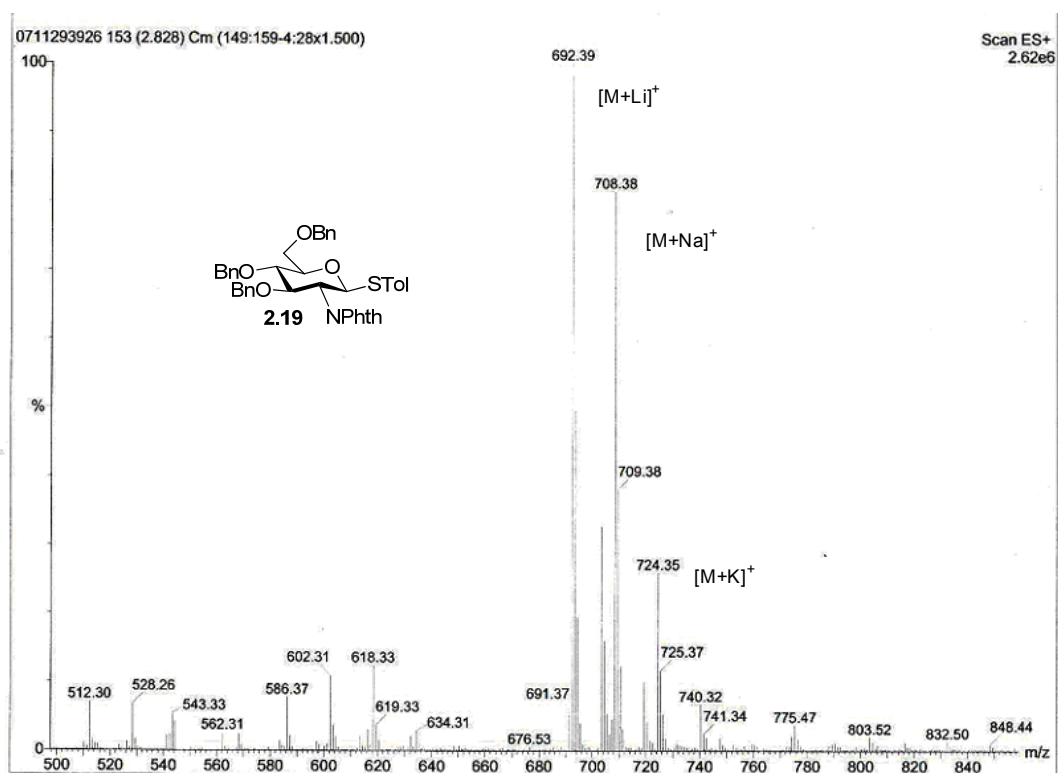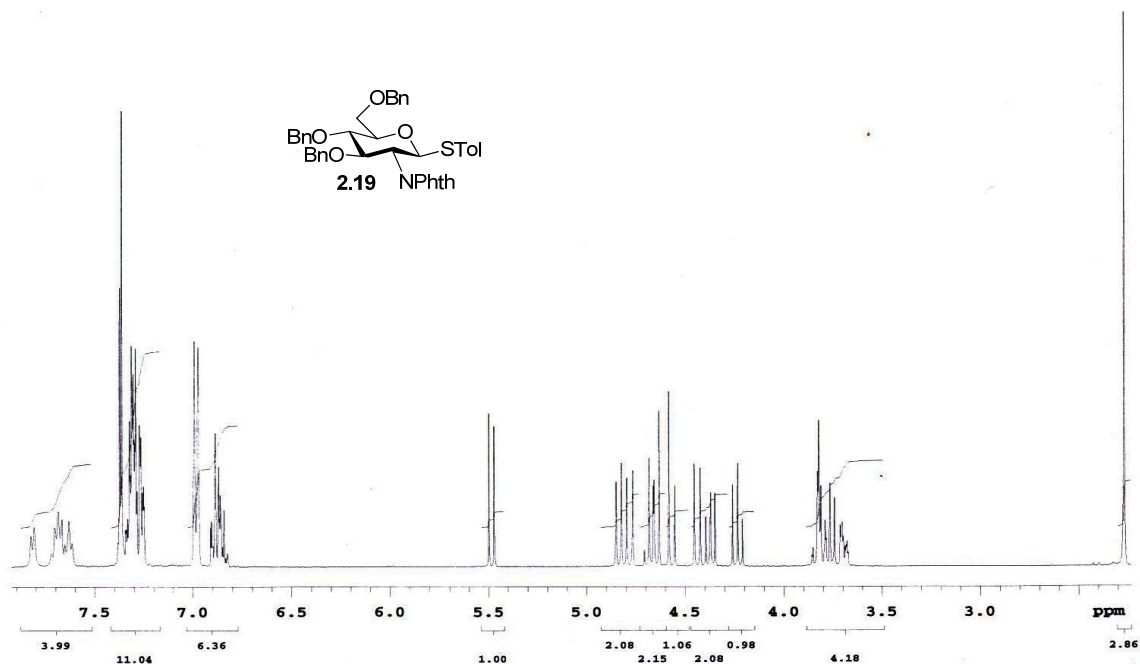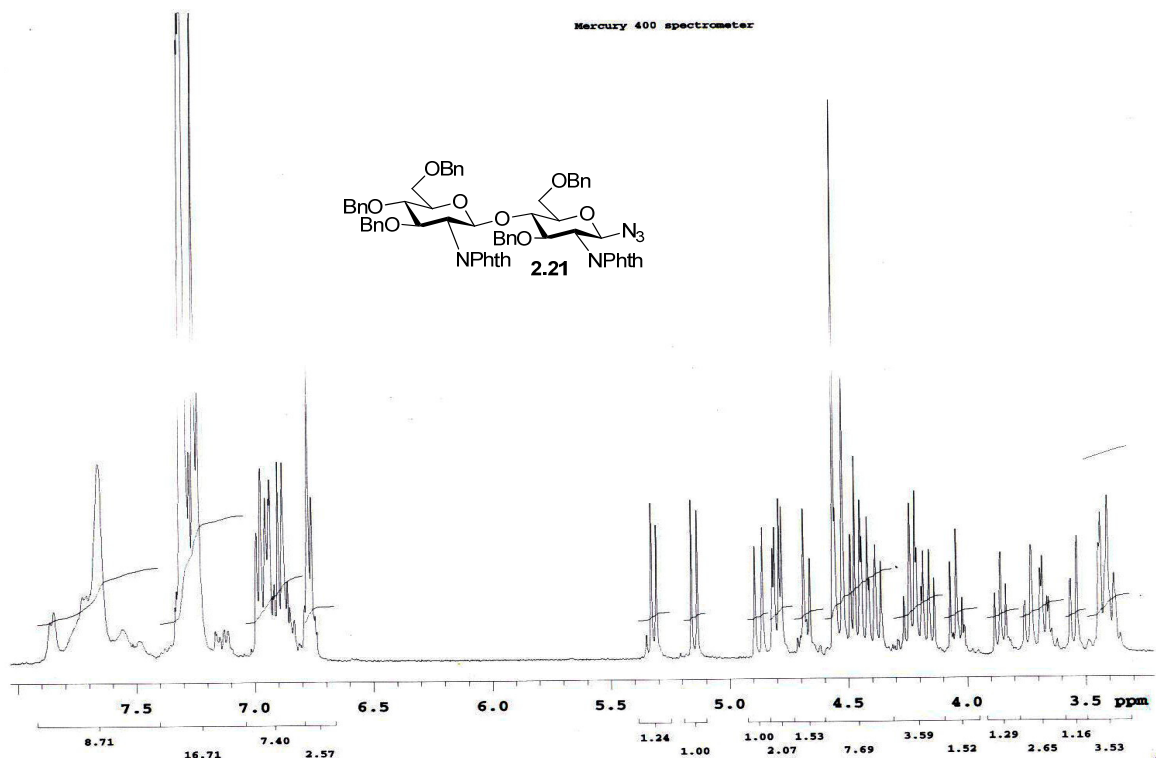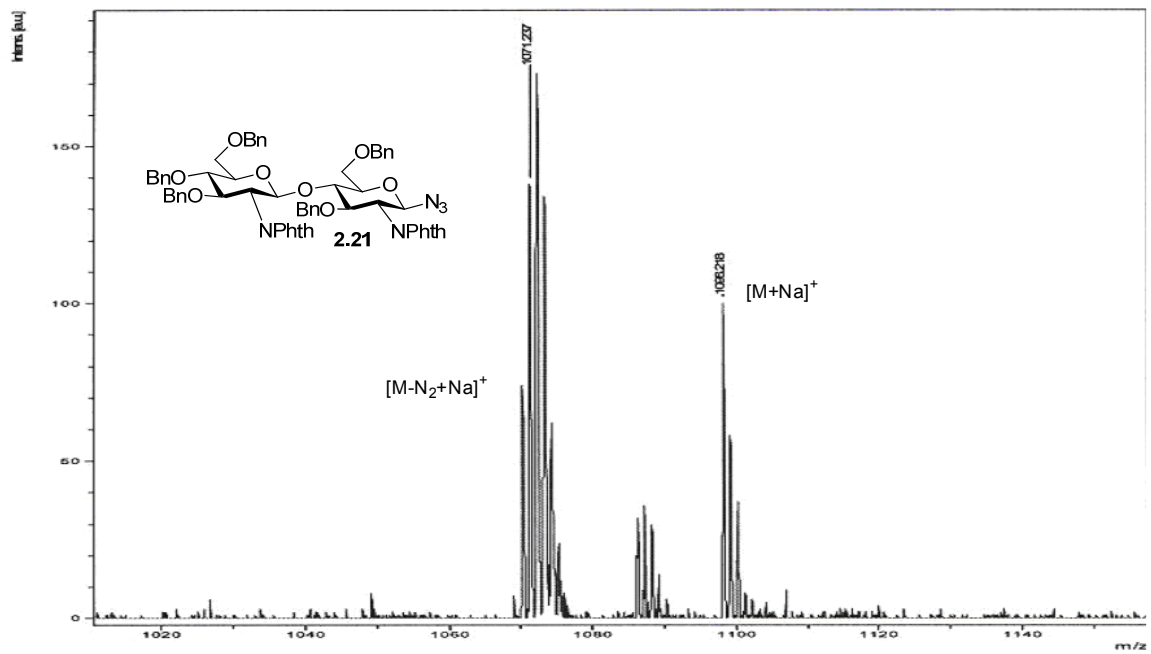
Mercury 400 spectrometer

7.5   7.0   6.5   6.0   5.5   5.0   4.5   4.0   3.5 ppm

8.71   7.40   1.24   1.00   1.53   3.59   1.29   1.16
     16.71   2.57   1.00   2.07   7.69   1.52   2.65   3.53

Comment 2

[M-N$_2$+Na]$^+$

[M+Na]$^+$

1020   1040   1060   1080   1100   1120   1140   m/z

Mercury 400 spectrometer

Varian 500 MHz spectrometer

Mercury 400 spectrometer

1.65 1.67   26.93   0.74   7.59 1.98   5.78 0.92   1.70   0.01 2.52
                                             3.77 2.89   4.76   2.71

1233.4211
[M+Na]+

1234.4419

1235.4384

1255.4540 [M-H+2Na]+
1256.4836

1236.4290   1257.5115

1247.4192
1157.3782 1172.4203   1237.3826 1250.4625 1263.3748   1309.5841 1324.5200

: s2pul

Varian 500 MHz spectrometer

2.15

5.5 5.0 4.5 4.0 3.5 3.0 2.5 2.0 1.5 1.0 0.5
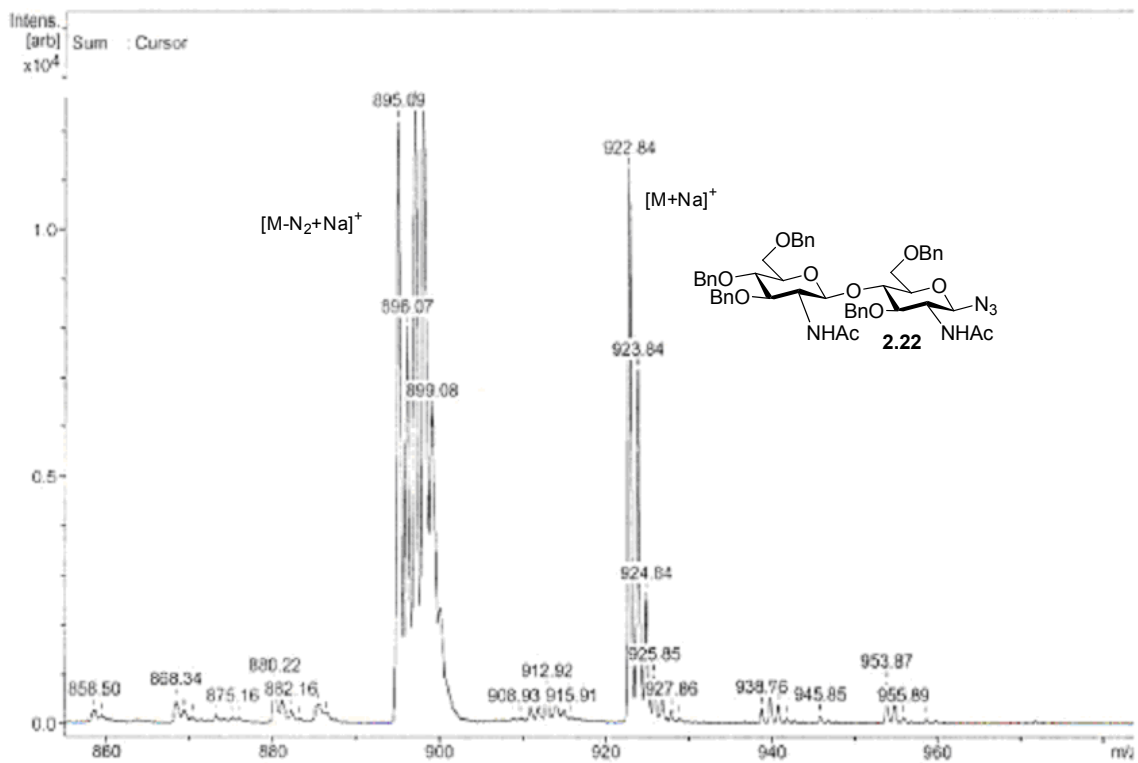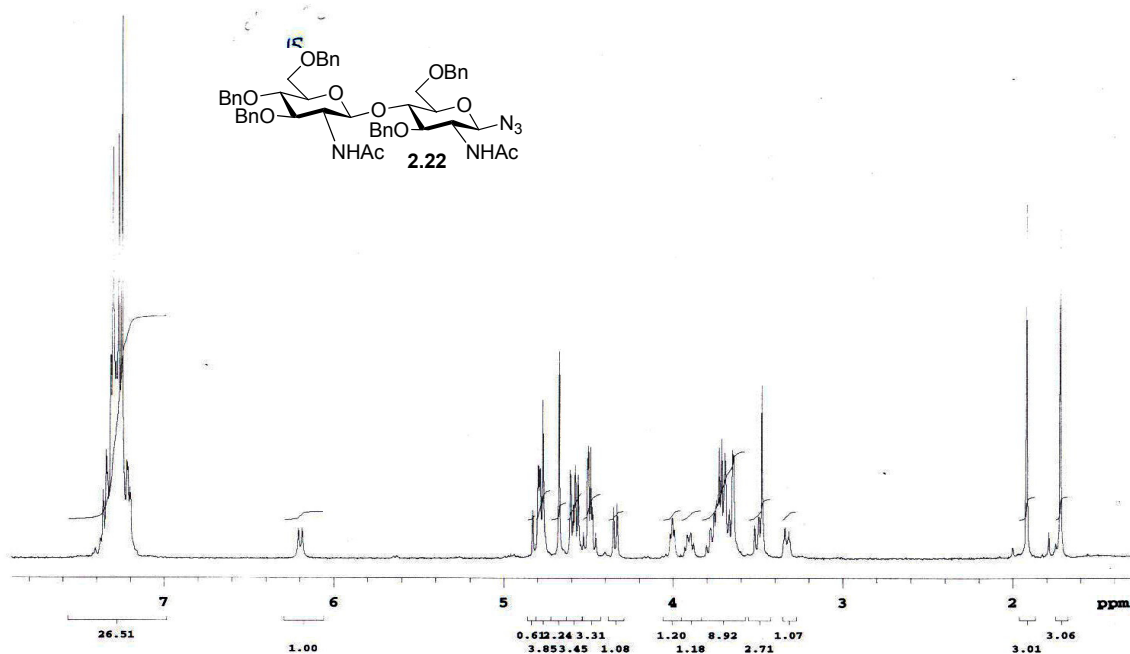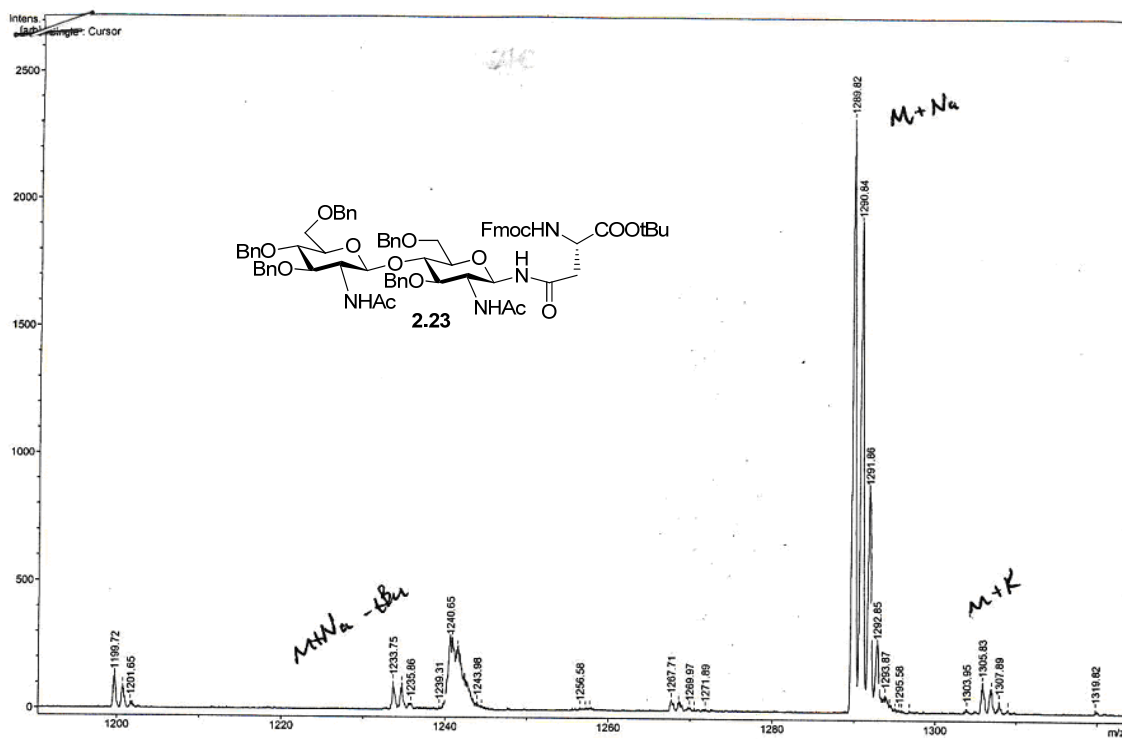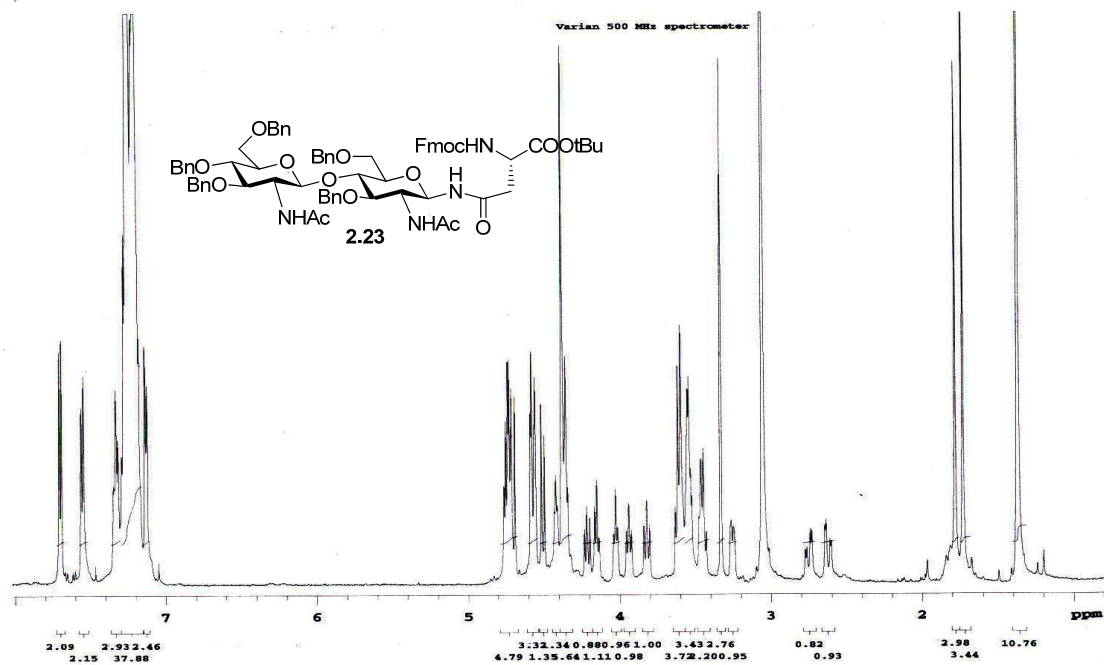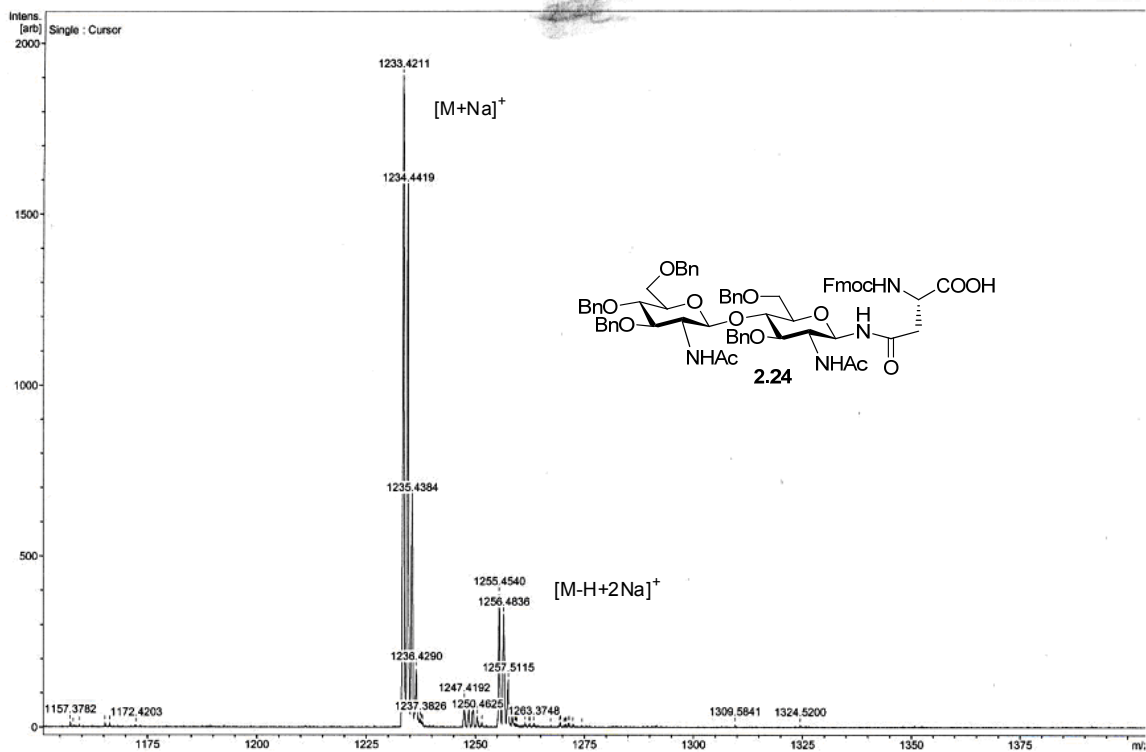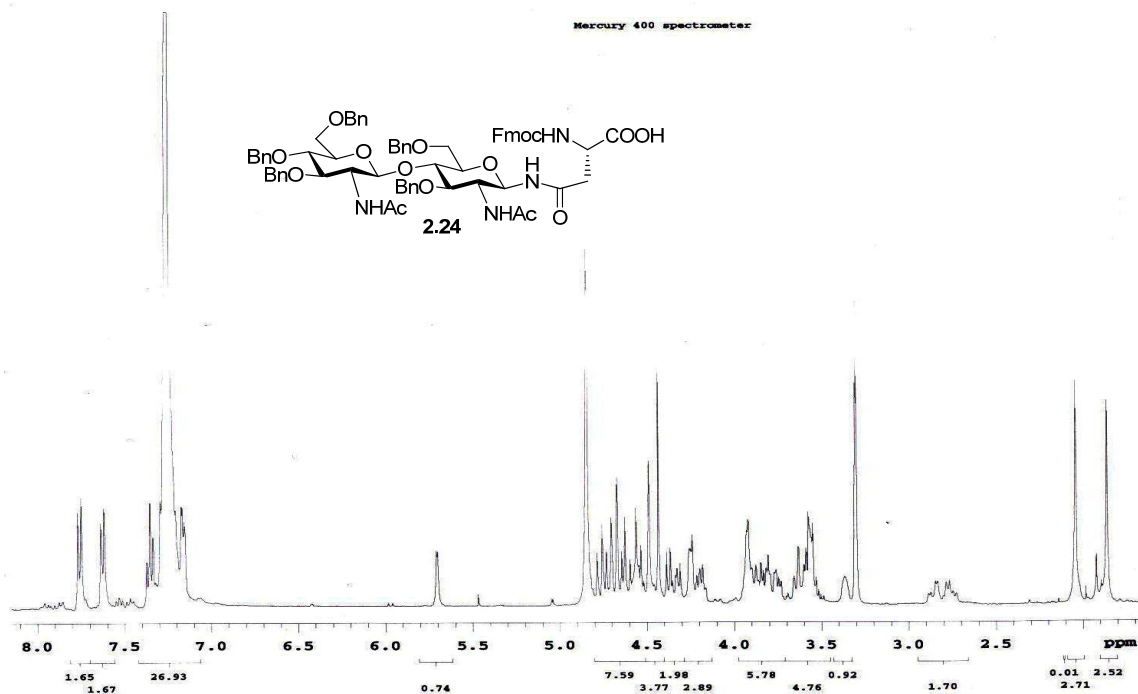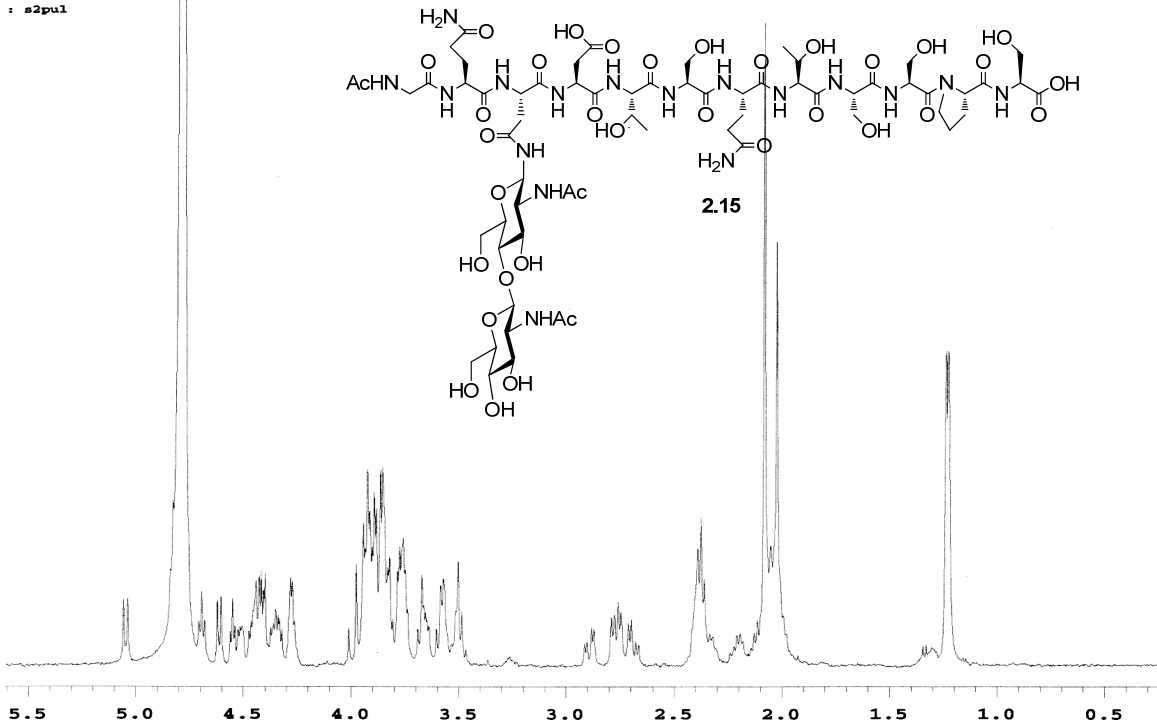
Guo- Ben Swarts Disac-CDS2-NHAc mw1655.7 LCT0078 3uL meoh:h2o st
Shay 2008-07b.pro **LCT Premier 15-Aug-2008 17:44:46**

2008_0815_0078_17 15 (0.300) Cm (12:19-38:47x2.000) 1: TOF MS ES+
2.71e3

100

839.8254

[M+H+Na]²⁺

828.8363

850.8186

829.3373

[M+2Na]²⁺ 851.3190

[M+2H]²⁺

%

837.3501   840.8282

851.8201

861.8107

841.3317   852.3223   862.8132   872.7935

888.7725

0
820   830   840   850   860   870   880   890   m/z
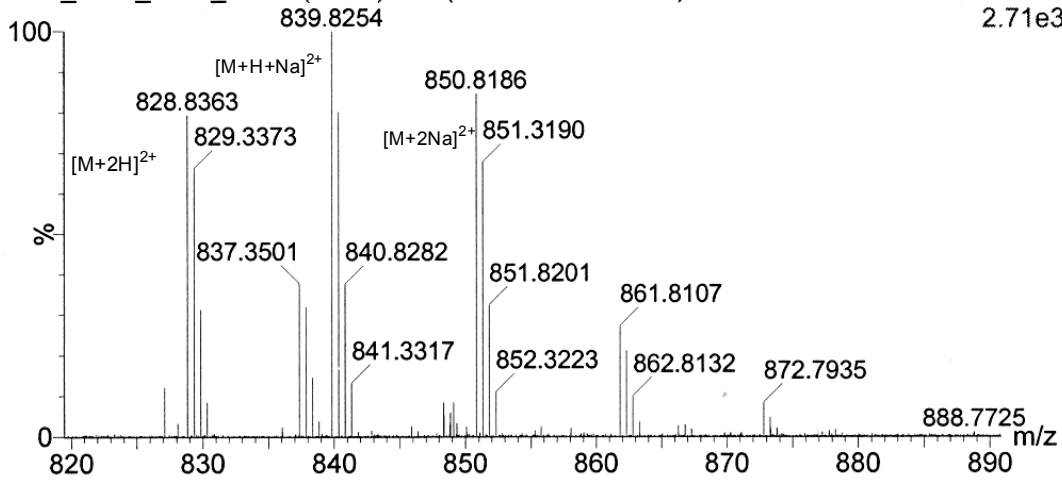
Heteronuclear polarization transfer experiment

DEPT SPECTRA
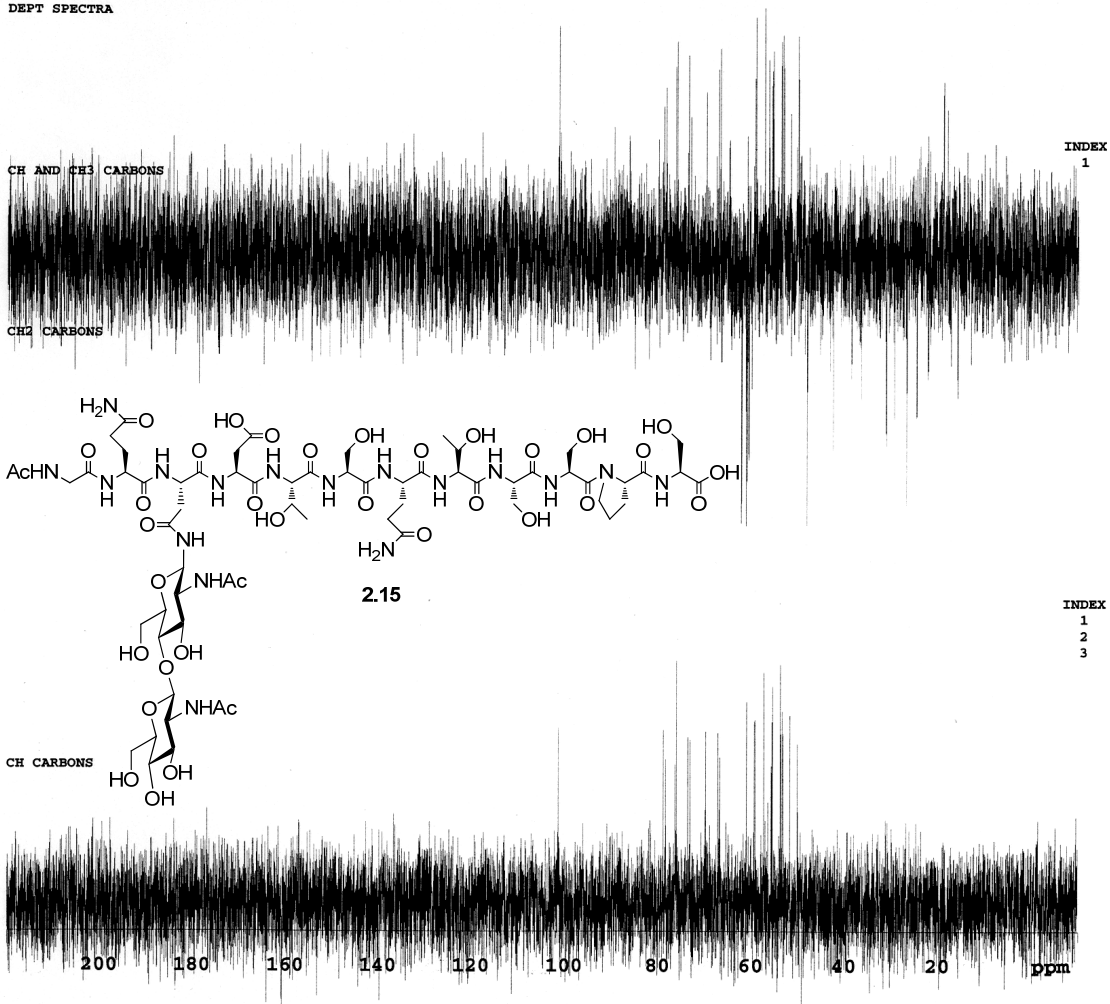
Varian 500 MHz spectrometer
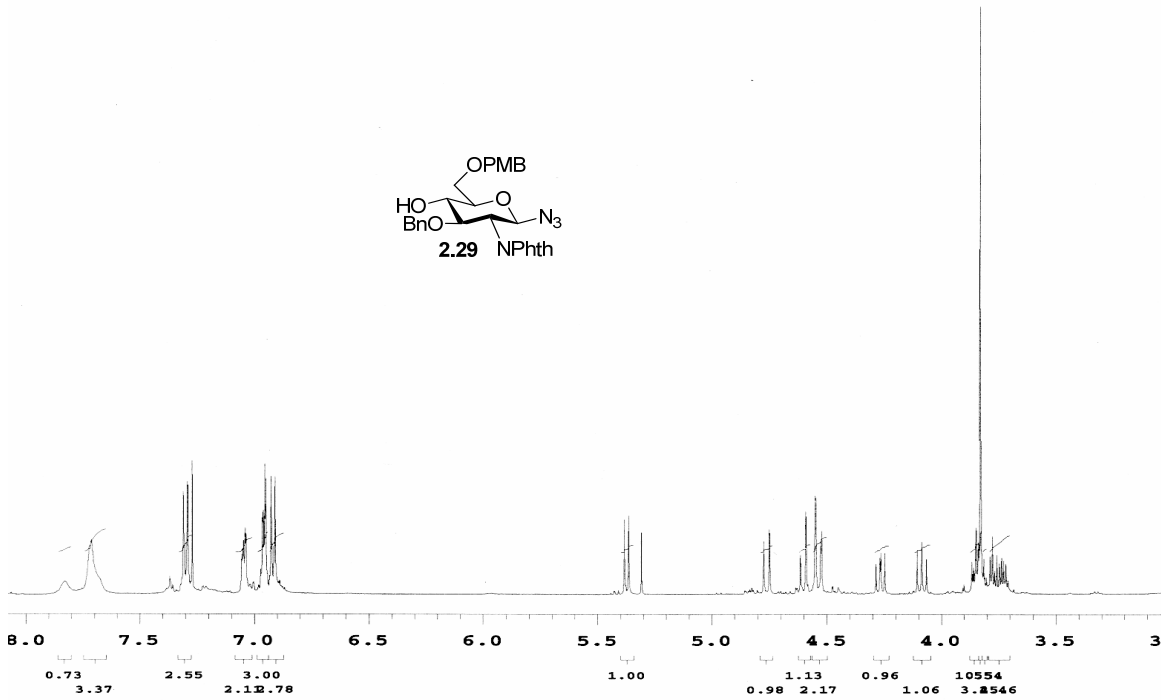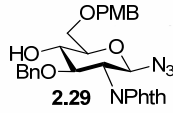
CH AND CH3 CARBONS

INDEX
1

CH2 CARBONS

2.15

INDEX
1
2
3

CH CARBONS

200 180 160 140 120 100 80 60 40 20 ppm

Varian 500 MHz spectrometer

8.0   7.5   7.0   6.5   6.0   5.5   5.0   4.5   4.0   3.5   3

0.73   2.55   3.00   1.00   1.13 0.96 10554
   3.37   2.12.78   0.98 2.17   1.06 3.8546

Elemental Composition Report

Page 1

Single Mass Analysis
Tolerance = 6.0 PPM   /   DBE: min = -1.5, max = 50.0
Element prediction: Off
Number of isotope peaks used for i-FIT = 3

Monoisotopic Mass, Even Electron Ions
746 formula(e) evaluated with 5 results within limits (up to 50 best isotopic matches for each mass)
Elements Used:
C: 0-500   H: 0-1000   N: 0-6   O: 0-7   23Na: 0-1

Guo- Ben Swarts BMS-II-23 mw544 LCT0073 1uL meoh 1cm stk
Shay 2008-07b.pro
2008_0813_0073_07 27 (0.582) Cm (26:34-1:6x6.000)
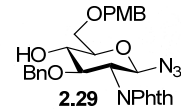
LCT Premier

14:45:48 13-Aug-2008

1: TOF MS ES+
9.84e+003
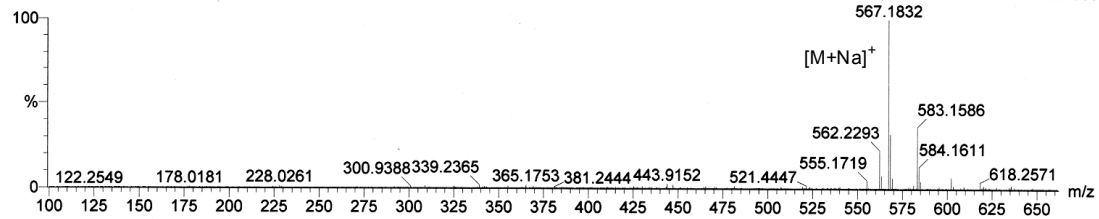
Minimum: -1.5
Maximum: 5.0   6.0   50.0

Mass	Calc. Mass	mDa	PPM	DBE	i-FIT	i-FIT (Norm)	Formula			
567.1832	567.1856	-2.4	-4.2	17.5	207.4	0.0	C29	H28	N4	O7 23Na
	567.1837	-0.5	-0.9	30.5	213.3	5.9	C41	H24	N2	23Na
	567.1821	1.1	1.9	29.5	213.3	6.0	C38	H23	N4	O2
	567.1808	2.4	4.2	24.5	213.5	6.2	C37	H27	O6	
	567.1861	-2.9	-5.1	33.5	215.2	7.8	C43	H23	N2	
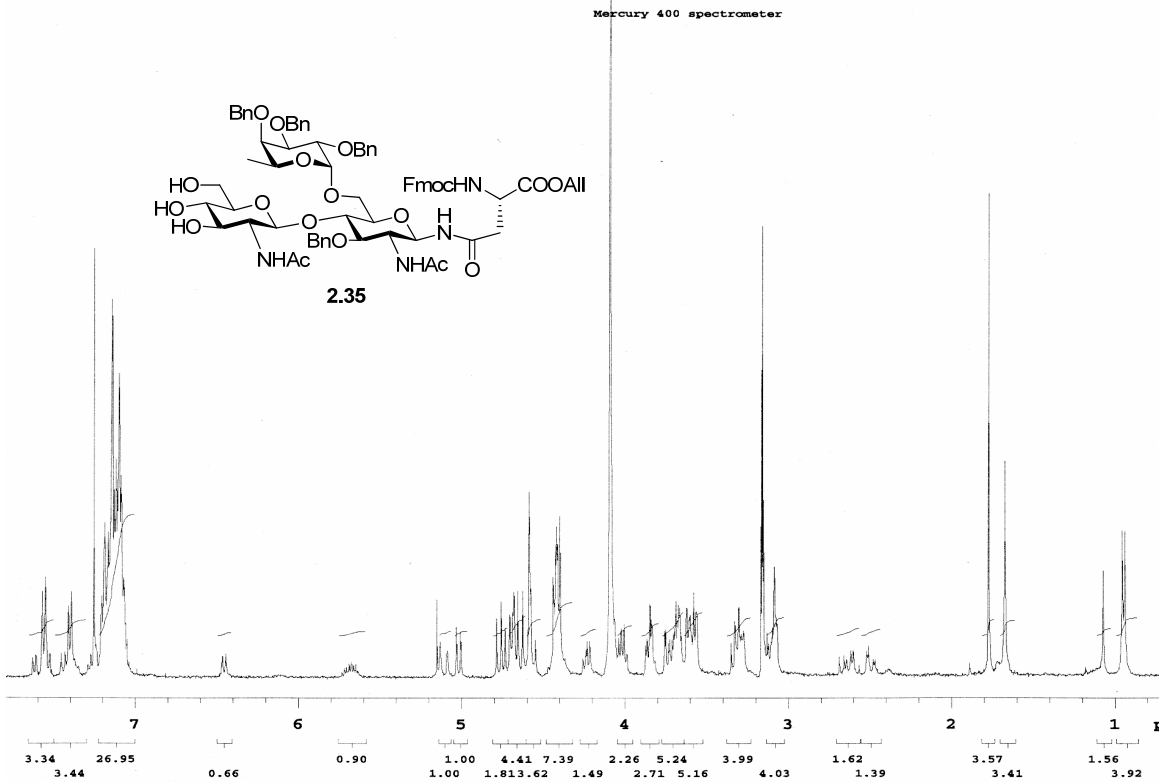
Mercury 400 spectrometer

2.35

	7			6		5			4		3			2		1		
3.34	26.95			0.90		1.00	4.41 7.39	2.26 5.24		3.99		1.62			3.57		1.56	
3.44		0.66				1.00	1.813.62 1.49	2.71 5.16	4.03		1.39				3.41			3.92

Elemental Composition Report

Page 1

Single Mass Analysis
Tolerance = 5.0 PPM / DBE: min = -1.5, max = 50.0
Element prediction: Off
Number of isotope peaks used for i-FIT = 3

Monoisotopic Mass, Even Electron Ions
506 formula(e) evaluated with 4 results within limits (up to 50 best isotopic matches for each mass)
Elements Used:
C: 0-72   H: 0-100   N: 0-5   O: 0-25   23Na: 0-1

Guo- Ben Swarts Bms-ii-85 mw1306 LCT0077 0.5uL meoh 1cm stk
Shay 2008-07b.pro   LCT Premier   16:06:53 13-Aug-2008
2008_0813_0077_16 13 (0.283) Cm (12:16-1:6x2.000)

1: TOF MS ES+
1.19e+004

$[M+Na]^+$ 1330.5422
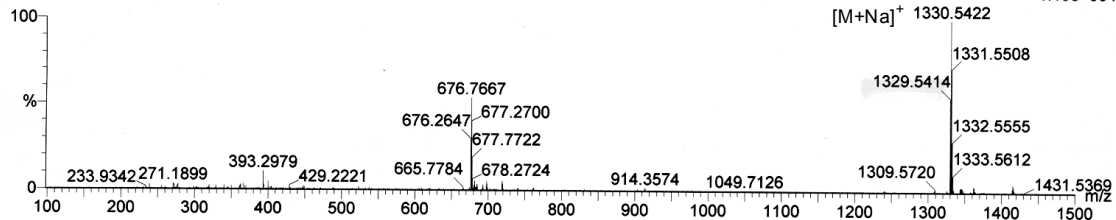
Minimum:				-1.5						
Maximum:		5.0	5.0	50.0						

Mass	Calc. Mass	mDa	PPM	DBE	i-FIT	i-FIT (Norm)	Formula			
1329.5414	1329.5417	-0.3	-0.2	24.5	98.8	1.1	C66	H86	N2	O25 23Na
	1329.5441	-2.7	-2.0	27.5	98.9	1.3	C68	H85	N2	O25
	1329.5458	-4.4	-3.3	28.5	99.2	1.5	C71	H86	O23	23Na
	1329.5471	-5.7	-4.3	33.5	99.4	1.8	C72	H82	N4	O19 23Na
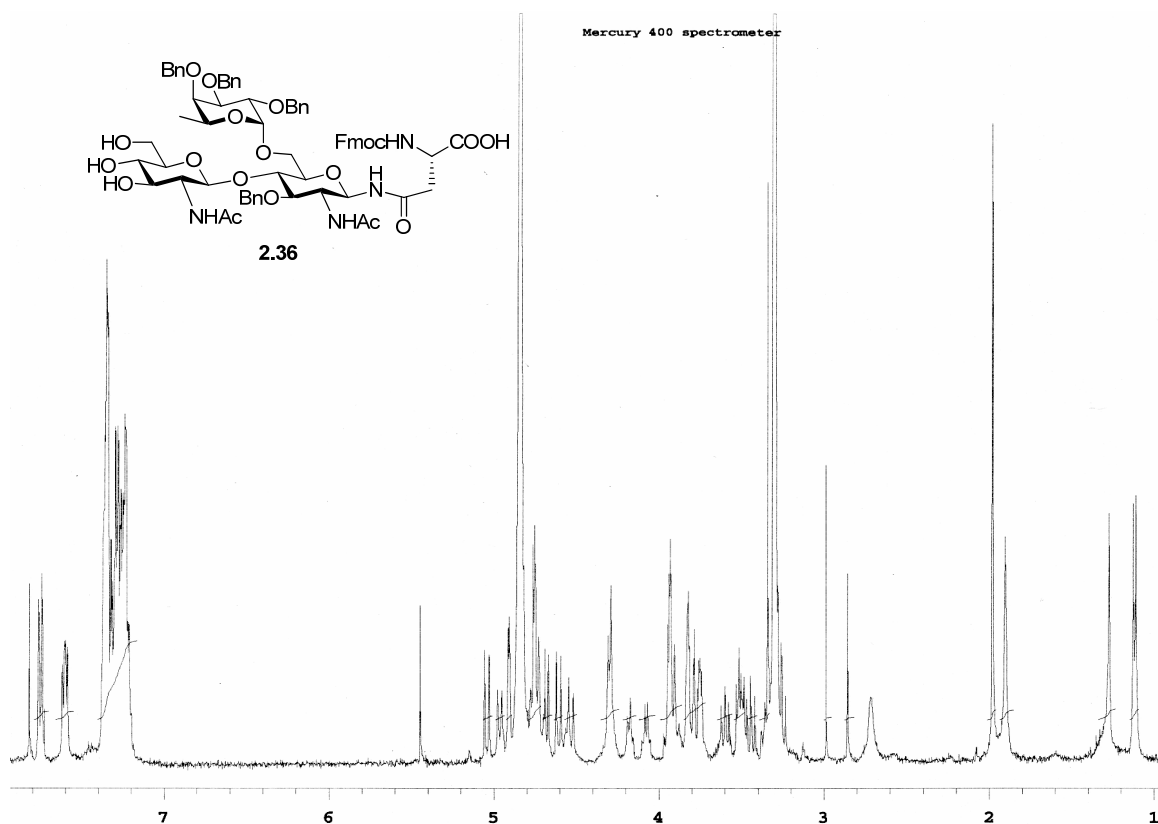
Mercury 400 spectrometer

2.36

7   6   5   4   3   2   1

Single Mass Analysis
Tolerance = 5.0 PPM   /   DBE: min = -1.5, max = 50.0
Element prediction: Off
Number of isotope peaks used for i-FIT = 3

Monoisotopic Mass, Even Electron Ions
588 formula(e) evaluated with 5 results within limits (up to 50 best isotopic matches for each mass)
Elements Used:
C: 0-70   H: 0-100   N: 0-5   O: 0-25   23Na: 0-1

Guo- Ben Swarts BUS-III-88 mw1266 LCT0076 0.2uL meoh 2mm stk
Shay 2008-07b.pro   LCT Premier
2008_0813_0076_15 17 (0.372) Cm (17:20-33:43x2.000)

2.36

15:54:14 13-Aug-2008

1: TOF MS ES+
4.35e+003

$[M+Na]^+$

100

%

0

199.1892   212.1197   303.1309   304.1357   305.1482   409.2913   645.2563   656.2485   656.7491   667.2402   671.7187   834.1784   873.3118   972.7915   1089.8285   1268.5304   1289.5116   1290.5137   1291.5190   1312.4995   1439.9535

100   200   300   400   500   600   700   800   900   1000   1100   1200   1300   1400   1500   m/z
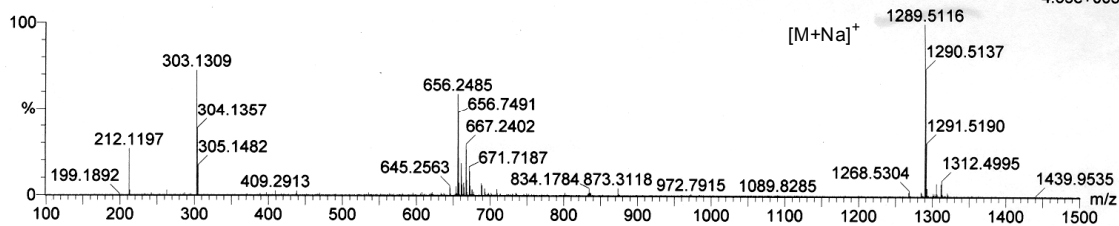
Minimum: -1.5
Maximum: 5.0   5.0   50.0

Mass	Calc. Mass	mDa	PPM	DBE	i-FIT	i-FIT (Norm)	Formula
1289.5116	1289.5104	1.2	0.9	23.5	47.3	0.3	C63 H82 N2 O25 23Na
	1289.5128	-1.2	-0.9	26.5	48.7	1.6	C65 H81 N2 O25
	1289.5145	-2.9	-2.2	27.5	51.1	4.0	C68 H82 O23 23Na
	1289.5158	-4.2	-3.3	32.5	52.9	5.9	C69 H78 N4 O19 23Na
	1289.5169	-5.3	-4.1	30.5	54.0	6.9	C70 H81 O23

2.16

.5   5.0   4.5   4.0   3.5   3.0   2.5   2.0   1.5   1.0   0.5
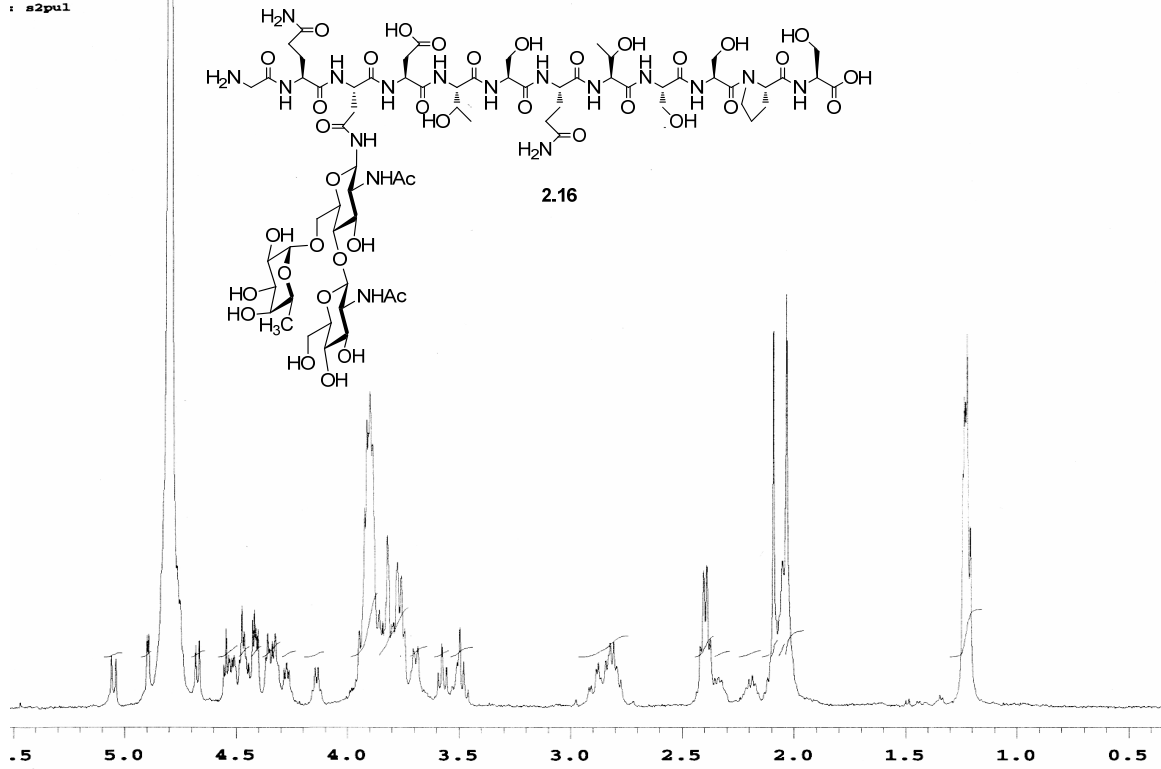
Comment 1   CD52_Trisac_NH2
Comment 2   DHB Positive
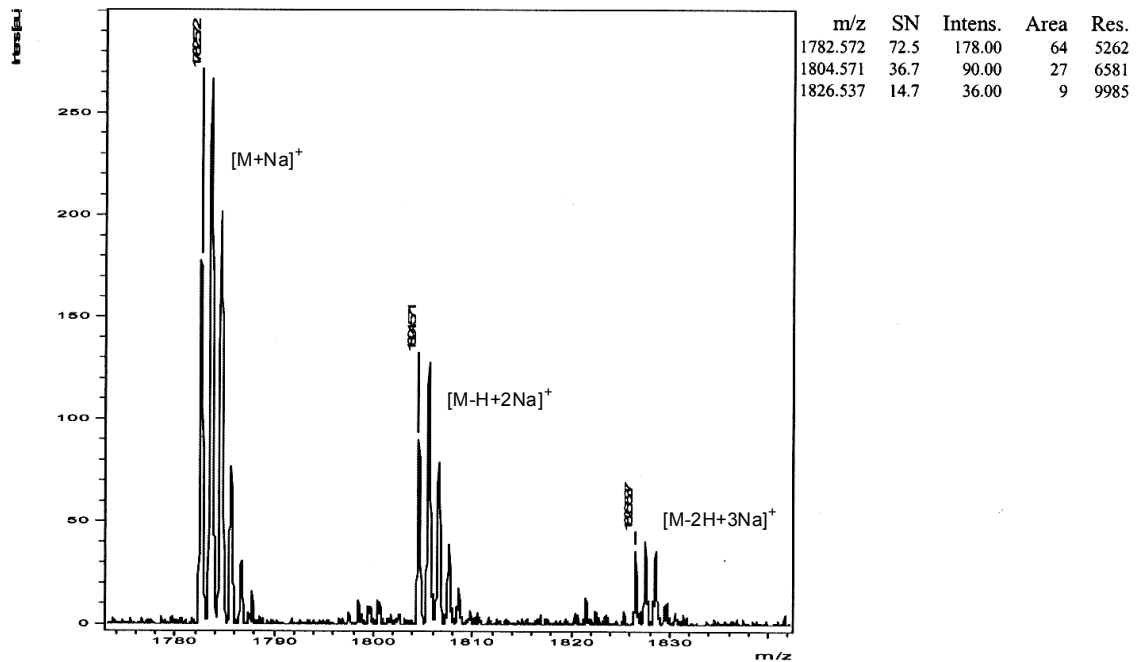
m/z	SN	Intens.	Area	Res.
1782.572	72.5	178.00	64	5262
1804.571	36.7	90.00	27	6581
1826.537	14.7	36.00	9	9985

[M+Na]⁺

[M-H+2Na]⁺

[M-2H+3Na]⁺

1780   1790   1800   1810   1820   1830   m/z

Varian 500 MHz spectrometer

Heteronuclear polarization transfer experiment

C13 AND DEPT SPECTRA

CH AND CH3 CARBONS

CH2 CARBONS

2.16

CH CARBONS

ALL CARBONS

INDEX
1
2
3
4
5
6
7
8
9
10
11
12
13
14
15
16
17
18
19
20
21
22
23
24
25

200   180   160   140   120   100   80   60   40   20   **ppm**
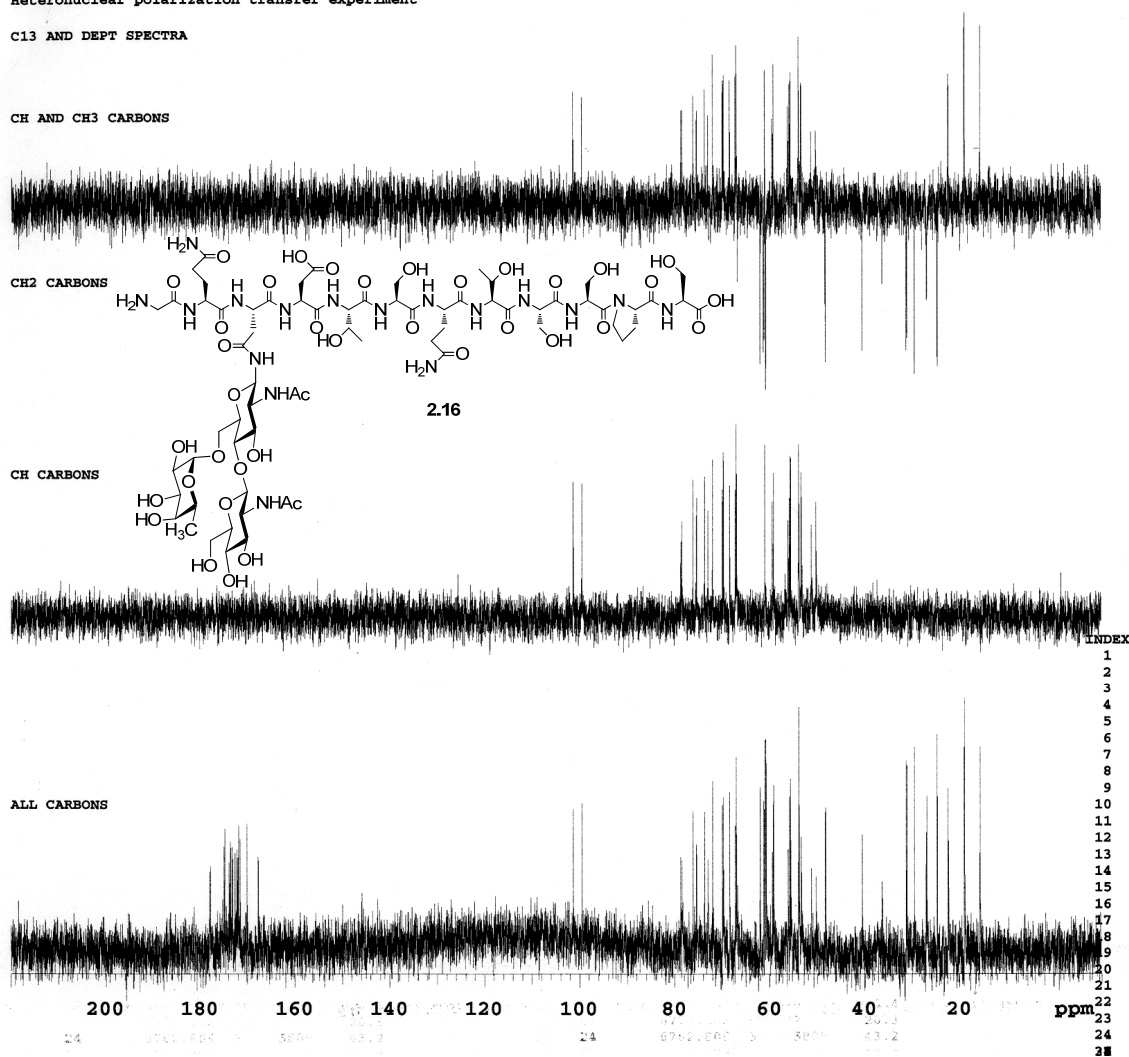
ABSTRACT

**SYNTHESIS OF FUNCTIONALIZED GPI ANCHORS
AND RELATED GLYCOCONJUGATES**

by

BENJAMIN M. SWARTS

March, 2010

Advisor: Zhongwu Guo, B.S, Ph. D.

Major: Chemistry (Organic)

Degree: Doctor of Philosophy

This dissertation is divided into two chapters describing the background, significance, and synthesis of GPI anchors and GPI-anchored molecules. GPI anchors are a class of complex glycolipids with the primary purpose of attaching cell surface proteins/glycoproteins to the cell membrane. The first chapter is focused on the synthesis of functionalized GPI anchors, and begins with an introductory look at the discovery, structure, biosynthesis, and biological functions of GPIs. Then, after surveying progress and achievements in GPI synthesis, including discussion about current strategic shortcomings in the field that prevent the chemical synthesis of various GPI derivatives, our approach to accessing uniquely functionalized GPI anchors is described. By employing the *para*-methoxybenzyl group for global hydroxyl protection, rather than traditional benzyl- or acyl-based protection, several functionalized GPI anchors were synthesized, including GPIs bearing unsaturated lipid chains, an alkyne-containing 'clickable' GPI anchor, and a biotinylated GPI anchor.

In the second chapter, the topic is shifted from the GPI itself to a GPI-anchored molecule, namely the human CD52 antigen, which is a 12-amino acid glycopeptide containing a single *N*-glycosylation site, to which complex glycans are attached. This glycoconjugate exists in two distinct functional forms, including lymphocyte and sperm CD52, which are involved in the human immune and reproductive systems, respectively. The contrasting biological functions arise from structural differences in their *N*-glycan and GPI anchor, raising the topic of how *N*-glycosylation and GPI-anchorage affect peptide structure, and consequently, activity. To probe this question, we synthesized several CD52 peptides and glycopeptides and compared their conformational profiles using circular dichroism. This work, as well as brief introductions to *N*-glycosylation, the CD52 antigen, and chemical synthesis of glycopeptides are discussed the second chapter.

Both chapters contain extensive experimental details for the preparation of all unknown compounds. Appendices A and B provide selected characterization data, including NMR, MS, and HPLC chromatograms, for chapters 1 and 2, respectively.

AUTOBIOGRAPHICAL STATEMENT

Education

- 8/2005-3/2010   Ph.D. in Organic Chemistry

                           Wayne State University, Detroit, MI

                           Advisor: Professor Zhongwu Guo

- 8/2000-5/2004   B. A. in Chemistry

                           College of Wooster, Wooster, OH

                           Advisor: Professor Judith C. Amburgey-Peters

Selected Publications

1. Benjamin M. Swarts, Yu-Cheng Chang, Honggang Hu, and Zhongwu Guo. Synthesis and CD Structural Studies of CD52 Peptides and Glycopeptides. *Carbohydr. Res.*, **2008**, *343*, 2894.

2. Benjamin M. Swarts and Zhongwu Guo. "Carbohyrate-Based Antiviral Vaccines" in *Carbohydrate-Based Vaccines and Immunotherapies*; Guo, Z., Boons, G.-J., Eds.; John Wiley & Sons, Inc.: Hoboken, 2009, p 167.

3. Zhimeng Wu, Xueqing Guo, Qianli Wang, Benjamin M. Swarts and Zhongwu Guo. Sortase-Catalyzed Peptide−Glycosylphosphatidylinositol Analogue Ligation. *J. Am. Chem. Soc.*, **2009**, *131*, 9878.

4. Xueqing Guo, Qianli Wang, Benjamin M. Swarts and Zhongwu Guo. Sortase A-Catalyzed Transpeptidation of GPI derivatives for Chemoenzymatic Synthesis of GPI-Anchored Proteins. *J. Am. Chem. Soc.*, **2010**, *132*, 1567.

5 Benjamin M. Swarts and Zhongwu Guo. Synthesis of GPI Anchors Bearing Unsaturated Lipid Chains. *J. Am. Chem. Soc.*, **2010**, accepted.